I. CATALYST DEVELOPMENT IN ASYMMETRIC PHASE TRANSFER CATALYSIS EMPLOYING QSAR METHODS
II. COMPUTATIONAL INVESTIGATIONS ON THE STEREOCHEMICAL COURSE OF THE ADDITION OF ALLYLSILANES TO ALDEHYDES

BY

LAWRENCE M. WOLF

DISSERTATION

Submitted in partial fulfillment of the requirements
for the degree of Doctor of Philosophy in Chemistry
in the Graduate College of the
University of Illinois at Urbana-Champaign, 2013

Urbana, Illinois

Doctoral Committee:

Professor Scott E. Denmark, Chair
Professor Martin D. Burke
Professor Paul J. Hergenrother
Professor Kenneth S. Suslick

Abstract

Part I of this dissertation describes the investigation in APTC employing a chemoinformatic analysis of the alkylation of a protected glycine imine with libraries of enantiomerically enriched quaternary ammonium ions. The synthesis of the quaternary ammonium ions follows a diversity oriented approach wherein the tandem inter[4+2]/intra[3+2] cycloaddition of nitroalkenes serves as the key transformation.. Catalyst activity and selectivity are rationalized in a qualitative way based on the effective positive potential of the ammonium ion. The next stage involved the development of quantitative structure -selectivity relationships (QSSR) for the alkylation of a protected glycine imine with libraries of quaternary ammonium ion catalysts. The variation in the observed enantioselectivity was rationalized employing a comparative molecular field analysis (CoMFA) using both the steric and electrostatic fields of the catalysts. A qualitative analysis of the developed model reveals preferred regions for catalyst binding to afford both configurations of the alkylated product.

In Part II, the diastereoselectivity of the addition allylsilanes to aldehydes is investigated using density functional theory. The interaction-distortion/activation-strain model of reactivity is used to rationalize the origin of the selectivity. Consistent with experimental model systems, the synclinal transition states are determined to be preferred over the antiperiplanar transition states in the electrophilic-activated manifolds and vice versa for the fluoride-activated manifold. The selectivity for the syn diastereomer in the electrophilic activation manifolds is accounted for by increased electrostatic and orbital interactions for a particular synclinal transition state at the expense of increased steric interactions relative to antiperiplanar transition states. The selectivity for the anti diastereomer in the nucleophilic manifold is explained by the lesser electrostatic repulsion in the antiperiplanar transition states which are favored relative to the synclinal transition states. Comparison of the transition states at constant distortion also reveals the origin of the variation in distortion in the transition states in terms of components of the interaction energy.

Acknowledgements

While graduate school does not necessarily lend the freedom to choose the people that surround us, I have been very fortuanate to have been surrounded by talented people with immearsurable kindness to whom I am indebted to for completing the following work.

I first must express my gratitude to a number of past Denmark group members for generously sacrificing much of their time torward my development for which special thanks are required for Chris Butler, Chris Regens, Nathan Gould, Tyler Wilson, and Nathan Werner. An additional appreciation is warranted for Nathan Gould for his exceptional mentorship and friendship. I have valued greatly his uniquely pragmatic, logical viewpoints and arguments on science and life in general.

Additional gratitude goes to all present Denmark group members for their continued friendship, support, and suggestions. I am especially grateful to past and present PTC subgroup members including Nathan Gould, Min Xie, Nici Bisek, Nick Anderson, Rob Weintraub, Lindsey Cullen, and Jeremy Henle for all of their helpful suggestions and for withstanding my longwinded reports and their occasional irrelavancy. A special thanks is needed for Tim Chang, who has been a good friend and has displayed commendable tolerance for my daily approach of either wacky ideas or some other positively inconsequential discussion. Others that I need to thank include Alex Jaunet (the Frog) for delightful conversation; my most recent lab mate Jeremy Henle who is more equipped and suited to pursue what was apparently beyond my capacity and for his guts for doing so; Andy Thomas for his “southern pragmatic” level of input; and anyone else that I apologize to for not mentioning here.

It would be difficult for me to envision reaching this point without the continued, unwavering support of my parents. Their encouragement and support has been paramount to this accomplishment as well as to me maintaining my marbles.

Finally, much gratitude is expressed toward my advisor Professor Scott E. Denmark. Prof. Denmark has instilled in me a level of confidence that I did not otherwise believe achievable. I am grateful to Prof. Denmark’s provision of the right amount of support and guidance per the freedom to pursue my own ideas. Lastly, while Prof. Denmark’s well known attention to detail is indeed of otherworldly rigor, I am a better scientist for the requisite attempted adherence to it.

To my Parents.

Table of Contents

Chapter 1: *Introduction and Background to Phase Transfer Catalysis*

1.1. Phase Transfer Catalysis and Catalyst Types.

Phase Transfer Catalysis (PTC) is an immerging methodology in organic synthesis that not only provides experimentally practical and environmentally benign alternatives to traditional techniques for performing ionic chemical reactions, but also exhibits the potential for addressing unsolved methodological problems. At the core, PTC can be loosely defined as a process that includes chemical reactions taking place in more than one phase.[1] The more typical application of PTC is toward the activity enhancement of nucleophilic anion reactants in the presence of a neutral electrophile (a nucleophilic activation mode). This mode of activation is in stark contrast to the much more common electrophilic mode of activation using conventional Lewis acids.[2] The overall reactivity enhancement is thought to arise in two general forms which are (1) increased collision frequency via interfacial transport (between phases) and (2) enhancement of negative partial charge on the anionic nucleophile through increased charge separation. A variety of phase transfer agents have been implemented for these purposes and among the most useful include ammonium salts, phosphonim salts, and crown ethers (Chart 1). Ammonium salts have received the most widespread use, due in part to their compatibility with a wider pKa range, and are the focus in this dissertation.

Chart 1.

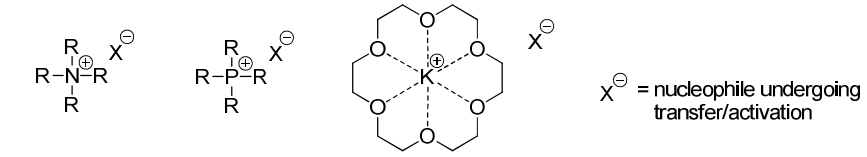

1.1.1. Early Demonstration of Synthetic Utility.

The reactions of hard nucleophilic anions with neutral (usually lipophilic) electrophiles in homogeneous media is burdened by poor solubility of the nucleophilic partner in typical organic solvents. In these situations of poor solubility, the effective concentration of the anion is very low which usually equates to little to no observed reactivity. The traditional solution is to use of

very polar aprotic solvents[3] (DMF, HMPA, DMSO, etc.) to solubilize the hard anionic nucleophile. However, the toxicity of such solvents is not particularly attractive and difficulties encountered with isolation are not uncommon, particularly if the desired product exhibits appreciable water solubility.

Alternatively, a biphasic system can be used (ie. toluene/water) in which each phase adequately dissolves each of the reactants (hard, hydrophilic anion dissolves in water and lipophilic electrophile dissolves in toluene). An example that illustrates this is the S_N2 displacement of an alkyl chloride with sodium cyanide (Scheme 1a). Although, in the absence of any other agents, the reactants will not be able to locate each other if there is no path for either of the reactants to traverse the boundary between the phases (interphase). The inclusion of an agent that is capable of modifying the properties of either of the reactants in such a way as to temporarily increase its affinity for the phase occupied by the other reactant would exponentially increase the collision frequency, effecting the desired chemical reaction. Modification of the alkyl chloride is not advantageous on account of the lack of strong intermolecular interactions inherent in alkyl halides. The ionic interaction between Na^+ and CN^- renders sodium cyanide more suitable for modification. If the hard, hydrophilic Na^+ can be exchanged with a more lipophilic cation, the associated CN^- would be theoretically more susceptible toward traversing the interfacial boundary to the organic layer where the desired reaction can occur.

Scheme 1.

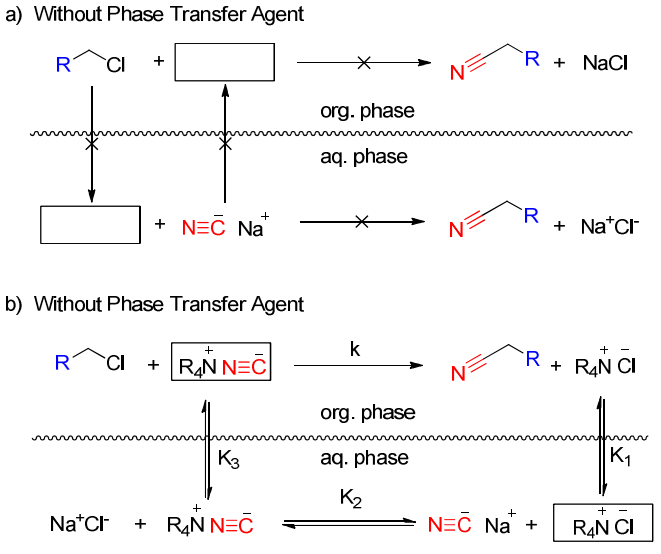

This has been performed and is among the earlier synthetically useful PTC reactions studied in detail in which an ammonium salt, $(C_6H_{13})_4N^+Cl^-$ (1wt%), was used as the phase transfer agent for the displacement of 1-chlorooctane (neat) with aqueous sodium cyanide.[4] Through counterion exchange of the ammonium chloride (Q^+Cl^-) with the sodium cyanide in the aqueous layer (K_2), Q^+CN^- is generated and this more lipophilic CN^- source is transported into the organic layer where the desired reaction can take place. The mechanism above outlines the extraction mechanism and will be discussed in more detail in Chapter 2.

1.1.2. PTC as an Alternative to Strong Base Chemistry.

Much of the synthetic potential of PTC can be manifested in the capacity to perform chemistry that typically requires strong base ($pk_a > 15$) under considerably milder conditions using inorganic hydroxide or carbonate bases. The Williamson ether synthesis[5] typically calls for the application of strong hydride bases (NaH or KH) in homogenous polar aprotic media. Alternatively, this reaction can be performed just as effectively using aqueous sodium hydroxide with an ammonium salt as the catalyst which greatly expands upon the rigorous conditions of the standard Williamson ether synthesis protocol (Scheme 2a).[6] Similarly, the alkylation of carbon-based acids such as phenylacetylnitrile ($pk_a > 25$) (Scheme 2b) is typically performed using strong hydride or lithium amide bases. The application of an ammonium salt in aqueous sodium hydroxide is sufficient for performing this reaction successfully. The formation of a stereogenic center in this case allows for the opportunity for enantioselectivie catalysis which greatly expands upon the synthetic utility and is the focus of a separate section.

Scheme 2.

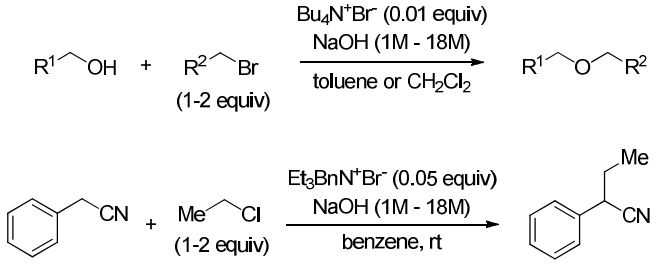

The rationale for the ability of PTC to access higher pK_a ranges can be attributed to chemistry taking place in the interfacial region is both catalyst and hydroxide rich. This

additional phase confers an added dimension of complexity to the overall mechanism and is discussed in greater detail in Chapter 2.

1.2. Catalyst Activity.

1.2.1. Catalyst Influence on Rate.

The efficacy of a PTC catalyst is thought to be linked to two principle components of a PTC process. The transfer or net delivery of the nucleophilic anion from the aqueous phase into the phase occupied by the electrophile, typically the organic phase, is one of these components. This overall transfer process may be comprised of numerous equilibria which depends on the mechanism operative. For the NaCN displacement of 1-clorooctane (Scheme 1), the transfer process is comprised of equilibria K_1, K_2, and K_3. The second component is the reaction of the quaternary ammonium cation/reacting anion ion pair with the organic substrate in the organic phase. This step is termed the intrinsic reaction . Any one of these components or a continuum thereof can limit the rate of a PTC reaction.

One can attain a rudimentary understanding on how these processes are interlinked via a mnemonic developed by Starks coined the PTC reaction rate matrix (Figure 2).[7] The PTC matrix consists of a plot of intrinsic reaction rate versus transfer. This plot is then divided into four quadrants. The fast quadrant in the upper right represents reactions in which both the transfer and intrinsic reactions are comparably fast. Reactions in this region need little optimization with respect to catalyst design. PTC reactions that are inherently slow for both transfer and intrinsic reaction belong in the lower left quadrant. Careful choice of catalyst as well as reaction optimization is necessary for these types of reactions. The lower-right and upper-left quadrants represent reactions where the overall reaction rate is limited by the intrinsic and transfer steps respectively.

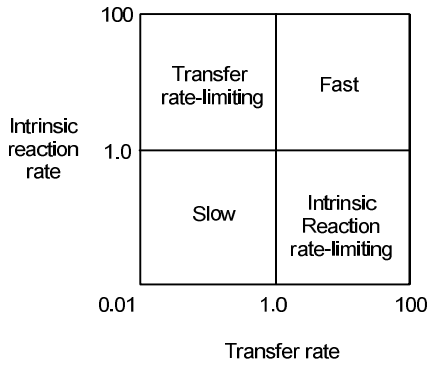

Figure 1.. PTC reaction rate matrix.

1.2.2. Mechanism of Hydroxide Initiated PTC

The broad utility of PTC has motivated numerous investigations from fields as for reaching as synthetic chemistry, chemical engineering, computational chemistry, physical chemistry and chemoinformatics. PTC reactions that use aqueous bases to generate carbanions are termed hydroxide-initiated PTC.[8] The mechanism of hydroxide-initiated PTC reactions is an intensely investigated subject that has been thoroughly reviewed from both a chemical[9] and engineering[10] perspective. Pioneering studies by Makosza[11] and Starks[12] led to two distinct mechanistic descriptions, later termed the interfacial (Makosza) and extraction (Starks) mechanisms. The mechanisms differ in the mode in which the substrate·ammonium ion pair enters the organic phase (Figure 2). Numerous studies have provided experimental support for *both* the extraction[13,14] and interfacial mechanisms.[15,16,17] These studies have accumulated a number of phenomenological observables that are used as indicators to decipher which mechanism is dominant.[9b] Reactions governed by the extraction mechanism show little dependence on stirring rate and first order kinetic behavior in substrate and catalyst. On the other hand, PTC reactions governed by the interfacial mechanism show a strong dependence on stirring rate, complex kinetic order in substrate, and fractional order in catalyst. The current understanding of hydroxide-initiated PTC reactions suggests a mechanistic continuum that is strongly dependent on substrate pKa and catalyst structure.[9b] To summarize, the extraction mechanism is dominant at the two extremes of substrate acidity (pKa < 16 and pKa > 23) and the interfacial mechanism is dominant when the pKa of the substrate is between 16-23. The rational is that reactions with highly acidic substrates are rate limited in extraction of the substrate

enolate and non-acidic substrates are rate limited by the rate of hydroxide extraction. Thus, the interfacial mechanism is proposed to be most relevant for enolate alkylations.[18]

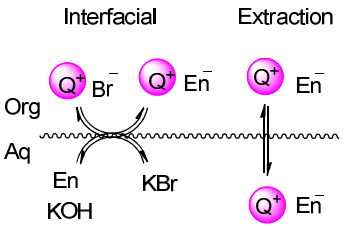

Figure 2. Simplified mechanistic views of the interfacial and extraction based mechanisms

1.2.3. Guidelines for the Design of Active Catalysts

The quaternary ammonium ion catalyst is the most critical element of a PTC reaction the selection of the "optimal" catalyst is crucial.[19,9b] The fact that there are two possible mechanisms, in combination with the possibility of many "off-cycle" pre-equilibria, all of which are a function of substrate and catalyst combination, has made identifying simple structure activity relationships difficult.[9a] For reactions strictly following an extraction mechanism (e.g. S_N2 displacements with N_3^-, CN^-, SCN^-, etc.) catalyst activity correlates well with lipophilicity.[14,13,20] No such generalizable structure activity relationships exist for hydroxide-initiated PTC reactions.

For hydroxide-initiated PTC reactions small hydrophilic ammonium ions are often superior catalysts, which is a compounding source of confusion.[21,22] For example, triethylbenzylammonium, a small hydrophilic quaternary ammonium ion is an efficient catalyst for a myriad of PTC enolate alkylations (e.g. nitriles, esters, ketones…etc.).[23] One approach has been to correlate a macroscopic observable such as interfacial surface tension to catalytic activity which unfortunately does not address the question of what catalyst attributes confer high activity.[24] In a rare SAR study, the ammonium ion accessibility (or size) *and* solubility were varied simultaneously and the most active symmetrical catalyst for alkylations was tetraethylammonium bromide.[25] A useful quantitative correlation of structure to catalyst activity was subsequently derived, namely the structural parameter, *q* (Equation 1).[26] The *q* parameter is defined as the sum of the reciprocals of the number of carbons on each chain.[27] For hydroxide-initiated PTC reactions, such as the alkylation of enolates, *q* values between 1.5 and 2.0 are optimal. This analysis is useful for simple quaternary ammonium ions containing only alkyl chains ($C_{1\text{-}4}$) but extension to catalysts containing functional groups, changes in hybridization, rings, branch points, or stereogenic centers has not been reported.

$$q = \frac{1}{n_1+1} + \frac{1}{n_2+1} + \frac{1}{n_3+1} + \frac{1}{n_4+1}$$

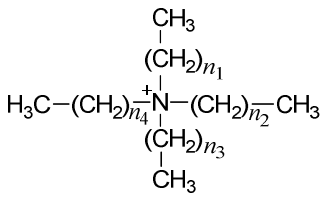

Equation 1. n_x (x=1,2,3,4) is the number of carbon atoms minus 1 along x of the 4 linear chains

1.3. Asymmetric Phase Transfer Catalysis

1.3.1. Enantioselective Alkylation Methods

The requirements for a catalytic, enantioselective, enolate alkylation are the in-situ generation of an enolate, alkylation in the presence of a stereochemical controlling element and stereochemical stability of the product (Scheme 3). Although auxiliary-based methods for the diastereoselective alkylation of enolates truly revolutionized the practice of organic synthesis in the 1970's.[28,29] A general and selective processes for catalytic enantioselective alkylations remains elusive.[30] In contrast to other carbon-carbon bond forming reactions of enolates (compare to e.g. aldol and Michael reactions), the rate of enolate alkylation is significantly less than addition to a π-system, thus the use of soft-enolization techniques which are crucial for catalytic π-addition reactions cannot be utilized for enolate alkylations.[31] The use of more reactive enolates, and strong bases to generate them, introduces a host of compatibility issues thus preventing the implementation of similar stereocontrol elements under catalytic conditions. Phase transfer catalysis relieves some of these compatibility issues and is thus ideally suited for approaching this problem.

Scheme 3.

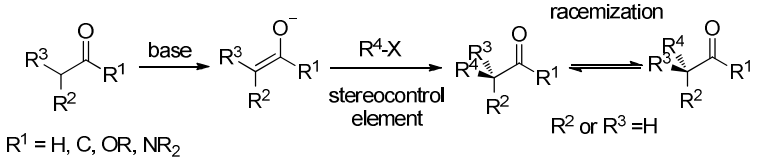

1.3.2. Early Examples of APTC

Phase transfer catalysis has already proven to be a broadly applicable and general method to perform strong base chemistry in a catalytically.[32] In particular, the catalytic, enantioselective alkylation of enolates has been extensively investigated in the context of APTC. In a landmark publication, the Merck Process Group reported the enantioselective alkylation of an indanone

under PTC conditions employing an *N*-4-trifluoromethylbenzyl cinchona alkaloid derivative.[33] Their detailed optimizations revealed a number of useful insights: (1) the use of a non-polar, polarizable solvent such as benzene or toluene was critical to achieving high enantioselectivity, (2) the enantioselectivity exhibited a small temperature dependence, while the reaction rate exhibited a large temperature dependence and (3) the presence of electron withdrawing groups on the N-benzyl substituent resulted in enhanced enantioselectivities.[33c]

Efforts to develop toward the development of synthetic routes to enantioenriched α-amino acids lead to a second critical advance in 1989 when O'Donnell demonstrated the selective alkylation of glycine imines under similar conditions (Scheme 4).[34] This discovery represented the first practical synthesis of enantioenriched α-amino acids through phase transfer catalysis. Conveniently, the different diastereomers, cinchonidine and cinchonine, were found to be enantio-complimentary in that each enantiomer of the product could be accessed in good enantioselectivity using each diastereomer. O'Donnell's alkylation has proven to be an operationally simple method for α-amino acid synthesis and has since served as a benchmark for the development of new asymmetric phase transfer catalysts.[35]

Scheme 4.

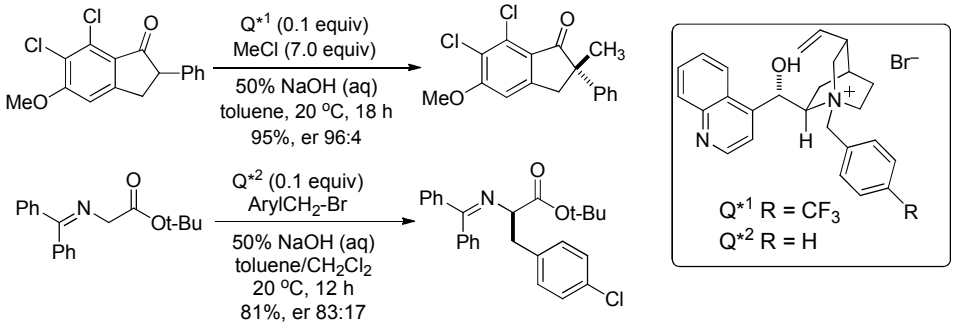

In the intervening 20 years many variations of cinchona alkaloid catalysts have been reported. The first notable advances were from independent studies by Lygo[36] and Corey,[37] in which the incorporation of a 9-anthracenylmethyl moiety as the nitrogen substituent markedly improved the enantioselectivity (Chart 1). Analogously, Park and Jew developed a tri-fluorinated *N*-benzyl quaternary ammonium catalysts[38a] and dimeric, meta-bridged cinchoninium catalysts.[38b] In recent years, Maruoka and Ooi have introduced a large number of novel, non-cinchona alkaloid catalyst systems based on a binaphthyl scaffold which allows introduction of substituents in the 3,3' positions.[39] Similarly, employing an in situ generation and screening

process, Lygo has discovered a useful locally C_2 (at the nitrogen) symmetric catalyst.[36c] Shibasaki/Ohshima,[40] Sasai,[41] Arai/Nishida,[42] and others have independently developed two-centered (and higher) APTC's by incorporation of quaternary ammonium ions, about a C_n axis. In addition to extensive catalyst development, significant advances in other typically strong-base-promoted reactions have been recorded including double alkylation of glycine imines, ketone alkylations, Michael, aldol, Mannich, and Darzens reactions as well as epoxidations and aziridinations.[32k,l,m,n]

Chart 2.

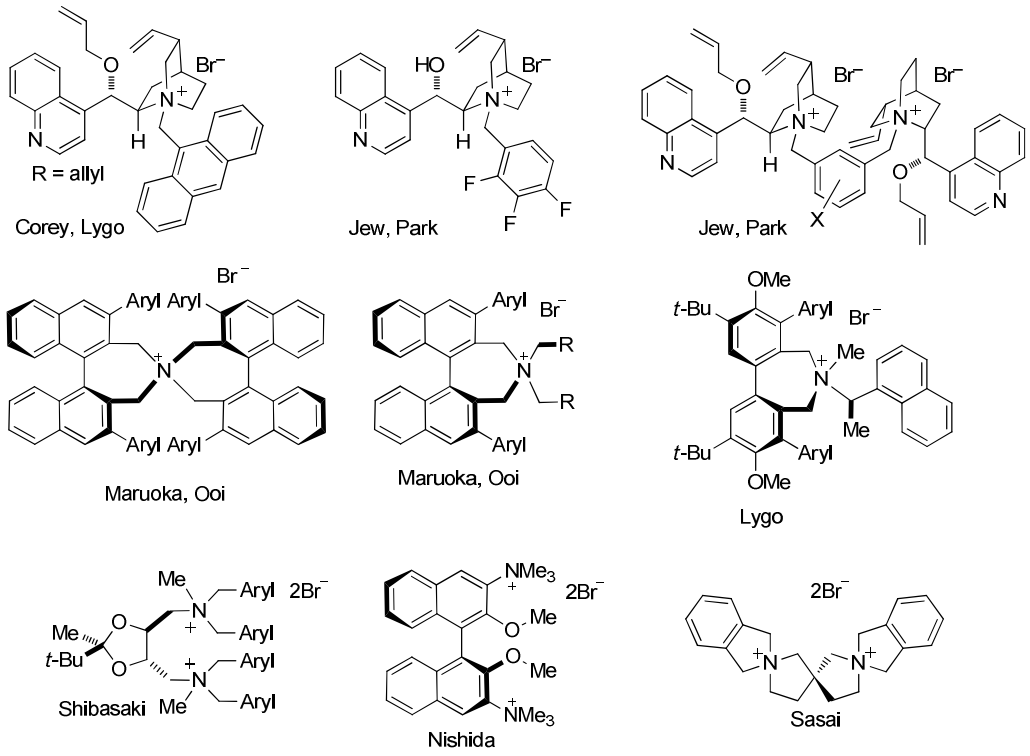

1.4. Stereochemical Models for Enantioselectivity (*chinchona alkaloid-derived*)

The rationalization of enantioselectivity and reduction to design criteria is of preeminent importance to the study of catalytic processes.[43] The alkylation of O'Donnell's imine is by far the most studied enolate alkylation and two general models have been proposed to rationalize the enantioselectivity observed with *cinchona* alkaloid derived catalysts (Figure 3).[44] In an early, thorough computational study, O'Donnell and Lipkowitz analyzed the enolate molecular recognition event and origin of enantioselectivity of this important transformation.[45] Computational results suggest selective binding of the catalyst to the *Si* face of the *Z*-enolate (a).

Subsequently, it has been proposed that catalysts bearing a 9-methylanthracenyl group on nitrogen react through the *E*-enolate (b).

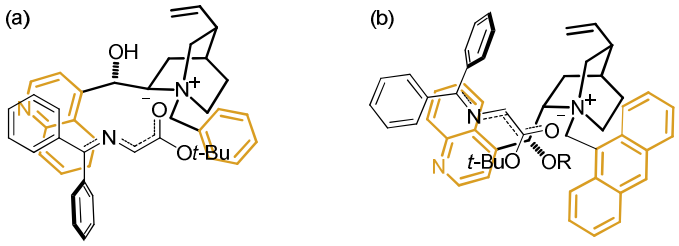

Figure 3 Stereochemical models using *cinchona* derived PTC catalysts.

The preferred region for anion association for the *cinchona* alkaloid derived catalysts has been performed using nOe correlations. [46] Using borohydride and fluoride as the counteranions, the nOe correlations suggested a stronger association with the left face (Figure 4a) on account of correlations with the H bound to C(1) and the quinoline hydrogens. The lack of strong correlations with the hydrogens bound to C(2) suggested only weak association with this region. These studies provide good support for strong hydrogen bonding interactions of the type $N^{+}CH\bullet\bullet\bullet O^{-}$ in solution which has also been identified in the solid state by X-ray crystallographic analysis of quaternary ammonium-enolate ion pairs.[47] High level calculations by Houk and Cannizarro further corroborate that in solution, ammonium ion ester enolates tend to orient "π-facial" to one of the faces of the ammonium (Figure 4b).[44b] The combination of these analyses lends to a useful design mnemonic by inscribing the ammonium nitrogen in a tetrahedron (red) where the vertices are the four carbons bound to it. The face proximal to the oxygen is the energetically more accessible region than the remaining three faces of the tetrahedron.

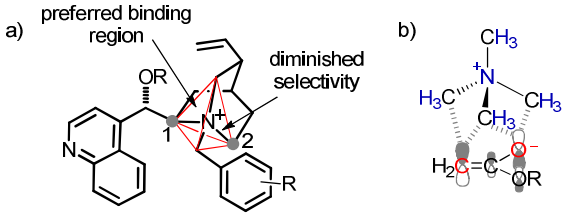

Figure 4. a) analysis of selectivie tetrahedral faces of *cinchona*-derived quaternary ammonium salts. b) facial association of enolate with ammonium cation

Very recently, a full DFT transition state modeling study has been performed on the cinchonidinium PTC enolate allylation to further refine the origins of enantioselectivity.[48] An

ensemble of several hundred transition states were searched systematically for both π-facial and oxyanion approaches of the enolate. The lowest energy transition state states exhibited oxyanion type binding rather than π-facial type (Figure 4b) as is observed for the ground state ion pairs. The change of binding from ground state to the transition state is consistent with the removal of negative partial atomic charge from the carbon atom toward the allyl electrophile. An important conformational controlling element in the transition state is purported to be a CH•••π interaction between the arene C-H of the out of plane phenyl group of the enolate with the π-system of the quinoline moiety. Increased Coulombic interaction is also believed to favor the lowest energy transition state through decreased separation between the oxygen of the enolate and the ammonium center due to the adoption of a sterically less encumbering conformation relative to the next closest in energy transition states. The increased enantioselectivity with the 9-anthracenyl group relative to groups with less π-surface area can be explained by creating a more well defined pocket for the enolate rather than exhibiting additional π-stacking interactions with the enolate as previously believed. The results are consistent with previous computational studies.[45]

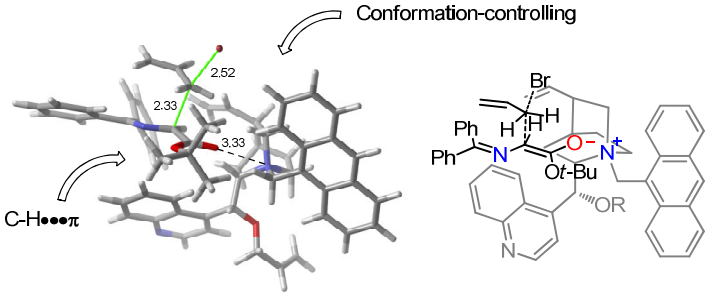

Figure 5. Lowest energy transition state for asymmetric alkylation with *cinchona*-derived catalyst.

The stereochemical models discussed help rationalize the enantioselecitivity for catalyst systems that perform well. However, the design criteria that can be learned from these studies may not translate as well to different enolate substrates, electrophiles, or alternative reaction types. Notwithstanding, the models do yield the most convenient and apparent starting guides for catalyst development. Methods that can be more intimately weaved in the catalyst development process may provide better opportunities for design and synthesis of more desirable catalysts. In-

as-such these methods should be capable of generating models that meet the pace at which the experimental data is accumulated. Strategies in chemoinformatics and quantitative structure-activity relationships are particularly useful for these purposes.

1.5. QSAR Modeling for Enantioselectivity.

Enantioselectivity in general has been modeled using geometrical descriptors such as steric size,[49] topological indices,[50] continuous chirality quantification methods[51] that indirectly account for 3-dimensionality, as well as various molecular interaction field (MIF) analyses. A MIF based approach was chosen to initiate these studies as it typically provides a more direct and more information-rich representation of the 3-dimensional features necessary to reflect the enantiotopic differentiating capacity of chiral catalysts.

MIF based approaches[52] are standard 3D-QSAR techniques employed in drug design. MIF algorithms encode variation in structure by positioning a probe atom and/or a point charge at fixed grid points around each molecule of interest and the interaction energies with the probe are recorded at each grid point. The dependent variable (typically a free energy of binding) is then linearly correlated with the interaction energies for which the coefficients are extracted from a multivariate linear regression analysis, commonly by Partial Least Squares (PLS) method. Although MIF approaches have enjoyed a long-standing history of greater than 20 years in medicinal chemistry for the development of drug candidates, only relatively recently (< 8 years) have they been applied to problems relating to asymmetric catalysis.

The most commonly employed MIF approach is Comparative Molecular Field Analysis (CoMFA). The method uses a molecular mechanics based force field to approximate van der Waals interactions and the standard Coulombic potential is used for electrostatic interactions for which the partial atomic charges are determined at the desired level of theory.[53] The appeal of this method stems from its predictive capacity and ability to allow one to visualize the developed model in terms of regions where field variation (either electrostatic or steric in origin) within the data set leads to a change in the dependent variable. In the field of asymmetric catalysis, this method was first applied in the analysis of the Diels-Alder reaction between cyclopentadiene and a 3-vinyloxazolidin-2-one using copper(II) Lewis acids with differing bisoxazoline and phosphinooxazoline ligands.[54] Methods that incorporate semi-empirical[55] as well as ab-initio quantum mechanical[56] interaction energies have also been developed and have found application in analyzing asymmetric diethylzinc additions using varying chiral amino alcohols[57] as well as

asymmetric lithiation using varying chiral sparteine surrogates.[56]

Two seminal reports employing CoMFA in the context of PTC involved the asymmetric alkylation of a protected glycine imine *tert*-butyl ester using different catalyst systems (Scheme 5).[58] In the first report,[58a] a model was developed employing varying cinchona alkaloid derived catalysts. In the second report,[58b] a model was generated for the same reaction while using different catalyst scaffolds developed by Lygo and coworkers.[59] The contributions of steric and electrostatic interactions to the variation in enantioselectivity were found to be roughly equivalent but the implications of electrostatic interactions were not discussed in detail in these reports, which are considered to be the predominate forces responsible for the ion-pair interaction strength.[60] Despite these important contributions, ambiguity is still present as to the dependence of electrostatic interactions on the observed enantioselectivity.

Scheme 5.

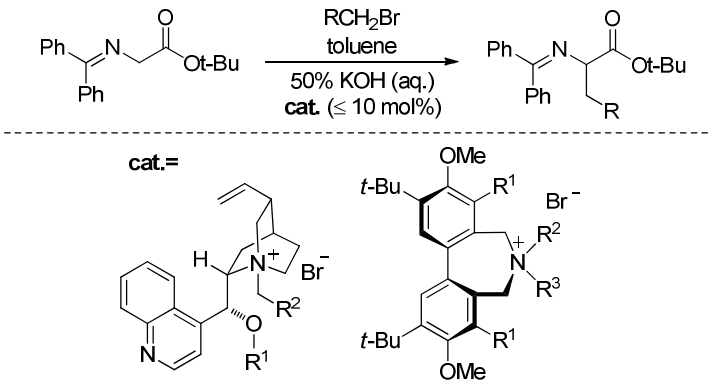

1.6. Research Objectives.

Part I of this dissertation involves the application of computer-aided design strategies toward the synthesis of enantioselective phase transfer catalysts. An enolate alkylation reaction was chosen for these studies for three reasons: (1) it is one of the oldest and most useful methods to form carbon-carbon bonds (2) many examples of PTC enolate alkylations are on record and (3) the methods to perform enolate alkylations in a catalytic enantioselective manner are very limited. The goals of this project involved a sequence of stages which involved: (1) synthesis of libraries of structurally diverse ammonium ions (2) collect rate and enantioselectivity data (3) construct mathematical models to reveal structural features that impart desirable enantioselectivity and activity (4) from these models develop mechanistic hypothesis and apply toward the synthesis of more active and enantioselective catalysts.

In Chapter 2 the synthesis of the catalyst librarires is discussed in detail. Synthetic strategies and protocols introduced that facilitate combinatorial synthesis. The collection of activity, in the form of half lives, and enantioselectivity data is elaborated. A discussion of the trends by qualitative analysis is also presented.

Chapter 3 concerns the development of QSAR/QSSR models. QSSR models for enantioselectivity were developed using the CoMFA method and the resulting models are discussed. Qualitative application of these models is presented.

The last chapter for Part I of this dissertation involves the development and application of alternative 3D-QSAR methods. The methods are discussed and applied to current data sets. Application of these models toward the synthesis of new catalysts is presented.

Chapter 2: *Synthesis and Evaluation of Catalysts*

2.1. Introduction.

Without testable hypotheses about what structural features will be dominant in conferring high phase transfer catalyst activity and selectivity, this project was necessarily initiated as a discovery oriented program. The initial focus was set on (1) identifying a suitable scaffold (or scaffolds) that could be prepared in enantiopure fashion and would allow for substitution in multiple positions followed by (2) developing suitably flexible parallel synthesis procedures for the elaboration of the scaffold to a diverse library of quaternary ammonium ions. Concurrently the scaffold and most easily substituted positions were evaluated in the context of known quaternary ammonium design principles. A strategy that was quickly identified as a reaction that embodies all of these requisite characteristics for scaffold selection was the tandem [4+2] / [3+2] cycloaddition of nitroalkenes, a methodology extensively studied in these laboratories (Scheme 6).[61]

Scheme 6.

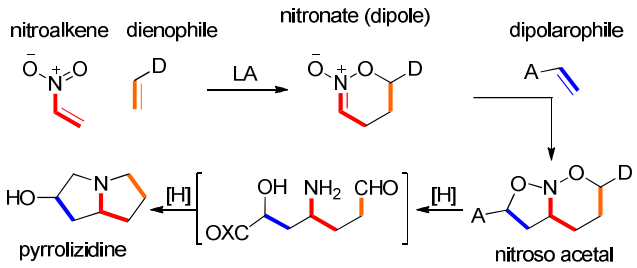

2.2. Synthetic Strategy.

2.2.1. Tandem [4+2]/[3+2] Cycloaddition.

In the tandem cycloaddition of nitroalkenes, three key components, a nitroalkene, a dienophile and a dipolarophile combine to construct a new six-carbon unit forging four bonds, up to six contiguous stereogenic centers, and four rings (Scheme 7). Lastly, the newly minted skeleton is transformed by hydrogenolysis, which proceeds by reductive N-O bond cleavage, followed by intramolecular reductive amination and lastly closure of the remaining ring to construct a pyrrolizidine ring system. Of the four possible permutations of inter- and intramolecularity, the tandem inter [4+2] / intra [3+2] family wherein the dipolarophile and

nitroalkene are covalently tethered is the most powerful (Scheme 7).[62] Tethering the dipolarophile to either the α- or β-position of the dienophile results in bridged cycloadducts and generates primary amines after hydrogenolysis. Tethering the dipolarophile to the nitroalkene results in either a spiro-mode (1-position) or a fused-mode (2-position) cycloaddition and generates tertiary lactams after hydrogenolysis. Extensive investigation of this family has revealed many advantages including: (1) ease of preparation of the precursors, (2) flexibility in the electronic nature and configuration of the components, (3) high levels of absolute stereocontrol with chiral dienophiles, and (4) diversity of product structure.[63]

Scheme 7.

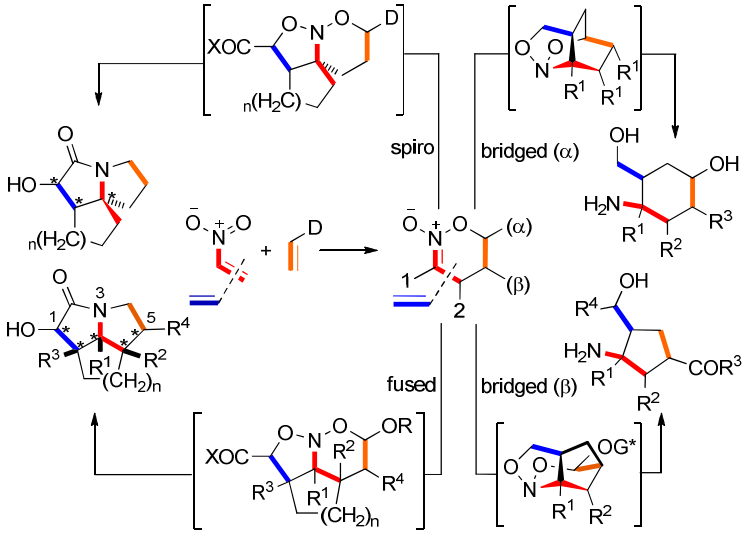

A key challenge to systematic investigation of APTC is the availability of catalyst scaffolds that allow for facile modification of sites proximal to the quaternary ammonium ion center.[64,65] Both the spiro- and fused-mode cycloadditions create skeletons where the nitrogen is fixed in a central position of a rigid ring system thereby providing potential for the controlled installation of groups in the vicinity of the nitrogen. The fused mode, tandem inter [4+2] / intra [3+2] cycloaddition with a two-carbon tether was chosen for initial studies. In this mode the tandem cycloaddition/hydrogenolysis sequence generates a tricyclic cyclopentapyrrolizidin-2-one ring system bearing a hydroxy group at C(1) and a substituent at C(5) (Scheme 7). Prior to elaboration of a detailed parallel synthesis strategy, the local environment around the ammonium nitrogen was considered in the context of known design principles.

2.2.2. Parallel Synthesis Design.

The tandem inter [4+2] / intra [3+2] cycloaddition of nitroalkenes in the fused mode allows for the stereoselective introduction of groups at C(5) (R^1) and a hydroxy group at C(1) while preserving the relative configuration of the scaffold ring system (Scheme 8). The variable groups R^1, R^2, and R^4 are situated on the convex face allowing for the evaluation of many different combinations of substituents. Because the C(5)-substituent (R^1) is the first point of diversification its variation was limited (either H or Me), thereby reducing the synthetic investment required for this initial survey. Moreover, the configuration of the C(1) center is dictated by the geometry of the dipolarophile thus introducing an additional element for diversification. After introduction of groups at C(1) and C(5) the scaffolds will be elaborated by means of parallel synthesis.

Scheme 8.

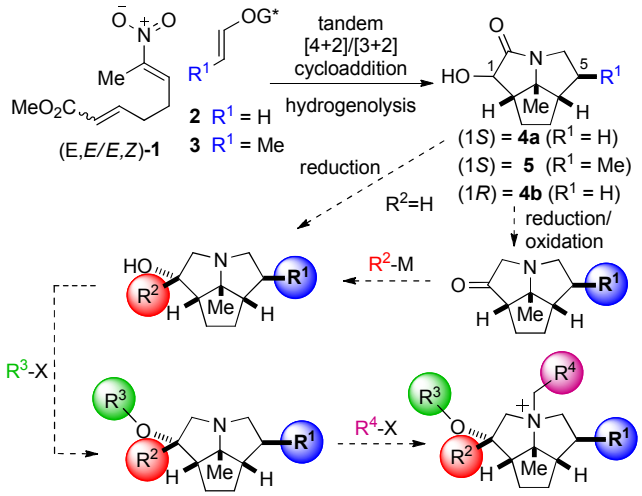

The forward synthetic analysis from the scaffold is outlined in Scheme 8. The hydroxyl group at C(1) was targeted for the next two points of diversification. Simple oxidation followed by addition of an organometallic reagent (R^2-M) would allow for the introduction of groups directly in the vicinity of the C(2)-C(7b)-C(9) face. Also, alkylation of the resulting alcohol (or the original secondary alcohol) with simple alkyl halides (R^3-X) would serve as a facile method for introducing groups on the concave face. Lastly, the nitrogen substituent (R^4) is installed by a second alkylation to afford the final quaternary ammonium salts. This analysis served as a general framework from which the order of synthetic steps suitable for parallel synthesis was worked out experimentally.

2.2.3. Library Design.

To facilitate description of the libraries, the catalysts are divided into focused sets of increasing substitution (**I-V**,Chart 3). The simplest members of this group (Library **I**) bear no oxygen containing functionality and vary only in the nitrogen substituent (R^4). Oxygen functionality is introduced in Libraries **II** and **III** whereas additional steric and conformation influencing groups are introduced in Libraries **IV** and **V**. Quaternary ammonium ion library members will be referred to by Roman numeral (Libraries **I-V**) followed by a braced number set designating the order and number of groups introduced {*X-X,X-X*}. For example, in Scheme 8 the intermediate free amine **X**{R^1,R^2,R^3} will be converted to library **V**{ R^1,R^2,R^3,*X-X*} through the action of reagents {*X-X*}.

Chart 3.

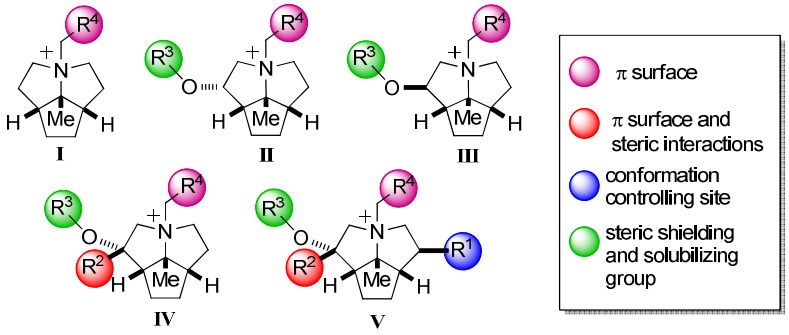

2.3. Synthesis Results.

2.3.1. Synthesis of Nitroalkenes.

To accurately determine the rate and enantioselectivity for each catalyst (ca. 3 runs/catalyst), approximately 30 mg of each quaternary ammonium salt would be required, thus mandating the synthesis of gram quantities of the scaffolds for Libraries **I-V**. Thus, the first phase of this investigation was to develop robust, scalable routes to the cycloaddition precursors (nitroalkenes (*E,E*)-**1** and (*E,Z*)-**1** and chiral vinyl ethers **2** and **3**, Scheme 8, above) in decagram quantities.

Nitroalkene (*E,E*)-**1** was synthesized by a known route with minor changes upon scale-up (Scheme 9). Thus, Wittig olefination of readily available 2-hydroxytetrahydrofuran[66] established the *E*-alkene geometry as well as the primary alcohol function in (*E*)-**6**. Oxidation by the Parikh von-Doering protocol,[67] (rather than the previously reported use of PCC), followed by immediate reaction of the aldehyde **7** under the standard Henry reaction conditions with nitroethane and

subsequent dehydration furnished nitroalkene (*E*)-**1** in excellent overall yield (86% over three steps). This route provided rapid access to tens of grams of nitroalkene (*E*)-**1**.

Scheme 9

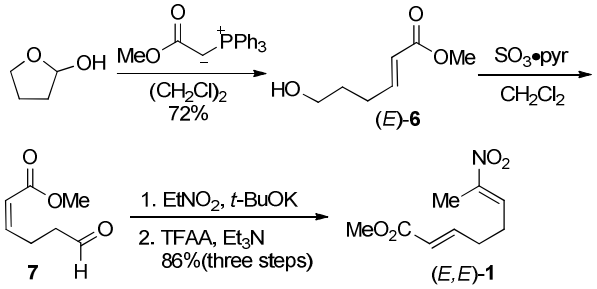

Large-scale preparation of the nitroalkene (*E,Z*)-**1** for these studies proved significantly more challenging. The previous synthesis of (*E,Z*)-**1** employed a Still-modified Horner-Wadsworth-Evans type olefination (Scheme 10).[68] Unfortunately, this method required tedious chromatographic purification to remove the minor geometrical isomer even on a sub-gram scale. Therefore, a new route to the enone (*Z*)-**6** was sought wherein the *Z*-double bond configuration would be controlled by inclusion in a 7-membered ring (Scheme 10). Thus, methanolysis of caprolactenone **8** was targeted. Sufficient quantities of the enoate **8** for the investigation of the methanolysis step were prepared by selenoxide elimination of caprolactone following the methods of either Reich or Fleming.[69,70]

Scheme 10.

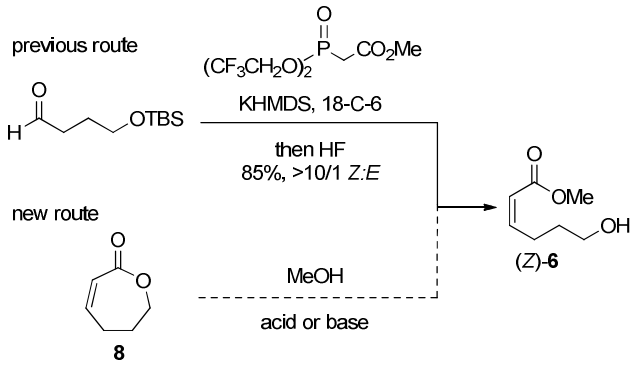

Because the acid-catalyzed alcoholysis of 7-membered lactones finds ample precedent,[71] a number of acids were surveyed (Table 1). Weak acids (pKa > 4) afforded little to no reaction within 24 h (entries 1 and 2). Stronger acids (pKa <4) such as sulfonic acids (entries 3 and 4) or

trifluoroacetic acid (entry 5) resulted in isomerization of the double bond at a rate competitive with ring opening. Reactions with hydrochloric acid (pKa <0) or silica gel or afforded the product with no apparent isomerization (entry 6, 8) however, neither reaction scaled well (entry 7). Treatment of the lactone with methanolic base led to a significantly faster reaction (on the order of minutes) in contrast to hours or days for acid promoters (both with 0.1 equiv). Whereas sodium methoxide led to rapid polymerization (entry 9), the use of a milder base such as potassium carbonate rapidly furnished the desired product with no apparent double bond isomerization or decomposition (entry 10). Fortunately, this process could be run on multigram scale to afford the geometrically pure enone **8** in good yield (entry 11). Upon scale-up, a small amount of a side product originating from conjugate addition of methanol could be detected (~5-10%). The use of sodium carbonate effectively suppressed the conjugate addition allowing for isolation of geometrically pure enone in good yield without the need for chromatographic purification (entry 12). With a robust method for alcoholysis of **8** in hand, the focus turned to developing a more scalable method for the preparation of the key lactenone **8**.

Table 1. Optimization of transesterifaction of lactone **8**.

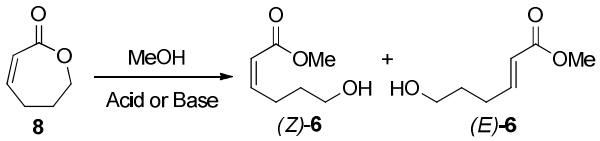

8 (*Z*)-**6** (*E*)-**6**

entry	additive	time, h	scale, g	*Z*/*E*[b]	yield, %[c]
1	2-$NO_2C_6H_4OH$	24	0.050	–	NR[d]
2	AcOH	24	0.050	–	NR
3	TsOH	20	0.050	4:3	ND[d]
4	CSA	20	0.050	4/1	ND
5	CF_3CO_2H	20	0.050	4/1	ND
6	silica gel	24	0.050	>10/1	ND
7	silica gel	24	0.473	>10/1	52
8	HCl	2	0.050	>10/1	ND
9	NaOMe	0.2	0.050	–	-[e]
10	K_2CO_3	0.2	0.050	>10/1	ND
11	K_2CO_3	0.5	5.20	>10/1	87
12	Na_2CO_3	0.5	10.0	>10/1	97

[a] General conditions: 50 mg **8**, 1 mL MeOH, 0.1 equiv acid or base, room temperature. [b] By ^{1}H-NMR integration. [c] Yield of chromatographically homogeneous material. [d] NR = no reaction and ND = not determined. [e] Only polymer was observed.

The preparation of caprolactenone **8** has been reported numerous times.[72] The method employed for the exploratory work (*vide supra*) was the selenoxide elimination of **9** developed by Reich and later scaled-up by Fleming and Chow (Scheme 11).[69,70] The advantages of this method are: (1) the full, contiguous carbon chain is readily available as caprolactone (~$0.07/g, Aldrich) (2) both terminal carbons of caprolactone are functionalized and (3) the sequence had already been scaled to 15 g (~6 mmol). Nevertheless, a more easily scalable route to this key intermediate was sought to avoid the use of selenium reagents and minimize the number of chromatographic purifications. For these reasons, a catalytic oxidation of silyl ketene acetal **10** was investigated (Scheme 11). The requisite ketene acetal **10** was prepared by deprotonation of caprolactone with LDA in the presence of TMSCl in 83% yield.[73] Notably, the process could be scaled to 20 g and the product directly purified by fractional distillation.

Scheme 11.

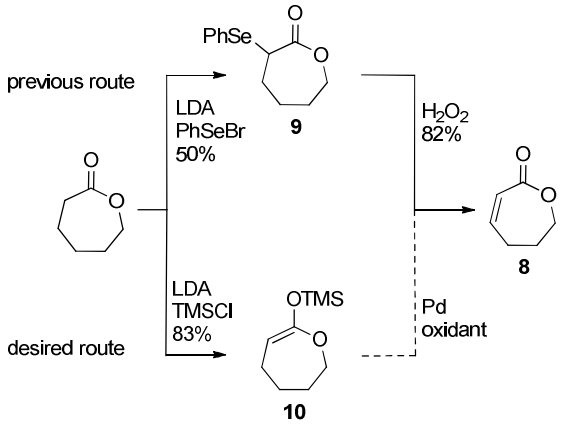

The dehydrogenation of silyl ketene acetals to provide lactones utilizing $Pd(OAc)_2$ (10 mol%) and allyl methyl carbonate as the oxidant has been reported by Tsuji.[74] To apply a palladium catalyzed dehydrogenation protocol on a large scale, a lower catalyst loading was required. Initially, a limited number of palladium sources and loadings were surveyed (Table 2). The desired product **8** was not detectable within 2 h with palladium (II) chloride (entry 1). Palladium (II) acetate gave a good yield that was enhanced slightly by the addition of an external ligand (entries 2-4). The preformed complex $Pd(dba)_2$ provided the best result with near quantitative conversion within 2 h (entry 6). Moreover, with $Pd(dba)_2$ the temperature could be

lowered and catalyst loading decreased to 1 mol % without a significant reduction in yield (entries 7 and 8). Under the optimal conditions, the reaction could be performed on decagram scale and the product isolated in greater than 95% yield.

Table 2. Optimization of Saegusa Oxidation.

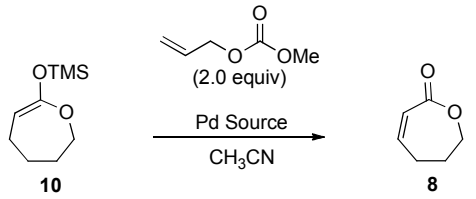

10 **8**

entry	Pd, source	Pd, mol%	yield, %[b]
1	$PdCl_2$	10	<1
2	$Pd(OAc)_2$	5	78
3	$Pd(OAc)_2$	10	84
4[c]	$Pd(OAc)_2$	5	87
5[c,d]	$Pd(OAc)_2$	5	77
6	$Pd(dba)_2$	5	96
7	$Pd(dba)_2$	1	95
8[e]	$Pd(dba)_2$	1	94

[a] Reaction conditions: 0.54 mmol of silyl ketene acetal, 0.2 M, 80 °C, 2 h. [b] Determined by ^{1}H-NMR spectroscopy. [c] 20 mol% DMSO added. [d] 0.8 M. [e] 40 °C.

2.3.2. Chiral Vinyl Ether Preparations.

Previous studies on the stereochemical course of the tandem cycloaddition of nitroalkenes identified (1*R*,2*S*)-2-phenylcyclohexanol **11** as an excellent chiral dienophile for this process.[75] Vinyl ether **2** has been prepared in 75% yield by equilibrium exchange with a donor vinyl ether (30 equiv) promoted by mercuric acetate (0.5 equiv).[76] Subsequent studies showed the same result could be obtained with only 0.05 equiv of Schlaf's catalyst ($Pd(OAc)_2$/1,10-phenanthroline).[77] Fortunately, the starting material **11** and product **2** are easily separated. (*E*)-Propenyl ether **3** was prepared following the published method.[75]

Scheme 12.

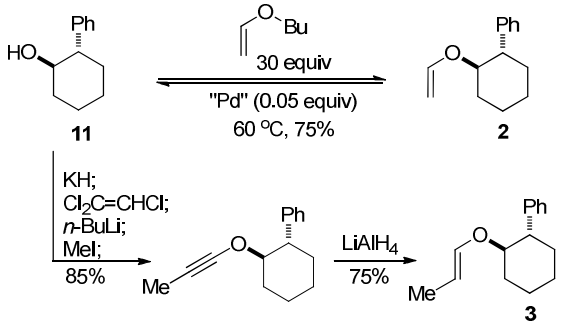

2.4. Scaffold Preparations by Tandem [4+2]/[3+2] Cycloaddition.

The centerpiece of the library synthesis was the use of the tandem cycloaddition of nitroalkenes to cast the polycyclic skeletons that will serve as parallel synthesis scaffolds. Known α-hydroxy lactam **4** was prepared in racemic form by tandem [4+2]/[3+2] cycloaddition of nitroalkene (*E,E*)-**1** with *n*-butyl via the intermediacy of nitronate **12** and nitroso acetal **13** (Scheme 13). Reductive hydrogenolysis afforded the tricyclic lactam **4a** in excellent overall yield (86% over three steps).

Scheme 13.

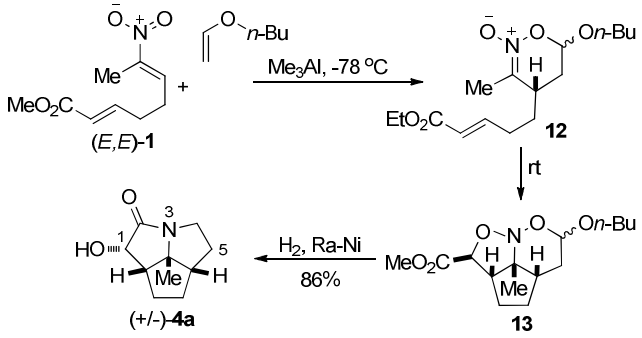

Likewise, α-hydroxy lactams **4a** and **5** were prepared as previously described in non-racemic form via the tandem cycloaddition with chiral vinyl and propenyl ethers **2** and **3** respectively (Scheme 14).[75,76] In this process, a standard set of reaction conditions was employed, namely exposure of a solution of nitroalkene and dienophile to $TiCl_2(O\textit{i}\text{-}Pr)_2$ at –78 °C to afford the intermediate nitronate. Subsequent, thermal cycloaddition occurred over the course of 2-3 h upon standing at room temperature. The resulting nitroso acetals were immediately subjected to hydrogenolysis with Raney nickel in methanol to afford the lactams in 76% and 89% respectively (three steps) with high enantioselectivity (e.r. 96:4).[78] The epimeric

α-hydroxy lactam **4b** (not previously described), was readily prepared in 63% yield following the standard protocol (e.r. 96:4). The elaboration of these scaffolds to the Libraries **I-V** respectively is detailed in the next section.

Scheme 14.

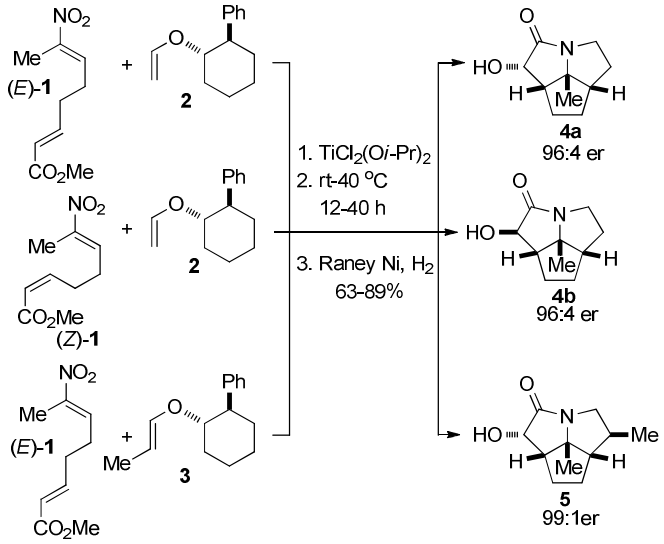

The next phase of these studies involved the development of a suitably versatile parallel synthesis route to allow for the introduction of various substituents on the core scaffold. The simplest scaffold (Library **I**), containing only a single site of variation, was first targeted to address the introduction of groups in the key N-alkylation step.

To complete the synthesis of the C_s symmetric scaffold, reduction of the two oxygen functional groups was required. Removal of the hydroxyl group was accomplished by activation as a phenyl(thiono)carbonate **14** followed by Barton type deoxygenation under the action of Bu_3SnH/AIBN to afford lactam **15** in good overall yield (64%, two steps) (Scheme 15).[79] Reduction of lactam **15** with borane•THF afforded the fully deoxygenated scaffold **16** for Library **I** as its borane adduct in 80% yield. With large quantities of borane adduct **16** in hand, N-quaternization conditions suitable for parallel synthesis could be investigated.

To facilitate the throughput of material, a method for the direct conversion of the amine borane adduct to the desired quaternary ammonium salts was sought that avoided the need for purification of intermediates. Heating amine·borane **16** in methanol in the presence of 1 M aq HCl led cleanly to the intermediate amine hydrochloride. The free base was liberated by partitioning the salt between 0.1 M aq NaOH and ether. Exposure of the free amine to a slight

excess of benzylic and primary aliphatic bromides {*1-6*} in acetonitrile at room temperature led smoothly to the quaternary ammonium ions **I**{*1-6*} in 72-90%. The excess electrophile could easily be removed by either filtration through silica gel or trituration with ether analogous to the methods of Dehmlow[80] and Maruoka respectively.[81] Ultimately, it was decided that silica gel plug filtration followed by trituration with ether could be used as the general conditions for purification for other ammonium salts.

Scheme 15.

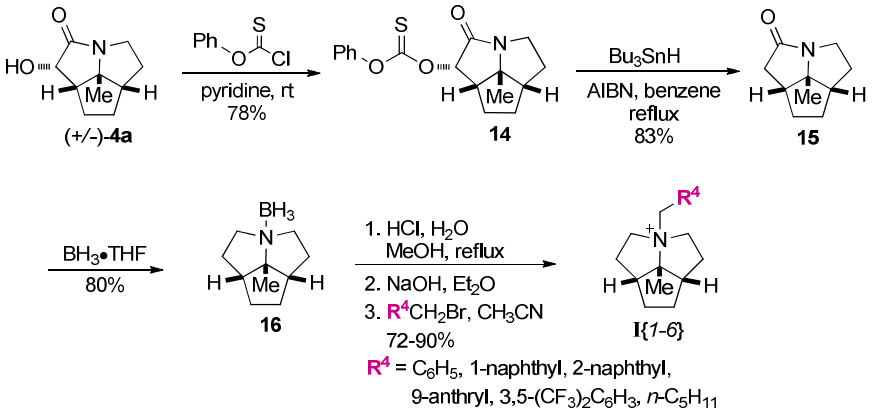

2.5. Preparation of Libraries II and III.

The next level of complexity called for the synthesis of libraries of chiral, non-racemic ammonium salts to study their effectiveness as *asymmetric* phase transfer catalysts. The construction of Libraries **II** and **III** introduces a second parallel synthesis step, namely O-alkylation. These two libraries embodied three objectives aimed at investigating *both* enantioselectivity and rate: (1) to introduce groups with variable solubilizing abilities (rate) and (2) introduce variable π-surfaces and steric bulk (selectivity) and (3) investigate the effect of configuration at C(1) (selectivity).

The diastereomeric lactams **4a** and **4b** were reduced to the pyrrolizidines **17a** and **17b** with BH_3·THF (>10 equiv) in good to excellent yield (Scheme 16). These amines were also isolated as their borane adducts, thus protecting the amine from air oxidation[82] and subsequent alkylation in the next step. This sequence allowed for the preparation of multi-gram quantities of borane complexes **17a** and **17b** as crystalline solids which was a convenient stage for storage of material. Application of standard Williamson ether synthesis conditions[83] (NaH, DMF) to borane complexes **17a** and **17b** allowed for facile elaboration to intermediates chemsets **II**{*1-5*} and

III{*1-5*}. The introduction of simple hydrophobic groups (*n*-hexyl), hydrophilic groups (methoxyethoxymethyl, MEM) as well as aromatic carbocycles and heterocycles, in good yield under a standard set of reaction conditions. It is noteworthy that the inclusion of a MEM ether in these series required the use of either neutral or base-promoted deborylation conditions because of the acid lability of this group. Accordingly, aq. HCl was replaced with aq. Na_2CO_3 under otherwise identical reaction conditions. Elaboration of the intermediate borane adducts as described in section 4.1 proceeded smoothly to afford quaternary ammonium salt libraries **II**{*1-5,1-6*} and **III**{*1-5,1-6*} in good yields over the three step process.

Scheme 16.

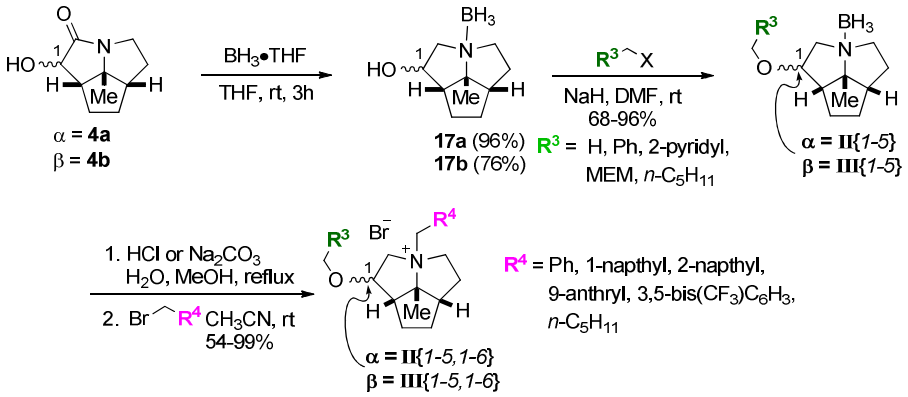

2.6. Preparation of Libraries IV and V.

2.6.1. Introduction of R^2 Substituents.

The presence of the hydroxyl group at C(1) allows for further diversification. This site was targeted for the introduction of different aliphatic and aromatic groups by organometallic addition to the corresponding C(1) ketone. Accordingly, Parikh von-Doering oxidation[67] of **17a** furnished the desired ketone **19** in 98% yield (Scheme 17). However, ketone **19** was not stable and was immediately carried on to the organometallic addition step. The increased acidity of the α-hydrogens, likely as a consequence of nitrogen complexation,[84] required the use of softer, less Brønsted basic organocerium reagents.[85] The resulting additions took place (40-98% yield) to form **21**{2,3,5} with complete β-diastereoselection as a consequence of the bowl shape of the core scaffold. Likewise, lactam **5** (an inseparable 12:1 mixture of C(5) diastereomers from cycloaddition with a propenyl ether) underwent the cerium-mediated addition to afford the tertiary alcohols **22**{2.3.5} in similar yields.

Scheme 17.

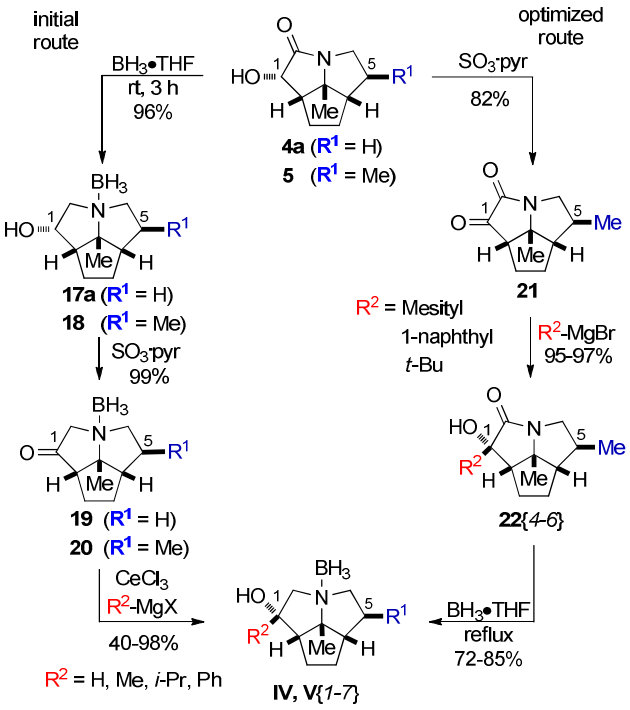

However, the inability to introduce bulky groups as well as poor reproducibility led to a modification of the synthetic route. Oxidation of alcohol **5** to α-keto lactam **23** afforded two important benefits over the initial route. First, the addition of Grignard reagents to this highly active dicarbonyl compound proceeded reproducibly and in excellent yields (95-97%) even with bulky nucleophiles. Second, the minor C(5) diastereomer could be removed by a single recrystallization. However, reduction of the resulting lactams **24**{*4,6,7*} required elevated temperatures, presumably a consequence of the additional steric bulk proximal to the site of reduction. In this way, the corresponding amine·borane adducts **21** and **22** could be isolated in respectable yields (72-85%) without increasing the number of steps in the synthetic route.

2.6.2. Parallel Synthesis Toward Libraries IV and V.

Extension of the developed parallel synthesis route to the more hindered tertiary alcohol at C(1) found in Libraries **IV** and **V** was straightforward (Scheme 18). The R^3 substituents in Libraries **IV** and **V** were limited to unfunctionalized aliphatic groups, electron rich (4-$MeOC_6H_4$) and electron deficient (3,5-$(CF_3)_2C_6H_3$) aromatic groups. Also, the 9-anthrylmethyl group at R^4 was removed from this set,[86] but a larger number of groups of varying electronic makeup and size were introduced for R^4 in Libraries **IV** and **V**.

Scheme 18.

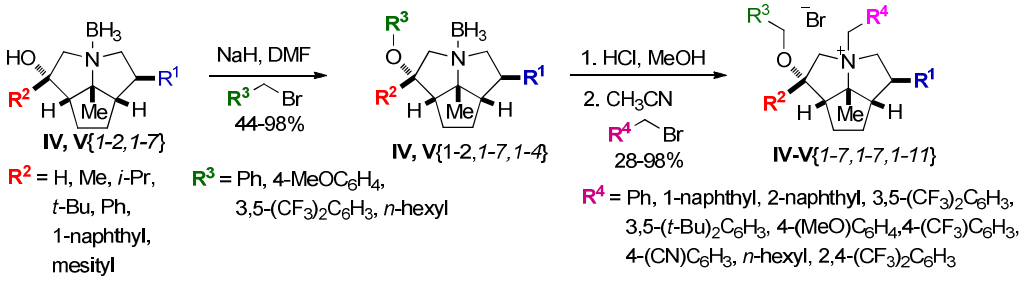

2.7. Summary of Library Synthesis.

A library of over 160 catalysts sharing the same core scaffold has been generated that incorporates the substituents below (Scheme 19). Although this number represents only a small fraction of the complete matrix of >1200 possible the library represents a good approximation on the basis of preliminary data. The groups shown reflect the need to evaluate the roles of steric and electronic contributions, π-surface, lipophilicity, and polar surface area on the catalyst structure for a given phase transfer catalyzed reaction.

Scheme 19.

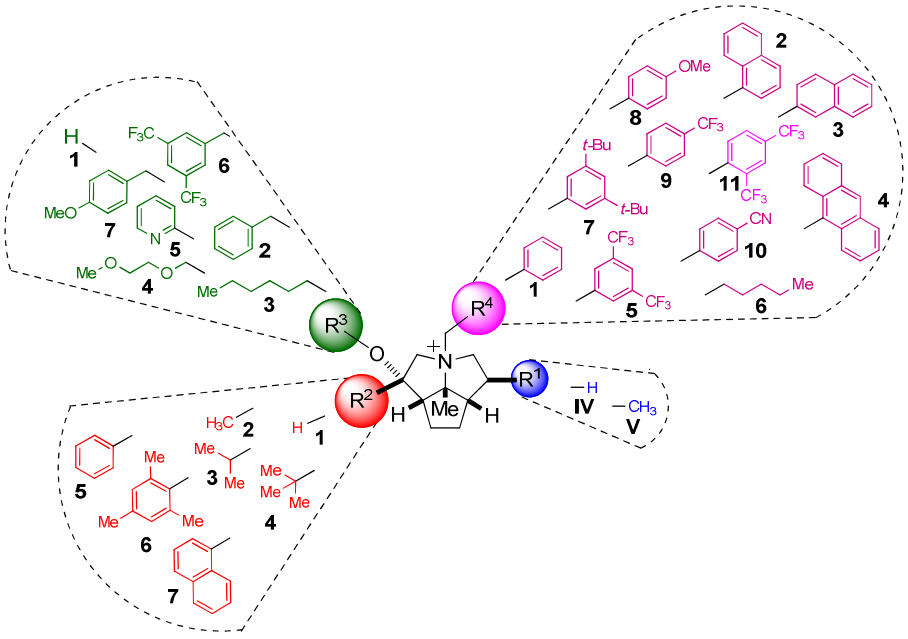

2.8. Collection of Kinetic Data.

2.8.1. Refining a Kinetic Analysis.

The base-promoted benzylation of glycine benzophenone imine *tert*-butyl ester **25** has

become the benchmark reaction for investigation of new catalyst structures.[32m] As such, a standard set of reaction conditions has been established, namely the use 50% aq. KOH solution and toluene.[34] Given the intrinsic biphasic nature of PTC reactions, efficient mixing is essential to promote efficient transport and to minimize the errors associated with precipitation. For these reasons, a 4-mL (1 cm x 3.5 cm) cylindrical vial was chosen as the reaction vessel together with a 1.5 cm egg-shaped stir bar. This stir bar was large enough such that it traversed the interface and yet was small enough to ensure mixing as a consistent shearing motion.[25,87] The scale of the reactions was dictated by the need to conduct multiple kinetic runs using 80-120 mg of starting ester **25** (thus dictating a minimally measurable amount of catalyst (4-8 mg)) and to maintain a reaction concentration of 0.33 M.

Under these conditions, orienting experiments utilizing 5 mol % of a catalyst at room temperature resulted in rapid reaction; most were complete within 1-3 min. Clearly this range of rates was not amenable to providing reproducible results. Decreasing the catalyst loading to 2.5 mol % and decreasing the temperature to 2-4 ^{o}C successfully slowed the reaction to a point where a range of rates could be obtained.[88]

Scheme 20.

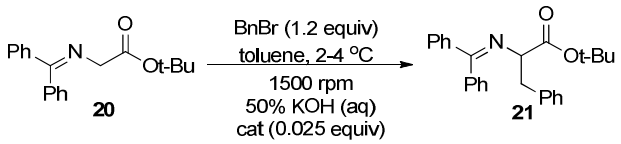

Initial experiments with tetrabutylammonium bromide allowed for an examination of sampling methods to ensure reproducibility. Sampling from the bulk mixture gave inconsistent results and the sampling needle clogged frequently. A more reliable protocol involved stopping the agitation momentarily to allow the biphasic mixture to separate (~2 s), and sampling from the organic layer. Utilizing this protocol the reaction profile was reproducible; two sample runs are shown in Figure 6a.

An important decision was to choose an appropriate value to represent the rate data (e.g. k_i, k_{obs}, $t_{1/2}$, …etc). Upon initial testing catalyst **I**{*1*}, a significant induction period was observed over the course of the first 5% conversion (Figure 7, red squares). This type of behavior has previously been reported as a function of ammonium counterion.**18**,[89] The induction period was seen under the protocol wherein the base was added last. However, if the order of addition of

reagents was changed such that the alkylating agent was added last, then the converse was observed and appearance of product was rapid at first, but quickly declined (a kinetic "burst"). Most importantly, regardless of the order of operations, the "time course" of the two reactions converges to a single rate (within 1%, Figure 6b). The implications of this observation will be discussed in the following section.

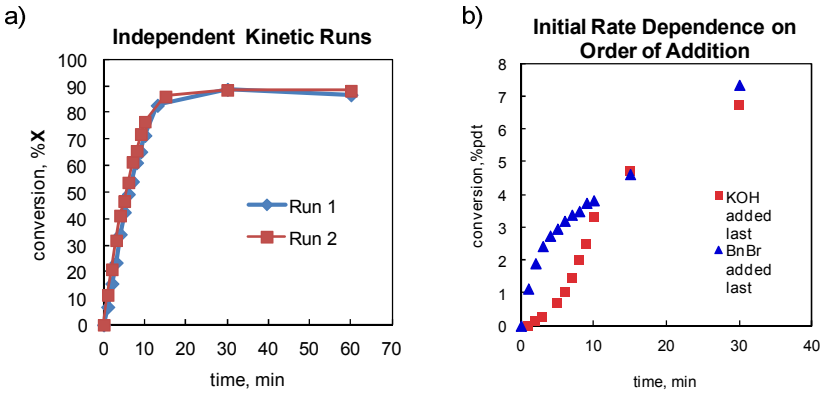

Figure 6. a) Kinetic profile of a TBAB catalyzed reaction. b) Affect of order of addition with catalyst **I**{1}.

Given the significant variation at the onset of the reaction, it was decided to extract data that would be independent of the initial rate, namely $t_{1/2}$. Although this determination is labor intensive, since it would require monitoring each reaction to greater than 50% conversion, it has the added advantage of showing the entire reaction profile.

2.9. Stir Rate Dependence.

The last critical decision to be made was a stirring rate that would sufficiently minimize errors from salting out and still allow for the differences in catalyst activities to be observed. Hydroxide initiated-PTC reactions can exhibit a rate dependence on stirring speed in excess of ~2000 rpm. At high enough stirring speeds there is little dependence which is consistent with the proposal that the influence of mixing is to increase the surface area to volume ratio (effectively concentration) of the biphase,[90] and that phase transfer reagents can decrease the interfacial surface tension.[91]

To determine a suitable stirring speed for application to the standard protocol, the dependence of catalytic activity on stirring speed was determined for a variety of variably active quaternary ammonium ions. Reaction half-lives were determined following the experimental

parameters noted above employing a range of stir rates (1038 – 2500 rpm). The resulting observed half lives are plotted as a log/log in analogy to a dose-response graph (Figure 7).[92,93] The top two curves represent catalysts with low catalytic activity while the two lower curves represent catalysts among the highest activity. Importantly, there is a sufficient range of stirring speeds, along which the activities of all of the catalysts surveyed are dependent (non-zero slope) on mixing rate. In choosing the stir rate with which all of the kinetic experiments were to be carried out, the important considerations were: (1) sufficient and consistent mixing, (2) operationally accessible, and (3) that the stir rate existed in a region where a reaction rate dependence was still observed. The stir rate of 1600 rpm fit within all three of these criteria (represented by the black vertical dotted line in Figure 7 and therefore, all of the remaining kinetic data were collected at this stir rate.

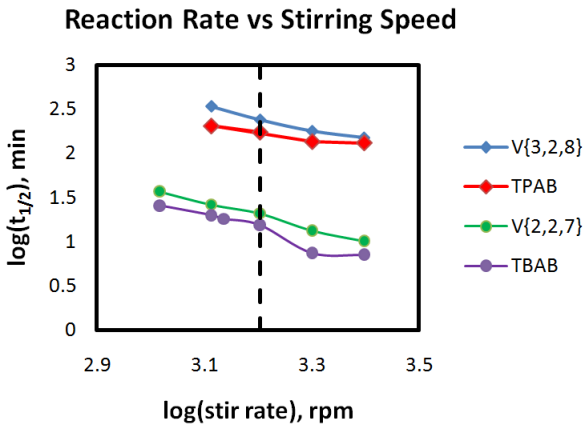

Figure 7. Effect of stir rate on reaction half-life with catalysts of varying structure and activity.

2.10. Summary of the Kinetic Data.

2.10.1. Statistical Description.

With a working analytical method in hand, a large subset of the ammonium salts was evaluated for their kinetic competence, represented as half-lives. The half-lives were determined by interpolation of the kinetic plot of percentage of product formation as a function of time. The reported half-life values represent averages over two runs with and average error of 4.5%.[94] Data from kinetic runs that resulted in errors exceeding 20% was discarded and repeated until an error of less than 20% was observed.

To date, half-lives for 102 of the 160 catalysts have been collected. The observed half-life

data covers four orders of magnitude of activity that was deemed suitable for the initial investigation of the structural effects of catalyst on rate. The half-life data collected from these experiments ranged from 5 min to over 15 h and is summarized in logarithmic scale below (Figure 8). Of the 98 catalysts surveyed to date 52 of them exhibited half-lives of 20 min or less. Twenty-three catalysts make up the data between 20 min and 1 h, and the half-lives of the remaining 23 catalysts range from 1 h to 15 h.

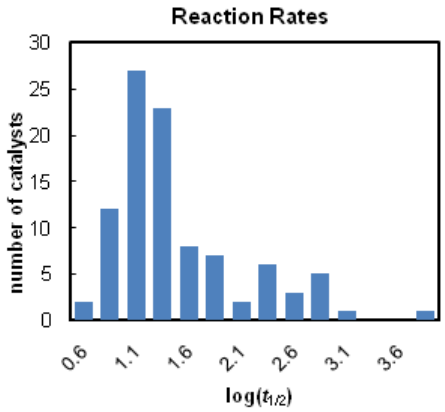

Figure 8 Histogram of $t_{1/2}$ data in logarithmic form.

2.10.2. Reaction Rates Results for Library I.

The half-life data for Library **I** is summarized in Table 3. These ammonium ions showed fairly poor catalytic activity exhibiting half-lives in the range of 5 to 12 h. The one exception was the catalyst containing an *n*-hexyl nitrogen substituent. In this case the half-life observed was only 13 min.

Table 3. Half-life Data for Library **I**.

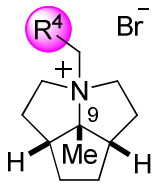

entry	Library #	R^4	$t_{1/2}$, min
1	**I**{*1*}	C_6H_5	940
2	**I**{*2*}	1-naphthyl	730
3	**I**{*3*}	2-naphthyl	na
4	**I**{*4*}	9-anthryl	324
5	**I**{*5*}	3,5-$(CF_3)_2C_6H_3$	na
6	**I**{*6*}	*n*-hexyl	12.8

2.10.3. Reaction Rates for Libraries II and III.

The half-life data for Libraries **II** and **III** is summarized in Table 4. These ammonium salts are generally more active catalysts than those lacking an oxygen substituent and exhibited half-life range from 6 min to 5.7 h. Catalysts containing a non-hydrogen substituent at R^3 are generally more active than the corresponding catalysts with hydrogen at R^3. However, no clear dependence of the nature of the R^3 substituent on catalyst activity was discernable. When R^3 = H, the rate was markedly dependent on the configuration at C(1) (entries 5 vs. 6). However, when $R^3 \neq$ H, the half-life was nearly independent on the C(1) configuration (entries 10 vs. 11, 12 vs. 13, 16 vs. 17, 21 vs. 22, and 23 vs. 24).

2.10.4. Reaction Rates for Libraries IV and V.

The half-life data for Libraries **IV** and **V** is summarized in

Table 5. The activity of these catalysts appears to be largely dependent on the R^2 substituent within the series. Comparing catalysts with fixed R^1, R^3, and R^4, substituents, but with varying R^2 substituents, the following trend in rates holds: R^2 = *i*-Pr > Me > Ph. However, there are important exceptions. For example, catalysts containing R^4 = 3,5-$(CF_3)_2C_6H_3$, R^1 = Me, R^3 = benzyl, the following trend in half-life holds for R^2: Me > *i*-Pr > *t*-Bu > Ph (entries 13, 26,

35, 39). Evidently, a compelling, but complex dependence of the bis(trifluoromethyl)phenyl group at R^4 on the catalyst activity is observed. Moreover, ammonium salts containing R^3 = *n*-hexyl are generally more active than catalysts with $R^3 \neq$ *n*-hexyl with all other substituents held constant, which suggests a dependence on lipophilicity.

Table 4 Half-life Data for Library II and III.

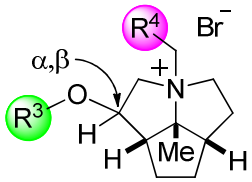

entry	Library #	R^3	R^4	C(1)-configuration	$t_{1/2}$, min
1	**II**{*1,1*}	H	C_6H_5	α	181
2	**II**{*1,2*}	H	1-naphthyl	α	179
3	**II**{*1,4*}	H	9-anthryl	α	298
4	**II**{*1,5*}	H	3,5-$(CF_3)_2C_6H_3$	α	346
5	**II**{*1,3*}	H	2-naphthyl	α	245
6	**III**{*1,3*}	H	2-naphthyl	β	72
7	**II**{*2,1*}	C_6H_5	C_6H_5	α	10
8	**II**{*2,2*}	C_6H_5	1-naphthyl	α	18
9	**II**{*2,3*}	C_6H_5	2-naphthyl	α	12.1
10	**II**{*3,1*}	*n*-hexyl	C_6H_5	α	11.7
11	**III**{*3,1*}	*n*-hexyl	C_6H_5	β	14.8
12	**II**{*3,2*}	*n*-hexyl	1-naphthyl	α	6.6
13	**III**{*3,2*}	*n*-hexyl	1-naphthyl	β	9.5
14	**III**{*3,3*}	*n*-hexyl	2-naphthyl	β	13.5
15	**II**{*3,5*}	*n*-hexyl	3,5-$(CF_3)_2C_6H_3$	α	12.7
16	**II**{3,6}	*n*-hexyl	*n*-hexyl	α	4.6
17	**III**{*3,6*}	*n*-hexyl	*n*-hexyl	β	5.5
18	**II**{*4,1*}	MEM	C_6H_5	α	17.5
19	**II**{*4,2*}	MEM	1-naphthyl	α	12.3
20	**II**{*4,3*}	MEM	2-naphthyl	α	22.8

Table 4. (cont.)

21	**II**{*5,1*}	2-pyridyl	C_6H_5	α	17.1
22	**III**{*5,1*}	2-pyridyl	C_6H_5	β	11.1
23	**II**{*5,2*}	2-pyridyl	1-naphthyl	α	6.6
24	**III**{*5,2*}	2-pyridyl	1-naphthyl	β	11
25	**II**{*5,3*}	2-pyridyl	2-naphthyl	α	12.7
26	**II**{*5,4*}	2-pyridyl	9-anthryl	α	21.1
27	**II**{*5,5*}	2-pyridyl	3,5-$(CF_3)_2C_6H_3$	α	31.8

Table 5. Half-life Data for Library IV and V.

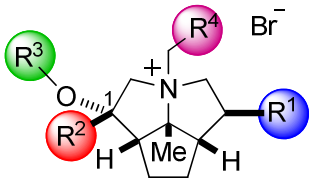

entry	Library #	R^1	R^2	R^3	R^4	C(1)-configuration	$t_{1/2}$, min
1	**IV**{*2,2,1*}	H	Me	C_6H_5	C_6H_5	α	93.5
2	**IV**{*2,2,2*}	H	Me	C_6H_5	1-naphthyl	α	51.1
3	**IV**{*3,2,1*}	H	*i*-Pr	C_6H_5	C_6H_5	α	19.5
4	**IV**{*3,2,5*}	H	*i*-Pr	C_6H_5	3,5-$(CF_3)_2C_6H_3$	α	26.1
5	**IV**{*5,2,5*}	H	C_6H_5	C_6H_5	3,5-$(CF_3)_2C_6H_3$	α	16.3
6	**V**{*1,2,1*}	Me	H	C_6H_5	C_6H_5	α	32.5
7	**V**{*1,2,8*}	Me	H	C_6H_5	4-$(MeO)C_6H_4$	α	51.8
8	**V**{*1,2,8*}	Me	H	C_6H_5	4-$(MeO)C_6H_4$	β	53.9
9	**V**{*1,2,7*}	Me	H	C_6H_5	3,5-(*t*-Bu)$_2C_6H_3$	β	9.78
10	**V**{*1,2,6*}	Me	H	C_6H_5	*n*-hexyl	α	24.7
11	V{*2,2,1*}	Me	Me	C_6H_5	C_6H_5	α	20.7
12	**V**{*2,2,3*}	Me	Me	C_6H_5	2-naphthyl	α	23.0
13	**V**{*2,2,5*}	Me	Me	C_6H_5	3,5-$(CF_3)_2C_6H_3$	α	899.7
14	**V**{*2,2,8*}	Me	Me	C_6H_5	4-$(MeO)C_6H_4$	α	19.9
15	**V**{*2,2,7*}	Me	Me	C_6H_5	3,5-(*t*-Bu)$_2C_6H_3$	α	15.1
16	**V**{*2,2,6*}	Me	Me	C_6H_5	*n*-hexyl	α	28.1
17	**V**{*2,3,1*}	Me	Me	*n*-hexyl	C_6H_5	α	23.0

Table 5. (cont.) Half-life Data for Library IV and V.

18	**V**{*2,3,2*}	Me	Me	*n*-hexyl	1-naphthyl	α	75.8
19	**V**{*2,3,3*}	Me	Me	*n*-hexyl	2-naphthyl	α	30.7
20	**V**{*2,3,5*}	Me	Me	*n*-hexyl	3,5-$(CF_3)_2C_6H_3$	α	236.0
21	**V**{*2,3,8*}	Me	Me	*n*-hexyl	4-$(MeO)C_6H_4$	α	26.5
22	**V**{*2,3,7*}	Me	Me	*n*-hexyl	3,5-(*t*-Bu)$_2C_6H_3$	α	28.9
23	**V**{*2,3,6*}	Me	Me	*n*-hexyl	*n*-hexyl	α	21.1
24	**V**{*2,7,1*}	Me	Me	4-$(MeO)C_6H_4$	C_6H_5	α	17.9
25	**V**{*3,2,1*}	Me	*i*-Pr	C_6H_5	C_6H_5	α	132.1
26	**V**{*3,2,5*}	Me	*i*-Pr	C_6H_5	3,5-$(CF_3)_2C_6H_3$	α	122.1
27	**V**{*3,2,7*}	Me	*i*-Pr	C_6H_5	3,5-(*t*-Bu)$_2C_6H_3$	α	28.6
28	**V**{*3,3,1*}	Me	*i*-Pr	*n*-hexyl	C_6H_5	α	41.8
29	**V**{*3,3,3*}	Me	*i*-Pr	*n*-hexyl	2-naphthyl	α	20.3
30	**V**{*3,3,5*}	Me	*i*-Pr	*n*-hexyl	3,5-$(CF_3)_2C_6H_3$	α	62.4
31	**V**{*3,3,8*}	Me	*i*-Pr	*n*-hexyl	4-$(MeO)C_6H_4$	α	42.7
32	**V**{*3,2,6*}	Me	*i*-Pr	C_6H_5	*n*-hexyl	α	86.0
33	**V**{*3,7,5*}	Me	*i*-Pr	4-$(MeO)C_6H_4$	3,5-$(CF_3)_2C_6H_3$	α	60.9
34	**V**{*3,7,8*}	Me	*i*-Pr	4-$(MeO)C_6H_4$	4-$(MeO)C_6H_4$	α	249.4
35	**V**{*4,2,5*}	Me	*t*-Bu	C_6H_5	3,5-$(CF_3)_2C_6H_3$	α	95.8
36	**V**{*5,2,1*}	Me	C_6H_5	C_6H_5	C_6H_5	α	10.6
37	**V**{*5,2,2*}	Me	C_6H_5	C_6H_5	1-naphthyl	α	12.2
38	**V**{*5,2,3*}	Me	C_6H_5	C_6H_5	2-naphthyl	α	10.3
39	**V**{*5,2,5*}	Me	C_6H_5	C_6H_5	3,5-$(CF_3)_2C_6H_3$	α	9.5
40	**V**{*5,2,8*}	Me	C_6H_5	C_6H_5	4-$(MeO)C_6H_4$	α	17.5
41	**V**{*5,2,9*}	Me	C_6H_5	C_6H_5	(4-CF_3)C_6H_4	α	16.0
42	**V**{*5,2,10*}	Me	C_6H_5	C_6H_5	(4-CN)C_6H_4	α	14.4
43	**V**{*5,3,1*}	Me	C_6H_5	*n*-hexyl	C_6H_5	α	9.5
44	**V**{*5,3,2*}	Me	C_6H_5	*n*-hexyl	1-naphthyl	α	18.7
45	**V**{*5,3,3*}	Me	C_6H_5	*n*-hexyl	2-naphthyl	α	13.1
46	**V**{*5,3,5*}	Me	C_6H_5	*n*-hexyl	3,5-$(CF_3)_2C_6H_3$	α	4.9

Table 5. (cont.) (cont.) Half-life Data for Library IV and V.

47	**V**{*5,3,8*}	Me	C_6H_5	*n*-hexyl	4-(MeO)C_6H_4	α	9.9
48	**V**{*5,3,7*}	Me	C_6H_5	*n*-hexyl	3,5-(*t*-Bu)$_2C_6H_3$	α	8.5
49	**V**{*5,6,1*}	Me	C_6H_5	3,5-$(CF_3)_2C_6H_3$	C_6H_5	α	7.9
50	**V**{*5,6,5*}	Me	C_6H_5	3,5-$(CF_3)_2C_6H_3$	3,5-$(CF_3)_2C_6H_3$	α	7.0
51	**V**{*5,6,8*}	Me	C_6H_5	3,5-$(CF_3)_2C_6H_3$	4-(MeO)C_6H_4	α	6.9
52	**V**{*5,7,1*}	Me	C_6H_5	4-(MeO)C_6H_4	C_6H_5	α	19.9
53	**V**{*5,7,2*}	Me	C_6H_5	4-(MeO)C_6H_4	1-naphthyl	α	19.2
54	**V**{*5,7,3*}	Me	C_6H_5	4-(MeO)C_6H_4	2-naphthyl	α	12.0
55	**V**{*5,7,5*}	Me	C_6H_5	4-(MeO)C_6H_4	3,5-$(CF_3)_2C_6H_3$	α	18.6
56	**V**{*5,7,7*}	Me	C_6H_5	4-(MeO)C_6H_4	3,5-(*t*-Bu)$_2C_6H_3$	α	14.6
57	**V**{*7,2,1*}	Me	1-naphthyl	C_6H_5	C_6H_5	α	13.7
58	**V**{*7,2,5*}	Me	1-naphthyl	C_6H_5	3,5-$(CF_3)_2C_6H_3$	α	28.7
59	**V**{*7,2,8*}	Me	1-naphthyl	C_6H_5	4-(MeO)C_6H_4	α	11.3
60	**V**{*7,2,9*}	Me	1-naphthyl	C_6H_5	(4-CF_3)C_6H_4	α	11.8
61	**V**{*7,2,10*}	Me	1-naphthyl	C_6H_5	(4-CN)C_6H_4	α	48.6
62	**V**{*6,2,1*}	Me	2,4,6-$(CH_3)_2C_6H_2$	C_6H_5	C_6H_5	α	12.2
63	**V**{*6,2,8*}	Me	2,4,6-$(CH_3)_2C_6H_2$	C_6H_5	4-(MeO)C_6H_4	α	11.8

2.10.5. Other Quaternary Ammonium Ions.

Varying the substituents on a common scaffold allowed for observation of a large range of rates. To determine how much of the "total possible" range of activity was being sampled tetramethylammonium bromide (TMAB, q = 4.0) was tested and exhibited a half-life of 1200

min (Table 6).[95] The similarly hydrophilic, but less accessible tetraethylammonium bromide (q = 2.0) exhibited a 20-fold rate increase over TMAB. The more lipophilic, but similarly accessible cation cetyltrimethyl (C_{19} total, q = 3.06) ammonium bromide was only three times faster than TMAB (entry 3). The rate increase from tetramethyl- to tetraethylammonium bromide was also seen in the use of tributylbenzylammonium bromide, which caused a further 20-fold rate increase. To directly address this dramatic effect of ammonium accessibility with catalysts more closely related to the common scaffold, one other small set of quaternary ammonium ions was constructed that replaces one of the pyrrolidine rings of the scaffold with an azetidine. As expected, the ammonium ions containing an azetidine ring exhibited overall poor catalytic activity with half-lives ranging from 900 to 1000 min.

Table 6. Half-life Data for other Quaternary Ammonium Ions.

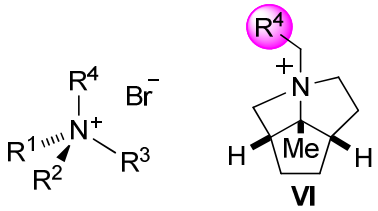

VI

entry	Library #	catalyst	R^4	$t_{1/2}$, min
1	-	Me_4N	-	12,000
2	-	Et_4N	-	480
3	-	$Me_3NC_{16}H_{33}$	-	2800
4	-	*n*-Bu_3NBn	-	21
5	**VI**{*1*}	-	C_6H_5	890
6	**VI**{*2*}	-	1-naphthyl	1000
7	**VI**{*3*}	-	2-naphthyl	1090

2.11. Enantioselectivity of the Catalysts.

In addition to determining the substituent effects on rate, those structural features that most strongly affect enantioselectivity were of equal interest. Summarized below is the enantioselectivity data for all 143 chiral, non-racemic catalysts constructed to date. The enantiomeric ratio of benzylated product **21** was measured by purifying a sample by silica gel chromatography from a separate experiment at 2-4 ^{o}C with 2.5 mol % catalyst loading. The enantiomeric ratios were determined by CSP-HPLC.

2.11.1. Enantioselectivity for Library II.

The enantioselectivity data for the α-series (Library **II**, $R^1 = R^2 = H$) is summarized in Table 7. For this series, when the oxygen substituent (R^3) was hydrogen, a small, but detectable selectivity for the *S* enantiomer was seen. However, this effect was only seen when the N-substituent was branched (entries 1 and 3 vs. 2, 4-6). Substituting R^3 with aliphatic (entries 7-12) and ethereal (entries 13-18) substituents did not result in a significant difference in the enantioselectivity. Installation of the 2-pyridyl group at the R^3 position led to a minor enrichment in the *R* enantiomer. The inclusion of a benzyl group at R^3 (entries 19-24) led to poor selectivity irrespective of the nitrogen substituent. In summary, only poor to moderate enrichment of the *S* enantiomer was observed with variable R^3 and R^4 substituents and where $R^1 = R^2 = H$ whereas catalysts with R^1 = Me in conjunction with R^4 bearing a 3,5-substitution pattern gave slightly higher selectivities in this series.

2.11.2. Enantioselectivity for Library III.

The enantioselectivity data for the β-series (Library **III**, $R^2 = H$) is summarized in Table 8. As was seen with the α-series, catalysts with $R^3 = H$ produced low to moderate enrichment of the *S* enantiomer of **21** with $R^4 = 3,5\text{-}(CF_3)_2C_6H_3$ (entry 4, e.r. 57:43) exhibiting the largest selectivity. Relative to the α-series, catalysts with R^3 = aliphatic consistently produced the *S* enantiomer in slightly greater enrichment (entries 7-12). Additionally, moderate enantioselectivity was observed in catalysts containing a 2-pyridyl group (where the point of attachment is the sp^2 carbon of the heteroaromatic ring) at R^3 (entries 19, 22, and 24) with the largest selectivity observed when R^4 = 1-naphthyl. Similar results were observed in catalysts with R^3 = benzyl within this series, apart from when R^4 = Ph (entry 18) which resulted in decreased selectivity. Overall, the enantioselectivity data for the catalysts in Library **III** was greater than their diastereomeric counterparts Library **II**.

Table 7. Enantioselectivity of Library **II**.

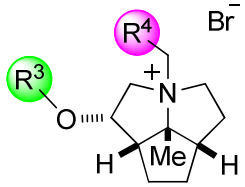

entry	Library #	R^3	R^4	er, *S*:*R*
1	**II**{*1,2*}	H	1-naphthyl	54:46
2	**II**{*1,3*}	H	2-naphthyl	51:49
3	**II**{*1,4*}	H	9-anthryl	54:46
4	**II**{*1,5*}	H	3,5-$(CF_3)_2C_6H_3$	53:47
5	**II**{*1,6*}	H	*n*-hexyl	51:49
6	**II**{*1,1*}	H	C_6H_5	52:48
7	**II**{*3,2*}	*n*-hexyl	1-naphthyl	52:48
8	**II**{*3,3*}	*n*-hexyl	2-naphthyl	51:49
9	**II**{*3,4*}	*n*-hexyl	9-anthryl	51:49
10	**II**{*3,5*}	*n*-hexyl	3,5-$(CF_3)_2C_6H_3$	51:49
11	**II**{*3,6*}	*n*-hexyl	*n*-hexyl	53:47
12	**II**{*3,1*}	*n*-hexyl	C_6H_5	52:48
13	**II**{*4,2*}	MEM	1-naphthyl	50:50
14	**II**{*4,3*}	MEM	2-naphthyl	51:49
15	**II**{*4,4*}	MEM	9-anthryl	50:50
16	**II**{*4,5*}	MEM	3,5-$(CF_3)_2C_6H_3$	50:50
17	**II**{*4,6*}	MEM	*n*-hexyl	50:50
18	**II**{*4,1*}	MEM	C_6H_5	51:49
19	**II**{*2,2*}	C_6H_5	1-naphthyl	50:50
20	**II**{*2,3*}	C_6H_5	2-naphthyl	48:52
21	**II**{*2,4*}	C_6H_5	9-anthryl	50:50
22	**II**{*2,5*}	C_6H_5	3,5-$(CF_3)_2C_6H_3$	50:50
23	**II**{*2,6*}	C_6H_5	*n*-hexyl	51:49
24	**II**{*2,1*}	C_6H_5	C_6H_5	47:53
25	**II**{*5,2*}	2-pyridyl	1-naphthyl	46:54
26	**II**{*5,3*}	2-pyridyl	2-naphthyl	48:52
27	**II**{*5,4*}	2-pyridyl	9-anthryl	45:55

Table. 7 (cont.) Enantioselectivity of Library **II**.

28	**II**{*5,5*}	2-pyridyl	3,5-$(CF_3)_2C_6H_3$	50:50
29	**II**{*5,6*}	2-pyridyl	*n*-hexyl	48:52
30	**II**{*5,1*}	2-pyridyl	C_6H_5	47:53

Table 8. Enantioselectivity of Library **II**.

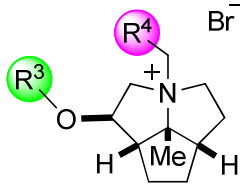

entry	Library #	R^3	R^4	er, *S:R*
1	**III**{*1,2*}	H	1-naphthyl	48:52
2	**III**{*1,3*}	H	2-naphthyl	55:45
3	**III**{*1,4*}	H	9-anthryl	50:50
4	**III**{*1,5*}	H	3,5-$(CF_3)_2C_6H_3$	57:43
5	**III**{*1,6*}	H	*n*-hexyl	52:48
6	**III**{*1,1*}	H	C_6H_5	55:45
7	**III**{*3,2*}	*n*-hexyl	1-naphthyl	48:52
8	**III**{*3,3*}	*n*-hexyl	2-naphthyl	55:45
9	**III**{*3,4*}	*n*-hexyl	9-anthryl	47:53
10	**III**{*3,5*}	*n*-hexyl	3,5-$(CF_3)_2C_6H_3$	52:48
11	**III**{*3,6*}	*n*-hexyl	*n*-hexyl	53:47
12	**III**{*3,1*}	*n*-hexyl	C_6H_5	54:46
13	**III**{*2,2*}	C_6H_5	1-naphthyl	64:36
14	**III**{*2,3*}	C_6H_5	2-naphthyl	48:52
15	**III**{*2,4*}	C_6H_5	9-anthryl	44:56
16	**III**{*2,5*}	C_6H_5	3,5-$(CF_3)_2C_6H_3$	57:43
17	**III**{*2,6*}	C_6H_5	*n*-hexyl	58:42
18	**III**{*2,1*}	C_6H_5	C_6H_5	53:47
19	**III**{*5,2*}	2-pyridyl	1-naphthyl	64:36
20	**III**{*5,3*}	2-pyridyl	2-naphthyl	48:52
21	**III**{*5,4*}	2-pyridyl	9-anthryl	54:46
22	**III**{*5,5*}	2-pyridyl	3,5-$(CF_3)_2C_6H_3$	58:42
23	**III**{*5,6*}	2-pyridyl	*n*-hexyl	57:43
24	**III**{*5,1*}	2-pyridyl	C_6H_5	60:40

2.11.3. Enantioselectivity for Libraries IV and V.

The enantioselectivities for catalysts with variable R^2, R^3, and R^4 groups while holding R^1 constant as a methyl group (excluding entry 1) are summarized in Table 9. Entries with the highest selectivities are highlighted. Introducing a methyl group at R^1 while maintaining a hydrogen and a benzyl group at R^2 and R^3 respectively did not lead to significant differences in the enantioselectivity apart from when the R^4 group was a 3,5-substited aryl ring (entries 7 and 8). In this case, inversion of the C(1) configuration resulted in a comparable enantioselectivity (entry 14).

The results for the catalysts with R^2 = Me are similar to those catalysts with R^2 = H. Likewise, catalysts with a 3,5-substitution pattern on the aryl ring of R^4 consistently resulted in the highest selectivities independent of the R^3 substituent (entries 1, 17, 21, 24, 28, 31, and 32). Increasing the size of the R^2 substituent to isopropyl and *tert*-butyl resulted in a reversal in the selectivity (entries 33-54). As was the case with catalysts with R^2 = Me, the catalysts exhibiting a 3,5-substitution pattern on the aryl ring of R^4 with R^2 = *i*-Pr and *t*-Bu produced the highest selectivities. Catalysts containing R^2 = phenyl are displayed in entries 55-76. These catalysts were variably selective for either the *S* or *R* enantiomer, apart from when R^4 was a 3,5-disubstitued aryl group. However, the maximum enantioselectivity was observed when R^4 = 3,5-$(CF_3)C_6H_3$ (entries 63, 69 and 74) This effect is independent of the oxygen substituent (R^3). Additionally, the substitution pattern of the trifluoromethyl groups on the aryl ring (R^4) proved to be important, as having groups at the 3- and 5- aryl position consistently resulted in greater enantioselectivity than having substituents at the 2- and 4-aryl positions (entry 64) or just the 4-aryl position (entry 65). Moreover, the presence of an alkyl group at R^1 (Me) is imperative as the analogous catalyst with R^1 = H afforded significantly decreased enantioselectivity (entry 1, e.r. 56:44). The installation of different groups at R^2 with π-surfaces while maintaining R^3 = 3,5-$(CF_3)C_6H_3$ produced similar results (1-naphthyl and mesityl, entries 77 and 83). When R^2 = *i*-propyl or *t*-butyl (entry 41) the enantioselectivity is significantly diminished in comparison to catalysts that contain an aromatic group is in this position. Together these results attest to the importance of π-surface rather than steric bulk at R^2 for higher enantioselectivity.

Table 9. Enantioselectivity of Libraries IV and V.

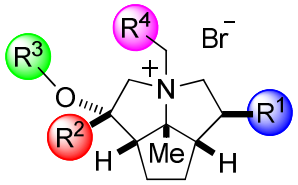

entry	Library #	R^1	R^2	R^3	R^4	C(1)-configuration	er, *S:R*
1	**IV**{*1,2,5*}	H	Ph	C_6H_5	3,5-$(CF_3)_2C_6H_3$	α	56:44
2	**V**{*1,2,2*}	Me	H	C_6H_5	1-naphthyl	α	54:46
3	**V**{*1,2,3*}	Me	H	C_6H_5	2-naphthyl	α	52:48
4	**V**{*1,2,1*}	Me	H	C_6H_5	C_6H_5	α	52:48
5	**V**{*1,2,3*}	Me	H	C_6H_5	*n*-hexyl	α	50:51
6	**V**{*1,2,8*}	Me	H	C_6H_5	4-(MeO)C_6H_4	α	52:48
7	**V**{*1,2,5*}	Me	H	C_6H_5	3,5-$(CF_3)_2C_6H_3$	α	56:44
8	**V**{*1,2,7*}	Me	H	C_6H_5	3,5-(*t*-Bu)$_2C_6H_3$	α	60:40
9	**V**{*1,2,2*}	Me	H	C_6H_5	1-naphthyl	β	49:51
10	**V**{*1,2,3*}	Me	H	C_6H_5	2-naphthyl	β	55:45
11	**V**{*1,2,5*}	Me	H	C_6H_5	3,5-$(CF_3)_2C_6H_3$	β	63:37
12	**V**{*1,2,3*}	Me	H	C_6H_5	*n*-hexyl	β	51:49
13	**V**{*1,2,8*}	Me	H	C_6H_5	4-(MeO)C_6H_4	β	56:44
14	**V**{*1,2,7*}	Me	H	C_6H_5	3,5-(*t*-Bu)$_2C_6H_3$	β	51:49
15	**V**{*2,3,2*}	Me	Me	*n*-hexyl	1-naphthyl	α	48:52
16	**V**{*2,3,3*}	Me	Me	*n*-hexyl	2-naphthyl	α	47:53
17	**V**{*2,3,5*}	Me	Me	*n*-hexyl	3,5-$(CF_3)_2C_6H_3$	α	57:43
18	**V**{*2,3,3*}	Me	Me	*n*-hexyl	*n*-hexyl	α	53:47
19	**V**{*2,3,8*}	Me	Me	*n*-hexyl	4-(MeO)C_6H_4	α	45:55
20	**V**{*2,3,1*}	Me	Me	*n*-hexyl	C_6H_5	α	46:54
21	**V**{*2,3,7*}	Me	Me	*n*-hexyl	3,5-(*t*-Bu)$_2C_6H_3$	α	58:42
22	**V**{*2,2,2*}	Me	Me	C_6H_5	1-naphthyl	α	45:55
23	**V**{*2,2,3*}	Me	Me	C_6H_5	2-naphthyl	α	49:51
24	**V**{*2,2,5*}	Me	Me	C_6H_5	3,5-$(CF_3)_2C_6H_3$	α	57:43
25	**V**{*2,2,3*}	Me	Me	C_6H_5	*n*-hexyl	α	51:49
26	**V**{*2,2,8*}	Me	Me	C_6H_5	4-(MeO)C_6H_4	α	47:53
27	**V**{*2,2,1*}	Me	Me	C_6H_5	C_6H_5	α	47:53
28	**V**{*2,2,7*}	Me	Me	C_6H_5	3,5-(*t*-Bu)$_2C_6H_3$	α	57:43
29	**V**{*2,7,2*}	Me	Me	4-(MeO)C_6H_4	1-naphthyl	α	48:52
30	**V**{*2,7,3*}	Me	Me	4-(MeO)C_6H_4	2-naphthyl	α	48:52
31	**V**{*2,7,5*}	Me	Me	4-(MeO)C_6H_4	3,5-$(CF_3)_2C_6H_3$	α	59:41
32	**V**{*2,7,7*}	Me	Me	4-(MeO)C_6H_4	3,5-(*t*-Bu)$_2C_6H_3$	α	57:43
33	**V**{*3,3,2*}	Me	*i*-Pr	*n*-hexyl	1-naphthyl	α	43:57
34	**V**{*3,3,3*}	Me	*i*-Pr	*n*-hexyl	2-naphthyl	α	42:58

Table 9. (cont.) Enantioselectivity of Libraries IV and V.

35	**V**{*3,3,5*}	Me	*i*-Pr	*n*-hexyl	3,5-$(CF_3)_2C_6H_3$	α	39:62
36	**V**{*3,3,3*}	Me	*i*-Pr	*n*-hexyl	*n*-hexyl	α	51:49
37	**V**{*3,3,8*}	Me	*i*-Pr	*n*-hexyl	4-$(MeO)C_6H_4$	α	40:60
38	**V**{*3,3,1*}	Me	*i*-Pr	*n*-hexyl	C_6H_5	α	40:60
39	**V**{*3,3,7*}	Me	*i*-Pr	*n*-hexyl	3,5-(*t*-Bu)$_2C_6H_3$	α	40:60
40	**V**{*3,2,2*}	Me	*i*-Pr	C_6H_5	1-naphthyl	α	42:58
41	**V**{*3,2,3*}	Me	*i*-Pr	C_6H_5	2-naphthyl	α	44:56
42	**V**{*3,2,5*}	Me	*i*-Pr	C_6H_5	3,5-$(CF_3)_2C_6H_3$	α	36:64
43	**V**{*3,2,3*}	Me	*i*-Pr	C_6H_5	*n*-hexyl	α	43:57
44	**V**{*3,2,8*}	Me	*i*-Pr	C_6H_5	4-$(MeO)C_6H_4$	α	44:56
45	**V**{*3,2,1*}	Me	*i*-Pr	C_6H_5	C_6H_5	α	43:57
46	**V**{*3,2,7*}	Me	*i*-Pr	C_6H_5	3,5-(*t*-Bu)$_2C_6H_3$	α	38:62
47	**V**{*3,7,2*}	Me	*i*-Pr	4-$(MeO)C_6H_4$	1-naphthyl	α	41:59
48	**V**{*3,7,3*}	Me	*i*-Pr	4-$(MeO)C_6H_4$	2-naphthyl	α	42:58
49	**V**{*3,7,5*}	Me	*i*-Pr	4-$(MeO)C_6H_4$	3,5-$(CF_3)_2C_6H_3$	α	40:60
50	**V**{*3,7,3*}	Me	*i*-Pr	4-$(MeO)C_6H_4$	*n*-hexyl	α	41:59
51	**V**{*3,7,8*}	Me	*i*-Pr	4-$(MeO)C_6H_4$	4-$(MeO)C_6H_4$	α	40:60
52	**V**{*3,7,1*}	Me	*i*-Pr	4-$(MeO)C_6H_4$	C_6H_5	α	44:56
53	**V**{*3,7,7*}	Me	*i*-Pr	4-$(MeO)C_6H_4$	3,5-(*t*-Bu)$_2C_6H_3$	α	39:61
54	**V**{*4,2,5*}	Me	*t*-Bu	C_6H_5	3,5-$(CF_3)_2C_6H_3$	α	37:63
55	**V**{*5,3,2*}	Me	C_6H_5	*n*-hexyl	1-naphthyl	α	48:52
56	**V**{*5,3,3*}	Me	C_6H_5	*n*-hexyl	2-naphthyl	α	49:51
57	**V**{*5,3,5*}	Me	C_6H_5	*n*-hexyl	3,5-$(CF_3)_2C_6H_3$	α	79:21
58	**V**{*5,3,8*}	Me	C_6H_5	*n*-hexyl	4-$(MeO)C_6H_4$	α	42:58
59	**V**{*5,3,1*}	Me	C_6H_5	*n*-hexyl	C_6H_5	α	45:55
60	**V**{*5,3,7*}	Me	C_6H_5	*n*-hexyl	3,5-(*t*-Bu)$_2C_6H_3$	α	61:39
61	**V**{*5,2,2*}	Me	C_6H_5	C_6H_5	1-naphthyl	α	49:51
62	**V**{*5,2,3*}	Me	C_6H_5	C_6H_5	2-naphthyl	α	51:49
63	**V**{*5,2,5*}	Me	C_6H_5	C_6H_5	3,5-$(CF_3)_2C_6H_3$	α	81:19
64	**V**{*5,2,11*}	Me	C_6H_5	C_6H_5	(2,4-$CF_3)_2C_6H_3$	α	56:44
65	**V**{*5,2,9*}	Me	C_6H_5	C_6H_5	(4-$CF_3)C_6H_4$	α	49:51
66	**V**{*5,2,10*}	Me	C_6H_5	C_6H_5	(4-CN)C_6H_4	α	50:50
67	**V**{*5,2,8*}	Me	C_6H_5	C_6H_5	4-$(MeO)C_6H_4$	α	44:56
68	**V**{*5,2,1*}	Me	C_6H_5	C_6H_5	C_6H_5	α	48:52
69	**V**{*5,6,5*}	Me	C_6H_5	3,5-$(CF_3)_2C_6H_3$	3,5-$(CF_3)_2C_6H_3$	α	81:19
70	**V**{*5,6,8*}	Me	C_6H_5	3,5-$(CF_3)_2C_6H_3$	4-$(MeO)C_6H_4$	α	46:54
71	**V**{*5,6,1*}	Me	C_6H_5	3,5-$(CF_3)_2C_6H_3$	C_6H_5	α	49:51
72	**V**{*5,7,2*}	Me	C_6H_5	4-$(MeO)C_6H_4$	1-naphthyl	α	50:50
73	**V**{*5,7,3*}	Me	C_6H_5	4-$(MeO)C_6H_4$	2-naphthyl	α	51:49
74	**V**{*5,7,5*}	Me	C_6H_5	4-$(MeO)C_6H_4$	3,5-$(CF_3)_2C_6H_3$	α	81:19

Table 9. (cont.) Enantioselectivity of Libraries IV and V.

75	**V**{*5,7,1*}	Me	C_6H_5	4-(MeO)C_6H_4	C_6H_5	α	48:52
76	**V**{*5,7,7*}	Me	C_6H_5	4-(MeO)C_6H_4	3,5-(*t*-Bu)$_2C_6H_3$	α	63:37
77	**V**{*7,2,5*}	Me	1-naphthyl	C_6H_5	3,5-$(CF_3)_2C_6H_3$	α	81:19
78	**V**{*7,2,9*}	Me	1-naphthyl	C_6H_5	(4-CF_3) C_6H_4	α	54:46
79	**V**{*7,2,10*}	Me	1-naphthyl	C_6H_5	(4-CN)C_6H_4	α	52:48
80	**V**{*7,2,8*}	Me	1-naphthyl	C_6H_5	4-(MeO)C_6H_4	α	48:52
81	**V**{*7,2,1*}	Me	1-naphthyl	C_6H_5	C_6H_5	α	51:49
82	**V**{*6,2,8*}	Me	mesityl	C_6H_5	4-(MeO)C_6H_4	α	47:54
83	**V**{*6,2,5*}	Me	mesityl	C_6H_5	3,5-$(CF_3)_2C_6H_3$	α	76:24

2.12. Discussion.

2.12.1. Summary of Ammonium Ion Preparations and Synthetic Strategies.

Since the discovery of asymmetric phase transfer catalysis with cinchona alkaloid derivatives, a significant level of effort has been devoted to the introduction of novel synthetic catalyst structures. Most of the synthetic endeavors fall into one of the following two synthetic strategies: (1) elaboration of a readily available source of chiral material by appending a non-stereogenic quaternary ammonium ion or (2) incorporation of a quaternary ammonium into a molecule in such a way that it lies on a symmetry axis. Although each of these approaches has seen some success, the synthetic strategy presented herein is significantly different and warrants discussion.

The approach presented here is unique in that the synthetic effort was focused on systematically varying the steric and electronic environment around a central stereogenic quaternary ammonium ion. To this end, the synthetic investment was divided into two different parts. The first part involved preparation of a nitrogen containing scaffold (a cyclopentapyrrolizidine) on a significant scale which was readily accomplished by application of the tandem inter [4+2]/intra [3+2] cycloaddition of nitroalkenes with only minor changes to the previously published routes. Notably, the tandem cycloaddition also served as a diversifying element in that it was in this step that the configuration at C(1) was set (Libraries **II** and **III**) and the R^1 group was introduced stereoselectively, which subsequently proved to be a critical catalyst structural feature.

The second synthetic component involved development of procedures amenable to parallel synthesis that introduced a variety of groups in the vicinity of the ammonium nitrogen.

Ultimately, three operationally simple bond forming reactions were utilized to accomplish this goal that allowed for the catalysts to be prepared in a parallel fashion. The tandem cycloaddition naturally installs a hydroxyl group at C(1) which served as a functional handle for two parallel synthesis steps; a Grignard addition and an O-alkylation, leaving only N-quaternization as the final parallel synthesis step. Including the previously installed R^1 substituent a total of four variable groups were introduced. The diversity and number of groups utilized was greatest for the positions that could be incorporated in parallel (R^2, 6; R^3, 7; R^4, 11) and the least for the group that required a recast skeleton (R^1, 2). A good appreciation for the shape of the catalyst(s) and disposition of the variable groups in relation to the ammonium nitrogen is necessary to facilitate a thorough analysis of the effect of each group (and combinations thereof) on catalytic activity and selectivity.

2.12.2. Summary of Results.

A brief summary of the rate and enantioselectivity data is necessary to facilitate the following discussion. The kinetic results are summarized in bar graph format in Figure 9. In general catalysts that bear an oxygen substituent at C(1) are more active than catalysts without this oxygen substituent, and the configuration of the oxygen functional group does not influence the reaction rate significantly. However, the catalytic activity is greater for ethers compared to alcohols. In addition, there is a decrease in catalytic activity when the substituent bonded to the nitrogen is strongly electron withdrawing (e.g. $R^4 = (3,5\text{-}CF_3)_2C_6H_3$). This effect is large when the R^2 substituent is small and aliphatic (R^2 = H, Me) and moderate when R^2 is bulky and aliphatic (R^2 = *i*-Pr, *t*-Bu). Significantly less dependence on the nitrogen substituent was observed when R^2 was aromatic (Ph, mesityl, 1-naphthyl). Quaternary ammonium ions containing a four membered ring (Library **VI**) displayed comparable activity to the parent scaffold (Library **I**). The catalytic activity of these unfunctionalized ring systems are not as high as tetraethylammonium but better than cetyltrimethyl ammonium in activity.

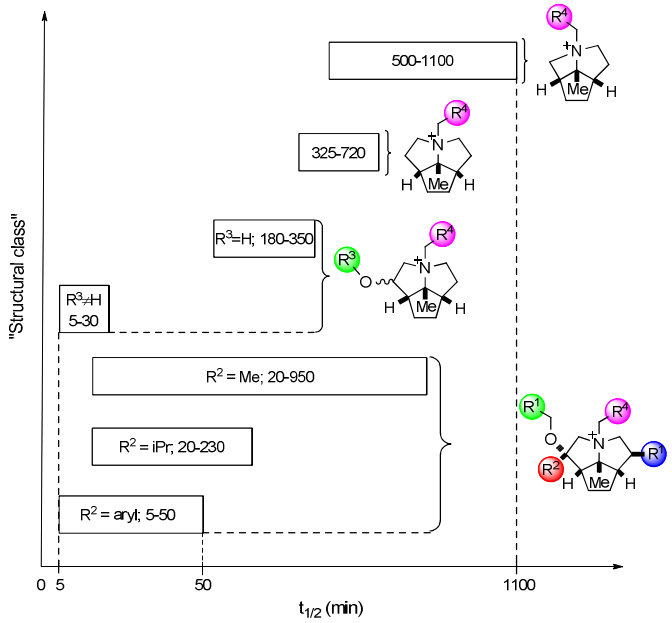

Figure 9. Structural Clustering of Kinetic Data.

Given the large volume of data presented herein, a concise statistical summary provides a good indication of which data is the most interesting and worthy of detailed analysis. The relative contribution of the groups to the variation in the observed data is estimated by examining the standard deviation as a function of each group (R^1-R^4).[96] That is the larger deviation in the observed rate (or selectivity) as a function of group positional substitution, then the greater is the relationship of that substituent (R^2-R^4) to the observed effect (rate or selectivity, Figure 10). Therefore, the variation approximates the sensitivity of the rate and selectivity to a structural change at the indicated substituent. Both catalyst activity and rate are influenced the most by the groups R^2 and R^4, with the greatest dependence on R^4. Also, in both cases, the R^3 group has the least influence. The R^1 group was not sufficiently varied for interpretation by this analysis.

The observation that the enantioselectivity is affected in a similar manner to the reaction rate may lead to interesting mechanistic interpretation. For instance, a possible consequence that is consistent with this analysis (but not unambiguously supported) is the direct relationship between the rate determining step and the selectivity-determining step (formation of a stable chiral ion-pair and/or alkylation of the enolate).

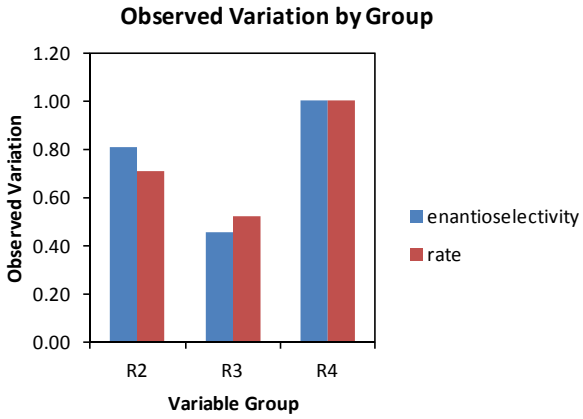

Figure 10. Variation in rate and selectivity as a function of positional group substitution.

2.12.3. Influence of the Alkoxy Group.

The presence of an oxygen at C(1) is a natural consequence of the tandem cycloaddition utilized to construct the scaffolds. However, inclusion of an oxygen substituent beta to the ammonium center appears to have an important effect on the catalytic activity (compare Libraries **I** and **II**). Similar observations have been reported previously for β-hydroxy quaternary ammonium ion phase transfer catalysts and rationalized by invoking a hydrogen bond donating interaction from the catalyst.[97] This analysis is consistent with the observation that β-hydroxy ammonium ions exhibit a high affinity for hydroxide ion.[98] Indeed, a β-oxygen substituent is a common structural motif employed in many asymmetric quaternary ammonium phase transfer catalysts.[99] Importantly, this substituent is a natural structural component of the cinchona alkaloids, but its inclusion in many other synthetic catalysts is likely a consequence of synthetic accessibility or serendipity. Because the rate enhancement that arises β-oxygenated ammonium ion catalysts has been observed previously and because it is a structural feature shared with cinchona derived catalysts, a more detailed analysis of the effect of β-oxygen substitution was sought. Insight to the origin of the rate enhancement effect could be gleaned by application of quantitative structure-activity relationships and will be discussed in the accompanying paper. However, changes in the local electronic environment of the ammonium upon inclusion of a β-oxygen substituent required some analysis to provide a stolid framework for even a qualitative rationalization of the rate and selectivities observed in this data set.

The electronic perturbation caused by an oxygen atom two carbons removed from the ammonium center is manifested in two related electronic effects, the electrostatic potential interaction and the direction of the dipole. Some insight is gleaned by comparison of the electrostatic potential maps of the oxygenated and unoxygenated catalyst scaffolds (Figure 11). For computational simplification, a methyl group is used at R^3. The directions of the dipoles are illustrated. The difference in the maximum electrostatic potential energies of the left and right faces of the oxygenated scaffold is 3.0 kcal/mol and 0 kcal/mol for the unoxygenated scaffold (Cs symmetric). In the C_s symmetric ammonium salts (Library **I**), the charge distribution is equally dispersed between the two convex faces, even though, in reality the lowest energy conformer (depicted) is not C_s symmetric. In contrast, inclusion of an alkoxy group two carbons removed from the ammonium nitrogen results in a considerable polarization of the positive potential toward the face to which it is attached (Library **II**, methoxy is included for simplicity). That is, the two convex faces of the ammonium ion are differentiated electronically, such that a greater positive potential resides on the left face. The same change in electronic distribution is manifested in the direction of the dipole vector (Figure 11). The dipole vector in the C_s symmetric scaffold bisects the R^4 substituent (the only polarizable group), reflecting the equal distribution of charge on the left and right faces of the pyrrolizidine unit. The dipole in the oxygenated analog is rotated 60^o clockwise such that the positive end is projected toward the left convex face of the ammonium ion. This analysis is consistent with a stronger electrostatic interaction with the left convex face than the right, which, in turn, is consistent with the experimental observation fact that the R^2 substituent has a large effect on the observed rate and selectivity. Since both rate and selectivity are highly dependent on the R^2 group and little to no selectivity is observed when R^1 = H, our data seems most consistent with a selective associations of the enolate to the left convex face of the ammonium. That is, the oxygen serves to increase the positive potential on the left convex face and the R^1 group acts to sterically shield the right convex face of the ammonium ion.

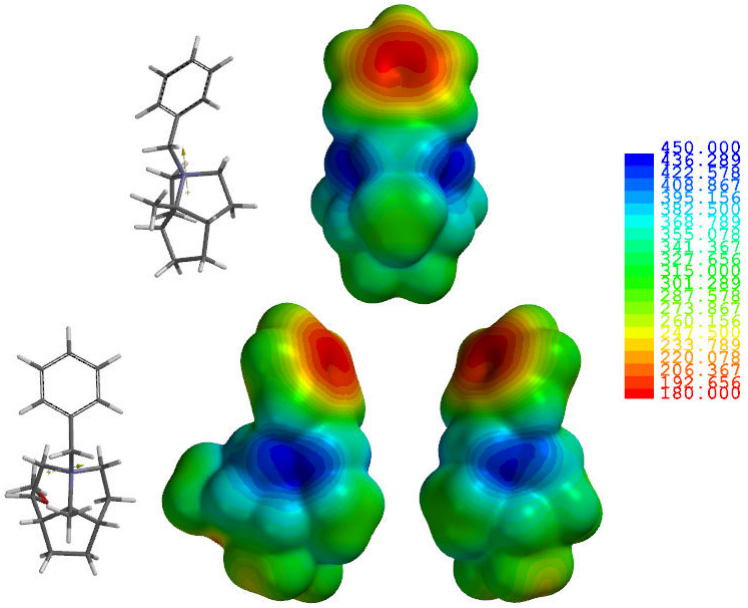

Figure 11. Electrostatic potential (ESP) maps (M062X/6-31G(d)) of scaffolds for Library I (unoxygenated) and Library II (oxygenated) where C(6) C(7) and N(3) C(9) dihedrals are constrained to 0 in the geometry optimization to exclude bias of a specific twist conformer. ESPs are mapped onto electron density isosurfaces (0.002 electrons/au^3). Legend is in units of kJ/mol.

2.13. Rate as a Function of Ammonium Ion Accessibility.

The reaction rate of PTC alkylation processes has been correlated with the accessibility of the ammonium nitrogen (in terms of q), where an optimum accessibility is found.[27] The observation of a maximum catalyst activity as a function of ammonium accessibility has two similar explanations. In the first, the accessibility of the ammonium nitrogen is related to the rate of exchange of anions, a kinetic phenomenon.[25] In the second, the accessibility of the ammonium nitrogen is related to the ability of the catalyst to decrease the interfacial tension and thereby facilitate enolate transfer, a thermodynamic phenomenon.[24,100]

The data collected herein are largely consistent with these proposals, with the added complexity that the magnitude of the exposed positive potential (δ^+) should be considered as well. On the basis of the analysis above, the accessibility of the positive potential (δ^+, left convex face) should be correlated with the steric bulk of the R^2 substituent. Regardless of the interpretation, the sensitivity of the rate to the R^2 substituent discussed above (Figure 10) advocates a strong dependence of the overall reaction rate on the nitrogen accessibility (steric nature of R^2).

The form of the observed dependence is partially revealed by examining the reaction half-lives as a function of the R^2 substituent for selected R^4 groups (Table 10, MR = molar refractivity).[101] The dependence is weak when the electronic character of R^4 is neutral to moderately electron rich (R^4 = C_6H_5, 4-$MeOC_6H_4$). However, a much stronger dependence is seen for catalysts containing the R^4 = 3,5-$(CF_3)_2C_6H_3$ group. In these catalysts an increase in steric bulk from *i*-Pr to *t*-Bu does not lead to a significant rate enhancement relative to the enhancement from Me to *i*-Pr. However, an increase in activity is observed for R^2 = Ph, which is somewhat diminished when the R^2 group is a larger aromatic group (mesityl or naphthyl). This disparity may be rationalized by ammonium accessibility, such that catalysts with R^2 = Ph have an optimum accessibility. Alternatively, the additional steric bulk on the left face of the pyrrolizidine unit may cause the enolate to associate more favorably on the right face of the scaffold when the R^2 substituent is larger than the R^1 substituent. The stereochemical course of the alkylation with these catalysts also support the latter rationale as a reversal in absolute configuration of the product was observed. However, it is not clear whether the enolate extraction step or the alkylation step is stereochemistry determining, or whether they occur in concert.

Table 10. Half-lives (min) of Selected Catalysts with R^1 = Me, R^3 = Ph and Variable R^2 and R^4.

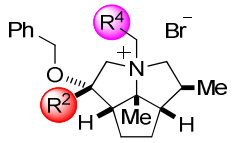

R^2		R^4		
	MR[a]	C_6H_5	3,5-$(CF_3)_2C_6H_3$	4-$(MeO)C_6H_4$
Me	6.88	21	900	18
i-Pr	16.08	132	122	174
t-Bu	20.85	-	96	-
phenyl	25.28	11	10	18
mesityl	42.97	12	62	12
1-naphthyl	42.45	14	29	11

[a]MR = molar refractivity of the R^2 substituent calculated by Chemdraw.

Rationalizing the effect of the R^2 substituent in terms of steric bulk makes intuitive sense because placing groups in this position modulates the relative accessibility of the positive potential at the two convex faces. However, other explanations are possible. For example, one could argue that the major structural perturbation upon replacing a branched aliphatic group with an aromatic group is the introduction of a π-surface. This line of reasoning is worth considering since the physical interpretation is different, which leads to a distinctly different conclusion. If introduction of a π-surface in the catalyst adds an additional binding force for the substrate anion (π-π interactions), then one may conclude that the equilibrium between catalyst$^+X^-$ (Br^- or HO^-) and catalyst$^+$enolate$^-$ ion pair is shifted toward the enolate complex. Therefore, the net rate enhancement could possibly be attributed to a greater proportion of catalyst being bound to enolate, a strictly thermodynamic phenomenon.

All of the comparisons in this section have been made with catalysts containing a 3,5-$(CF_3)_2C_6H_3$ group at R^4. The same interpretations cannot be readily applied to catalysts without a 3,5-$(CF_3)_2C_6H_3$ group at R^4. Most consistent with the above analysis of charge polarization, the 3,5-$(CF_3)_2C_6H_3$ group must impart sufficient charge polarization to amplify the effect of the variable R^2 group. Interpretation of these observations in the context of a transfer rate limiting regime has led to the conclusion that an optimum ammonium accessibility, or charge exposure is likely. In other words, a greater charge exposure will increase the ammonium ions association with the anionic hydroxide surface. However, if the exposed δ+ area or charge density is too great, then the catalyst will not dissociate away from the interface as readily.

Three important elements can be inferred from the discussion of rate:

(1) the observed increase in catalyst activity upon the inclusion of an oxygen substituent is attributed to the increase in the rate of ion pair formation and/or a decrease in interfacial tension,

(2) the observed decrease in catalyst activity upon the inclusion of the 3,5-$(CF_3)_2C_6H_3$ group at R^4 for small groups at R^2 (H, Me, *i*-Pr) is attributed to a diminished tendency of the ion-pair to transport from the interface to the organic phase for alkylation due to greater charge density at the ammonium center,

(3) the observed increase in catalyst activity upon the inclusion of aryl groups at R^2 with R^4= 3,5-$(CF_3)_2C_6H_3$ is attributed to an enhanced ability of the ion-pair to transport from the interface into the organic phase for alkylation because of an optimum

surface exposure of the ammonium ion (kinetic) or a change in enolate binding equilibrium (thermodynamic).

2.13.1. Enantioselectivity.

The intermolecular forces that have been proposed to contribute to enantioselectivity in APTC reactions include: (1) ROH•••$^{-}$O–CR=CR_2 hydrogen bonding[33a,c] (2) R_3N^{+}-CHR–H•••$^{-}$O–CR=CR_2 (α-CH hydrogen bonding)[44b] (3) π-π interactions.[33a,c] The most selective catalysts in this study do not contain OH hydrogen bond donating sites, therefore intermolecular force (1) can be eliminated as a stereocontrolling element. The results here support the operation of interactions (2) and potentially (3).

The unique structural features of the catalyst scaffold include the intrinsic shielding of two of the four faces of the imaginary tetrahedron encompassing the nitrogen and the capacity to differentiate the two remaining exposed faces (c.f. Figure 12). The second feature arises from the modular nature of the cycloaddition-based construction which allows both exposed front faces to be differentiated electronically (β-oxygenation) and sterically (relative steric bulk of R^1 and R^2). Although those factors that control the topicity of the enolate reactivity are difficult to predict, the factors that dictate the relative binding strengths of the enolate to each of the tetrahedral faces are more easily controlled and predicted. Initially, these factors were the primary focus for the design and construction of the libraries.

The observed enantioselectivities are largely dependent on the substituents that influence the binding of the anion to the face of the hypothetical tetrahedron around the ammonium ion with the largest concentration of positive potential (R^2 and R^4, Figure 12). The observation that the enantioselectivity is greatest for catalysts that bear strongly electron withdrawing groups on the nitrogen is consistent with the need for one or both of the following potential interactions: (1) α-CH-hydrogen bonding or (2) a tighter ion pair resulting from increased Coulombic interaction. Additionally, a π-surface is necessary at the R^2 substituent, presumably to engage in π-stacking interactions with the phenyl rings of the reacting enolate. Moreover, the presence of an alkyl group at R^1 is necessary to decrease the accessibility of the right hand face of the pyrrolizidine moiety because in its absence, the enantioselectivity is poor. This observation suggests that binding to the right hand face leads to lower selectivity because of the pseudo-enantiotopic local chirality. The aforementioned interactions seem to operate in concert as the absence of one of the interactions leads to significantly diminished enantioselectivities.

2.14. Conclusions.

A synthetic strategy for the synthesis of diverse libraries of quaternary ammonium ions has been developed. The key feature of the synthetic strategy was to divide the preparative work into two distinct stages: (1) scaffold preparation and (2) diversity oriented parallel synthesis. In this way, a total of 160 structurally diverse quaternary ammonium ions were prepared that share a common scaffold constructed by a tandem inter[4+2]/intra[[3+2] cycloaddition of a nitroalkene. A method was developed for the collection of kinetic data of a biphasic reaction that is applicable over a wide range of catalyst activities (half-lives ranging from days to minutes). The range of data collected covers many orders of magnitude and therefore is well suited for analysis by the application of quantitative structure-activity relationships. Inclusion of an oxygen atom in the vicinity of the quaternary ammonium ion affects the catalytic activity. The catalyst enantioselectivity is strongly dependent on the substituent attached to the same carbon as the oxygen atom. These observations were rationalized in terms of a selective polarization of the positive potential on one of the faces of the tetrahedral ammonium over the other. The inclusion of a 3,5-substituted aromatic substituent on nitrogen proved crucial for catalyst enantioselectivity. With strongly electron withdrawing 3,5-trifluoromethyl groups, the previously observed dependencies on rate were amplified. The proposed dependencies of rate on the ammonium accessibility are consistent with the data reported herein with the added complexity that the magnitude of the “ammonium charge” or charge density should be considered as well. Quantitative models have been developed to describe both the reactivity and selectivity trends discussed herein and constitute the focus of the following sections.

Chapter 3: *Ion-Pair QM Modeling and the Development of CoMFA Models for Enantioselectivity*

3.1. Introduction.

The formulation of relationships between molecular structure and chemical function has always been and remains area of intense research within the physical and life sciences. Relating single substituent effects on reactivity has been widely studied in the form of linear free energy relationships (LFER) pioneered by Hammett.[102] However, these analyses are limited to minor structural changes, namely single substitution patterns. Methods to correlate function with a myriad of molecular properties, i.e. descriptors, have been developed in the form of multi-dimensional QSAR[103] due in part to the seminal contributions from Hansch[104] and Wilson.[105] Medicinal chemistry has benefitted immensely since the advent of these techniques. While QSAR methods have found the widest utility in relating the activity of a drug to its structure, theoretically, the same principles can be applied toward correlating function with any response, even the rate or selectivity of a chemical reaction.

Not until recently have such methods been used in correlating structure with *enantioselectivity*.[43f] Such methods include comparative molecular field analysis (CoMFA),[54] stereocartography,[43b] functional group mapping[43c] and others.[43f] These methods have been implemented for a number of systems and were found to provide some success in predicting the selectivity of catalysts with good predictability. New applications of simple LFER's has also recently been implemented toward rationalizing[43i,49,106,107] and predicting[108] catalysts. Nevertheless, PTC has received only moderate attention employing such approaches and is the focus of the following sections in this chapter.[58] But before doing so, it will be beneficial to gain an understanding of the preferred arrangement of an ammonium cation and the enolate in the ion pair geometry. This knowledge will facilitate the formulation of stereochemical models for which future catalyst design criteria can be based from.

3.2. Ion-Pair Modeling

Information on the geometry of the ground state ammonium enolate ion pair is crucial to understanding asymmetric induction. Because less than a handful of computational studies on ammonium enolate ion pairs exist in the literature,[44b,45,48] it was deemed worthwhile to establish

some principles on the geometry of the ion pair computationally. The ion pair between timethylammonium and methyl acetate enolate has been investigated computationally and a facial orientation was obtained.[44b] The enolate studied here is complicated by considerable delocalization and the presence of an additional electronegative atom (imine nitrogen) relative to a simple ester enolate. Consequentially, its own investigation was warranted.

The lowest energy ion pairs should be those that maximize the number of C-H•••$^{-}$En interactions.[44b] Four possible ion pair arrangements can be envisioned when including the *E*/*Z* geometry of the enolate (Scheme 21). The enolate can either orient in a facial manner ((*Z*/*E*)-face) or in a manner by which the plane of the enolate bisects the plane created by the three α-hydrogens ((*Z*/*E*)-edge).

Scheme 21.

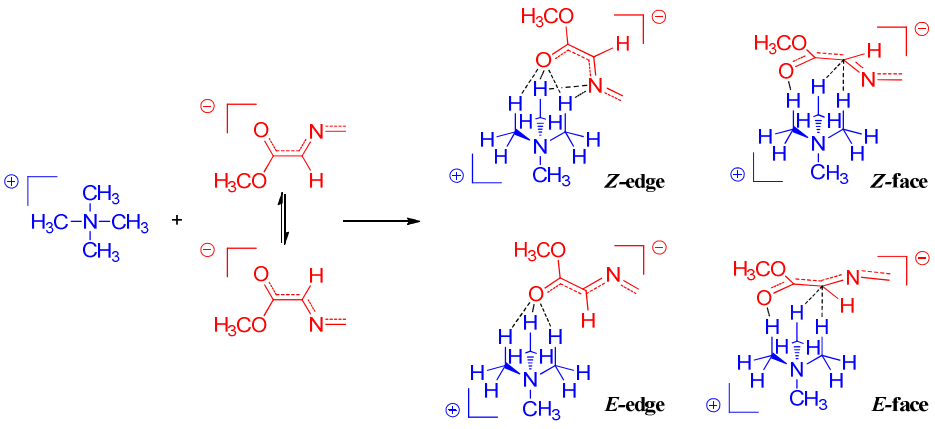

Three of the four ion pair arrangements were located using the M06-2X density functional (Figure 12). The ***Z*-face-H** geometry could not be located as it converged to the ***Z*-edge-H** geometry. The lowest energy geometry is ***Z*-edge-H** by 3.0 kcal/mol over ***E*-face-H**. ***E*-edge-H** is the highest energy geometry at ΔE_{rel} = 5.4 kcal/mol. The edge geometries are tilted causing them to be between planar and orthogonal with respect to the plane adopted by the three hydrogen atoms and the plane of the enolate. Interestingly, the geometry with the smallest separation between the charged oxygen of the enolate and the three hydrogen atom of the ammonium ion is ***E*-edge-H** which possesses the highest energy. The origins of the differences in energy can be illuminated by decomposing the binding energy between the ammonium cation and the enolate for each geometry into unique energy terms.

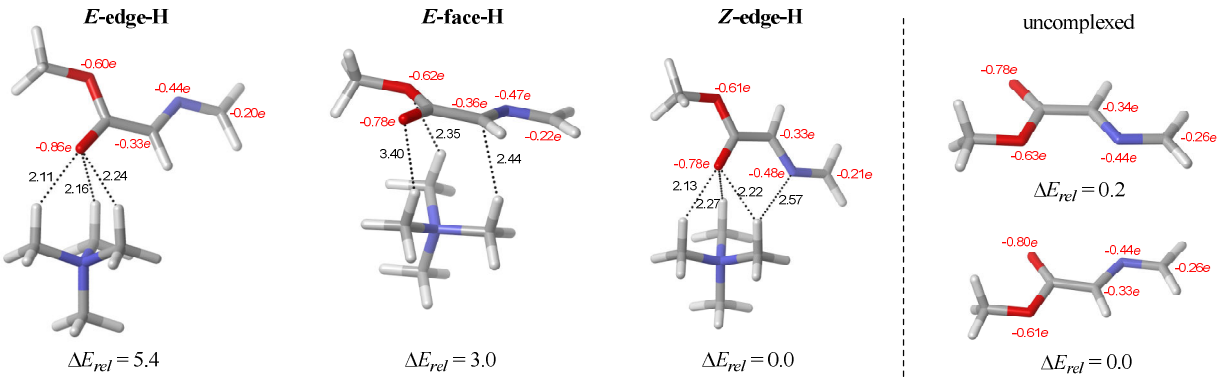

Figure 12. Ammonium enolate ion-pair geometries. Distances are in Å. Energies (ΔE_{rel}) are in kcal/mol. Calculated at the CPCM(toluene)-M06-2X/6-311+G(2d,2p)//CPCM(toluene)-M06-2X/6-31+G(d,p). Values in red represent NBO partial atomic charges.

A localized molecular orbital based energy decomposition analysis (LMO-EDA)[109] is implemented for interpreting the origin of the differences in energy of the complexes. The results of the energy decomposition analysis are illustrated in Table 11. The energy required to distort the fragments to the geometry of the complex is low throughout (< 2 kcal/mol) which is consistent with the resulting low geometrical distortion from the isolated fragments (which can be observed by qualitative inspection). Complex ***Z*-edge-H** is energetically preferred over ***E*-edge-H** in large part due to the difference in the electrostatic term ($\Delta\Delta E_{es}$ = -10.9 kcal/mol) which is likely due to additional Coulombic attraction between the nitrogen of the imine and the α-hydrogen atoms. Complex ***E*-edge-H** exhibits the most polarized charge distribution relative to the uncomplexed enolate which is consistent with only the oxygen atom of the enolate interacting significantly with the ammonium cation. Complex ***E*-edge-H** is preferred over ***E*-face-H** by electrostatic interactions ($\Delta\Delta E_{es}$ = -11.6 kcal/mol) at a cost of unfavorable orbital interactions ($\Delta\Delta E_{orb}$ = 4.7 kcal/mol), which can be mostly attributed to polarization.

Table 11. LMO-EDA Analysis. Calculated at the CPCM(toluene)-M06-2X/6-311+G(2d,2p). Energies are in units of kcal/mol. $\Delta E = \Delta E_{int} + \Delta E_{d}$.

	ΔE_{es}	ΔE_{exrep}	ΔE_{orb}	ΔE_{disp}	ΔE_{d}	ΔE_{int}	ΔE
***E*-edge-H**	-26.1	28.1	-29.5	-14.0	1.7	-41.5	-39.8
***E*-face-H**	-25.4	27.4	-26.8	-18.6	1.1	-43.4	-44.5
***Z*-edge-H**	-37.0	32.3	-24.8	-17.4	1.9	-46.9	-45.0

The influence of phenyl substitution on the imine was probed next to more closely mimic the actual substrate (Table 12). For purposes of computational efficiency, only the trans-phenyl ring is added since that is the ring that is likely to be in conjugation. The cis-phenyl ring is expected to be out of plane (thus a much lower degree of conjugation) on account of $A^{1,3}$ strain. Complex ***Z*-edge-ph** is still the favored complex but to a lower extent relative to the complexes lacking the phenyl substitution (Figure 12). The lower preference for ***Z*-edge-ph** can be traced back to decreased electrostatic interactions. The inclusion of the phenyl ring causes the nitrogen to be further away from the α-hydrogen atoms thus leading to a decreased Coulombic attraction. Increased dispersion interactions compensates for the electrostatic difference between ***E*-edge-ph** and ***Z*-edge-ph** causing the difference in energy to be nearly equivalent ($\Delta E_{(\textbf{\textit{Z}-edge-ph – \textit{E}-edge-ph})}$ = -5.4 kcal/mol; $\Delta E_{(\textbf{\textit{Z}-edge- – \textit{E}-edge})}$ = -5.2 kcal/mol). The smaller difference between ***E*-face-ph** and ***Z*-edge-ph** can be attributed to a more favorable dispersion component for ***E*-face-ph** and a less favorable electrostatic component for ***Z*-edge-ph**. The significantly smaller electrostatic preference ($\Delta E_{es(\textbf{\textit{Z}-edge-ph – \textit{E}-edge-ph})}$ = -7.5 kcal/mol; $\Delta E_{es(\textbf{\textit{Z}-edge- – \textit{E}-edge})}$ = -12.4 kcal/mol) can be attributed to Me_3N^+-CH_2-H····π type interactions as there is some curvature present in the enolate in complex ***E*-face-ph** causing a slight folding around the ammonium cation. Since ***Z*-edge-ph** is the energetically preferred complex in both systems investigated, this arrangement was applied toward the study of model systems of the 5-5-5 scaffold.

Table 12. Ammonium enolate ion-pair geometries. Distances are in Å. Energies (ΔE_{rel}) are in kcal/mol. Calculated at the CPCM(toluene)-M06-2X/6-311+G(2d,2p)//CPCM(toluene)-M06-2X/6-31+G(d,p). Values in red represent NBO partial atomic charges.

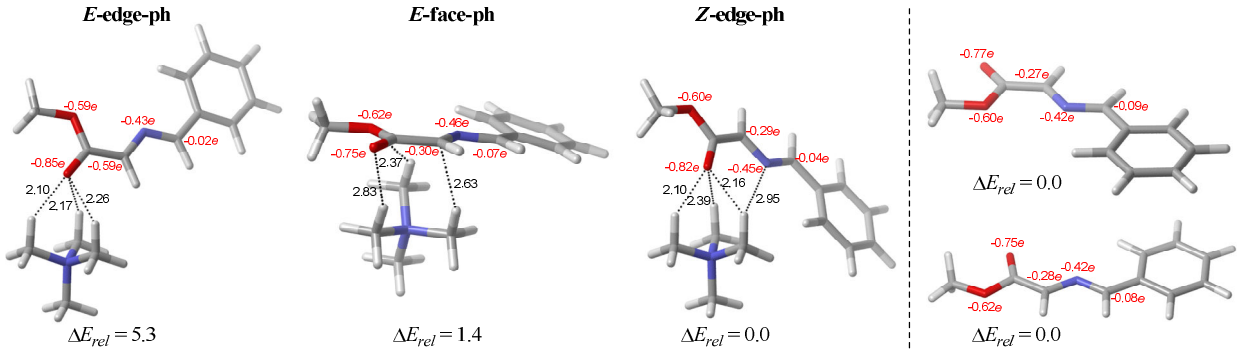

	ΔE_{es}	ΔE_{exrep}	ΔE_{orb}	ΔE_{disp}	ΔE_{d}	$\Delta E_{int,}$	ΔE
***E*-edge-ph**	-24.5	26.4	-29.6	-13.2	3.5	-40.8	-37.3
***E*-face-ph**	-26.3	29.3	-25.4	-21.4	2.5	-43.7	-41.2
***Z*-edge-ph**	-33.8	31.4	-24.8	-18.3	2.8	-45.5	-42.7

With the knowledge that complex *Z*-edge is the lowest energy arrangement, a model system for the core 555 scaffold (introduced in Chapter 2) can be investigated computationally. Two faces of the catalysts are considered to be available for enolate association based on electrostatic potential arguments (Figure 11 from Chapter 2). The complex that results from enolate association with the left face (**cat-L**) is 1.7 kcal/mol lower in energy than the complex that results from enolate association with the right face (**cat-R**). Most of this energy difference can be attributed to electrostatic interactions ($\Delta\Delta E_{es(L\text{-}R)}$ = –2.8 kcal/mol) (which is very close to the value based on qualitative inspection of the ESP maps (Figure 11 from Chapter 2)) which is the energy component that exhibits the largest difference. This difference provides the most compelling support for the polarization of electrostatic potential induced by the β-alkoxy group and its ability to lower the energy of complex formation. The concepts established from this investigation will aid in future catalyst design in combination with results from the next sections.

Table 13. Ammonium enolate ion-pair geometries. Energies (ΔE_{rel}) are in kcal/mol. Calculated at the CPCM(toluene)-M06-2X/6-311+G(2d,2p)//CPCM(toluene)-M06-2X/6-31+G(d,p).

cat-L **cat-R**

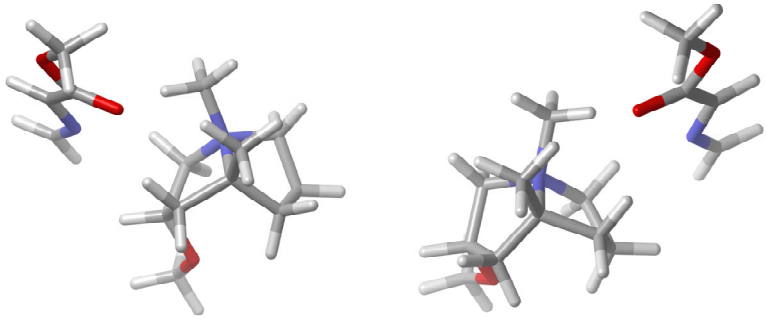

$\Delta E_{rel} = 0.0$ $\Delta E_{rel} = 1.7$

	ΔE_{es}	ΔE_{exrep}	ΔE_{orb}	ΔE_{disp}	ΔE_{d}	$\Delta E_{int,}$	ΔE
cat-L	-36.3	36.5	-26.5	-21.3	3.3	-47.6	-44.3
cat-R	-33.5	34.8	-26.7	-20.8	3.1	-45.5	-42.4
$\Delta\Delta E_{(L-R)}$	-2.8	1.2	0.2	-0.5	0.2	-2.1	-1.9

3.3. QSAR Modeling.

Quantitative models for activity and enantioselectivity were developed in parallel in this investigation. The reader is referred to the dissertation of Nathan Duncan-Gould for a detailed account of quantitative structure-activity relationships employing relevant 2-d descriptors such as clogP, XSA, electrostatic potential, molar refractivity, and others as applied to interpreting catalyst activity data.[110]

3.3.1. Conformations of Catalysts.

The choice of catalyst conformation is relevant for descriptors that are conformer-dependent including principle moment of inertia, dipole, surface area, and the spatial distribution of the interaction energies in the CoMFA analysis. Some ambiguity arises when considering the appropriate ring flip geometry for each catalyst, and thus a conformational analysis proved necessary. Minimum conformers for each catalyst were generated using the MMFF force field and a Monte-Carlo based conformation search as implemented in Spartan '08 v1.2.0.[111.] To ensure that the MMFF conformers were converging to reasonably stable minima, full geometry optimizations were carried out at B3LYP/6-31G(d) for each ring-flip conformer obtained from the MMFF conformation distribution analysis which resulted in 3 stable local minima using

MMFF. Gratifyingly, none of the three optimizations changed the ring flip conformations identified by MMFF. Moreover, the local minima maintained the same relative energies, validating the use of the MMFF conformers (See Experimental Section). Additionally, single point energies were determined including and excluding solvation (SM8[112] solvation model) in the absence of a counterion, again, the energetic ordering of the conformers was equivalent.

The lowest energy conformers of the isolated cations may not accurately reflect the major reactive conformation for the ammonium ion in the reaction medium. To address this deficiency, CoMFA analyses were performed on multiple conformer libraries with varying scaffold geometries obtained from the MMFF minimizations. The consequences of each developed model will be addressed in the Results Section.

3.3.2. Enantioselectivity Model Development.

Models for enantioselectivity were generated using CoMFA to generate the interaction fields and Partial Least Squares regression for the model development as implemented in SYBYL-X 1.1. The dependent variable was represented as a free energy term, $\Delta G = -RT \ln (R/S)$, because it is expressed as a linear combination of energy terms in the PLS model. Although representation of the data as enantiomeric excess (%ee)[50,54] would suffice given the nearly linear relationship with ΔG within the energy range of this study (1.2 kcal/mol), the model would not translate well in extrapolating to higher enantioselectivities where the linear relationship breaks down. Therefore, the representation of the dependent variable as an energy seemed appropriate and fundamentally justified.

The electrostatic fields were calculated from the partial atomic charges on all of the atoms. During preliminary studies, different partial charge methods were investigated including MMFF, Gasteiger-Marsili, and semi-empirical methods (AM1, MNDO, and PM3). Models using MNDO charges generally provided better correlations. CoMFA models developed from semi-empirical based charges have been demonstrated to provide consistently more predictive models than models developed from Partial Equalization of Orbital Electronegativity (PEOE, Gasteiger) and molecular mechanics based methods.[113] Thus, all of the remaining discussion of CoMFA model development will have incorporated MNDO ESP based partial atomic charges as determined from single point calculations on the MMFF conformers.

The structures were aligned employing a simple RMS rigid-body alignment. The rigidity of the scaffold led to a relatively straightforward decision on how to align the molecules in an

effort to minimize the variation in their fields (maximize the ratio of variation accountable versus variation that is unaccountable). The common substructure used for the alignment is represented by the nine atoms that make up the core 5-5-5 ring scaffold. An example of an alignment for one of the conformation libraries (in the Results Section) is illustrated (Figure 13).

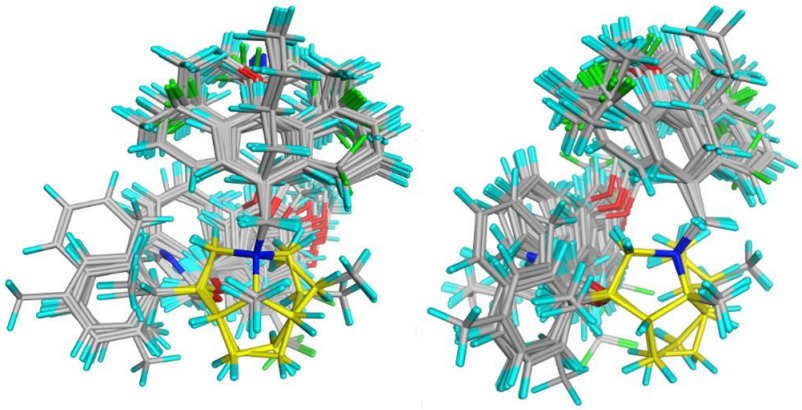

Figure 13. Rigid RMS alignment for a representative conformation library (101 catalysts) from two perspectives**.** The core 5-5-5 scaffold is highlighted in yellow.

The electrostatic and steric fields were calculated using two separate methods: Tripos Standard and Indicator field[114] classes. Under the Tripos Standard field method, the potentials at each lattice point are evaluated from the Lennard-Jones (6-12) and the Coulomb potentials. Cutoff energies are applied so that energies are not evaluated well within the Van der Waals surface of the atoms. Under the indicator field method, grid points are assigned as having either the pre-assigned cutoff value or zero. If the energy is calculated (by the LJ or Coulomb potentials) to be above the cutoff value, the energy at that grid point is set to the cutoff value. If the energy is calculated to be below the cutoff value, the energy at that grid point is set to zero. The indicator field method has the advantage of selecting only grid points of intermediate energy and has a tendency to reduce model noise.[58]

The resultant CoMFA models were further refined by placing weights on grid points that were more pertinent to the model through the region focusing technique as implemented in Sybyl-X 1.1. The grid points were weighted by the discriminate power option which weights each grid point by its contribution to the variation in the components of the model. This effectively enhances grid points with larger contributions while attenuating grid points that are less pertinent to the model. The exponent that gauges the steepness of the applied weights was

varied between 0.2 and 0.8. Application of the region focusing procedure was carried out iteratively until no improvement in the q^2_{LOO} was observed.

3.4. Model Validation.

The predictive capacity of the models was assessed through internal and external cross-validation.[115] The internal cross-validation was performed employing the leave-one-out (LOO) and leave-multiple-out (LMO) cross-validation methods. The q^2_{LMO} is subject to variation, especially for smaller training and prediction set splits. Thus, 100 LMO cross-validation runs were performed and the corresponding q^2_{LMO} is reported as the average over the 100 runs. External validation was performed upon the judicious division of the entire data set into training and test sets. This method will be discussed in more detail in the ensuing results section.

The model robustness was assessed through y-scrambling analysis.[116] The dependent variable data were completely scrambled such that each half-life or enantioselectivity value is paired up with the incorrect set of descriptors that are calculated for a particular catalyst. This process was performed 100 times and the average R^2 and q^2_{LOO} are reported.

3.5. Results.

The CoMFA modeling required multiple stages of development. The first stage involved the choice of conformers to use to represent each catalyst. Preliminary CoMFA modeling was then performed on each conformer library to obtain knowledge on the optimal representations of the catalysts for which the greatest variation in selectivity may be explained by the variation in their fields. Since both the rate and enantioselectivity models include conformation-dependent descriptors, the conformations identified from the preliminary CoMFA modeling may be used for the model development for reaction rate. After the ideal conformational representations for each catalyst was established from preliminary CoMFA modeling, the different CoMFA parameters (cutoff energies, field types, dielectric, etc.) were explored on the optimal conformer library to generate the best models as determined from internal cross-validation methods. To further validate the model, external cross-validation was then performed.

3.5.1. Establishing Catalyst Conformations.

Choosing appropriate conformational representations often represents a significant challenge for 3-D QSAR development and various approaches have been adopted.[117] The

catalysts studied herein have relatively few degrees of freedom at ambient temperature (within the scaffold) allowing for a relatively unambiguous conformational investigation. The most significant conformational differences are those represented as the "**up**" and "**dn**" conformers (Table 14). The preference for ring **a** to be in the "down" conformation is large enough that the "up" conformer for this ring need not be considered.[118] The preference for either the **up** or **dn** conformation as shown is primarily a function of the identities of the R^1 and R^2 substituents and the libraries in Table 14 (Libraries, **A** thru **E**) are organized as such. A first approximation of reasonable conformations was the global minimum for each catalyst (Library **A**, Table 14).[119] The geometry optimization for each catalyst was carried out in the absence of a counterion and thus the probability with which they represent active conformations is uncertain. Hence, alternative conformational representations and different combinations thereof were investigated. Taking into consideration the minimal energy difference between the "**up**" and "**dn**" conformers,[119] two additional conformer libraries were generated; one with all of the catalysts in the "**dn**" conformation (Library **B**), and another with all of the catalysts in the "**up**" conformation (Library **C**). The investigation of libraries **D** and **E** only became apparent after the initial CoMFA modeling was carried out and will be described in that order.

Table 14. Two primary conformational representations of catalysts and table of libraries representing differing combinations of conformers **up** and **dn** dependent on R^1 and R^2.

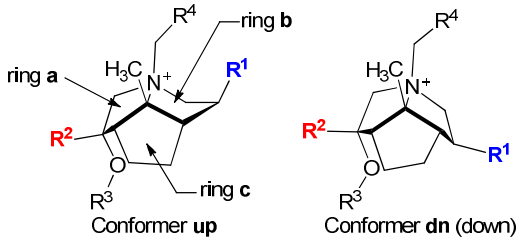

	R^2/R^1				
Library	H/H	H/Me	Me/Me	(*i*-Pr or *t*-Bu)/Me	Aryl[a]/Me
A[b]	**up**[c]	**up**	**dn**	**dn**	**dn**
B	**dn**	**dn**	**dn**	**dn**	**dn**
C	**up**	**up**	**up**	**up**	**up**
D	**up**	**up**	**up**	**dn**	**up**
E	**dn**	**dn**	**dn**	**up**	**up**

CoMFA modeling of the enantioselectivity was carried out using a limited number of cutoff energy combinations (15 or 30 kcal/mol) for both electrostatic and steric fields of standard

or indicator field types. An example of a rigid body alignment is illustrated in Figure 13 (conformer Library **D**). A condensed summary of these results in terms of their coefficients of determination (R^2/q^2_{LOO}) is compiled in Table 15. Generally, MNDO semi-empirical based ESP partial charges provided models with the highest correlations and are considered here in calculating the electrostatic energies for the CoMFA analysis (Table 15).[120] The correlations for libraries **A**, **B**, and **C** fall short of the minimum for statistically significant predictions ($q^2_{LOO} \geq 0.6$). Inspection of the residuals for the cross-validated runs (q^2_{LOO}) revealed that catalysts with R^2 = *i*-Pr and the most selective catalysts (R^2 = aryl, R^4 = 3,5-bis(trifluoromethyl)benzyl) exhibited the largest error in the predictions. Although, Library **C** does contain one model with a $q^2_{LOO} > 0.6$, the result is quite sensitive to the cutoff energies. Therefore, additional conformer libraries were envisioned to address the low correlations.

Table 15. CoMFA modeling (R^2 / q^2_{LOO}) of different conformer libraries from Table 14 with varying cutoff energies and field types (standard and indicator).

Cutoff Energy (field type)	Conformation Library[a]				
	A	**B**	**C**	**D**	**E**
30/30[b] Std[c]	0.728[d]/0.547[e]	0.697/0.465	0.711/0.493	0.815/0.612	0.794/0.574
30/15 Std	0.729/0.551	0.700/0.481	0.711/0.485	0.814/0.598	0.794/0.586
15/30 Std	0.734/0.545	0.705/0.498	0.709/0.460	0.803/0.641	0.812/0.636
30/30 Ind[f]	0.724/0.474	0.697/0.423	0.712/0.477	0.835/0.648	0.768/0.527
30/15 Ind	0.797/0.484	0.754/0.442	0.835/0.619	0.924/0.778	0.782/0.474
15/30 Ind	0.711/0.462	0.693/0.416	0.724/0.466	0.810/0.604	0.795/0.557

[a] See Table 1. [b] Steric cutoff energy (kcal/mol) / electrostatic cutoff energy (kcal/mol) [c] Standard Tripos field. [d] R^2. [e] q^2_{LOO}. [f] Indicator field.

Conformer library **D** (Table 14), in which $R^2 \neq$ *i*-Pr or *t*-Bu possesses the **up** conformation while catalysts with R^2 = *i*-Pr or *t*-Bu possesses the **dn** conformation, was envisioned to address the error in predictions for these catalysts. Additionally, Library **E** which possesses the opposite ring-flip geometries with respect to Library **D**, was investigated for purposes of comparison. Clearly conformer library **D** consistently provided the highest correlations, with one model (30/15; Indicator field) exhibiting a correlation that may be statistically relevant ($q^2_{LOO} > 0.778$).

Interestingly conformer library **E** (possessing conformers opposite to that of **D**) provided the second highest correlations, alluding to the importance of the conformational difference between ring **a** and ring **b** of the catalysts at the extremes of the e.r. spectrum. The physical justification for the nature of the conformations in library **D** will be addressed in the Discussion Section.

To attest to the statistical prevalence of the conformations present in Library **D**, 500 libraries of random (but unique) distributions of **up** and **dn** conformers were generated. The average q^2_{LOO} over the 500 runs was 0.409 with a maximum q^2_{LOO} of 0.679. Reassuringly, the library with $q^2_{LOO} = 0.679$ contained conformers that closely mimicked that present in Library **D** in that the most selective catalysts (> 75:25) possessed the **up** conformation and the most selective in the opposite direction (< 38:62) possessed the **dn** conformation.

3.5.2. Internal Cross-validation.

With conformations that lead to models possessing statistically significant correlations (represented by Library **D**, Table 14), optimization of the various CoMFA parameters (cutoff energies, dielectric, exponent of the repulsive term in the Lennard-Jones potential, etc.) can be carried out. Models incorporating both indicator and standard field types were generated. Additionally, models incorporating only the electrostatic or steric field, individually, were generated. The assumption in the development of models with individual fields is that all of the interaction responsible for the variation in enantioselectivity is either electrostatic or steric in origin. As it is conceivable that there can be overlap in these fields (an interaction energy at a grid point may be interpreted as steric but also be interpreted as electrostatic and *vice-versa*), analysis of models constructed from individual fields may be informative.

In a typical CoMFA analysis, the descriptors significantly outnumber the dependent variables, thus rigorous cross-validation methods are necessary to substantiate the predictive capacity of the models. Accordingly, different internal cross-validation methods were carried out (q^2_{LOO} and q^2_{LMO}) in conjunction with y-scrambling (which assesses model robustness) (Table 16). The coefficients in the absence and in the presence of region focusing are presented. The results clearly show that indicator fields provide models that exhibit better overall correlations. The y-scrambling results (low average R^2 and q^2 over 100 runs) suggest that the models are statistically significant and are not subject to chance correlation between the randomized enantioselectivities and the descriptors as the $q^2_{LOO,scramb}$ for each model is never a positive value and the corresponding R^2_{scramb} values are minimal ($R^2_{scramb.} < R^2/2$). Additionally, external cross-

validation has been performed through analysis of successive training and test set splits and further supports the sufficient predictive capacity of the model ($R^2_{test,avg} = 0.880$).[121]

Table 16. CoMFA models with optimal cutoff energies, standard and indicator field types, internal cross-validation , y-scrambling, with and without the application of region focusing.

Field(s)_field type	Cutoff energy[a] (steric/elec.)	R^2	q^2_{LOO}	q^2_{LMO}[b]	y-scramb.[c] $R^2_{scramb.}$	y-scramb. $q^2_{LOO,scramb.}$
Both[d]_STD[e]	35/5	0.846[f]/ 0.875[g]	0.669/ 0.738	0.615/ 0.705	0.383/ 0.338	-0090/ -0.050
elec[h]_STD[i]	15/30	0.865[j]	0.543	0.506	0.413	-0.073
Steric[k]_STD	40	0.794/ 0.829	0.605/ 0.710	0.583/ 0.697	0.350/ 0.301	-0.103/ -0.084
Both_IND[l]	20/5	0.940/ 0.944	0.794/ 0.890	0.760/ 0.878	0.579/ 0.429	-0.137/ -0.096
elec_IND	10/5	0.923/ 0.887	0.750/ 0.799	0.705/ 0.766	0.594/ 0.388	-0.069/ -0.030
steric_IND	25	0.840/ 0.867	0.648/ 0.749	0.627/ 0.732	0.431/ 0.378	-0.122/ -0.102

[a] kcal/mol. [b] Leave 20% out cross-validation average over 100 runs [c] average correlation coefficient over 100 completely scrambled iterations. [d] Both = electrostatic and steric fields. [f] R^2 for model constructed from an unfocused region. [g] R^2 for model constructed from a focused region. [h] electrostatic field only. [i] STD = Standard Tripos Field. [j] Unfocused region only. Region focusing did not improve the correlations. [k] steric field only. [l] IND = Indicator field

3.6. Discussion.

3.6.1. Conformation from CoMFA Modeling.

As noted previously, the catalysts in this study exhibit two primary conformational preferences manifested as the **up** and **dn** conformers (Table 14). The distribution of the conformers in a given library significantly impacts the integrity of the CoMFA models as illustrated in Table 15. These conformational preferences in the CoMFA models necessitate further analysis and physical justification.

The underlying hypothesis is that the preference for the catalyst to exist in the **up** or **dn** conformation depends largely on the face of the catalyst to which the enolate associates. As illustrated in the accompanying paper, the oxygen substituent at C(1) polarizes a larger amount of positive potential to the face over ring **a** relative to the face over ring **b** of the catalyst scaffold. Thus, association of the enolate with the face over ring **a** would be expected with small groups as

the R^2 substituent (Table 14). If R^2 is isopropyl or *tert*-butyl, it may be expected that the enolate would associate preferentially with the face over ring **b** of the catalyst as less positive potential is "screened" by a methyl group (at R^1) relative to the isopropyl or *tert*-butyl groups (at R^2). Association with the face over ring **b** would require the catalyst to exist in the **dn** conformation to maximize exposed positive potential and hence the Coulombic interaction. The conformational preference (**dn** or **up**) for catalysts with R^2 not equal to isopropyl or *tert*-butyl does not have a strong Coulombic component and may primarily be dictated by the energy intrinsic to the scaffold geometry. These energy differences vary depending on R^1, but it is not expected to greatly influence the enantioselectivity.

When taking the reaction medium into consideration, it is unlikely that the strength of the interaction with the enolate (when R^2 is not equal to isopropyl or *tert*-butyl) would be affected by the conformation of ring **b** significantly if the catalyst is in the toluene layer. On the other hand, if the catalyst is present in the aqueous or interfacial layer, it is probable that the catalyst would prefer to adopt the **dn** conformation to enable partial solvation with water molecules. However, of primary concern is the thermodynamic preference of the ammonium enolate in the toluene layer as that is primarily the medium where the intrinsic alkylation step (and also the stereodetermining step) is believed to occur.

The complication of unknown reactive conformations may be alleviated by including a distribution of both conformers weighted by their corresponding energies. However, this approach would require modeling in the presence of an anion as the energies would not reflect the desired Boltzmann distributions in the absence of an anion (since the **dn** conformation would be largely preferred if the enolate is associating with the face over ring **b** which is presumed to be occurring for catalysts with R^2 = *i*-Pr, *t*-Bu), which would be outside the computational rigor intended for this study.

3.6.2. Contour Maps.

The CoMFA models may be physically interpreted in the form of contours encompassing the catalysts. The most common method for illustrating the contours are as products of the standard deviation of the interaction action energies and the coefficients in the PLS model at each grid point (StDev*Coeff). This product represents regions where and how the variation in the interaction energies can be explained by the variation in the enantioselectivity. The contours produced can be physically interpreted as spatial regions encompassing the catalyst where an

increase or decrease in steric bulk (green for increase, yellow for decrease) and positive charge (blue for increase, red for decrease) leads to an increase and decrease in enantioselectivity respectively. Both the steric and electrostatic contour maps derived from indicator fields (boxed model in Table 16) are illustrated below (Figure 14 and Figure 15). It is noteworthy that contour maps from models derived from Tripos standard fields display information that is similar to the contour maps derived from indicator based fields below.

3.6.3. Steric Contour Maps.

Upon inspection of the steric contour maps (Figure 14), the relationship between the substitution pattern and the contours becomes immediately apparent. A catalyst among the most selective is illustrated to serve as a template for interpreting how the contours are manifested. Two 3-D representations of different perspectives are illustrated for gauging relative depth. The location of the contours will be discussed with respect to the perspective of the left illustration in which the 5-5-5 scaffold is presented. The green contour on the front of ring **b** overlaps with the methyl group which is necessary for higher selectivity. The data is consistent with the hypothesis that this methyl group is necessary to shield the right front of ring **b** from anion association. The green contours overlapping with the substituents at the 3 and 5 positions of the phenyl ring of the benzyl group attached to the nitrogen atom are consistent with increased enantioselectivity with substitution at those positions. Only *tert*-butyl and trifluoromethyl groups were explored with latter groups bestowing greater enantioselectivity. The green contour in the back, overlapping with the phenyl ring of the benzyl group attached to the oxygen atom is an indirect indicator of the presence of a non-hydrogen group at the R^2 substituent. If the R^2 substituent is hydrogen, the benzyl group attached to the oxygen atom occupies the region of space after rotation of ~90^o counterclockwise about the O- CH_2Ph bond with respect to the conformation adopted by the corresponding catalyst with $R^2 \neq$ hydrogen.[122] All catalysts possessing a hydrogen atom at R^2 exhibit poor enantioselectivity in which case the phenyl ring would not overlap with the green contour of interest. The yellow contours surrounding the group attached to the nitrogen atom (R^4) reflect substitution patterns (1-naphthyl, hexyl, and 9-anthracenyl groups) unfavorable for enantioselectivity. The large yellow contour over ring **A** may reflect both unfavorable interactions with the 9-anthracenyl substituent as well as bulky aliphatic groups at the R^2 position (*i*-Pr and *t*-Bu groups). The effect of this steric contour will be further rationalized in conjunction with the electrostatic contours as discussed below.

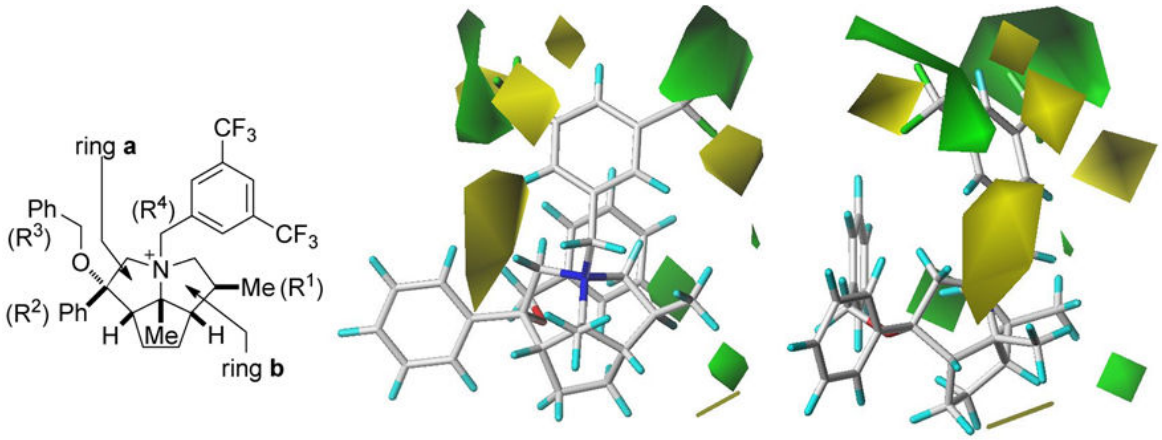

Figure 14. Steric contour maps from two different perspectives. Green contours indicate regions where increased steric bulk leads to increased enantioselectivity while yellow contours indicate regions where decreased steric bulk leads to increased enantioselectivity.

3.6.4. Electrostatic Contour Maps.

Although the steric contours enabled the rationalization of the direct influence of specific substitution patterns, the electrostatic contours tend to reveal more indirect information relating to stereocontrolling features including differential binding affinities. After eliminating the grid points with minimal field variation (1.3 kcal/mol column filtering), only two primary contours remain. The presence of a large blue contour over ring **a** suggests the potential for this region to serve as a reasonable binding site for the reactive enolate. This conclusion is consistent with the fact that the largest degree of positive potential is localized over this ring in accordance with electrostatic potential (ESP) maps determined using ab-initio theory.[123] The blue contour may additionally reflect the enantioselectivity enhancing effects of an aryl group at the R^1 position as the quadrupole moment of arenes results in a region of positive potential along the circumference of the ring and may serve as an indicator for the regression analysis.[124] The ESP partial charges should reflect this region of increased positive potential (relative to catalysts with $R^2 \neq$ arene) which is thus detected by the indicator fields. The red contour is coincident with a trifluoromethyl group on the right side and is consonant with the enantioselectivity enhancing effects of this group in conjunction with previously mentioned substitution requirements necessary for enantioselectivity. Interestingly, a red contour does not overlap with the trifluoromethyl group on the left hand side which may be a result of the nearby blue contour and it having a larger contribution to the model. The absence of a contour in this position may suggest the undesirable negative electrostatic potential and that the enantioselectivity might be

enhanced in its absence. These two electrostatic contours may also reveal an intrinsic dipole preference of the catalyst for enantioselectivity. The yellow steric contour on the front of ring **a** in Figure 14 is complementary to the electrostatic contours in that increased positive potential and decreased steric potential should lead to a more favorable binding interaction with an associating anion. The combined effects of the steric and electrostatic contours are supportive of the conclusion that the most favorable binding site for increased enantioselectivity is that on the convex side of ring **a** for an associating enolate.

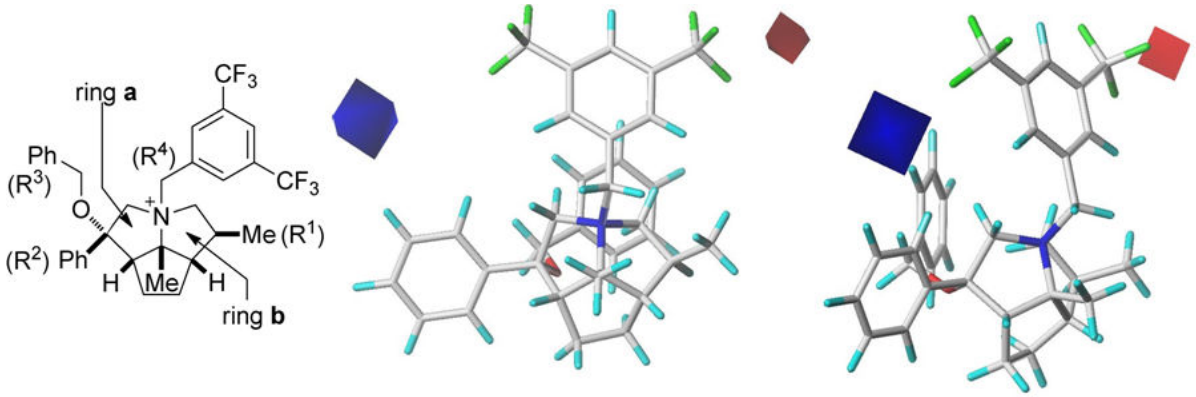

Figure 15. Electrostatic contour maps from two different perspectives. Blue contours indicate regions where increased positive charge leads to increased enantioselectivity while red contours indicate regions where decreased positive charge (increased negative charge) leads to increased enantioselectivity.

The information revealed by considering both the steric and electrostatic fields allows some generalizations to be drawn regarding the mode with which the enolate should associate with the catalyst that leads to increased enantioselectivity. The blue contour coincident with the R^2 group (Figure 15), the green contour coincident with the R^1 substituent (Figure 14), and the large yellow contour on the front of ring **a** of the catalyst (Figure 14) are all consistent with the preferred region of the catalyst for association that leads to increased enantioselectivity to be the front of ring **a** of the catalyst scaffold. The red contour (Figure 15) may enforce a preferred dipole orientation of the catalyst for aligning the enolate.

The observed enantioselectivity may be explained by considering one of two limiting scenarios assuming a thermodynamic dependence of the outcome: (1) the binding of the enolate to the catalyst is completely selective for one of the four faces of the imaginary tetrahedron inscribing the ammonium nitrogen and the enantioselectivity is directly related to the capacity of

the face of the catalyst in question to differentiate the *Re* or *Si* faces of the enolate or (2) the capacity with which the catalyst differentiates the *Re* or *Si* faces of the enolate with respect to the faces of the ammonium ion is maximal (each face selects either *Re* or *Si* completely), and the enantioselectivity is directly related to the binding selectivity of the enolate to one of the four faces of the catalyst. A combination of (1) and (2) is likely operative, however the observation that bulky aliphatic groups at R^2 result in a reversal in enantioselectivity suggests that a large portion of the observed enantioselectivity is governed by limiting scenario (2).

Assuming that limiting scenario (2) is primarily operative, some generalizations about relative binding affinities and enantioselectivity can be drawn. Both the electrostatic and steric contours are then consistent with the relative association preferences outlined below (Figure 16). Because of the polarization effects of the oxygen substituent, association mode (**A**) is preferred in structures of type **5** and to a lesser extent for **1**, **2**, and **3** (preferred pathway is indicated by a larger arrow). When the face over ring **a** is significantly sterically hindered, as in structures of type **4**, association mode (**B**) is preferred even though the electrostatic preference favors association mode (**A**). The ordering outlined in Figure 16 is most consistent with the enantiomeric ratios when R^4 is significantly electron withdrawing such as a bis(trifluoromethyl)phenyl group. Presumably, this group serves to create a stronger Coulombic interaction (decreased separation distance) with the enolate which enhances the steric influence of the R^1 and R^2 substituents with respect to catalysts with less electron withdrawing groups at R^4. The stronger interaction for catalysts with R^2 = aryl is not likely a consequence of increased steric or Coulombic interactions but may be attributed to the intervention of π-stacking interactions. An alternative to this analysis (limiting scenario (1)), would be that the erosion of enantioselectivity may be attributed to decreased enantiotopic differentiation of the faces of ring **a** or ring **b** of the catalyst for the *Re* and *Si* faces of the enolate which lends to a more challenging stereochemical rationalization.

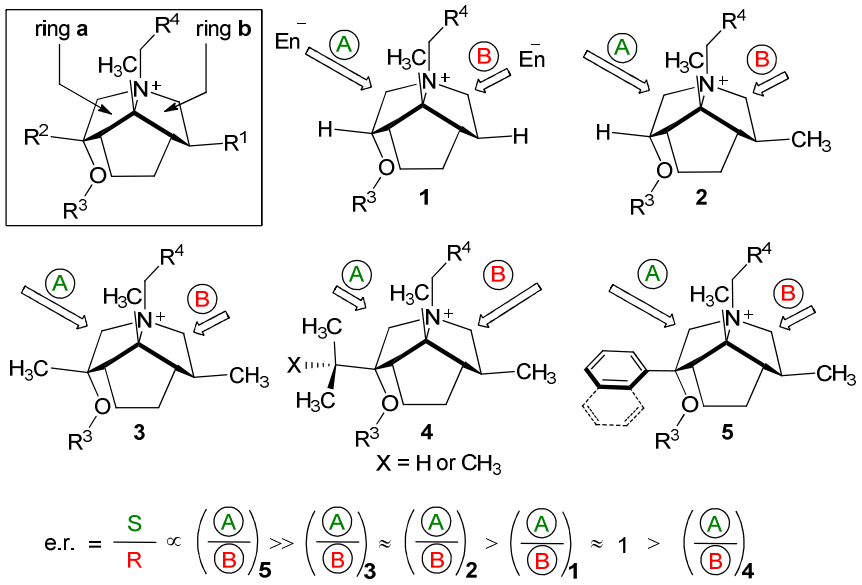

Figure 16. Association preferences for the enolate (En^-) as a function of the R^1 and R^2 groups.

Although the highest enantioselectivity observed in this report (e.r. = 81:19) does not currently allow for the development of a well-defined stereochemical model for this catalyst system, the contour maps do allow the generation of *qualitative* assessments of how to increase the enantioselectivity further by introducing substituents that render the interactions noted above even more favorable. The model may also be used to make *semi-quantitative* predictions regarding the extent of enantioselectivity to which certain substituents may provide. While such extrapolation can be susceptible to erroneous predictions, some confidence may be placed in the predictions if the catalysts identified to be more selective are proximal to the structural and dependent variable domain of the training set. For example, this model would be incapable of predicting enantioselectivities imparted by cinchona derived quaternary ammonium ions and any catalysts that furnish enantioselectivities significantly greater than 81:19.

3.6.5. Summary of CoMFA Analysis.

Correlations of the enantioselectivity with the steric and electrostatic fields (55% steric; 45% electrostatic) of the catalysts were statistically significant as determined by rigorous cross-validation. The model was readily interpreted qualitatively as relating to the differential binding preferences of the reactive enolate for the catalyst in accordance with contour maps represented as multiplicative products of coefficients of the model and the variation in the molecular interaction fields of the catalysts. The steric field revealed differential van der Waals repulsive

interactions between the two active faces of the catalysts available for binding as being relevant in explaining the observed reversal in enantioselectivity with the inclusion of bulky aliphatic groups shielding one of the two faces. The electrostatic field revealed that higher enantioselectivity for the (*S*) configured product is obtained by further differentiating one face over the other through charge polarization. The inclusion of aryl groups at one of the faces selectively introduces positive potential in this region as a result of the quadrupole moment imparted by arenes, which enforces the preference for the (*S*) configured product. This observation may indicate an important role for π-stacking interactions at this position for this reaction system. Additionally, the inclusion of a region of preferred negative potential for the (*S*) configured product, coupled with the region of preferred positive potential, may reveal a preferred dipole orientation that allows for facial discrimination of the enolate. Future development of more enantioselective catalysts based on the current scaffold would involve enhancing substrate interaction with the desired face for binding through the qualitative and quantitative application of the QSSR model developed here. The principles borne from this QSSR study may serve as criteria for the rational design of future APTC catalysts.

3.6.6. Proposals for Stereochemical Model.

The results from density functional ion pair modeling and the CoMFA analysis suggests that a stronger preference for the enolate exists to associate with the left face of the catalyst, and that this is the region where the enanioselectivity is most sensitive to structural variation. Upon accepting this to be the case, four ion-pair arrangements can be envisioned which have been optimized at the PM6 semiempirical level to provide only qualitative insight (the relative energies do not warrant discussion due to inaccuracy from poor inclusion of dispersion and solvation effects) (Figure 17). Only the *Z*-enolates have been considered here on the basis of earlier findings (Section 3.2).

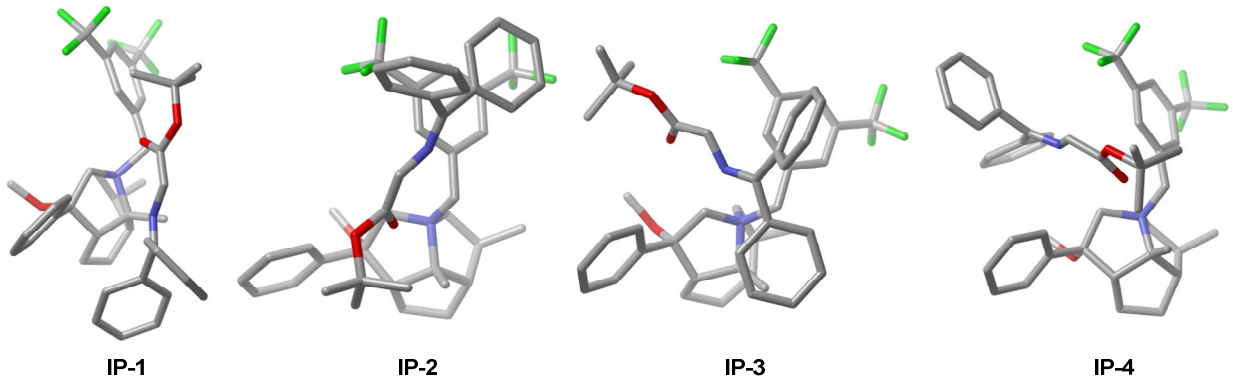

Figure 17. Geometries of ion-pairs optimized at the PM6 semiempirical level.

Ion pairs **IP-1** and **IP-2** are expected to lead to opposite enantiomers predominately. The *Re* face of the enolate in **IP-1** is shielded by the aryl group at R^2, thus the *S*-configured product is expected to form predominately, consistent with experimental results. **IP-1** also appears to be capable of engaging in π-stacking interactions between one of the phenyl groups of the enolate with the aryl group at R^2 of the catalyst. Conversely, the *Si* face of the enolate in **IP-2** is hindered by both the aryl group at R^2 and the aryl group at R^4 thus favoring the *R*-configured product. An apparent π-stacking interaction could exist between one of the electron-rich phenyl rings of the enolate with the electron poor 3,5-bis-trifluoromethylphenyl group at R^4 of the catalyst. Nevertheless this ion pair seems to favor the opposite enantiomer which is inconsistent with the observed positive influence of the 3,5-bis-trifluoromethyl phenyl group.

The preferred enantiomer formed from alkylation of ion pairs **IP-3** and **IP-4** is not as clear. Ion pair **IP-3** is expected to be higher in energy since the oxygen of the enolate is furthest from the ammonium nitrogen. Ion pair **IP-4** would furnish the observed product if the electrophile approached from the direction of the aryl group at R^2. This ion pair seems energetically feasible as there appears to be an available ArH⋯π interaction between the π electrons of the enolate and one of the $C(sp^2)$-H bonds of the phenyl ring ring at R^2.

Overall, ion pairs **IP-1** and **IP-4** appear to be the arrangements most consistent with the experimental results. Future catalyst design criteria would then reflect modifications in the catalyst that would increase the facial selectivity of ion pairs **IP-1** and **IP-4**. This effect would entail introducing varying degrees electronic perturbations of the π-surface areas electronics at R^2 and modification of the electronic properties of the aryl group at R^4.

Chapter 4: *Synthesis of New catalysts Guided by Quantitative Models*

4.1. Synthesis of New Catalysts.

According to the structure activity relationships introduced in the previous chapter, the catalyst scaffold requires highly specific substituent patterns to obtain reasonable enantioselectivity. The substituent at R^1 should be a non-hydrogen group, although only methyl and hydrogen have been explored up to this point. The R^2 group needs to contain an arene. The enantioselectivity is relatively independent of the R^3 group. Lastly, the enantioselectivity is quite sensitive to the R^4 group which is should be 3,5-$(CF_3)_2C_6H_3$ for moderate enantioselectivity from the groups explored. Groups R^2 and R^4 were initially chosen for further exploration since R^1 would require a greater synthetic investment as its introduction is at the earliest stage of the four groups.

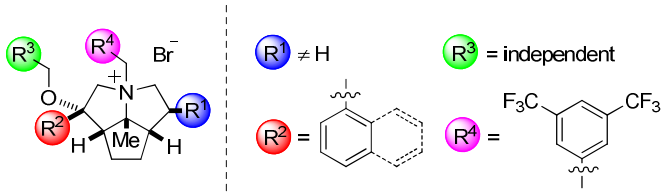

Figure 18. Conditions on R groups for e.r. > 80:20.

The variation envisioned at the R^2 for further exploration was based on electronic contributions and π-surface area. The catalysts displayed in Figure 19 represent a brief investigation on this variation. Catalysts **23** and **24** exhibit some modification of electronic properties of the substituent at the R^2 position. The levels of enantioselectivity are similar to those for the analogous catalysts with a phenyl or 1-naphthyl group at this position with all other groups held constant. Upon introduction of alternative groups at R^4 with varying electronic properties, significant reduction in enantioselectivities are observed throughout relative to R^4= 3,5-$(CF_3)_2C_6H_3$. Catalyst **29** with a 2,4-$(CF_3)_2C_6H_3$ exhibited no reactivity. This result is likely due to the decomposition of the catalyst because of pKa lowering of the alpha hydrogens of the benzylic hydrogens.

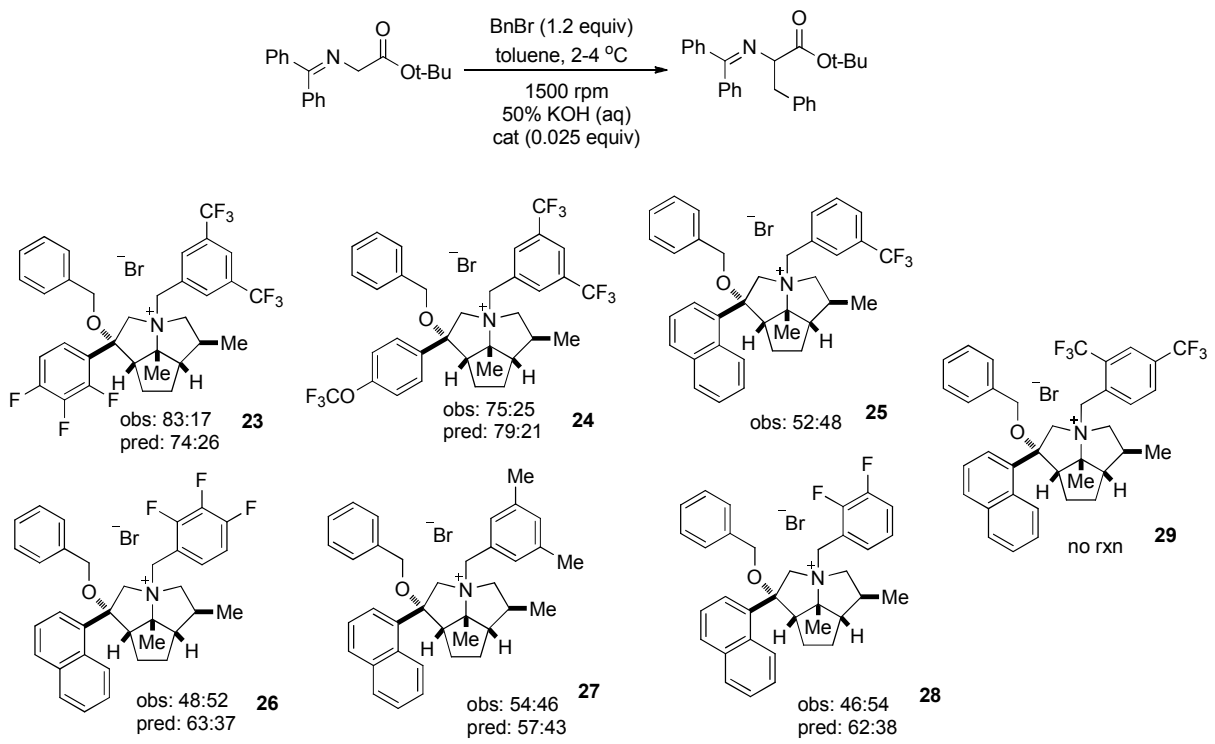

Figure 19. Predicted and observed enantiomeric ratios. The predicted values are based on the best CoMFA model from Table 16 (Chapter 3).

From this initial set of newly acquired data, it is not clear how the current stereochemical model can be improved. Thus, to move forward, inspiration was sought from alternative, effective catalyst scaffolds such as the *cinchona* alkaloids. From Figure 20, it is apparent that a common substitution pattern exists that contains the ammonium nitrogen, the alkoxy group and the aryl group (quinoline group). In an effort to better resemble the *cinchona* alkaloid structure in this aspect, a quinoline group was considered for introduction at R^2 in the 5-5-5 system. However, because of restrictions in the synthetic sequence, a nucleophilic quinoline source is necessary for addition to the electrophilic α-keto amide (Scheme 7), and methods are lacking for this construction. With this in mind, the 3-quinoline substituted catalyst was sought instead.

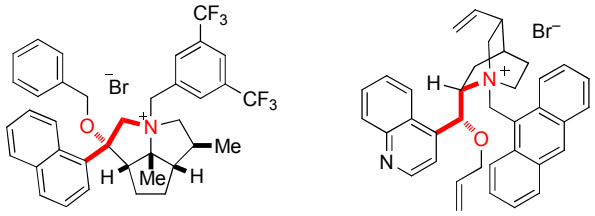

Figure 20. Comparison between 5-5-5 scaffold and a *cinchona* alkallid derived catalyst. The substitution pattern of the ammonium nitrogen, the alkoxy group, and the aryl group (quinoline group) is the same.

The synthesis departs significantly from the established protocol (Scheme 17). The Grignard addition was replaced by an organolithium addition. Reduction of the amide required some additional exploration. Applying the standard BH_3•THF reduction protocol led to a complex mixture of products that included reduction of the quinoline group. A lithium aluminum hydride reduction was attempted on both the hydroxyamide **30** and the benzylated amide **31** but furnished only complex mixtures. A fundamentally different strategy was adopted which first involved benzylation of the hydroxyl group *via* the standard Williamson ether synthesis conditions. In view of the failure of nucleophilic hydride reduction, hydrogenolytic reduction was envisioned. An attractive option was to incorporate carbon-sulfur bonds because their lability toward hydrogen mediated cleavage. In this regard, the amide was first converted to the thioamide using Lawesson's reagent.[125] The addition of DMAP was found to be necessary for liberating any excess Lawesson's reagent that was bound to the qunoline nitrogen. Cleavage of the carbon-sulfur double bond proceeded in modest yield (50%) to furnish the desired amine. The final quaternization was carried out at room temperature over an extended period of time to avoid over benzylation of the quinoline nitrogen, which account for the diminished yield (38%).

Scheme 22.

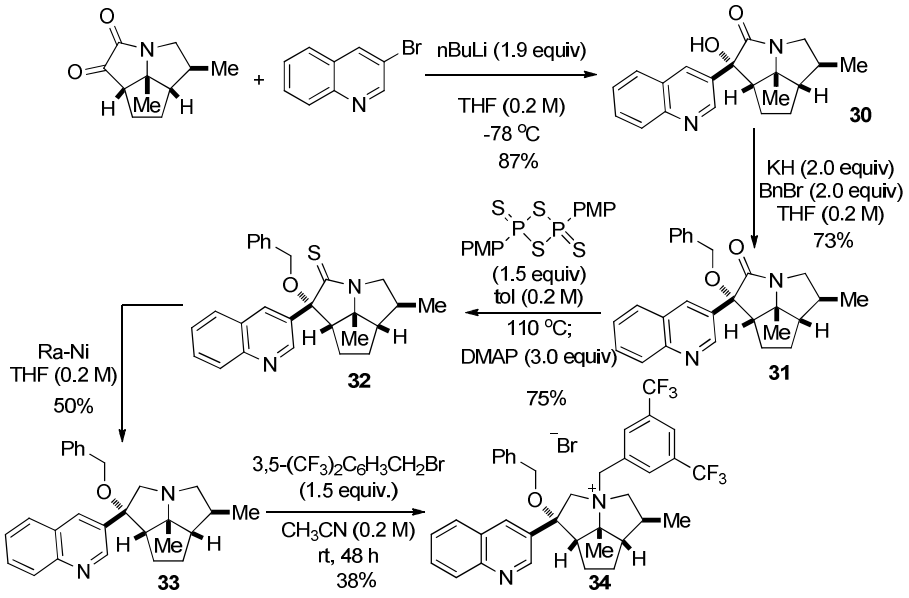

The resulting quinoline-substituted catalyst **34** was next applied in the model PTC reaction and afforded an enantiomeric ratio of 87:13 which is greater than the maximum observed previously (82:18 – 83:17 e.r.) (Scheme 23). To probe whether the quinoline group is important or if the presence of the π-surface was sufficient, the 2-naphthyl group was introduced *via* the established sequence (Scheme 17). Interestingly, the same enantioselectivity was oberserved for this catalyst **36** as the quinoline substituted catalyst **35 (**Scheme 23**)**. These results suggest that the presence of the π-surface is more relevant and the effects of the nitrogen atom are inconsequential. This development caused our strategy to focus more on variation in π-surface area.

Scheme 23.

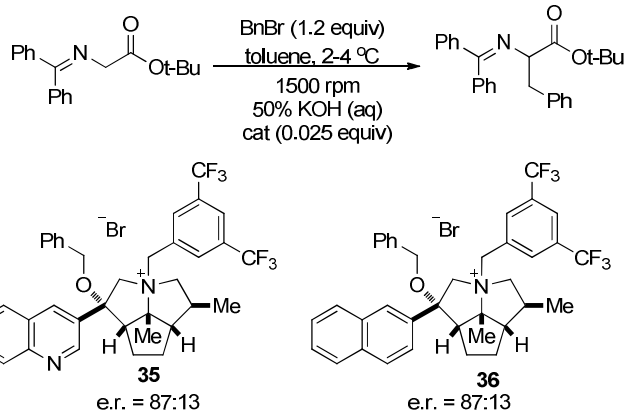

Before the investigation of new catalysts, a modeling strategy that might be more amenable toward small extrapolations was pursued. The currently used CoMFA method is not well suited for extrapolation, because of the generation of highly parameterized models (very large number of descriptors). Thus, a strategy that is capable of isolating only a handful of descriptors that are the most relevant to a 3D-QSAR model was explored.

4.2. Development and Application of an Alternative 3D-QSAR Approach.

4.2.1. Descriptor Types.

In the standard CoMFA approach, the electrostatic energies and steric energies are determined from the Coulomb potential and the Lennard-Jones potential respectively. The Coulomb energy terms are determined using partial atomic charges. These partial atomic charges are typically derived by molecular mechanics or from semi-empirical methods. Rarely are quantum mechanical methods used since the error associated with using partial atomic charges for determining the electrostatic energy is comparable to the error between semi-empirical and QM partial charges.

An alternative, more accurate approach to determine the electrostatic energy is to use the electron density ρ, rather than partial charges, which is calculated from the square of the QM wavefunction $\rho = \int \psi^2 d\mathbf{r}$. The electrostatic potential $V(\mathbf{r})$ can then be expressed as the following;

$$V(\mathbf{r}) = \sum_{i=1}^{n} \frac{Z_i}{|\mathbf{r} - \mathbf{R}_i|} - \int \frac{\rho(\mathbf{r}')}{|\mathbf{r} - \mathbf{r}'|} \, d\mathbf{r}' \qquad (\text{eq. } 2)$$

where Z_i and $\mathbf{R}_i$ are the charge and the position of the nucleus i, n is the total number of nuclei, $\rho(\mathbf{r}')$ is the electron density at position $\mathbf{r}'$, and $\mathbf{r}$ is the position of the test charge. The first term represents the electrostatic potential felt by a test charge due to all of the nuclei and the second term is the potential due to the electronic distribution. (It should be mentioned that the quantity defined in eq.1 is the *potential*, not the *potential energy* of the interaction with the test charge. The actual potential energy is obtained by multiplying $V(\mathbf{r})$ by the magnitude of the test charge, $U(\mathbf{r}) = q_{\text{test}}V(\mathbf{r})$. Because the test charge typically has a magnitude of one, and since the electrostatic potential is used solely for comparing energies at points within the same molecule, the inclusion of q_{test} is inconsequential.)

The van der Waals potential is complex, and more accurate models have been empirically derived to approximate this energy term. Instead of using the Lennard-Jones 6-12 potential, for the purposes of this investigation, a "Buffered-14-7" form of the potential was used as implemented in the MMFF94 force field.[126] The MMFF94 force field provides relatively low errors and was deemed suitable. A description of how these models are performed and the corresponding scripts are provided in the experimental section.

4.2.2. Descriptor Selection.

The CoMFA model is quite adept at explaining the variation within a training set, however the complexity (large number of grid points) of the model precludes confident application towards extrapolation due to possible over-parameterization. Therefore, a strategy that includes a smaller number of descriptors of greater quality (quantum mechanical) was adopted. The descriptor selection procedure relies on a simulated annealing based algorithm. The optimization algorithm was built to select combinations of grid points that lead the best models according to a procedure merging PLS with cross validation. This allows the effective selection of only the most pertinent grid points rather than the entire grid point pool (i.e. CoMFA). The number of PLS components used is dependent of the number of chosen descriptors.

The strategy developed draws parallels to both CoMFA and QMQSAR[55] where the electrostatic interaction energies are determined from the ESP maps derived from DFT electron densities and the van der Waals interaction energies (vdW) are derived from the vdW potential function of the MMFF94 force field[126] where the probe atom is a C(sp^2) atom. The model may represent either of the following forms:

$$\Delta G = C_0 + \sum_{i=1}^{n} C_i\left(\mathrm{E}_i^{ele} + \alpha \mathrm{E}_i^{vdw}\right) \qquad \text{(eq. 3)}$$

$$\Delta G = C_0 + \sum_{i=1}^{n} C_i \mathrm{E}_i^{ele} + \sum_{j=1}^{m} C_j \mathrm{E}_j^{vdw} \qquad \text{(eq. 4)}$$

where for eq. 3, at each grid point the calculated electrostatic and vdW energies are summed with a scaling factor operating on the vdW term, which is determined from the regression. This operation ensures that the grid point energy is analogous or proportional to a total interaction energy (elec + vdW) and the ratio of the steric and electrostatic terms is not altered in the regression. The model from eq. 4 is similar to the CoMFA approach in the sense that the electrostatic and van der Waals energy terms contain unique regression coefficients.

4.2.3. Test Applications.

The newly developed models were applied to a test set of 50 catalysts from the library that contained only a phenyl group at R^3 since the enantioselectivity was insensitive to variation at this group. Both descriptor selection methods were applied to garner how well the resulting models would compare to the CoMFA models and whether they correspond well with qualitative expectations (Figure 21). The correlation statistics and the number of PLS components are provided. The position of the grid points of the best model overlaid with the most enantioselective catalyst is shown.

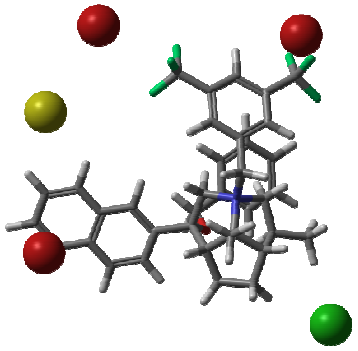

Blue:
inc. (+) → inc. e.r.
Red:
inc. (-) → inc. e.r.
Green:
inc. (vdw) → inc. e.r.
Yellow:
dec. (vdw) → inc. e.r.

Method	Comp.	R^2	Q_{LOO}^2	esp:vdw
eq. 3	2	0.826	0.781	45:55
eq. 4	4	0.817	0.772	-

Figure 21. The model from eq. 2 is illustrated graphically with the location of the grid points overlaid with the most enantioselective catalyst.

The electrostatic grid points are confluent with qualitative expectations and differ somewhat from the CoMFA model which is not surprising considering data points not included in the CoMFA model have been included in these models (catalysts **35** and **36**). The red spheres represent the requirement for having electronegative groups at the 3,5 positions of the aromatic ring of R^2. The green sphere on the right indicates the requirement for a non-hydrogen group at R^1. The yellow contour may represent the enantioselectivity decreasing influence of an 9-anthracenyl group at R^4. Finally, the lower red sphere indicates a preference for π-electron density at the R^2 group. Also, the contributions of the electrostatic and steric fields to the model are similar to that from the CoMFA model (esp:vdw = 45:55).

The extrapolative potential for this modeling strategy was evaluated with a reduced training set size of 12 catalysts. Only the catalysts with R^4 = 3,5-$(CF_3)_2C_6H_3$ were retained since this group produced the most significant variation in enantioselectivity and since groups that have greater electron withdrawing capacity would likely lead to catalyst decomposition. The top 2 catalysts were removed from the training set from the training set and a model, employing the strategy from eq. 1, was developed. The resulting 2 grid point model exhibited an R^2 = 0.965 and Q^2 = 0.819. The top two predictions, based on this model, are provided (Figure 22). It is important to emphasize that these 2 catalysts were not included in the model development. The prediction for the 2-naphthyl catalyst is close to the observed value. However, the prediction for 3-quinonline substituted catalyst was poor.

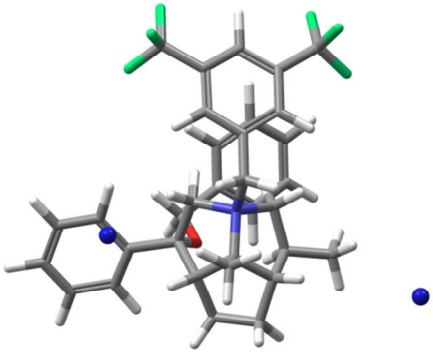

R^2	e.r.$_{obs}$	e.r.$_{pred}$
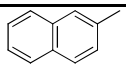	87:13	88.6:11.4
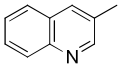	86.5:12.5	60:40

Figure 22. Two Grid point model with a training set size of 10 catalysts. R^2 = 0.965, Q^2_{LOO} = 0.819.

The poor prediction for catalyst **35** suggests that this catalyst is too far removed from the training set. This breakdown can be understood from difference in electrostatic potential between these two catalysts at the left grid point that is not accounted for by a corresponding difference in enantioselectiviy (Table 17). The model take the following form; ln(R/S) = 0.597 – 0.586(g1) + 0.175(g2) where g1 and g2 are each the sum of the electrostatic and steric energies at the left grid point and right grid point respectively. The values for the catalyst with R^2 = Ph is provided for reference purposes. The quinoline substituted catalyst exhibits a much lower esp (-2.6 kcal/mol) which indicates that a positive point charge interacts less favorably than with either the 2-naphthyl or Ph substituted catalysts. The less favorable interaction is due to the electron deficient nature of the quinoline π-system. A model was then developed with a training set that includes the top two catalysts. The left grid point in this model is now relocated to a region that does not lead to a significant variation in the electrostatic potential. This process of prediction and inclusion illustrates how the training set can be trained with the incorporation of newly acquired data.

Table 17. Relative electrostatic potential energy values (kcal/mol) for models excluding catalysts (n=10) and including (n=12) the top two catalysts. (R^1 = Me, R^3 = Ph, R^4 = 3,5-$(CF_3)_2C_6H_3$). R^2 = 0.965, Q^2_{LOO} = 0.938.

R^2	n=10	n=12	$e.r._{pred}$
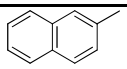	4.3	0.9	87.5:12.5
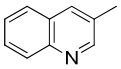	-2.6	1.3	85.7:14.3
	0	0	

4.2.4. Prediction and Synthesis of New Catalysts.

The π-surface at R^2 is clearly important and thus additional catalysts with variation at this position were envisioned that were readily synthetically accessible (Table 18). Catalysts that could not be synthesized are not discussed here. Groups that possessed greater degrees of π-surface and π-electron density were explored. Each new catalyst is predicted to have a greater e.r. than the maximum in the training set. However, the observed values were lower than that predicted, closer to the maximum values in the training set. These were somewhat disappointing results and as a consequence the R^1 group was chosen for further elaboration.

Table 18. Predicted and observed enantiomeric ratios. The predicted values are based on the model from Table 18.

Catalyst	R^2	$e.r._{pred}$	$e.r._{obs}$
37	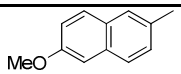	91:9	87:13
38	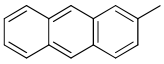	91:9	85:15
39	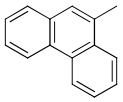	91:9	85:15

The hypothesis at this point was that the catalyst may still experience some association with the enolate on the right face which may result in erosion of enantioselectivity. A slightly altered strategy for the modeling was necessary to accommodate the new catalysts. First, the fact that both the ethyl and isopropyl substituted catalysts can exist in different conformations needed to be factored in. This adjustment was done by taking the sum of the Boltzmann weighted electrostatic and steric energies at each grid point. The Boltzmann weighting was determined

from the overall energies of the cations from the single point B3LYP/6-31G(d,p) calculations. Second, to avoid accepting grid points too close to the van der Waals surface of the *t*-Bu group (grid points could be selected within this surface since both the ethyl and isopropyl groups have hydrogens that are within this surface), a cutoff distance was applied. The predictions of the resulting models are shown (Table 19).

Table 19. Predicted enantiomeric ratios. The predicted values are based on the model from Table 18.

Catalyst	R^2	R^1	$e.r._{pred}$
40	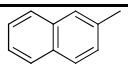	Et	91:9
41	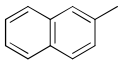	*i*-Pr	92:8
42	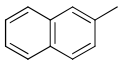	*t*-Bu	97:3

The synthesis of the ethyl substituted catalyst follows the same sequence as the methyl substituted catalyst and is provided in the experimental section. The isopropyl and *tert*-butyl substituted catalysts required different routes for preparation of the chiral alkenyl ethers for the [4+2]/[3+2] sequence.

A number of sequences have been explored for the isopropyl substituted alkenyl ether and most consisted of either less than desirable length or yields. The sequence that was finally accepted (Scheme 25. first involved prenylation of chiral alcohol **11** to form **43**. The double bond was then isomerized to **44** following a modified protocol using Wilkinson's catalysts.[127] Unfortunately this step was very low yielding (20% yield) as unreacted starting material remained and side products including equal amounts of the (*Z*)-isomer and the saturated product from over reduction. The remaining unreacted starting material was a consequence of a small equilibrium constant for this reaction as added catalyst and longer reaction times only led to the formation of more of the saturated product. Nevertheless, this sequence was accepted in view of the practicality relative to other investigated routes. The synthesis of the final catalysts follows the same protocol used for the synthesis of the catalyst with R^1 = Me and is provided in the experimental section.

Scheme 24.

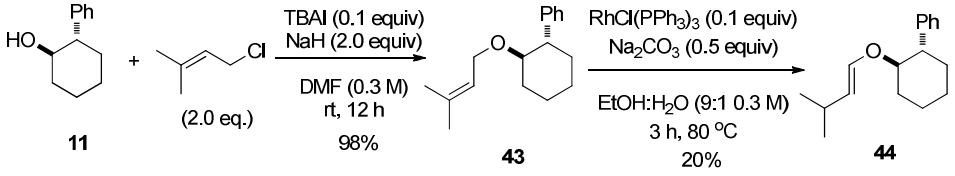

The synthesis of the *tert*-butyl substituted chiral enol ether first involved diazotization of pinacolone *via* the use of a diazo-transfer reagent. The diazo ketone **46** is than added to chiral alcohol **11** through an indium triflate catalyzed O-H insertion.[128] The carbonyl is then reduced with the aid of sodium borohydride. The hydroxyl group is then eliminated following a modified Chugaev protocol[129] that involves first generation of the thiocarbonate followed by thermal elimination to furnish enol ether **51**. The synthesis of the final catalyst follows precisely that for the catalyst with R^2 = Me which is provided in the experimental section.

Scheme 25.

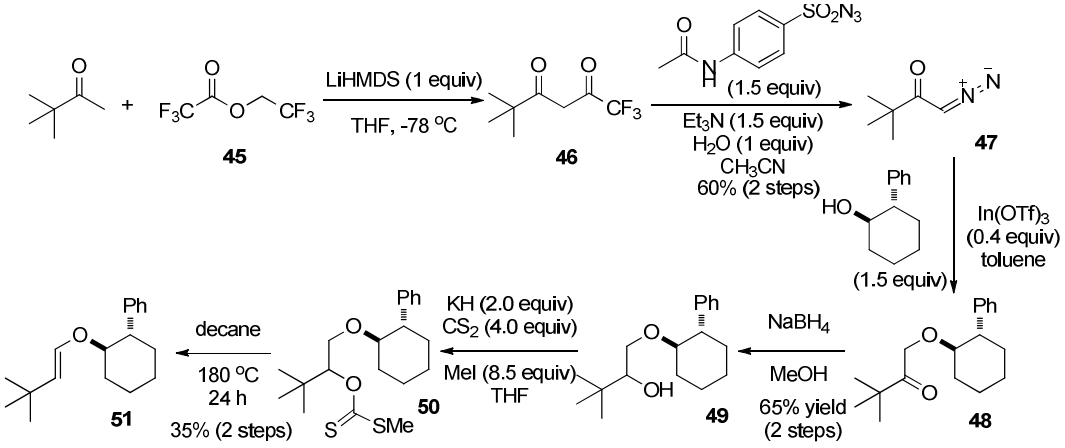

The catalysts from Table 19 were employed in the model PTC alkylation reaction and the enantioselectivity was measured. The observed results were again quite different than the predicted values (Table 20). The ethyl and isopropyl substituted catalysts furnished the same e.r. as the methyl substituted catalyst. Interestingly, the *tert*-butyl substituted catalyst furnished a *lower* e.r. than the methyl substituted catalyst. These results suggest that the enolate is not associating with the right face of the catalyst to a significant extent. The negative influence of the *tert*-butyl group may suggest a conformational dependence of the R^4 group. If the enolate is primarily associating with the right face, the R^4 group may need to rotate to the right to

accommodate this association. Moreover, the *tert*-butyl group may compress the R^4 group toward the left face thus impeding enolate association. This effect may suggest that ion pair model **IP-4** (Figure 17) might be operative since it exhibits some rotation of the R^4 group toward the right face.

Table 20. Predicted and observed enantiomeric ratios. The predicted values are based on the model from Table 18.

Catalyst	R^2	R^1	e.r.$_{pred}$	e.r.$_{obs}$
40	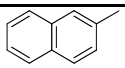	Et	91:9	87:13
41	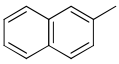	*i*-Pr	92:8	86:14
42	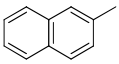	*t*-Bu	97:3	70:30

4.3. Hammett-Type Analysis.

The 3,5-$(CF_3)_2C_6H_3$ group at R^4 is obviously important for enantioselectivity, however the nature of this influence is unclear. To provide additional insight on whether the origin is related to inductive or resonance effects, a Hammett-type analysis was performed. The additional catalysts in Figure 23 were prepared for this analysis. A plot of the energy associated with the enantioselectivity as a function of sigma constant reveals a much stronger correlation with σ_p over σ_m. The difference in correlation suggests that influence of the substituents on the arene at the R^4 group is better associated with ability of the group to donate electron density into the π-system rather than the inductive influence.

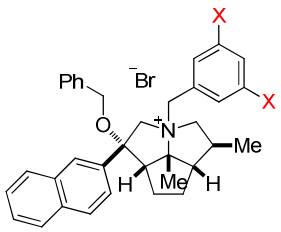

Catalyst	X	e.r.	σ_p	σ_m
49	OMe	45:55	-0.27	0.12
50	F	66.3:33.8	0.06	0.34
51	Me	55.8:44.2	-0.17	-0.07
36	CF3	87:13	0.54	0.43

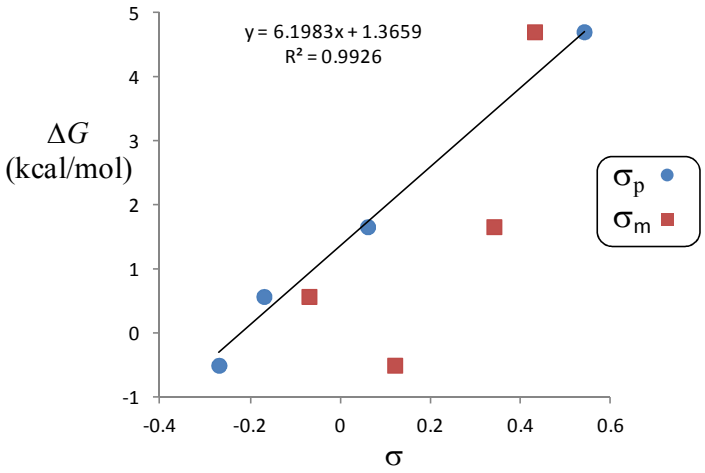

Figure 23. Enantioselectivity data for catalysts with variable groups at the 3,5 positions of the arene at R^4 and plot of the free energy versus different Hammett constants.

These results suggest that groups that withdraw more electron density would lead to higher enantioselectivity. Substituents that are more electron withdrawing than CF_3 include CN and NO_2. The 3,5-$(CN)_2C_6H_3$ catalyst was prepared but was not an effective catalyst for the reaction as there was no observed product formation over a number of hours. It is likely that group is too electron withdrawing thus causing the catalyst to decompose *via* Hoffmann elimination

4.4. Summary and Future Directions.

The objective outlined in the chapter was to improve the enantioselectivity induced by the 5-5-5 scaffold on the model PTC reaction using quantitative models. Initially, the CoMFA model was used for purposes of qualitative design. Focus was directed on the R^2 group and the 2-

naphthyl group provided the highest enantioselectivity to date (e.r. = 87:13). Alternative modeling strategies were developed with the intent on increasing chances for minor extrapolation as the CoMFA model may exhibit over parameterization of the training set that diminishes the opportunity for extrapolation. These modeling strategies provided similar insight as the CoMFA model, which served to validate these approaches.

The models formulated from these new strategies were applied toward prediction of new catalysts. Modifications to the R^2 group were initially investigated (Table 18). The new modeling methods that predicted catalysts with additional π-surface area and greater π-electron density to have enantiomeric ratios greater than the maximum observed in the training set (87:13). However, the experimentally determined values were very close to the maximum of 87:13 from the training set. This result may suggest that the arene at R^2 is simply provided a cleft for th association of the enolate. Any additional π-surface beyond what is necessary for serving as a cleft will not result in an e.r. increase (e.g. 2-anthracenyl group in Table 18). Only modest changes in the electronic properties were made in R^2, but the e.r. appears to be relatively insensitive this aspect of the π-surface.

Attention was directed toward structural variation at the R^1 substituent. Increasing steric bulk at this position was predicted to lead to an increase in enantioselectivity. However, the observed values for R^1 = Et and *i*Pr were both very close to the corresponding catalyst with R^1 = Me. Moreover, the enantioselectivity actually diminished for the catalyst with R^1 = *t*-Bu (e.r. = 70:30). This result is also consistent with ion pair model **IP-4** as the R^4 group is slightly tilted to the right face. The *t*-Bu group would disfavor this tilt because of its considerable steric bulk.

If further improvements in this catalyst scaffold were to be pursued, focus should likely be placed on investigating how to differentiate the enantiotopic faces of the enolate in ion-pair model **IP-4** since this model appears to most coincide with experimental observation. If ion pair model **IP-1** is believed to be operative, a 9-anthracenyl group may be sufficient for blocking the *Re* face of the enolate.

In retrospect, the method by which this project was initially approached may not have been the most efficient demonstration of a computer model guided strategy. A very large library was constructed with less than ideal rational design elements. The kind of groups worked well for other catalyst systems were understood, and these types of groups were introduced in the 5-5-5 scaffold. Moreover, a significant portion of the structural space was already sampled without

the aid of a computer model. A more efficient demonstration would be to design an initial training set based on structural diversity, with a common core scaffold, which can be measured by similarity metrics[130] such as Tanimoto similarity. A computer model can be constructed from this initial training set and used to guide the synthesis of more optimal catalysts (Figure 24). From the initial training set model, a virtual screen of catalysts with structural variation at the location of the model coefficients (ie. grid points) is performed. The large virtual library is then filtered based on a combination of predicted e.r. and the similarity to the training set (higher e.r. and higher similarity to the training set). The filtered catalysts are then synthesized and evaluated based on the predicted enantiomeric ratio. If the e.r. is less than the maximum observed in previous iterations, then a new training set is devised based on e.r. and similarity including the newly acquired catalyst data and the cycle is repeated. If a number of iterations (k) have been completed without an increase in e.r., then a new, more diverse training set needs to be constructed or a new scaffold should be explored. If the maximum e.r. is greater than previous iterations and is the optimal e.r. desired, then the cycle is complete. This procedure would ideally allow the research to reach the ideal catalyst more quickly with less synthetic investment.

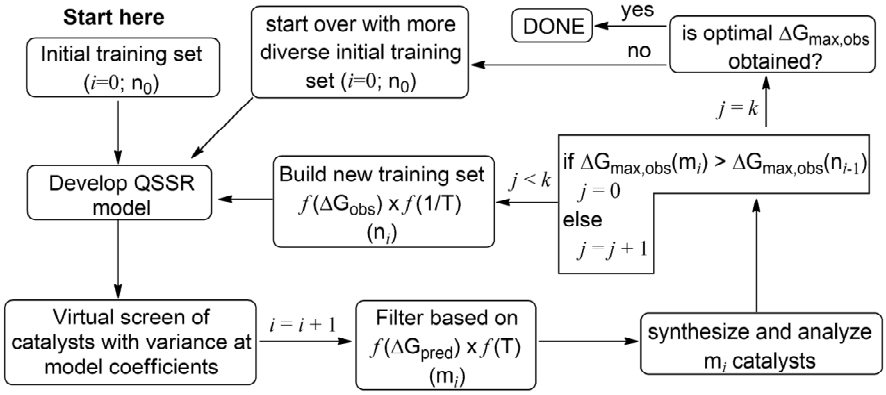

Figure 24. Optimization flowchart representing the proposed strategy. i=iterations; n_i=i^{th} training set; m_i=i^{th} set filtered from the in-silico screen; $f(\Delta G_{pred})$ represents a function of the e.r. and f(T) is a function of the Tanimoto similarity metric; $\Delta G_{max,obs}(m_i)$ represents the maximum e.r. oberseved within the m_i set; k=pre-defined limit without an increase in observed e.r.

These strategies can be applied toward the optimization of any reaction. The methods outlined here would probably be more suitable for catalysts that operate by noncovalent interactions as strong orbital interactions may not be described readily by electrostatic and steric

fields alone. For applications that make use of strong orbital interactions, HOMO and LUMO fields (or any orbital of appropriate symmetry for the desired reaction) could be applied.

Chapter 5: *Introduction to Allylation of Aldehydes with Allylsilanes*

The controlled construction of contiguous stereocenters is of primary importance in the synthesis of natural and non-natural products. A significant number of methods developed for this purpose involve the combination of two π systems, specifically those of electron-rich alkenes with aldehydes and ketones. The stereochemical course of the bond-forming event is dictated by the relative topicity of prostereogenic carbons in the transition state (Scheme 1). Each pairwise combination leads to a unique stereoisomer, for which three, limiting, staggered arrangements of the double bonds are possible, antiperiplanar, (+)-synclinal and (–)-synclinal. The ability to *reliably* predict the stereochemical outcome of such reactions is vital for synthetic planning and requires an understanding of the physical origins underlying the way in which the structural and electronic properties of the two π systems (A, D, R^1, R^2) influence their relative orientations in the competing transition structures. Effective stereocontrol mechanisms often rely on strong organizational elements that enforce propinquity of the reacting components such as metal coordination or dative association with directing groups. On the other hand, some of the most challenging reactions to rationalize are typically those that are believed to proceed through open transition state structures, in which selectivity controlling factors pertain primarily to nonbonding interactions. Such reactions are the focus of this study.

Scheme 26.

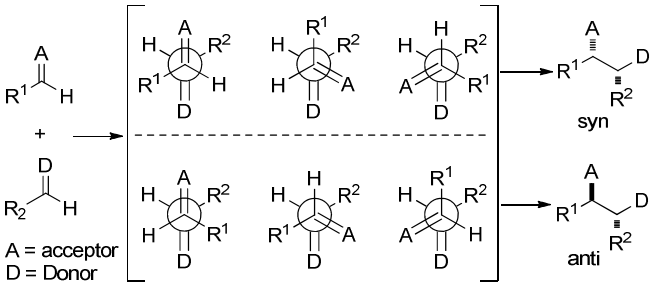

An early phenomenological analysis of the stereochemical course of these types of reactions formulated a set of topological rules,[131] which are summarized here because they will be referred to frequently in the following sections (Scheme 2):

i. All vicinal bonds are staggered

ii. A synclinal arrangement of the donor (C=D) and acceptor (C=A) bonds is preferred

iii. The smaller group on the donor (H) is placed antiperiplanar with respect to the C=A bond

iv. The synclinal orientation adopted is that which positions the donor and acceptor atoms in the closest possible proximity

Rules **i** and **iii** address the minimization of steric interactions whereas rules **ii** and **iv** have electronic implications. Rule **ii** has received the most scrutiny experimentally.

Scheme 27.

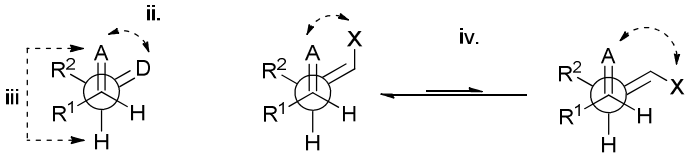

A host of interactions have been suggested to explain these preferences, including minimization and/or maximization of unlike and like charge separation respectively (Coulombic),[132] steric effects,[133] orbital control,[134] and dispersion forces.[135] However, the dominant selectivity-controlling interactions that are related to the structure of the π systems still remain unclear. Each of the suggested effects is to some extent associated with the components of the interaction energy of the two fragments in the transition state. The aim of this investigation was to computationally identify the interactions that are most accountable for the diastereoselective preference in pathways thought to proceed through open transition states using theoretical methods.

The addition of electron rich π systems to activated carbonyl groups constitutes a large body of reactions.[136] The stereochemical course of these reactions is often highly predictable through the use of cyclic transition state models. Conversely, a physical understanding of stereochemical control in acyclic transition structures is less well developed. However, this has not prevented the accumulation of substantial amounts of experimental data that have allowed for the formulation of rules and generalities that possess some qualitative predictive capacity.[137] The immense synthetic utility of the addition of allylsilanes to aldehydes made it ideally suited to serve as the platform for this study.

5.1. Background.

5.1.1. Experimental Studies.

Beyond the edifice of preparative studies on the Lewis acid mediated addition of allylsilanes to aldehydes, the reaction mechanism and stereochemical course have been extensively investigated. Thorough stereochemical studies have established that the reaction of allylic *trialkyl*silanes proceeds through acyclic (open) transition states (Scheme 3).[138] This behavior is in contrast to the reactions of allylboron reagents that proceed through closed transition states because of the Lewis acidic nature of the tricoordinate boron atom.[139] Consequently, six limiting transition structures can be envisioned that possess staggered orientations of all bonds to minimize steric interactions (rule **i**). Additionally, the Lewis acid is coordinated to the aldehyde oxygen on the side of the hydrogen atom as has been amply demonstrated in spectroscopic and computational studies.[140]

Scheme 28.

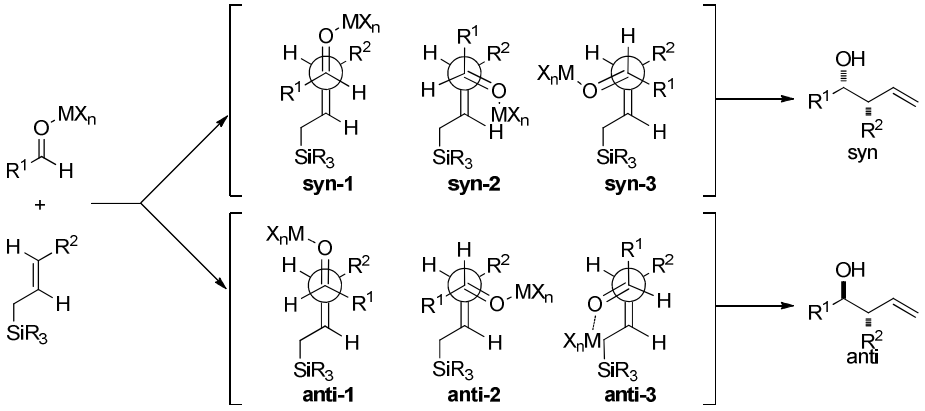

The silicon group and the electrophile are located on opposite sides of the allyl moiety (i.e. anti S_E2') which established the open nature of the transition state.[138] A syn disposition (established for allyl *trihalo*silanes)[141] would likely perturb the energies of the synclinal transition states more profoundly.

Scheme 29.

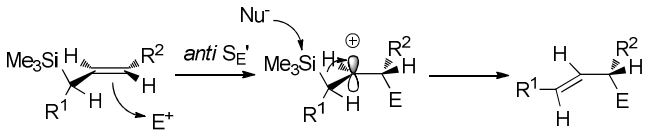

The syn diastereomer is often produced in these reactions with high diastereoselectivity. A common rationale for the observed diastereoselectivity invokes the minimization of steric repulsion by proceeding through antiperiplanar transition states.[136f] The antiperiplanar transition state leading to the anti diastereomer (**anti-1**, Scheme 3) is considered to exhibit more severe gauche interactions between R^1 and R^2 than the corresponding synclinal transition state (**syn-1**, Scheme 3). Unfortunately, for intermolecular reactions, it is impossible to determine the precise orientation of the reactants that lead to the observed products. Accordingly, to unambiguously determine the relative orientation of the reactants, a number of models that incorporate both reactants in a single molecule have been devised and examined.

The two most studied models are the subject of a number of detailed investigations from these laboratories (Scheme 4).[142] Model system **A** was designed to probe the preference between transition structures **syn-3** and **anti-1** in the reaction of an *E*-crotylsilane whereas model system **B** was designed to probe the analogous *Z*-crotylsilane system. The results of these studies revealed that the Lewis acid promoted reactions afforded predominately the product resulting from a synclinal disposition of double bonds in the transition state. The fluoride-promoted pathway was also investigated and, interestingly, the product resulting from the antiperiplanar transition state is generated in greater amounts. This intriguing divergence in selectivity clearly suggests that multiple factors are operative. Clearly, model systems of this type will be limited in the number of different transition states that can be accessed given the structural constraints of intramolecularity.

Scheme 30.

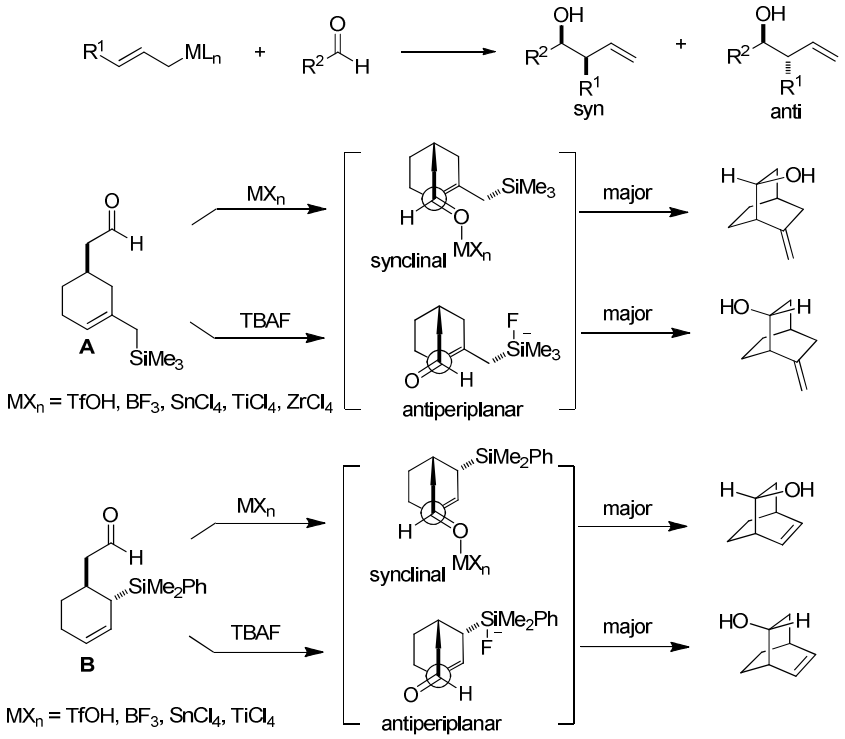

5.1.2. Computational Studies.

The allylation of activated carbonyl compounds has also been investigated computationally using quantum mechanical methods.[143] An early gas phase DFT study using BFH_2 as the Lewis acid and trihydridoallylsilane suggests a pseudo-cyclic transition state in which the fluorine atom is closely associated with the silicon atom.[144] Intrinsic reaction coordinate (IRC) calculations imply bond formation between the silicon and the fluorine atoms. Only synclinal transition states could be located which is a direct consequence of the proposed Si---F interaction. The model simplifications introduce an unjustified bias toward a cyclic transition state due to a lack of solvation (unquenched potential on the fluorine atom) and the use of a less hindered, electron deficient silicon atom than used experimentally. Moreover, the conclusion of such an interaction is invalidated by the experimental demonstration of an anti S_E2' process for allylsilane additions.[142d]

A thorough, combined computational and experimental study on the crotylation of O-methyloxocarbenium ions has also been reported.[145] Canonical ensembles of the calculated B3LYP transition states are relatively consistent with the experimentally observed

diastereoselectivities that, for the most part, favor the syn diastereomer. Steric repulsion primarily accounts for the formation of the major syn diastereomer. The relative agreement between the predicted and the experimental diastereoselectivities suggests a stepwise process.

3. Goals of this Study. The nature and magnitude of the interactions governing the selectivity preferences in open transition structures remains obscure. The deconstruction of the interaction energies in the transition state and/or along the reaction coordinate into physically recognizable quantities such as steric, electrostatic, orbital, and dispersion should provide additional insights into the stereochemical controlling factors. Such a decomposition process was conceived[146] and implemented[147] by Kitaura and Morukuma a number of years ago. This method essentially teases out the electrostatic ΔE_{elec}, polarization ΔE_{pol}, charge transfer ΔE_{CT} exchange repulsion ΔE_{exrep} and dispersion ΔE_{disp} energetic contributions from the total interaction energy ΔE_{int} of the interacting components;

$$\Delta E_{int} = \Delta E_{elec} + \Delta E_{pol} + \Delta E_{exrep} + \Delta E_{CT} + \Delta E_{disp}$$

Although energy decomposition analysis (EDA) methods have been applied to understand weak and strong chemical binding and bonding,[148] the method has seen only limited application toward understanding reactivity and selectivity in chemical reactions. Bickelhaupt and Houk have pioneered the activation-strain model[149] or synonymously the activation-distortion model[150] of reactivity to analyze a number of chemical reactions. This method decomposes the energy difference between a point along the reaction coordinate and the minimum from which it originates $\Delta E(\xi)$ (ξ, extent of reaction) to the sum of the interaction energy of the distorted reactants (ΔE_{int}) and the energy required to distort the fragments to that geometry in the absence of any interaction (ΔE_{dist}).

$$\Delta E(\xi) = \Delta E_{int} + \Delta E_{dist}$$

A significant number of reactions have been investigated for which $\Delta E(\xi)$ as a function of structure is more strongly correlated with the distortion energy rather than the energy of interaction ΔE_{int}. This situation will most often obtain for reactions with late transition states and those that have high frequency bending modes along the reaction coordinate.[150a,150b] Reactions with earlier transition states are expected to better correlate with the interaction energy component of the total energy (FMO theory).

The goal of this study was to reveal which components of the interaction energy

contributed most to the observed diastereoselectivity for the addition of (*E*)-2-butenyltrimethylsilane to acetaldehyde under activation by BF_3, hydronium ion, and fluoride ion. The first stage in the program required locating the six staggered transition structures for which density functional theory was the chosen theoretical approach. Next, the energies for each transition structure were decomposed along their respective reaction coordinates employing a recently-developed localized molecular orbital EDA method.[151] Then for each reaction, the components of the interaction energy that contributed most to the diastereoselectivity were identified and the EDA results were validated through assessment of geometrical and electron density properties. The analysis would ideally provide a better understanding of the selectivity controlling factors in the allylation of aldehydes and other open transition state reactions such as Mukaiyama-type aldol[152] and Michael[153] addition reactions.

Chapter 6: *Computational Investigations on the Addition of Allylsilanes to Aldehydes*

6.1. Reaction Mechanism.

6.1.1. BF_3-Promoted Addition.

Previous computational studies on the reaction mechanism of BF_3-promoted addition of (*E*)-2-butenyltrimethylsilane to acetaldehyde (Scheme 31) have focused on simplified systems and did not probe the entire transformation from reactants to products. For example, side processes such as oxetane[154] formation have not been accounted for and the desilylation step remains uninvestigated. Moreover, the experimentally documented formation of fluorotrimethylsilane at a temperature of -80 ^{o}C needs to be reconciled.[155] More importantly, the potential influence of steps subsequent to carbon-carbon bond formation on the diastereoselectivity has not been considered in detail.

Scheme 31.

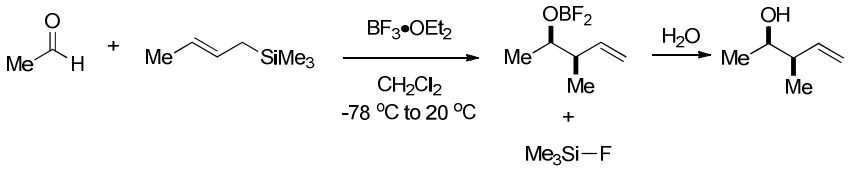

A potential energy diagram was mapped out for the BF_3-promoted crotylation of acetaldehyde (Figure 25) to gain a better understanding of the reaction mechanism, particularly the fate of the intermediate after C-C bond formation. Initial complexation of BF_3•OMe_2 to acetaldehyde is thermodynamically unfavorable ($\Delta G_{\mathbf{1}\rightarrow\mathbf{2a}}$ = 3.3 kcal/mol; $\Delta G_{\mathbf{1}\rightarrow\mathbf{2b}}$ = 4.7 kcal/mol) which is consistent with the stronger Lewis basicity of ethers relative to aldehydes[156] and more than compensates for the partial charge delocalization from aldehyde complexation. Formation of the anti isomer **2a**[157] is more favorable than the corresponding syn isomer **2b** ($\Delta\Delta G$ = 1.4 kcal/mol). This well-established thermodynamic preference[158] together with the attendant, enhanced activation of the carbonyl group (evidenced by the greater LUMO lowering (~0.04 eV) of **2a** compared to **2b**, resulting from more effective complexation), suggests that the reaction is primarily proceeding through anti isomer, **2a**.

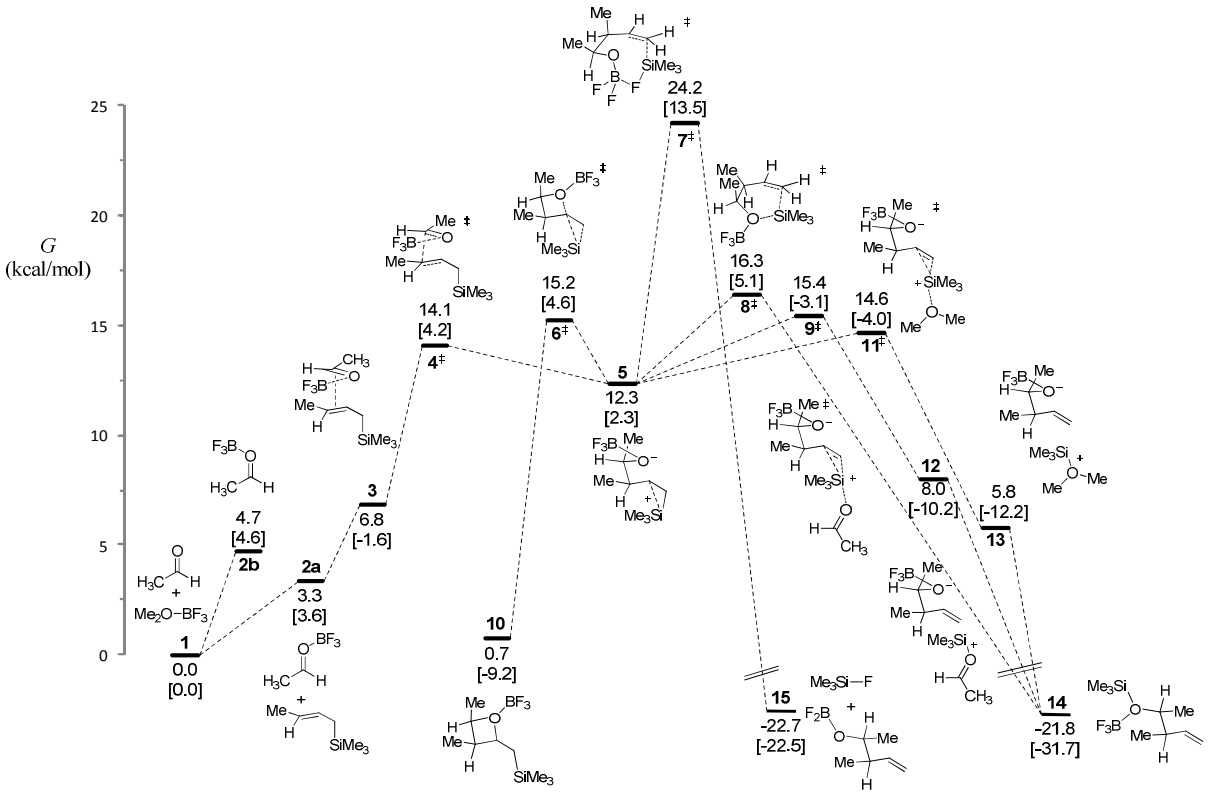

Figure 25. Energy diagram illustrating reaction pathways investigated for the BF_3•OMe_2 promoted crotylation of acetaldehyde. Relative energy values are represented as free energies *G* (kcal/mol) and are calculated at the CPCM(CH_2Cl_2)-M06-2X/6-311+G(2d,2p)//CPCM(CH_2Cl_2)-M06-2X/6-31+G(d,p) level. Energies in brackets represent enthalpies *H* (kcal/mol). Thermodynamic quantities are determined at 195 K.

Association of the aldehyde-BF_3 complex **2a** with (*E*)-2-butenyltrimethylsilane results in the formation of pre-transition state complex **3**. A transition state connecting **2a** to **3** was not investigated. The physical nature of complex **3** was probed through an energy decomposition analysis of the reactants (Figure 26). The primary intermolecular NBO donor-acceptor stabilization interaction is the $\pi_{C=C} \rightarrow \pi^*_{C=O}$ and amounts to 9.3 kcal/mol. No other intermolecular NBO donor-acceptor interactions were found that are greater than 0.5 kcal/mol. The NBO charge transfer (Δq), which is likely exclusively associated with the $\pi_{C=C} \rightarrow \pi^*_{C=O}$ interaction, amounts to 0.06 *e*. The angle of approach of the aldehyde (110^o) is close to that for optimal frontier orbital overlap (107^o, Burgi-Dunitz approach).[159] Complex **3** is sterically and electrostatically unfavorable, however, through orbital interactions and dispersion forces, an overall favorable electronic interaction energy results ($\Delta E_{int} = -8.1$ kcal/mol). A low level of distortion ($\Delta E_d = 1.42$ kcal/mol) is necessary to form complex **3** from the isolated optimized reactants. Thus, orbital

interactions and dispersion forces more than compensate for the unfavorable electrostatic, steric, and distortion components of the overall energy. Complex **3** can best be described as a charge transfer / van der Waals complex since both favorable energetic components (ΔE_{orb} and ΔE_{disp}) are nearly equal. However, the overall enthalpy of association ($\Delta H = \Delta E + \Delta H_{corr} = -5.2$ kcal/mol) is not sufficient to offset the entropic penalty of $-T\Delta S = 8.7$ kcal/mol which causes the overall Gibbs free energy of association to be positive ($\Delta G = \Delta E + \Delta H_{corr} - T\Delta S = 3.5$ kcal/mol). Similar pre-transition state complexes have been invoked in the structurally similar Mukaiyama aldol reaction in gas phase computational studies,[160] but should also exist in solution of moderate polarity in view of the smaller frontier orbital energy difference in the reactants relative to crotylation examined in this study (ε_{HOMO}(silyl enol ether) > ε_{HOMO}(crotylsilane)).

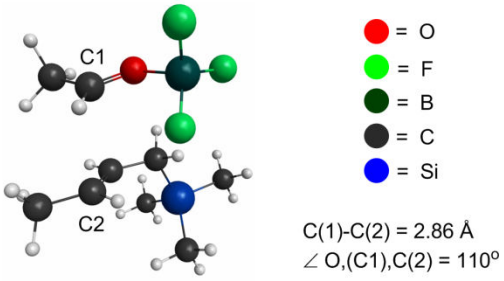

ΔE_{es}	ΔE_{ste}	ΔE_{orb}	ΔE_{disp}	ΔE_{int}	ΔE_{d}	ΔE^{a}	$\Delta H_{corr}{}^{b}$	$-T\Delta S$	$\pi\rightarrow\pi^{*c}$	Δq
2.9	26.5	-19.3	-18.2	-8.1	1.4	-6.7	1.5	8.7	9.3	0.06

Figure 26. Geometry of complex **3** and an energy decomposition analysis. Energy values are in units of kcal/mol. [a] $\Delta E = \Delta E_{int} + \Delta E_{d}$. [b] Enthalpic correction including zero point energy. [c] NBO donor-acceptor stabilization energy.

Complex **3** next proceeds through transition state $\mathbf{4}^{\ddagger}$ to form intermediate **5** in a considerably endergonic step ($\Delta G_{\mathbf{3}\rightarrow\mathbf{5}} = 5.5$ kcal/mol) (Figure 25). Intermediate **5** may proceed through at least six readily accessible pathways ($\mathbf{4}^{\ddagger}$, $\mathbf{6}^{\ddagger}$, $\mathbf{7}^{\ddagger}$, $\mathbf{8}^{\ddagger}$, $\mathbf{9}^{\ddagger}$, $\mathbf{11}^{\ddagger}$). Reversion (via $\mathbf{4}^{\ddagger}$) is actually the lowest energy pathway with a barrier of only $\Delta G^{\ddagger}_{\mathbf{5}\rightarrow\mathbf{4}} = 1.8$ kcal/mol. Desilylation of **5** is necessary to proceed toward the observed products, and multiple pathways can be envisioned to effect this process. Intramolecular transfer of the silyl group to the fluorine atom with concomitant Si-F cleavage via an eight-membered transition state $\mathbf{7}^{\ddagger}$ to generate product **15** and fluorotrimethylsilane directly is the highest energy pathway ($\Delta G^{\ddagger}_{\mathbf{5}\rightarrow\mathbf{7}} = 11.9$ kcal/mol) and is thus less likely to contribute. This finding is in contrast to previous computational studies

suggesting direct fluorine to silicon transfer.[155] Intramolecular transfer of the silyl group to the oxygen atom via a six-membered transition state **8**‡ is a more favorable pathway ($\Delta G^{\ddagger}_{\mathbf{5\rightarrow 8}}$ = 4.0 kcal/mol) but there are still accessible lower energy pathways. Alternatively, external nucleophiles can serve as desilylating agents in bimolecular steps. However, the only stable nucleophiles present in solution are the aldehyde reactant and the dimethyl ether that is decomplexed. Free fluoride ion is unlikely to be present in solution to effect desilylation. Desilylation carried out by dimethyl ether ($\Delta G^{\ddagger}_{\mathbf{5\rightarrow 11}}$ = 2.3 kcal/mol) or acetaldehyde ($\Delta G^{\ddagger}_{\mathbf{5\rightarrow 9}}$ = 3.1 kcal/mol) provide lower energy alternatives to the intramolecular transfer via **7**‡ and **8**‡. Acetaldehyde and dimethyl ether serve to shuttle the silyl group to the oxygen via intermediate ion pairs **13** and **12** respectively to form highly stable product **14**. Conversion of ion pairs **12** and **13** to product **14** is expected to be near barrierless, and thus transition states were not investigated that lead to **14**.

The formation of fluorotrimethylsilane suggests the need for the conversion of product **14** to product **15**. Deprotection of silyl ethers with BF_3 can be performed experimentally supporting the conversion of **14** to **15**. Product **15** likely either dimerizes[161] or coordinates with dimethyl ether to increase the thermodynamic preference.

6.1.2. Pathways Toward Active BF_3 Consumption.

Experimental evidence for the formation of fluorotrimethylsilane and the requirement for a stoichiometric amount of $BF_3{\bullet}OEt_2$ for full conversion of the aldehyde, requires the consumption of product **13**. The transfer of the BF_3 group from **13** to **14** is more preferred ($\Delta G_{\mathbf{13\rightarrow 14}}$ = −1.1 kcal/mol) which is consistent with the stronger lewis basicity of dialkyl ethers relative to silyl thers.[162]Two pathways for consumption of product **13** have been considered and investigated here. The first involves progression via a 4-membered σ-bond metathesis transition state **15**‡ to generate product **18**. Similar transition states have been invoked in the deprotection of *t*-butyldimethylsilyl ethers with $BF_3{\bullet}OEt_2$.[163] However, this is a high barrier process ($\Delta G^{\ddagger}_{\mathbf{13\rightarrow 15}}$ = 24.0 kcal/mol) and is only mildly exergonic ($\Delta G_{\mathbf{13\rightarrow 15}}$ = –0.9 kcal/mol). An alternative pathway involves first association of BF_3 with one of the fluorine atoms on **13** to generate **16** which then can undergo fluorine transfer to the silicon group via a six membered transition state **17**‡. This pathway is also high in energy ($\Delta G_{\mathbf{13\rightarrow 16}}$ = 15.8 kcal/mol and $\Delta G^{\ddagger}_{\mathbf{16\rightarrow 17}}$ =

24.8 kcal/mol) and is not expected to occur at low temperatures. Decomposition through a bimolecular process may provide a lower energy pathway but was not investigated.

There is not a strong thermodynamic driving force for the formation of fluorotrimethylsilane and product **18** ($\Delta G_{\mathbf{13}\rightarrow\mathbf{18}}$ = -0.9 and $\Delta G_{\mathbf{14}\rightarrow\mathbf{18}}$ = 0.2 kcal/mol). The potential of the tricoordinate boron atom in **18** can be quenched by either dimerization to form **19** ($\Delta G_{\mathbf{18}\rightarrow\mathbf{19}}$ = -0.2 kcal/mol) or coordination with dimethylether ($\Delta G_{\mathbf{18}\rightarrow\mathbf{20}}$ = -2.5 kcal/mol). Dimerization is highly enthalpically favorable ($\Delta G_{\mathbf{18}\rightarrow\mathbf{19}}$ = −11.0 kcal/mol) but a low driving force due to the high entropic cost ($-T\Delta S_{\mathbf{18}\rightarrow\mathbf{19}}$ = 10.8 kcal/mol). Hence, coordination with dimethylether is probably the most viable pathway for deactivation of any source of active BF_3.

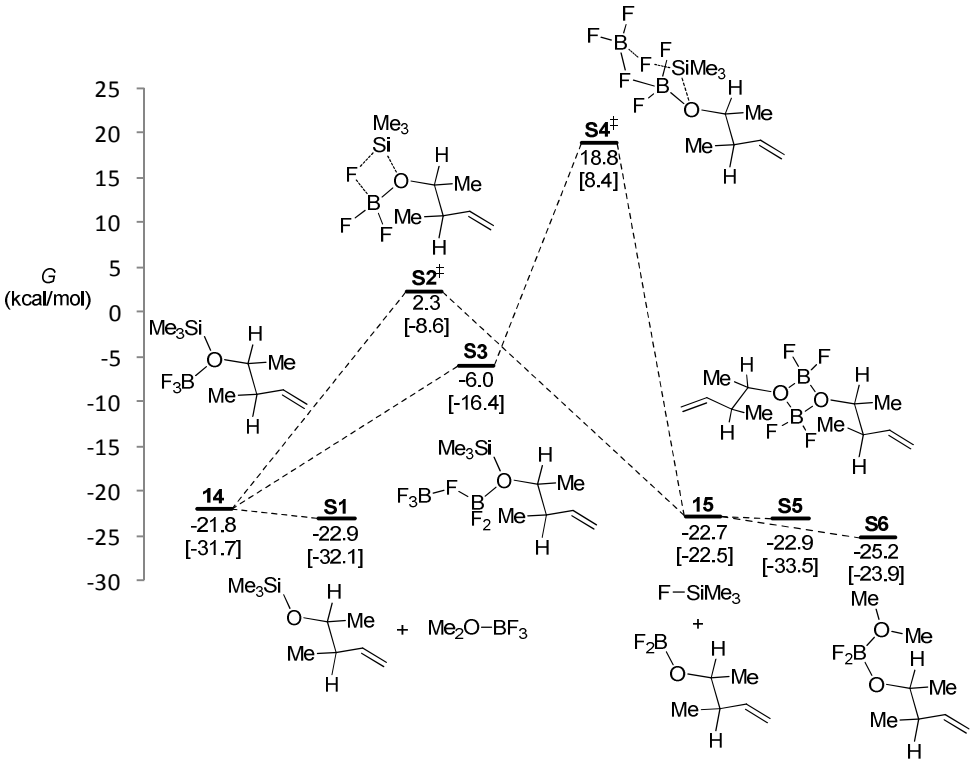

Figure 27. Energy diagram for consumption of active BF_3.

6.1.3. Formation of Side Products.

Experimentally, side products have been observed in this reaction that include oxetanes[154], acetals[164], tetrahydrofurans[165] and tetrahydropyrans[166] the formation of which are all highly dependent on the substrate and reaction conditions. Each of these side products contains the silyl group and thus their formation is favorable if desilylation is inhibited, usually achieved

by the use of sterically bulky silyl groups. Oxetane formation provides a low energy pathway from intermediate **5** via transition state $\mathbf{6}^{\ddagger}$ ($\Delta G^{\ddagger}_{\mathbf{5}\rightarrow\mathbf{6}}$ = 2.9 kcal/mol) to intermediate **10** which is considerably exergonic ($\Delta G_{\mathbf{5}\rightarrow\mathbf{10}}$ = −11.6 kcal/mol) and which is competitive with desilylation via $\mathbf{8}^{\ddagger}$, $\mathbf{9}^{\ddagger}$, and $\mathbf{11}^{\ddagger}$. Because the barrier to reversion ($\Delta G^{\ddagger}_{\mathbf{10}\rightarrow\mathbf{6}}$ = 14.5 kcal/mol) is similar to the barrier from uncomplexed acetaldehyde to intermediate **5** via $\mathbf{4}^{\ddagger}$ ($\Delta G^{\ddagger}_{\mathbf{1}\rightarrow\mathbf{4}}$=14.1 kcal/mol), oxetane **10** is expected to funnel to product **14** and eventually **15**, as long as an energetically feasible pathway exists between **14** and **15**.

6.1.4. Minimum Energy Pathway.

The lowest energy pathway from the diagram in Figure 25 is reproduced in Scheme 32. After initial coordination of acetaldehyde to BF_3 to generate complex **2a**, crotylsilane associates to form pre-transition state complex **3**. Complex **3** proceeds through the C-C bond forming transition state $\mathbf{4}^{\ddagger}$ to form intermediate **5**. Although a number of pathways are accessible to intermediate **5**, the lowest energy is desilylation promoted by dimethyl ether via transition state $\mathbf{11}^{\ddagger}$ to form intermediate ion pair **13** which quickly transfers the silyl group to the oxygen atom to form intermediate **14**. The experimental requirement for stoichiometric quantities of $BF_3{\bullet}OEt_2$ suggests that intermediate **14** is converted to final product **15** through a mechanism that is beyond the scope of the present discussion.[167]

Scheme 32.

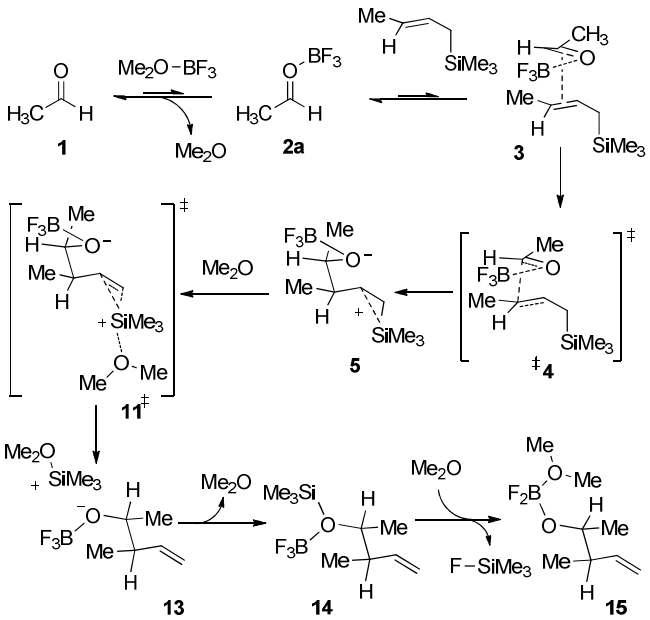

6.1.5. $TiCl_4$-Promoted Addition.

The broad energy landscape accessible to intermediate **5** equates to a complex dependence of the diastereoselectivity on the energies of multiple stationary points including transition state energies to C-C bond formation that lead to **5** and the transition state energies of desilylation. To address the impact of these factors on the diastereoselectivity of addition, a different Lewis acid was evaluated in the hope that the energy landscape would be more favorable (less likely to revert).

Titanium (IV) tetrachloride is another commonly used Lewis acid for this reaction which furnishes higher diastereoselectivities than $BF_3{\bullet}OEt_2$.[136k] The $TiCl_4$-mediated crotylation reaction was also modeled to understand the origins of the higher diastereoselectivity with $TiCl_4$ relative to $BF_3{\bullet}OEt_2$.

Titanium (IV) chloride carbonyl complexes can exist in various titanium/carbonyl stoichiometries including 1:1, 1:2, 2:1, and 2:2.[168] The 1:1 complex is chosen for this study on the basis of likely greater reactivity as well as computational efficiency. The $TiCl_4$ promoted pathway begins with an exergonic ($\Delta G^{\ddagger}_{\mathbf{16}\rightarrow\mathbf{17}}$ = –2.5 kcal/mol) association with acetaldehyde which translates to a near stoichiometric complexation consistent with experimental observation[168] (Figure 28). The effective concentration of the activated aldehyde is thus greater in the $TiCl_4$ pathway compared to the $BF_3{\bullet}OEt_2$ pathway. However, the barrier to C-C bond formation ($\Delta G^{\ddagger}_{\mathbf{17}\rightarrow\mathbf{19}}$ = 11.8 kcal/mol) is not much different than that for the $BF_3{\bullet}OEt_2$ pathway ($\Delta G^{\ddagger}_{\mathbf{2a}\rightarrow\mathbf{4}}$ = 10.8 kcal/mol). This difference is seemingly contradictory with the lower LUMO of the activated aldehyde$\bullet TiCl_4$ complex **17** (–3.46 eV) compared with the aldehyde$\bullet BF_3$ complex **2a** (–2.54 eV) (Figure 29). However, the LUMO of aldehyde$\bullet TiCl_4$ complex **17** is considerably more delocalized through mixing of the $\pi^*_{C=O}$ with an empty *d* orbital on the titanium metal center. Additionally, the NBO and electrostatic potential fitted charges on the carbon atom of the aldehyde are both more positive for the aldehyde$\bullet BF_3$ complex ($q(C)_{NBO}$ = 0.587, $q(C)_{ESP}$ = 0.601) compared to the aldehyde$\bullet TiCl_4$ complex ($q(C)_{NBO}$ = 0.560, $q(C)_{ESP}$ = 0.539).

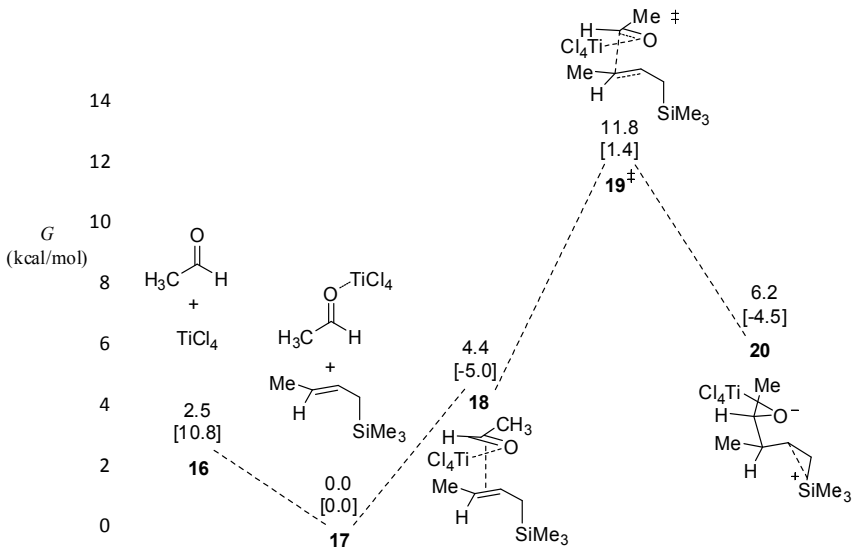

Figure 28. Energy diagram illustrating reaction pathways investigated for the $TiCl_4$-promoted crotylation of acetaldehyde. Relative energy values are represented as free energies *G* (kcal/mol) and are calculated at the CPCM(CH_2Cl_2)-M06/TZV(2f),6-311+G(2d,2p)//CPCM(CH_2Cl_2)-M06/TZV(2f),6-31+G(d,p) level. Energies in brackets represent enthalpies *H* (kcal/mol). Thermodynamic quantities are determined at 195 K.

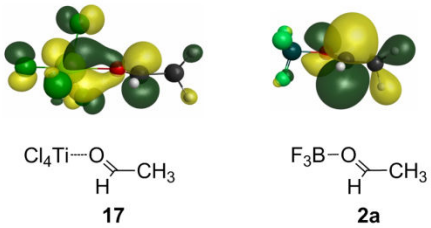

	LUMO[a]	$q(C)_{NBO}$[b]	$q(C)_{ESP}$[c]
$TiCl_4$	-3.46	0.560	0.539
BF_3	-2.54	0.587	0.601

Figure 29. LUMO for **17** and **2a** [a] LUMO energy in eV [b] NBO partial atomic charges at C(1) [c] electrostatic potential fitted charges according to the CHelpG scheme.

It is important to note that the barrier to reversion is significantly greater in the $TiCl_4$-promoted pathway ($\Delta G^{\ddagger}_{\mathbf{20}\rightarrow\mathbf{19}}$ = 5.6 kcal/mol) compared to the BF_3 pathway ($\Delta G^{\ddagger}_{\mathbf{5}\rightarrow\mathbf{4}}$ = 1.8 kcal/mol, Figure 25). Moreover, the ground state energy difference is less unfavorable for $TiCl_4$ ($\Delta G_{\mathbf{17}\rightarrow\mathbf{20}}$ = 6.2 kcal/mol) than for BF_3 ($\Delta G_{\mathbf{2a}\rightarrow\mathbf{5}}$ = 9.0 kcal/mol). The difference in barrier energies ($\Delta\Delta G^{\ddagger}$ = 3.8 kcal/mol) may have important consequences for diastereoselectivity. The barrier to desilylation of intermediate **20** in the $TiCl_4$ pathway is likely to be similar to the barrier for

desilylation of **5** since the lability of the silyl group is unlikely to be dependent on the group bound to the oxygen atom. Intermediate **20** is likely to be consumed by chloride-promoted desilylation.[169] Even though the BF_3-promoted pathway may be complicated by reversibility, the critical, stereodetermining C-C bond forming step was investigated more thoroughly with respect to the topological approach of the activated aldehyde as a model for systems that do not exhibit potential reversibility such as was found for $TiCl_4$.

6.2. Computational Investigation on the Selectivity of Model Systems.

Model system B (Scheme 30) and a simplified intermolecular system were modeled using density functional theory for purposes of comparison and to judge whether or not the intramolecular case introduces unwanted bias for the synclinal conformation (Scheme 33).[170] It was judged that if the calculated energy difference between the synclinal and antiperiplanar transition states for the intramolecular and intermolecular cases were similar to each other as well as to the experimental values, model system **5** would indeed be suggested to intrinsically reflect the synclinal preference in the transition state.

Scheme 33.

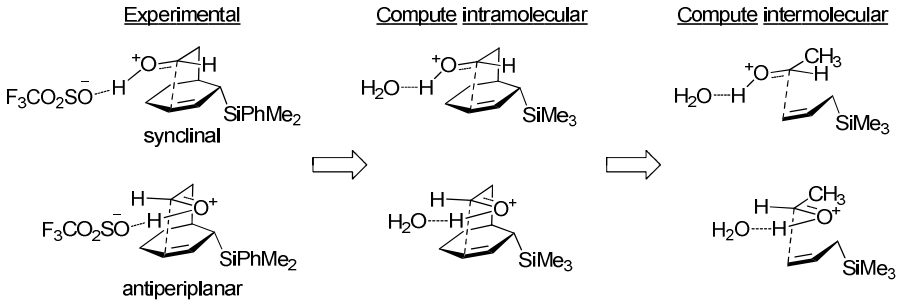

Initially moldel system B (Scheme 30) was computed in which CF_3SO_3H was substituted with H_3O^+. The preferred transition state is predicted to proceed through the synclinal conformation (**TS-a**, $\Delta G^{\ddagger}$=2.1 kcal/mol) in qualitative agreement with the experimental results ($\Delta G^{\ddagger}$=1.14 kcal/mol). The electronic energy difference in the intermolecular analogue (**TS-b**, $\Delta E^{\ddagger}$=1.1 kcal/mol) qualitatively compares well to the calculated electronic intramolecular case (**TS-a**, $\Delta E^{\ddagger}$=1.9 kcal/mol). This agreement suggests that the intramolecular case reflects the electronic preference for the synclinal orientation in the intermolecular case satisfactorily. The internal nuclear coordinates of the relevant atoms are also similar. The distance of the forming

bond is smaller by ~0.2 Å likely reflecting minor intramolecular constraints rather than an earlier transition state.

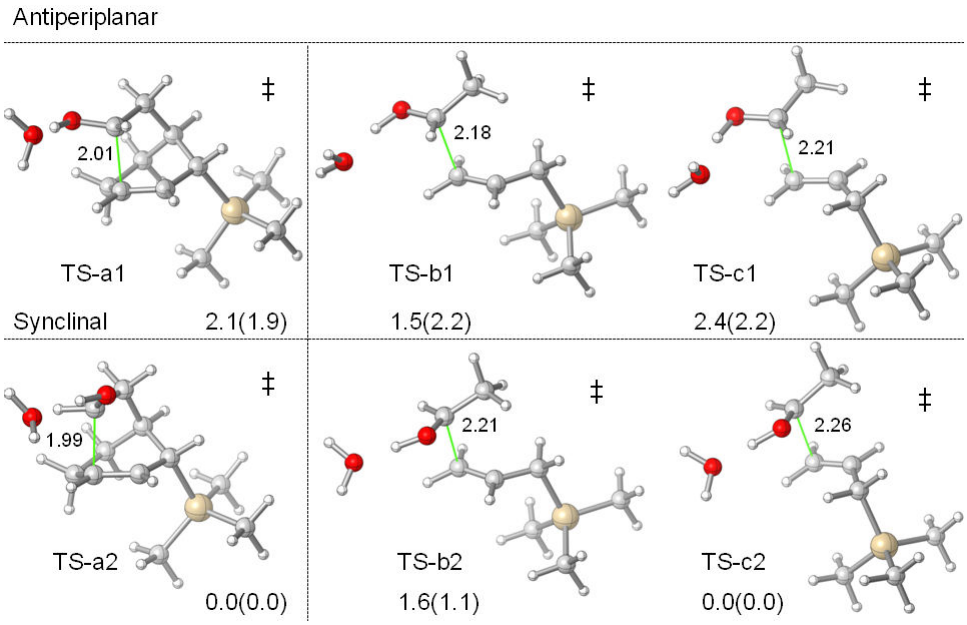

Figure 30. Relative free energies (kcal/mol) at 195 K and electronic energies in parentheses; structures **TS-a** are relative to **TS-a2**; structures **TS-b** and **TS-c** are relative to **TS-c2**; selected distances are labeled in Å; CPCM-M06-2X/6-311++G(2d,2p)//M06-2X/6-31+G(d,p).

Perhaps, a more relevant comparison can be made with **TS-c** in which the face of the π-system of the allylsilane approaching the aldehyde is switched (Figure 25). The presence of differential steric interactions would be minimal. There does appear to be much better agreement to the predicted free energy difference in this case (**TS-c**, $\Delta G^{\ddagger}$=2.4 kcal/mol). However, a counter argument for this being a relevant comparison is that the arrangement allows for secondary orbital overlap which may control the synclinal preference. To address this counter argument, previous work from the authors employing a model system in which the constitution in **TS-c** was retained (Model system A, Scheme 30), leaving secondary orbital overlap available if stabilizing, afforded the same degree of synclinal preference as model system **5** ($\Delta G^{\ddagger}$=1.1 kcal/mol), in which the secondary orbital overlap of consideration is geometrically unavailable. These results clearly suggest that secondary orbital overlap can only be at most a minor contributor to the selectivity.

While the difference between the predicted and experimental selectivity in **5** may be considered significant (0.96 kcal/mol), the correctly predicted conformation as well as the excellent agreement between the predicted selectivity in **5** and **TS-c** supports a lack of bias in the probing interactions of **5**. Additionally, the fact that **TS-c2** is predicted to be the lowest energy transition state by 1.5 kcal/mol provides further support for the relevance of comparing **TS-c** to **5**. Collectively, this investigation suggests that the selectivity in **5** is reflective of the intrinsically preferred synclinal preference in the transition state.

6.3. Stereodetermining Transition States for Addition of (*E*)-2-Butenyltrimethylsilane to Acetaldehyde.

6.3.1. BF_3-Promoted Pathway.

All six transition state structures for the BF_3-promoted crotylation of acetaldehyde were located and are provided in Figure 31. For the synclinal conformations, all bonds are arranged with roughly staggered orientations. The anti conformations are perturbed slightly from the idealized 180^o dihedral angle for staggered orientations displaying dihedral angles of 173^o and 176^o. The distances between the carbon atoms undergoing bond formation are very similar (1.97 ± 0.02 Å). The predicted energies reveal a preference for the transition states leading to the syn diastereomer, particularly through transition state **syn-T3-L**[171] that possesses a synclinal arrangement of double bonds. The two antiperiplanar transition states (**syn-T1-L** and **anti-T1-L**), which are commonly invoked as providing lower energy channels because of minimized steric interactions,[136f] possess the highest energies of the six structures. These relative energy values suggest that steric interactions may not be important contributors to the overall diastereoselectivity compared to other energetic components.

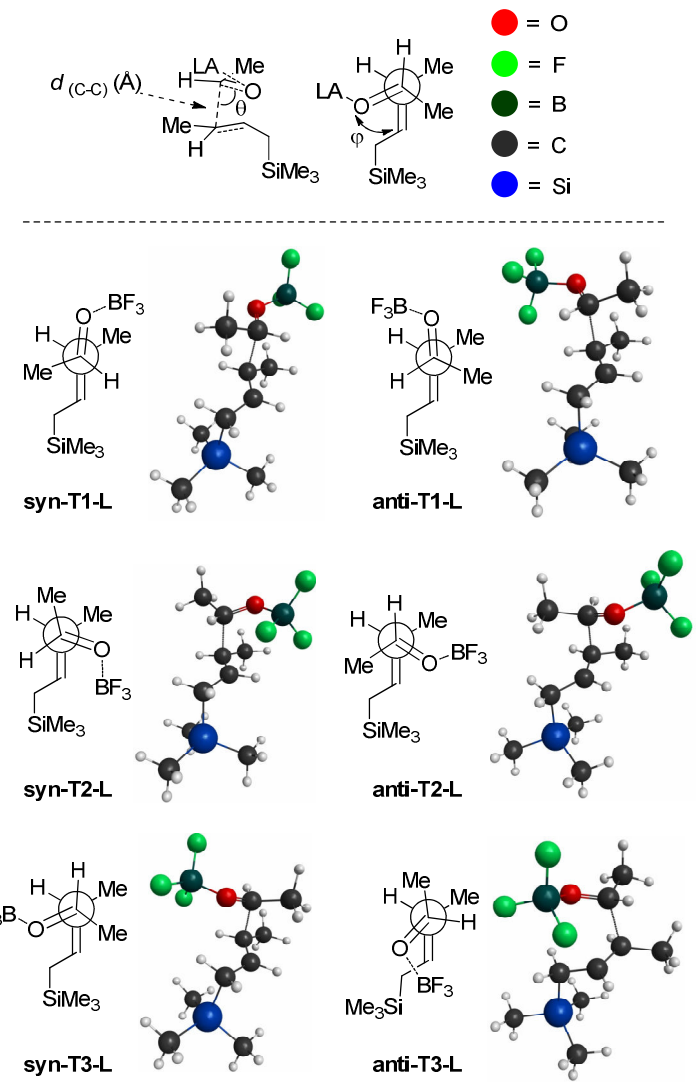

	$\Delta G^{\ddagger}$ [$\Delta H^{\ddagger}$]^a	d ^{b}	θ ^{c}	φ ^{d}
syn-T1-L	4.2 [4.7]	1.99	101.7	187.2
syn-T2-L	0.8 [0.9]	1.96	108.7	273.2
syn-T3-L	0.0 [0.0]	1.95	110.9	66.9
anti-T1-L	2.0 [2.1]	1.96	102.1	184.5
anti-T2-L	3.0 [3.1]	1.96	112.1	296.9
anti-T3-L	1.0 [1.8]	2.00	113.3	42.6

Figure 31. Six transition states for BF_3-promoted crotylation. ^{a} Relative transition state energies ($\Delta G^{\ddagger}$ and $\Delta H^{\ddagger}$) in kcal/mol. ^{b} C(1)-C(2) bond distance (Å). ^{c} Approach angle (deg). ^{d} Dihedral angle (deg).

6.3.2. Brønsted Acid Promoted Pathway.

The crotylsilane addition through Brønsted acid activation was also investigated. This mode effectively removes any steric influence that the Lewis acid may impart. A single water molecule was used to attenuate its level of activation as relaxed coordinate scans in the absence of a water molecule suggest a barrierless bond formation. The location of the proton in the activated carbonyl group presents some ambiguity, however its position has little influence on the energies of either the reactants or the transition states.[172] To be geometrically consistent with other Lewis acids, the proton is situated synperiplanar to the aldehydic hydrogen.[173]

Some of the transition states deviate from idealized staggered conformations (Figure 32). Antiperiplanar transition state **syn-T1-H** adopts a 170^{o} dihedral angle, likely in an effort to relieve unfavorable interaction between the methyl group of the aldehyde and the TMS-CH_2 group. Whereas all the synclinal transition states for the BF_3-mediated allylation exhibit a smaller dihedral angle in which the oxygen atom is positioned close to the partially positively charged carbon atom of the crotylsilane, all of the synclinal conformations for the proton-mediated pathway deviate from this orientation by maximizing the distance between the protonated oxygen and carbon atom C(1) gaining the positive charge. This preference likely results from electrostatic repulsion considering the fact that **anti-T3-H** positions the two methyl groups in a near eclipsed conformation to provide sufficient distance between the partially positively charged atoms. The electrostatic gain in energy by avoiding repulsion more than compensates for the loss in energy from unfavorable steric interactions.

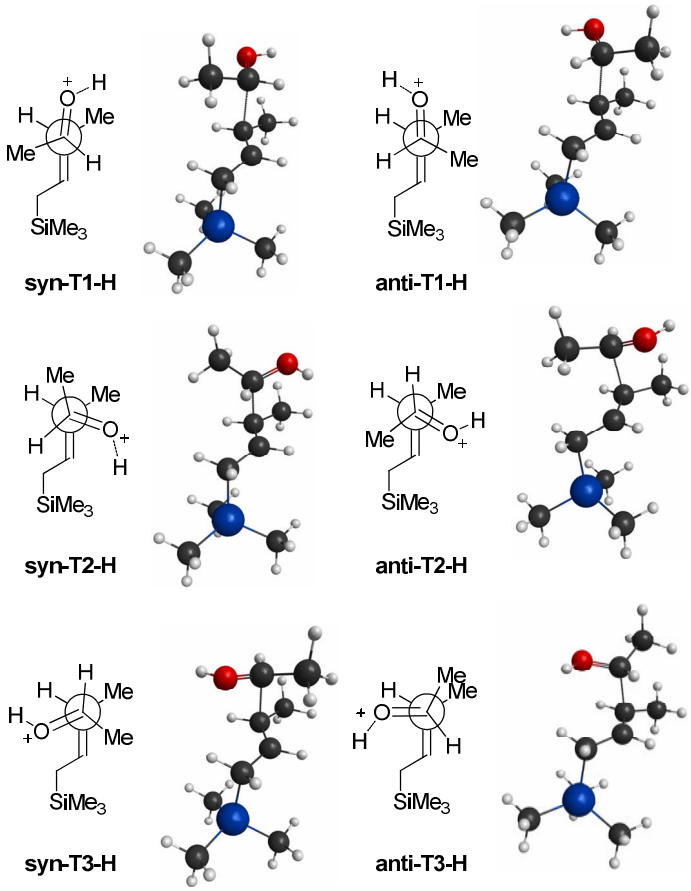

	$\Delta G^{\ddagger}$ [$\Delta H^{\ddagger}$]	*d*	θ	φ
syn-T1-H	3.0 [3.0]	2.16	98.4	189.9
syn-T2-H	1.7 [1.6]	2.08	104.9	256.0
syn-T3-H	0.0 [0.0]	2.24	106.9	76.9
anti-T1-H	2.8 [2.2]	2.13	98.7	175.8
anti-T2-H	1.8 [1.6]	2.16	107.5	281.9
anti-T3-H	3.1 [2.6]	2.13	103.1	92.8

Figure 32. Six transition states for Brønsted acid-promoted crotylation. See Figure 31 for legend.

6.3.3. Fluoride-Promoted Pathway.

The fluoride-promoted pathway was next investigated to identify how a different mode of activation (nucleophilic as opposed to electrophilic) influences the topology of the approach. This investigation is intended to embody characteristics of the Brønsted acid activated pathway because of the lack of a bulky group bound to the aldehyde oxygen atom but representing opposing electronic activation modes.

The fluoride-promoted pathway illustrates interesting contrasts with the BF_3 and Brønsted acid-promoted pathways (Figure 33). Both antiperiplanar transition states are lower in energy than all four synclinal transition states, in contradistinction to the Lewis acid containing transition states. As was seen in the Lewis acid promoted reactions, **anti-T1-F** is the lower energy of the two antiperiplanar transition states. Generally the dihedral angles more closely resemble those of the BF_3 bound transition states. Structure **syn-T3-F** is the lowest energy synclinal transition state as was also observed for both Lewis acid bound transition states.

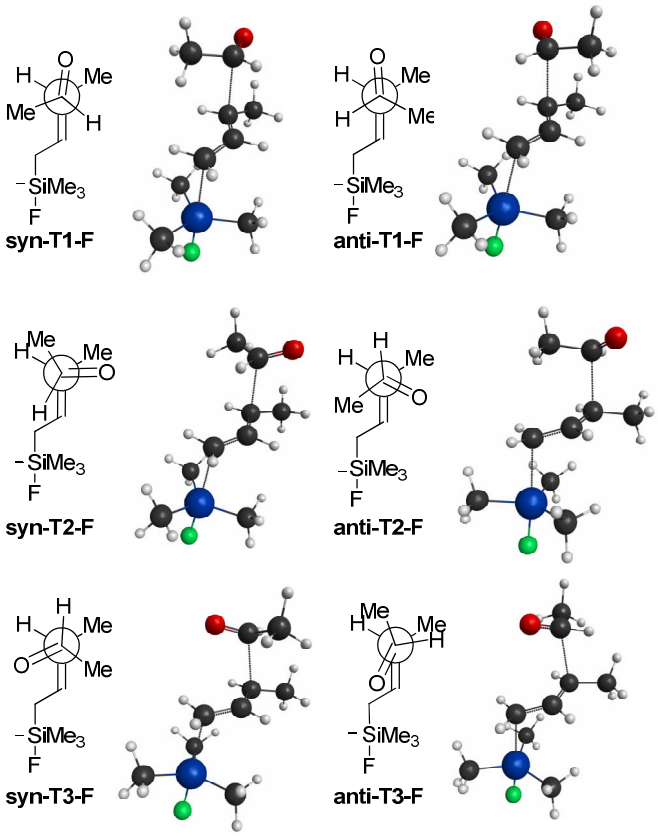

	$\Delta G^{\ddagger}$ [$\Delta H^{\ddagger}$]	*d*	θ	φ
syn-T1-F	1.1 [0.9]	2.30	105.6	206.1
syn-T2-F	2.4 [2.3]	2.28	108.6	265.6
syn-T3-F	1.4 [1.4]	2.22	109.4	68.5
anti-T1-F	0.0 [0.0]	2.23	105.0	175.0
anti-T2-F	2.5 [2.3]	2.22	110.2	284.9
anti-T3-F	4.0 [3.7]	2.30	113.2	27.5

Figure 33. Six transition states for F^- promoted crotylation. See Figure 31 for legend.

To summarize this section, the activation energies reveal that the electrophilically-activated pathways show a preference for the formation of the syn diastereomer specifically through the **syn-T3** transition state. The formation of the competing anti diastereomer takes place via **anti-T2-L** and **anti-T1-H**. In comparison, the nucleophilically-activated pathway exhibits a preference for formation of the anti diastereomer via the antiperiplanar **anti-T1-F** transition state. These results are in accord with experimental findings.[136k] The factors that influence the reactivity differences in each pathway as well as the divergence in diastereoselectivity between the electrophilically and nucleophilically activated pathways will be addressed using energy decomposition analysis in the following sections.

6.4. Energy Decomposition Analysis (EDA) of Transition States.

The interaction energies between the aldehyde and allylsilane partners for all transition states were decomposed to reveal the relative contributions of the individual components of the interaction energy as well as the distortion energy to the total energy $\Delta E^{\ddagger}$. For completeness, the energies of distortion of each reactant are also included in the analysis. With the inclusion of reactant distortion energies, the total electronic activation barrier $\Delta E^{\ddagger}$ can be expressed as $\Delta E^{\ddagger} = \Delta E_{int}^{\ddagger} + \Delta E_d^{\ddagger}(A) + \Delta E_d^{\ddagger}(B)$.[174]

The transition states for the BF_3-promoted reaction are the latest along the reaction coordinate as well as being the most endergonic, hence a greater degree of distortion is necessary to achieve suitable levels of interaction as is observed (Table 21). The lowest energy transition state **syn-T3-L** does possess the second highest interaction energy behind **syn-T2-L** as well as the lowest energy of distortion of the crotylsilane component $\Delta E_d(B)$. Transition state **anti-T1-L**, however, has the next lowest energy required to distort the crotylsilane component $\Delta E_d(B)$. The antiperiplanar transition states **syn-T1-L** and **anti-T1-L** have the lowest steric contribution $\Delta E_{ste}^{\ddagger}$ which is the traditional rationale for its status as the preferred transition state.[136f] Although **syn-T1-L** is sterically the most preferred transition state, it suffers from a relatively low preference in terms of orbital $\Delta E_{orb}^{\ddagger}$ and electrostatic interactions $\Delta E_{es}^{\ddagger}$. Overall, the energetic preference for transition state **syn-T3-L**, can be attributed to a combination of favorable electrostatic interactions, orbital interactions, and a low energy of distortion of the allylsilane component.

The energy breakdown in the Brønsted acid mediated pathway is similar to the BF_3-mediated pathway. A marked distinction is the earlier nature of the lowest energy transition state

syn-3-H (d = 2.24 Å) which is the lowest energy transition state. Counterintuitively, **syn-T3-H** also possesses the most unfavorable interaction energy. For every component of the interaction energy, excluding a substantially favorable steric component ($\Delta E_{ste}^{\ddagger}$), **syn-T3-H** exhibits the weakest interaction. The smaller favorable energies in **syn-T3-H** are compensated for by highly favorable distortion energies for both the aldehyde and allylsilane components.

The fluoride-promoted pathway generally has high reaction barriers, but the reaction is concerted, after pre-equilibrium formation of a pentacoordinated fluorosilicate. The lowest energy transition states are antiperiplanar (**syn-T1-F** and **anti-T1-F)** with **anti-T1-F** being slightly lower (0.9 kcal/mol). Analysis of the energetic contributions of this pathway is complex because all components of the interaction energy influence $\Delta E^{\ddagger}$ to a similar extent. However, the antiperiplanar transition states do appear to benefit from decreased steric ($\Delta E_{ste}^{\ddagger}$) and favorable electrostatic ($\Delta E_{es}^{\ddagger}$) interactions whereas the synclinal transition states **syn-T3-F** and **anti-T2-F** exhibit the strongest orbital interactions ($\Delta E_{orb}^{\ddagger}$). The electrostatic preference for antiperiplanar TS's contrasts the electrophilically activated pathways in which the synclinal transition states are electrostatically preferred. The role of distortion energy is not as significant in the fluoride promoted pathway.

Table 21. Energy decomposition analysis of reactants in transition states for all three modes of activation.

TS	$\Delta E_{es}^{\ddagger}$	$\Delta E_{ste}^{\ddagger}$	$\Delta E_{orb}^{\ddagger}$	$\Delta E_{disp}^{\ddagger}$	$\Delta E_{d}^{\ddagger}$(A)[a]	$\Delta E_{d}^{\ddagger}$(B)[b]	$\Delta E_{int}^{\ddagger}$	$\Delta E^{\ddagger}$[c]
syn-T1-L[d]	-34.2	120.5	-84.6	-29.6	21.8	10.2	-27.9	4.1
syn-T2-L	-44.5	143.7	-98.2	-33.2	24.0	8.0	-32.2	-0.2
syn-T3-L	-42.0	137.8	-96.5	-30.8	23.1	7.5	-31.5	-0.9
anti-T1-L	-38.6	128.3	-90.1	-28.7	22.4	7.8	-29.1	1.1
anti-T2-L	-42.9	139.7	-96	-31.3	23.9	9.1	-30.5	2.4
anti-T3-L	-33.3	122.9	-86.4	-31.3	21.4	8.3	-28.1	1.6
syn-T1-H[e]	11.5	84	-91.9	-25.0	14.0	5.5	-21.4	-1.9
syn-T2-H	-4.21	120.1	-117.7	-27.7	21.5	4.0	-29.5	-4.0
syn-T3-H	15.5	77.2	-86.4	-24.0	10.3	2.3	-17.7	-5.0
anti-T1-H	9.7	89.9	-96.7	-24.9	14.3	4.1	-22.0	-3.6
anti-T2-H	7.2	94.5	-97.6	-26.9	14.7	4.3	-22.7	-3.7
anti-T3-H	0.9	107.0	-106.7	-28.0	19.0	4.8	-26.8	-3.0
syn-T1-F[f]	5.8	74.8	-71.7	-20.5	6.5	10.0	-11.6	4.9
syn-T2-F	4.9	78.3	-74.2	-19.9	7.2	9.9	-10.9	6.2
syn-T3-F	7.9	83.9	-81.3	-21.7	7.5	9.0	-11.2	5.2
anti-T1-F	3.6	80.3	-74.6	-21.6	7.2	9.0	-12.2	4.0
anti-T2-F	2.1	86.9	-78.3	-21.4	7.9	9.4	-10.7	6.6
anti-T3-F	13.5	72.8	-76.7	-19.5	6.8	10.4	-9.9	7.2

All energies are in units of kcal/mol [a] Distortion energy of aldehyde component [b] Distortion energy of crotylsilane component [c] $\Delta E^{\ddagger} = \Delta E_{d}^{\ddagger}$ (A) + $\Delta E_{d}^{\ddagger}$ (B) + $\Delta E_{int}^{\ddagger}$ [d] BF_3-promoted pathway [e] Bronsted acid promoted pathway [f] Fluoride-promoted pathway

In summary, for the BF_3-promoted pathway, the antiperiplanar transition states are preferred sterically whereas the synclinal transition states are preferred through electrostatic and orbital interactions. The combination of these factors renders **syn-T3-L** the energetically preferred transition state overall. The Brønsted acid promoted pathway is complicated by significant variation in distortion energy. For the fluoride-promoted pathway antiperiplanar transition states are preferred overall because of favorable steric and electrostatic (contrary to the

BF_3-promoted pathway) interactions while favoring the synclinal transition states through orbital interactions.

6.4.1. Rationalization of Diastereoselectivity.

To a first approximation, the overall diastereoselectivity can be rationalized by the difference between the lowest energy transition state leading the syn diastereomer and the lowest energy transition state leading to the anti diastereomer (Table 21). Each bar in the graphs in Figure 34 represents the difference for the indicated component of the overall energy ($\Delta E^{\ddagger}$) between the lowest energy syn transition state versus the lowest energy anti transition state ($\Delta\Delta E_x < 0$ reflects a preference for the syn transition state for energy component x while $\Delta\Delta E_x > 0$ reflects an anti preference).

The transition states for the BF_3-promoted process exhibit a small difference in distortion energy ($\Delta E_d^{\ddagger}$) reflecting similar extents of bond formation at the transition state. Although sterically unfavorable, transition state **syn-T3-L** benefits from considerably favorable electrostatic and orbital interactions. The diastereoselectivity for the BF_3-promoted process is thus largely attributed to favorable electrostatic ΔE_{es} and orbital ΔE_{orb} terms for **syn-T3-L**.

For the Brønsted acid promoted pathway, the lowest energy transition state is particularly early ($d_{C(1)\text{-}C(2)} = 2.24$ Å) compared to all other transition states for this pathway (Figure 32). The early nature is reflected in a smaller ΔE_d. The low energy of distortion and steric interactions for **syn-T3-H** account for the diastereoselectivity observed in the Brønsted acid promoted pathway. The origin of the favorable distortion level for **syn-T3-H** is the subject of a forthcoming section.

The diastereoselectivity in the fluoride-promoted reaction is largely accounted for by the difference in the energies of the antiperiplanar transition states. The greatest energetic contributor to the transition state energy difference is steric interactions (ΔE_{ste}) in preference for transition state **syn-T1-F**. However the combination of favorable electrostatic (ΔE_{es}), orbital (ΔE_{orb}), and dispersion (ΔE_{disp}) terms results in the overall energetic preference for **anti-T1-F**.

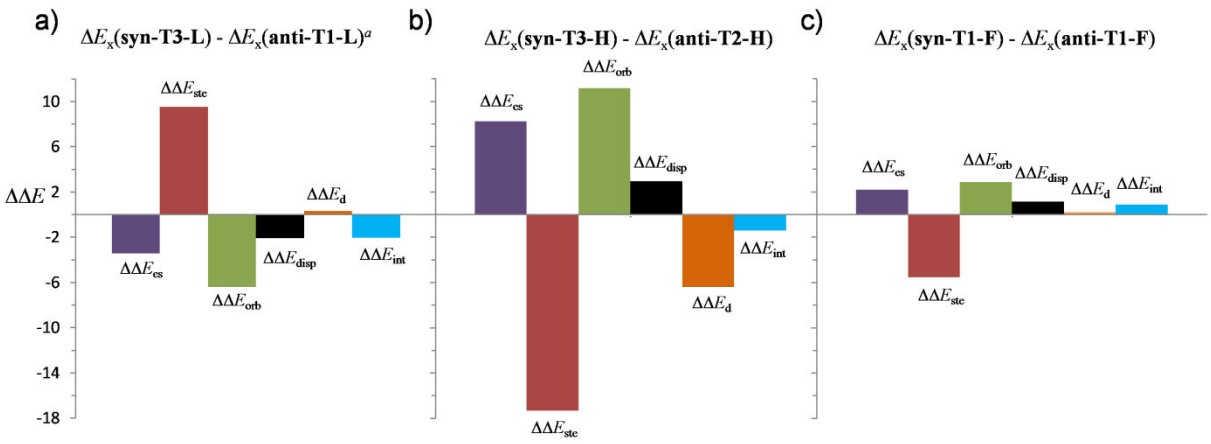

Figure 34. Differences in components of interaction energy between two lowest energy different transition states in each activation mode in kcal/mol: (a) BF_3, (b) H^+, (c) F^-. [a] x = es (electrostatic), ste (steric), orb (orbital), disp (dispersion), d (distortion), int (interaction).

The variation in distortion has a significant impact on the energies of competing transition state conformations and consequentially the diastereoselectivity. Decomposition of the interaction energy alone is not sufficient for a complete understanding of this variation. Uncovering the origin of the variation in the distortion energies would provide a more complete rationalization of the observed diastereoselectivities and is the focus of the following sections.

6.5. Origin of Variation in Distortion.

The appearance of reaction barriers depends on a balance between both ΔE_d and ΔE_{int}. The amount of energy necessary to distort the nuclei in the transition state is dependent on how much energy from interaction is gained from this distortion. Once the point at which an infinitesimal gain in interaction energy is balanced by an infinitesimal loss in the energy from distortion, the downward slope of the transition state is initiated. With these considerations in mind, points along respective reaction coordinates ($\Delta E(\xi)$) at constant levels of distortion may be compared with respect to ΔE_{int} and its components. As long as the change in energy from $\Delta E^{\ddagger}$ to $\Delta E(\xi)$ is small, this comparison is possible. The comparison of the ΔE_{int} at constant distortion ($\Delta E_{int,d}$) among multiple transition states is an option when a linear relationship exists between $\Delta E_{int,d}$ and $\Delta E^{\ddagger}$. This allows the investigation of the components of the interaction energy close to the transition state that best account for the variation in $\Delta E_d(\xi)$.

For each transition state, an EDA was performed on selected points along the reaction coordinate. Each component of the energy was plotted as a function of $\Delta E_d(\xi)$ and fitted to a parabolic curve. The energies were interpolated on the basis of a parabolic fit (all fits contained ≥ 5 points with $R^2>0.99$, see Supporting Information). The optimal $\Delta E_d(\xi)$ was chosen based on the correlation between $\Delta E^{\ddagger}$ and $\Delta E_{int,d}(\xi)+\Delta E_d(\xi)$ for all of the pathways. The interaction energy components at the interpolated transition states are listed in Table 22.

Table 22. Energetic Components at Constant Levels of Distortion.[a, b, c]

TS	$\Delta E_{es,d}^{\ddagger}$	$\Delta E_{ste,d}^{\ddagger}$	$\Delta E_{orb,d}^{\ddagger}$	$\Delta E_{disp,d}^{\ddagger}$	$\Delta E_{int,d}^{\ddagger}$
syn-T1-L[a]	-35.3	123.2	-87.1	-29.5	-28.9
syn-T2-L	-45.7	146.7	-101.0	-33.4	-33.2
syn-T3-L	-44.4	144.1	-102.4	-31.1	-33.9
anti-T1-L	-41.6	135.8	-97.0	-29.1	-31.8
anti-T2-L	-43.1	140.1	-96.2	-31.4	-30.6
anti-T3-L	-36.7	131.3	-94.1	-31.8	-31.3
syn-T1-H[b]	13.5	79.4	-87.9	-24.6	-19.6
syn-T2-H	7.0	94.7	-97.8	-25.9	-21.9
syn-T3-H	8.0	94.2	-99.3	-25.6	-22.7
anti-T1-H	10.6	87.9	-95.0	-24.8	-21.3
anti-T2-H	8.9	90.9	-94.5	-26.6	-21.4
anti-T3-H	9.7	87.6	-91.7	-26.4	-20.8
syn-T1-F[c]	2.9	80.0	-75.1	-20.8	-13.1
syn-T2-F	2.8	81.9	-76.4	-20.2	-11.8
syn-T3-F	4.9	89.2	-85.0	-22.0	-12.9
anti-T1-F	0.4	86.1	-78.6	-21.9	-14.0
anti-T2-F	0.5	89.6	-80.1	-21.5	-11.5
anti-T3-F	12.4	73.6	-77.0	-19.6	-10.6

[a] Values for BF_3 pathway are interpolated at $\Delta E_d(\xi)$ = 33.0 kcal/mol. [b] Values for Brønsted acid pathway are interpolated at $\Delta E_d(\xi)$ = 17.7 kcal/mol. [c] Values for fluoride pathway are interpolated at $\Delta E_d(\xi)$ = 18.1 kcal/mol.

A linear relationship is expected between $\Delta E^{\ddagger}$ and $\Delta E_{int,d}(\xi)+\Delta E_d(\xi)$ if the change in energy from distortion at small variations in ξ near the transition state is approximately equal to the energy gained by interaction ($dE_{int}/d\xi \approx -dE_d/d\xi$) for all transition states (low curvature at the transition state). All three pathways exhibit $\Delta E_d(\xi)$ values in the range of the distortion levels at the transition states $\Delta E_d^{\ddagger}$ for their respective reactions (Figure 35). The strong linear trends

validate the comparison of the components of the interaction energy (ΔE_{int}) at the corresponding constant levels of distortion.

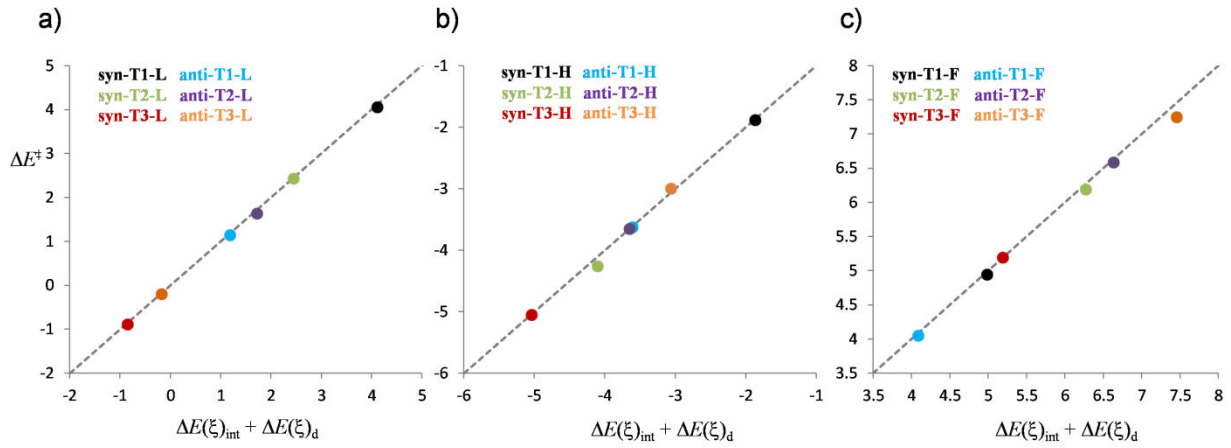

Figure 35. Plots of $\Delta E^{\ddagger}$ versus $\Delta E(\xi)_{int,d}$. (a) BF_3 with $\Delta E_d(\xi)$ = 33.0 kcal/mol; R^2=0.9999 (b) H^+ with $\Delta E_d(\xi)$=17.7; R^2=0.996 (c) F^- with $\Delta E_d(\xi)$=18.1; R^2=0.998.

Conceptually different conclusions can be inferred from the interaction at constant distortion compared to variable distortion when the conversion of energy between distortion and interaction is not equal via all pathways (Figure 36). The differences in the interaction energy components for the lowest energy transition states leading to the syn and anti diastereomers at constant distortion are compared to those at variable distortion in Figure 36 (for each $\Delta\Delta E_x$, the left bar, labeled with a *d*, corresponds to the difference in the energy at the distortion level from Table 22 while the right bar corresponds to the energies from Table 21). For the BF_3 pathways, the difference in the distortion energy at the transition states is only 0.4 kcal/mol favoring **anti-T1-L** ($[\Delta E_d^{\ddagger}(A) + \Delta E_d^{\ddagger}(B)]_{\textbf{anti-T1-L}} - [\Delta E_d^{\ddagger}(A) + \Delta E_d^{\ddagger}(B)]_{\textbf{syn-T3-L}}$ = 0.4 kcal/mol, Table 21). This distortion energy is distributed among the different interaction energies and results in only a small lowering in each of the energy components for **syn-T3-L** compared to **anti-T1-L**.

The difference in distortion for the Brønsted acid mediated pathway between the synclinal transition state pathways **syn-T3-H** and **anti-T2-H** is significant at a value of 6.4 kcal/mol (Table 21 and Figure 34) favoring the **syn-T3-H** pathway. This large difference in distortion leads to a very different interaction energy landscape at constant distortion than at the distortion level of the transition state (Figure 36b). Whereas, the only energy components that favor **syn-T3-H** at the transition state are ΔE_{ste} and ΔE_d (6.4 kcal/mol, Figure 34b), all of the

energy components favor **syn-T3-H** at constant distortion except for ΔE_{ste} and ΔE_{disp}. Thus, the origin of the large distortion energy difference favoring **syn-T3-H** at the transition state is accounted for mostly by a large favorable orbital term ΔE_{orb}. The difference in distortion energy for the fluoride mediated pathway at the transition states between **syn-T1-F** and **anti-T1-F** is only 0.3 kcal/mol and hence only a small difference in the interaction energy components results.

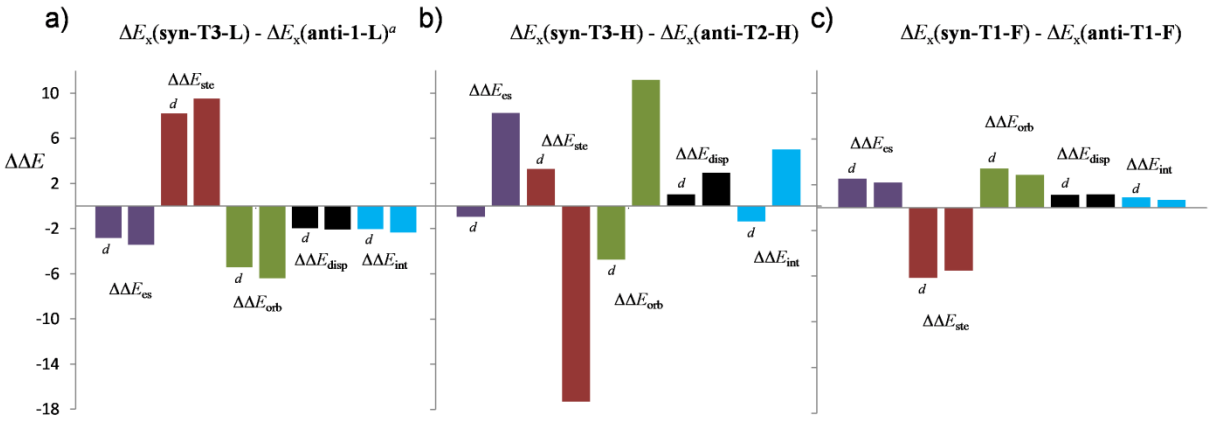

Figure 36. Left bar of for each colored pair (labeled with a *d* for constant distortion) corresponds to $\Delta\Delta E_x$ at distortion energy from Figure 9 while right bar corresponds to $\Delta\Delta E_x$ from Figure 8; (a) BF_3, (b) H^+, (c) F^-.

To summarize, the activation energy is readily correlated with the interaction energy at constant levels of distortion. A necessary condition is that $dE_{int}/d\xi \approx -dE_d/d\xi$ in the vicinity of the transition states that are being compared. The rationalizations for the diastereoselectivity in the BF_3- and fluoride-promoted reactions do not change very much because the difference in distortion energy between the lowest energy transition states leading to each diastereomer is small.

However, this situation is not the case for the Brønsted acid promoted reaction in which the difference in distortion energy between the lowest energy transition states leading to each diastereomer is significant and different conclusions can be reached. The analysis shows that the origin of the large difference in distortion of the nuclei in the Brønsted acid promoted pathway can be mostly attributed to a more favorable change in the orbital interaction energy (ΔE_{orb}), which is a distinctly different conclusion than would otherwise be drawn from the energy values at the transition states (Table 21).

The origin of the enhanced orbital interactions favoring **syn-T3** for all activation manifolds remains unclear at this point.[175] A frontier orbital energy analysis can be used to dissect the orbital interactions into contributions from orbital overlap and frontier orbital energy differences in the reacting components, which is the focus of the following sections

6.6. Orbital Energy Analysis.

6.6.1. Rationalizing Synclinal Selectivity.

The foregoing analysis revealed that: (1) in the electrophilic activation manifolds, the preference for **syn-T3-L** and **syn-3T-H** pathways is attributed to increased orbital interactions and to a lesser extent, electrostatic interactions and (2) in the nucleophilic activation manifold, the preference for antiperiplanar **anti-T1-F** is attributed to decreased steric and electrostatic repulsion. Nevertheless, the most favorable transition state leading to a syn product, **syn-T3-F**, possesses greater orbital interactions. Thus, the three most favorable synclinal transition states (**T3**) are characterized by greater orbital interactions. The origin of this increased orbital interaction term for those synclinal transition states is next elucidated by a frontier orbital energy analysis.

The figure (a) in Table 23 depicts the orbital energy diagram for the BF_3-promoted and Brønsted acid-promoted pathways and figure (b) depicts the fluoride-promoted pathway. The HOMO for the undistorted crotylsilane is shown on the far left and the LUMO of the undistorted aldehyde component is shown on the far right in both figures. The nuclei are then allowed to distort to the transition state geometries and the energies of the resulting distorted orbitals are then determined. The resulting distorted orbitals are allowed to mix causing the orbital splitting in the transition states which is shown in the center of the diagrams, corresponding to $HOMO^{‡}$ and $LUMO^{‡}$.

Table 23. Orbital Energy Differences (Δ_x[a] and $\Delta_x^{\ddagger}$[b]) and Charge Transfer (Δq_x[c]).

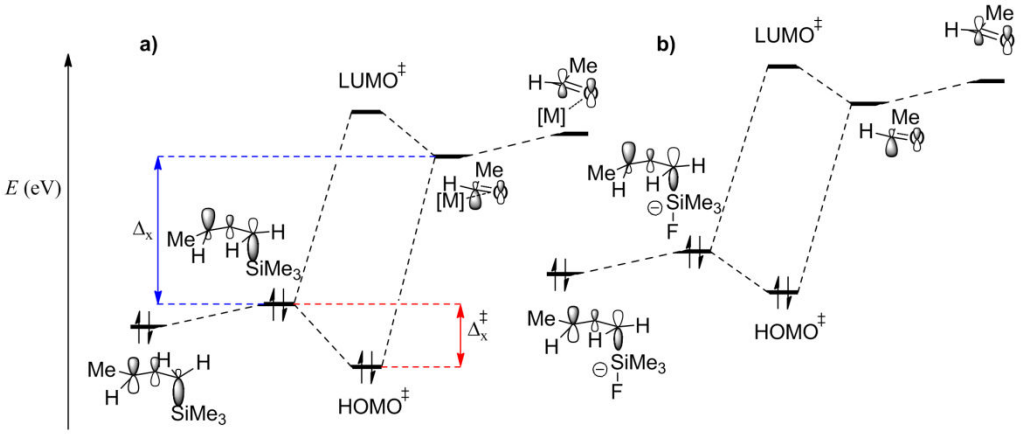

	syn-T1	syn-T2	syn-T3	anti-T1	anti-T2	anti-T3
$\Delta_L^{\ddagger}$	1.39	1.50	1.60	1.54	1.47	1.50
Δ_L	4.18	4.18	4.07	4.07	4.18	4.19
Δq_L	0.473	0.528	0.541	0.522	0.526	0.525
$\Delta_H^{\ddagger}$	1.59	1.72	1.75	1.67	1.66	1.63
Δ_H	4.08	4.00	4.02	4.02	4.08	4.08
Δq_H	0.363	0.395	0.406	0.389	0.393	0.373
$\Delta_F^{\ddagger}$	0.64	0.60	0.69	0.71	0.53	0.64
Δ_F	3.81	3.81	3.85	3.79	3.98	3.80
Δq_F	0.316	0.315	0.330	0.318	0.326	0.293

[a] Frontier orbital energy difference of distorted reactants (eV) [b] Difference in energy between HOMO of the distorted reactant and the HOMO of the transition state (eV). [c] charge transfer determined from NBO charges

Under second order perturbation theory[176], the amount that the HOMO‡ energy is lowered relative to the HOMO of the crotylsilane component ($\Delta_x^{\ddagger}$) is dependent on both the HOMO-LUMO gap (Δ_x) of the reactants, the resonance energy associated with the overlap region, and the exchange-corrected Coulombic repulsion contributions. The amount of charge transfer (Δq_x) in the transition state from the crotylsilane to the activated aldehyde component is listed in Table 23. The charge transfer includes effects from both resonance energy from orbital overlap and Δ_x.

In comparing synclinal transition state **syn-T3-L** to antiperiplanar transition state **anti-T1-L** the orbital energy differences Δ_L are equivalent (Δ_L(**syn-T3**) = Δ_L(**anti-T1**), Table 23). This equivalence means that the distortion of the reactants leads to equivalent frontier orbital energy

separation. However, the charge transfer is greater for **syn-T3-L** (Δq_L = 0.541) than for **anti-T1-L** (Δq_L = 0.522). This greater charge transfer is confluent with the lowering of the HOMO‡ for **syn-T3-L** ($\Delta_L^{\ddagger}$ = 1.60 eV) compared to **anti-T1-L** ($\Delta_L^{\ddagger}$ = 1.54 eV). Thus, the preference for the **syn-T3-L** transition state arises from greater charge transfer which is in turn due to greater orbital overlap rather than a narrowing of the frontier orbital energy gap of the distorted reactants.[177]

Within the Brønsted acid-promoted manifold, the lowest energy transition states leading to the anti diastereomer are similar ($\Delta E^{\ddagger}$(**anti-T1-H**) = -3.6 kcal/mol ; $\Delta E^{\ddagger}$(**anti-T2-H**) = -3.7 kcal/mol, Table 1). Thus it is necessary to compare both of these transition states to the lowest energy transition state leading to the syn diastereomer (**syn-T3-H**) to gain a more complete understanding of the diastereoselectivity. Both **syn-T3-H** and **anti-T1-H** possess the same orbital energy gap Δ_H and similar differences in $\Delta\Delta q_H$ (0.017 *e*), $\Delta\Delta_H^{\ddagger}$ (0.08 eV), and $\Delta\Delta E_{orb}$ (-4.3 kcal/mol) as compared to the BF_3-promoted manifold. Thus, roughly half of the diastereoselectivity is controlled by greater charge transfer from orbital overlap rather than from FMO energy differences for **syn-T3-H** and **anti-T1-H**. For comparison of **syn-T3-H** to **anti-T2-H**, all three descriptors in Table 3 ($\Delta\Delta q_H$ = 0.013 *e*, $\Delta\Delta_H$ = -0.06, $\Delta\Delta_H^{\ddagger}$ = 0.09 eV) favor **syn-T3-H**. Thus, the remaining contribution to the diastereoselectivity arises from the orbital preference for **syn-T3-H** over **anti-T2-H** which may be derived from orbital overlap or decreased orbital energy difference (Δ_H).

Under fluoride activation, the energetically preferred pathways are both antiperiplanar, **syn-T1-F** and **anti-T1-F** with a slight preference for **anti-T1-F** ($\Delta\Delta E^{\ddagger}$ = 0.9 kcal/mol, Table 1). Pathway **anti-T1-F** has a slightly smaller Δ_F ($\Delta\Delta_F$ = –0.02 eV), slightly larger charge transfer Δq_F ($\Delta\Delta q_F$ = 0.002 *e*), and a larger $\Delta_F^{\ddagger}$ ($\Delta_F^{\ddagger}$ = 0.07 eV) which all contribute to an overall preference for **anti-T1-F**. Although **syn-T3-F** is less favorable than both antiperiplanar transition states, it still has the greatest overall charge transfer (Δq_F = 0.330 *e*) illustrating its superior overlap energy. Thus, the primary contributors to the diastereoselectivity in the fluoride-promoted pathway are: (1) the steric and electrostatic repulsions that disfavor all four synclinal transition states and (2) the enhanced orbital interactions in **anti-T1-F** compared to **syn-T1-F** that favor formation of the anti diastereomer.

Although enhanced orbital interactions accompany all three (–)-synclinal pathways (**syn-T3**), the reasons for this preferred arrangement are not certain. Two possible contributors can be identified: (1) greater intrinsic overlap in the primary interacting orbitals or (2) in-phase overlap of orbitals not engaged in primary interaction (secondary orbital overlap). In fact, as early as 1986, Ahn and Thanh suggested that secondary orbital overlap could be responsible for the preferred synclinal arrangement of double bonds in the aldol addition reaction.[178] In the following section, the importance of this contribution is investigated.

6.7. Do Secondary Orbital Interactions Contribute to the Preference for syn-T3?

Secondary orbital interactions (SOIs) are characterized by in-phase orbital overlap between atoms not directly involved in bonding in the HOMO of the transition state. The HOMO of the **syn-3T** transition states for each reaction type qualitatively suggests a region of in-phase overlap between the oxygen atom of the aldehyde and the methylene group of the crotylsilane (Figure 37). If this overlap is sufficiently energetically stabilizing, one might expect enhanced charge transfer and/or a larger $\Delta_L^{\ddagger}$ compared to transition states that do not possess this interaction.

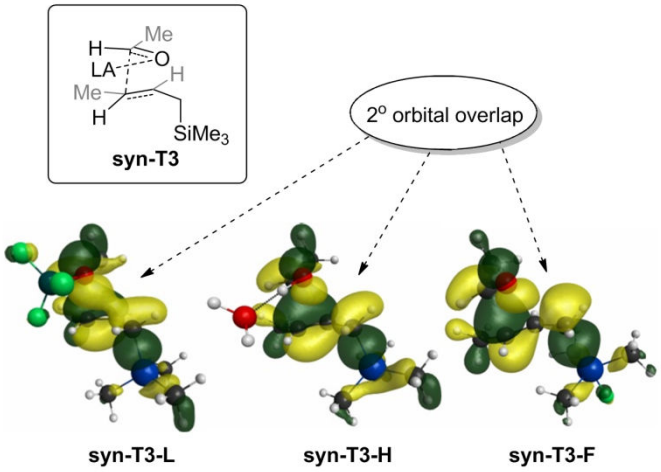

Figure 37. HOMO of transition states (HOMO‡) for **syn-3T-L**, **syn-3T-H**, and **syn-3T-F** with isodensity = 0.03 au.

The approximate contribution from SOIs can be teased out by making relevant transition state comparisons as illustrated in Figure 38. The quantities that may gauge SOI contributions and their determinations are shown at the bottom of Figure 38 (Δq^{SOI}, $\Delta^{\ddagger,SOI}$, $\Delta E_{orb}{}^{SOI}$, and

ΔE_{int}^{SOI}).[179] The difference in energy between **syn-T3** and **anti-T2** could furnish the contribution from SOIs because they are both synclinal transition states and the former contains overlap between the aldehyde oxygen and the silylmethylene whereas the latter does not. However, they also experience different contributions to the four parameters alluded to above because of different steric interactions. These different contributions are: (a) the gauche relationship of the methyl groups in **syn-T3** and (b) the gauche relationship of the methyl group and the Lewis acid in **anti-T2** and (c) the steric interaction between the methyl and silylmethylene groups in **anti-T2.** To adumbrate the existence of SOIs, the contributions that these parameters make can be factored out by: (1) subtracting the contributions that they make to **anti-T1** from the contributions they make to **synT-3** to account for interaction (a) above, (2) subtracting the contributions that they make to **syn-T1** from the contributions they make to **anti-T2** to account for interactions (b) and (c) above.[180]

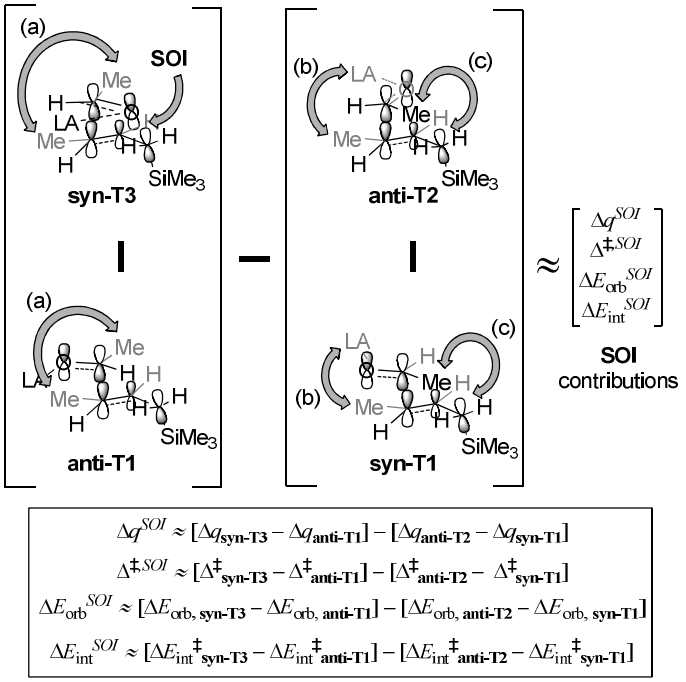

$$\Delta q^{SOI} \approx [\Delta q_{\textbf{syn-T3}} - \Delta q_{\textbf{anti-T1}}] - [\Delta q_{\textbf{anti-T2}} - \Delta q_{\textbf{syn-T1}}]$$

$$\Delta^{\ddagger,SOI} \approx [\Delta^{\ddagger}_{\textbf{syn-T3}} - \Delta^{\ddagger}_{\textbf{anti-T1}}] - [\Delta^{\ddagger}_{\textbf{anti-T2}} - \Delta^{\ddagger}_{\textbf{syn-T1}}]$$

$$\Delta E_{orb}^{SOI} \approx [\Delta E_{orb,\,\textbf{syn-T3}} - \Delta E_{orb,\,\textbf{anti-T1}}] - [\Delta E_{orb,\,\textbf{anti-T2}} - \Delta E_{orb,\,\textbf{syn-T1}}]$$

$$\Delta E_{int}^{SOI} \approx [\Delta E_{int}{}^{\ddagger}_{\textbf{syn-T3}} - \Delta E_{int}{}^{\ddagger}_{\textbf{anti-T1}}] - [\Delta E_{int}{}^{\ddagger}_{\textbf{anti-T2}} - \Delta E_{int}{}^{\ddagger}_{\textbf{syn-T1}}]$$

Figure 38. Scheme for determining the contribution from secondary orbital interactions.

The comparison of the **syn-T3** and **anti-T2** transition states for the BF_3 pathway provides the following results: Δq_L^{SOI} = -0.034 *e*, $\Delta_L^{\ddagger,SOI}$ = -0.02 eV, ΔE_{orb}^{SOI} = 3.7 kcal/mol, ΔE_{int}^{SOI} = -0.4 kcal/mol. All of these descriptors except ΔE_{int}^{SOI} indicate that SOIs do not make a stabilizing contribution to transition state **syn-T3**.[181] Similar data is obtained from the Brønsted acid-

promoted manifold; Δq_H^{SOI} = -0.013 *e*, $\Delta_H^{\ddagger,SOI}$ = 0.01 eV, ΔE_{orb}^{SOI} = 2.3 kcal/mol, ΔE_{int}^{SOI} = 0.4 kcal/mol. *From these results, it can be concluded that SOIs do not contribute significantly to the synclinal preference for* ***syn-T3***.

The elimination of SOIs as a significant contributor to the diastereoselectivity suggests that the preference can be attributed to enhanced, primary orbital interactions. To identify the contribution of primary orbital interactions, inspection of the transition state geometries provides valuable insights. For example, differences in geometrical coordinates between two transition states may reveal how achieving optimal primary orbital interactions (as reflected in the near equality of the orbital interaction energies ($\Delta\Delta E_{orb}^{\ddagger}$**(anti-T2-L − syn-T3-L)** = 0.5 kcal/mol)) requires different levels of distortion. Inspection of the crotylsilane fragment in the transition state reveals that an additional amount of distortion is present in **anti-T2-L** that is absent in **syn-T3-L** ($\Delta\Delta E_d^{\ddagger}$**(anti-T2-L − syn-T3-L)** = 1.6 kcal/mol), namely the distortion of the π-system (Figure 39).[182] This distortion in the crotylsilane is necessary so that the aldehyde can adopt an appropriate approach trajectory in **anti-T2-L** for ideal overlap. The distortion is induced by the steric interaction between the methyl group of the aldehyde and the silylmethylene group. This observation explains why the orbital interactions at a constant level of distortion favor **syn-T3-L** more significantly ($\Delta\Delta E_{orb,d}^{\ddagger}$**(anti-T2-L − syn-T3-L)** = 6.2 kcal/mol). These conclusions are also consistent with the results from model systems investigated experimentally (Scheme 30).[138c]

In summary, the overall transition state energy for **syn-T3-L** is lower than **anti-T2-L** because a lesser degree of distortion is required in **syn-T3-L** to achieve the same level of primary orbital overlap compared to **anti-T2-L**. Similar conclusions are reached upon comparing Brønsted acid mediated transition states (**syn-T3-H** and **anti-T2-H**).

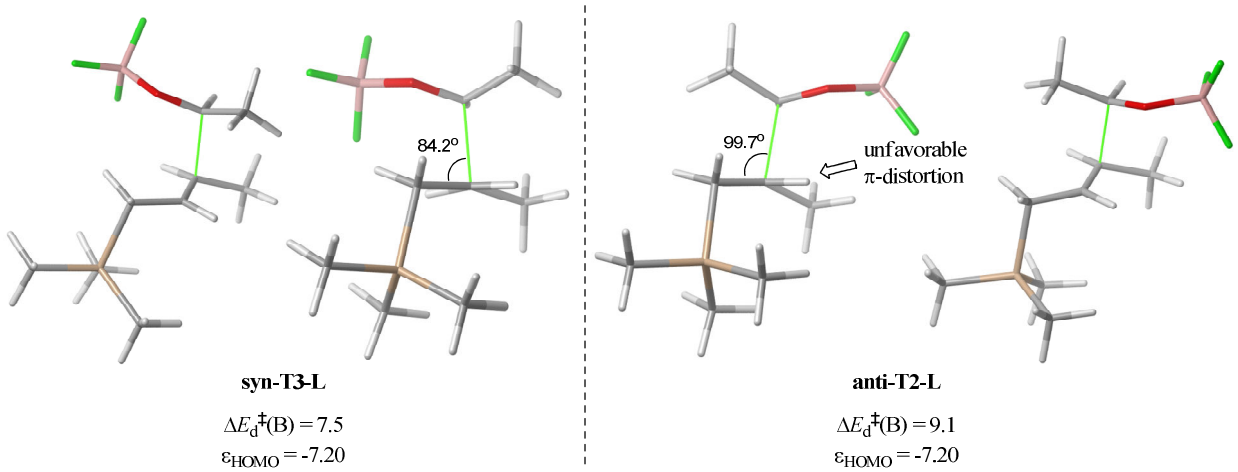

Figure 39. Transition states for **syn-T3-L** and **anti-T2-L** from the perspective of the internuclear axis of the C-C bond of the alkene from the silylmethylene bound carbon.

6.8. Which Orbital Interactions Favor Synclinal Over Antiperiplanar Transition States?

The origin of the enhanced orbital interactions present in synclinal transition state **syn-T3** compared to **anti-T1** or **anti-T2** compared to **syn-T1** has not yet been fully addressed. The contribution of SOI's involving an in-phase interaction between the oxygen of the aldehyde and the silylmethylene carbon was ruled out because of insignificant energetic contributions.

A reasonable alternative for the enhanced orbital overlap could be differential primary $\pi \rightarrow \pi^*$ interactions. The differences in the orbital overlap of the FMO's can be seen qualitatively from Figure 40. The distorted FMO's for **syn-T3-L** (a) and **anti-T1-L** (b) as well as the corresponding transition state HOMO's are shown. The HOMO's of the crotylsilane are very similar for both **syn-T3-L** and **anti-T1-L**. The major difference is the approach of the aldehyde. The portion of the electrophile LUMO localized on the carbonyl carbon in **syn-T3-L** is directed inward, toward the alkene π-system because of the tilted approached of the aldehyde. The corresponding portion of the electrophile LUMO localized on the carbonyl carbon in **anti-T1-L** is directed away from the alkene π-system. The requirement for a Burgi-Dunitz approach angle imposes additional geometrical constraints in antiperiplanar transition states that diminsh overlap of the carbonyl carbon with the internal alkene carbon relative to synclinal transition states. The difference in overlap is also borne out by inspection of the transition state HOMO's. The overlap between the aldehyde carbon and the alkene π-system of the crotylsilane is more centered while that for **anti-T1-L** is more off-centered which may be expected to translate to a decreased overlap energy for **anti-T1-L**.

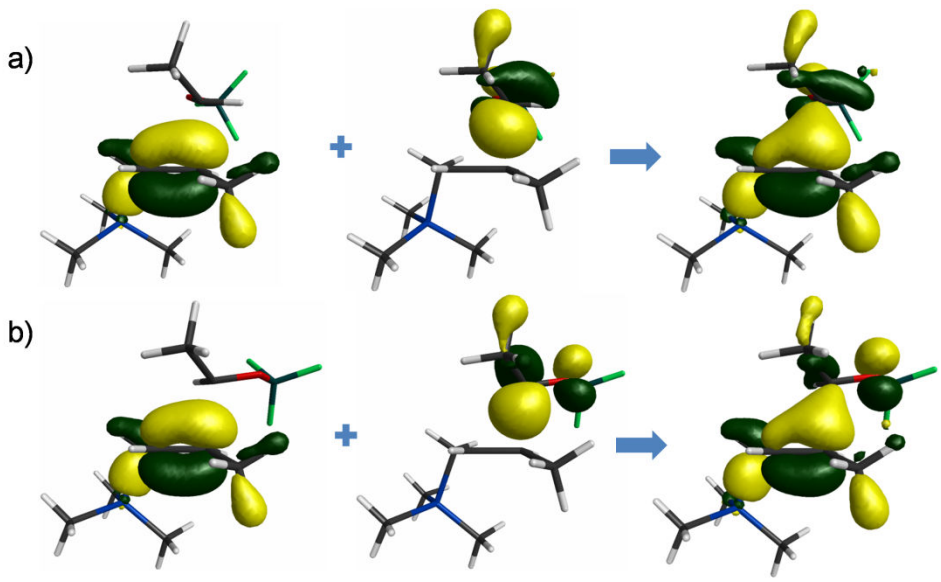

Figure 40. Distorted HOMO of crotylsilane, distorted LUMO of crotylsilane and transition state HOMO for a) **syn-T3-L** and b) **anti-T1-L**. The HOMO's and LUMO's have values of isodensity = 0.06 while the transition state HOMO's have an isodensity = 0.05.

The π→π* interaction of interest can be quantified using second order perturbation theory through an NBO analysis. The separation of the reactants in the transition state is too small to accurately quantify this interaction using the NBO localization scheme. Thus, the π→π* interaction was quantified at earlier points along the reaction coordinate for each pathway (**syn-T3-L** and **anti-T1-L**), where extensive orbital polarization and mixing has not yet taken place, to approximate the π→π* interaction difference at the transition state (Figure 12). Graph a) is a plot of the energy difference ($\Delta\Delta E_{\pi\rightarrow\pi^*}$) between the π→π* interaction for **syn-T3-L** and **anti-T1-L** respectively. The energy difference increases to $\Delta\Delta E_{\pi\rightarrow\pi^*}$ = 5.3 kcal/mol as the distance approaches $d_{c\text{-}c}$ = 2.28Å. The energy difference also favors **syn-T3-L** upon comparison as a function of distortion (Figure 12, graph b). The energy difference $\Delta\Delta E_{\pi\rightarrow\pi^*}$ is approximated to be 6.0 kcal/mol, favoring **syn-T3-L**, at a distortion level of ΔE_d = 11.0 kcal/mol based on linear fits of the two curves. Thus, as a function of both distance and distortion, the **syn-T3-L** pathway exhibits a greater π→π* interaction energy than the **anti-T1-L** pathway. Similar conclusions can be drawn when comparing synclinal **anti-T2-L** to antiperiplanar **syn-T1-L**.

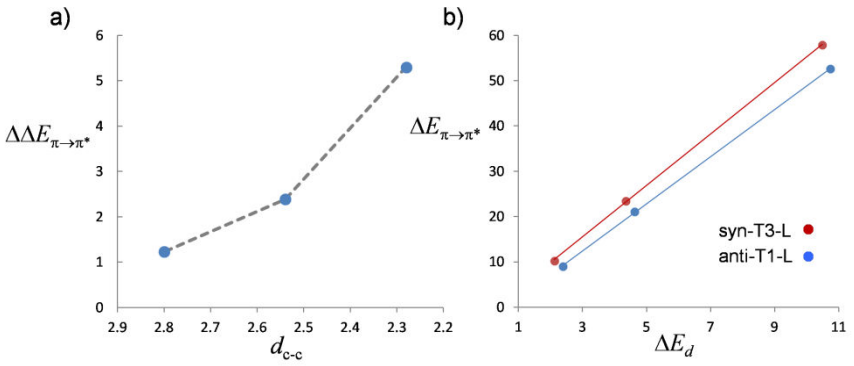

Figure 41. a) $\Delta\Delta E_{\pi\rightarrow\pi^*}$ (kcal/mol) = $\Delta E_{\pi\rightarrow\pi^*}$(**syn-T3-L**) – $\Delta E_{\pi\rightarrow\pi^*}$(**anti-T1-L**) and is plotted versus $d_{c\text{-}c}$ (Å). b) $\Delta E_{\pi\rightarrow\pi^*}$ (kcal/mol) as a function of the distortion energy ΔE_d (kcal/mol).

In conclusion, the enhanced orbital interactions in synclinal versus antiperiplanar transition states is attributed to increased primary π→π* interactions. This greater overlap can be explained by the tilted trajectory of the activated aldehyde in synclinal transition states which directs the aldehyde LUMO toward the center of the π system of the crotylsilane. Moreover, the geometrical mandates of the Burgi-Dunitz approach trajectory prevent the aldehyde in antiperiplanar transition states to engage in additional overlap between the carbonyl carbon and the internal alkene carbon atom resulting in diminished overall orbital overlap relative to synclinal transition states.

6.9. Summary and Conclusions.

The diastereoselectivity in the additions of nucleophilic π-systems to aldehydes and ketones that proceed through open transition states has historically been challenging to rationalize because strong, directionality-controlling interactions are absent. In this study, the origin of diastereoselectivity in the crotylation of acetaldehyde has been examined by energy decomposition based theoretical methods. The BF_3-promoted crotylation reaction is complicated by potential reversible carbon-carbon bond formation. Alternative Lewis acids, $TiCl_4$, exhibited a higher barrier to reversion ameliorating concerns about and might account for higher, experimentally observed diastereoselectivities.

Under electrophilic activation (BF_3 and Brønsted acid), the syn diastereomer is obtained experimentally with high selectivity and that selectivity is reproduced in these calculations. In particular, the preferred pathway proceeds via (–)-synclinal transition state **syn-T3** for both activation modes. Under nucleophilic activation (fluoride), the anti diastereomer is observed

experimentally and is also found computationally. However, unlike in the electrophilic activation modes, the antiperiplanar transition states are preferred.

The most informative transition state comparisons (from the data in Tables 21 and 22) illustrated in Figure 40.

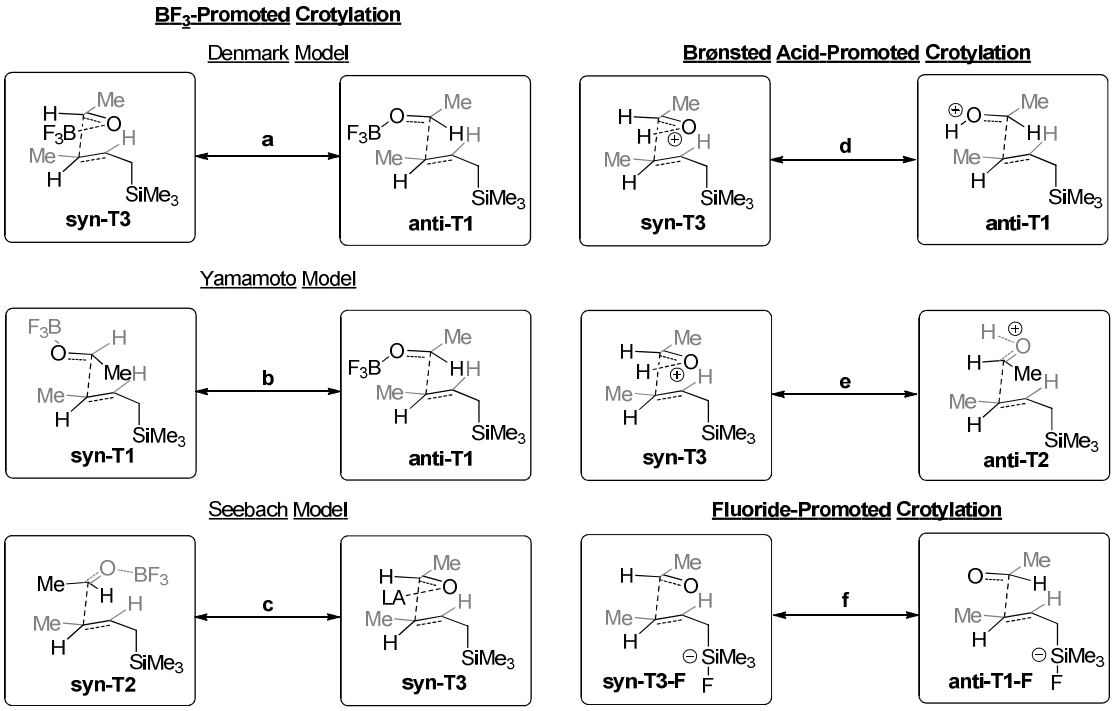

Figure 42. Most relevant transition state comparisons for crotylation of aldehydes.

The comparisons of the transition state illustrated in Figure 40 are summarized as follows (the letters beginning each paragraph correspond to the letters labeling the comparisons in Figure 40):

(a) The observed syn diastereoselectivity in the BF_3-promoted pathway arises from the energetic preference for **syn-T3** compared to **anti-T1.** Transition state **syn-T3** is favored electrostatically and through orbital interactions but disfavored sterically relative to **anti-T1**. The preferred orbital interactions for **syn-T3** can be accounted for by favorable orbital overlap conducive to greater charge transfer since the orbital energy difference of the separated reactants is identical in the two transition states ($\Delta\Delta_L$=0). The reader should make careful note that these two transition states correspond precisely to the synclinal and antiperiplanar transition states evaluated in the Denmark model system **A**, Scheme 30. The computationally validated discovery

that these two limiting transition states are actually those most relevant to acyclic stereoselection provides a highly satisfying vindication of the significance of that model system. At the time of its disclosure in 1983, the model was heavily criticized as being flawed because it did not compare the synclinal and antiperiplanar transition states that were believed to be relevant in acyclic systems (see (b) below).

(b) The reigning dogma in the field of allylmetal aldehyde additions[136f] posited that the diastereoselectivity could be explained by the difference in energy of the limiting antiperiplanar transition states on the basis of steric considerations. The calculated results suggest otherwise as the lower energy antiperiplanar transition state (**anti-T1**) leads to the anti diastereomer ($\Delta\Delta E^{\ddagger}_{(\textbf{anti-T1-L} - \textbf{syn-T1-L})}$ = –3.0 kcal/mol; $\Delta\Delta E^{\ddagger}_{(\textbf{anti-T1-H} - \textbf{syn-T1-H})}$ = –1.7 kcal/mol), not the observed syn diastereomer under electrophilic activation. Although the steric contribution to these transition states does indeed favor **syn-T1-L** ($\Delta\Delta E_{\text{ste}}{}^{\ddagger}_{(\textbf{syn-T1-L} - \textbf{anti-T1-L})}$ = –7.8 kcal/mol), this preference does not compensate for the additional contribution from the electrostatic ($\Delta\Delta E_{\text{es}}{}^{\ddagger}_{(\textbf{anti-T1-L} - \textbf{syn-T1-L})}$ = –4.4 kcal/mol) and orbital interactions ($\Delta\Delta E_{\text{orb}}{}^{\ddagger}_{(\textbf{anti-T1-L} - \textbf{syn-T1-L})}$ = –5.5 kcal/mol) that favor **anti-T1-L.** The origin of the lesser electrostatic and orbital interaction energies for the sterically favored **syn-T1-L** transition state can be ascribed to the greater π-distortion of the crotylsilane component present in **syn-T1-L** (Figure 41). Compared to **anti-T1-L**, the energy required to distort the crotylsilane component is higher ($\Delta\Delta E_{\text{orb,d}}{}^{\ddagger}_{(\textbf{syn-T1-L} - \textbf{anti-T1-L})}$ = 2.4 kcal/mol) and causes an unfavorable alignment of the primary orbitals in the individual components, thus reducing the stabilizing interactions. Similar conclusions are reached by comparing the analogous Brønsted acid transition states (**anti-T1-H** and **syn-T1-H**) albeit with a lesser magnitude.

The greater distortion in transition state **syn-T1-L** arises from the attempted avoidance of steric interactions between the aldehyde methyl group and the silylmethylene group. However, this causes a tilt that leads to an unfavorable compression between the methyl group of the crotylsilane and the BF_3 unit. Because of this second compression, a favorable orbital alignment cannot be achieved thus accounting for the considerable orbital interaction and electrostatic energy difference. In transition state **anti-T1-L**, the distortion arises from avoidance of the steric interactions between the aldehyde and crotylsilane methyl groups. However, in this case, that interaction causes a tilt that compresses the two gauche hydrogens and the BF_3 unit thus

requiring less distortion to achieve transition state. This tilt is easily seen in the acute dihedral angle between the silylmethylene (C-C) bond and the forming sigma bond (Figure 41).

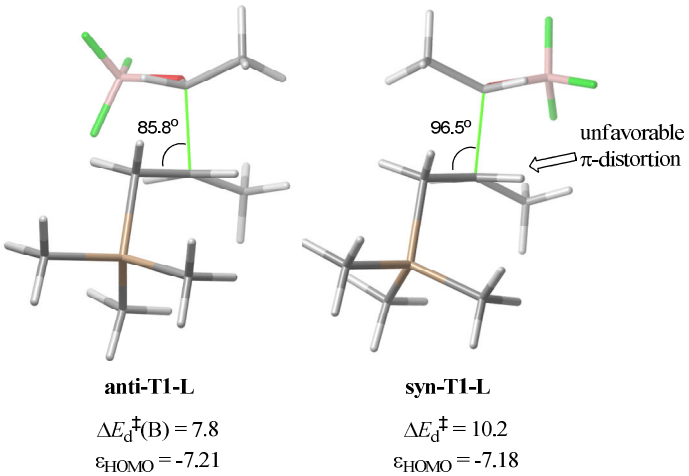

Figure 43. Transition states for **anti-T1-L** and **syn-T1-L** from the perspective of the internuclear axis of the C-C bond of the alkene from the silylmethylene bound carbon.

(c) According to the empirical rules developed by Seebach (Scheme 27),[131] either the **syn-T2** or the **syn-T3** transition states should be the most favored for these reactions (depending upon whether Rule iii or Rule iv is dominant). Interestingly, these two transition states are very close in energy ($\Delta\Delta E^{\ddagger}_{(\textbf{syn-T3-L} - \textbf{syn-T2-L})}$ = –0.7 kcal/mol; $\Delta\Delta E^{\ddagger}_{(\textbf{syn-T3-H} - \textbf{syn-T2-H})}$ = –1.0 kcal/mol) and are both lower in energy than the lowest energy transition states leading to the anti diastereomer. It is interesting to note that at the transition states, both **syn-T3-L** and **syn-T3-H** exhibit less favorable interaction energies as compared to **syn-T2-L** and **syn-T2-H** and it is the lower distortion energies that cause the **syn-T3** transition states to be energetically favorable overall. The lower degree of distortion in **syn-T3** is manifested in lower steric and orbital interactions in **syn-T3-L** ($\Delta\Delta E_{ste,d}$ = -2.6 kcal/mol; $\Delta\Delta E_{orb,d}$ = -1.4 kcal/mol) and mostly orbital interactions in **syn-T3-H** ($\Delta\Delta E_{orb,d}$ = -1.5 kcal/mol) (Table 2). Thus, the modest preference for **syn-T3-L** arises from the significantly lower steric repulsion energy that more than compensates for slightly unfavorable electrostatic and orbital interaction energies.

(d) and (e) The observed syn diastereoselectivity in the Brønsted acid-promoted pathway arises from the energetic preference for **syn-T3** compared to **anti-T1** and **anti-T2**. In this case **anti-T2-H** is a more important contributor to this pathway than **anti-T2-L** is to the BF_3 promoted pathway. This change is a consequence of the lesser steric interactions between the H^+

on the aldehyde oxygen and the methyl group of the crotylsilane compared to the same interaction of the BF_3 moiety in **anti-T2-L.** The rationalization for the preference of **syn-T3-H** compared to **anti-T1-H** is similar to that for the comparison made in (a).

Transition state **syn-T3-H** is favored over **anti-T2-H** mostly through orbital interactions that are accounted for through a decreased frontier orbital energy difference in the separated reactants rather than an enhanced spatial orbital overlap (Table 23). The orbital energy separation may be a result of unfavorable distortion arising from the steric interaction between the aldehyde methyl group and the crotylsilane methylene group (Figure 39). These conclusions are similar to those drawn from the discussion of SOIs (Section 6.7).

(f) The observed anti diastereoselectivity in the fluoride-promoted pathway arises from the energetic preference for **anti-T1-F** compared to **syn-T1-F.** The basis for this preference mirrors the analysis for the energetic differences between the antiperiplanar transition states in the electrophilically activated additions (b). An interesting comparison can be made between **anti-T1-F** and **syn-T3-F** because the latter is close in energy to **syn-T1-F** and is favored in both electrophilic activation modes. Whereas synclinal transition structure **syn-T3-F** does exhibit increased charge transfer and orbital interactions, the electrostatic repulsion between the negatively charged oxygen atom and the negatively charged silylmethylene group in **syn-T3-F** offsets the stabilizing effects from increased orbital interactions and charge transfer. Thus, the repulsion in transition state **syn-T3-F** leads to an overall energetic preference for antiperiplanar transition structure **anti-T1-F**. This conclusion is supported by the experimentally observed preference for the **anti-T1-F** transition state in model system **A** (Scheme 4).

The results of this investigation can be extended to the qualitative design or rationalization of systems for the addition of other π-donors including enamines, silyl enol ethers, or silyl ketene acetals, to aldehydes, nitroalkenes or other π-acceptors.

Chapter 7: *Experimental Section*

7.1. General Experimental.

All reactions were performed in oven-dried (145 °C) or flame-dried glassware under an inert atmosphere of dry N_2. Reaction solvents THF (Fisher, HPLC grade), Et_2O (Fisher, BHT stabilized ACS grade) and methylene chloride (Fisher, unstabilized HPLC grade) were dried by percolation through two columns packed with neutral alumina under a positive pressure of argon. Reaction solvents hexane (Fisher, OPTIMA grade) and toluene (Fisher, ACS grade) were dried by percolation through a column packed with neutral alumina and a column packed with Q5 reactant, a supported copper catalyst for scavenging oxygen, under a positive pressure of argon. Reactions were carried out at the temperature indicated (internal temperature) as measured by an internal thermocouple device unless otherwise indicated. Parallel synthesis was performed on a Buchi Synchor reactor fittet with a 96 well block and a standard Argon/vacuum manifold.

Column chromatography was performed using Merck grade 9385, 60 Å silica gel. Visualization was accomplished by UV light, ceric ammonium molybdate (CAM), potassium permanganate (KmnO4), sulfuric acid (H_2SO_4), ceric ammonium nitrate (CAN), or iodine (I_2) as indicated. Analytical and preparative thin-layer chromatography was performed on Merck silica gel plates with F-254 indicator. Distillations were performed using a short-path with a 3 cm, Vigreux column. Bulb-to-bulb distillations were conducted using a Buchi GKR-50 Kugelrohr apparatus at the pressure specified and air bath temperature (ABT).

^{1}H NMR and ^{13}C NMR spectra were acquired at 500 MHz and 126 MHz respectively and referenced to residual solvent ($CHCl_3$ at 7.26 (^{1}H) and 77.00 (^{13}C) or MeOH (3.31 (^{1}H), 49.00 (^{13}C) ppm). Assignments were obtained by reference to COSY and HETCOR and DEPT(135) correlations. Chemical shifts are reported in ppm ; multiplicities are indicated by s (singlet), d (doublet), t (triplet), q (quartet), p, (pentet), m (multiplet) and br (broad). Coupling constants, *J,* are reported in Hertz. Mass Spectrometry was performed by the University of Illinois Mass Spectrometer Center. EI mass spectra were performed on a 70-VSE spectrometer. CI mass spectra were performed on a 70-VSE-B spectrometer with methane as the carrier gas. ESI mass spectra were performed on a Waters Q-Tof Ultima instrument. Data are reported in the form of *m/z* (intensity relative to base peak = 100). Infared spectra (IR) were recorded on a Mattson Galaxy 5020 spectrophotometer using NaCl plates. Peaks are reported in cm^{-1} with indicated

relative intensities: s (strong, 67-100%); m (medium, 34-66%); w (weak, 0-33%). Analytical capillary gas chromatography (GC) was performed using a gas chromatograph fitted with a flame ionization detector (H_2 carrier gas, 1 mL/min). GC Method 1: Injections were made onto a Hewlett-Packard HP-5 50-m cross-linked 5%-phenyl methyl silicone gum phase column. The detector temperature was 300 °C. The column temperatures was maintained at 140 ^oC isotherm over 20 min then ramped to 250 ^oC over 10 min. Analytical high pressure liquid chromatography (HPLC) was performed using a Hewlett Packard 1090L Chromatograph equipped with a variable wavelength diode array detector and an autosampler. The chromatograph was equipped with a reverse phase Phenomenex Luna C18(2) column (3μm, 4.6x150mm, lampcurrent = 1). Method 1: Linear Gradient; flow rate = 1.0 mL/min, λ = 254 nm, solvent = CH_3CN/H_2O (30/70) to CH_3CN/H_2O (90/10) over 10 min, then isocratic for 7 min. A 3 min re-equilibration time was utilized between runs. The water eluent contained 0.1% v/v acetic acid. Chiral Stationary phase HPLC (CSP-HPLC) Method 1: *R,R*-Welk-O, 1.0 mL/min, IPA/Hexanes 5:95. Analytical supercritical fluid chromatography (SFC) was performed on a Berger Instruments SFC with spectrophotometric detector (220 nm) using Daicel Chiralpak AD, AS, OD, OJ, and Welk-O columns. Optical rotations were measured in Fischer Optima grade EtOH, MeOH and CH_2Cl_2 and are reported as follows: concentration (c = g/dL), and solvent. Melting points were conducted in vacuum-sealed glass tubes using a Thomas-Hoover Uni-Melt™ melting point apparatus and are corrected.

7.2. Literature Procedures

The following compounds were synthesized following the published procedures: Ethyl pent-4-enoate, 4-penten-1-ol, 1-bromomethylnaphthalene, 2-bromomethylnaphthalene, 9-bromomethylanthracene, *N,N,N,N*-tributyl-(1-benzyl) quaternary ammonium bromide, Phenylselenenyl chloride, (*E*)-methyl 6-hydroxyhex-2-enoate (*E*-**6**), tert-butyl 2-(diphenylmethyleneamino) acetate (**25**), dichlorotitanium diisopropoxide, (1*S*,3*R*,5a*S*,7a*S*,7b*R*)-Octahydro-1-[*N*-(3,5-dinitrophenyl)carbamoxy]-7b-methyl-*2H*-cyclopenta**[*gh*]pyr**rolizin-2-one.

7.3. Experimental Procedures for Chapter 2

7.3.1. Tandem Cycloaddition Precursors and Scaffolds

Scale up of Alcohol (*Z*)-6. Preparation of Trimethyl(4,5,6,7-tetrahydrooxepin-2-yloxy)silane (10)

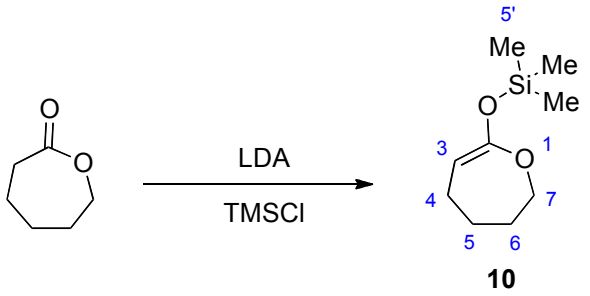

10

A jacketed 500-mL, three-necked, liquid addition flask fitted with a a nitrogen inlet adaptor, and two rubber septa was fitted to a 1-L, two-necked, round-bottomed flask fitted with a magnetic stir bar, a rubber septum and an internal temperature probe (through rubber septum). To the addition flask was added diisopropylamine (36.5 mL, 209 mmol, 1.3 equiv) and THF (300 mL). The resulting solution was cooled to -78 ^{o}C (bath temp) by addition of an acetone/$CO_{2(s)}$ bath to the jacket reservoir. Then, *n*-butyllithium (2.56 M in hexanes, 81.8 mL, 1.3 equiv) was added dropwise over 20 min. To the 1-L, two-necked, flask was added ε-caprolactone (18.4 g, 161 mmol), THF (150 mL) and trimethylsilyl chloride (26.5 mL, 209 mmol, 1.3 equiv) via syringe. The reaction vessel was brought to < -80 ^{o}C by immersion in a hexanes/N_2 bath. The freshly generated solution of LDA (above) was added dropwise at a rate that maintained an internal temperature < –75 ^{o}C (ca. 1 h). The resulting turbid solution was allowed to warm to –25 ^{o}C, and was then concentrated by rotary evaporation (15 mm Hg, 20-25 ^{o}C). The resulting mixture was triturated with pentane (~100 mL) and filtered (Celite). The filtrate was again concentrated by rotary evaporation (15 mm Hg, 20-25 ^{o}C). Purification by distillation (0.5 mm Hg, 43 ^{o}C) afforded ketene acetal **10** (24.8 g, 83%) as a clear colorless oil.

Data for **10**:

bp: 58-60 ˚C / 2-3 torr

^{1}H-NMR: (500 MHz, $CDCl_3$)

4.12 (t, *J* = 5.9, 1 H, HC(3)), 3.99 (dd, *J* = 5.4, 5.6, 2 H, $H_2C(7)$), 2.02 (dd, *J* = 5.9, 11.6, 2 H, $H_2C(4)$) 1.83 (ddd, *J* = 5.7, 10.7, 11.5, 2 H, $H_2C(6)$), 1.65-

1.59 (m, 2 H, $H_2C(5)$), 0.22 (s, 9 H, $H_3C(5')$)

^{13}C-NMR: (126 MHz, $CDCl_3$)

160.0 (C(2)), 83.1 (C(3)), 71.5 (C(7)), 31.3 (C(4)), 26.2 (C(6)), 23.3 (C(5)), 0.16 (C(5'))

IR: (neat, NaCl plate)

2931 (s), 2837 (m), 1682 (s), 1455 (m), 1355 (m)

MS: (ESI, Q-tof)

187 (21) [M+1], 171 (38), 147 (14), 132 (12), 129 (13), 117 (30), 75 (100), 69 (32), 55 (23), 54 (23)

TLC: R_f 0.77 (hexanes/Et_2O, 4:1) [UV, $KmnO_4$]

Palladium Catalyzed Oxidation Silyl Ketene Acetal 10. Preparation of 6,7-dihydro-5*H*-oxepin-2-one (8).

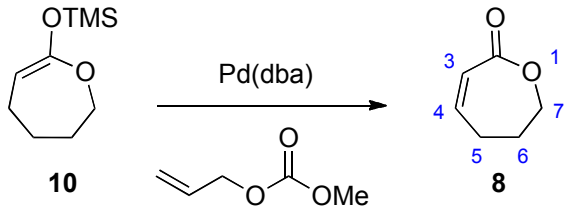

To a 1.0-L, one-necked, round-bottomed flask fitted with a reflux condenser, a magnetic stir bar, and a nitrogen inlet adapter, fitted with a rubber septum, was added sequentially, palladium(0)bisdibenzylideneacetone (309 mg, 0.537 mmol, 0.01 equiv), allyl methyl carbonate (12.2 mL, 107 mmol, 2.0 equiv), and acetonitrile (268 mL). Silyl ketene acetal **10** (1.0 g, 21.5 mmol) was then added via syringe. The resulting solution was placed in an oil bath pre-heated to 40^{o}C and allowed to stir. After being stirred for 30 min at 40 ^{o}C, the reaction mixture was removed from the oil bath and allowed to cool to room temperature. The solution was concentrated to approximately one-quarter of the total volume (~70 mL). This solution was passed through a plug of silica gel (20mm x 5 cm) using hexanes/Et_2O (1:4, 3 x 50 mL). The filtrate was concentrated by rotary evaporation (15 mm Hg, 20-25^{o}C) to afford 5.13 g (97%) of **8** as a pale-yellow oil. This material is carried on to the next step without further purification.

Data for **8**:

bp: 70 ^{o}C @ 0.1 mm Hg

^{1}H-NMR: (500 MHz, $CDCl_3$)

6.41 (td, J = 4.4, 12.1, 1 H, HC(4)), 5.98 (d, J = 12.4, 1 H, HC(3)),4.28 (m, 2 H, H_2C(7)), 2.50 (dd, J = 5.4, 10.2, 2 H, H_2C(5)), 2.12 (td, J = 6.6, 12.9, 2 H, H_2C(6))

^{13}C-NMR: (126 MHz, $CDCl_3$)

169.2 (C(2)), 144.0 (C(4)), 121.9 (C(3)), 67.3 (C(7)), 30.1 (C(5)), 27.0 (C(6))

TLC: R_f 0.20 (pentane/MTBE, 1:1) [$KMNO_4$]

Methanolysis of ε-Caprolactenone 8. Preparation of (*Z*)-Methyl 6-Hydroxy-2-hexenoate ((*Z*)-6)

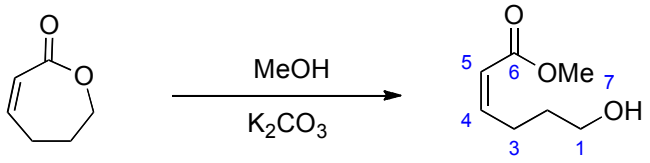

8 (*Z*)-**6**

To a 100-mL, one-necked, round-bottomed flask fitted with a rubber septum, a large a magnetic stir bar, and a nitrogen inlet adaptor, was added ester **8** (4.5 g, 40.1 mmol) *via* syringe. Methanol (80 mL) was then added followed by potassium carbonate (554 mg, 4 mmol, 0.1 equiv). The suspension was stirred vigorously for 20 min, during which the solution gradually became opaque. The resulting suspension was poured into a 500-mL separatory funnel containing water (100 mL) and diluted with dichloromethane (100 mL). The layers were separated and the aqueous was extracted with dichloromethane (5 x 50 mL). The combined organic extracts were dried ($MgSO_4$), filtered (cotton plug), and concentrated *via* rotary evaporation (15 mm Hg, 20-25 ^{o}C). The resulting clear oil was filtered through a small plug of silica gel (1.8 cm x 2 cm) with 25 mL EtOAc to remove any remaining base impurities. Concentration of the resulting solution yielded 5.19 g (89%) of geometrically pure (Z)-6 as determined by ^{1}H-NMR analysis.

Data for (Z)-6:

^{1}H-NMR: (500 MHz, $CDCl_3$)

6.24 (td, J = 8.3, 11.5, 1 H, HC(4)), 5.87 (td, J = 1.4, 11.5, 1 H, HC(5)), 3.72 (s, 3 H, H_3C(7)), 3.61 (t, J = 5.9, 2 H, H_2C(1)), 2.74 (dt, J = 1.4, 8.2, 2 H, H_2C(C(3)), 1.73 (td, J = 8.3, 11.5, 1 H, H_2C(2))

^{13}C-NMR: (126 MHz, $CDCl_3$)

167.5 (C(6)), 149.8 (C(4)), 120.2 (C(5)), 61.1 (C(1)), 51.3 (C(7)), 31.2 (C(2)), 25.1 (C(3))

IR: (neat)

3423 (br), 2950 (m), 2870 (m), 2343 (w), 2361 (w), 1723 (s), 1645 (m), 1439 (s), 1408 (m), 1202 (s), 1173 (s)

MS: (ESI, Q-tof)

167(100), 145(35), 127(15)

TLC: R_f 0.22 (hexanes/EtOAc, 4:1) [UV, $KmnO_4$]

A. Preparation of Nitroalkenes (*E,Z*)-1 and (*E,E*)-1. Preparation of Methyl (2*Z*,6*E*)-7-Nitro-2,6-octadienoate ((*E,Z*)-1)

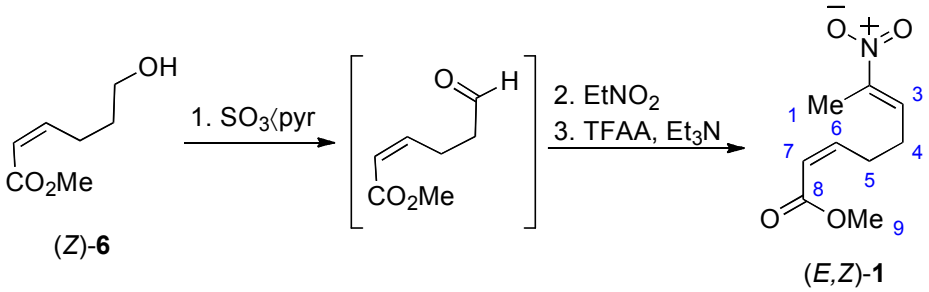

(*Z*)-**6** (*E,Z*)-**1**

To a 500-mL, two-necked, round-bottomed flask fitted with a rubber septum and a nitrogen inlet adaptor was added alcohol (Z)-6 (3.0 g, 20.8 mmol) along with CH_2Cl_2 and DMSO (100 mL each). Triethylamine (17.4 mL, 125 mmol, 6.0 equiv) was added and the flask was immersed in a ice/NaCl(s) bath. Once the internal temperature reached –5 °C, SO_3•pyridine complex was added in a single portion (5.5 g, 31 mmol, 1.5 equiv). After two hours at < 0 °C an additional portion of SO_3•pyridine complex (5.5 g, 31 mmol, 1.5 equiv) was added. After another 2 h the reaction was quenched by pouring into a 500-mL separatory funnel containing 100 mL sat. aq. NH_4Cl. The organic phase was diluted with another 100 mL of CH_2Cl_2 and rinsed with NH_4Cl (3 x 50 mL) followed by $CuSO_4$ (1 x 50 mL), brine (100 mL) and H_2O (100 mL). The combined organic extracts were dried ($MgSO_4$), filtered over a silica gel plug (3 x 1 cm) and concentrated to afford 2.98 g (89%) of crude intermediate aldehyde as a light-yellow oil. The aldehyde was carried on directly to nitroalkene (E,Z)-1 without further purification as previously described.[183]

Data for (E,Z)-1:

^{1}H-NMR: (500 MHz, $CDCl_3$)

7.10 (t, J = 7.8, 1 H, HC(3)), 6.19 (dd, J = 8.2, 10.9, 1 H, HC(6)), 5.85 (d, J = 11.4, 1 H, HC(7)), 3.70 (s, 3 H, H_3C(9)), 2.84 (dq, J = 1.6, 7.6, 2 H, H_2C(4)), 2.38 (m, 2 H, H_2C(5)), 2.16 (s, 3 H, H_3C(1))

^{13}C-NMR: (126 MHz, $CDCl_3$)

166.4 (C(8)), 147.1 (C(2)), 134.6 (C(6)), 121.1 (C(3)), 51.2 (C(7)), 27.3 (C(9, 1)), 12.5 (C(4,5))

IR: (neat)

3054 (w), 2987 (w), 2954 (w), 2254 (m), 1719 (s), 1650 (m), 1521 (s), 1440 (m)

MS: (EI, 70eV)

197 (5), 182 (12), 168 (25), 150 (42), 149 (45), 93 (100), 91

TLC: R_f 0.57 (hexanes/EtOAc, 4:1) [UV, $KmnO_4$]

Preparation of Methyl (2*E*,6*E*)-7-Nitro-2,6-octadienoate ((*E,E*)-1)

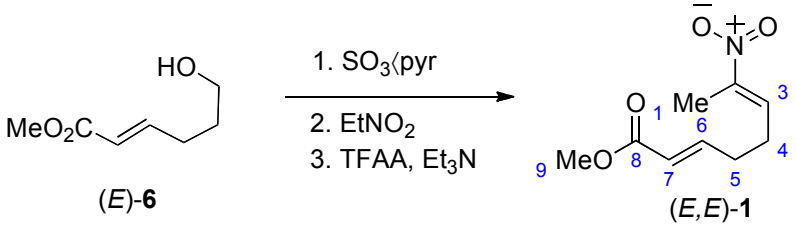

(*E*)-**6** (*E,E*)-**1**

To a 1-L, three-necked, round-bottomed flask fitted with two rubber septa and a nitrogen inlet adaptor and an internal temperature probe (through a septum) was added alcohol (*E,E*)-**6** (21 g, 147 mmol) along with CH_2Cl_2 and DMSO (147 mL each). Triethylamine (12 mL, 874 mmol, 6.0 equiv) was added and the flask was immersed in a ice/NaCl(s) bath. Once the internal temperature reached –5 ^{o}C, SO_3•pyridine complex was added in a single portion (29.4 g, 184 mmol, 1.25 equiv). After two hours at < 0 ^{o}C an additional portion of SO_3•pyridine complex (29.4 g, 184 mmol, 1.25 equiv) was added. After another 2 h the reaction was quenched by pouring into a 1-L separatory funnel containing 200 mL sat. aq. NH_4Cl. The organic phase was diluted with 150 mL of Et_2O and rinsed with NH_4Cl (3 x 100 mL) followed by $CuSO_4$ (2 x 100 mL), brine (100 mL) and sat. aq, $NaHCO_3$ (100 mL). The combined organic extracts were dried

($MgSO_4$), filtered over a silica gel plug (3 x 1 cm) and concentrated to afford the crude aldehyde (*E*)**-7** as a light-yellow oil. The aldehyde was carried on directly to the nitroalkene without further purification as previously described to give 22.9 g (80%) of nitroalkene (E,E)-1 as a light-yellow oil. The data collected was consistent with that previously reported.

Data for (E,E)-1:

^{1}H-NMR: (500 MHz, $CDCl_3$)

7.14 (t, J = 7.7, 1 H, HC(6)), 6.19 (td, J = 11.4, J = 7.6, 1 H, HC(3)), 5.85 (d, J = 11.9, 1 H,HC(2)), 3.70 (s, 3 H, H_3C(9)), 2.85 (m, 2 H), 2.38 (m, 2 H), 2.16 (s, 3 H, H_3C(8)).

^{13}C-NMR: (126 MHz, $CDCl_3$)

166.5 (C(8)), 148.4 (C(2)), 146.2 (C(6)), 133.9 (C(3)), 122.5 (C(7)), 51.6 (C(9)), 26.5 (C(4)), 22.4 (C(5)), 12.6 (C(1))

IR: (neat)

2992 (w), 2953 (w), 2843 (w), 2255 (m), 1721 (s), 1662 (m), 1523 (s), 1438 (m), 1391 (m), 1334 (s), 1284 (m), 1213 (m), 1173 (m), 1042 (w), 971 (w), 906 (s)

TLC: R_f 0.6 (hexanes/EtOAc, 4:1) [UV, $KMnO_4$]

Preparation of (1*S*,3*R*,5a*S*,7a*S*,7b*R*)-Octahydro-1-hydroxy-7b-methyl-2*H*cyclopenta[*gh*] pyrrolizin•Borane (17a)

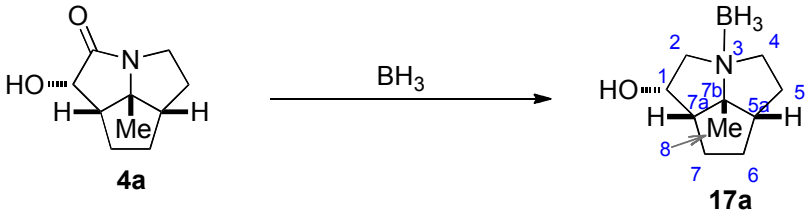

To a 50-mL, two-necked, round-bottomed flask fitted with a rubber septum, a nitrogen inlet adaptor, a magnetic stir bar and an internal temperature probe (inserted through a rubber septum) was added lactam **4a** (181 mg, 1.0 mmol) and THF (1 mL). The flask was cooled to 0 ºC in an ice bath, and BH_3•THF complex (5.0 equiv, 1.0 M solution, 5 mL) was added dropwise over 10 min (bubbling observed). The cooling bath was removed and the resulting clear solution was stirred for 2 h. The reaction was quenched by the addition of 20 mL of MeOH and the

mixture was concentrated by rotary evaporation (15 mm Hg, 20-25 ^{o}C). This process was repeated three more times to afford the crude product as a white solid. Purification by silica gel column chromatography ((2 cm x 7 cm), hexanes/EtOAc, 95:5, 85:15, 3:1, 150 mL each) afforded ~185 mg of **17a**. Recrystallization from hexanes/MTBE (5:1) afforded 175 mg (96%) of the borane complex **17a** as white needles.

Data for **17a**:

mp: 164-165˚C (MTBE/hexanes)

^{1}H-NMR: (500 MHz, $CDCl_3$)

4.75 (dd, *J* = 8.1, 15.3, 1 H, HC(1)), 3.44 (dd, *J* = 6.5, 10.9, 1 H, HC(2)), 3.28 (ddd, *J* = 2.5, 6.7, 12.1, 1 H, HC(4)), 3.16 (dt, *J* = 6.6, 11.7, 1 H, HC(4)), 3.03 (m, 1 H, HC(2)), 2.39 (m, 2 H HC(5a), HC(7a)), 2.07-2.00 (m, 1 H, HC(7)), 1.99-1.90 (m, 1 H, HC(6)), 1.89-1.73 (m, 2 H, HC(6), HC(5)), 1.74-1.58 (M, 2 H, HC(7), HC(5)), 2.10-1.25 (s, broad, 3 H, H_3B), 1.48 (s, 3 H, H_3C(8))

^{13}C-NMR: (126 MHz, $CDCl_3$)

87.8 (C(7b)), 69.4 (C(1)), 66.0 (C(2)), 63.1 (C(4)), 55.1 (C(7a)), 53.1 (C(5a)), 32.1 (C(5)), 28.0 (C(7)), 26.4 (C(6)), 25.2 (C(8))

IR: (NaCl plate, film)

3018 (m), 2969 (m), 2872 (w), 2367 (m), 2363 (m), 2333 (m), 2276 (w), 1215 (s)

MS: (ESI, Q-tof)

180 (42), 167 (21), 152 (100), 96 (59)

Opt. rot.: $[\alpha]_D^{24}$ -1.74^{o} (c = 1.0, CH_2Cl_2)

TLC: R_f 0.33 (hexanes/EtOAc, 3:1) [I_2]

Analysis: $C_{10}H_{20}BNO$ (181.08)

Calcd:	C, 66.33;	H, 11.13;	N, 7.73
Found:	C, 66.05;	H, 10.95;	N, 7.52

Preparation of Scaffold for Library IV.

Preparation of (3*R*,5a*S*,7a*S*,7b*R*)-Octahydro-7b-methyl-2*H*cyclopenta[*gh*]pyrrolizin-1-one ●Borane (19)

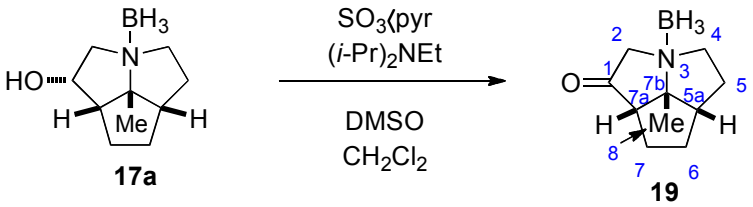

To a 100-mL, three-necked, round-bottomed flask fitted with a nitrogen inlet adapter, a magnetic stir bar, and an internal temperature probe was added **17a** (500 mg, 2.76 mmol), CH_2Cl_2 (11.5 mL), and DMSO (2.3 mL). The resulting solution was cooled to –12 °C in an ice/salt bath. To this solution was added diisopropylethylamine (2.41 mL, 13.8 mmol, 5.0 equiv) followed by a solution of SO_3•pyridine complex (1.32 g, 8.28 mmol, 3.0 equiv) in DMSO (4.6 mL) at rate such that the internal temperature remained < –5 °C (~5 min). After stirring for an additional 20 min at –10 °C, the cooling bath was removed and the solution was allowed to warm to room temperature (~10 min), then cooled to 0 °C by re-immersion in the ice/salt bath. The solution was diluted with Et_2O (10 mL) and quenched with H_2O (10 mL). This mixture was poured into a 250-mL separatory funnel and the layers were separated. The aqueous extract was washed with Et_2O (2 x 25 mL). The organic extracts were washed with sat. aq. $CuSO_4$ solution (2 x 25 mL), sat. aq. $NaHCO_3$ solution (1 x 25 mL), brine (25 mL), the combined organic extracts dried over $MgSO_4$, filtered through Celite (20 mm x 5 cm), and rinsed with TBME (3 x 10 mL). The filtrate was concentrated by rotary evaporation (15 mm Hg, 20-25 °C) to afford 498 mg (99%) of **19** as a white solid without further purification.

Data for **19**:

^{1}H-NMR: (500 MHz, $CDCl_3$)

3.89 (d, J = 17.6, 1 H, HC(2)), 3.55 (ddd, J = 7.6, 7.6, 12.2, 1 H, HC(4)), 3.48 (d, J = 17.6, 1 H, HC(2)), 3.16 (ddd, J = 6.5, 1 H, HC(4)), 2.63-2.57 (m, 2 H, HC(7a), HC(5a)), 2.40 (147et, J = 6.0, 7.4, 9.4, 13.6, 1 H, HC(5)), 2.16-2.03 (m, 3 H, HC(7), HC(7)), 1.65 (s, 3 H, H_3C(8)), 1.65-1.58 (m, 2 H, HC(5)), 1.48-1.41 (m, 1 H, HC(6)), 0.8-2.5 (br, 3 H, $(H_3B)^3$)

^{13}C-NMR: (126 MHz, $CDCl_3$)

212.1 (C(1)), 86.5 (C(7b)), 70.0 (C(2)), 64.9 (C(4)), 58.4 (C(7a)), 51.8 (C(5a)), 35.1 (C(6)), 32.3 (C(7)), 29.9 (C(5)), 24.4 (C(8))

IR: (NaCl plate, thin film)

2964 (s), 2865 (w), 2381 (s), 2333 (s), 2273 (s), 1755 (s), 1468 (m), 1419 (w),

1383 (m), 1195 (s), 1164 (s), 1071 (m), 913 (s), 732 (s)

MS: (EI, 70eV)

179 (12), 178 (100), 165 (28), 150 (24), 137 (48), 121 (15), 108 (16), 95 (27)

Mol. Formula: $C_{10}H_{18}BNO$ (179.07)

HRMS: $C_{10}H_{17}ONB^{+}$: (179.1403)

Calcd: 179.1403

Found: 178.1406

TLC: R_f 0.35 (hexanes/EtOAc, 3:2) [I_2, CAM]

Preparation of Scaffold for Library V (*via* 20 and 21).

Preparation of (1*S*,3*S*,5*S*,5a*S*,7a*S*,7b*R*)-Octahydro-1-hydroxy-5-methyl-7b-methyl-2*H*cyclopenta[*gh*]pyrrolizin-2-one ((+)-5)

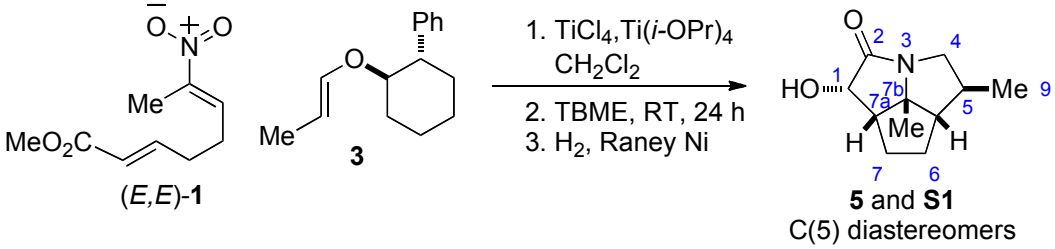

To a 100-mL, three-necked, round-bottomed flask fitted with two rubber septa, a magnetic stir bar, a nitrogen inlet adaptor and an internal temperature probe, was added nitroalkene (E,E)-1 (1.0 g, 5.02 mmol) and chiral propenyl ether **3** (1.63 g, 7.53 mmol, 1.5 equiv) *via* syringe. The resulting yellow oil was then evacuated under high vacuum (~0.1 mm Hg) for 30 min. The flask was backfilled with N_2 and charged with CH_2Cl_2 (22 mL). The solution was cooled to –85 °C (internal temperature) using hexanes/N_2 bath. This yellow solution was sirred for 15 min, then freshly prepared $TiCl_2(O\textit{i}\text{-Pr})_2$ solution (1.2 M in CH_2Cl_2, 12.6 mL, 15.1 mmol, 3.0 equiv) was added dropwise *via* syringe while maintaining an internal temperature ≤ –70 °C (ca. 15 min). After addition of the Lewis acid, the cooling bath was replaced with an acetone/$CO_{2(s)}$ bath and the resulting bright yellow solution was stirred for another 5 h while maintaining an internal temperature ≤ –75 °C. During the course of the reaction, the yellow color gradually faded and a white precipitate formed. After 5 h the reaction was quenched with triethylamine (30.6 mL, 6.1 equiv, 1 M in MeOH) *via* syringe while maintaining an internal temperature of < –40 °C. The cooling bath was then removed and the reaction mixture was

allowed to warm to 0 °C (ca. 15 min). The resulting white suspension was then diluted with ethyl acetate (50 mL) and poured onto a biphasic mixture of sat. aq. NH_4Cl and ethyl acetate (75 mL) in a 500-mL separatory funnel. The aqueous extract was washed with ethyl acetate (3 x 75 mL). The organic extracts were washed with sat. aq. NH_4Cl solution (2 x 50 mL), H_2O (2 x 50 mL) and brine (2 x 50 mL). The combined organic extracts were dried over $NaHCO_3/MgSO_4$ (1/1), filtered (cotton plug), and concentrated by rotary evaporation (15 mm Hg, 20-25 °C). The resulting residue was filtered through a pad of silica gel (3 x 3 cm), eluting with ethyl acetate (100 mL) to remove any remaining amine impurities. The resulting clear solution was concentrated by rotary evaporation (15 mm Hg, 20-25 °C) to a pale-yellow residual oil in a 1-L one-necked, round-bottomed flask. TBME (100 mL) was added followed by $NaHCO_3$ (5 g, 50.0 mmol, 10.0 equiv). The flask was equipped with a nitrogen inlet adaptor, a magnetic stir bar, and evacuated and backfilled with N_2 (3x). The suspension was stirred at room temperature for 12 h, then filtered through Celite (3 x 3 cm, cotton plug) and concentrated by rotary evaporation (15 mm Hg, 20-25 °C). The resulting mixture of nitroso acetals was diluted in EtOAc/MeOH (9:1, 25 mL) and added to a test tube (6 cm x 14 cm) containing a spatula tip (~200 mg) of Raney Ni (previously washed with H_2O, MeOH, and EtOAc, 2 x 15 mL each) along with a magnetic stir bar. The tube was placed in a steel autoclave, which was then pressurized with H_2 (350 psi). After 2 days the autoclave was *carefully* vented in a fume hood and the solution was filtered through a plug of Celite (5 cm x 5 cm, cotton plug) with EtOAc (100 mL). The resulting clear solution was concentrated by rotary evaporation (15 mm Hg, 20-25 °C) and purified by silica gel column chromatography (2 cm x 8 cm, hexanes/EtOAc, 9:1, 4:1, 7:3, 2:3, 1:4, 100 mL each) affording 870 mg (89%) of a mixture of epimeric α-hydroxy lactams **5** and **S2** as a white solid (11:1 by ^{1}H-NMR analysis).

Data for **5**:

^{1}H-NMR: (500 MHz, $CDCl_3$)

4.63 (dd, J = 6.8, 1.5, 1 H, HC(4)), 4.05 (dd, J = 11.8, 7.4, 1 H, HC(4)), 2.73 (br, s, 1 H, OH), 2.59-2.46 (m, 2 H), 1.86–1.73 (m, 3 H), 1.67–1.55 (m, 1 H), 1.53–1.40 (m, 2 H), 1.34 (s, 3 H, H_3C(8)), 1.07 (d, J = 6.7, 3 H, H_3C(9)).

^{13}C-NMR: (126 MHz, $CDCl_3$)

176.0 (C(2)), 75.4 (C(7b)), 72.4 (C(1)), 58.1 (C(5a)), 51.9 (C(7a)), 50.5 (C(4)), 42.1 (C(5)), 30.8 (C(6)), 25.2 (C(7)), 24.8 (C(9)), 17.5 (C(8))

IR: (NaCl plate, film)

3338 (br), 2959 (s), 2870 (s), 1685 (s), 1462 (m), 1412 (m), 1334 (m), 1269 (w), 1223 (s), 1142 (m), 1115 (w), 1097 (w), 1044 (w), 964 (w), 880 (w)

MS: (ESI, Q-tof)

195.1 (67), 180.1 (100), 167.1 (12), 152.1 (56), 138.1 (14), 111 (43), 96.1 (15), 81.1 (24)

TLC: R_f 0.20 (Hexanes/EtOAc, 1:1) [I_2]

Analysis: $C_{11}H_{17}NO_2$ (195.26)

Calcd:	C, 67.66;	H, 8.78;	N, 7.17
Found:	C, 67.41;	H, 9.05;	N, 7.19

Preparation of (1*R*,3*R*,5*R*,5a*S*,7a*S*,7b*R*)-Octahydro-1-[*N*-(3,5-Dinitrophenyl)carbamoxy]-7b-methyl-2H-cyclopenta[*gh*]pyrrolizin-2-one (S7)

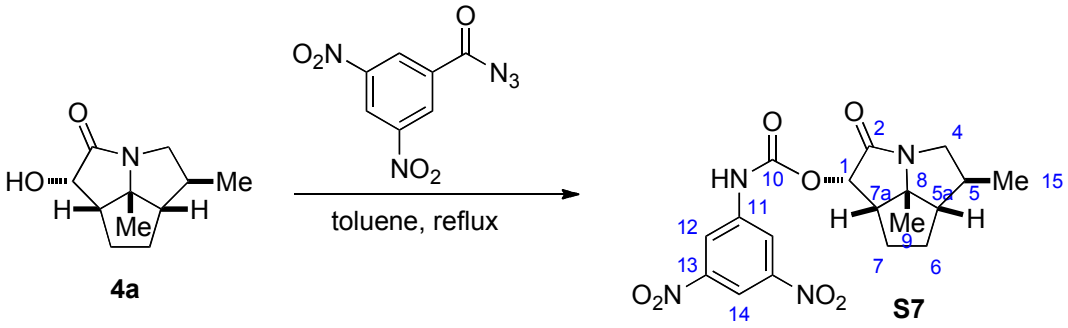

A 25 mL round-bottomed flask (A) was fitted with a reflux condenser, a nitrogen inlet adaptor, a rubber rubber septum and a magnetic stir bar. The apparatus was opened and 3,5-dinitrobenzoylazide (25 mg, 0.11 mmol, 1.1 equiv) was added as a solid. The apparatus was evacuated and backfilled with N_2 three times and toluene (4.8 mL) was added. The clear solution was immersed in a preheated (115 ^oC) oil bath and stirred at reflux for 30 min. In a separate, two-neck, 5 mL conical flask (B) fitted with a triangular a magnetic stir bar, rubber septum and a nitrogen inlet adaptor the starting alcohol was added (18.9 mg, 0.096 mmol) followed by toluene (1.0 mL). The resulting solution (B) was transferred to flask (A) *via* cannula. The resulting light yellow solution was heated to reflux for 2 h and then allowed to cool to room temperature. The reaction mixture was concentrated *in vacuo*, and the crude product was purified by column chromatography (hexane/EtOAc (3/1, 1/1)) to afford 38 mg (98%) of enantioenriched **S7** as a white solid. The sample was compared to racemate as previously described.

Data for **S7**:

^{1}H-NMR: (500 MHz, $CDCl_3$)

9.90 (s, 1 H, NH), 8.61 (s, 1 H, HC(14)), 8.56 (s, 2 H, HC(12)), 5.89 (d, *J* = 6.7, 1 H, HC(1)), 4.12 (dd, *J* = 7.4, 11.9, 1 H, HC(4)), 2.71 (dd, *J* = 9.5, 14.1, 1 H), 2.69 (dd, *J* = 10.7, 23.5, 1 H), 1.96 (dd, *J* = 7.0, 7.0, 1 H), 1.93-1.81 (m, 2 H), 1.63-1.50 (m, 3 H), 1.46 (s, 3 H, H_3C(9)), 1.14 (d, *J* = 6.7, 3 H, H_3C(15))

^{13}C-NMR: (126 MHz, $CDCl_3$)

220.6, 171.5, 152.6, 148.8, 141.2, 118.3, 118.2, 112.6, 75.9, 75.0, 58.3, 50.9, 42.7, 31.3, 26.3, 24.3, 17.7

TLC: R_f 0.34 (hexanes/EtOAc, 3:1) [I_2]

CSFC: *t*R= 7.98 min (1%) and 9.88 (99%) (Chiralpak AD, 125 bar, 40 °C, 15 % MeOH in CO_2, 3.0 mL/min, 220 nm)

Preparation of (3*R*,5a*S*,7a*S*,7b*R*)-Octahydro-5-methyl-7b-methyl-2*H*cyclopenta[*gh*]pyrrolizin-1-one (20)

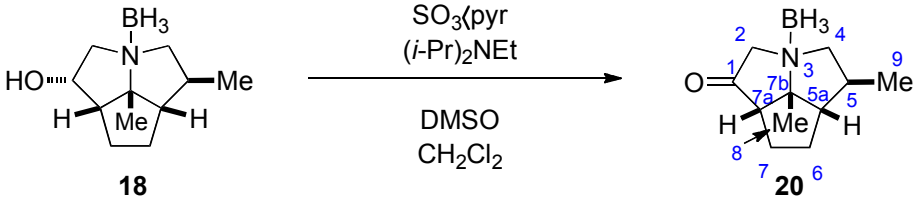

To a 50-mL, three-necked, round-bottomeded flask fitted with a nitrogen inlet adapter, a magnetic stir bar, and an internal temperature probe was added **18** (505 mg, 2.59 mmol), CH_2Cl_2 (10.8 mL), and DMSO (2.2 mL). The resulting solution was cooled to –12 °C in an ice/NaCl bath. To this solution was added diisopropylethylamine (2.25 mL, 12.9 mmol, 5.0 equiv) followed by the dropwise addition of a solution of SO_3•pyridine complex (1.24 g, 7.76 mmol, 3 equiv) in DMSO (4.3 mL) while maintaining an internal temperature < –5 °C. After being stirred for 20 min at –10 °C, the cooling bath was removed and the mixture was allowed to warm to room temperature. This mixture was poured into a 250-mL separatory funnel and the layers were separated. The aqueous extract was washed with Et_2O (2 x 25 mL). The organic extracts were washed with sat. aq. $CuSO_4$ solution (2 x 25 mL), sat. aq. $NaHCO_3$ solution (1 x 25 mL), brine (25 mL), the combined organic extracts dried over $MgSO_4$, filtered through a Celite (20

mm x 5 cm, cotton plug), and rinsed with TBME (3 x 10 mL).The filtrate is concentrated in vacuo (15 mm Hg, 20-25 ^{o}C) to afford 498 mg (99%) of **20** as a white solid.

Data for **20**:

^{1}H-NMR: (500 MHz, $CDCl_3$)

3.98 (d, J = 18.1, 1 H, HC(2)), 3.49 (d, J = 18.1, 1 H, HC(2)), 3.39 (dd, J = 6.4, 12.8, 1 H, HC(4)), 3.23 (dd, J = 12.4, 12.4, 1 H, HC(4)), 2.59 (d, J = 8.1, 1 H, HC(7a)), 2.28-2.23 (m, 1 H, HC(7)), 2.15-2.07 (m, 2 H, HC(6), HC(5a)), 2.09-1.96 (m, 2 H, HC(7), HC(5)), 1.66 (s, 3 H, H_3C(8)), 1.46-1.38 (m, 1 H, HC(6)), 1.10 (d, J = 6.5, 3 H, H_3C(9)), 0.8-2.5 (br, 3 H, $(H_3B)^3$)

^{13}C-NMR: (126 MHz, $CDCl_3$)

212.4 (C(1)), 87.3 (C(7b)), 72.0 (C(4)), 70.3 (C(2)), 60.9 (C(5a)), 57.9 (C(7a)), 38.1 (C(5)), 32.54 (C(7 or 6)), 32.45 (C(7 or 6)), 24.8 (C(8)), 17.5 (C(9))

IR: (NaCl plate, film)

2965 (s), 2964(s), 2963 (s), 2962 (m), 1757 (s), 1457 (w), 1383 (w), 1215 (s), 1163 (s), 745 (s)

MS: (EI, 70 eV)

192 (100), 180 (50), 166 (32), 151 (71), 149 (67), 136 (32), 123 (19), 95 (44), 81 (100)

Mol. Formula: $C_{11}H_{20}BNO$ (193.09)

HRMS: $C_{11}H_{19}BNO^{+}$: (192.1560)

Calcd: 193.1560

Found: 192.1560

TLC: R_f 0.45 (CH_2Cl_2/Et_2O, 19:1) [I_2, CAM]

Preparation of Scaffold for Library V via (α-Keto Lactam 23).

Preparation of (3*R*,5*S*,5a*S*,7a*S*,7b*R*)-Octahydro-5-methyl-7b-methyl-2*H*cyclopenta[*gh*]pyrrolizin-1,2-one (23)

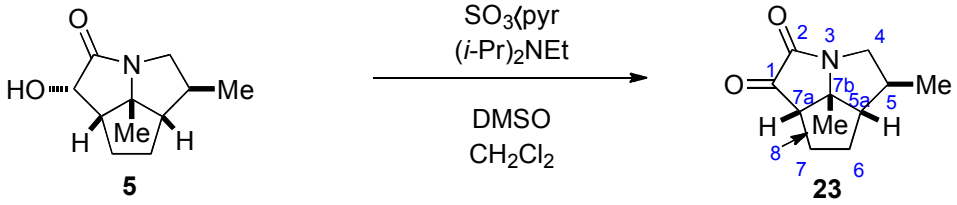

To a 50-mL, three-necked, round-bottomed flask fitted with a nitrogen inlet adapter, a magnetic stir bar, and an internal temperature probe was added **5** (491 mg, 2.51 mmol), CH_2Cl_2 (10.5 mL), and DMSO (2.1 mL). The resulting solution was cooled to –12 °C in an ice/salt bath. To this solution was added diisopropylethylamine (2.2 mL, 12.6 mmol, 5.0 equiv) followed by the dropwise addition of a solution of SO_3•pyridine complex (1.2 g, 7.54 mmol, 3.0 equiv) in DMSO (5.2 mL) while maintaining an internal temperature < –5 °C. After being stirred for 20 min at –10 °C, the mixture was allowed to warm to room temperature. The mixture was then cooled to 0 °C and diluted with CH_2Cl_2 (25 mL) and H_2O (25 mL). This mixture was poured into a 250-mL separatory funnel and the layers were separated. The aqueous extract was washed with CH_2Cl_2 (2 x 25 mL). The organic extracts were washed with sat. aq. $CuSO_4$ solution (2 x 25 mL), sat. aq. $NaHCO_3$ solution (1 x 25 mL), brine (25 mL), the combined organic extracts dried over $MgSO_4$, filtered (cotton plug), and rinsed with TBME (3 x 10 mL). The resulting pale-yellow oil was purified by silica gel column chromatography ((10 mm x 10 cm column,) gradient elution, hexanes/EtOAc, 3:1, 1:1, 1:3, 1:9, 100 mL each) followed by recrystallization (hexanes/TBME, 1:1, 25 mL) to afford 485 mg (82%) of **23** as white needles and as a single diastereomer.

Data for **23:**

mp: 83-84 °C (MTBE/Hexanes)

^{1}H-NMR: (500 MHz, $CDCl_3$)

4.36 (ddd, *J* = 1.2, 7.7, 12.3, 1 H, HC(4)), 2.98 (dd, *J* = 7.8, 12.0, 1 H, HC(4)), 2.71 (dd, *J* = 5.6, 9.0, 1 H, HC(7a)), 2.13-2.04 (m, 1 H, HC(7)), 2.06-1.97 (m, 3 H, HC(6), HC(5a), HC(5)), 1.77-1.70 (m, 1 H, HC(7)), 1.45 (s, 3 H, H_3C(8)), 1.40-1.32 (m, 1 H, HC(6)), 1.20 (d, *J* = 5.9, 3 H, H_3C(9))

^{13}C-NMR: (126 MHz, $CDCl_3$)

203.6 (C(1)), 160.4 (C(2)), 74.4 (C(7b)), 57.0 (C(5a)), 55.8 (C(7a)), 51.9 (C(4)), 41.0 (C(5)), 32.8 (C(6)), 30.7 (C(7)), 25.1 (C(8)), 19.8 (C(9))

IR: (NaCl plate, film)

3496 (w), 3404 (w), 2961 (s), 2873 (s), 1760 (s), 1713 (s), 1462 (s), 1401 (s), 1332 (w), 1226 (s), 1180 (s), 1084 (m), 678 (w)

MS: (EI, 70 eV)

193 (26), 165 (26), 150 (32), 122 (6), 107 (11), 93 (5), 81 (100)

TLC: R_f 0.35 (hexanes/EtOAc, 3:1) [I_2]

Analysis: $C_{11}H_{15}N$: (193.24)

Calcd:	C, 68.37;	H, 7.82;	N, 7.25
Found:	C, 68.57;	H, 8.02;	N, 7.31

Preparation of (1*R*,3*R*,5*S*,5a*S*,7a*S*,7b*R*)-Octahydro-1-hydroxy-5-methyl-7b-methyl-2*H*cyclopenta[*gh*]pyrrolizin•Borane (18) and (1*S*,3*R*,5*S*,5a*S*,7a*S*,7b*R*)-Octahydro-1-hydroxy-5-methyl -7b-methyl-2*H*cyclopenta[*gh*]pyrrolizin•Borane (S3)

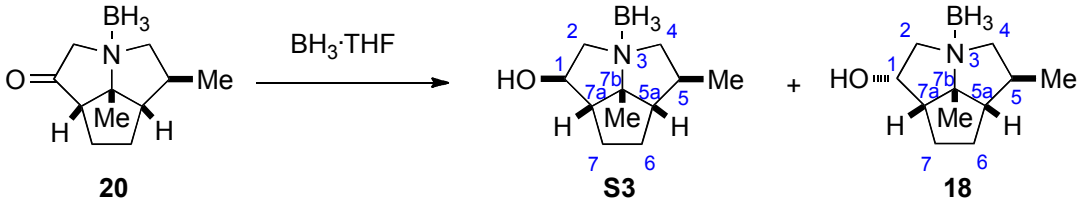

To a 25-mL, two-necked, round-bottomed flask equipped with a nitrogen adapter, a rubber septum and a magnetic stir bar was added sequentially **20** (63 mg, 0.326 mmol), THF (1.6 mL, 0.2 M), and BH_3•THF complex (1.6 mL, 1.0 M solution, 5.0 equiv) dropwise over 5 min during which gas evolution was observed. After being stirred for 2 h at room temperature, the reaction was quenched with methanol (5 mL) and the resulting solution was concentrated by rotary evaporation (15 mm Hg, 20-25°C) to afford crude **S3** as a mixture of diastereomers (5/9, ^{1}H-NMR). The crude mixture was purified by silica gel column chromatography (1.8 cm x 8 cm column, gradient elution, CH_2Cl_2/ether, 99:1, 49:1, 24:1, 47:3, 9:1, 25 mL each) to afford 22 mg (35%) of **S3** as a white solid.

Data for **S3**:

^{1}H-NMR: (500 MHz, $CDCl_3$)

3.88 (dd, J = 4.4, 10.6, 1 H, HC(1)), 3.74 (d, J = 10.8, 1 H, OH)), 3.56 (d, J =

12.7, 1 H, HC(2)), 3.37 (dd, *J* = 4.4, 12.7, 1 H, HC(2)), 3.24 (dd, *J* = 5.2, 12.7, 1 H, HC(4)), 2.85 (dd, *J* = 12.2, 12.2, 1 H, HC(4)), 2.39 (dd, *J* = 9.1, 9.1, 1 H, HC(7a)), 2.11-2.04 (m, 1 H, HC(7)), 1.91-1.84 (m, 2 H, HC(5a), HC(5)), 1.77-1.68 (m, 1 H, HC(6)), 1.66-1.63 (m, 1 H, HC(6)), 1.60 (s, 3 H, $H_3C(8)$), 1.41-1.32 (m, 1 H, HC(7)), 1.01 (d, *J* = 5.8, 3 H, $H_3C(9)$), 0.8-2.5 (br, 3 H, $(H_3B)^3$)

^{13}C-NMR: (126 MHz, $CDCl_3$)

88.5 (C(7b)), 76.0 (C(1)), 71.1 (C(4)), 69.2 (C(2)), 62.1 (C(5a)), 61.4 (C(7a)), 34.8 (C(5)), 31.2 (C(7)), 29.6 (C(6)), 26.0 (C(8)), 16.5 (C(9))

IR: ($CDCl_3$)

3492 (s), 2964 (s), 2922 (s), 2869 (s), 2369 (s), 2318 (s), 2270 (s), 1454 (s), 1412 (m), 1381 (m), 1348 (m), 1250 (m), 1186 (s), 1160 (m) 1121 (m), 1048 (s), 1023 (m), 996 (m), 973 (m), 925 (m), 869 (m), 844 (w), 818 (w), 802 (w)

MS: (EI, 70 eV)

194.2 (78), 181 (24), 166 (100), 150 (3), 138 (12), 124 (10), 110 (44), 96 (11), 84 (14)

Mol. Formula: $C_{11}H_{22}BNO$ (195.11)

HRMS: $C_{11}H_{21}BNO$, (194.1716)

Calcd: 194.1716

Found: 194.1720

TLC: R_f 0.61 (CH_2Cl_2/ether, 9:1) [I_2]

Preparation of (1*S*,3*S*,5*S*,5a*S*,7a*S*,7b*R*)-Octahydro-1-hydroxy-5-methyl-7b-methyl-2*H*cyclopenta[*gh*]pyrrolizin•Borane (18)

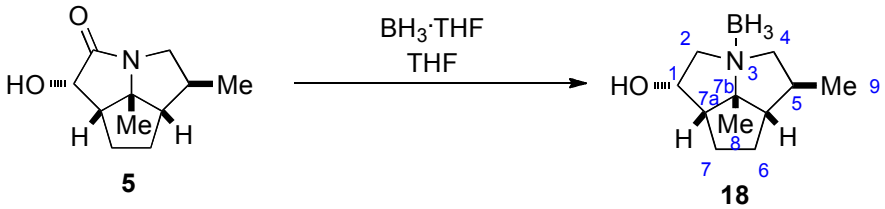

To a 250-mL round-bottomed flask equipped with a nitrogen inlet adapter, a rubber septum and a magnetic stir bar was added sequentially **5** (931 mg, 4.77 mmol), THF (23.9 mL, 0.2 M), and BH_3•THF complex (23.9 mL, 1.0 M solution, 10.0 equiv) dropwise over 5 min

during which gas evolution was observed. After being stirred for 4 h at room temperature, the reaction was quenched with methanol (40 mL) and the mixture was concentrated by rotary evaporation (15 mm Hg, 20-25 ^{o}C). The resulting colorless oil was purified by silica gel column chromatography (2 cm x 15 cm column, gradient elution, CH_2Cl_2/ether, 99:1, 49:1, 24:1, 47:3, 9:1, 100 mL each) to afford 875 mg (94%) of **18** as a white solid.

Data for **18**:

mp: 86.5-87.5 ^{o}C

^{1}H-NMR: (500 MHz, $CDCl_3$)

4.81 (ddd, *J* = 7.2, 7.2, 10.5, 1 H, HC(1)), 3.46 (dd, *J* = 6.6, 10.3, 1 H, HC(2)), 3.17 (dd, *J* = 6.2, 12.5, 1 H, HC(4)), 3.02 (dd, *J* = 10.5, 10.5, 1 H, HC(2)), 2.82 (dd, *J* = 12.5, 12.5, 1 H, HC(4)), 2.34 (dd, *J* = 8.2, 17.0, 1 H, HC(7a)), 2.11-2.01 (m, 1 H, HC(5)), 1.94-1.85 (m, 2 H, HC(7), HC(5a)), 1.81-1.76 (m, 1 H, HC(6)), 1.76-1.67 (m, 2 H, HC(7), HC(6)), 1.56 (br, s, 1 H, OH), 1.50 (s, 3 H, H_3C(8)), 1.03 (d, *J* = 6.4, 3 H, H_3C(9)), 0.8-2.5 (br, 3 H, $(H_3B)^3$)

^{13}C-NMR: (126 MHz, $CDCl_3$)

88.1 (C(7b)), 70.0 (C(4)), 68.8 (C(1)), 65.7 (C(2)), 62.0 (C(5a)), 55.1 (C(7a)), 34.6 (C(5)), 29.7 (C(7)), 26.4 (C(6)), 25.7 (C(8)), 16.4 (C(9))

IR: ($CHCl_3$ film)

3447 (br), 2962 (s), 2963 (s), 2964 (s), 2965 (m), 2378 (s), 2377 (s), 2375 (s), 1474 (m), 1457 (m), 1381 (w), 1214(s), 1166 (s), 1118 (m), 1088 (m), 141 (w), 1010 (w), 995 (w), 946 (w), 755 (s),

MS: (EI, 70 eV)

194 ([M^{+}-1],8), 181 (16), 166 (100), 110 (60), 96 (12), 82 (8)

TLC: R_f 0.36 (CH_2Cl_2/ether, 9:1) [I_2]

Analysis: $C_{11}H_{22}BNO$, (195.1095)

Calcd: C, 67.71; H, 11.37; N, 7.18

Found: C, 67.8%; H, 11.31; N, 7.06

Opt. Rot.: $[\alpha]_D^{24}$ -11.14^{o} (c = 1.0, $CHCl_3$)

III. Parallel Syntheses: Library Intermediates and Quaternary Ammonium Bromides.

7.3.2. A. Variable Group R^2: Organometal Ketone Additions.

Cerium-Mediated Additions to Keto Amine 19. Preparation of (1*S*,3*S*,5a*S*,7a*S*,7b*R*)-Octahydro-1-hydroxy-1-methyl-7b-methyl-2*H*cyclopenta[*gh*]pyrrolizine•Borane (21{*2*})

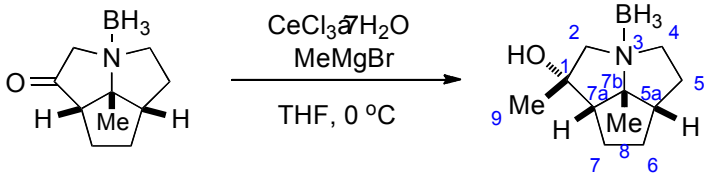

19 **21**{*2*}

To a 25-mL, two-necked, round-bottomed flask equipped with a nitrogen inlet adapter, a rubber septum and a magnetic stir bar was added $CeCl_3$•$7H_2O$ (559 mg, 1.50 mmol, 1.5 equiv). The flask was immersed in a preheated oil bath (140 °C) under vacuum (< 0.1 mm Hg) for 2 h. The flask was backfilled with nitrogen, allowed to cool to room temperature, and then immersed in an ice bath. To the solid was added THF (4.0 mL), via syringe, and the resulting milky, heterogenous mixture was allowed to stir vigorously at room temperature for 2 h. The mixture was then sonicated and stirred intermittently for 15 min intervals over a 2 h time period. The flask was then immersed in an ice bath and methylmagnesium bromide (2.7 M, 556 µL, 1.5 mmol, 1.5 equiv) was added via syringe. The ice bath was removed and the solution was stirred at room temperature for 1.5 h. The flask was immersed in an ice bath and ketone **19** (179 mg, 1.0 mmol) was added as a solution in THF (1.0 mL) via syringe. After stirring for 30 min while immersed in an ice bath, the reaction was quenched with sat. aq. NH_4Cl solution (5.0 mL). The biphasic mixture was poured into a 125-mL separatory funnel containing sat. aq. NH_4Cl solution (20 mL) and Et_2O (20 mL). The layers were separated and the aqueous extract was washed with Et_2O (2 x 25 mL). The organic extracts were washed with sat. aq. $NaHCO_3$ (1 x 25 mL), brine (1 x 25 mL), and the combined organic extracts were dried over $MgSO_4$, filtered (cotton plug), and concentrated by rotary evaporation (15 mm Hg, 20-25°C). The resulting pale-yellow oil was purified by silica gel column chromatography (2 cm x 8 cm, gradient elution, CH_2Cl_2/EtOAc, 1:0, 99:1, 49:1, 19:1, 50 mL each) to afford **21**{*2*} (134 mg, 68%) as a white solid.

Data for **21**{*2*}:

^{1}H-NMR: (500 MHz, $CDCl_3$)

3.88 (ddd, *J* = 6.3, 10.6, 10.3, 1 H, HC(4)), 3.37 (d, *J* = 13.4, 1 H, HC(2)), 3.33 (d, *J* = 13.6, 1 H, HC(2)), 3.31-3.27 (m, 1 H, HC(4)), 2.35-2.34 (m, 1 H, HC(5a), HC(5)), 2.16-2.13 (m, 1 H, HC(7a)), 1.96-1.89 (m, 2 H, HC(7),

HC(6)), 1.80-1.68 (m, 2 H, HC(7), HC(6)), 1.54-1.49 (m, 1 H, HC(5)), 1.50 (s, 3 H, $H_3C(8)$, 1.41 (s, 3 H, $H_3C(9)$), 0.8-2.5 (br, 3 H, $(H_3B)^3$)

^{13}C-NMR: (126 MHz, $CDCl_3$)

89.2 (C(7b)), 78.1 (C(1)), 74.7 (C(2)), 63.7 (C(7a)), 63.6 (C(4)), 52.2 (C(5a)), 34.6 (C(6)), 30.5 (C(8 or 9)), 29.6 (C(5)), 27.3 (C(7)), 25.8 (C(8 or 9))

IR: (thin film)

3503 (s), 2383 (s), 2329 (s), 2277 (s), 1301 (m), 1258 (m), 1178 (m), 1124 (w), 1070 (m), 1018 (w), 953 (w), 850 (w)

MS: (EI, 70eV)

194.2 (93), 181 (34), 166 (50), 138 (6), 110 (57), 96 (100), 81 (18)

Mol. Formula: $C_{11}H_{22}BNO$ (195.18)

HRMS: $C_{11}H_{21}BNO^+$ (194.1716)

Calcd: 194.1716

Found: 194.1714

TLC: R_f 0.25 (CH_2Cl_2/EtOAc, 19:1) [I_2, CAM]

Preparation of (1*S*,3*S*,5a*S*,7a*S*,7b*R*)-Octahydro-1-hydroxy-1-isopropyl-7b-methyl-2*H*cyclopenta[*gh*]pyrrolizine•Borane (21{*3*})

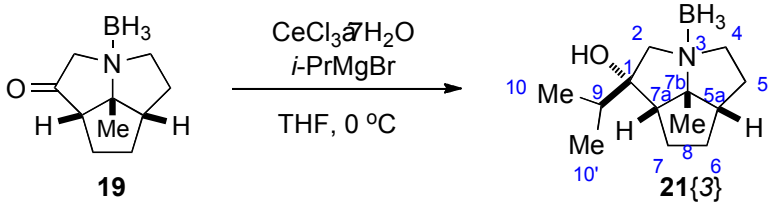

To a 25-mL, two-necked, round-bottomed flask equipped with a nitrogen inlet adapter, a rubber septum and a magnetic stir bar was added $CeCl_3$•$7H_2O$ (559 mg, 1.50 mmol, 1.5 equiv). The flask was immersed in a preheated oil bath (140 °C) and stirred under vacuum (< 0.1 torr) for 2 h. The flask was backfilled with nitrogen, allowed to cool to room temperature, and then immersed in an ice bath. To the solid was added THF (4.0 mL), and the resulting milky, heterogenous mixture was allowed to stir vigorously at room temperature for 2 h. The mixture was then sonicated and stirred intermittently for 15 min intervals over a 2 h time period. The flask was then immersed in an ice bath and isopropylmagnesium chloride (1.9 M, 811 µL, 1.5

mmol, 1.5 equiv) was added via syringe. The ice bath was removed and the solution was stirred at room temperature for 1.5 h. The flask was immersed in an ice bath and ketone **19** (179 mg, 1.0 mmol) was added as a solution in THF (1.0 mL) via syringe. After stirring for 30 min while immersed in an ice bath, the reaction was quenched with sat. aq. NH_4Cl solution (5.0 mL). The biphasic mixture was poured into a 125-mL separatory funnel containing sat. aq. NH_4Cl solution (20 mL) and Et_2O (20 mL). The layers were separated and the aqueous extract was washed with Et_2O (2 x 25 mL). The organic extracts were washed with sat. aq. $NaHCO_3$ (1 x 25 mL), brine (1 x 25 mL), and the combined organic extracts were dried over $MgSO_4$, filtered (cotton plug), and concentrated by rotary evaporation (15 mm Hg, 20-25°C). The resulting pale-yellow oil was purified by silica gel column chromatography (1.8 cm x 8 cm, gradient elution, CH_2Cl_2/EtOAc, 1:0, 99:1, 49:1, 19:1, 50 mL each) to afford **21**{*3*} (89 mg, 40%) as a white solid.

Data for **21**{*3*}:

^{1}H-NMR: (500 MHz, $CDCl_3$)

3.98 (ddd, *J* = 6.6, 11.1, 11.5, 1 H, HC(4)), 3.39 (d, *J* = 13.8, 1 H, HC(2)), 3.35 (d, *J* = 9.0, 1 H, HC(2)), 3.34-3.31 (m, 1 H, HC(4)), 2.46-2.43 (m, 2 H, HC(5a), HC(5)), 2.20-2.17 (m, 1 H, HC(7a)), 2.00-1.90 (m, 2 H, HC(7), HC(6)), 1.80 (m, 1 H, HC(6)), 1.74-1.67 (m, 1 H, HC(7)), 1.67-1.60 (m, 1 H, HC(9)), 1.53-1.49 (m, 1 H, HC(5)), 1.48 (s, 3 H, H_3C(8)), 1.40 (br, s, 1 H, OH), 0.91 (d, *J* = 2.4, 3 H, H_3C(10), 0.90 (d, *J* = 2.5, 3 H, H_3C(10')), 0.8-2.5 (br, 3 H, $(H_3B)^3$)

^{13}C-NMR: (126 MHz, $CDCl_3$)

89.0 (C(7b), 82.4 (C(1)), 74.2 (C(2)), 63.2 (C(4)), 62.5 (C(7a)), 51.4 (C(5a)), 39.7 (C(9)), 35.5 (C(6)), 30.0 (C(5)), 27.9 (C(7)), 25.5 (C(8)), 16.9 (C(10)), 16.7 (C(10`))

IR: (thin film)

3433 (s), 2411 (m), 2319 (s), 2270 (s), 1309 (w), 1280 (S), 1162 (m), 1070 (w), 988 (m), 975 (w), 849 (w), 703 (w)

MS: (ESI, Q-tof)

222 (89), 209 (50), 194 (34), 178 (18), 166 (16), 124 (21), 110 (65), 96 (100), 81 (20)

Mol. Formula:	$C_{13}H_{26}BNO$	(223.16)
HRMS:	$C_{13}H_{25}BNO$	(222.2029)
	Calcd:	222.2029
	Found:	222.2030
TLC:	R_f 0.40 (hexanes/EtOAc, 4:1) [I_2, CAM]	

Preparation of (1*S*,3*S*,5a*S*,7a*S*,7b*R*)-Octahydro-1-hydroxy-1-phenyl-7b-methyl-2*H*cyclopenta[*gh*]pyrrolizine•Borane (21{*5*})

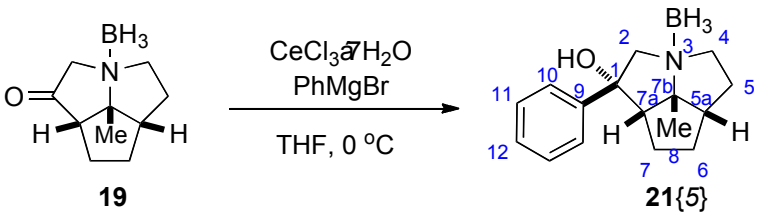

19 **21**{*5*}

To a 25-mL, two-necked, round-bottomed flask equipped with a nitrogen inlet adapter, a rubber septum and a magnetic stir bar was added $CeCl_3$•$7H_2O$ (559 mg, 1.50 mmol, 1.5 equiv). The flask was immersed in a preheated oil bath (140 °C) and stirred under vacuum (< 0.1 torr) for 2 h. The flask was backfilled with N_2, allowed to cool to room temperature, and then immersed in an ice bath. To the solid was added THF (4.0 mL), and the resulting milky, heterogenous mixture was allowed to stir vigorously at room temperature for 2 h. The mixture was then sonicated and stirred intermittently for 15-min intervals over a 2 h time period. The flask was then immersed in an ice bath and phenylmagnesium bromide (3.0 M, 500 µL, 1.5 mmol, 1.5 equiv). The ice bath was removed and the solution was stirred at room temperature for 1.5 h. The flask was immersed in an ice bath and ketone **19** (179 mg, 1.0 mmol) was added as a solution in THF (1.0 mL) via syringe. After stirring for 30 min while immersed in an ice bath, the reaction was quenched with sat. aq. NH_4Cl solution (5.0 mL). The biphasic mixture was poured into a 125-mL separatory funnel containing sat. aq. NH_4Cl solution (20 mL) and Et_2O (20 mL). The layers were separated and the aqueous extract was washed with Et_2O (2 x 25 mL). The organic extracts were washed with sat. aq. $NaHCO_3$ (1 x 25 mL), brine (1 x 25 mL), and the combined organic extracts were dried over $MgSO_4$, filtered (cotton plug), and concentrated by rotary evaporation (15 mm Hg, 20-25°C). The resulting pale-yellow oil was purified by silica gel column chromatography (1.8 cm x 8 cm, gradient elution, CH_2Cl_2/EtOAc, 1:0, 99:1, 49:1, 19:1, 50 mL each) to afford **21**{*5*} (131 mg, 51%) as a white solid.

Data for **21**{*5*}:

^{1}H-NMR: (500 MHz, $CDCl_3$)

7.42-7.36 (m, 4 H, HC(10), HC(11)), 7.33-7.28 (m, 1 H, HC(12)), 4.28-4.20 (m, 1 H, HC(4)), 3.81 (d, *J* = 13.9, 1 H, HC(2)), 3.68 (d, *J* = 13.9, 1 H, HC(2)), 3.45-3.40 (m, 1 H, HC(4)), 2.75 (dd, *J* = 3.0, 8.3, 1 H, HC(7a)), 2.45-2.36 (m, 2 H, HC(5a), HC(5)), 2.12-2.02 (m, 2 H, HC(7), HC(6)), 1.94-1.78 (m, 3 H, HC(7), HC(6), OH), 1.63-1.58 (m, 1 H, HC(5)), 1.58 (s, 3 H, H_3C(8)), 0.8-2.5 (br, 3 H, $(H_3B)^3$)

^{13}C-NMR: (126 MHz, $CDCl_3$)

145.1 (C(9)), 129.0 (C(10 or 11)), 128.0 (C(10 or 11)), 124.9 (C(12)), 89.2 (C(7b)), 82.1 (C(1)), 74.9 (C(2)), 64.3 (C(7a)), 63.3 (C(4)), 52.2 (C(5a)), 35.2 (C(6)), 29.7 (C(5)), 27.3 (C(7)), 25.9 (C(8))

IR: (thin film)

3433 (s), 2411 (m), 2319 (s), 2270 (s), 1309 (w), 1280 (S), 1162 (m), 1070 (w), 988 (m), 975 (w), 849 (w), 703 (w)

MS: (EI, 70 eV)

254.2 (62), 243.2 ([M^+], 66), 228 (20), 210 (10), 178 (8), 158 (48), 149 (15), 138 (11), 123 (46), 110 (100)

Mol. Formula: $C_{16}H_{24}BNO$; 257.18

HRMS: $C_{16}H_{21}NO$: (243.1623)

Calcd: 243.16232

Found: 243.16251

TLC: R_f 0.20 (CH_2Cl_2/EtOAc, 19:1) [I_2, CAM]

Cerium Mediated Additions to 20. Preparation of (1*S*,3*S*,5*S*,5a*S*,7a*S*,7b*R*)-Octahydro-1-hydroxy-1-methyl-5-methyl-7b-methyl-2*H*cyclopenta[*gh*]pyrrolizine•Borane (22{*2*})

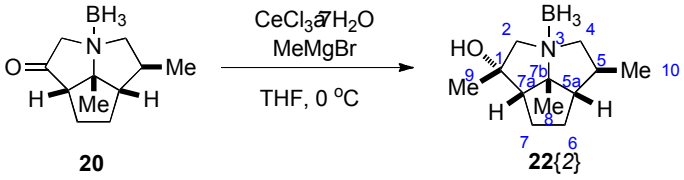

20 **22**{*2*}

To a 100-mL, two-necked, round-bottomed flask equipped with a nitrogen inlet adapter, a rubber septum and a magnetic stir bar was added $CeCl_3$•$7H_2O$ (2.30 g, 8.70 mmol, 1.5 equiv). The flask was immersed in a preheated oil bath (140 °C) and stirred under vacuum (~0.1 torr). After 2 h the flask was backfilled with nitrogen, allowed to cool to room temperature, and then immersed in an ice bath. To the solid was added THF (25 mL), and the resulting milky, heterogenous mixture was allowed to stir vigorously at room temperature for 2 h. The mixture was then sonicated and stirred intermittently for 15 min intervals over a 2 h time period. The flask was then immersed in an ice bath and methylmagnesium bromide (3.0 M, 3.0 mL, 1.50 mmol, 1.5 equiv). The ice bath was removed and the solution was stirred at room temperature for 1.5 h. The flask was immersed in an ice bath and ketone **20** (1.12 g, 5.80 mmol) was added as a solution in THF (4.0 mL). After being stirred for 30 min while immersed in an ice bath, the reaction was quenched with sat. aq. NH_4Cl solution (20 mL). The biphasic mixture was poured into a 250-mL separatory funnel containing sat. aq. NH_4Cl solution (30 mL) and Et_2O (40 mL). The layers were separated and the aqueous extract was washed with Et_2O (2 x 50 mL). The organic extracts were washed with sat. aq. $NaHCO_3$ (1 x 50 mL), brine (1 x 50 mL), and the combined organic extracts were dried over $MgSO_4$, filtered (cotton plug), and concentrated by rotary evaporation (15 mm Hg, 20-25°C). The resulting pale-yellow oil was purified by silica gel column chromatography (2 cm x 12 cm, gradient elution, CH_2Cl_2/ether, 1:0, 99:1, 49:1, 24:1, 9:1, 4:1, 100 mL each) to afford **22**{*2*} (1.1 g, 87%) as a white solid.

Data for **22**{*2*}:

mp: 84-85 °C (MTBE:Hexanes)

^{1}H-NMR: (500 MHz, $CDCl_3$)

3.43 (d, *J* = 12.0, 1 H, HC(2)), 3.28 (dd, *J* = 6.8, 12.6, 1 H, HC(4)), 3.25 (d, *J* = 12.3, 1 H, HC(2)), 2.97 (dd, *J* = 12.2, 12.2, 1 H, HC(4)), 2.13 (162et, *J* = 4.8, 8.1, 9.6, 12.7, 1 H, HC(5)), 2.06 (ddd, *J* = 8.2, 8.2, 7.8, 1 H, HC(7a)), 2.02-1.96 (m, 1 H, HC(7)), 1.85 (dd, *J* = 7.0, 7.0, 1 H, HC(5a)), 1.83-1.70 (m,

3 H, HC(7), HC(6), HC(6)), 1.61 (s, 3 H,$H_3C(9)$), 1.52 (s, 3 H, $H_3C(8)$), 1.38 (d, *J* = 4.7, 1 H, OH), 0.99 (d, J = 6.5, 3 H, H3C(10)), 0.8-2.5 (br, 3 H, $(H_3B)^3$)

^{13}C-NMR: (126 MHz, $CDCl_3$)

88.9 (C(7b)), 75.5 (C(1)), 74.9 (C(2)), 73.4 (C(4)), 61.9 (C(7a)), 61.8 (C(5a)), 34.0 (C(5)), 31.0 (C(9)), 29.7 (C(6)), 27.1 (C(7)), 26.0 (C(8)), 16.5 (C(10))

IR: ($CHCl_3$)

3969 (br), 2962 (s), 2870 (s), 2380 (s), 2331 (s), 2276 (s), 1459 (s), 1381 (s), 1340 (m), 1180 (s), 1134 (s), 1064 (s), 1049 (w), 1019 (w), 960 (s), 871 (w), 826 (m)

MS: (EI, 70 eV)

208 (4), 195 (16), 180 (48), 124 (28), 110 (100), 96 (16), 81 (8)

Mol. Formula: $C_{12}H_{24}BNO$ (209.14)

HRMS: $C_{12}H_{23}BNO$: (208.1873)

Calcd: 208.1873

Found: 208.1875

TLC: R_f 0.33 (CH_2Cl_2/Et_2O, 19:1) [I_2, CAM]

Preparation of (1*S*,3*S*,5*S*,5a*S*,7a*S*,7b*R*)-Octahydro-1-hydroxy-1-isopropyl-5-methyl-7b-methyl-2*H*cyclopenta[*gh*]pyrrolizine•Borane (22{*3*})

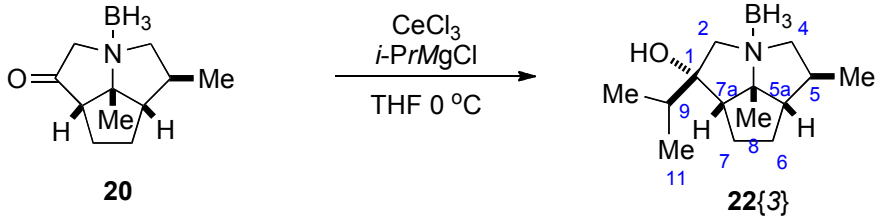

To a 100-mL, two-necked, round-bottomed flask equipped with a nitrogen inlet adapter, a rubber septum and a magnetic stir bar was added $CeCl_3$•$7H_2O$ (2.90 g, 7.77 mmol, 1.5 equiv). The flask was immersed in a preheated oil bath (140 °C) and stirred under vacuum (~0.1 torr). After 2 h the flask was backfilled with nitrogen, allowed to cool to room temperature, and then immersed in an ice bath. To the solid was added THF (22 mL), and the resulting milky, heterogenous mixture was allowed to stir vigorously at room temperature for 2 h. The mixture

was then sonicated and stirred intermittently for 15 min intervals over a 2 h time period. The flask was then immersed in an ice bath and isopropyl magnesium chloride (1.8 M, 4.3 mL, 1.50 mmol, 1.5 equiv) was added via syringe. The ice bath was removed and the solution was stirred at room temperature for 1.5 h. The flask was immersed in an ice bath and ketone **20** (1.0 g, 5.18 mmol) was added as a solution in THF (4.0 mL). After stirring for 30 min while immersed in an ice bath, the reaction was quenched with sat. aq. NH_4Cl solution (20 mL). The biphasic mixture was poured into a 250-mL separatory funnel containing sat. aq. NH_4Cl solution (30 mL) and Et_2O (40 mL). The layers were separated and the aqueous extract was washed with Et_2O (2 x 50 mL). The organic extracts were washed with sat. aq. $NaHCO_3$ (1 x 50 mL), brine (1 x 50 mL), and the combined organic extracts were dried over $MgSO_4$, filtered (cotton plug), and concentrated by rotary evaporation (15 mm Hg, 20-25°C). The resulting pale-yellow oil was purified by silica gel column chromatography (2 cm x 10 cm, gradient elution, CH_2Cl_2/ether, 1:0, 99:1, 49:1, 24:1, 47:3, 9:1, 17:3, 100 mL each) to afford **22**{*3*} (931 mg, 79%) as a pale yellow oil.

Data for **22**{*3*}:

^{1}H-NMR: (500 MHz, $CDCl_3$)

3.60 (d, *J* = 13.5, 1 H, HC(2)), 3.51 (dd, *J* = 7.9, 12.2, 1 H, HC(4)), 3.31 (d, *J* = 13.5, 1 H, HC(2)), 3.16 (dd, *J* = 10.7, 12.1, 1 H, HC(4)), 2.42–2.32 (m, 1 H, HC(5)), 2.18 (dd, *J* = 7.0, 9.1, 1 H, HC(7a)), 2.09–1.98 (m, 1 H, HC(7)), 1.89–1.83 (m, 3 H, HC(6), HC(6), HC(5a)), 1.82–1.69 (m, 2 H, HC(7), HC(9)), 1.49 (s, 3 H, H_3C(8)), 1.37 (br, s, 1 H, OH), 0.99 (d, *J* = 6.6, 3 H, H_3C(12)), 0.91 (d, *J* = 6.8, 3 H, H_3C(10)), 0.87 (d, *J* = 6.9, 3 H, H_3C(11)), 0.8–2.5 (br, 3 H, $(H_3B)^3$)

^{13}C-NMR: (126 MHz, $CDCl_3$)

89.4 (C(7b)), 80.2 (C(1)), 77.1 (C(2)), 74.1 (C(4)), 60.9 (C(7a)), 60.0 (C(5a)), 38.3 (C(9)), 34.5 (C(5)), 31.3 (C(6)), 25.4 (C(7)), 25.3 (C(8)), 17.6 (C(12)), 17.0 (C(10)), 16.8 (C(11)),

IR: ($CHCl_3$)

3507 (br), 2964 (s), 2866 (m), 2380 (s), 2326 (s), 2268 (s), 1465 (m), 1171 (m), 1000 (w)

MS: (EI, 70 eV)

236 (18), 234 (24), 223 (23), 208 (30), 192 (7), 180 (15), 124 (36), 110 (100), 96 (12), 81 (10)

Mol. Formula: $C_{14}H_{28}BNO$ (237.19)

HRMS: $C_{14}H_{27}BNO$: (236.2186)

Calcd: 236.2186

Found: 236.2183

TLC: R_f 0.40 (CH_2Cl_2/ether, 19:1) [I_2, CAM]

Preparation of (1*S*,3*S*,5*S*,5a*S*,7a*S*,7b*R*)-Octahydro-1-hydroxy-1-phenyl-5-methyl-7b-methyl-2*H*cyclopenta[*gh*]pyrrolizine•Borane (22{*5*})

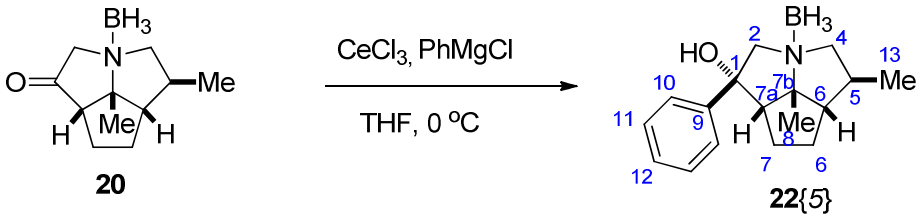

To a 50-mL, two-necked, round-bottomed flask equipped with a nitrogen inlet adapter, a rubber septum and a magnetic stir bar was added $CeCl_3$•$7H_2O$ (1.74 g, 4.66 mmol, 1.5 equiv). The flask was immersed in a preheated oil bath (140 °C) and stirred under vacuum (~0.1 torr). After 2 h the flask was backfilled with nitrogen, allowed to cool to room temperature, and then immersed in an ice bath. To the solid was added THF (14 mL), and the resulting milky, heterogenous mixture was allowed to stir vigorously at room temperature for 2 h. The mixture was then sonicated and stirred intermittently for 15 min intervals over a 2 h time period. The flask was then immersed in an ice bath and phenylmagnesium bromide (2.9 M, 1.6 mL, 1.50 mmol, 1.5 equiv) was added via syringe. The ice bath was removed and the solution was stirred at room temperature for 1.5 h. The flask was immersed in an ice bath and ketone **20** (600 mg, 3.11 mmol) was added as a solution in THF (2.0 mL) via syringe. After stirring for 30 min while immersed in an ice bath, the reaction was quenched with sat. aq. NH_4Cl solution (15 mL). The biphasic mixture was poured into a 250-mL separatory funnel containing sat. aq. NH_4Cl solution (30 mL) and Et_2O (40 mL). The layers were separated and the aqueous extract was washed with Et_2O (2 x 50 mL). The organic extracts were washed with sat. aq. $NaHCO_3$ (1 x 50 mL), brine (1 x 50 mL), and the combined organic extracts were dried over $MgSO_4$, filtered (cotton plug), and concentrated by rotary evaporation (15 mm Hg, 20-25°C). The resulting pale-yellow oil was

purified by silica gel column chromatography (1.8 cm x 10 cm, gradient elution, hexanes/TBME, 9:1, 4:1, 7:3, 1:1, 1:4, 50 mL each) to afford **22**{*5*} (828 mg, 98%) as a white solid.

Data for **22**{*5*}:

mp: 81.5-82 ^{o}C (MTBE:Hexanes)

^{1}H-NMR: (500 MHz, $CDCl_3$)

7.37 (d, *J* = 4.3, 1 H, HC(10), HC(11)), 7.31 (m, 1 H, HC(12)), 4.10 (d, *J* = 13.7, 1 H, HC(2)), 3.70 (d, *J* = 13.6, 1 H, HC(2)), 3.68 (dd, *J* = 8.3, 12.0, 1 H, HC(4)), 3.29 (dd, *J* = 10.8, 12.1, 1 H, HC(4)), 2.75 (dd, *J* = 6.1, 9.3, 1 H, HC(7a)), 2.64–2.55 (m, 1 H, HC(5)), 2.34–2.37 (m, 1 H, HC(5a)), 1.99–1.93 (m, 3 H, $H_2C(7)$, HC(6)), 1.93–1.83 (m, 1 H, HC(6)), 1.80 (br, s, 1 H, OH), 1.55 (s, 3 H, $H_3C(8)$), 1.02 (d, *J* = 6.6, 3 H, $H_3C(13)$), 0.8–2.5 (br, 3 H, $(H_3B)^3$)

^{13}C-NMR: (126 MHz, $CDCl_3$)

146.0 (C(9)), 128.9 (C(11)), 128.0 (C(12)), 125.1 (C(10)), 89.6 (C(7b), 79.3 (C(1)), 78.8 (C(2)), 74.5 (C(4)), 62.6 (C(5a)), 59.8 (C(7a)), 34.7 (C(5)), 31.5 (C(7)), 25.1 (C(8)), 24.1 (C(6)), 17.7 (C(13))

IR: ($CHCl_3$ film)

3475 (br), 2960 (s), 2871 (s), 2377 (s), 2327 (s), 2271 (s), 1494 (w), 1447 (m), 1266 (w), 1172 (s), 1131 (m), 1067 (w), 1004 (m), 954 (w), 876 (w), 700 (s)

MS: (EI, 70 eV)

268.2 (24), 257.2 (23), 242.1 (11), 224.1 (3), 192.1 (4), 178.1 (4), 158 (14), 137.1 (11), 124.1 (26), 110.1 (100)

Mol. Formula: $C_{17}H_{26}BNO$ (271.21)

HRMS: $C_{17}H_{23}NO$: (257.1780)

Calcd: 257.1780

Found: 257.1775

TLC: R_f 0.58 (hexanes/TBME, 1:1) [I_2, CAM]

Grignard Additions to Keto Amide 23. Preparation of (1*R*,3*S*,5*S*,5a*S*,7a*S*,7b*R*)-Octahydro-1-hydroxy-1-(*tert*-butyl)-5-methyl-7b-methyl-2*H*cyclopenta[*gh*]pyrrolizin-2-one (24{*4*}):

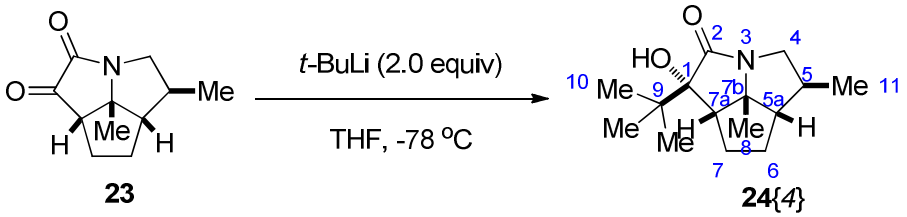

To a 25-mL, two-necked, round-bottomed flask equipped with a nitrogen inlet adapter, a rubber septum and a magnetic stir bar was added **23** (100 mg, 0.518 mmol) followed by THF (5.0 mL). The flask was immersed in an acetone/$CO_{2(s)}$ and stirred for 20 min. Then, *t*-BuLi (1.6 M, 648 µL, 2.0 equiv) was added dropwise over 5 min via syringe. After being stirred for 10 min, the acetone/$CO_{2(s)}$ bath was replaced with an ice bath and the reaction was stirred for 1 hr. The reaction was quenched by the dropwise addition of sat. aq. NH_4Cl solution (15 mL) and further diluted with Et_2O (10 mL). The biphasic mixture was poured into a 125-mL separatory funnel containing sat. aq. NH_4Cl solution (10 mL) and Et_2O (30 mL). The layers were separated and the aqueous extract was washed with Et_2O (2 x 25 mL). The organic extracts were washed with H_2O (1 x 25 mL), brine (1 x 25 mL), and the combined organic extracts were dried over Na_2SO_4, filtered (cotton plug), and concentrated by rotary evaporation (15 mm Hg, 20-25°C). The resulting pale-yellow oil was purified by silica gel column chromatography (1.8 cm x 6cm, gradient elution, hexanes/TBME, 17:3, 5:1, 3:1, 3:1, 3:2, 25 mL each) to afford **24{*4*}** (43 mg, 33%) as a white solid.

Data for **24{*4*}**:

^{1}H-NMR: (500 MHz, $CDCl_3$)

4.30 (dd, *J* = 8.6, 12.2, 1 H, HC(4)), 2.63 (dd, *J* = 7.3, 12.2, 1 H, HC(4)), 2.55 (s, 1 H, HC(OH)), 2.38 (d, *J* =8.0, 1 H, HC(7a)), 2.07 (dd, *J* = 5.3, 12.7, 1 H, HC(7)), 1.99 (dd, *J* = 7.3, 15.3, 1 H, HC(5)), 1.86 (ddd, *J* = 6.4, 6.4, 12.8, 1 H, HC(6)), 1.78 (ddd, *J* = 2.1, 7.4, 9.8, 1 H, HC(5a)), 1.64–1.56 (m, 1 H, HC(7)), 1.40 (s, 3 H, H_3C(8)), 1.11 (d, *J* = 7.1, 3 H, H_3C(11)), 1.09–1.02 (m, 1 H, HC(6)), 0.97 (s, 9 H, H_3C(10))

^{13}C-NMR: (126 MHz, $CDCl_3$)

179.3 (C(2)), 83.2 (C(1 or 7b)), 76.6 (C(1 or 7b)), 59.3 (C(5a)), 51.4 (C(4)), 49.6 (C(7a)), 37.8 (C(5)), 37.3 (C(10)), 33.9 (C(6)), 29.8 (C(7)), 25.0 (C(11)), 23.9 (C(8)), 21.3 (C(9))

IR: ($CDCl_3$, film)

3404 (br), 2958 (s), 2865 (s), 2248 (w), 1678 (s), 1464 (m), 1395 (m), 1365 (m), 1340 (m), 1230 (w), 1181 (w), 1147 (w), 1115 (w), 1087 (w), 1057 (w), 1015 (w), 994 (w), 910 (w), 766 (w)

MS: (EI, 70 eV)

251.2 (1), 236.2 (1.8), 218 (1.9), 195.1 (100), 166.1 (2.7), 152.1 (3.1), 140.1 (2.8), 110.1 (8.7)

Mol. Formula: $C_{15}H_{25}NO_2$ (251.36)

HRMS: $C_{21}H_{23}NO_2$, (251.1885)

Calcd: 251.1885

Found: 251.1883

TLC: R_f 0.25 (hexanes/TBME, 3:1) [I_2]

Preparation of (1*S*,3*S*,5*S*,5a*S*,7a*S*,7b*R*)-Octahydro-1-hydroxy-1-(2,4,6-trimethly-phenyl)-5-methyl-7b-methyl-2*H*cyclopenta[*gh*]pyrrolizine•Borane (24{*6*})

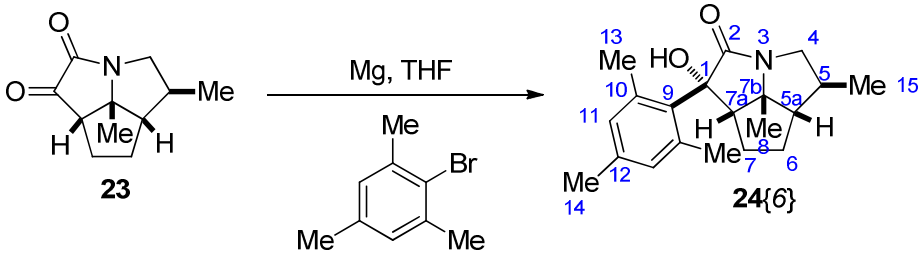

To a 25-mL, two-necked, round-bottomed flask equipped with a nitrogen inlet adapter, a rubber septum and a magnetic stir bar was added **23** (100 mg, 0.517 mmol) followed by THF (2.7 mL). The flask was immersed in an ice bath and mesitylmagnesium bromide (0.39 M, 2.0 mL, 1.5 equiv) was added dropwise via syringe. After being stirred for 10 min, the cooling bath was removed and the solution was stirred at room temperature for 20 min. The reaction flask was immersed in an ice bath and the reaction was quenched with sat. aq. NH_4Cl solution (15 mL). The biphasic mixture was poured into a 125-mL separatory funnel containing sat. aq. NH_4Cl solution (10 mL) and Et_2O (30 mL). The layers were separated and the aqueous extract was washed with Et_2O (2 x 25 mL). The organic extracts were washed with H_2O (1 x 25 mL), brine (1 x 25 mL), and the combined organic extracts were dried over $MgSO_4$, filtered (cotton plug), and concentrated by rotary evaporation (15 mm Hg, 20-25°C). The resulting pale-yellow oil was purified by silica gel column chromatography (1.8 cm x 8 cm, gradient elution,

hexanes/EtOAc, 9:1, 4:1, 7:3, 1:1, 25 mL each) to afford **24**{*6*} (157 mg, 97%) as a white solid.

Data for **24**{*6*}:

mp: 101-102 °C (hexanes:EtOAc)

^{1}H-NMR: (500 MHz, $CDCl_3$)

6.92 (s, 1 H, HC(11)), 6.68 (s, 1 H, HC(11)), 4.17 (dd, *J* = 7.3, 11.7, 1 H, HC(4)), 3.47 (s, 1 H, OH), 2.65 (dd, *J* = 7.6, 10.1, 1 H, HC(4)), 2.64 (dd, *J* = 10.4, 11.6, 1 H, HC(5)), 2.48 (s, 3 H, H_3C(8, 13, or 14), 2.41 (s, 3 H, H_3C(8, 13, or 14)), 2.22 (s, 3 H, H_3C(8, 13, or 14)), 1.98-1.92 (m, 1 H, HC(7)), 1.84-1.79 (m, 1 H, HC(7a)), 1.78-1.66 (m, 3 H, HC(7), HC(6), HC(5a)), 1.55-1.48 (m, 1 H, HC(6)), 1.09 (d, *J* = 6.7, 3 H, H_3C(15)), 1.08 (s, 3 H, H_3C(8, 13, or 14))

^{13}C-NMR: (126 MHz, $CDCl_3$)

179.1 (C(2)), 139.4 (C(9)), 138.3 (C(10 or 12)), 136.6 (C(10 or 12)), 133.9 (C(10 or 12)), 131.9 (C(11)), 130.8 (C(11)), 82.3 (C(1)), 75.3 (C(7b)), 60.2 (C(5)), 58.9 (C(7a)), 50.9 (C(4)), 41.7 (C(5a)), 29.9 (C(6)), 27.1 (C(7)), 23.8 (C(8, 13 or 14)), 22.3 (C(8, 13, or 14)), 21.2 (C(8, 13, or 14)), 20.7 (C(8, 13, or 14)), 17.7 (C(15))

IR: (NaCl plate, film)

3404 (br), 3000 (s), 2959 (s), 2922 (s), 2870 (s), 1693 (s), 1610 (m), 1560 (w), 1460 (s), 1407 (s), 1379 (m), 1351 (m), 1280 (w), 1232 (m), 1120 (m), 1072 (m), 1035 (m), 978 (w), 851 (m)

MS: (EI, 70 eV)

313 (10), 295 (84), 285 (4), 280 (6), 270 (3), 252 (5), 147 (100), 138 (10), 124 (21), 119 (29), 110 (90)

Mol. Formula: $C_{20}H_{27}NO_2$ (313.43)

HRMS: $C_{20}H_{27}NO_2$: (313.2042)

Calcd: 313.2042

Found: 313.2045

TLC: R_f 0.32 (hexanes/EtOAc, 3:1) [I_2, CAM]

Preparation of (1*R*,3*S*,5*S*,5a*S*,7a*S*,7b*R*)-Octahydro-1-hydroxy-1-[1]naphthyl-5-methyl-7b-

methyl-2*H*cyclopenta[*gh*]pyrrolizin-2-one (24{*7*}):

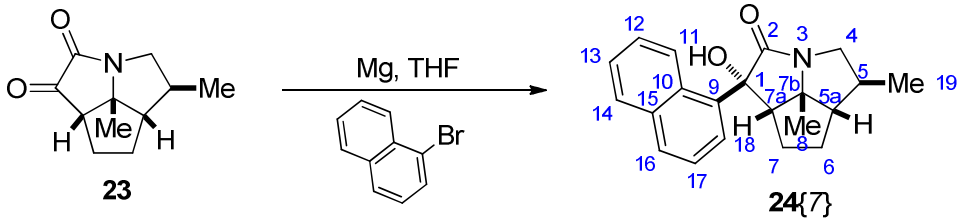

To a 25-mL, two-necked, round-bottomed flask equipped with a nitrogen inlet adapter, a rubber septum and a magnetic stir bar was added **23** (100 mg, 0.517 mmol) followed by THF (2.7 mL). The flask was immersed in an ice bath and 1-naphthylmagnesium bromide (0.4 M, 2.0 mL, 1.5 equiv) was added dropwise via syringe. After being stirred for 10 min, the cooling bath was removed and the reaction was stirred at room temperature for 20 min. The biphasic mixture was poured into a 125-mL separatory funnel containing sat. aq. NH_4Cl solution (10 mL) and Et_2O (30 mL). The layers were separated and the aqueous extract was washed with Et_2O (2 x 25 mL). The organic extracts were washed with H_2O (1 x 25 mL), brine (1 x 25 mL), and the combined organic extracts were dried over $MgSO_4$, filtered (cotton plug), and concentrated by rotary evaporation (15 mm Hg, 20-25^{o}C). The resulting pale-yellow oil was purified by silica gel column chromatography (1.8 cm x 8 cm, gradient elution, hexanes/EtOAc, 9:1, 4:1, 7:3, 1:1, 25 mL each) to afford **24{*7*}** (157 mg, 95%) as a white solid.

Data for **24{*7*}**:

mp: 150-151 ^{o}C (hexanes/EtOAc)

^{1}H-NMR: (500 MHz, $CDCl_3$)

8.43 (d, J = 8.4, 1 H, HC(11)), 7.87 (d, J = 7.9, 1 H, HC(14)), 7.78 (d, J = 7.9, 1 H, HC(16)), 7.56-7.48 (m, 2 H, HC(12), HC(13)), 7.34-7.28 (m, 2 H, HC(17), HC(18)), 4.27 (dd, J = 6.8, 11.5, 1 H, HC(4)), 3.44 (br, s, 1 H, OH), 2.96 (dd, J = 7.6, 10.1, 1 H, HC(7a)), 2.69 (dd, J = 10.0, 11.5, 1 H, HC(4)), 2.21-2.14 (m, 1 H, HC(7)), 2.00-1.92 (m, 1 H, HC(7)), 1.83-1.73 (m, 3 H, HC(6), HC(5a), HC(5)), 1.60-1.55 (m, 1 H, HC(6)), 1.11 (d, J = 6.4, 3 H, H_3C(19)), 0.87 (s, 3 H, H_3C(8))

^{13}C-NMR: (126 MHz, $CDCl_3$)

177.2 (C(2)), 138.9 (C(9)), 135.0 (C(15)), 131.1 (C(10)), 129.3 (C(16)), 129.1 (C(14)), 126.6 (C(11)), 126.0 (C(12 or 13)), 125.7 (C(12 or 13)), 124.7 (C(17 or 18)), 124.7 (C(17 or 18)), 84.1 (C(1 or 7b)), 75.9 (C(1 or 7b)), 58.9 (C(5a)),

57.9 (C(7a)), 51.2 (C(4)), 41.9 (C(5)), 30.0 (C(6)), 27.0 (C(7)), 24.4 (C(8)), 17.7 (C(19))

IR: (NaCl plate, film)

3386 (s), 3050 (w), 3007 (m), 2959 (s), 2871 (s), 1693 (s), 1596 (w), 1509 (m), 1461 (s), 1411 (s), 1352 (m), 1376 (m), 1330 (m), 1280 (m), 1230 (s), 1213 (m), 1174 (w), 1131 (s), 1074 (s), 1030 (w), 967 (w), 915 (w), 862 (w), 802 (s)

MS: (EI, 70 eV)

321 (19), 293 (6), 183 (9), 165 (13), 155 (68), 127 (46), 110 (100)

Mol. Formula: $C_{21}H_{23}NO_2$ (321.41)

HRMS: $C_{21}H_{23}NO_2$: (321.1729)

Calcd: 321.1729

Found: 321.1732

TLC: R_f 0.28 (hexanes/EtOAc, 3:1) [I_2, CAM]

Preparation of (1*R*,3*S*,5*S*,5a*S*,7a*S*,7b*R*)-Octahydro-1-hydroxy-1-(*tert*-butyl)-5-methyl-7b-methyl-2*H*cyclopenta[*gh*]pyrrolizine•Borane (22{*4*}):

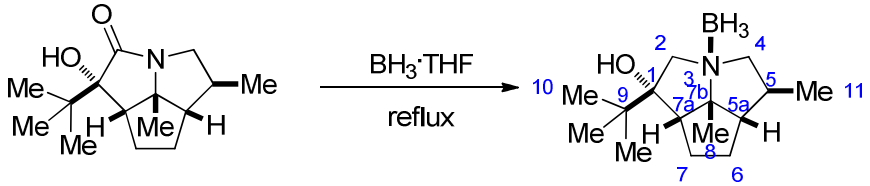

24{*4*} **22**{*4*}

To a 25-mL, single-necked, round-bottomed flask equipped with a nitrogen inlet adapter, a rubber septum, a reflux condenser, and a magnetic stir bar was added sequentially **24**{*4*} (29 mg, 0.115 mmol), THF (200 µL), and BH_3•THF complex (3.3 mL, 1.0 M solution, 20 equiv). The reaction flask was immersed in an oil bath and heated to reflux (70 °C). After being stirred for 12 h at reflux, the solution was allowed to reach room temperature, then quenched by dropwise addition of methanol (10 mL) and then concentrated by rotary evaporation (15 mm Hg, 20-25°C). The resulting colorless oil was purified by silica gel column chromatography (1.8 cm x 8 cm column, gradient elution, hexanes/TBME, 19:1, 9:1, 3:1, 3:2, 25 mL each) to afford 27 mg (93%) of **22**{*4*} as a white solid.

Data for **22**{*4*}:

^{1}H-NMR: (500 MHz, $CDCl_3$)

3.80 (d, *J* = 13.9, 1 H, HC(2)), 3.63 (dd, *J* =8.5, 12.0, 1 H, HC(4)), 3.23 (d, *J* =13.8, 1 H, HC(2)), 3.23–3.18 (m, 1 H, HC(4)), 2.48–2.40 (m, 1 H, HC(7a)), 2.41 (dd, *J* = 6.8, 9.2, 1 H, HC(5)), 2.09–1.99 (m, 1 H, HC(7)), 1.91–1.84 (m, 3 H, H_2C(6), HC(5a)), 1.72–1.63 (m, 1 H, HC(7)), 1.62 (br, s, 1 H, HO), 1.46 (s, 3 H, H_3C(8)), 0.99 (d, *J* = 6.6, 3 H, H_3C(9)), 0.92 (s, 3 H, H_3C(11)), 0.8–2.5 (br, 3 H, $(H_3B)^3$)

^{13}C-NMR: (126 MHz, $CDCl_3$)

89.7 (C(1 or 7b)), 83.0 (C(1 or 7b)), 75.7 (C(2)), 74.6 (C(4)), 59.6 (C(5a)), 56.5 (C(7a)), 37.5 (C(10)), 35.0 (C(5)), 32.1 (C(6)), 25.5 (C(10)), 25.4 (C(7)), 24.7 (C(8)), 18.1 (C(11))

IR: ($CDCl_3$ film)

3503 (s), 2961 (s), 2872 (s), 2376 (s), 2327 (s), 2271 (s), 1465 (m), 1400 (w), 1378 (m), 1335 (w), 1267 (w), 1174 (m), 1140 (m), 1091 (w), 1057 (w), 1002 (w), 980 (w), 958 (w), 940 (w), 910 (s), 882 (w), 841 (w), 733 (s), 649 (w)

MS: (ESI, Q-tof)

422.2 (10), 344.2 (25), 318.2 (40), 308.2 (100)

Mol. Formula: $C_{15}H_{30}BNO$ (251.22)

HRMS: $C_{21}H_{26}NO$: (308.2014)

Calcd: 308.2014

Found: 308.2011

TLC: R_f 0.27 (hexanes/TBME, 3:1) [I_2, CAM]

Preparation of (1*R*,3*S*,5*S*,5a*S*,7a*S*,7b*R*)-Octahydro-1-hydroxy-1-mesityl-5-methyl-7b-methyl-2*H*cyclopenta[*gh*]pyrrolizine•Borane (22{*6*}):

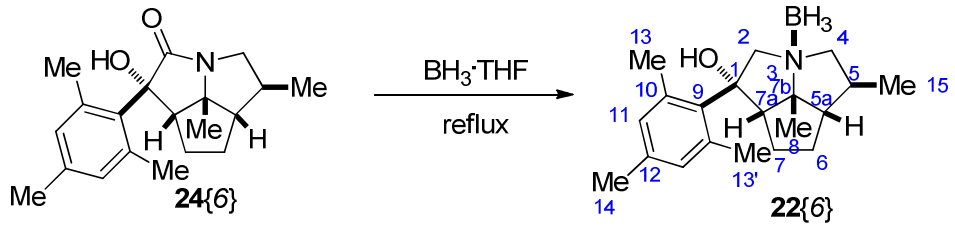

To a 25-mL round-bottomed flask equipped with a nitrogen inlet adapter, a rubber

septum, a reflux condenser, and a magnetic stir bar was added sequentially **24**{*6*} (50 mg, 0.160 mmol), THF (200 μL), and BH_3•THF complex (3.2 mL, 1.0 M solution, 20 equiv). The reaction flask was immersed in an oil bath and heated to reflux (70 ^oC). After being stirred for 12 h at reflux, the solution was allowed to reach room temperature and was quenched with methanol (5 mL) and concentrated by rotary evaporation (15 mm Hg, 20-25^oC). The resulting colorless oil was purified by silica gel column chromatography (1.8 cm x 8 cm column, gradient elution, hexanes/TBME, 19:1, 9:1, 4:1, 3:1,25 mL each) to afford 36 mg (72%) of **22**{*6*} as a white solid.

Data for **22**{*6*}:

mp: 131-132 ^oC (MTBE/hexanes)

^{1}H-NMR: (500 MHz, $CDCl_3$)

6.81 (s, 2 H, HC(11)), 4.09 (d, *J* = 14.1, 1 H, HC(9)), 4.02 (d, *J* = 14.1, 1 H, HC(9)), 3.72 (dd, *J* = 8.2, 12.1, 1 H, HC(4)), 3.29 (dd, *J* = 9.9, 12.0, 1 H, HC(4)), 3.10 (dd, *J* = 6.0, 8.5, 1 H, HC(7a)), 2.62–2.52 (m, 1 H, HC(5)), 2.52 (s, 6 H, H_3C(13), H_3C(13)), 2.40–2.31 (m, 1 H, HC(7)), 2.22 (s, 3 H, H_3C(14)), 2.06–1.98 (m, 1 H, HC(7)), 1.99–1.93 (m, 3 H, H_2C(6), HC(5a)), 1.51 (s, 3 H, H_3C(8)), 1.04 (d, *J* = 6.7, 3 H, H_3C(14)), 0.8–2.5 (br, 3 H, $(H_3B)^3$)

^{13}C-NMR: (126 MHz, $CDCl_3$)

139.1 (C(12)), 136.9 (C(9)), 136.4 (C(10)), 132.5 (C(11)), 88.4 (C(7b)), 82.4 (C(1)), 79.9 (C(2)), 75.1 (C(4)), 62.5 (C(7a)), 60.6 (C(5a)), 35.4 (C(5)), 31.8 (C(6)), 27.0 (C(7)), 25.6 (C(8)), 25.1 (C(13 or 14)), 20.4 (C(13 or 14)), 18.2 (C(15))

IR: (thin film)

3508 (s), 2383 (s), 2319 (s), 2274 (s), 1606 (m), 1378 (s), 1309 (w), 1287 (w), 1187 (s), 1128 (w), 1071 (m), 1034 (m), 943 (m), 860 (w), 734 (w)

MS: (ESI, Q-tof)

314.2 (12), 300.2 (30), 296.2 (100), 268.2 (25)

Mol. Formula: $C_{20}H_{32}BNO$ (313.29)

HRMS: $C_{20}H_{30}NO$: (300.2327)

Calcd: 300.2327

Found: 300.2332

TLC: R_f 0.33 (hexanes/TBME, 9:1) [I_2, CAM]

Preparation of (1*R*,3*S*,5*S*,5a*S*,7a*S*,7b*R*)-Octahydro-1-hydroxy-1-[1]naphthyl-5-methyl-7b-methyl-2*H*cyclopenta[*gh*]pyrrolizine•Borane (22{*7*}):

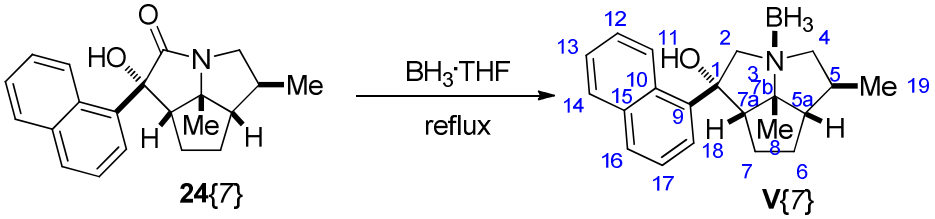

To a 25-mL, round-bottomed flask equipped with a nitrogen inlet adapter, a rubber septum, a reflux condenser, and a magnetic stir bar was added sequentially **24**{*7*} (50 mg, 0.156 mmol), THF (200 µL), and BH_3•THF complex (3.1 mL, 1.0 M solution, 20 equiv). The reaction flask was immersed in an oil bath and heated to reflux (70 °C). After being stirred for 12 h at reflux, the solution was allowed to reach room temperature, then quenched with methanol (5 mL) and then concentrated by rotary evaporation (15 mm Hg, 20-25°C). The resulting colorless oil was purified by silica gel column chromatography (1.8 cm x 8 cm column, gradient elution, hexanes/TBME, 19:1, 9:1, 3:1, 3:2, 25 mL each) to afford 42 mg (85%) of **22**{*7*} as a white solid.

Data for **22**{*7*}:

mp: 151-153 °C (MTBE:Hexanes)

^{1}H-NMR: (500 MHz, $CDCl_3$)

8.44 (d, *J* = 8.5, 1 H, HC(11)), 7.87 (d, *J* = 7.9, 1 H, HC(14)), 7.81 (d, *J* = 8.2, 1 H, HC(16)), 7.67 (d, *J* = 7.3, 1 H, HC(18)), 7.55–7.47 (m, 2 H, HC(12), HC(17)), 7.40 (dd, *J* = 7.8, 7.8, 1 H, HC(13)), 4.23 (d, *J* = 13.4, 1 H, HC(2)), 4.04 (d, *J* = 13.5, 1 H, HC(2)), 3.66 (dd, *J* = 7.5, 12.2, 1 H, HC(4)), 3.25–3.19 (m, 2 H, HC(7a), HC(4)), 2.60–2.50 (m, 1 H, HC(5)), 2.40–2.32 (m, 1 H, HC(7)), 2.22 (br, s, 1 H, OH), 2.10–2.01 (m, 1 H, HC(7)), 2.00–1.93 (m, 3 H, H_2C(6), HC(5a)), 1.54 (s, 3 H, H_3C(8)), 1.05 (d, *J* = 6.5, 3 H, H_3C(19)), 0.8–2.5 (br, 3 H, $(H_3B)^3$)

^{13}C-NMR: (126 MHz, $CDCl_3$)

139.2 (C(9)), 135.3 (C(15)), 131.2 (C(10)), 130.0 (C(16)), 129.6 (C(14)), 126.4 (C(11)), 126.3 (C(12 or 17)), 125.9 (C(12 or 17)), 124.8 (C(13)), 124.2 (C(18)), 88.1 (C(7b)), 80.9 (C(1)), 76.5 (C(2)), 74.6 (C(4)), 61.3 (C(5a)), 60.4 (C(7a)), 34.8 (C(5)), 31.0 (C(6)), 26.8 (C(7)), 25.7 (C(8)), 17.5 (C(19))

IR: (thin film)

3475 (m), 2383 (s), 2332 (s), 2269 (s), 1596 (w), 1444 (w), 1309 (w), 1202 (w), 1163 (m), 1134 (m), 1067 (w), 1040 (w), 1000 (w), 933 (w), 872 (w), 808 (m), 782 (s)

MS: (ESI, Q-tof)

422.2 (10), 344.2 (25), 318.2 (40), 308.2 (100)

Mol. Formula: $C_{21}H_{28}BNO$ (321.26)

HRMS: $C_{21}H_{26}NO$, (308.2014)

Calcd: 308.2014

Found: 308.2011

TLC: R_f 0.39 (hexanes/TBME, 3:1) [I_2, CAM]

7.3.3. B. Variable Group R^3: Williamson Ether Synthesis

General Procedure (I) for the Preparation of Library Intermediates

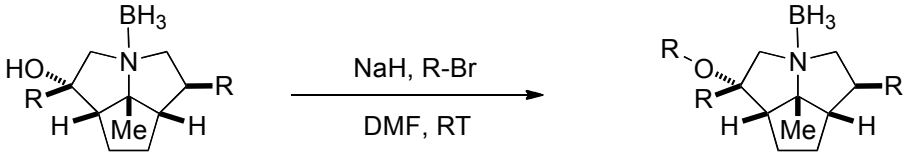

To a two-necked, 25-mL, round-bottomed flask equipped with a nitrogen inlet adapter, a rubber septum and a magnetic stir bar was added sequentially alcohol X (X mg, 0.X mmol) and DMF (2.74 mL, ~0.35 M). The flask was then immersed in an ice/NaCl bath for 15 min. Sodium hydride (xx mg, 0.xx mmol, 1.2 equiv) was weighed into a vial in a glove box then transferred to the flask in one portion (bubbling was observed). The resulting solution was allowed to stir for 15 min then alkyl bromide (X μL, 0.X mmol, 1.2 equiv) was added via syringe in a single portion. The resulting cloudy mixture was stirred for 2 h, then quenched by pouring onto onto ice water (20 mL). This mixture was transferred to a 125-mL separatory funnel where an additional 20 mL of water was added and the aqueous phase was extracted with dichloromethane (3 x 20 mL). The organic extracts were washed with water (2 x 20 mL), and

brine (2x 20 mL), then the combinded organic extracts were dried ($MgSO_4$). The floculant suspension was filtered through a small pad of Celite (1 cm x 2 cm) and concentrated by rotary evaporation (15 mm Hg, 20-25°C) to afford a thick oil. Purification by silica gel chromatography (1.8 cm x 8 cm column, gradient elution, hexanes/EtOAc, 1:9, 1:3, 1:1) afforded X mg (XX%) of ether **X**{*x*}.

Preparation of Amino•Borane Intermediates IV{*2-5, 2-3*}. Preparation of (1*S*,3*S*,5a*S*,7a*S*,7b*R*) Octahydro-1-benzyloxy-1-methyl-7b-methyl-2*H*cyclopenta[*gh*]pyrrolizine•Borane (IV{*2,2*})

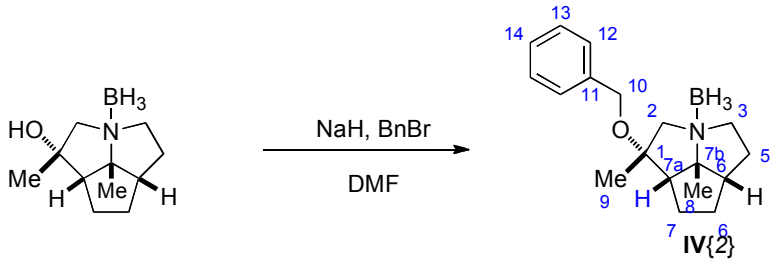

Following General Procedure I, to a two-necked, 10-mL round-bottomed flask equipped with a nitrogen inlet adapter, rubber septum and a magnetic stir bar was added sequentially alcohol **21**{*2*} (49 mg, 0.250-mmol), dimethylformamide (2.5 mL, ~0.1 M), then sodium hydride (9.0 mg, 0.375 mmol, 1.2 equiv) at 0 °C. After 15 min, benzyl bromide (60 µL, 0.500 mmol, 1.2 equiv) was added via syringe. The solution was stirred for 2 hr then quenched onto ice water (10 mL). Extraction and purification by silica gel column chromatography as described in General Procedure I afforded 64 mg (89%) of benzyl ether **IV**{*2,2*} as a clear, viscous oil.

Data for **IV**{*2,2*}:

^{1}H-NMR: (500 MHz, $CDCl_3$)

7.37–7.26 (m, 5 H, HC(12), HC(13), HC(14)), 4.40 (s, 2 H, H_2C(10)), 3.64 (dd, J = 6.7, 10.3, 1 H, HC(4)), 3.56 (d, J = 13.5, 1 H, HC(2)), 3.25 (dd, J = 4.5, 11.0, 1 H, HC(4)), 3.24 (d, J = 13.4, 1 H, HC(2)), 2.39–2.33 (m, 1 H, HC(5a)), 2.29–2.22 (m, 2 H, HC(7a), HC(5)), 2.22–2.13 (m, 1 H, HC(7)), 1.86–1.78 (m, 1 H, HC(6)), 1.77–1.69 (m, 2 H, HC(7), HC(6)), 1.49 (s, 3 H, H_3C(8 or 9)), 1.47 (s, 3 H, H_3C(8 or 9)), 1.47–1.43 (m, 1 H, HC(5)), 0.8–2.5 (br, 3 H, $(H_3B)^3$)

^{13}C-NMR: (126 MHz, $CDCl_3$)

139.0 (C(11)), 129.0 (C(12, 13, or 14)), 128.0 (C(12, 13, or 14)), 127.0 (C(12, 13, or 14)), 88.7 (C(7b)), 81.8 (C(1)), 70.8 (C(2)), 65.3 (C(10)), 64.4 (C(7a)), 64.0 (C(4)), 52.1 (C(5a)), 34.3 (C(6)), 29.5 (C(5)), 27.3 (C(7)), 25.6 (C(8 or 9)), 25.5 (C(8 or 9)),

IR: (NaCl plate, film)

2966 (s), 2858 (m), 2375 (s), 2326 (s), 2279 (s), 1454 (m), 1382 (m), 1172 (s), 1087 (m), 1028 (m), 933 (w) 905 (w), 855 (w), 754 (s) (696 (m)

MS: (EI, 70 eV)

284 (5), 271 (1), 256 (2), 180 (100), 165 (28), 149 (3), 138 (2), 122 (4), 109 (8)

Mol. Formula: $C_{18}H_{28}BNO$ (285.23)

HRMS: $C_{18}H_{27}BNO$, (284.2186)

Calcd: 284.2186

Found: 284.2184

TLC: R_f 0.23 (hexanes/TBME, 9:1) [I_2, CAM]

Preparation of (1*S*,3*S*,5a*S*,7a*S*,7b*R*) Octahydro-1-hexyloxy-1-methyl-7b-methyl-2*H*cyclopenta[*gh*]pyrrolizine•Borane (IV{*2*,*3*})

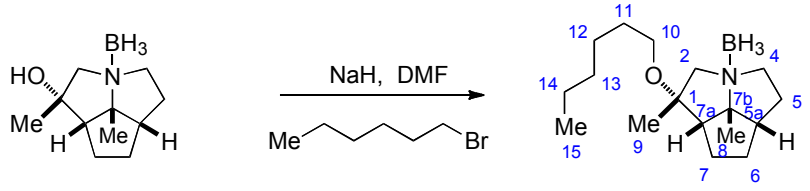

21{*2*} **22**{*3*}

To a one-necked, round-bottomed flask equipped with a nitrogen inlet adapter, rubber septum and a magnetic stir bar is added sequentially **21**{*2*} (49 mg, 0.250 mmol), dimethylformamide (2.5 mL, 0.1 M) and sodium hydride (6 mg, 0.250 mmol). After being stirred for 15 min, 1-bromohexane (41 µL, 0.250 mmol) was added. After being stirred for 2 h, NaH (6 mg, 0.250 mmol) was added. After being stirred for 15 min, 1-bromohexane (41 µL, 0.250 mmol) was added. After being stirred for 2 h, NaH (6 mg, 0.250 mmol) was added. After being stirred for 15 min, 1-bromohexane (41 µL, 0.250 mmol) was added. After 2 h, the reaction was quenched with water (10 mL) at 0 °C. Extraction and purification by silica gel column chromatography as described in General Procedure I afforded 47 mg (69%) of hexyl ether

IV{*2*,*3*} as a clear, viscous oil.

Data for **IV**{*2*,*3*}:

^{1}H-NMR: (500 MHz, $CDCl_3$)

3.64 (ddd, *J* = 6.5*,* 10.2*,* 10.0, 1 H, HC(4)), 3.48 (d, *J* = 13.4, 1 H, HC(2)), 3.29 (ddd, *J* = 1.6*,* 6.6*,* 6.6, 2 H, H_2C(10)), 3.28 (m, 1 H, HC(4)), 3.14 (d, *J* = 13.4, 1 H, HC(2)), 2.33 (m, 1 H, HC(5a)), 2.25 (m, 1 H, HC(5)), 2.15 (dd, *J* = 6.3*,* 8.1, 1 H, HC(7a)), 2.07 (ddd, *J* = 6.2*,* 6.2*,* 13.1, 1 H, HC(7)), 1.85 (dddd, *J* = 7.3*,* 7.3*,* 7.2*,* 12.6, 1 H, HC(6)), 1.77–1.71 (m, 1 H, HC(6)), 1.71–1.64 (m, 1 H, HC(6)),1.54–1.49 (m, 3 H, HC(5), H_2C(11)) 1.49 (s, 3 H, H_3C(8)), 1.35 (s, 3 H, H_3C(9)), 1.35–1.25 (m, 6 H, H_2C(12), H_2C(13), H_2C(14)), 0.88 (dd, *J* = 6.9*,* 6.9, 3 H, H_3(15)), 0.8–2.5 (br, 3 H, $(H_3B)^3$)

^{13}C-NMR: (126 MHz, $CDCl_3$)

88.6 (C(7b)), 81.1 (C(1)), 70.3 (C(2)), 64.6 (C(7a)), 63.7 (C(4)), 62.9 (C(10)), 52.1 (C(5a)), 34.5 (C(6)), 31.8 (C(13)), 30.3 (C(11)), 29.6 (C(5)), 27.0 (C(7)), 26.1 (C(12 or 14)), 25.7 (C(8)), 25.1 (C(9)), 22.7 (C(12 or 14)), 14.2 (C(15))

IR: (NaCl plate, film)

2931 (s), 2865 (s), 2376 (s), 2326 (s), 2279 (s), 1456 (s), 1378 (s), 1301 (m), 1172 (s), 1086 (s), 1021 (m), 965 (w), 924 (w), 851 (w), 756 (s)

MS: (EI, 70 eV)

278 (13), 265 (6), 250 (16), 194 (10), 180 (100), 165 (38), 150 (6), 138 (10), 123 (13), 110 (41)

Mol. Formula: $C_{17}H_{34}BNO$ (279.27)

HRMS: $C_{17}H_{33}BNO$, (278.2655)

Calcd: 278.2655

Found: 278.2656

TLC: R_f 0.35 (hexanes/TBME, 9:1) [I_2, CAM]

Preparation of (1*S*,3*S*,5a*S*,7a*S*,7b*R*) Octahydro-1-benzyloxy-1-isopropyl-7b-methyl-2*H*cyclopenta[*gh*]pyrrolizine•Borane (IV{*3*,*2*}**)**

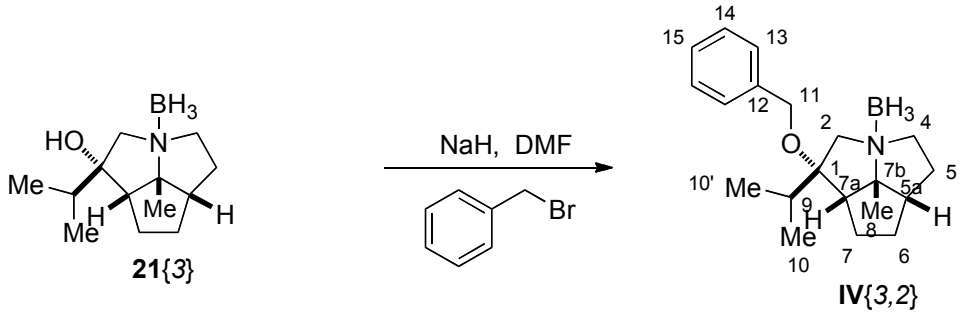

Following General Procedure I, to a two-necked, 10-mL round-bottomed flask equipped with a nitrogen inlet adapter, rubber septum and a magnetic stir bar was added sequentially alcohol **21**{*3*} (30 mg, 0.134 mmol), dimethylformamide (1.3 mL, ~0.1 M), then sodium hydride (4.8 mg, 0.202 mmol, 1.5 equiv) at 0 °C. After 15 min, benzyl bromide (24 μL, 0.202 mmol, 1.5 equiv) was added via syringe. The solution was stirred for 2 hr then quenched onto ice water (10 mL). Extraction and purification by silica gel column chromatography as described in General Procedure I afforded 39 mg (92%) of benzyl ether **IV**{*3,2*} as a clear, viscous oil.

Data for **IV**{*3,2*}:

^{1}H-NMR: (500 MHz, $CDCl_3$)

7.37–7.33 (m, 4 H, HC(13), HC(14)), 7.31–7.27 (m, 1 H, HC(15)), 4.49 (d, *J* = 11.3, 1 H, HC(11)), 4.42 (d, *J* = 11.3, 1 H, HC(11)), 3.84–3.77 (m, 1 H, HC(4)), 3.63 (d, *J* = 14.5, 1 H, HC(2)), 3.39 (d, *J* = 14.5, 1 H, HC(1)), 3.29 (dd, *J* = 8.5, 8.5, 1 H, HC(4)), 2.41–2.32 (m, 3 H, HC(7a), HC(5a), HC(5)), 2.27–2.20 (m, 1 H, HC(6)), 2.22–2.16 (m, 1 H, HC(9)), 1.96–1.88 (m, 1 H, HC(7)), 1.78–1.66 (m, 2 H, HC(7), HC(6)), 1.49 (s, 3 H, H_3C(8)), 1.44–1.40 (m, 1 H, HC(5)), 1.00 (d, J = 6.8, 3 H, H_3C(10)), 0.96 (d, J = 6.8, 3 H, H_3C(10')), 0.8–2.5 (br, 3 H, $(H_3B)^3$)

^{13}C-NMR: (126 MHz, $CDCl_3$)

138.5 (C(12)), 128.7 (C(13)), 127.6 (C(15)), 127.1 (C(14)), 88.6 (C(1)), 87.5 (C(7b)), 65.1 (C(11)), 64.1 (C(2)), 63.1 (C(4)), 58.4 (C(7a)), 51.5 (C(5a)), 35.9 (C(7)), 30.6 (C(9)), 30.4 (C(5)), 28.3 (C(6)), 25.1 (C(8)), 18.4 (C(10)), 17.6 (C(11))

IR: ($CHCl_3$)

3071 (w), 3028 (w), 2964 (s), 2379 (s), 2326 (s), 2278 (s), 2234 (w), 1957 (w), 1876 (w), 1812 (w), 1727 (w), 1599 (w), 1496 (m), 1468 (m), 1454 (s),

1379 (s), 1330 (w), 1264 (m), 1168 (s), 1085 (s), 1063 (s), 1028 (m), 970 (w), 912 (s), 850 (w), 794 (w), 734 (s), 697 (s)

MS: (EI, 70 eV)
312 (41), 299 (4), 268 (6), 256 (8), 220 (5), 208 (100), 193 (27), 164 (8), 149 (16), 126 (24)

Mol. Formula: $C_{20}H_{32}BNO$ (313.29)

HRMS: $C_{20}H_{31}BNO$, (312.2499)
Calcd: 312.2499
Found: 312.2497

TLC: R_f 0.25 (hexanes/TBME, 4:1) [I_2, CAM]

Preparation of (1*R*,3*S*,5a*S*,7a*S*,7b*R*) Octahydro-1-benzyloxy-1-phenyl-7b-methyl-2*H*cyclopenta[*gh*]pyrrolizine•Borane (IV{*5,2*})

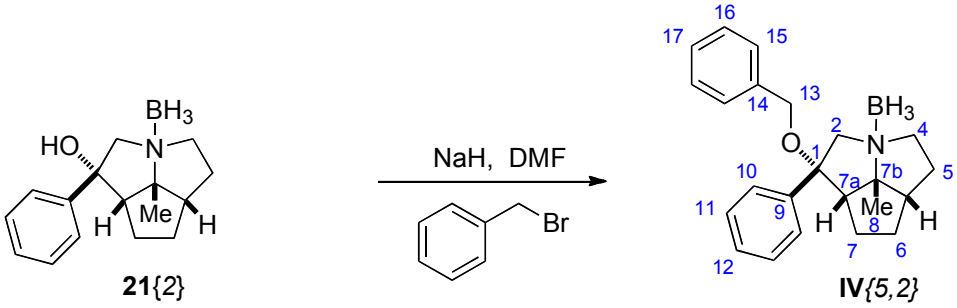

Following General Procedure I, to a two-necked, 10-mL round-bottomed flask equipped with a nitrogen inlet adapter, rubber septum and a magnetic stir bar was added sequentially alcohol **21**{*5,2*} (60 mg, 0.233 mmol), dimethylformamide (2.3 mL, ~0.1 M), then sodium hydride (8.4 mg, 0.350 mmol, 1.5 equiv) at 0 °C. After 15 min, benzyl bromide (42 µL, 0.350 mmol, 1.5 equiv) was added via syringe. The solution was stirred for 2 hr then quenched onto ice water (10 mL). Extraction and purification by silica gel column chromatography as described in General Procedure I afforded 80 mg (98%) of benzyl ether **IV**{*5,2*} as a clear, viscous oil.

Data for **IV**{*5,2*}:

^{1}H-NMR: (500 MHz, $CDCl_3$)
7.41–7.36 (m, 4 H), 7.34–7.30 (m, 3 H), 7.30–7.23 (m, 3 H), 4.32 (d, J = 11.5,

1 H, HC(2)), 4.01 (ddd, J = 14.3, 14.3, 14.2, 2 H, HC(13)), 3.98 (d, J = 11.9, 1 H, HC(2)), 4.00–3.95 (m, 1 H, HC(4)), 3.46–3.42 (m, 1 H, HC(4)), 2.68 (dd, J = 3.9, 8.3, 1 H, HC(7a)), 2.58–2.53 (m, 1 H, HC(7)), 2.44–2.46 (m, 2 H, HC(5a), HC(5)), 2.05–2.01 (m, 1 H, HC(6)), 1.94–1.83 (m, 2 H, HC(7), HC(6)), 1.57 (dd, 7.9, 10.5, 1 H, HC(5)), 1.51 (s, 3 H, $H_3C(8)$), 0.8–2.5 (br, 3 H, $(H_3B)^3$)

^{13}C-NMR: (126 MHz, $CDCl_3$)

142.2 (C(9)), 138.1 (C(14)), 128.9, 128.5, 128.1, 127.5, 127.0, 126.0, 88.6 (C(7b)), 85.9 (C(1)), 66.1 (C(2)), 65.6 (C(13)), 65.4 (C(4)), 62.7 (C(7a), 52.0 (C(5a)), 35.5 (C(6)), 29.9 (C(5)), 27.2 (C(7)), 25.7 (C(8))

IR: ($CHCl_3$)

30064 (w), 3031 (w), 2965 (s), 2869 (m), 2376 (s), 2332 (s), 2277 (s), 2243 (m), 1497 (m), 1448 (m), 1379 (w), 1177 (s), 1132 (w), 1088 (m), 1059 (s), 1027 (w), 911 (s), 849 (w), 732 (s), 699 (s)

MS: (EI, 70 eV)

333.2 (1), 332.2 (1), 318.2 (1), 242.1 (100), 227.1 (9), 105 (32)

Mol. Formula: $C_{23}H_{30}BNO$ (347.30)

HRMS: $C_{23}H_{27}NO$, (333.2093)

Calcd: 333.20927

Found: 333.20927

TLC: R_f 0.28 (hexanes/TBME, 9:1) [I_2, CAM]

Preparation of Amino•Borane Intermediates V{*2-7, 2-7*}. Preparation of (1*S*,3*S*,5*S*,5a*S*,7a*S*,7b*R*)-Octahydro-1-benzyloxy-5-methyl-7b-methyl-2*H*cyclopenta[*gh*]pyrrolizine•Borane (V{*1,2*})

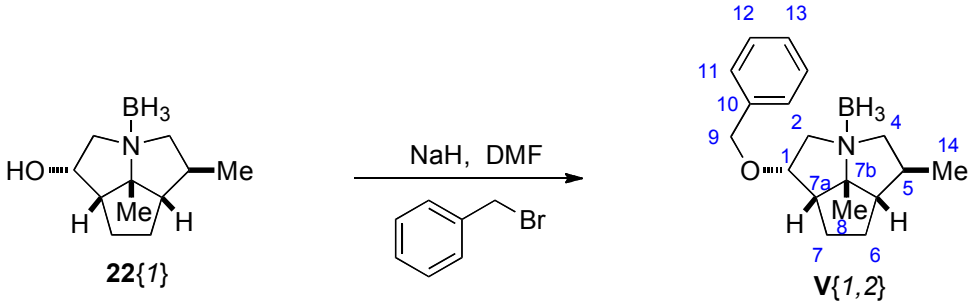

22{*1*} **V**{*1,2*}

Following General Procedure I, to a two-necked, 10-mL round-bottomed flask equipped with a nitrogen inlet adapter, rubber septum and a magnetic stir bar was added sequentially alcohol **18** (30 mg, 0.154 mmol), dimethylformamide (1.5 mL, ~0.1 M), then sodium hydride (5.5 mg, 0.231 mmol, 1.2 equiv) at 0 °C. After 15 min, benzyl bromide (27 μL, 0.231 mmol, 1.2 equiv) was added via syringe. The solution was stirred for 2 hr then quenched onto ice water (10 mL). Extraction and purification by silica gel column chromatography as described in General Procedure I afforded 40 mg (91%) of benzyl ether **V**{*1*,*2*} as a clear, viscous oil.

Data for **V**{*1*,*2*}:

^{1}H-NMR: (500 MHz, $CDCl_3$)

7.33 (m, 5 H, HC(11), HC(12), HC(13)), 4.53 (ddd, *J* = 6.6, 6.6, 10.7, 1 H, HC(1)), 4.51 (d, *J* = 11.7, 1 H, HC(1)), 4.45 (d, *J* = 11.4, 1 H, HC(9)), 3.51 (dd, *J* = 6.5, 10.4, 1 H, HC(2)), 3.16 (dd, *J* = 6.1, 12.5, 1 H, HC(4)), 3.06 (dd, *J* = 10.6, 10.6, 1 H, HC(2)), 2.82 (dd, *J* = 12.5, 12.5, 1 H, HC(4)), 2.42 (dd, *J* = 8.0, 17.0, 1 H, HC(7a)), 2.09–2.00 (m, 1 H, HC(5)), 2.00–1.92 (m, 1 H, HC(7)), 1.89–1.85 (m, 1 H, HC(5a)), 1.82–1.76 (m, 1 H, HC(7)), 1.75–1.70 (m, 2 H, $H_2C(6)$), 1.51 (s, 1 H, $H_3C(8)$), 1.02 (d, *J* = 6.4, 3 H, $H_3C(14)$), 0.8–2.5 (br, 3 H, $(H_3B)^3$)

^{13}C-NMR: (126 MHz, $CDCl_3$)

138.1 (C(10)), 128.6 (C(13)), 128.0 (C(12)), 127.8 (C(11)), 88.1 (C(7b)), 76.0 (C(1)), 72.0 (C(9)), 70.0 (C(4)), 64.3 (C(2)), 62.0 (C(5a)), 53.3 (C(7a)), 34.6 (C(5)), 29.6 (C(6)), 26.7 (C(7)), 25.9 (C(8)), 16.4 (C(16))

IR: (NaCl plate, film)

3064 (w), 3021 (w), 2960 (s), 2922 (s), 2872 (s), 2379 (s), 2326 (s), 2276 (s), 2234 (w), 1654 (w), 1497 (w), 1472 (m), 1456 (s), 1380 (m), 1364 (s), 1326 (w), 1305 (w), 1234 (w), 1186 (s), 1167 (s), 1142 (s), 1124 (s), 1054 (m), 1018 (w), 991 (m), 956 (w), 913 (s), 844 (w), 810 (w), 698 (s)

MS: (EI, eV)

284 (18), 256 (19), 228 (5), 180 (100), 165 (31), 110 (30), 91 (71), 84 (13)

Mol. Formula: $C_{18}H_{28}BNO$ (285.23)

HRMS: $C_{18}H_{27}BNO$, (284.2186)

Calcd: 284.21858

Found: 284.21909

TLC: R_f 0.25 (hexanes/TBME, 9:1) [I_2, CAM]

Preparation of (1*S*,3*S*,5*S*,5a*S*,7a*S*,7b*R*)-Octahydro-1-benzyloxy-1-methyl-5-methyl-7b-methyl-2*H*cyclopenta[*gh*]pyrrolizine•Borane (V{*2*,*2*}):

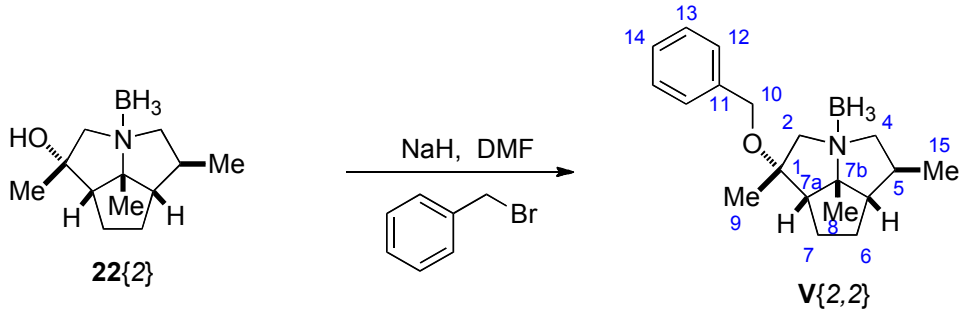

Following General Procedure I, to a two-necked, 10-mL round-bottomed flask equipped with a nitrogen inlet adapter, rubber septum and a magnetic stir bar was added sequentially alcohol **22**{*2*} (42 mg, 0.200 mmol), dimethylformamide (2.0 mL, ~0.1 M), then sodium hydride (7.2 mg, 0.300 mmol, 1.5 equiv) at 0 °C. After 15 min, benzyl bromide (48 µL, 0.4 mmol, 2.0 equiv) was added via syringe. The solution was stirred for 2 hr then quenched onto ice water (10 mL). Extraction and purification by silica gel column chromatography as described in General Procedure I afforded 58 mg (97%) of benzyl ether **V**{*2*,*2*} as a clear, viscous oil.

Data for **V**{*2*,*2*}:

^{1}H-NMR: (500 MHz, $CDCl_3$)

7.36–7.27 (m, 5 H, HC(12), HC(13), HC(14)), 4.43 (d, J = 11.1, 1 H, HC(10)), 4.35 (d, J = 11.1, 1 H, HC(10)), 3.50 (d, J = 11.6, 1 H, HC(2)), 3.35 (d, J = 11.6, 1 H, HC(2)), 3.23 (dd, J = 6.3, 12.5, 1 H, HC(4)), 2.96 (dd, J = 12.4, 12.4, 1 H, HC(4)), 2.21–2.12 (m, 2 H, HC(7a), HC(7)), 2.10–2.01 (m, 1 H, HC(5)), 1.88–1.83 (m, 2 H, HC(5a), HC(7)), 1.78–1.74 (m, 1 H, HC(6)), 1.75 (s, 3 H, H_3C(9)), 1.71–1.64 (m, 1 H, HC(6)), 1.57 (s, 3 H, H_3C(8)), 0.99 (d, J = 6.4, 3 H, H_3C(15)), 0.8–2.5 (br, 3 H, $(H_3B)^3$)

^{13}C-NMR: (126 MHz, $CDCl_3$)

138.7 (C(11)), 128.5 (C(13)), 127.6 (C(12)), 127.2 (C(14)), 88.7 (C(7b)), 79.9 (C(1)), 73.5 (C(4)), 73.3 (C(2)), 65.8 (C(10)), 62.1 (C(5a)), 61.3 (C(7a)), 33.5

(C(5)), 29.0 (C(6)), 27.3 (C(7)), 26.3 (C(8)), 25.9 (C(9)), 16.0 (C(15))

IR: ($CHCl_3$)

2961 (s), 2398 (s), 2282 (s), 1497 (w), 1457 (s), 1384 (m), 1152 (s), 1063 (m), 1028 (m), 956 (w), 697 (m)

MS: (EI, 70 eV)

298 (4), 270 (4), 194 (100), 179 (20), 110 (28), 91 (28)

Mol. Formula: $C_{19}H_{30}BNO$ (299.26)

HRMS: $C_{19}H_{29}BNO$, (298.2342)

Calcd: 298.2342

Found: 298.2341

TLC: R_f 0.30 (hexanes/TBME, 9:1) [I_2, CAM]

Preparation of (1*S*,3*S*,5*S*,5a*S*,7a*S*,7b*R*) Octahydro-1-(4-methoxybenzyloxy)-1-methyl-5-methyl-7b-methyl-2*H*cyclopenta[*gh*]pyrrolizine•Borane (V{*2*,*7*})

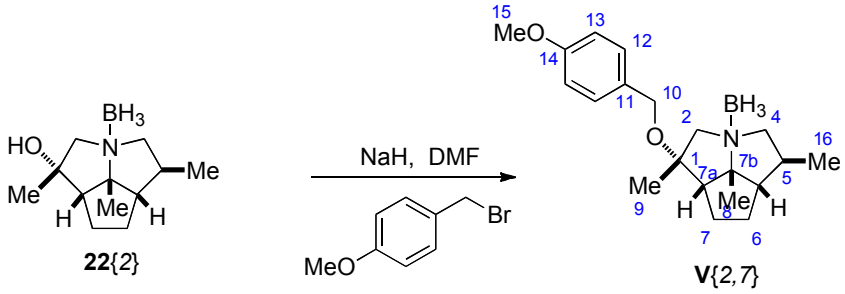

Following General Procedure I, to a two-necked, 10-mL round-bottomed flask equipped with a nitrogen inlet adapter, rubber septum and a magnetic stir bar was added sequentially alcohol **22**{*2*} (42 mg, 0.200 mmol), dimethylformamide (2.0 mL, ~0.1 M), then sodium hydride (7.2 mg, 0.300 mmol, 1.5 equiv) at 0 °C. After 15 min, 4-methoxybenzyl bromide (32 µL, 0.220 mmol, 1.1 equiv) was added via syringe. The solution was stirred for 2 hr then quenched onto ice water (10 mL). Extraction and purification by silica gel column chromatography as described in General Procedure I afforded 58 mg (86%) of 4-methoxybenzyl ether **V**{*2*,*7*} as a clear, viscous oil.

Data for **V**{*2*,*7*}:

^{1}H-NMR: (500 MHz, $CDCl_3$)

7.23 (d, J = 8.6, 2 H, HC(13)), 6.87 (d, J = 8.7, 2 H, HC(12)), 4.35 (d, J =

10.6, 1 H, HC(10)), 4.26 (d, *J* = 10.6, 1 H, HC(10)), 3.80 (s, 1 H, $H_3C(13)$), 3.48 (d, *J* = 11.6, 1 H, HC(2)), 3.32 (d, *J* = 11.6, 1 H, HC(2)), 3.21 (dd, *J* = 6.3, 12.4, 1 H, HC(4)), 2.95 (dd, *J* = 12.4, 12.4, 1 H, HC(4)), 2.19–2.10 (m, 2 H, HC(7a), HC(7)), 2.08–2.00 (m, 1 H, HC(5)), 1.90–1.82 (m, 2 H, HC(7), HC(5a)), 1.77–1.74 (m, 1 H, HC(6)), 1.74 (s, 3 H, $H_3C(9)$), 1.70–1.62 (m, 1 H, HC(6)), 1.56 (s, 3 H, $H_3C(8)$), 0.98 (d, *J* = 6.4, 3 H, $H_3C(16)$), 0.8–2.5 (br, 3 H, $(H_3B)^3$)

^{13}C-NMR: (126 MHz, $CDCl_3$)

159.2 (C(14)), 130.7 (C(11)), 128.9 (C(13)), 113.9 (C(12)), 88.7 (C(7b)), 79.8 (C(1)), 73.5 (C(4)), 73.3 (C(2)), 65.5 (C(10)), 62.1 (C(5a)), 61.2 (C(7a)), 55.4 (C(15)), 33.4 (C(5)), 29.0 (C(6)), 27.3 (C(7)), 26.3 (C(8)), 25.9 (C(9)), 16.0 (C(16))

IR: (NaCl plate, film)

2958 (s), 2929 (s), 2835 (s), 2396 (s), 2330 (s), 2282 (s), 1612 (s), 1586 (w), 1514 (s), 1457 (s), 1384 (s), 1349 (w), 1337 (w), 1302 (m), 1249 (s), 1166 (s), 1152 (s), 1108 (w), 1092 (m), 1064 (s), 1036 (s), 956 (m), 910 (w), 873 (w), 823(s)

MS: (EI, 70 eV)

328 (8), 194 (100), 179 (49), 164 (3), 151 (3), 121 (52), 110 (34)

Mol. Formula: $C_{20}H_{32}BNO_2$ (329.28)

HRMS: $C_{20}H_{31}BNO_2$, (328.2448)

Calcd: 328.2448

Found: 328.2448

TLC: R_f 0.28 (hexanes/TBME, 9:1) [I_2, CAM]

Preparation of (1*S*,3*S*,5*S*,5a*S*,7a*S*,7b*R*) Octahydro-1-hexyloxy-1-methyl-5-methyl-7b-methyl-2*H*cyclopenta[*gh*]pyrrolizine•Borane (V{*2,3*})

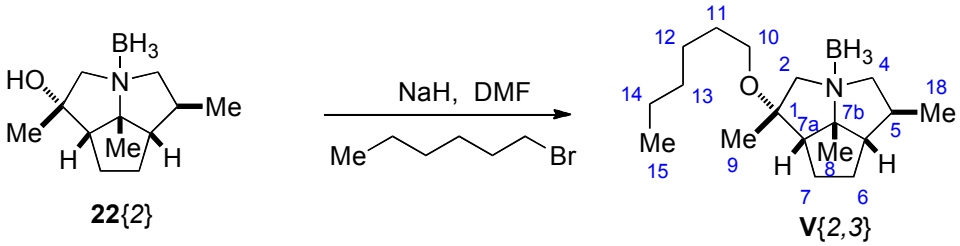

To a one-necked, round-bottomed flask equipped with a nitrogen inlet adapter, rubber septum and a magnetic stir bar is added sequentially **22**{*2*} (40 mg, 0.191 mmol), dimethylformamide (1.9 mL, 0.1 M) and sodium hydride (5 mg, 0.191 mmol). After being stirred for 15 min, 1-iodohexane (28 μL, 0.191 mmol) was added. After being stirred for 2 h, NaH (5 mg, 0.191 mmol), was added. After being stirred for 15 min, 1-iodoohexane (28 μL, 0.191 mmol) was added. After being stirred for 2 h, NaH (5 mg, 0.191 mmol) was added. After being stirred for 15 min, 1-iodohexane (28 μL, 0.191 mmol) was added. After 2 h, the reaction was quenched with water (10 mL) at 0 °C. Extraction and purification by silica gel column chromatography as described in General Procedure I afforded 31 mg (55%) of hexyl ether **V**{*2*,*3*} as a clear, viscous oil.

Data for **V**{*2*,*3*}:

^{1}H-NMR: (500 MHz, $CDCl_3$)

3.40 (d, J = 11.7, 1 H, HC(2)), 3.25 (m, 4 H, HC(10), HC(2), HC(4)), 2.95 (dd, J = 12.4, 12.4, 1 H, HC(4)), 2.11–2.02 (m, 3 H, HC(7a), HC(7), HC(5)), 1.81 (dd, J = 6.4, 9.8, 1 H, HC(5a)), 1.73 (m, 2 H, HC(7), HC(6)), 1.69–1.62 (m, 1 H, HC(6)), 1.59 (s, 1 H, H_3C(9)), 1.52 (s, 3 H, H_3C(8)), 1.52–1.46 (m, 2 H, HC(11)), 1.33–1.22 (m, 6 H, HC(12), HC(13), HC(14)), 0.98 (d, J = 6.4, 3 H, H_3C(16)), 0.88 (dd, J = 6.9, 6.9, 3 H, H_3C(15)), 0.8–2.5 (br, 3 H, $(H_3B)^3$)

^{13}C-NMR: (126 MHz, $CDCl_3$)

88.65 (C(9)), 79.08 (C(2)), 73.55 (C(1 or 12)), 73.36 (C(1 or 12)), 63.69 (C(8)), 62.05 (C(3)), 61.47 (C(6)), 33.56 (C(7)), 31.85 (C(14, 15 or 16), 30.37 (C(13)), 29.11 (C(5)), 26.89 (C(4)), 26.24 (C(10)), 26.05 (C(14, 15, or 16)), 25.63 (C(11)), 22.74 (C(14, 15, or 16)), 16.12 (C(18)), 14.19 (C(17))

IR: ($CDCl_3$, film)

2957 (s), 2931 (s), 2872 (s), 2396 (s), 2284 (s), 2241 (w), 1730 (w), 1459 (s), 1381 (m), 1348 (w), 1184 (s), 1168 (s), 1149 (s), 1064 (m), 913 (s)

MS: (ESI, 70 eV)

292 (51), 279 (7), 264 (20), 250 (5), 222 (3), 208 (13), 194 (100), 184 (30), 179 (41), 164 (8), 137 (6), 124 (22), 110 (67)

Mol. Formula: $C_{18}H_{36}BNO$ (293.30)

HRMS: $C_{18}H_{35}BNO$, (292.2812)

Calcd: 292.28118

Found: 292.28154

TLC: R_f 0.35 (hexanes/TBME, 9:1) [I_2, CAM]

Preparation of (1*S*,3*S*,5*S*,5a*S*,7a*S*,7b*R*) Octahydro-1-benzyloxy-1-isopropyl-5-methyl-7b-methyl-2*H*cyclopenta[*gh*]pyrrolizine•Borane (V{*3,2*})

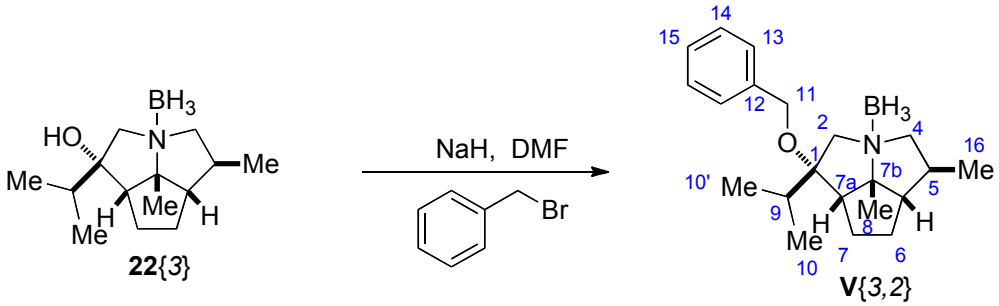

Following General Procedure I, to a two-necked, 10-mL round-bottomed flask equipped with a nitrogen inlet adapter, rubber septum and a magnetic stir bar was added sequentially alcohol **22**{*3*} (59 mg, 0.250 mmol), dimethylformamide (2.5 mL, ~0.1 M), then sodium hydride (9.0 mg, 0.375 mmol, 2.0 equiv) at 0 °C. After 15 min, benzyl bromide (60 µL, 0.500 mmol, 2.0 equiv) was added via syringe. The solution was stirred for 2 hr then quenched onto ice water (10 mL). Extraction and purification by silica gel column chromatography as described in General Procedure I afforded 80 mg (98%) of benzyl ether **V**{*3,2*} as a clear, viscous oil.

Data for **V**{*3,2*}:

^{1}H-NMR: (500 MHz, $CDCl_3$)

7.37–7.28 (m, 5 H, HC(13), HC(14), HC(15)), 4.51 (d, J = 11.1, 1 H, HC(11)), 4.38 (d, J = 11.1, 1 H, HC(11)), 3.63 (d, J = 14.3, 1 H, HC(2)), 3.60 (d, J = 14.3, 1 H, HC(2)), 3.36 (dd, J = 8.3, 12.1, 1 H, HC(4)), 3.14 (dd, J = 10.3, 12.1, 1 H, HC(4)), 2.45–2.38 (m, 1 H, HC(7)), 2.37 (dd, J = 7.7,16.4, 1

H, HC(7a)), 2.29–2.21 (m, 1 H, HC(5)), 2.21–2.13 (m, 1 H, HC(9)), 1.84–1.77 (m, 3 H, $H_2C(6)$, HC(5a)), 1.67–1.61 (m, 1 H, HC(7)) ,1.48 (s, 3 H, $H_3C(8)$), 0.99 (d, J = 6.8, 1 H, $H_3C(10)$), 0.93 (d, J = 6.8, 3 H, $H_3C(10')$), 0.84 (d, J = 6.7, 3 H, $H_3C(16)$), 0.8–2.5 (br, 3 H, $(H_3B)^3$)

^{13}C-NMR: (126 MHz, $CDCl_3$)

138.3 (C(12)), 128.6 (C(13) or C(15)), 127.6 (C(14)), 127.3 (C(13) or C(15)), 88.8 (C(7b) or C(1)), 85.1 (C(7b) or C(1)), 74.0 (C(4)), 69.4 (C(2)), 64.8 (C(11)), 59.6 (C(5a)), 57.1 (C(7a)), 34.7 (C(5)), 31.6 (C(6)), 30.3 (C(9)), 24.8 (C(7)), 24.7 (C(8)), 18.2 (C(10)), 17.7 (C(10')), 17.6 (C(16))

IR: ($CDCl_3$, film)

2962 (s), 2922 (s), 2870 (s), 2374 (s), 2327 (s), 2272 (s), 1497 (w), 1454 (s), 1379 (m), 1170 (s), 1147 (m), 1131 (m), 1057 (m), 1027 (m), 868 (w), 697 (m)

MS: (EI, 70 eV)

326 (6), 234 (6), 270 (11), 222 (s), 207 (21)

Mol. Formula: $C_{21}H_{34}BNO$ (327.31)

HRMS: $C_{21}H_{33}BNO$, (326.2655)

Calcd: 326.2655

Found: 326.2652

TLC: R_f 0.24 (hexanes/TBME, 9:1) [I_2]

Preparation of (1*S*,3*S*,5*S*,5a*S*,7a*S*,7b*R*) Octahydro-1-hexyloxy-1-isopropyl-5-methyl-7b-methyl-2*H*cyclopenta[*gh*]pyrrolizine•Borane (V{*3,3*})

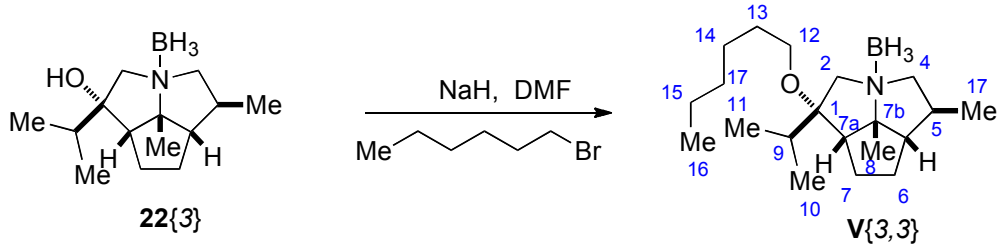

To a one-necked, round-bottomed flask equipped with a nitrogen inlet adapter, rubber septum and a magnetic stir bar is added sequentially **22**{*3*} (59 mg, 0.250 mmol), dimethylformamide (2.5 mL, 0.1 M) and sodium hydride (6 mg, 0.250 mmol). After being

stirred for 15 min, 1-bromohexane (35 μL, 0.250 mmol) was added. After being stirred for 2 h, NaH (6 mg, 0.250 mmol), was added. After being stirred for 15 min, 1-bromohexane (35 μL, 0.250 mmol) was added. After being stirred for 2 h, NaH (6 mg, 0.250 mmol) was added. After being stirred for 15 min, 1-bromohexane (35 μL, 0.250 mmol) was added. After 2 h, the reaction was quenched with water (10 mL) at 0 ^{o}C. Extraction and purification by silica gel column chromatography as described in General Procedure I afforded 37 mg (44%) of hexyl ether **V**{*3*,*3*} as a clear, viscous oil.

Data for **V**{*3*,*3*}:

^{1}H-NMR: (500 MHz, $CDCl_3$)

3.51 (d, *J* = 14.2, 1 H, HC(2)), 3.45 (d, *J* = 14.2, 1 H, HC(2)), 3.40-3.26 (m, 3 H, HC(4), H_2C(14), 3.18 (dd, *J* = 10.5, 12.0, 1 H, HC(4)), 2.42-2.32 (m, 2 H, HC(7), HC(5)), 2.27 (dd, *J* = 7.0, 9.3, 1 H, HC(7a)), 2.01 (hept, *J* = 6.8, 1 H, HC(9)), 1.87-1.77 (m, 3 H, H_2C(6), HC(5a)), 1.60-1.51 (m, 3 H, HC(7), H_2C(13)), 1.45 (s, 3 H, H_3C(8)), 1.38-1.32 (m, 2 H, H_2C(14)), 1.36-1.25 (m, 4 H, H_2C(15), H_2C(16)), 0.96 (d, *J* = 6.7, 3 H, H_3C(10)), 0.91 (d, *J* = 6.8, 3 H, H_3C(10)), 0.89 (dd, *J* = 6.9, 6.9, 3 H, H_3C(11)), 0.82 (d, *J* = 6.8, 3 H, H_3C(17)), 0.8-2.5 (br, 3 H, $(H_3B)^3$)

^{13}C-NMR: (126 MHz, $CDCl_3$)

88.7 (C(1) or C(7b)), 84.1 (C(1) or C(7b)), 74.2 (C(4)), 69.3 (C(2)), 62.1 (C(12)), 59.6 (C(5a)), 57.0 (C(7a)), 34.7 (C(5)), 31.9 (C(15)), 31.6 (C(6)), 30.2 (C(13)), 29.9 (C(9)), 26.2 (C(14)), 24.6 (C(8)), 24.4 (C(7)), 22.7 (C(16)), 18.2 (C(10) or C(11)), 17.6 (C(10) or C(11) or C(17)), 17.6 (C(10) or C(11) or C(17)), 14.2 (C(16))

IR: ($CDCl_3$, film)

2957 (s), 2230 (s), 2870 (s), 2376 (s), 2327 (s), 2273 (s), 1457 (s), 1378 (s), 1270 (w), 1170 (s), 1147 (m), 1084 (s),

MS: (EI, 70 eV)

320 (25), 318 (50), 307 (7), 292 (6), 278 (9), 276 (10), 264 (49), 236 (9), 222 (100), 207 (47), 192 (19), 180 (17), 164 (13), 137 (7), 124 (30), 110 (77)

Mol. Formula: $C_{20}H_{40}BNO$ (321.35)

HRMS: $C_{20}H_{39}BNO$, (320.3125)

Calcd: 320.3125

Found: 320.3125

TLC: R_f 0.34 (hexanes/TBME, 9:1) [I_2]

Preparation of (1*R*,3*S*,5*S*,5a*S*,7a*S*,7b*R*) Octahydro-1-benzyloxy-1-phenyl-5-methyl-7b-methyl-2*H*cyclopenta[*gh*]pyrrolizine•Borane (V{*5,2*})

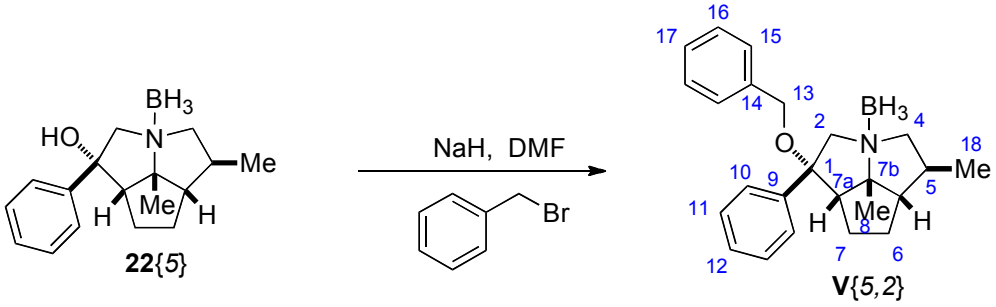

Following General Procedure I, to a two-necked, 10-mL round-bottomed flask equipped with a nitrogen inlet adapter, rubber septum and a magnetic stir bar was added sequentially alcohol **22**{*5*}(68 mg, 0.250 mmol), dimethylformamide (2.5 mL, ~0.1 M), then sodium hydride (9.0 mg, 0.375 mmol, 2.0 equiv) at 0 °C. After 15 min, benzyl bromide (60 µL, 0.500 mmol, 2.0 equiv) was added via syringe. The solution was stirred for 2 hr then quenched onto ice water (10 mL). Extraction and purification by silica gel column chromatography as described in General Procedure I afforded 80 mg (89%) of benzyl ether **V**{*5,2*} as a clear, viscous oil.

Data for **V**{*5,2*}:

^{1}H-NMR: (500 MHz, $CDCl_3$)

7.39 (m, 4 H), 7.33 (m, 3 H), 7.28 (d, J = 7.1, 1 H), 7.21 (d, J = 6.8, 2 H), 4.17 (d, J = 11.3, 1 H, HC(13)), 4.14 (d, J = 13.8, 1 H, HC(2)), 3.97 (d, J = 11.1, 1 H, HC(13)), 3.96 (d, J = 13.5, 1 H, HC(2)), 3.46 (dd, J = 7.9, 12.3, 1 H, HC(4)), 3.21 (dd, J = 11.2, 12.2, 1 H, HC(4)), 2.79 (dd, J = 8.0, 8.0, 1 H, HC(7a)), 2.73–2.63 (m, 1 H, HC(7)), 2.52–2.42 (m, 1 H, HC(5)), 1.97–1.88 (m, 4 H, HC(7), H_2C(6), HC(5a)), 1.52 (s, 3 H, H_3C(8)), 0.96 (d, J = 6.6, 3 H, H_3C(18)), 0.8–2.5 (br, 3 H, $(H_3B)^3$)

^{13}C-NMR: (126 MHz, $CDCl_3$)

141.8 (C(9) or C(14)), 138.0 (C(9) or C(14)), (128.7, 128.5, 128.1, 127.6, 127.4, 126.4) (C(10), C(11), C(12), C(15), C(16), C(17)), 88.8 (C(1) or C(7b)), 83.4 (C(1) or C(7b)), 73.6 (C(4)), 70.6 (C(2)), 66.3 (C(13)), 62.2

(C(7a)), 60.3 (C(5a)), 34.4 (C(5)), 30.9 (C(6)), 25.0 (C(8)), 24.2 (C(7)), 17.3 (C(18))

IR: (NaCl plate, film)

2960 (s), 2329 (s), 1497 (m), 1172 (s), 1136 (w), 1058 (s), 931 (w), 700 (s)

MS: (EI, 70 eV)

358.2 (3), 256.1 (100), 241.1 (11), 105 (35)

Mol. Formula: $C_{24}H_{32}BNO$ (361.33)

HRMS: $C_{24}H_{29}BNO$, (358.2342)

Calcd: 358.2342

Found: 358.2336

TLC: R_f 0.25 (hexanes/TBME, 9:1) [I_2]

Preparation of (1*R*,3*S*,5*S*,5a*S*,7a*S*,7b*R*) Octahydro-1-(4-methoxy-benzyloxy)-1-phenyl-5-methyl-7b-methyl-2*H*cyclopenta[*gh*]pyrrolizine•Borane (V{*5,7*})

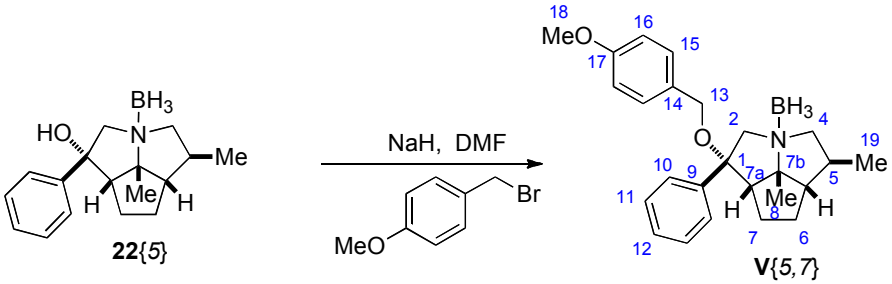

Following General Procedure I, to a two-necked, 10-mL round-bottomed flask equipped with a nitrogen inlet adapter, rubber septum and a magnetic stir bar was added sequentially alcohol **22**{*5*} (68 mg, 0.250 mmol), dimethylformamide (2.5 mL, ~0.1 M), then sodium hydride (9.0 mg, 0.375 mmol, 2.0 equiv) at 0 °C. After 15 min, 4-methoxybenzyl bromide (40 µL, 0.275 mmol, 1.1 equiv) was added via syringe. The solution was stirred for 2 hr then quenched onto ice water (10 mL). Extraction and purification by silica gel column chromatography as described in General Procedure I afforded 89 mg (91%) of 4-methoxybenzyl ether **V**{*5,7*} as a clear, viscous oil.

Data for **V**{*5,7*}:

^{1}H-NMR: (500 MHz, $CDCl_3$)

7.39 (m, 4 H, HC(10), HC(11)), 7.33 (m, 1 H, HC(12)), 7.11 (d, J = 8.7, 2 H,

HC(15)), 6.84 (d, *J* = 8.7, 2 H, HC(16)), 4.12 (d, *J* = 13.4, 1 H, HC(13)), 4.09 (d, *J* = 10.7, 1 H, HC(2)), 3.94 (d, *J* = 13.4, 1 H, HC(13)), 3.89 (d, *J* = 10.6, 1 H, HC(2)), 3.79 (s, 3 H, $H_3C(18)$), 3.45 (dd, *J* = 7.9, 12.3, 1 H, HC(4)), 3.20 (dd, *J* = 11.2, 12.1, 1 H, HC(4)), 2.77 (dd, *J* = 7.9, 7.9, 1 H, HC(7a)), 2.70–2.61 (m, 1 H, HC(7)), 2.50–2.40 (m, 1 H, HC(5)), 1.96–1.83 (m, 4 H, HC(7), $H_2C(6)$, HC(5a)), 1.51 (s, 3 H, $H_3C(8)$), 0.96 (d, *J* = 6.6, 3 H, $H_3C(19)$)

^{13}C-NMR: (126 MHz, $CDCl_3$)

159.2 (C(19)), 141.9 (C(11)), 130.1 (C(16)), 129.0 (C(17)), 128.7 (C(12) or C(11)), 128.1 (C(12)), 126.5 (C(10) or C(11)), 113.9 (C(16)), 88.8 (C(1) or C(7b)), 83.2 (C(1) or C(7b)), 73.6 (C(4)), 70.6 (C(13)), 66.0 (C(2)), 62.0 (C(7a)), 60.3 (C(5a)), 55.4 (C(18)), 34.4 (C(5)), 30.8 (C(6)), 25.0 (C(8)), 24.1 (C(7)), 17.3 (C(19)), 0.8-2.5 (br, 3 H, $(H_3B)^3$)

IR: ($CDCl_3$, film)

2957 (s), 2922 (s), 2869 (s), 2369 (s), 2329 (s), 2274 (s), 1613 (s), 1585 (w), 1514 (s), 1457 (s), 1379 (m), 1301 (m), 1249 (s), 1173 (s), 1136 (m), 1116 (w), 1033 (s), 823 (m), 756 (s), 700 (s)

MS: (EI, 70 eV)

388.2 (1), 256.2 (100), 241.2 (17), 105 (38)

Mol. Formula: $C_{25}H_{34}BNO_2$ (391.35)

HRMS: $C_{25}H_{31}BNO_2$, (388.2448)

Calcd: 388.2448

Found: 388.2444

TLC: R_f 0.22 (hexanes/TBME, 9:1) [I_2]

Preparation of (1*R*,3*S*,5*S*,5a*S*,7a*S*,7b*R*) Octahydro-1-hexyloxy-1-phenyl-5-methyl-7b-methyl-2*H*cyclopenta[*gh*]pyrrolizine•Borane (V{*5,3*})

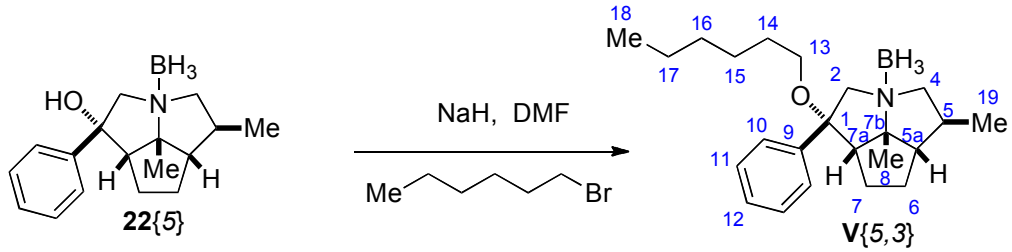

To a one-necked, round-bottomed flask equipped with a nitrogen inlet adapter, rubber septum and a magnetic stir bar is added sequentially **22**{*5*} (64 mg, 0.236 mmol), dimethylformamide (2.4 mL, 0.1 M) and sodium hydride (6 mg, 0.250 mmol). After being stirred for 15 min, 1-bromohexane (33 μL, 0.236 mmol) was added. After being stirred for 2 h, NaH (6 mg, 0.250 mmol), was added. After being stirred for 15 min, 1-bromohexane (33 μL, 0.236 mmol) was added. After being stirred for 2 h, NaH (6 mg, 0.250 mmol) was added. After being stirred for 15 min, 1-bromohexane (33 μL, 0.236 mmol) was added. After 2 h, the reaction was quenched with water (10 mL) at 0 °C. Extraction and purification by silica gel column chromatography as described in General Procedure I afforded 63 mg (75%) of hexyl ether **V**{*5,3*} as a clear, viscous oil.

Data for **V**{*5,3*}:

^{1}H-NMR: (500 MHz, $CDCl_3$)

7.33 (dd, *J* = 7.3, 7.3, 2 H, HC(10)), 7.29–7.24 (m, 3 H, HC(11), HC(12)), 4.03 (d, *J* = 13.6, 1 H, HC(2)), 3.85 (d, *J* = 13.6, 1 H, HC(2)), 3.45 (dd, *J* = 8.1, 12.2, 1 H, HC(4)), 3.24 (dd, *J* = 11.1, 12.0, 1 H, HC(4)), 3.13 (ddd, *J* = 6.4, 6.4, 8.9, 1 H, HC(13)), 2.82 (ddd, *J* = 6.5, 6.5, 8.9, 1 H, HC(13)), 2.70–2.61 (m, 2 H, HC(7a), HC(7)), 2.59–2.50 (m, 1 H, HC(5)), 1.90 (m, 4 H, HC(7), H_2C(6), HC(5a)), 1.47 (s, 3 H, H_3C(8)), 1.47–1.41 (m, 2 H, H_2C(14)), 1.32–1.20 (m, 4 H, H_2C(15), H_2C(16)), 1.23–1.15 (m, 2 H, H_2C(17)), 1.00 (d, *J* = 6.6, 3 H, H_3C(19)), 0.86 (t, *J* = 7.2, 3 H, H_3C(18)), 0.8–2.5 (br, 3 H, $(H_3B)^3$)

^{13}C-NMR: (126 MHz, $CDCl_3$)

142.3 (C(9)), 128.5 (C(10)), 127.8 (C(11)), 126.3 (C(12)), 88.8 (C(7b) or C(1)), 82.4 (C(7b) or C(1)), 73.8 (C(4)), 70.2 (C(2)), 63.8 (C(13)), 63.2 (C(7a)), 56.0 (C(5a)), 34.5 (C(5)), 31.7 (C(7b)), 31.1 (C(6)), 29.9 (C(14)), 26.1 (C(16)), 24.9 (C(8)), 23.4 (C(7)), 22.7 (C(15)), 17.4 (C(18)), 14.1 (C(19))

IR: (NaCl plate, film)

2950 (s), 2929 (s), 2869 (s), 2377 (s), 2329 (s), 2274 (s), 1457 (s), 1337 (m), 1379 (m), 1173 (s), 1137 (m), 1092 (m), 1064 (m), 924 (w), 868 (w), 751 (w), 700 (s)

MS: (EI, 70 eV)

352.2 (3), 341.2 (6), 326.2 (4), 270.1 (4), 256.1 (100), 241.1 (29), 110.1 (24)

Mol. Formula: $C_{23}H_{38}BNO$ (355.36)

HRMS: $C_{23}H_{35}NO$ (341.2719)

Calcd: 341.2719

Found: 341.2722

TLC: R_f 0.35 (hexanes/TBME, 9:1) [I_2]

Preparation of (1*R*,3*S*,5*S*,5a*S*,7a*S*,7b*R*) Octahydro-1-(3,5-bistrifluoromethyl-benzyloxy)-1-phenyl-5-methyl-7b-methyl-2*H*cyclopenta[*gh*]pyrrolizine•Borane (V{*5,6*})

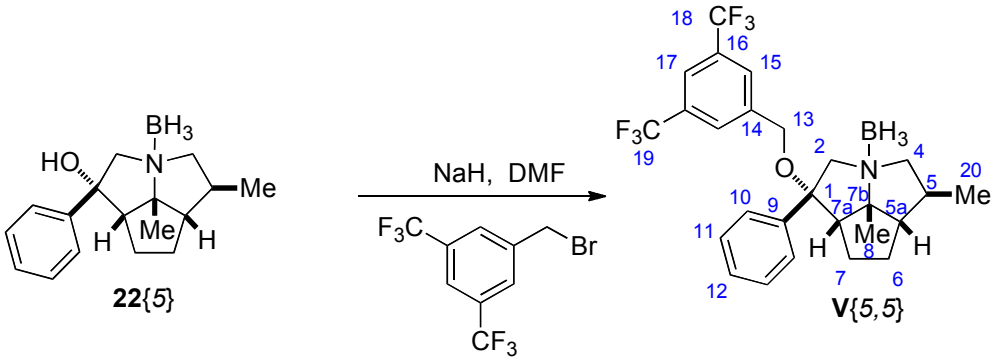

To a two-necked, 25-mL round-bottomed flask equipped with a nitrogen inlet adapter, rubber septum and a magnetic stir bar was added sequentially alcohol **22**{*5*} (105 mg, 0.287 mmol), THF (2.0 mL, 0.1 M), then potassium hydride (19 mg, 0.474 mmol, 1.22 equiv). The flask was immersed in an ice/NaCl cooling bath. To the resulting mixture was added 3,5-bis(trifluoromethyl)benzyl bromide dropwise, via syringe, as a solution in THF (2.0 mL). The bath was removed and the reaction was allowed to reach room temperature. After being stirred for 2 h at room temperature, the flask was immersed in an ice bath and the reaction was quenched with sat. aq. ammonium chloride (5.0 mL). Extraction and purification by silica gel column chromatography as described in General Procedure I afforded 146 mg (76%) of 3,5-bis(trifluomethyl)benzyl ether **V**{*5,6*} as a clear, viscous oil.

Data for **V**{*5,6*}:

^{1}H-NMR: (500 MHz, $CDCl_3$)

7.75 (s, 1 H, HC(17)) , 7.60 (s, 2 H, HC(15)), 7.39-7.38 (m, 4 H, HC(10), HC(11)), 7.36-7.31 (m, 1 H, HC(12)), 4.24 (d, *J* = 12.4, 1 H, HC(13)), 4.16 (d, *J* = 13.2, 1 H, HC(2)), 4.07 (d, *J* = 12.4, 1 H, HC(13)), 3.93 (d, *J* = 13.2, 1 H, HC(2)), 3.42 (dd, *J* = 7.7, *J* = 12.4, 1 H, HC(4)), 3.21 (dd, *J* = 11.8, *J* = 11.8, 1 H, HC(4)), 2.91 (dd, *J* = 8.4, *J* = 8.4, 1 H, HC(7a)), 2.64-2.55 (m, 1 H, HC(7)), 2.45-2.35 (m, 1 H, HC(5)), 2.03-2.87 (m, 4 H, HC(7), H_2C(6), HC(5a)), 1.53 (s, 3 H, H_3C(8)), 1.00 (d, *J* = 6.5, 3 H, H_3C(20)), 0.8-2.5 (br, 3 H, $(H_3B)^3$)

^{13}C-NMR: (126 MHz, $CDCl_3$)

140.9 (C(9 or 14)), 140.8 (C(9 or 14)), 130.2 (q, *J* = 33.2, C(19)), 127.1 (C(10)), 127.1 (C(11)), 127.1 (C(12), 126.7 (C(15)), 121.5 (hept, *J* = 3.8, C(17)), 88.9 (C(7b)), 84.1 (C(1)), 73.4 (C(4)), 71.2 (C(2)), 65.1 (C(13)), 60.6 (C(7a or 5a)), 60.6 (C(7a or 5a)), 34.5 (C(5)), 30.7 (C(6)), 25.1 (C(7)), 25.0 (C(8)), 17.0 (C(20))

IR: ($CDCl_3$, film)

3063 (w), 2962 (s), 2931 (s), 2874 (s), 2376 (s), 2331 (s), 2277 (s), 2243 (s), 1808 (w), 1624 (m), 1497 (m), 1461 (s), 1448 (s), 1366 (s), 1279 (s), 1174 (s), 1134 (s), 1091 (s), 1016 (m), 994 (m), 957 (w), 911 (s), 844 (s), 812 (w), 704 (s)

MS: (ESI, Q-tof)

494.2 (75), 484.2 (100)

Mol. Formula: $C_{26}H_{30}BF_6NO$ (497.32)

HRMS: $C_{26}H_{28}NOF_6$, (484.2075)

Calcd: 484.2075

Found: 484.2064

TLC: R_f 0.38 (hexanes/TBME, 9:1) [I_2]

Preparation of (1*R*,3*S*,5*S*,5a*S*,7a*S*,7b*R*) Octahydro-1-benzyloxy-1-(2,4,6-trimethyl-phenyl)-5-methyl-7b-methyl-2*H*cyclopenta[*gh*]pyrrolizine•Borane (V{*6,2*})

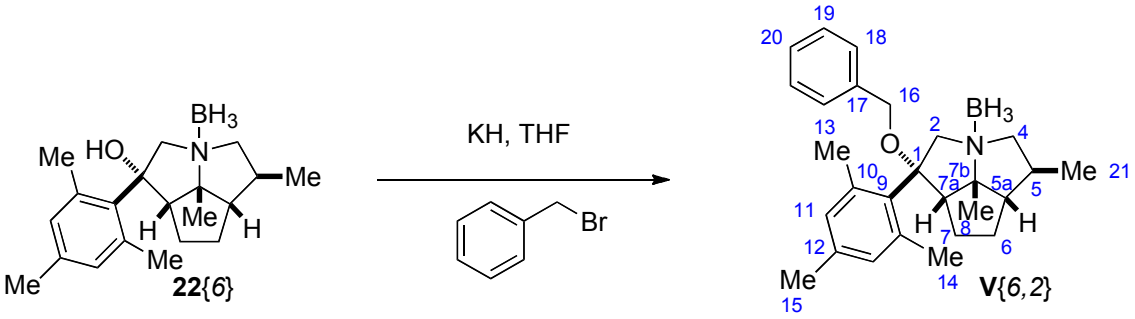

Following General Procedure I, to a two-necked, 10-mL round-bottomed flask equipped with a nitrogen inlet adapter, rubber septum and a magnetic stir bar was added sequentially alcohol **22**{*6*} (31 mg, 0.099 mmol), dimethylformamide (1.0 mL, ~0.1 M), then sodium hydride (3.6 mg, 0.148 mmol, 1.5 equiv) at 0 °C. After 15 min, benzyl bromide (18 μL, 0.148 mmol, 1.5 equiv) was added via syringe. The solution was stirred for 2 hr then quenched onto ice water (10 mL). Extraction and purification by silica gel column chromatography as described in General Procedure I afforded 39 mg (98%) of benzyl ether **V**{*6,2*} as a clear, viscous oil.

Data for **V**{*6,2*}:

^{1}H-NMR: (500 MHz, $CDCl_3$)

7.32 (dd, *J* = 7.2, 7.2, 1 H, HC(19)), 7.29-7.25 (m, 1 H, HC(20)), 7.23 (d, *J* = 7.2, 1 H, HC(18)), 6.86 (s, 2 H, HC(11)) 4.28 (d, *J* = 11.1, 1 H, HC(16)), 4.25 (d, *J* = 14.1, 1 H, HC(2)), 4.17 (d, *J* = 11.0, 1 H, HC(16)), 4.07 (d, *J* = 13.8, 1 H, HC(2)), 3.94 (dd, *J* = 9.3, 11.6, 1 H, HC(4)), 3.25 (dd, *J* = 6.9, 11.8, 1 H, HC(4)), 2.99 (dd, *J* = 9.1, 9.1, 1 H, HC(7a)), 2.54 (s, 3 H, H_3C(13)) 2.52 (s, 3 H, H_3C(14)), 2.25 (s, 3 H, H_3C(15)), 2.26-2.19 (m, 1 H, HC(5)), 2.15-2.09 (m, 1 H, HC(7)), 2.01-1.98 (m, 1 H, HC(5a)), 1.90-1.84 (m, 2 H, H_2C(6), 1.41 (s, 3 H, H_3C(8)), 1.13 (d, *J* = 6.9, 3 H, H_3C(21)), 0.8-2.5 (br, 3 H, $(H_3B)^3$)

^{13}C-NMR: (126 MHz, $CDCl_3$)

138.4, 138.0, 137.0, 137.0, 132.3, 132.1, 128.5, 127.6, 127.3, 87.5 (C(1 or 7b)), 87.4 (C(1 or 7b)), 74.6 (C(4)), 71.8 (C(2)), 66.9 (C(16)), 64.4 (C(7a)), 59.5 (C(5a)), 36.2 (C(5)), 33.0 (C(6)), 28.5 (C(15)), 25.6 (C(8)), 25.0 (C(13 or 14)), 24.6 (C(13 or 14)), 20.5 (C(7)), 19.9 (C(21))

IR: ($CDCl_3$, film)

3028 (w), 2950 (s), 2930 (s), 2865 (s), 2376 (s), 2330 (s), 2277 (m), 2241 (m), 1610(m), 1454 (s), 1379 (m), 1348 (w), 1277 (w), 1173 (s), 1086 (s), 1063 (s),

1028 (s), 993 (w), 911 (s), 872 (w)

MS: (EI, 70 eV)

400.3 (1), 389.2 (2), 298.2 (100), 281.2 (4), 147.1 (47), 124.1 (26)

Mol. Formula: $C_{27}H_{38}BNO$ (403.41)

HRMS: $C_{27}H_{35}NO$, 389.2719)

Calcd: 389.2719

Found: 389.2719

TLC: R_f 0.25 (hexanes/TBME, 9:1) [I_2]

Preparation of (1*R*,3*S*,5*S*,5a*S*,7a*S*,7b*R*) Octahydro-1-benzyloxy-1-(1-naphthyl)-5-methyl-7b-methyl-2*H*cyclopenta[*gh*]pyrrolizine•Borane V{*7,2*}

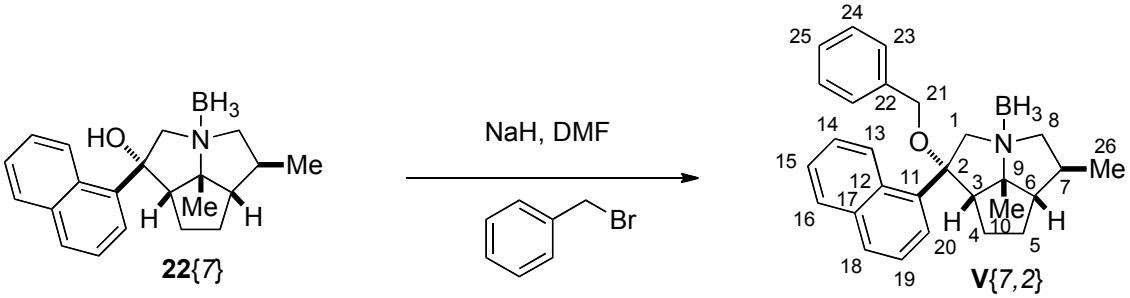

Following General Procedure I, to a two-necked, 10-mL round-bottomed flask equipped with a nitrogen inlet adapter, rubber septum and a magnetic stir bar was added sequentially alcohol **22**{*7*} (38 mg, 0.118 mmol), dimethylformamide (1.2 mL, ~0.1 M), then sodium hydride (4.3 mg, 0.177 mmol, 1.5 equiv) at 0 ^{o}C. After 15 min, benzyl bromide (21 μL, 0.177 mmol, 1.5 equiv) was added via syringe. The solution was stirred for 2 hr then quenched onto ice water (10 mL). Extraction and purification by silica gel column chromatography as described in General Procedure I afforded 45 mg (93%) of benzyl ether **V**{*7,2*} as a clear, viscous oil.

Data for **V**{*7,2*}:

^{1}H-NMR: (500 MHz, $CDCl_3$)

8.58 (d, *J* = 8.0, 0.6 H) , 8.53-8.50 (m, 1 H), 7.95-7.85 (m, 4 H), 7.54-7.48 (m, 4 H), 7.31-7.25 (m, 4 H), 7.16-7.13 (m, 3 H), 4.71 (d, *J* = 13.5, 0.6 H), 4.47 (d, *J* = 11.4, 1 H), 4.21 (d, *J* = 11.1, 0.6 H), 4.05-3.98 (m, 1.6 H), 3.91-3.84 (m, 1.6 H), 3.78 (d, *J* = 10.5, 1 H), 3.73 (dd, *J* = 8.2, 11.8, 0.6 H), 3.60 (dd, *J* = 9.3, 9.3, 1 H), 3.30 (dd, *J* = 11.2, 11.2, 0.6 H), 3.25 (dd, *J* = 6.2, 12.5, 1 H),

3.04-2.95 (m, 0.6 H), 2.89 (dd, *J*=12.5, 12.5, 1 H), 2.79 (dd, *J* = 8.7, 8.7, 0.6 H), 2.59-2.50 (m, 1 H), 2.45-2.37 (m, 0.6 H), 2.26-2.11 (m, 3 H), 2.03-1.80 (m, 5H), 1.72 (s, 3 H), 1.35 (s, 1.8 H), 1.09 (d, *J* = 6.5, 1.8 H), 1.06 (d, *J* = 6.3, 3 H)

^{13}C-NMR: (126 MHz, $CDCl_3$)

138.13, 138.08, 136.6, 136.0, 135.1, 134.8, 131.4, 130.3, 129.8, 129.6, 129.2, 128.4, 128.0, 127.7, 127.6, 126.4, 126.3, 126.2, 126.0, 125.9, 125.8, 125.78, 126.76, 125.7, 124.6, 124.3, 88.8, 86.9, 85.3, 85.0, 73.5, 72.8, 72.4, 70.6, 67.2, 66.8, 64.1, 63.4, 60.3, 54.8, 34.5, 33.7, 31.1, 28.7, 28.6, 27.7, 25.0, 25.3, 17.8, 16.1

IR: ($CDCl_3$, film)

3050 (w), 2959 (s), 2929 (s), 2870 (m), 2397 (s), 2326 (s), 2279 (m), 2242 (m), 1602 (w), 1509 (w), 1498 (w), 1455 (s), 1380 (s), 1336 (w), 1287 (w), 1241 (w), 1173 (s), 1142 (m), 1113 (m), 1059 (s), 1026 (m), 959 (w), 911 (s), 865 (w), 804 (s), 780 (s), 733 (s), 699 (s), 648 (m)

MS: (EI, 70 eV)

426.2 (9), 408.2 (5), 398.2 (64), 382.2 (8), 306.1 (100), 290.1 (94), 270.1 (8), 155.0 (11)

Mol. Formula: $C_{28}H_{34}BNO$ (411.3867)

HRMS: $C_{27}H_{35}NO$, 412.2812)

Calcd: 412.2812

Found: 412.2640

TLC: R_f 0.40 (hexanes/TBME, 4:1) [I_2, CAM]

Preparation of (1*R*,3*S*,5*S*,5a*S*,7a*S*,7b*R*)-Octahydro-1-benzyloxy-5-methyl-7b-methyl-2*H*cyclopenta[*gh*]pyrrolizine•Borane (β-V{*2*})

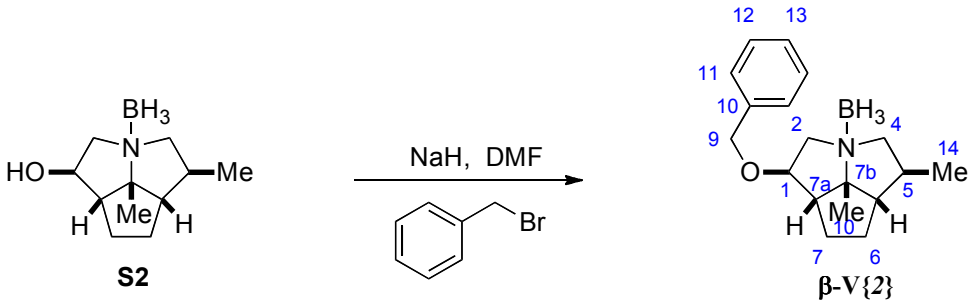

Following General Procedure I, to a two-necked, 10-mL round-bottomed flask equipped with a nitrogen inlet adapter, rubber septum and a magnetic stir bar was added sequentially alcohol **S3** (22 mg, 0.113 mmol), dimethylformamide (1.1 mL, ~0.1 M), then sodium hydride (4 mg, 0.17 mmol, 1.5 equiv) at 0 °C. After 15 min, benzyl bromide (20 μL, 0.17 mmol, 1.5 equiv) was added via syringe. The solution was stirred for 2 hr then quenched onto ice water (10 mL). Extraction and purification by silica gel column chromatography as described in General Procedure I afforded 28 mg (88%) of benzyl ether β-**V**{*3*} as a clear, viscous oil.

Data for β-**V**{*2*}:

^{1}H-NMR: (500 MHz, $CDCl_3$)

7.35 (m, 4 H, HC(11), HC(12)), 7.28 (m, 1 H, HC(13)), 4.63 (d, J = 11.7, 1 H, HC(9)), 4.38 (d, J = 11.7, 1 H, HC(9)), 3.79–3.75 (m, 2 H, HC(2), HC(1)), 3.26–3.21 (m, 2 H, HC(2), HC(4)), 3.04 (dd, J = 12.2, 12.2, 1 H, HC(4)), 2.40 (dd, J = 7.9, 7.9, 1 H, HC(7a)), 2.07–2.01 (m, 1 H, HC(7)), 1.86–1.81 (m, 2 H, HC(5a), HC(5)), 1.81–1.73 (m, 1 H, HC(6)), 1.71–1.66 (m, 1 H, HC(6)), 1.60 (s, 3 H, H_3C(8)), 1.60–1.52 (m, 1 H, HC(7)), 1.00 (d, J = 5.9, 3 H, H_3C(14)), 0.8–2.5 (br, 3 H, $(H_3B)^3$)

^{13}C-NMR: (126 MHz, $CDCl_3$)

138.1 (C(10)), 128.5 (C(12)), 127.8 (C(13)), 127.7 (C(11)), 88.0 (C(7b)), 81.8 (C(1)), 73.0 (C(4)), 70.8 (C(9)), 67.7 (C(2)), 60.9 (C(5a)), 58.2 (C(7a)), 35.4 (C(5)), 30.6 (C(7)), 29.7 (C(6)), 25.0 (C(8)), 16.6 (C(14))

IR: ($CDCl_3$, film)

2956 (s), 2915 (s), 2872 (s), 2383 (s), 2328 (s), 2262 (s), 1496 (w), 1455 (s), 1379 (m), 1316 (w), 1273 (w), 1234 (w), 1177 (s), 1106 (m), 1067 (m), 1014 (w), 913 (m), 862 (w), 798 (w)

MS: (ESI, Q-tof)

284.2 (70), 272.2 (100), 192.2 (35), 141 (12)

Mol. Formula: $C_{18}H_{28}BNO$ 285.23

HRMS: $C_{18}H_{26}NO$, (272.2014)

Calcd: 272.2014

Found: 272.2008

TLC: R_f 0.24 (hexanes/TBME, 9:1) [I_2]

Preparation of (1*R*,3*S*,5*S*,5a*S*,7a*S*,7b*R*) Octahydro-1-benzyloxy-1-(*tert*-butyl)-5-methyl-7b-methyl-2*H*cyclopenta[*gh*]pyrrolizine•Borane (V{*4,2*})

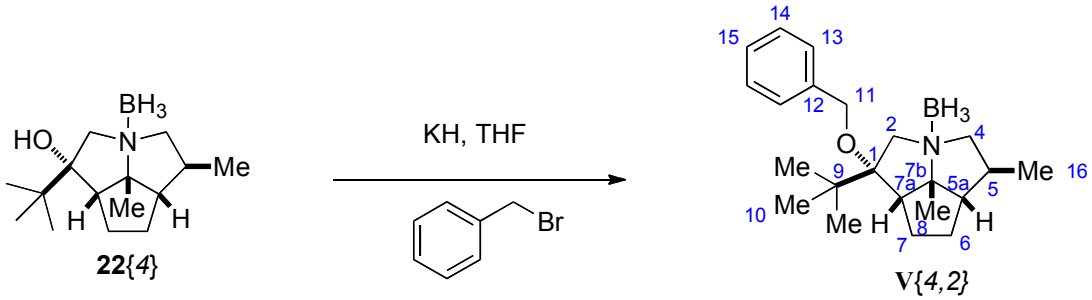

Following General Procedure I, to a two-necked, 10-mL round-bottomed flask equipped with a nitrogen inlet adapter, rubber septum and a magnetic stir bar was added sequentially alcohol **24**{*4*}(25 mg, 0.100 mmol), tetrahydrofuran (1.0 mL, ~0.1 M), then potassium hydride (6 mg, 0.149 mmol, 1.5 equiv) at 0 °C. After 15 min, benzyl bromide (26 µL, 0.149 mmol, 1.5 equiv) was added via syringe. The solution was stirred for 2 hr then quenched onto ice water (10 mL). Extraction and purification by silica gel column chromatography as described in General Procedure I afforded 33 mg (97%) of benzyl ether **V**{*4,2*} as a clear, viscous oil.

Data for **V**{*4,2*}:

^{1}H-NMR: (500 MHz, $CDCl_3$)

7.38–7.33 (m, 4 H, HC(13), HC(14)), 7.30–7.27 (m, 1 H, HC(15)), 4.83 (d, *J* = 11.2, 1 H, HC(2)), 4.56 (d, *J* = 11.2, 1 H, HC(2)), 3.81 (d, *J* = 15.2, 1 H, HC(11)), 3.77 (d, *J* = 15.1, 1 H, HC(11)), 3.32 (dd, *J* = 8.0, 12.4, 1 H, HC(4)), 3.15 (dd, *J* = 11.2, 12.0, 1 H, HC(4)), 2.59 (dd, *J* = 6.9, 9.6, 1 H, HC(7a)), 2.57–2.48 (m, 1 H, HC(7)), 2.09–2.01 (m, 1 H, HC(5)), 1.80–1.72 (m, 3 H, H_2C(6), HC(5a)), 1.65–1.59 (m, 1 H, HC(7)), 1.48 (s, 3 H, H_3C(8)), 1.00 (s, 9 H, H_3C(10)), 0.72 (d, *J* = 6.6, 3 H, H_3C(16)), 0.8–2.5 (br, 3 H, $(H_3B)^3$)

^{13}C-NMR: (126 MHz, $CDCl_3$)

138.5 (C(12)), 128.6 (C(14)), 127.6 (C(15)), 127.2 (C(13)), 88.7 (C(1 or 7b)), 86.8 (C(1 or 7b)), 74.0 (C(4)), 68.6 (C(2)), 68.5 (C(11)), 59.7 (C(5a)), 59.5 (C(7a)), 39.2 (C(9)), 34.3 (C(5)), 31.4 (C(6)), 27.6 (C(10)), 24.6 (C(7)), 24.4 (C(8)), 16.9 (C(16))

IR: ($CDCl_3$, film)

2960 (s), 2871 (s), 2382 (s), 2328 (s), 2274 (s), 1728 (w), 1604 (w), 1497 (w), 1455 (s), 1401 (w), 1378 (m), 1318 (w), 1285 (w), 1235 (w), 1175 (s), 1133 (m), 1092 (s), 1061 (m), 1028 (m), 1007 (w), 977 (w), 955 (w), 926 (m), 913 (m), 869 (w), 735 (s), 698 (s)

MS: (EI, 70 eV)

338.2 (13), 270.1 (12), 236.2 (100), 221.2 (3.9), 204.1 (3), 178.1 (10), 164.1 (3), 138.1 (3), 124.1 (4), 110.1 (10.2)

Mol. Formula: $C_{22}H_{36}BNO$ (341.34)

HRMS: $C_{22}H_{33}NO^+$, (327.2562)

Calcd: 327.2562

Found: 327.2556

TLC: R_f 0.28 (hexanes/TBME, 9:1) [I_2]

Variable Group R^4: Deborylation and *N*-Quaternization

Parallel Synthesis Step II-III: General Procedure II

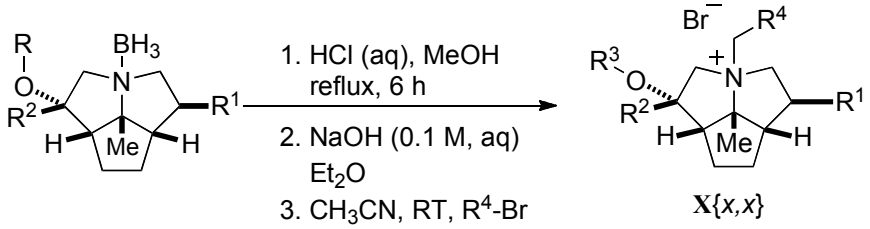

X{*x,x*}

A solution of borane adduct **X** (**XX** mg, **XX** mmol) in CH_3OH (0.03 M) was transferred to a 250-mL, round-bottomed, flask fitted with a reflux condenser, a magnetic stir-bar, and a nitrogen inlet adapter with a rubber septum. Lastly, 1.0 M aq. HCl solution (x.x mL, 5.0 equiv) was added via syringe. The resulting clear solution was immersed in an oil bath (preheated, 60 ^oC) and stirred for 12 h. The mixture was allowed to cool to room temperature and was concentrated by rotary evaporation (15 mm Hg, 20-25 ^oC) whereupon a 0.1 M aq. NaOH solution (xx.x mL, 6.0 equiv) was added. The resulting solution was tested to assure basicity by pH paper (typically pH ~11-14). The basic solution was extracted with Et_2O (3 x 100 mL) and the combined extracts were dried (K_2CO_3). The resulting floculant suspension was filtered (cotton plug), and concentrated by rotary evaporation (15 mm Hg, 20-25 ^oC) to furnish the crude intermediate amine as a pale-yellow oil. The amine was dissolved in acetonitrile (0.2 M) and distributed among five 20-mL test tubes fitted in a Büchi SynCore reactor (Figure X) which were then evacuated and backfilled with N_2. An alkyl bromide (x.x mL, x.x mmol, 1.2 equiv) was added to each test tube *via* syringe (the solid bromides were added as solids) and the reactor was set to agitate at 200 rpm. After 12 h, the individual reaction mixtures were concentrated by rotary evaporation (15 mm Hg, 20-25^oC). Each salt was purified by silica gel plug filtration (1.8 cm x 5 cm, CH_2Cl_2/EtOAc, 1:1 (50 mL), then CH_2Cl_2/methanol 49:1, 24:1, 9:1 (50 mL each) afforded the product ammonium salts as a clear, sticky residues. The residues were triturated with Et_2O (~10 mL) in a 20-mL scintillation vial to free flowing solids which were then concentrated by rotary evaporation (15 mm Hg, 20-25^oC). The resulting solids were dried under vacuum (0.1 mm Hg, 20-25 ^oC) for 12 h to afford the final quaternary ammonium bromides **X***{x}* as free flowing powers.

.

Preparation of Quaternary Ammonium Bromides IV{2-7,1-7,1-11}. Preparation of Quaternary Ammonium Bromides IV{*2*,*2*,R^4}

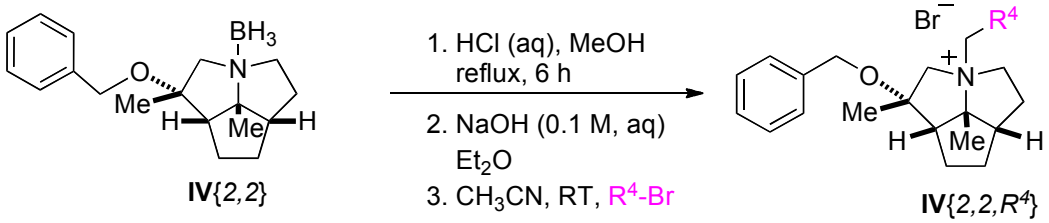

IV{*2,2*} **IV**{*2,2,R*^{4}}

Following General Procedure II, amino borane **V**{*2,2*} (210 mg, 0.74 mmol) was added to a 250-mL, round-bottomed flask as a solution in 150 mL of MeOH (~0.03 M). The flask was fitted with a reflux condenser, a magnetic stir bar, and a nitrogen inlet adapter. Lastly, 1.0 M aq. HCl solution (24 mL, 5.0 equiv) was added via syringe. The resulting solution was heated and then concentrated by rotary evaporation (15 mm Hg, 20-25 ^{o}C) as described General Procedure II. The resulting free amine was dissolved in acetonitrile and was distributed among six test tubes that were subsequently charged with benzyl bromide (tube 1, 23 mg, 0.30 mmol, 1.2 equiv), 1-bromomethylnaphthalene (tube 2, 80 mg, 0.3 mmol, 1.2 equiv), 2-bromomethylnaphthalene (tube 3, 80 mg, 0.3 mmol, 1.2 equiv). After being agitated for 12 h, the reaction mixtures were worked up and the products isolated and purified as described in General Procedure II.

Preparation of *rel*-(1*S*,3*R*,5a*S*,7a*S*,7b*R*) Octahydro-1-benzyloxy-1-methyl-3-benzyl-7b-methylcyclopenta[*gh*]pyrrolizinium Bromide (IV{*2,2,1*})

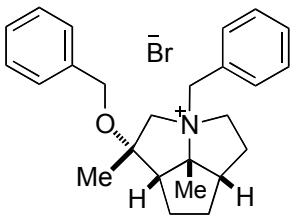

IV{*2,2,1*}

Data for **IV**{*2,2,1*}:

Yield: 63 mg (57%), free-flowing white powder

^{1}H-NMR: (500 MHz, $CDCl_3$)

7.78-7.75 (m, 2 H), 7.48-7.42 (m, 3 H), 7.31-7.24 (m, 3 H), 7.18 (d, *J* = 7.1, 2 H), 5.38 (d, *J* = 12.4, 1 H), 5.34 (d, *J* = 13.0, 1 H), 4.45 (d, *J* = 11.4, 1 H),

4.26-4.21 (m, 2 H), 3.86-3.78 (m, 1 H), 3.72 (dd, *J* = 6.8, 12.2, 1 H), 3.44 (d, *J* = 13.1, 1 H), 2.83-2.79 (m, 1 H), 2.68 (dd, *J* = 6.4, 13.5, 1 H), 2.49-2.40 (m, 1 H), 2.27-2.20 (m, 1 H), 2.12 (s, 3 H), 2.12-2.04 (m, 1 H), 1.91-1.80 (m, 1 H), 1.80-1.75 (m, 1 H), 1.75 (s, 3 H)

MS: (ESI, Q-tof)

362.2 (100)

Mol. Formula: $C_{25}H_{32}BrNO$, (442.43)

HRMS: $C_{25}H_{32}NO^+$: (362.2484)

Calcd: 362.2484

Found: 362.2479

TLC: R_f 0.22 (CH_2Cl_2/MeOH, 9:1) [I_2]

Preparation of *rel*-(1*S*,3*R*,5a*S*,7a*S*,7b*R*) Octahydro-1-benzyloxy-1-methyl-3-(1-naphthylmethyl)-7b-methylcyclopenta[*gh*]pyrrolizinium Bromide (IV{*2,2,2*})

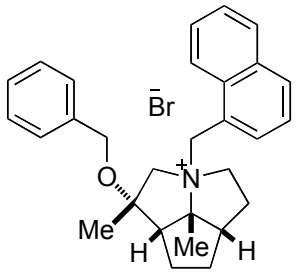

IV{*2,2,2*}

Data for **IV**{*2,2,2*}:

Yield: 71 mg (58%), free-flowing white powder

^{1}H-NMR: (500 MHz, $CDCl_3$)

8.44-8.35 (m, 1 H), 8.17-8.10 (m, 1 H), 7.88-7.74 (m, 2 H), 7.59 (t, *J* = 7.2, 1 H), 7.53-7.47 (m, 1 H), 7.34 (s, 1 H), 7.25-7.16 (m, 3 H), 7.12-7.07 (m, 2 H), 5.60-5.42 (m, 2 H), 5.17-4.97 (m, 1 H), 4.41 (d, *J* = 11.4, 1 H), 4.13 (d, *J* = 11.6, 1 H), 3.83-3.73 (m, 1 H), 3.51-3.44 (m, 1 H), 3.36-3.28 (m, 1 H), 2.93-3.67 (m, 3 H), 2.33 (s, 3 H), 2.26-2.18 (m, 1 H), 2.11 (s, 1 H), 1.91-1.71 (m, 3 H), 1.75 (s, 3 H)

MS: (ESI, Q-tof)

412.3 (100)

Mol. Formula: $C_{29}H_{34}BrNO$ (492.49)

HRMS: $C_{29}H_{34}NO^+$: (412.2640)

Calcd: 412.2640

Found: 412.2636

TLC: R_f 0.25 (CH_2Cl_2/MeOH, 9:1) [I_2]

Preparation of *rel*-(1*S*,3*R*,5a*S*,7a*S*,7b*R*) Octahydro-1-benzyloxy-1-methyl-3-(2-naphthylmethyl)-7b-methylcyclopenta[*gh*]pyrrolizinium Bromide (IV{*2,2,3*})

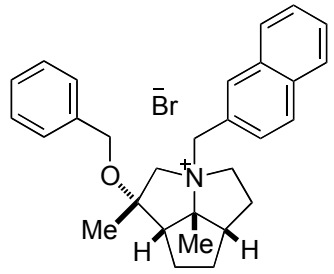

IV{*2,2,3*}

Data for **IV**{*2,2,3*}:

Yield: 64 mg (53%), free-flowing white powder

^{1}H-NMR: (500 MHz, $CDCl_3$)

8.21 (s, 1 H), 7.94-7.88 (m, 1 H), 7.83-7.74 (m, 3 H), 7.56-7.48 (m, 2 H), 7.28-7.17 (m, 3 H), 7.13 (d, *J* = 7.4, 2 H), 5.56-5.34 (m, 2 H), 4.45-4.40 (m, 1 H), 4.42 (d, *J* = 11.0, 1 H), 4.17 (d, *J* = 11.4, 1 H), 3.85-3.70 (m, 2 H), 3.47 (d, *J* = 13.0, 1 H), 2.88-2.69 (m, 2 H), 2.64-2.50 (m, 1 H), 2.28-2.17 (m, 1 H), 2.19 (s, 3 H), 2.12-2.04 (m, 1 H), 1.91-1.73 (m, 3 H), 1.75 (s, 3 H)

MS: (ESI, Q-tof)

412.3 (100)

Mol. Formula: $C_{29}H_{34}BrNO$ (492.49)

HRMS: $C_{29}H_{34}NO^+$: (412.2640)

Calcd: 412.2640

Found: 412.2631

TLC: R_f 0.25 (CH_2Cl_2/MeOH, 9:1) [I_2]

Preparation of Quaternary Ammonium Bromides IV{*2,3,1-3*}

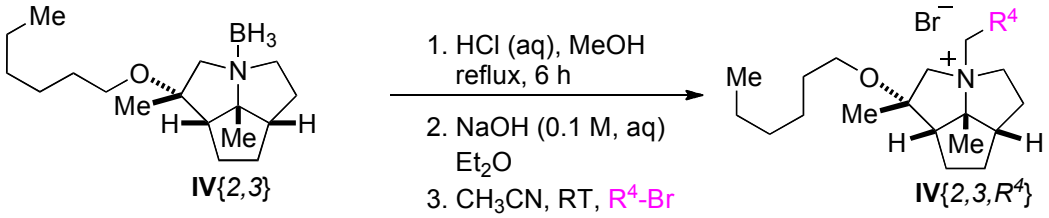

Following General Procedure II, amino borane **IV**{*2*,*3*} (103 mg, 0.37 mmol) was added to a 50-mL round-bottomed flask as a solution in 12 mL of MeOH (0.03 M). The flask was fitted with a reflux condenser, a magnetic stir bar, and a nitrogen inlet adapter. Lastly, 1.0 N aq. HCl solution (3.68 mL, 5.0 equiv) was added via syringe. The resulting solution was heated and then concentrated by rotary evaporation (15 mm Hg, 20-25 ^{o}C) as described General Procedure II. The resulting free amine was dissolved in acetonitrile and was distributed among six test tubes that were subsequently charged with benzyl bromide (tube 1, 82 mg, 0.478 mmol, 4.0 equiv), 1-bromomethylnaphthalene (tube 2, 79 mg, 0.358 mmol, 3.0 equiv), 2-bromomethylnaphthalene (tube 3, 79 mg, 0.358 mmol, 3.0 equiv). After being agitated for 12 h, the reaction mixtures were worked up and the products isolated and purified as described in General Procedure II.

Preparation of *rel*-(1*S*,3*R*,5a*S*,7a*S*,7b*R*) Octahydro-1-hexyloxy-1-methyl-3-benzyl-7b-methylcyclopenta[*gh*]pyrrolizinium Bromide (IV{*2,3,1*})

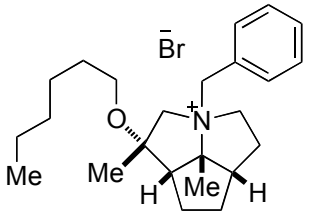

IV{*2,3,1*}

Data for **IV**{*2,3,1*}:

Yield: 41 mg (51%), free-flowing white powder

^{1}H-NMR: (500 MHz, $CDCl_3$)

7.79-7.73 (m, 2 H), 7.48-7.42 (m, 3 H), 5.35 (d, *J* = 12.3, 1 H), 5.17 (d, *J* = 13.0, 1 H), 4.27-4.18 (m, 1 H), 3.84 (ddd, *J* = 6.0, 12.1, 12.1, 1 H), 3.79–3.73 (m, 1 H), 3.32 (d, *J* = 12.9, 2 H), 3.30 (dd, *J* = 6.9, 15.2, 1 H), 3.11 (dd, *J* = 6.4, 15.1, 1 H), 2.76-2.70 (m, 1 H), 2.66 (dd, *J* = 7.2, 14.7, 1 H), 2.53-2.42 (m, 1 H), 2.19-2.00 (m, 2 H), 2.09 (s, 3 H), 1.86-1.72 (m, 3 H), 1.60 (s, 3 H), 1.47-1.38 (m, 2 H), 1.30-1.15 (m, 6H), 0.84 (t, *J* = 6.9, 3 H).

MS: (ESI, Q-tof)

356.3 (100)

Mol. Formula: $C_{24}H_{38}BrNO$ (436.47)

HRMS: $C_{24}H_{38}NO^+$: (356.2953)

Calcd: 356.2953

Found: 356.2951

TLC: R_f 0.32 (CH_2Cl_2/MeOH, 9:1) [I_2]

Preparation of *rel*-(1*S*,3*R*,5a*S*,7a*S*,7b*R*) Octahydro-1-hexyloxy-1-methyl-3-(1-naphthyl methyl)-7b-methylcyclopenta[*gh*]pyrrolizinium Bromide (IV{*2,3,2*})

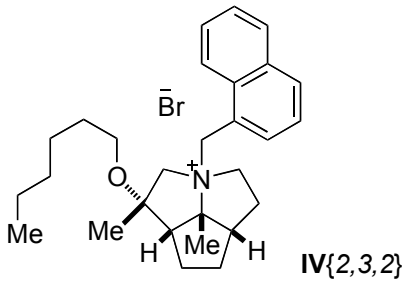

IV{*2,3,2*}

Data for **IV**{*2,3,2*}:

Yield: 45 mg (51%), free-flowing white powder

^{1}H-NMR: (500 MHz, $CDCl_3$)

8.42-8.36 (m, 1 H), 8.16-8.10 (m, 1 H), 7.85 (d, *J* = 7.7, 1 H), 7.82-7.76 (m, 1 H), 7.61 (dd, *J* = 7.6, 7.6, 1 H), 7.51 (dd, *J* = 7.5, 7.5, 1 H), 7.41-7.33 (m, 1 H), 5.53 (d, *J* = 12.5, 1 H), 5.31 (d, *J* = 12.9, 1 H), 5.06 (d, *J* = 12.6, 1 H), 3.84-3.75 (m, 1 H), 3.35 (d, *J* = 12.9, 2 H), 3.25 (dd, *J* = 7.1, 15.2, 1 H), 2.99 (dd, *J* = 6.3, 15.0, 1 H), 2.84-2.69 (m, 3 H), 2.30 (s, 3 H), 2.15-2.05 (m, 2 H), 1.83-1.74 (m, 3 H), 1.60 (s, 3 H), 1.38-1.25 (m, 2 H), 1.22-1.09 (m, 6H), 0.79 (t, *J* = 7.0, 3 H).

MS: (ESI, Q-tof)

406.3 (100)

Mol. Formula: $C_{28}H_{40}BrNO$ (486.53)

HRMS: $C_{28}H_{40}NO^+$: (406.3110)

Calcd: 406.3110

Found: 406.3099

TLC: R_f 0.35 (CH_2Cl_2/MeOH, 9:1) [I_2]

Preparation of *rel*-(1*S*,3*R*,5a*S*,7a*S*,7b*R*) Octahydro-1-hexyloxy-1-methyl-3-(2-naphthylmethyl)-7b-methylcyclopenta[*gh*]pyrrolizinium Bromide (IV{*2,3,3*})

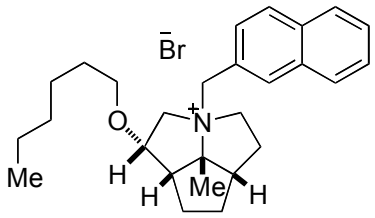

IV{*2,3,3*}

Data for **IV**{*2,3,3*}:

Yield: 51 mg (57%), free-flowing white powder

^{1}H-NMR: (500 MHz, $CDCl_3$)

8.21 (s, 1 H), 7.94-7.89 (m, 1 H), 7.83-7.74 (m, 3 H), 7.56-7.48 (m, 2 H), 5.53-5.46 (m, 1 H), 5.27-5.17 (m, 1 H), 4.55-4.39 (m, 1 H), 3.87-3.73 (m, 2 H), 3.35 (d, J = 12.9, 1 H), 3.26 (dd, J = 7.2, 13.6, 1 H), 3.04 (dd, 1 H, J = 6.9, 13.3), 2.78-2.67 (m, 2 H), 2.65-2.54 (m, 1 H), 2.18-2.02 (m, 2 H), 2.16 (s, 3 H), 1.88-1.72 (m, 3 H), 1.60 (s, 3 H), 1.45-1.29 (m, 2 H), 1.24-1.11 (m, 6H), 0.80 (t, J = 6.8, 3 H)

MS: (ESI, Q-tof)

406.3 (100)

Mol. Formula: $C_{28}H_{40}BrNO$ (486.53)

HRMS: $C_{28}H_{40}NO^+$: (406.3110)

Calcd: 406.3110

Found: 406.3109

TLC: R_f 0.35 (CH_2Cl_2/MeOH, 9:1) [I_2]

Preparation of Quaternary Ammonium Bromides IV{*3,2,R*^{4}}

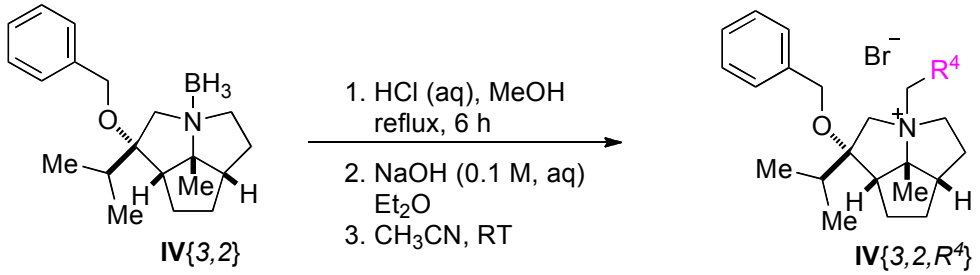

Following General Procedure II, amino borane **IV{*2,3*}** (533 mg, 1.68 mmol) was added to a 50-mL round-bottomed flask as a solution in 56 mL of MeOH (0.03 M). The flask was fitted with a reflux condenser, a magnetic stir bar, and a nitrogen inlet adapter. Lastly, 1.0 N aq. HCl solution (8.4 mL, 5.0 equiv) was added via syringe. The resulting solution was heated and then concentrated by rotary evaporation (15 mm Hg, 20-25 ^{o}C) as described General Procedure II. The resulting free amine was dissolved in acetonitrile and was distributed among four test tubes that were subsequently charged with benzyl bromide (tube 1, 87 mg, 0.509 mmol, 1.2 equiv), 1-bromomethylnaphthalene (tube 2, 116 mg, 0.509 mmol, 1.2 equiv), 2-bromomethylnaphthalene (tube 3, 116 mg, 0.509 mmol, 1.2 equiv), 3,5-bis(trifluoromethyl)benzyl bromide (tube 4, 156 mg, 0.509 mmol, 1.2 equiv). After being agitated for 12 h, the reaction mixtures were worked up and the products isolated and purified as described in General Procedure II.

Preparation of *rel*-(1*R*,3*R*,5a*S*,7a*S*,7b*R*) Octahydro-1-benzyloxy-1-isopropyl-3-benzyl-7b-methylcyclopenta[*gh*]pyrrolizinium Bromide (IV{*3,2,1*})

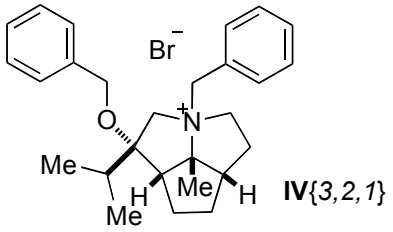

IV{*3,2,1*}

Data for **IV**{*3,2,1*}:

Yield: 235 mg (99%), free-flowing white powder

^{1}H-NMR: (500 MHz, $CDCl_3$)

7.82-7.77 (dd, *J* = 2.2, 7.2, 2 H), 7.44-7.37 (s, 3 H), 7.30-7.21 (m, 3 H), 7.19-7.15 (m, 2 H), 5.50 (d, *J* = 12.5, 1 H), 4.77 (d, *J* = 13.4, 1 H), 4.62-4.53 (m, 1 H), 4.46 (d, *J* = 11.3, 1 H), 4.21 (d, *J* = 11.3, 1 H), 3.91-3.82 (m, 1 H), 3.72 (d, *J* = 13.5, 1 H), 3.49 (dd, *J* = 7.2, 12.3, 1 H), 2.83-2.76 (m, 1 H), 2.73 (dd, *J* = 8.2, 8.2, 1 H), 2.67-2.56 (m, 1 H), 2.42-2.32 (m, 1 H), 2.31-2.21 (m, 1 H), 2.09-1.99 (m, 1 H), 1.96 (s, 3 H), 1.86-1.76 (m, 2 H), 1.69-1.59 (m, 1 H), 1.28 (d, *J* = 6.8, 3 H), 1.05 (d, *J* = 6.8, 3 H)

MS: (ESI, Q-tof)

390.3 (100)

Mol. Formula: $C_{27}H_{36}BrNO$ (470.48)

HRMS: $C_{27}H_{36}NO^+$: (390.2797)

Calcd: 390.2797

Found: 390.2789

TLC: R_f 0.21 (CH_2Cl_2/MeOH, 9:1) [I_2]

Preparation of *rel*-(1*R*,3*R*,5a*S*,7a*S*,7b*R*) Octahydro-1-benzyloxy-1-isopropyl-3-(1-naphthylmethyl)-7b-methylcyclopenta[*gh*]pyrrolizinium Bromide (IV{*3,2,2*})

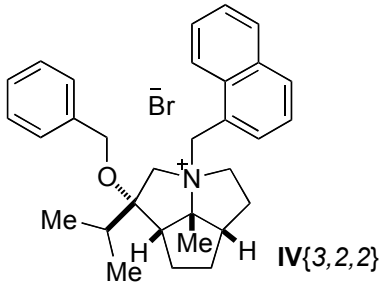

IV{*3,2,2*}

Data for **IV**{*3,2, 2*}:

Yield: 194 mg (74%), free-flowing white powder

^{1}H-NMR: (500 MHz, $CDCl_3$)

8.35 (s, 1 H), 8.24 (s, 1 H), 7.66 (s, 1 H), 7.53 (dd, *J* = 7.9, 7.9, 1 H), 7.45-7.40 (m, 2 H), 7.18-7.13 (m, 3 H), 7.02 (d, *J* = 5.9, 2 H), 6.99-6.89 (m, 1 H), 5.62-5.49 (m, 2 H), 4.82 (d, *J* = 13.8, 1 H), 4.37 (d, *J* = 11.2, 1 H), 4.00 (d, *J* = 11.3, 1 H), 3.76-3.67 (m, 1 H), 3.54 (d, *J* = 13.9, 1 H), 3.26-3.16 (m, 1 H), 3.03-2.94 (m, 2 H), 2.78 (dd, *J* = 7.3, 7.3, 1 H), 2.39-2.16 (m, 2 H), 2.30 (s, 3 H), 2.11-2.02 (m, 1 H), 1.85-1.75 (m, 2 H), 1.63-1.55 (m, 1 H), 1.35 (d, *J* = 6.8, 3 H), 1.04 (d, *J* = 6.8, 3 H)

MS: (ESI, Q-tof)

440.3 (100)

Mol. Formula: $C_{31}H_{38}BrNO$ (520.54)

HRMS: $C_{31}H_{38}NO^+$: (440.2953)

Calcd: 440.2953

Found: 440.2960

TLC: R_f 0.25 (CH_2Cl_2/MeOH, 9:1) [I_2]

Preparation of *rel*-(1*R*,3*R*,5a*S*,7a*S*,7b*R*) Octahydro-1-benzyloxy-1-isopropyl-3-(2-naphthylmethyl)-7b-methylcyclopenta[*gh*]pyrrolizinium Bromide (IV{*3,2,3*})

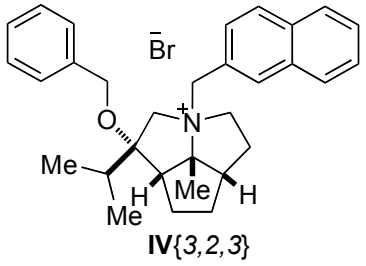

IV{*3,2,3*}

Data for **IV**{*3,2,3*}:

Yield: 195 mg (75%), free-flowing white powder

^{1}H-NMR: (500 MHz, $CDCl_3$)

8.22 (s, 1 H), 7.86-7.81 (m, 1 H), 7.74 (d, *J* = 8.3, 1 H), 7.64-7.55 (m, 2 H), 7.45-7.42 (m, 2 H), 7.20-7.14 (m, 3 H), 7.11-7.08 (m, 2 H), 5.62 (d, *J* = 12.8, 1 H), 4.92-4.82 (m, 1 H), 4.83 (d, *J* = 13.4, 1 H), 4.41 (d, *J* = 11.3, 1 H), 4.11 (d, *J* = 11.2, 1 H), 3.87-3.78 (m, 1 H), 3.69 (d, *J* = 13.4, 1 H), 3.49-3.41 (m, 1 H), 2.95-2.89 (m, 1 H), 2.82-2.71 (m, 2 H), 2.37 (hept, *J* = 6.9, 1 H), 2.29-2.21 (m, 1 H), 2.10-2.02 (m, 1 H), 2.07 (s, 3 H), 1.86-1.75 (m, 2 H), 1.68-1.60 (m, 1 H), 1.33 (d, *J* = 6.8, 3 H), 1.03 (d, *J* = 6.7, 3 H)

MS: (ESI, Q-tof)

440.3 (100)

Mol. Formula: $C_{31}H_{38}BrNO$ (520.54)

HRMS: $C_{31}H_{38}NO^+$: (440.2953)

Calcd: 440.2953

Found: 440.2960

TLC: R_f 0.25 (CH_2Cl_2/MeOH, 9:1) [I_2]

Preparation of *rel*-(1*R*,3*R*,5a*S*,7a*S*,7b*R*) Octahydro-1-benzyloxy-1-isopropyl-3-(3,5-trifluoromethyl benzyl)-7b-methylcyclopenta[*gh*]pyrrolizinium Bromide (IV{*3,2,5*})

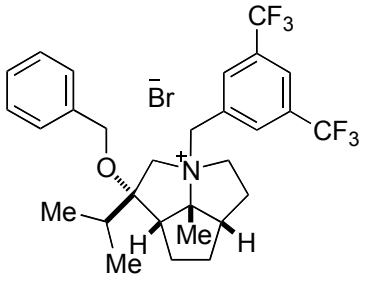

IV{*3,2,5*}

Data for **IV**{*3,2,5*}:

Yield: 199 mg (66%), free-flowing white powder

^{1}H-NMR: (500 MHz, $CDCl_3$)

8.32 (s, 2 H), 7.83 (s, 1 H), 7.25-7.19 (m, 3 H), 7.15-7.10 (m, 2 H), 5.88 (d, *J* = 12.7, 1 H), 5.17-5.09 (m, 1 H), 4.88 (d, *J* = 13.2, 1 H), 4.47 (d, *J* = 11.5, 1 H), 4.16 (d, *J* = 11.5, 1 H), 3.94-3.85 (m, 1 H), 3.47 (d, *J* = 13.1, 1 H), 3.02-2.93 (m, 2 H), 2.80-2.70 (m, 2 H), 2.38 (hept, *J* = 6.7, 1 H), 2.31-2.22 (m, 1 H), 2.12-1.99 (m, 1 H), 2.04 (s, 3 H), 1.91-1.77 (m, 2 H), 1.74-1.65 (m, 1 H), 1.31 (d, *J* = 6.7, 3 H), 1.02 (d, *J* = 6.7, 3 H)

MS: (ESI, Q-tof)

526.3 (100)

Mol. Formula: $C_{29}H_{34}BrF_6NO$ (606.48)

HRMS: $C_{29}H_{34}NOF_6^+$: 526.2545)

Calcd: 526.2545

Found: 526.2549

TLC: R_f 0.30 (CH_2Cl_2/MeOH, 9:1) [I_2]

Preparation of *rel*-(1*R*,3*R*,5a*S*,7a*S*,7b*R*) Octahydro-1-benzyloxy-1-phenyl-3-(3,5-trifluoromethylbenzyl)-7b-methylcyclopenta[*gh*]pyrrolizinium Bromide (IV{*5,2,5*})

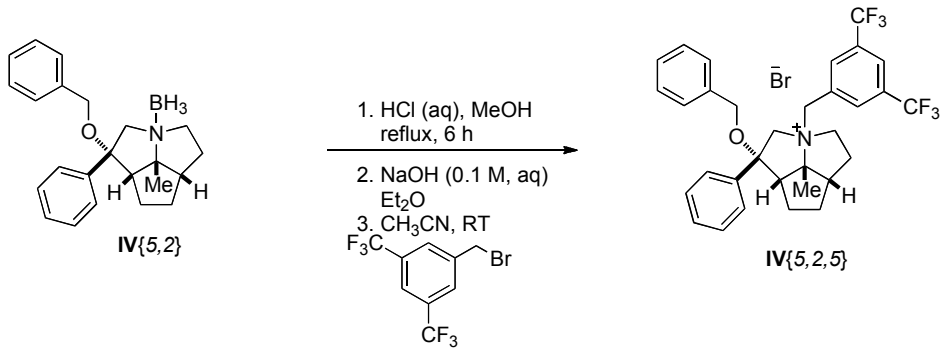

Following General Procedure II, benzyl ether **IV{*5,2*}** (69 mg, 0.268 mmol) was added to a 50-mL round-bottomed flask as a solution in 8.9 mL of MeOH (0.03 M). The flask was fitted with a reflux condenser, a magnetic stir bar, and a nitrogen inlet adapter. Lastly, 1.0 N aq. HCl solution (1.3 mL, 5.0 equiv) was added via syringe. The resulting solution was heated and then concentrated by rotary evaporation (15 mm Hg, 20-25 ^{o}C) as described General Procedure II. The resulting free amine (30 mg, 0.09 mmol) was dissolved in acetonitrile along with 3,5-bis(trifluoromethyl)benzyl bromide (33 mg, 0.108 mmol, 2.0 equiv) and was allowed to react for 12 h. Purification of described in General Procedure II afforded 44 mg (75%) of the quaternary ammonium ion **IV{*5,2,5*} a**s a free flowing white power.

Data for **IV**{*5,2,5*}:

Yield: 44 mg (75%), free-flowing white powder

^{1}H-NMR: (500 MHz, $CDCl_3$)

8.12 (s, 1 H), 7.93 (s, 1 H), 7.76 (d, *J* = 7.5, 1 H), 7.64 (dd, *J* = 7.6, 7.6, 1 H), 7.55 (dd, *J* = 7.3, 7.3, 1 H), 7.30-7.24 (m, 1 H), 7.12 (dd, *J* = 2.1, 7.5, 1 H), 5.59 (d, *J* = 12.5, 1 H), 4.80 (s, 1 H), 4.59 (d, *J* = 13.0, 1 H), 4.37 (d, *J* = 11.6, 1 H), 4.07 (d, *J* = 11.0, 1 H), 3.91 (d, *J* = 11.0, 1 H), 3.62 (d, *J* = 13.1, 1 H), 3.44-3.39 (m, 1 H), 3.32 (dd, *J* = 8.1, 8.1, 1 H), 3.15-3.08 (m, 1 H), 2.61-2.45 (m, 1 H), 2.26 (s, 3 H), 2.16-2.03 (m, 1 H), 2.01-1.95 (m, 1 H), 1.87 (ddd, *J* = 7.8, 14.5, 14.3, 1 H)

MS: (ESI, Q-tof)

560.2 (100)

Mol. Formula: $C_{32}H_{32}BrF_6NO$ (640.50)

HRMS: $C_{20}H_{38}NO_3^{+}$: (560.2388)

Calcd: 560.2388

Found: 560.2388

TLC: R_f 0.32 (CH_2Cl_2/MeOH, 9:1) [I_2]

Preparation of Quaternary Ammonium Bromides V{1-7,1-7,1-11}.

Preparation of Quaternary Ammonium Bromides V{1,2,R^4}

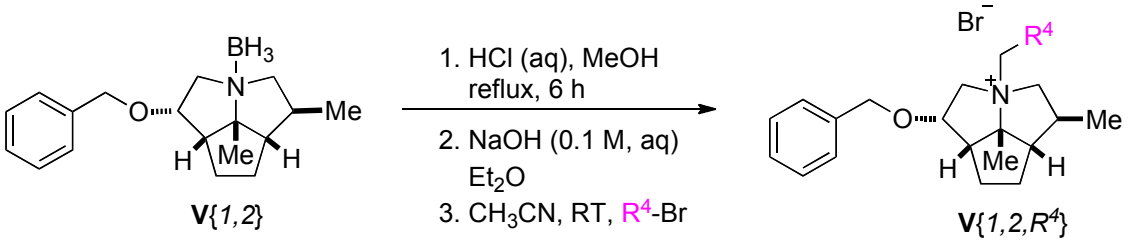

V{*1,2*} **V**{*1,2,R^4*}

Following General Procedure II, amino borane **V**{*1,2*} (533 mg, 1.68 mmol) was added to a 50-mL round-bottomed flask as a solution in 37 mL of MeOH (0.03 M). The flask was fitted with a reflux condenser, a magnetic stir bar, and a nitrogen inlet adapter. Lastly, 1.0 N aq. HCl solution (5.5 mL, 5.0 equiv) was added via syringe. The resulting solution was heated and then concentrated by rotary evaporation (15 mm Hg, 20-25 ^oC) as described General Procedure II. The resulting free amine was dissolved in acetonitrile and was distributed among seven test tubes that were subsequently charged with benzyl bromide (tube 1, 40 mg, 0.235 mmol, 1.5 equiv), 1-bromomethylnaphthalene (tube 2, 42 mg, 0.188 mmol, 1.2 equiv), 2-bromomethylnaphthalene (tube 3, 42 mg, 0.188 mmol, 1.2 equiv), 3,5-bis(trifluoromethyl)benzyl bromide (tube 4, 58 mg, 0.188 mmol, 1.2 equiv), 3,5-bis(*t*-butyl)benzyl bromide (tube 5, 54 mg, 0.188 mmol, 1.2 equiv), 4-methoxybenzyl bromide (tube 6, 38 mg, 0.188 mmol, 1.2 equiv), 1-bromohexane (tube 7, 129 mg, 0.785 mmol, 5.0 equiv). After being agitated for 12 h, the reaction mixtures were worked up and the products isolated and purified as described in General Procedure II.

Preparation of *rel*-(1*S*,3*R*,5*S*,5a*S*,7a*S*,7b*R*) Octahydro-1-benzyloxy-3-benzyl-5-methyl-7b-methylcyclopenta[*gh*]pyrrolizinium Bromide (V{*1,2,1*})

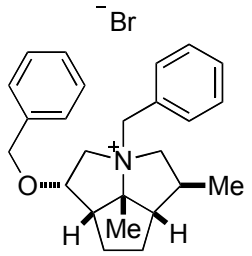

V{*1,2,1*}

Data for **V**{*1,2,1*}:

Yield: 63 mg (90%), free-flowing white powder

^{1}H-NMR: (500 MHz, $CDCl_3$)

7.64 (d, *J* = 6.7, 2 H), 7.43-7.31 (m, 8H), 5.14 (d, *J* = 12.3, 1 H), 4.99-4.93 (dd, *J* = 6.9, 17.2, 1 H), 4.65 (d, *J* = 12.3, 1 H), 4.63 (d, *J* = 11.7, 1 H), 4.57 (d, *J* = 11.7, 1 H), 4.37 (dd, *J* = 11.9, 11.9, 1 H), 3.87 (dd, *J* = 6.2, 12.5, 1 H), 3.10 (dd, *J* = 6.1, 11.5, 1 H), 2.88-2.82 (m, 2 H), 2.45-2.40 (s, 1 H), 2.15-2.06 (m, 1 H), 2.06-1.95 (m, 1 H), 2.04 (s, 3 H), 1.93-1.78 (m, 3 H), 1.20 (d, *J* = 6.4, 3 H)

MS: (ESI, Q-tof)

362.2 (100)

Mol. Formula: $C_{25}H_{32}BrNO$ (442.43)

HRMS: $C_{25}H_{32}NO^+$: (362.2484)

Calcd: 362.2484

Found: 362.2484

TLC: R_f 0.20 (CH_2Cl_2/MeOH, 9:1) [I_2]

Preparation of *rel*-(1*S*,3*R*,5*S*,5a*S*,7a*S*,7b*R*) Octahydro-1-benzyloxy-3-(1-naphthylmethyl)-5-methyl-7b-methylcyclopenta[*gh*]pyrrolizinium Bromide (V{*1,2,2*})

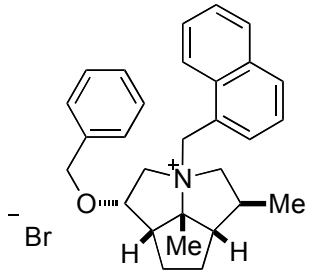

V{*1,2,2*}

Data for **V**{*1,2,2*}:

Yield: 77 mg (99%), free-flowing white powder

^{1}H-NMR: (500 MHz, $CDCl_3$)

8.25-8.16 (m, 2 H), 7.85-7.73 (m, 2 H), 7.53-7.47 (m, 1 H), 7.49 (dd, *J* = 7.6, 14.6, 1 H), 7.40-7.26 (m, 7H), 5.54 (d, *J* = 13.0, 1 H), 5.25 (d, *J* = 13.0, 1 H), 5.17-5.08 (m, 1 H), 4.72 (dd, *J* = 11.9, 11.9, 1 H), 4.64 (d, *J* = 11.8, 1 H), 4.49 (d, *J* = 11.8, 1 H), 3.56 (dd, *J* = 6.1, 12.4, 1 H), 3.06 (dd, *J* = 5.9, 11.3, 1 H), 2.91 (dd, *J* = 8.4, 16.9, 1 H), 2.74 (t, *J* = 11.8, 11.8, 1 H), 2.59-2.53 (m, 1 H), 2.31 (s, 3 H), 2.04-1.75 (m, 5 H), 1.59 (s, 3 H), 1.21 (d, *J* = 6.3, 3 H)

MS: (ESI, Q-tof)

412.3 (100)

Mol. Formula: $C_{29}H_{34}BrNO$ (492.49)

HRMS: $C_{29}H_{34}NO^+$: (412.2640)

Calcd: 412.2640

Found: 412.2633

TLC: R_f 0.23 (CH_2Cl_2/MeOH, 9:1) [I_2]

Preparation of *rel*-(1*S*,3*R*,5*S*,5a*S*,7a*S*,7b*R*) Octahydro-1-benzyloxy-3-(2-naphthylmethyl)-5-methyl-7b-methylcyclopenta[*gh*]pyrrolizinium Bromide (V{*1,2,3*})

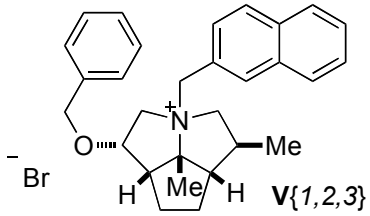

V{*1,2,3*}

Data for **V**{*1,2,3*}:

Yield: 65 mg (84%), free-flowing white powder

^{1}H-NMR: (500 MHz, $CDCl_3$)

8.15 (s, 1 H), 7.91-7.82 (m, 1 H), 7.73-7.62 (m, 3 H), 7.52-7.44 (m, 2 H), 7.39-7.28 (m, 5 H), 5.33 (d, *J* = 12.3, 1 H), 5.10 (dd, *J* = 6.9, 17.2, 1 H), 4.93 (d, *J* = 12.4, 1 H), 4.65 (d, *J* = 14.1, 1 H), 4.62 (d, *J* =14.1, 1 H), 4.42 (dd, *J* = 11.9, 11.9, 1 H), 3.94 (dd, *J* = 6.2, 12.4, 1 H), 3.11 (dd, *J* = 6.0, 11.4, 1 H), 2.89 (dd, *J* = 8.5, 16.9, 1 H), 2.83 (dd, *J* = 11.4, 11.4, 1 H), 2.47-2.41 (m, 1 H), 2.15-1.94 (m, 2 H), 2.13 (s, 3 H), 1.92-1.74 (m, 3 H), 1.20 (d, *J* = 6.4, 3 H).

MS: (ESI, Q-tof)

412.3 (100)

Mol. Formula: $C_{29}H_{34}BrNO$ (492.49)

HRMS: $C_{29}H_{34}NO^+$: (412.2640)

Calcd: 412.2640

Found: 412.2625

TLC: R_f 0.24 (CH_2Cl_2/MeOH, 9:1) [I_2]

Preparation of *rel*-(1*S*,3*R*,5*S*,5a*S*,7a*S*,7b*R*) Octahydro-1-benzyloxy-3-(3,5-trifluoromethyl-benzyl)-5-methyl-7b-methylcyclopenta[*gh*]pyrrolizinium Bromide (V{*1*,*2*,*5*})

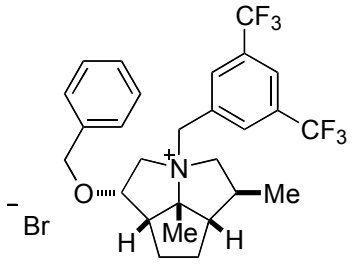

V{*1,2,5*}

Data for **V**{*1*,*2*,*5*}:

Yield: 84 mg (98%), free-flowing white powder

^{1}H-NMR: (500 MHz, $CDCl_3$)

8.40 (s, 2 H), 7.90 (s, 1 H), 7.38-7.27 (m, 5 H), 5.58 (d, *J* = 12.4, 1 H), 5.32-5.24 (m, 1 H), 5.13-5.04 (m, 1 H), 4.61 (d, *J* = 11.6, 1 H), 4.58 (d, *J* = 11.6, 1 H), 4.44 (dd, *J* = 11.6, 11.6, 1 H), 3.83 (dd, *J* = 6.1, 12.5, 1 H), 3.06-3.00 (m, 1 H), 2.95-2.84 (m, 2 H), 2.42-2.36 (m, 1 H), 2.26-2.15 (m, 1 H), 2.00-1.97 (m, H), 2.09 (s, 3 H), 1.89-1.79 (m, 3 H), 1.19 (d, *J* = 6.2, 3 H).

MS: (ESI, Q-tof)

498.2 (100)

Mol. Formula: $C_{27}H_{30}BrF_6NO$ (578.43)

HRMS: $C_{27}H_{30}F_6NO^+$: (498.2232)

Calcd: 498.2232

Found: 498.2222

TLC: R_f 0.28 (CH_2Cl_2/MeOH, 9:1) [I_2]

Preparation of *rel*-(1*S*,3*S*,5*S*,5a*S*,7a*S*,7b*R*) Octahydro-1-benzyloxy-3-hexyl-5-methyl-7b-methylcyclopenta[*gh*]pyrrolizinium Bromide (V{*1,2,6*})

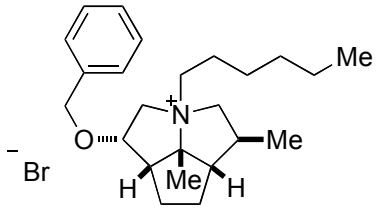

V{*1,2,6*}

Data for **V**{*1,2,6*}:

Yield: 65 mg (95%), free-flowing white powder

^{1}H-NMR: (500 MHz, $CDCl_3$)

7.40–7.30 (m, 5 H), 4.63 (dd, *J* = 7.9, 14.6, 1 H), 4.60 (d, *J* = 11.5, 1 H), 4.57 (d, *J* = 11.5, 1 H), 4.11 (dd, *J* = 6.2, 12.5, 1 H), 3.71–3.58 (m, 3 H), 3.49 (ddd, *J* = 4.4, 4.4, 12.2, 1 H), 3.31 (dd, *J* = 8.9, 12.5, 1 H), 2.84–2.78 (m, 1 H), 2.37–2.20 (m, 2 H), 2.17 (s, 2 H), 2.13–2.02 (m, 1 H), 1.92–1.81 (m, 3 H), 1.84 (s, 3 H), 1.80–1.64 (m, 2 H), 1.51–1.40 (m, 2 H), 1.36–1.27 (m, 4 H), 1.16 (d, *J* = 6.3, 3 H), 0.89 (t, *J* = 7.1, 3 H)

MS: (ESI, Q-tof)

356.3 (100)

Mol. Formula: $C_{24}H_{38}BrNO$ (436.47)

HRMS: $C_{24}H_{38}NO^+$: (356.2953)

Calcd: 356.2953

Found: 356.2947

TLC: R_f 0.25 (CH_2Cl_2/MeOH, 9:1) [I_2]

Preparation of *rel*-(1*S*,3*R*,5*S*,5a*S*,7a*S*,7b*R*) Octahydro-1-benzyloxy-3-(3,5-*tert*-butyl-benzyl)-5-methyl-7b-methylcyclopenta[*gh*]pyrrolizinium Bromide (V{*1,2,7*})

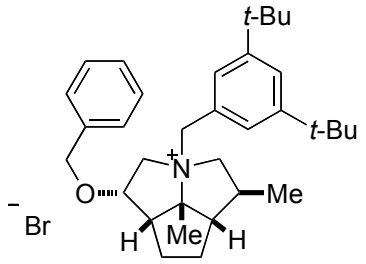

V{*1,2,7*}

Data for **V**{*1,2,7*}:

Yield: 84 mg (96%), free-flowing white powder

^{1}H-NMR: (500 MHz, $CDCl_3$)

7.52–7.48 (m, 3 H), 7.40–7.28 (m, 5 H), 5.08 (d, *J* = 12.4, 1 H), 4.83 (dd, *J* = 6.9, 16.8, 1 H), 4.62 (d, *J* = 11.9, 1 H), 4.54 (d, *J* = 11.9, 1 H) 4.52 (d, *J* = 11.9, 1 H), 4.42 (dd, *J* = 11.7, 11.7, 1 H), 4.17 (dd, *J* = 6.2, 12.5, 1 H), 3.19 (dd, *J* = 6.2, 11.6, 1 H), 3.00 (dd, *J* = 11.2, 11.2, 1 H), 2.90 (dd, *J* = 8.2, 16.4, 1 H), 2.50–2.45 (m, 1 H), 2.22–2.12 (m, 1 H), 2.12–1.99 (m, 1 H), 2.10 (s, 3 H), 1.95–1.80 (m, 3 H), 1.34 (s, 18H), 1.24 (d, *J* = 6.5, 3 H)

MS: (ESI, Q-tof)

474.4 (100)

Mol. Formula: $C_{33}H_{48}BrNO$ (554.64)

HRMS: $C_{33}H_{48}NO^+$: 474.3736)

Calcd: 474.3736

Found: 474.3723

TLC: R_f 0.32 (CH_2Cl_2/MeOH, 9:1) [I_2]

Preparation of *rel*-(1*S*,3*R*,5*S*,5a*S*,7a*S*,7b*R*) Octahydro-1-benzyloxy-3-(4-methoxy-benzyl)-5-methyl-7b-methylcyclopenta[*gh*]pyrrolizinium Bromide (V{*1,2,8*})

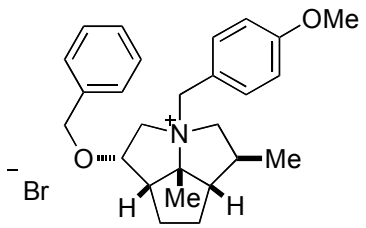

V{*1,2,8*}

Data for **V**{*1,2,8*}:

Yield: 77 mg (99%), free-flowing white powder

^{1}H-NMR: (500 MHz, $CDCl_3$)

7.56 (d, *J* = 8.6, 2 H), 7.40–7.31 (m, 5 H), 6.85 (d, *J* = 8.4, 2 H), 5.07 (d, *J* = 12.4, 1 H), 5.00–4.90 (m, 1 H), 4.65–4.52 (m, 3 H), 4.31 (dd, *J* = 11.9, 1 H), 3.90–3.82 (m, 1 H), 3.80 (s, 3 H), 3.07 (dd, *J* = 6.5, 11.2, 1 H), 2.83 (dd, *J* = 8.03, 15.8, 2 H), 2.44–2.38 (m, 1 H), 2.14–2.05 (m, 1 H), 2.05–1.93 (m, 1 H), 2.03 (s, 3 H), 1.91–1.76 (m, 3 H), 1.20 (d, *J* = 6.4, 3 H)

MS: (ESI, Q-tof)

392.3 (100)

Mol. Formula: $C_{26}H_{34}BrNO_2$ (472.46)

HRMS: $C_{26}H_{34}NO_2^+$: (392.2590)

Calcd: 392.2590

Found: 392.2578

TLC: R_f 0.18 (CH_2Cl_2/MeOH, 9:1) [I_2]

Preparation of Quaternary Ammonium Bromides V{*2,2,R*^{4}}

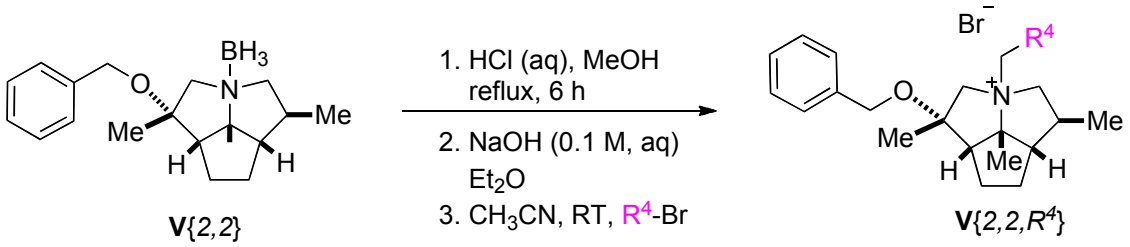

V{*2,2*} **V**{*2,2,R*^{4}}

Following General Procedure II, amino borane **V**{*2,2*} (397 mg, 1.33 mmol) was added to a 50-mL round-bottomed flask as a solution in 44 mL of MeOH (0.03 M). The flask was fitted with a reflux condenser, a magnetic stir bar, and a nitrogen inlet adapter. Lastly, 1.0 N aq. HCl solution (6.6 mL, 5.0 equiv) was added via syringe. The resulting solution was heated and then concentrated by rotary evaporation (15 mm Hg, 20-25 ^{o}C) as described General Procedure II. The resulting free amine was dissolved in acetonitrile and was distributed among seven test tubes that were subsequently charged with benzyl bromide (tube 1, 48 mg, 0.279 mmol, 1.2 equiv), 1-bromomethylnaphthalene (tube 2, 50 mg, 0.279 mmol, 1.2 equiv), 2-bromomethylnaphthalene (tube 3, 50 mg, 0.279 mmol, 1.2 equiv), 3,5-bis(trifluoromethyl)benzyl bromide (tube 4, 70 mg, 0.279 mmol, 1.2 equiv), 3,5-bis(*t*-butyl)benzyl bromide (tube 5, 64 mg, 0.279 mmol, 1.2 equiv), 4-methoxybenzyl bromide (tube 6, 70 mg, 0.279 mmol, 1.2 equiv), 1-bromohexane (tube 7, 70 mg, 0.279 mmol, 1.2 equiv). After being agitated for 12 h, the reaction mixtures were worked up and the products isolated and purified as described in General Procedure II.

Preparation of *rel*-(1*S*,3*R*,5*S*,5a*S*,7a*S*,7b*R*) Octahydro-1-benzyloxy-1-methyl-3-benzyl-5-methyl-7b-methylcyclopenta[*gh*]pyrrolizinium Bromide (V{*2,2,1*})

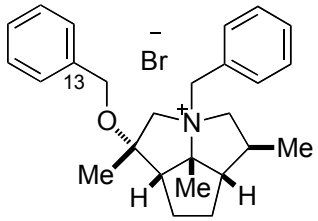

V{*2,2,1*}

Data for **V**{*2,2,1*}:

Yield: 79 mg (74%), free-flowing white powder

^{1}H-NMR: (500 MHz, $CDCl_3$)

7.80-7.77 (m, 2 H), 7.51–7.43 (m, 3 H), 7.38–7.29 (m, 3 H), 7.24 (d, *J* = 6.7, 2 H), 5.20 (d, *J* = 12.2, 1 H), 4.86 (d, *J* = 12.2, 1 H), 4.51 (d, *J* = 13.5, 1 H), 4.49 (d, *J* = 11.1, 11.1, 1 H), 4.41 (d, *J* = 11.0, 1 H), 4.37 (d, *J* = 11.0, 1 H), 3.24 (d, *J* = 13.3, 1 H), 3.18 (dd, *J* = 6.7, 11.7, 1 H), 2.71 (dd, *J* = 8.4, 8.4, 1 H), 2.59–2.52 (m, 1 H), 2.39–2.19 (m, 2 H), 2.16 (s, 3 H), 1.96 (m, 1 H), 1.89 (m, 2 H), 1.84 (s, 3 H), 1.20 (d, *J* = 6.6, 3 H).

MS: (ESI, Q-tof)

376.3 (100)

Mol. Formula: $C_{26}H_{34}BrNO$ (456.46)

HRMS: $C_{26}H_{34}NO^+$: (376.2640)

Calcd: 376.2640

Found: 376.2638

TLC: R_f 0.22 (CH_2Cl_2/MeOH, 9:1) [I_2] [I_2]

Preparation of *rel*-(1*S*,3*R*,5*S*,5a*S*,7a*S*,7b*R*) Octahydro-1-benzyloxy-1-methyl-3-(1-naphthylmethyl)-5-methyl-7b-methylcyclopenta[*gh*]pyrrolizinium Bromide (V{*2,2,2*})

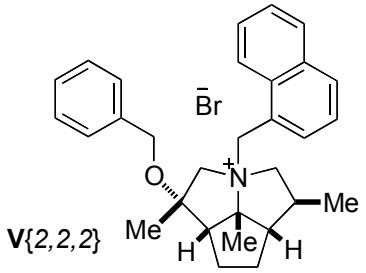

V{*2,2,2*}

Data for **V**{*2,2,2*}:

Yield: 91 mg (77%), free-flowing white powder

^{1}H-NMR: (500 MHz, $CDCl_3$)

8.42 (d, *J* = 8.6, 1 H), 8.30 (d, *J* = 7.1, 1 H), 7.92-7.87 (m, 2 H), 7.66 (dd, *J* = 7.6, 7.6, 1 H), 7.52 (m, 2 H), 7.30–7.21 (m, 3 H), 7.18–7.12 (m, 2 H), 5.53 (d, *J* = 12.9, 1 H), 5.43 (d, *J* = 12.9, 1 H), 4.61 (d, *J* = 13.2, 1 H), 4.44 (dd, *J* = 11.7, 11.7, 1 H), 4.38 (d, *J* = 11.1, 1 H), 4.29 (d, *J* = 11.1, 1 H), 3.24 (d, *J* = 13.3, 1 H), 2.98 (dd, *J* = 6.8, 11.6, 1 H), 2.78 (dd, *J* = 8.3, 8.3, 1 H), 2.62 (d, *J* = 9.5, 1 H), 2.36–2.20 (m, 2 H),2.31 (s, 3 H), 1.98–1.83 (m, 3 H), 1.92 (s, 3 H), 1.10 (d, *J* = 6.5, 3 H)

MS: (ESI, Q-tof)

426.3 (100)

Mol. Formula: $C_{30}H_{36}BrNO$ (506.52)

HRMS: $C_{30}H_{36}NO^+$: (426.2797)

Calcd: 426.2797

Found: 426.2801

TLC: R_f 0.24 (CH_2Cl_2/MeOH, 9:1) [I_2]

Preparation of *rel*-(1*S*,3*R*,5*S*,5a*S*,7a*S*,7b*R*) Octahydro-1-benzyloxy-1-methyl-3-(2-naphthylmethyl)-5-methyl-7b-methylcyclopenta[*gh*]pyrrolizinium Bromide (V{*2,2,3*})

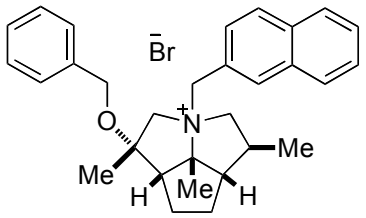

V{*2,2,3*}

Data for **V**{*2,2,3*}:

Yield: 96 mg (81%), free-flowing white powder

^{1}H-NMR: (500 MHz, $CDCl_3$)

8.27 (s, 1 H), 7.95 (d, *J* = 8.3, 1 H), 7.86–7.82 (m, 3 H), 7.57–7.52 (m, 2 H), 7.31–7.22 (m, 3 H), 7.21-7.18 (m, 2 H), 5.32 (d, *J* = 12.2, 1 H), 5.07 (d, *J* = 12.3, 1 H), 4.60 (d, *J* = 13.2, 1 H), 4.54 (dd, *J* = 11.4, 1 H), 4.40 (d, *J* = 11.0, 1 H), 4.34 (d, *J* = 11.0, 1 H), 3.23 (d, *J* = 13.2, 1 H), 3.19 (dd, *J* = 7.2, 12.0, 1 H), 2.73 (dd, *J* = 8.3, 8.3, 1 H), 2.59–2.52 (m, 1 H), 2.36–2.27 (m, 1 H), 2.27–2.15 (m, 1 H), 2.2 (s, 3 H), 1.98–1.90 (m, 1 H), 1.90–1.85 (m, 2 H), 1.87 (s, 3 H), 1.19 (d, *J* = 6.5, 3 H)

MS: (ESI, Q-tof)

426.3 (100)

Mol. Formula: $C_{30}H_{36}BrNO$ (506.52)

HRMS: $C_{30}H_{36}NO^+$: (426.2797)

Calcd: 426.2797

Found: 426.2806

TLC: R_f 0.25 (CH_2Cl_2/MeOH, 9:1) [I_2]

Preparation of *rel*-(1*S*,3*R*,5*S*,5a*S*,7a*S*,7b*R*) Octahydro-1-benzyloxy-1-methyl-3-(3,5-trifluoromethylbenzyl)-5-methyl-7b-methylcyclopenta[*gh*]pyrrolizinium Bromide (V{*2,2,5*})

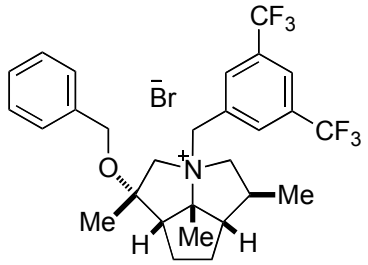

V{*2,2,5*}

Data for **V**{*2,2,5*}:

Yield: 98 mg (71%), free-flowing white powder

^{1}H-NMR: (500 MHz, $CDCl_3$)

8.40 (s, 2 H), 7.98 (s, 1 H), 7.34–7.27 (m, 3 H), 7.23–7.18 (m, 2 H), 5.43 (d, *J* = 12.5, 1 H), 5.37 (d, *J* = 12.5, 1 H), 4.55 (d, *J* = 13.1, 1 H), 4.44 (d, *J* =11.1, 1 H), 4.38 (d, *J* =11.1, 1 H), 4.36 (dd, *J* = 10.6, 10.6, 1 H), 3.24 (d, *J* = 13.1, 1 H), 3.11 (dd, *J* = 6.1, 11.3, 1 H), 2.76 (dd, *J* = 8.0, 8.0, 1 H), 2.51–2.41 (m, 2 H), 2.32–2.23 (m, 1 H), 2.16 (s, 3 H), 1.99–1.87 (m, 3 H), 1.82 (s, 3 H), 1.16 (d, *J* = 6.2, 3 H)

MS: (ESI, Q-tof)

512.2 (100)

Mol. Formula: $C_{28}H_{32}BrF_6NO$ (592.45)

HRMS: $C_{28}H_{32}NOF_6^+$: (512.2388)

Calcd: 512.2388

Found: 512.2395

TLC: R_f 0.30 (CH_2Cl_2/MeOH, 9:1) [I_2]

Preparation of *rel*-(1*S*,3*S*,5*S*,5a*S*,7a*S*,7b*R*) Octahydro-1-benzyloxy-1-methyl-3-hexyl-5-methyl-7b-methylcyclopenta[*gh*]pyrrolizinium Bromide (V{*2,2,6*})

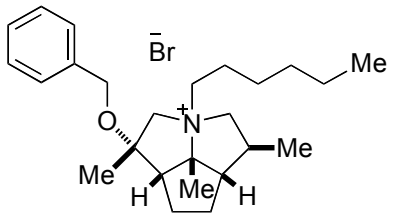

V{*2,2,6*}

Data for **V**{*2,2,6*}:

Yield: 30 mg (28%), free-flowing white powder

^{1}H-NMR: (500 MHz, $CDCl_3$)

7.33 (m, 5 H), 4.47 (d, *J* = 11.1, 1 H), 4.37 (d, *J* = 11.0, 1 H), 3.41 (dd, *J* = 6.9, 6.9, 2 H), 3.01 (d, *J* = 8.9, 1 H), 2.92 (d, *J* = 8.9, 1 H), 2.82 (dd, *J* = 6.0, 12.2, 1 H), 2.49 (dd, *J* = 11.8, 11.8, 1 H), 2.07-2.00 (m, 2 H), 1.94-1.81 (m, 5 H), 1.72-1.63 (m, 3 H), 1.46-1.40 (m, 3 H), 1.36-1.34 (m, 8H), 0.97 (d, *J* = 6.5, 3 H), 0.90 (t, *J* = 7.0, 3 H)

MS: (ESI, Q-tof)

370.3 (100)

Mol. Formula: $C_{25}H_{40}BrNO$ (450.50)

HRMS: $C_{25}H_{40}NO^+$: (370.3110)

Calcd: 370.3110

Found: 370.3109

TLC: R_f 0.40 (CH_2Cl_2/MeOH, 9:1) [I_2]

Preparation of *rel*-(1*S*,3*R*,5*S*,5a*S*,7a*S*,7b*R*) Octahydro-1-benzyloxy-1-methyl-3-(3,5-*tert*-butyl-benzyl)-5-methyl-7b-methylcyclopenta[*gh*]pyrrolizinium Bromide (V{*2,2,7*})

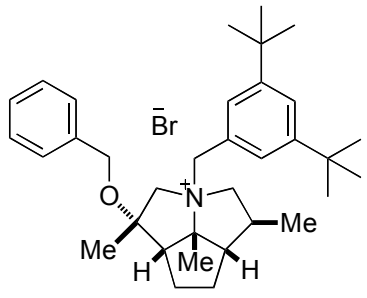

V{*2,2,7*}

Data for **V**{*2,2,7*}:

Yield: 109 mg (82%), free-flowing white powder

^{1}H-NMR: (500 MHz, $CDCl_3$)

7.57 (d, *J* = 1.7, 2 H), 7.50 (s, 1 H), 7.34–7.27 (m, 3 H), 7.24-7.22 (m, 2 H), 5.22 (d, *J* = 12.3, 1 H), 4.74 (d, *J* = 12.3, 1 H), 4.58 (dd, *J* = 11.2, 11.2, 1 H), 4.47 (d, *J* = 13.2, 1 H), 4.41 (s, 2 H), 3.22 (d, *J* = 11.9, 1 H), 3.21 (d, *J* = 12.8, 1 H), 2.65 (dd, *J* = 8.6, 8.6, 1 H), 2.61–2.56 (m, 1 H), 2.32–2.18 (m, 2 H), 2.16 (s, 3 H), 2.00–1.92 (m, 1 H), 1.90–1.86 (m, 2 H), 1.84 (s, 3 H), 1.35 (s, 18H), 1.23 (d, *J* = 6.6, 3 H)

MS: (ESI, Q-tof)

488.4 (100)

Mol. Formula: $C_{34}H_{50}BrNO$ (569.67)

HRMS: $C_{20}H_{38}NO_3^+$: (488.3892)

Calcd: 488.3892

Found: 488.3893

TLC: R_f 0.33 (CH_2Cl_2/MeOH, 9:1) [I_2]

Preparation of *rel*-(1*S*,3*R*,5*S*,5a*S*,7a*S*,7b*R*) Octahydro-1-benzyloxy-1-methyl-3-(4-methoxy-benzyl)-5-methyl-7b-methylcyclopenta[*gh*]pyrrolizinium Bromide (V{*2,2,8*})

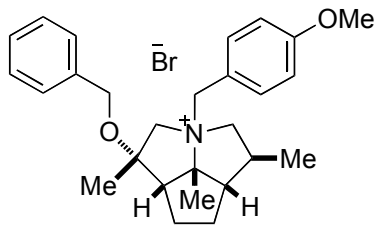

V{*2,2,8*}

Data for **V**{*2,2,8*}:

Yield: 88 mg (77%), free-flowing white powder

^{1}H-NMR: (500 MHz, $CDCl_3$)

7.71 (d, *J* = 8.7, 2 H), 7.34–7.28 (m, 3 H), 7.22 (d, *J* = 6.7, 2 H), 6.94 (d, *J* = 8.4, 2 H), 5.11 (d, *J* = 12.3, 1 H), 4.78 (d, *J* = 12.4, 1 H), 4.48–4.40 (m, 2 H), 4.41 (d, *J* = 11.0, 1 H), 4.37 (d, *J* = 11.0, 1 H), 3.82 (s, 3 H), 3.20 (d, *J* = 13.3, 1 H), 3.14 (dd, *J* = 6.7, 11.7, 1 H), 2.67 (dd, *J* = 8.4, 8.4, 1 H), 2.55–2.48 (m, 1 H), 2.33–2.17 (m, 2 H), 2.11 (s, 3 H), 1.97–1.89 (m, 1 H), 1.88–1.83 (m, 2 H), 1.81 (s, 3 H), 1.17 (d, *J* = 6.5, 3 H)

MS: (ESI, Q-tof)

406.3 (100)

Mol. Formula: $C_{27}H_{36}BrNO_2$ (486.48)

HRMS: $C_{27}H_{36}NO_2^+$: (406.2746)

Calcd: 406.2746

Found: 406.2748

TLC: R_f 0.20 (CH_2Cl_2/MeOH, 9:1) [I_2]

Preparation of Quaternary Ammonium Bromides V{*2,3,R*^{4}}

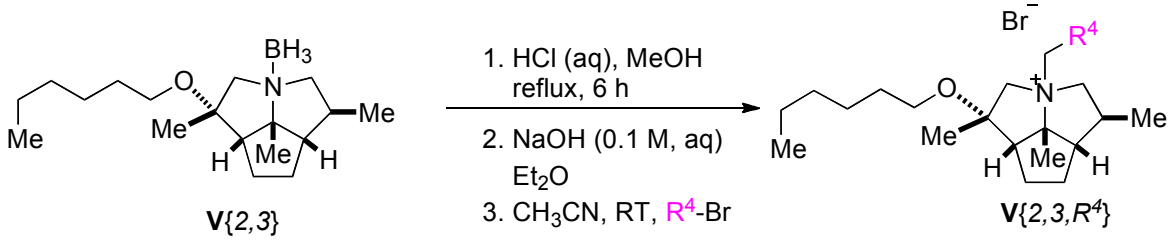

V{*2,3*} **V**{*2,3,R*^{4}}

Following General Procedure II, amino borane **V**{*2,3*} (397 mg, 1.35 mmol) was added to a xxx-mL round-bottomed flask as a solution in 45 mL of MeOH (0.03 M). The flask was fitted with a reflux condenser, a magnetic stir bar, and a nitrogen inlet adapter. Lastly, 1.0 N aq. HCl solution (6.8 mL, 5.0 equiv) was added via syringe. The resulting solution was heated and then concentrated by rotary evaporation (15 mm Hg, 20-25 ^{o}C) as described General Procedure II. The resulting free amine was dissolved in acetonitrile and was distributed among seven test tubes that were subsequently charged with benzyl bromide (tube 1, 38 mg, 0.220 mmol, 1.2 equiv), 1-bromomethylnaphthalene (tube 2, 48 mg, 0.220 mmol, 1.2 equiv), 2-bromomethylnaphthalene (tube 3, 48 mg, 0.220 mmol, 1.2 equiv), 3,5-bis(trifluoromethyl)benzyl bromide (tube 4, 67 mg, 0.220 mmol, 1.2 equiv), 3,5-bis(*t*-butyl)benzyl bromide (tube 5, 62 mg, 0.220 mmol, 1.2 equiv), 4-methoxybenzyl bromide (tube 6, 44 mg, 0.220 mmol, 1.2 equiv), 1-bromohexane (tube 7, 90 mg, 0.549 mmol, 3.0 equiv). After being agitated for 12 h, the reaction mixtures were worked up and the products isolated and purified as described in General Procedure II.

Preparation of *rel*-(1*S*,3*R*,5*S*,5a*S*,7a*S*,7b*R*) Octahydro-1-hexyloxy-1-methyl-3-benzyl-5-methyl-7b-methylcyclopenta[*gh*]pyrrolizinium Bromide (V{*2,3,1*})

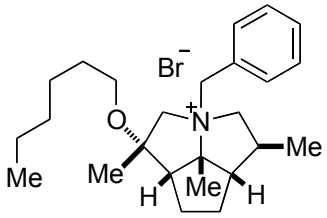

V{*2,3,1*}

Data for **V**{*2,3,1*}:

Yield: 76 mg (92%), free-flowing white powder

^{1}H-NMR: (500 MHz, $CDCl_3$)

7.80–7.76 (m, 2 H), 7.47–7.42 (m, 3 H), 5.17 (d, *J* = 12.2, 1 H), 4.80 (d, *J* = 12.2, 1 H), 4.49 (dd, *J* = 11.3, 11.3, 1 H), 4.40 (d, *J* = 13.2, 1 H), 3.26 (t, *J* = 6.6, 2 H), 3.18 (dd, *J* = 6.6, 11.6, 1 H), 3.13 (d, *J* = 13.2, 1 H), 2.58 (t, *J* = 8.1, 8.1, 1 H), 2.55–2.51 (m, 1 H), 2.40–2.30 (m, 1 H), 2.21–2.08 (m, 1 H), 2.11 (s, 3 H), 1.90–1.81 (m, 3 H), 1.68 (s, 3 H), 1.49–1.42 (m, 2 H), 1.32–1.19 (m, 6H), 0.86 (t, *J* = 6.9, 3 H)

MS: (ESI, Q-tof)

370.3 (100)

Mol. Formula: $C_{25}H_{40}BrNO$ (450.50)

HRMS: $C_{25}H_{40}NO^+$: (370.3110)

Calcd: 370.3110

Found: 370.3101

TLC: R_f 0.28 (CH_2Cl_2/MeOH, 9:1) [I_2]

Preparation of *rel*-(1*S*,3*R*,5*S*,5a*S*,7a*S*,7b*R*) Octahydro-1-hexyloxy-1-methyl-3-(1-naphthylmethyl)-5-methyl-7b-methylcyclopenta[*gh*]pyrrolizinium Bromide (V{*2,3,2*})

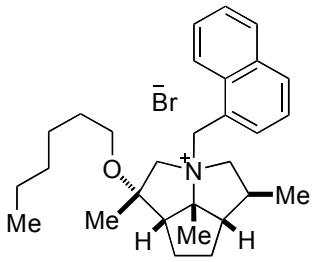

V{*2,3,2*}

Data for **V**{*2,3,2*}:

Yield: 90 mg (98%), free-flowing white powder

^{1}H-NMR: (500 MHz, $CDCl_3$)

8.37 (d, *J* = 8.6, 1 H), 8.34 (d, *J* = 6.4, 1 H), 7.93 (dd, *J* = 8.2, 14.1, 1 H), 7.67 (dd, *J* = 7.7, 7.7, 1 H), 7.55 (dd, *J* = 6.4, 14.3, 2 H), 5.51 (d, *J* = 12.9, 1 H), 5.40 (d, *J* = 12.9, 1 H), 4.58 (d, *J* = 13.2, 1 H), 4.45 (dd, *J* = 11.6, 11.6, 1 H), 3.30–3.21 (m, 1 H), 3.20–3.14 (m, 2 H), 3.02 (dd, *J* = 6.8, 11.7, 1 H), 2.70 (dd, *J* = 8.1, 8.1, 1 H), 2.64–2.58 (m, 1 H), 2.42–2.30 (m, 1 H), 2.27 (s, 3 H), 2.25–2.12 (m, 1 H), 1.93–1.79 (m, 3 H), 1.76 (s, 3 H), 1.44–1.34 (m, 2 H), 1.27–1.12 (m, 9H), 0.83 (t, *J* = 6.8, 3 H)

MS: (ESI, Q-tof)

420.3 (100)

Mol. Formula: $C_{29}H_{42}BrNO$ (500.55)

HRMS: $C_{29}H_{42}NO^+$: (420.3266)

Calcd: 420.3266

Found: 420.3265

TLC: R_f 0.30 (CH_2Cl_2/MeOH, 9:1) [I_2]

Preparation of *rel*-(1*S*,3*R*,5*S*,5a*S*,7a*S*,7b*R*) Octahydro-1-hexyloxy-1-methyl-3-(2-naphthylmethyl)-5-methyl-7b-methylcyclopenta[*gh*]pyrrolizinium Bromide (V{*2*,*3*,*3*})

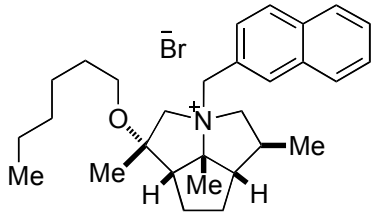

V{*2*,*3*,*3*}

Data for **V**{*2*,*3*,*3*}:

Yield: 82 mg (90%), free-flowing white powder

^{1}H-NMR: (500 MHz, $CDCl_3$)

8.26 (s, 1 H), 7.96 (d, *J* = 7.3, 1 H), 7.91–7.83 (m, 3 H), 7.59–7.52 (m, 2 H), 5.29 (d, *J* = 12.3, 1 H), 5.02 (d, *J* = 12.3, 1 H), 4.55 (dd, *J* = 11.5, 11.5, 1 H), 4.52 (d, *J* = 13.3, 1 H), 3.29–3.18 (m, 3 H), 3.15 (d, *J* = 13.2, 1 H), 2.66–2.60 (m, 1 H), 2.56–2.53 (m, 1 H), 2.42–2.33 (m, 1 H), 2.21–2.12 (m, 1 H), 2.17 (s, 3 H), 1.91–1.82 (m, 3 H), 1.72 (s, 3 H), 1.48–1.40 (m, 2 H), 1.30–1.17 (m, 9H), 0.84 (t, *J* = 6.9, 3 H)

MS: (ESI, Q-tof)

420.3 (100)

Mol. Formula: $C_{29}H_{42}BrNO$ (500.55)

HRMS: $C_{29}H_{42}NO^+$: (420.3266)

Calcd: 420.3266

Found: 420.3271

TLC: R_f 0.31 (CH_2Cl_2/MeOH, 9:1) [I_2]

Preparation of *rel*-(1*S*,3*R*,5*S*,5a*S*,7a*S*,7b*R*) Octahydro-1-hexyloxy-1-methyl-3-(3,5-trifluoromethylbenzyl)-5-methyl-7b-methylcyclopenta[*gh*]pyrrolizinium Bromide (V{*2,3,5*})

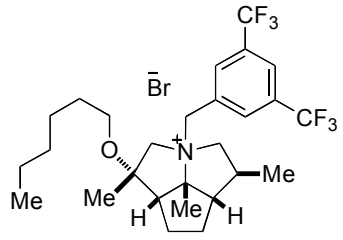

V{*2,3,5*}

Data for **V**{*2,3,5*}:

Yield: 101 mg (95%), free-flowing white powder

^{1}H-NMR: (500 MHz, $CDCl_3$)

8.26 (s, 1 H), 7.96 (d, *J* = 7.3, 1 H), 7.91–7.83 (m, 3 H), 7.59–7.52 (m, 2 H), 5.29 (d, *J* = 12.3, 1 H), 5.02 (d, *J* = 12.3, 1 H), 4.55 (dd, *J* = 11.5, 11.5, 1 H), 4.52 (d, *J* = 13.3, 1 H), 3.29–3.18 (m, 3 H), 3.15 (d, *J* = 13.2, 1 H), 2.66–2.60 (m, 1 H), 2.56–2.53 (m, 1 H), 2.42–2.33 (m, 1 H), 2.21–2.12 (m, 1 H), 2.17 (s, 3 H), 1.91–1.82 (m, 3 H), 1.72 (s, 3 H), 1.48–1.40 (m, 2 H), 1.30–1.17 (m, 9H), 0.84 (t, *J* = 6.9, 3 H)

MS: (ESI, Q-tof)

506.3 (100)

Mol. Formula: $C_{27}H_{38}BrF_6NO$ (586.49)

HRMS: $C_{27}H_{38}NOF_6^+$: (506.2858)

Calcd: 506.2858

Found: 506.2859

TLC: R_f 0.39 (CH_2Cl_2/MeOH, 9:1) [I_2]

Preparation of *rel*-(1*S*,3*S*,5*S*,5a*S*,7a*S*,7b*R*) Octahydro-1-hexyloxy-1-methyl-3-hexyl-5-methyl-7b-methylcyclopenta[*gh*]pyrrolizinium Bromide (V{*2,3,6*})

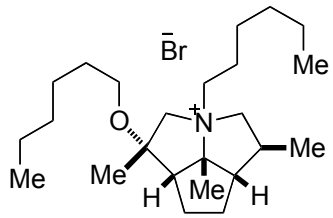

V{*2,3,6*}

Data for **V**{*2,3,6*}:

Yield: 36 mg (44%), free-flowing white powder

^{1}H-NMR: (500 MHz, $CDCl_3$)

4.31 (d, *J* = 13.1, 1 H), 3.80 (ddd, *J* = 5.7, 11.4, 11.4, 1 H), 3.73–3.61 (m, 4 H), 3.55 (ddd, *J* = 5.0, 11.7, 11.7, 1 H), 3.36 (t, *J* = 6.7, 2 H), 2.65–2.50 (m, 2 H), 2.33–2.15 (m, 2 H), 1.96–1.74 (m, 5 H), 1.88 (s, 3 H), 1.62–1.41 (m, 5 H), 1.52 (s, 3 H), 1.38–1.24 (m, 7H), 1.13 (d, *J* = 6.7, 3 H), 0.91–0.87 (m, 6H)

MS: (ESI, Q-tof)

364.4 (100)

Mol. Formula: $C_{24}H_{46}BrNO$ (444.53)

HRMS: $C_{24}H_{46}NO^+$: (364.3579)

Calcd: 364.3579

Found: 364.357

TLC: R_f 0.42 (CH_2Cl_2/MeOH, 9:1) [I_2]

Preparation of *rel*-(1*S*,3*R*,5*S*,5a*S*,7a*S*,7b*R*) Octahydro-1-hexyloxy-1-methyl-3-(3,5-*tert*-butylbenzyl)-5-methyl-7b-methyl-cyclopenta[*gh*]pyrrolizinium Bromide (V{*2,3,7*})

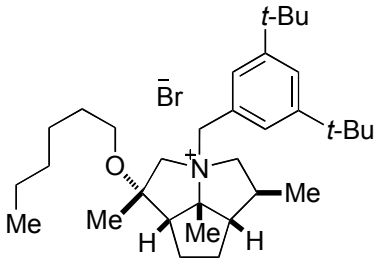

V{*2,3,7*}

Data for **V**{*2,3,7*}:

Yield: 101 mg (99%), free-flowing white powder

^{1}H-NMR: (500 MHz, $CDCl_3$)

7.55 (d, *J* = 1.7, 2 H), 7.49 (s, 1 H), 5.21 (d, *J* = 12.3, 1 H), 4.68 (d, *J* = 12.3, 1 H), 4.59 (dd, *J* = 11.3, 11.3, 1 H), 4.33 (d, *J* = 13.1, 1 H), 3.27 (t, *J* = 6.7, 2 H), 3.22 (dd, *J* = 6.5, 11.6, 1 H), 3.10 (d, *J* = 13.2, 1 H), 2.60–2.55 (m, 1 H), 2.53 (dd, *J* = 8.6, 1 H), 2.31–2.22 (m, 1 H), 2.17–2.08 (m, 1 H), 2.12 (s, 3 H), 1.90–1.80 (m, 3 H), 1.70 (s, 3 H), 1.52–1.44 (m, 2 H), 1.35 (s, 18H), 1.31–1.20 (m, 6H), 1.26 (d, *J* = 6.5, 3 H), 0.86 (t, *J* = 6.9, 3 H)

MS: (ESI, Q-tof)

482.4 (100)

Mol. Formula: $C_{33}H_{65}BrNO$ (562.71)

HRMS: $C_{33}H_{56}NO^+$: (482.4362)

Calcd: 482.4362

Found: 482.4358

TLC: R_f 0.41 (CH_2Cl_2/MeOH, 9:1) [I_2]

Preparation of *rel*-(1*S*,3*R*,5*S*,5a*S*,7a*S*,7b*R*) Octahydro-1-hexyloxy-1-methyl-3-(4-methoxybenzyl)-5-methyl-7b-methyl-cyclopenta[*gh*]pyrrolizinium Bromide (V{*2*,*3*,*8*})

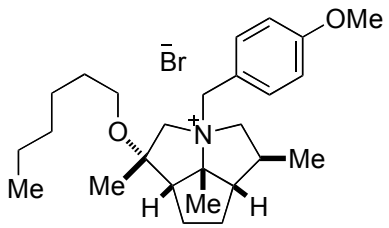

V{*2,3,8*}

Data for **V**{*2*,*3*,*8*}:

Yield: 85 mg (98%), free-flowing white powder

^{1}H-NMR: (500 MHz, $CDCl_3$)

7.70 (d, *J* = 8.7, 2 H), 6.94 (d, *J* = 8.7, 2 H), 5.09 (d, *J* = 12.4, 1 H), 4.73 (d, *J* = 12.4, 1 H), 4.44 (dd, *J* = 11.4, 11.4, 1 H), 4.36 (d, *J* = 13.2, 1 H), 3.82 (s, 3 H), 3.26 (t, *J* = 6.6, 2 H), 3.16 (dd, *J* = 6.6, 11.7, 1 H), 3.11 (d, *J* = 13.2, 1 H), 2.56 (dd, *J* = 8.1, 8.1, 1 H), 2.54–2.49 (m, 1 H), 2.38–2.29 (m, 1 H), 2.19–2.09 (m, 1 H), 2.08 (s, 3 H), 1.88–1.81 (m, 3 H), 1.66 (s, 3 H), 1.51–1.40 (m, 2 H), 1.33–1.19 (m, 9H), 0.86 (t, *J* = 6.9, 3 H)

MS: (ESI, Q-tof)

400.3 (100)

Mol. Formula: $C_{26}H_{42}BrNO_2$ (480.52)

HRMS: $C_{26}H_{42}NO_2^+$: (400.3216)

Calcd: 400.3216

Found: 400.3212

TLC: R_f 0.23 (CH_2Cl_2/MeOH, 9:1) [I_2]

Preparation of Quaternary Ammonium Bromides V{*2,7,R*^{4}}

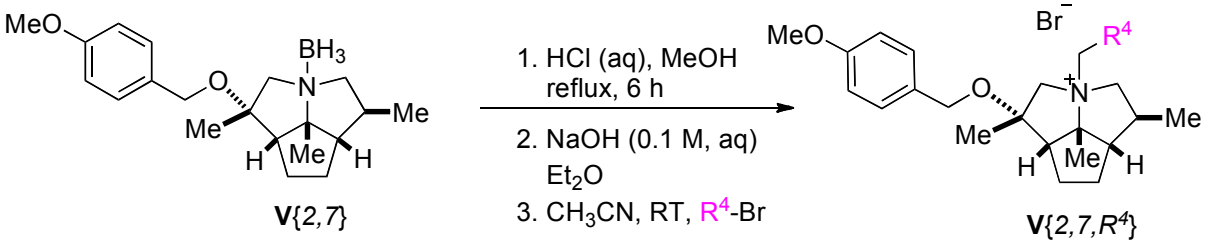

V{*2,7*} **V**{*2,7,R*^{4}}

Following General Procedure II, amino borane **V**{*2*,7} (163 mg, 0.495 mmol) was added to a 50-mL round-bottomed flask as a solution in 17 mL of MeOH (0.03 M). The flask was fitted with a reflux condenser, a magnetic stir bar, and a nitrogen inlet adapter. Lastly, 1.0 N aq. HCl solution (2.5 mL, 5.0 equiv) was added via syringe. The resulting solution was heated and then concentrated by rotary evaporation (15 mm Hg, 20-25 ^{o}C) as described General Procedure II. The resulting free amine was dissolved in acetonitrile and was distributed among five test tubes that were subsequently charged with benzyl bromide (tube 1, 14 mg, 0.08 mmol, 1.2 equiv), 1-bromomethylnaphthalene (tube 2, 17 mg, 0.08 mmol, 1.2 equiv), 2-bromomethylnaphthalene (tube 3, 17 mg, 0.08 mmol, 1.2 equiv), 3,5-bis(trifluoromethyl)benzyl bromide (tube 4, 25 mg, 0.08 mmol, 1.2 equiv), 3,5-bis(*t*-butyl)benzyl bromide (tube 5, 23 mg, 0.08 mmol, 1.2 equiv). After being agitated for 12 h, the reaction mixtures were worked up and the products isolated and purified as described in General Procedure II.

Preparation of *rel*-(1*S*,3*R*,5*S*,5a*S*,7a*S*,7b*R*) Octahydro-1-(4-methoxy-benzyloxy)-1-methyl-3-benzyl-5-methyl-7b-methylcyclopenta[*gh*]pyrrolizinium Bromide (V{*2,7,1*})

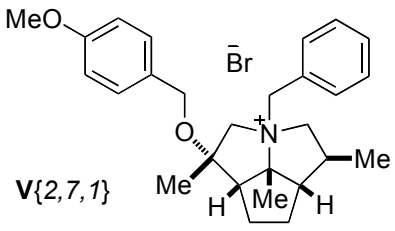

V{*2,7,1*}

Data for **V**{*2,7,1*}:

Yield: 25 mg (76%) free-flowing white powder

^{1}H-NMR: (500 MHz, $CDCl_3$)

7.79-7.76 (m, 2 H), 7.47-.7.44 (m, 3 H), 7.14 (d, *J* = 8.6, 2 H), 6.84 (d, *J* = 8.6, 2 H), 5.19 (d, *J* = 12.3, 1 H), 4.79 (d, *J* = 12.2, 1 H), 4.49 (dd, *J* = 11.5, 11.5,1 H), 4.34 (d, *J* = 10.6, 1 H), 4.31 (d, *J* = 10.6, 1 H), 3.78 (s, 3 H), 3.18 (d, *J* = 13.4, 1 H), 3.15 (dd, *J* = 7.5, 12.4, 1 H), 2.66 (dd, *J* = 8.5, 8.5, 1 H), 2.56-2.52 (m, 1 H), 2.32-2.18 (m, 2 H), 2.14 (s, 3 H), 1.98-1.91 (m, 1 H), 1.88-1.84 (m, 2 H), 1.82 (s, 3 H), 1.19 (d, *J* = 6.5, 3 H)

MS: (ESI, Q-tof)

406.3 (100)

Mol. Formula: $C_{27}H_{36}BrNO_2$ (486.48)

HRMS: $C_{27}H_{36}NO_2^+$: (406.2746)

Calcd: 406.2746

Found: 406.2749

TLC: R_f 0.21 (CH_2Cl_2/MeOH, 9:1) [I_2]

Preparation of *rel*-(1*S*,3*R*,5*S*,5a*S*,7a*S*,7b*R*) Octahydro-1-(4-methoxy-benzyloxy)-1-methyl-3-(1-naphthylmethyl)-5-methyl-7b-methylcyclopenta[*gh*]pyrrolizinium Bromide (V{*2,7,2*})

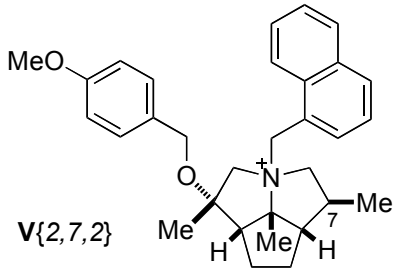

V{*2,7,2*}

Data for **V**{*2,7,2*}:

Yield: 30 mg (85%), free-flowing white powder

^{1}H-NMR: (500 MHz, $CDCl_3$)

8.39 (d, *J* = 8.6, 1 H), 8.32 (d, *J* = 6.5, 1 H), 7.97–7.86 (m, 2 H), 7.67 (dd, *J* = 7.1, 7.1, 2 H), 7.57–7.51 (m, 2 H), 7.08 (d, *J* = 8.7, 2 H), 6.77 (d, *J* = 8.8, 2 H), 5.54 (d, *J* = 12.9, 1 H), 5.39 (d, *J* = 12.9, 1 H), 4.56 (d, *J* = 13.3, 1 H), 4.46 (dd, *J* = 11.7, 11.7, 1 H), 4.31 (d, *J* = 10.6, 1 H), 4.23 (d, *J* = 10.6, 1 H), 3.75 (s, 3 H), 3.20 (d, *J* = 13.3, 1 H), 2.97 (dd, *J* = 6.8, 11.7, 1 H), 2.76 (dd, *J* = 8.5, 8.5, 1 H), 2.65–2.60 (m, 1 H), 2.32–2.19 (m, 2 H), 2.30 (s, 3 H), 1.98–1.84 (m, 3 H), 1.91 (s, 3 H), 1.11 (d, *J* = 6.5, 3 H)

MS: (ESI, Q-tof)

456.3

Mol. Formula: $C_{31}H_{38}BrNO_2$ (536.54)

HRMS: $C_{31}H_{38}NO_2^+$: (456.2903)

Calcd: 456.2903

Found: 456.2906

TLC: R_f 0.25 (CH_2Cl_2/MeOH, 9:1) [I_2]

Preparation of *rel*-(1*S*,3*R*,5*S*,5a*S*,7a*S*,7b*R*) Octahydro-1-(4-methoxy-benzyloxy)-1-methyl-3-(2-naphthylmethyl)-5-methyl-7b-methylcyclopenta[*gh*]pyrrolizinium Bromide (V{*2,7,3*})

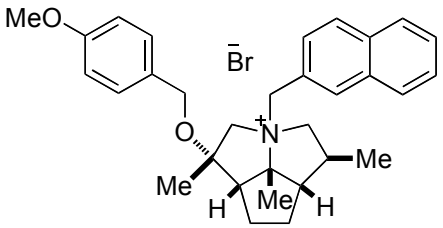

V{*2,7,3*}

Data for **V**{*2,7,3*}:

Yield: 30 mg (85%), free-flowing white powder

^{1}H-NMR: (500 MHz, $CDCl_3$)

8.26 (s, 1 H), 7.96 (d, *J* = 8.4, 1 H), 7.91–7.80 (m, 3 H), 7.60–7.51 (m, 2 H), 7.12 (d, *J* = 8.6, 2 H), 6.80 (d, *J* = 8.6, 2 H), 5.32 (d, *J* = 12.3, 1 H), 5.03 (d, *J* = 12.3, 1 H), 4.60–4.50 (m, 2 H), 4.33 (d, *J* = 10.6, 1 H), 4.29 (d, *J* = 10.6, 1 H), 3.74 (s, 3 H), 3.21–3.13 (m, 2 H), 2.71 (dd, *J* = 8.4, 8.4, 1 H), 2.58–2.53 (m, 1 H), 2.36–2.15 (m, 2 H), 2.19 (s, 3 H), 1.98–1.90 (m, 1 H), 1.90–1.83 (m, 2 H), 1.86 (s, 3 H), 1.20 (d, *J* = 6.5, 3 H)

MS: (ESI, Q-tof)

456.3 (100)

Mol. Formula: $C_{31}H_{38}BrNO_2$ (536.54)

HRMS: ($C_{20}H_{38}NO_3^+$: (456.2903)

Calcd: 456.2903

Found: 456.2900

TLC: R_f 0.24 (CH_2Cl_2/MeOH, 9:1) [I_2]

Preparation of *rel*-(1*S*,3*R*,5*S*,5a*S*,7a*S*,7b*R*) Octahydro-1-(4-methoxybenzyloxy)-1-methyl-3-(3,5-trifluoromethylbenzyl)-5-methyl-7b-methylcyclopenta[*gh*]pyrrolizinium Bromide (V{*2*,*7*,*5*})

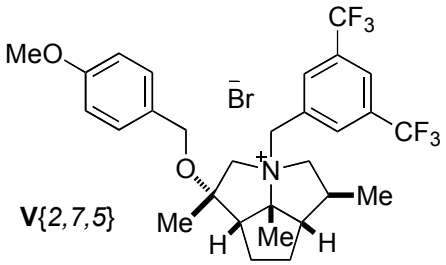

V{*2*,*7*,*5*}

Data for **V**{*2*,*7*,*5*}:

Yield: 33 mg (80%), free-flowing white powder

^{1}H-NMR: (500 MHz, $CDCl_3$)

8.40 (s, 2 H), 7.97 (s, 1 H), 7.13 (d, *J* = 8.6, 2 H), 6.82 (d, *J* = 8.6, 2 H), 5.37 (d, *J* = 12.5, 1 H), 5.37 (d, *J* = 12.5, 1 H), 4.37 (d, *J* = 10.9, 1 H), 4.37 (dd, *J* = 7.2, 10.9, 1 H), 4.31 (d, *J* = 10.7, 1 H), 3.77 (s, 3 H), 3.21 (d, *J* = 13.1, 1 H), 3.09 (dd, *J* = 6.2, 11.3, 1 H), 2.74 (dd, *J* = 8.0, 8.0, 1 H), 2.53–2.38 (m, 2 H), 2.30–2.21 (m, 1 H), 2.15 (s, 3 H), 1.98–1.85 (m, 3 H), 1.81 (s, 3 H), 1.15 (d, *J* = 6.2, 3 H)

MS: (ESI, Q-tof)

542.3 (100)

Mol. Formula: $C_{29}H_{34}BrF_6NO_2$ (622.48)

HRMS: $C_{29}H_{34}F_6NO_2^+$: (542.2494)

Calcd: 542.2494

Found: 542.2488

TLC: R_f 0.28 (CH_2Cl_2/MeOH, 9:1) [I_2]

Preparation of *rel*-(1*S*,3*R*,5*S*,5a*S*,7a*S*,7b*R*) Octahydro-1-(4-methoxybenzyloxy)-1-methyl-3-(3,5-*tert*-butylbenzyl)-5-methyl-7b-methylcyclopenta[*gh*]pyrrolizinium Bromide (V{*2*,*7*,*7*})

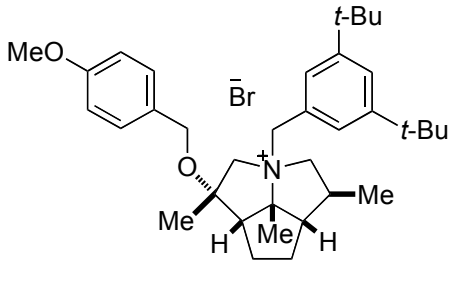

V{*2,7,7*}

Data for **V**{*2*,*7*,*7*}:

Yield: 33 mg (82%), free-flowing white powder

^{1}H-NMR: (500 MHz, $CDCl_3$)

7.57 (d, *J* = 1.7, 2 H), 7.50 (dd, *J* = 1.7, 1.7, 1 H), 7.16 (d, *J* = 8.7, 2 H), 6.85 (d, *J* = 8.8, 2 H), 5.22 (d, *J* = 12.3, 1 H), 4.71 (d, *J* = 12.3, 1 H), 4.59 (dd, *J* = 11.3, 1 H), 4.43 (d, *J* = 13.2, 1 H), 4.33 (s, 2 H), 3.79 (s, 3 H), 3.25–3.08 (m, 2 H), 2.63 (dd, *J* = 8.7, 8.7, 1 H), 2.61-2.56 (m, 1 H), 2.30–2.12 (m, 2 H), 2.16 (s, 3 H), 2.00–1.92 (m, 1 H), 1.90–1.84 (m, 2 H), 1.83 (s, 3 H), 1.35 (s, 18H), 1.23 (d, *J* = 6.6, 3 H)

MS: (ESI, Q-tof)

518.4 (100)

Mol. Formula: $C_{35}H_{52}BrNO$ (598.70)

HRMS: $C_{35}H_{52}NO_2^+$: (518.3998)

Calcd: 518.3998

Found: 518.3997

TLC: R_f 0.31 (CH_2Cl_2/MeOH, 9:1) [I_2]

Preparation of Quaternary Ammonium Bromides V{*3,2,R*^{4}}

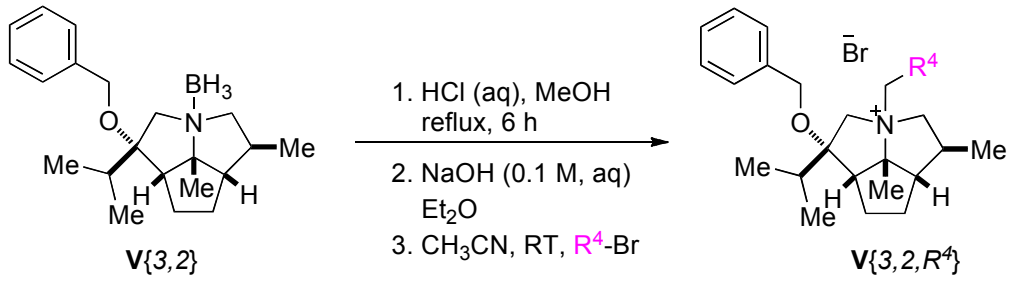

V{*3,2*} **V**{*3,2,R*^{4}}

Following General Procedure II, amino borane **V**{*3,2*} (456 mg, 1.39 mmol) was added to a 100-mL round-bottomed flask as a solution in 50 mL of MeOH (0.03 M). The flask was fitted with a reflux condenser, a magnetic stir bar, and a nitrogen inlet adapter. Lastly, 1.0 N aq. HCl solution (7.0 mL, 5.0 equiv) was added via syringe. The resulting solution was heated and then concentrated by rotary evaporation (15 mm Hg, 20-25 ^{o}C) as described General Procedure II. The resulting free amine was dissolved in acetonitrile and was distributed among seven test tubes that were subsequently charged with benzyl bromide (tube 1, 40 mg, 0.230 mmol, 1.2 equiv), 1-bromomethylnaphthalene (tube 2, 51 mg, 0.230 mmol, 1.2 equiv), 2-bromomethylnaphthalene (tube 3, 51 mg, 0.230 mmol, 1.2 equiv), 3,5-bis(trifluoromethyl)benzyl bromide (tube 4, 71 mg, 0.230 mmol, 1.2 equiv), 3,5-bis(*t*-butyl)benzyl bromide (tube 5, 65 mg, 0.230 mmol, 1.2 equiv), 4-methoxybenzyl bromide (tube 6, 66 mg, 0.230 mmol, 1.2 equiv), 1-bromohexane (tube 7, 95 mg, 0.573 mmol, 3.0 equiv). After being agitated for 12 h, the reaction mixtures were worked up and the products isolated and purified as described in General Procedure II.

Preparation of *rel*-(1*S*,3*R*,5*S*,5a*S*,7a*S*,7b*R*) Octahydro-1-benzyloxy-1-isopropyl-3-benzyl-5-methyl-7b-methylcyclopenta[*gh*]pyrrolizinium Bromide (V{*3,2,1*})

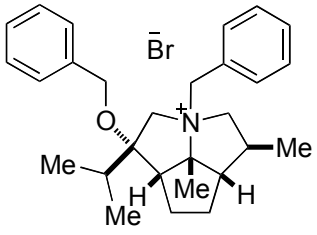

V{*3,2,1*}

Data for **V**{*3,2,1*}:

Yield: 91 mg (98%), free-flowing white powder

^{1}H-NMR: (500 MHz, $CDCl_3$)

7.90–7.85 (m, 2 H), 7.45 (d, *J* = 5.3, 3 H), 7.32–7.25 (m, 3 H), 7.20–7.16 (m, 2 H), 5.35 (d, *J* = 12.1, 1 H), 4.83 (d, *J* = 12.0, 1 H), 4.77 (d, *J* = 13.7, 1 H), 4.53 (d, *J* = 11.0, 1 H), 4.18 (d, *J* = 11.0, 1 H), 3.83 (dd, *J* = 9.6, 12.2, 1 H), 3.70 (d, *J* = 13.7, 1 H), 3.19 (dd, *J* = 9.9, 9.9, 1 H), 2.77 (dd, *J* = 8.0, 8.0, 1 H), 2.53–2.33 (m, 4 H), 2.00 (s, 3 H), 1.96–1.86 (m, 2 H), 1.81–1.74 (m, 1 H), 1.23 (d, *J* = 6.8, 3 H), 1.01 (d, *J* = 6.5, 6 H)

MS: (ESI, Q-tof)

404.3 (100)

Mol. Formula: $C_{28}H_{38}BrNO$ (484.51)

HRMS: $C_{28}H_{38}NO^+$: (404.2953)

Calcd: 404.2953

Found: 404.2955

TLC: R_f 0.23 (CH_2Cl_2/MeOH, 9:1) [I_2]

Preparation of *rel*-(1*S*,3*R*,5*S*,5a*S*,7a*S*,7b*R*) Octahydro-1-benzyloxy-1-isopropyl-3-(1-naphthylmethyl)-5-methyl-7b-methylcyclopenta[*gh*]pyrrolizinium Bromide (V**{*3*,*2*,*2*})**

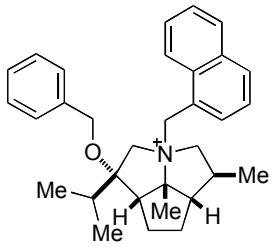

V{*3,2,2*}

Data for **V**{*3*,*2*,*2*}:

Yield: 95 mg (93%), free-flowing white powder

^{1}H-NMR: (500 MHz, $CDCl_3$)

8.37–8.30 (m, 2 H), 7.83 (d, *J* = 7.9, 1 H), 7.79 (d, *J* = 7.7, 1 H), 7.60 (t, *J* = 7.6, 1 H), 7.49 (t, *J* = 7.4, 1 H), 7.45–7.36 (m, 1 H), 7.24–7.18 (m, 3 H), 7.11–7.06 (m, 2 H), 5.73 (d, *J* = 12.8, 1 H), 5.61 (d, *J* = 12.7, 1 H), 4.90 (d, *J* = 13.6, 1 H), 4.45 (d, *J* = 10.9, 1 H), 4.01 (d, *J* = 10.9, 1 H), 3.90 (dd, *J* = 11.4, 11.4, 1 H), 3.66 (d, *J* = 13.6, 1 H), 2.89 (dd, *J* = 8.5, 11.9, 1 H), 2.81 (dd, *J* = 6.6, 9.7, 1 H), 2.60–2.55 (m, 1 H), 2.54–2.43 (m, 2 H), 2.35–2.26 (m, 1 H), 2.19 (s, 3 H), 2.02–1.85 (m, 2 H), 1.80–1.70 (m, 1 H), 1.24 (d, *J* = 6.8, 3 H), 0.94 (d, *J* = 6.8, 3 H), 0.88 (d, *J* = 6.5, 3 H)

MS: (ESI, Q-tof)

454.3 (100)

Mol. Formula: $C_{32}H_{40}BrNO$ (534.57)

HRMS: $C_{32}H_{40}NO^+$: (454.3110)

Calcd: 454.3110

Found: 454.3105

TLC: R_f 0.25 (CH_2Cl_2/MeOH, 9:1) [I_2]

Preparation of *rel*-(1*S*,3*R*,5*S*,5a*S*,7a*S*,7b*R*) Octahydro-1-benzyloxy-1-isopropyl-3-(2-naphthylmethyl)-5-methyl-7b-methylcyclopenta[*gh*]pyrrolizinium Bromide (V{*3*,*2*,*3*})

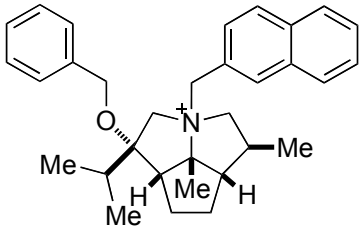

V{*3,2,3*}

Data for **V**{*3*,*2*,*3*}:

Yield: 94 mg (92%), free-flowing white powder

^{1}H-NMR: (500 MHz, $CDCl_3$)

8.35 (s, 1 H), 7.97–7.92 (m, 1 H), 7.90 (dd, *J* = 1.7, 8.5, 1 H), 7.81–7.77 (m, 2 H), 7.55–7.48 (m, 2 H), 7.24–7.19 (m, 3 H), 7.14–7.10 (m, 2 H), 5.49 (d, *J* = 12.1, 1 H), 5.07 (d, *J* = 12.1, 1 H), 4.82 (d, *J* = 13.7, 1 H), 4.48 (d, *J* = 11.0, 1 H), 4.10 (d, *J* = 10.9, 1 H), 3.91 (dd, *J* = 9.7, 12.1, 1 H), 3.71 (d, *J* = 13.6, 1 H), 3.18 (dd, *J* = 7.1, 12.3, 1 H), 2.78 (dd, *J* = 6.9, 9.5, 1 H), 2.54–2.33 (m, 4 H), 2.05 (s, 3 H), 1.97–1.87 (m, 2 H), 1.81–1.72 (d, *J* = 4.0, 1 H), 1.26 (d, *J* = 6.8, 3 H), 1.04 (d, *J* = 6.2, 3 H), 1.00 (d, *J* = 6.8, 3 H)

MS: (ESI, Q-tof)

454.3 (100)

Mol. Formula: $C_{32}H_{40}BrNO$ (534.57)

HRMS: $C_{32}H_{40}NO^+$: (454.3110)

Calcd: 454.3110

Found: 454.3104

TLC: R_f 0.27 (CH_2Cl_2/MeOH, 9:1) [I_2]

Preparation of *rel*-(1*S*,3*R*,5*S*,5a*S*,7a*S*,7b*R*) Octahydro-1-benzyloxy-1-isopropyl-3-(3,5-trifluoromethyl-benzyl)-5-methyl-7b-methylcyclopenta[*gh*]pyrrolizinium Bromide (V**{*3*,*2*,*5*})**

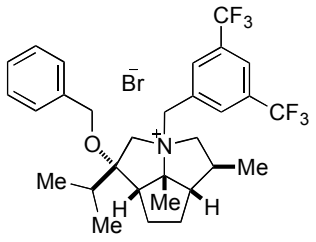

V{*3,2,5*}

Data for **V**{*3*,*2*,*5*}:

Yield: 110 mg (93%), free-flowing white powder

^{1}H-NMR: (500 MHz, $CDCl_3$)

8.48 (s, 2 H), 7.96 (s, 1 H), 7.31–7.23 (m, 2 H), 7.20–7.12 (m, 2 H), 5.84 (d, *J* = 12.3, 1 H), 5.25–5.18 (m, 1 H), 4.88 (d, *J* = 13.3, 1 H), 4.56 (d, *J* = 11.2, 1 H), 4.18 (d, *J* = 11.2, 1 H), 3.61 (t, *J* = 11.9, 2 H), 3.57 (dd, *J* = 11.9, 11.9, 1 H), 3.15–3.09 (m, 1 H), 2.77 (dd, *J* = 8.3, 8.3, 1 H), 2.60–2.49 (m, 1 H), 2.49–2.32 (m, 3 H), 2.03 (s, 3 H), 1.96–1.89 (m, 2 H), 1.82–1,74 (m, 1 H), 1.25 (d, *J* = 6.7, 3 H), 1.04 (d, *J* = 6.6, 3 H), 0.99 (d, *J* = 6.8, 3 H)

MS: (ESI, Q-tof)

540.3 (100)

Mol. Formula: $C_{30}H_{36}BrF_6NO$ (620.51)

HRMS: $C_{30}H_{36}F_6NO^+$: (540.2701)

Calcd: 540.2701

Found: 540.2692

TLC: R_f 0.31 (CH_2Cl_2/MeOH, 9:1) [I_2]

Preparation of *rel*-(1*S*,3*S*,5*S*,5a*S*,7a*S*,7b*R*) Octahydro-1-benzyloxy-1-isopropyl-3-hexyl-5-methyl-7b-methylcyclopenta[*gh*]pyrrolizinium Bromide (V{*3,2,6*})

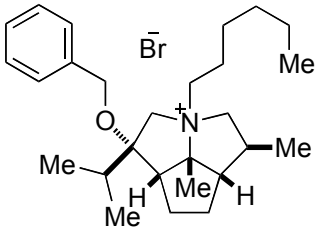

V{*3,2,8*}

Data for **V**{*3,2,6*}:

Yield: 66 mg (73%), free-flowing white powder

^{1}H-NMR: (500 MHz, $CDCl_3$)

7.44 (d, *J* = 7.1, 2 H), 7.36 (t, *J* = 7.3, 2 H), 7.31 (t, *J* = 7.3, 1 H), 4.64 (dt, *J* = 10.8, 20.1, 2 H), 4.16 (d, *J* = 14.0, 1 H), 3.97 (ddd, *J* = 5.0, 12.0, 12.0, 1 H), 3.88 (dd, *J* = 8.4, 12.3, 1 H), 3.25-3.16 (m, 2 H), 2.60 (dd, *J* = 6.7, 9.6, 1 H), 2.57–2.56 (m, 2 H), 2.39–2.31 (m, 1 H), 2.13–2.00 (m, 2 H), 1.94–1.84 (m, 2 H), 1.77–1.66 (m, 2 H), 1.66 (s, 3 H), 1.57–1.51 (m, 1 H), 1.43–1.30 (m, 5 H), 1.11 (d, *J* = 6.7, 3 H), 0.96 (d, *J* = 6.8, 3 H), 0.89 (t, *J* = 6.9, 3 H), 0.83 (d, *J* = 6.6, 3 H)

MS: (ESI, Q-tof)

398.3 (100)

Mol. Formula: $C_{27}H_{44}BrNO$ (478.55)

HRMS: $C_{27}H_{44}NO^+$: (398.3423)

Calcd: 398.3423

Found: 398.3417

TLC: R_f 0.39 (CH_2Cl_2/MeOH, 9:1) [I_2]

Preparation of *rel*-(1*S*,3*R*,5*S*,5a*S*,7a*S*,7b*R*) Octahydro-1-benzyloxy-1-isopropyl-3-(3,5-*tert*-butylbenzyl)-5-methyl-7b-methylcyclopenta[*gh*]pyrrolizinium Bromide (V{*3,2,7*})

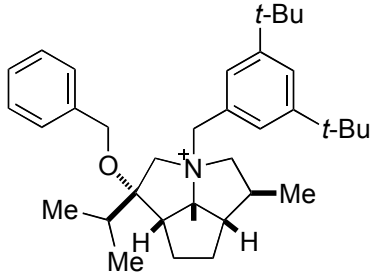

Data for **V**{*3*,*2*,*7*}:

Yield: 115 mg (99%), free-flowing white powder

^{1}H-NMR: (500 MHz, $CDCl_3$)

7.67 (d, *J* = 1.7, 2 H), 7.51 (s, 1 H), 7.32–7.24 (m, 3 H), 7.21–7.17 (m, 2 H), 5.41 (d, *J* = 12.2, 1 H), 4.92 (d, *J* = 13.7, 1 H), 4.59 (d, *J* = 12.2, 1 H), 4.54 (d, *J* = 11.1, 1 H), 4.24 (d, *J* = 11.1, 1 H), 3.78 (dd, *J* = 8.2, 12.4, 1 H), 3.68 (d, *J* = 13.7, 1 H), 3.37 (dd, *J* = 8.1, 12.6, 1 H), 2.79 (dd, *J* = 8.2, 8.2, 1 H), 2.47–2.31 (m, 4 H), 2.04 (s, 3 H), 2.00–1.88 (m, 2 H), 1.87–1.79 (m, 1 H), 1.37 (s, 18H), 1.22 (d, *J* = 6.8, 3 H), 1.07 (t, *J* = 6.7, 6 H)

MS: (ESI, Q-tof)

516.4 (100)

Mol. Formula: $C_{36}H_{54}BrNO$ (596.72)

HRMS: $C_{36}H_{54}NO^+$: (516.4205)

Calcd: 516.4205

Found: 516.4190

TLC: R_f 0.35 (CH_2Cl_2/MeOH, 9:1) [I_2]

Preparation of *rel*-(1*S*,3*R*,5*S*,5a*S*,7a*S*,7b*R*) Octahydro-1-benzyloxy-1-isopropyl-3-(4-methoxy-benzyl)-5-methyl-7b-methylcyclopenta[*gh*]pyrrolizinium Bromide (V{*3,2,8*})

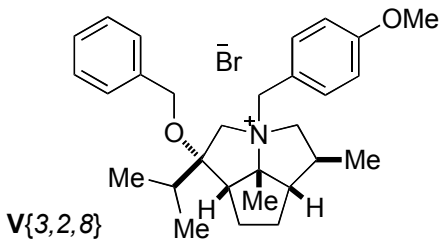

V{*3,2,8*}

Data for **V**{*3,2,8*}:

Yield: 93 mg (94%), free-flowing white powder

^{1}H-NMR: (500 MHz, $CDCl_3$)

7.80 (d, *J* = 8.7, 2 H), 7.34–7.25 (m, 3 H), 7.21–7.17 (m, 2 H), 6.96 (d, *J* = 8.6, 2 H), 5.27 (d, *J* = 12.3, 1 H), 4.72 (d, *J* = 13.6, 2 H), 4.53 (d, *J* = 10.9, 1 H), 4.19 (d, *J* = 10.9, 1 H), 3.84 (s, 3 H), 3.80 (dd, *J* = 9.5, 12.3, 1 H), 3.69 (d, *J* = 13.7, 1 H), 3.22 (dd, *J* =7.9, 12.1, 1 H), 2.76 (dd, *J* = 7.0, 9.2, 1 H), 2.53–2.41 (m, 2 H), 2.41–2.34 (m, 2 H), 1.98 (s, 3 H), 1.95–1.87 (m, 2 H), 1.82–1.73 (m, 1 H), 1.23 (d, *J* = 6.8, 3 H), 1.02 (d, *J* = 6.9, 3 H), 1.01 (d, *J* = 6.7, 3 H)

MS: (ESI, Q-tof)

434.3 (100)

Mol. Formula: $C_{29}H_{40}BrNO_2$ (514.54)

HRMS: $C_{29}H_{40}NO_2^+$: (434.3059)

Calcd: 434.3059

Found: 434.3055

TLC: R_f 0.20 (CH_2Cl_2/MeOH, 9:1) [I_2]

Preparation of Quaternary Ammonium Bromides V{*3,3,R*^{4}}

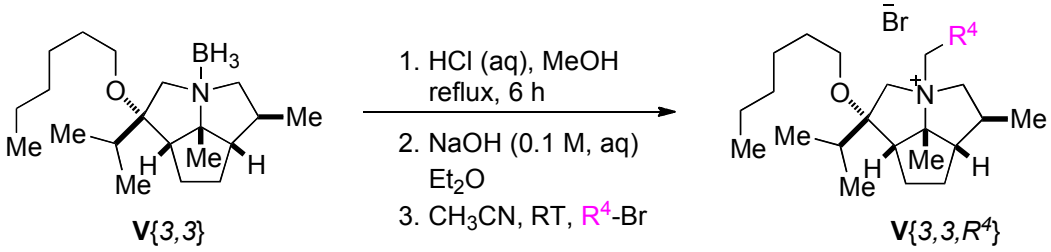

V{*3,3*} **V**{*3,3,R*^{4}}

Following General Procedure II, amino borane **V**{*3,3*} (245 mg, 0.762 mmol) was added to a 100-mL round-bottomed flask as a solution in 23 mL of MeOH (0.03 M). The flask was fitted with a reflux condenser, a magnetic stir bar, and a nitrogen inlet adapter. Lastly, 1.0 N aq. HCl solution (3.5 mL, 5.0 equiv) was added via syringe. The resulting solution was heated and then concentrated by rotary evaporation (15 mm Hg, 20-25 ^{o}C) as described General Procedure II. The resulting free amine was dissolved in acetonitrile and was distributed among seven test tubes that were subsequently charged with benzyl bromide (tube 1, 20 mg, 0.115 mmol, 1.2 equiv), 1-bromomethylnaphthalene (tube 2, 25 mg, 0.115 mmol, 1.2 equiv), 2-bromomethylnaphthalene (tube 3, 25 mg, 0.115 mmol, 1.2 equiv), 3,5-bis(trifluoromethyl)benzyl bromide (tube 4, 35 mg, 0.115 mmol, 1.2 equiv), 3,5-bis(*t*-butyl)benzyl bromide (tube 5, 32 mg, 0.115 mmol, 1.2 equiv), 4-methoxybenzyl bromide (tube 6, 23 mg, 0.115 mmol, 1.2 equiv), 1-bromohexane (tube 7, 48 mg, 0.288 mmol, 3.0 equiv). After being agitated for 12 h, the reaction mixtures were worked up and the products isolated and purified as described in General Procedure II.

Preparation of *rel*-(1*S*,3*R*,5*S*,5a*S*,7a*S*,7b*R*) Octahydro-1-hexyloxy-1-isopropyl-3-benzyl-5-methyl-7b-methylcyclopenta[*gh*]pyrrolizinium Bromide (V{*3,3,1*})

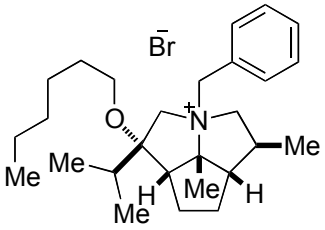

V{*3,3,1*}

Data for **V**{*3,3,1*}:

Yield: 46 mg (99%), free-flowing white powder

^{1}H-NMR: (500 MHz, $CDCl_3$)

7.90–7.82 (m, 2 H), 7.47–7.41 (m, 3 H), 5.17 (d, *J* = 12.1, 1 H), 5.00–4.94 (m, 1 H), 4.54 (d, *J* = 13.6, 1 H), 4.00 (dd, *J* = 11.1, 11.1, 1 h), m, 2 H), 2.56–2.46 (m, 1 H), 2.44–2.34 (m, 1 H), 2.24–2.16 (m, 1 H), 2.00–1.91 (m, 2 H), 1.96 (s, 3 H), 1.77–1.67 (m, 1 H), 1.64–1.56 (m, 3 H), 1.48–1.40 (m, 2 H), 1.34–1.17 (m, 3 H), 1.20 (d, *J* = 6.6, 3 H), 1.14 (d, *J* = 6.8, 3 H), 0.90 (d, *J* = 6.8, 3 H), 0.85 (dd, *J* = 6.0, 7.0, 3 H)

MS: (ESI, Q-tof)

398 (100)

Mol. Formula: $C_{26}H_{41}BrNO$ (463.51)

HRMS: $C_{20}H_{38}NO_3^+$: (398.3423)

Calcd: 398.3423

Found: 398.3416

TLC: R_f 0.25 (CH_2Cl_2/MeOH, 9:1) [I_2]

Preparation of *rel*-(1*S*,3*R*,5*S*,5a*S*,7a*S*,7b*R*) Octahydro-1-hexyloxy-1-isopropyl-3-(1-naphthylmethyl)-5-methyl-7b-methylcyclopenta[*gh*]pyrrolizinium Bromide (V**{*3,3,2*})**

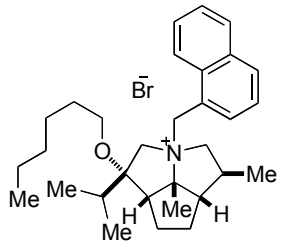

V{*3,3,2*}

Data for **V**{*3,3,2*}:

Yield: 50 mg (99%), free-flowing white powder

^{1}H-NMR: (500 MHz, $CDCl_3$)

8.37 (d, *J* = 7.2, 1 H), 8.27 (d, *J* = 8.5, 1 H), 7.87 (t, *J* = 8.5, 2 H), 7.62 (t, *J* = 7.7, 1 H), 7.54–7.44 (m, 2 H), 5.67 (d, *J* = 12.9, 1 H), 5.63 (d, *J* = 12.9, 1 H), 4.72 (d, *J* = 13.6, 1 H), 4.09 (dd, *J* = 11.5, 11.5, 1 H), 3.50 (d, *J* = 13.5, 1 H), 3.26 (dd, *J* = 6.9, 15.4, 1 H), 3.02 (dd, *J* = 8.1, 12.0, 1 H), 2.94 (dd, *J* = 6.1, 14.9, 1 H), 2.74 (dd, *J* = 6.5, 9.7, 1 H), 2.72–2.60 (m, 2 H), 2.45 (m, 2 H), 2.48–2.39 (m, 1 H), 2.18–2.08 (m, 1 H), 2.15 (s, 3 H), 2.00–1.94 (m, 2 H), 1.75–1.65 (m, 1 H), 1.44–1.30 (m, 2 H), 1.27– 1.14 (m, 6H), 1.16 (d, *J* = 6.7, 3 H), 1.10 (d, *J* = 6.4, 3 H), 0.84 (d, *J* = 6.8, 3 H), 0.81 (t, *J* = 6.9, 3 H)

MS: (ESI, Q-tof)

448.3 (100)

Mol. Formula: $C_{31}H_{46}BrNO$ (528.61)

HRMS: $C_{31}H_{46}NO^+$: (448.3579)

Calcd: 448.3579

Found: 448.3573

TLC: R_f 0.28 (CH_2Cl_2/MeOH, 9:1) [I_2]

Preparation of *rel*-(1*S*,3*R*,5*S*,5a*S*,7a*S*,7b*R*) Octahydro-1-hexyloxy-1-isopropyl-3-(2-naphthylmethyl)-5-methyl-7b-methylcyclopenta[*gh*]pyrrolizinium Bromide (V**{*3,3,3*})**

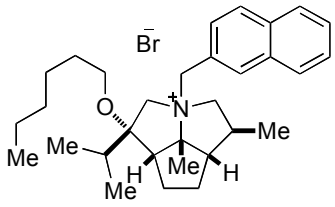

V{*3,3,3*}

Data for **V**{*3,3,3*}:

Yield: 46 mg (91%), free-flowing white powder

^{1}H-NMR: (500 MHz, $CDCl_3$)

8.34 (s, 1 H), 7.95–7.92 (m, 1 H), 7.90 (dd, *J* = 1.7, 8.5, 1 H), 7.80–7.75 (m, 2 H), 7.55–7.48 (m, 2 H), 5.36 (d, *J* = 12.1, 1 H), 5.20 (d, *J* = 12.0, 1 H), 4.62 (d, *J* = 13.5, 1 H), 4.11–4.06 (dd, *J* = 10.8, 10.8, 1 H), 3.55 (d, *J* = 13.5, 1 H), 3.30 (dd, *J* = 6.9, 15.4, 1 H), 3.20 (dd, *J* = 8.0, 12.0, 1 H), 3.00 (dd, *J* = 6.3, 14.8, 1 H), 2.72–2.61 (m, 1 H), 2.70 (dd, *J* = 7.0, 9.7, 1 H), 2.60–2.56 (m, 1 H), 2.44–2.33 (m, 1 H), 2.25–2.15 (m, 1 H), 2.02 (s, 3 H), 1.97–1.91 (m, 2 H), 1.76–1.66 (m, 1 H), 1.44–1.32 (m, 2 H), 1.27–1.14 (m, 6H), 1.22 (d, *J* = 6.7, 3 H), 1.18 (d, *J* = 6.7, 3 H), 0.89 (d, *J* = 6.8, 3 H), 0.81 (t, *J* = 7.0, 3 H)

MS: (ESI, Q-tof)

448.4 (100)

Mol. Formula: $C_{31}H_{46}BrNO$ (513.57)

HRMS: $C_{31}H_{46}NO^+$: (448.3579)

Calcd: 448.3579

Found: 448.3577

TLC: R_f 0.29 (CH_2Cl_2/MeOH, 9:1) [I_2]

Preparation of *rel*-(1*S*,3*R*,5*S*,5a*S*,7a*S*,7b*R*) Octahydro-1-hexyloxy-1-isopropyl-3-(3,5-trifluoromethyl-benzyl)-5-methyl-7b-methyl-cyclopenta[*gh*]pyrrolizinium Bromide (V{*3,3,5*})

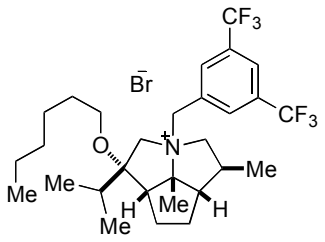

V{*3,3,5*}

Data for **V**{*3,3,5*}:

Yield: 59 mg (99%), free-flowing white powder

^{1}H-NMR: (500 MHz, $CDCl_3$)

8.49 (s, 2 H), 7.94 (s, 1 H), 5.70 (d, *J* = 12.2, 1 H), 5.37 (d, *J* = 12.3, 1 H), 4.70 (d, *J* = 13.2, 1 H), 3.83 (dd, *J* = 11.0, 11.0, 1 H), 3.44 (d, *J* = 13.1, 1 H), 3.36 (dd, *J* = 6.9, 15.3, 1 H), 3.26 (dd, *J* = 7.9, 11.9, 1 H), 3.08 (dd, *J* = 6.3, 14.7, 1 H), 2.75–2.66 (m, 2 H), 2.58–2.53 (m, 1 H), 2.45–2.34 (m, 1 H), 2.23–2.16 (m, 1 H), 2.01 (s, 3 H), 1.98–1.92 (m, 2 H), 1.76–1.68 (m, 1 H), 1.51–1.38 (m, 2 H), 1.36–1.18 (m, 6 H), 1.21 (s, 3 H, *J* = 6.1), 1.16 (d, *J* = 6.8, 3 H), 0.88 (d, *J* = 6.8, 3 H), 0.85 (t, *J* = 6.9, 3 H)

MS: (ESI, Q-tof)

534.3 (100)

Mol. Formula: $C_{29}H_{42}BrF_6NO$ (599.51)

HRMS: $C_{29}H_{42}F_6NO^+$: (534.3171)

Calcd: 534.3171

Found: 534.3167

TLC: R_f 0.32 (CH_2Cl_2/MeOH, 9:1) [I_2]

Preparation of *rel*-(1*S*,3*S*,5*S*,5a*S*,7a*S*,7b*R*) Octahydro-1-hexyloxy-1-isopropyl-3-hexyl-5-methyl-7b-methyl-cyclopenta[*gh*]pyrrolizinium Bromide (V{*3,3,6*})

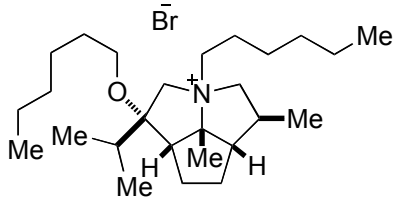

V{*3,3,6*}

Data for **V**{*3,3,6*}:

Yield: 43 mg (98%), free-flowing white powder

^{1}H-NMR: (500 MHz, $CDCl_3$)

4.25 (d, *J* = 13.8, 1 H), 4.07 (d, *J* = 13.8, 1 H), 4.00–3.82 (m, 2 H), 3.56–3.33 (m, 6H), 2.81–2.70 (m, 1 H), 2.55 (dd, *J* = 6.6, 9.6, 1 H), 2.49–2.40 (m, 1 H), 2.21–2.12 (m, 3 H), 2.04–1.84 (m, 4 H), 1.81–1.64 (m, 2 H), 1.69 (s, 3 H), 1.64–1.48 (m, 4 H), 1.48–1.20 (m, 6H), 1.09 (d, *J* = 6.7, 3 H), 1.05 (d, *J* = 6.7, 3 H), 0.91–0.87 (m, 6H), 0.85 (d, *J* = 6.8, 3 H)

MS: (ESI, Q-tof)

392.4 (100)

Mol. Formula: $C_{26}H_{50}BrNO$ (457.55)

HRMS: $C_{26}H_{50}NO^+$: (392.3892)

Calcd: 392.3892

Found: 392.3882

TLC: R_f 0.40 (CH_2Cl_2/MeOH, 9:1) [I_2]

Preparation of *rel*-(1*S*,3*R*,5*S*,5a*S*,7a*S*,7b*R*) Octahydro-1-hexyloxy-1-isopropyl-3-(3,5-*tert*-butylbenzyl)-5-methyl-7b-methylcyclopenta[*gh*]pyrrolizinium Bromide (V{*3,3,7*})

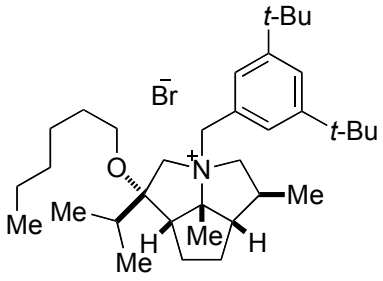

V{*3,3,7*}

Data for **V**{*3,3,7*}:

Yield: 56 mg (99%), free-flowing white powder

^{1}H-NMR: (500 MHz, $CDCl_3$)

7.65 (d, *J* = 1.5, 2 H), 7.49 (s, 1 H), 5.25 (d, *J* = 12.2, 1 H), 4.71 (t, *J* = 12.8, 2 H), 3.96 (dd, *J* = 8.8, 12.3, 1 H), 3.54 (d, *J* = 13.6, 1 H), 3.42 (dd, *J* = 8.1, 12.3, 1 H), 3.39–3.33 (m, 1 H), 3.15 (dd, *J* = 6.0, 14.5, 1 H), 2.70 (dd, *J* = 7.0, 9.0, 1 H), 2.60–2.50 (m, 1 H), 2.47–2.40 (m, 1 H), 2.40–2.32 (m, 1 H), 2.29–2.20 (m, 1 H), 2.01 (s, 3 H), 1.99–1.92 (m, 2 H), 1.81–1.73 (m, 1 H), 1.49–1.42 (m, 2 H), 1.38–1.20 (m, 6H), 1.36 (s, 18H), 1.22 (d, *J* = 6.8, 3 H), 1.14 (d, *J* = 6.8, 3 H), 0.97 (d, *J* = 6.8, 3 H), 0.85 (t, *J* = 6.8, 3 H)

MS: (ESI, Q-tof)

510.5 (100)

Mol. Formula: $C_{35}H_{60}BrNO$ (605.80)

HRMS: $C_{35}H_{60}NO^+$: (510.4675)

Calcd: 510.4675

Found: 510.4674

TLC: R_f 0.35 (CH_2Cl_2/MeOH, 9:1) [I_2]

Preparation of *rel*-(1*S*,3*R*,5*S*,5a*S*,7a*S*,7b*R*) Octahydro-1-hexyloxy-1-isopropyl-3-(4-methoxy-benzyl)-5-methyl-7b-methylcyclopenta[*gh*]pyrrolizinium Bromide (V{*3,3,8*})

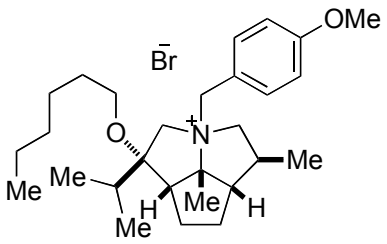

V{*3,3,8*}

Data for **V**{*3,3,8*}:

Yield: 48 mg (98%), free-flowing white powder

^{1}H-NMR: (500 MHz, $CDCl_3$)

7.78 (d, *J* = 8.7, 2 H), 6.93 (d, *J* = 8.6, 2 H), 5.10 (d, *J* = 12.0, 1 H), 4.92–4.86 (m, 1 H), 4.48 (d, *J* = 13.6, 1 H), 3.95 (dd, *J* = 10.4, 10.4, 1 H), 3.82 (s, 3 H), 3.52 (d, *J* = 13.6, 1 H), 3.34 (dd, *J* = 6.8, 15.3, 1 H), 3.26–3.20 (m, 1 H), 3.09 (dd, *J* = 6.2, 14.7, 1 H), 2.72–2.57 (m, 2 H), 2.51–2.46 (m, 1 H), 2.45–2.33 (m, 1 H), 2.24–2.13 (m, 1 H), 1.97–1.91 (m, 2 H), 1.95 (s, 3 H), 1.75–1.67 (m, 1 H), 1.48–1.41 (m, 2 H), 1.33–1.18 (m, 6H), 1.19 (d, *J* = 6.0, 3 H), 1.14 (d, *J* = 6.8, 3 H), 0.90 (d, *J* = 6.8, 3 H), 0.85 (t, *J* = 6.9, 3 H)

MS: (ESI, Q-tof)

428.4 (100)

Mol. Formula: $C_{28}H_{46}BrNO_2$ (493.54)

HRMS: $C_{28}H_{46}NO_2^+$: (428.3529)

Calcd: 428.3529

Found: 428.3529

TLC: R_f 0.21 (CH_2Cl_2/MeOH, 9:1) [I_2]

Preparation of Quaternary Ammonium Bromides V{*3*,7,R^4}

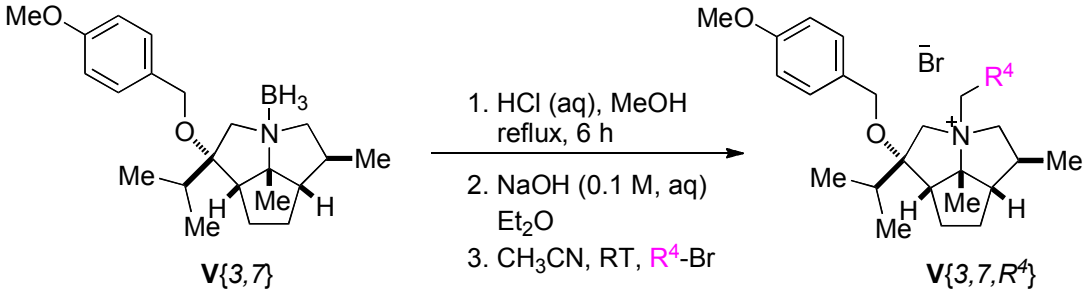

Following General Procedure II, amino borane **V**{*3*,7} (502 mg, 1.40 mmol) was added to a 100-mL round-bottomed flask as a solution in 50 mL of MeOH (0.03 M). The flask was fitted with a reflux condenser, a magnetic stir bar, and a nitrogen inlet adapter. Lastly, 1.0 N aq. HCl solution (7.0 mL, 5.0 equiv) was added via syringe. The resulting solution was heated and then concentrated by rotary evaporation (15 mm Hg, 20-25 ^{o}C) as described General Procedure II. The resulting free amine was dissolved in acetonitrile and was distributed among six test tubes that were subsequently charged with benzyl bromide (tube 1, 20 mg, 0.116 mmol, 1.2 equiv), 1-bromomethylnaphthalene (tube 2, 26 mg, 0.116 mmol, 1.2 equiv), 2-bromomethylnaphthalene (tube 3, 26 mg, 0.116 mmol, 1.2 equiv), 3,5-bis(trifluoromethyl)benzyl bromide (tube 4, 35 mg, 0.116 mmol, 1.2 equiv), 3,5-bis(*t*-butyl)benzyl bromide (tube 5, 33 mg, 0.116 mmol, 1.2 equiv), 4-methoxybenzyl bromide (tube 6, 23 mg, 0.116 mmol, 1.2 equiv). After being agitated for 12 h, the reaction mixtures were worked up and the products isolated and purified as described in General Procedure II.

Preparation of *rel*-(1*S*,3*R*,5*S*,5a*S*,7a*S*,7b*R*) Octahydro-1-(4-methoxy-benzyloxy)-1-isopropyl-3-benzyl-5-methyl-7b-methylcyclopenta[*gh*]pyrrolizinium Bromide (V{*3*,7,*1*})

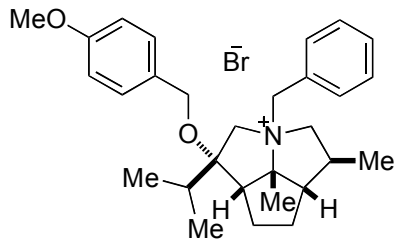

V{*3,7,1*}

Data for **V**{*3*,7,*1*}:

Yield: 38 mg (75%), free-flowing white powder

^{1}H-NMR: (500 MHz, $CDCl_3$)

7.90–7.82 (m, 2 H), 7.49–7.42 (m, 3 H), 7.08 (d, *J* = 8.6, 2 H), 6.80 (d, *J* = 8.6, 2 H), 5.31 (d, *J* = 12.1, 1 H), 4.83 (d, *J* = 12.1, 1 H), 4.72 (d, *J* = 13.7, 1 H), 4.45 (d, *J* = 10.6, 1 H), 4.11 (d, *J* = 10.6, 1 H), 3.83 (dd, *J* = 9.62, 12.0, 1 H), 3.77 (s, 3 H), 3.69 (d, *J* = 13.6, 1 H), 3.19 (dd, *J* = 7.9, 12.2, 1 H), 2.74 (dd, *J* =6.86, 9.45, 1 H), 2.54–2.30 (m, 4 H), 1.98 (s, 3 H), 1.96–1.84 (m, 2 H), 1.79–1.70 (m, 1 H), 1.22 (d, *J* = 6.8, 3 H), 1.01 (t, *J* = 7.1, 6 H).

MS: (ESI, Q-tof)

434.3 (100)

Mol. Formula: $C_{29}H_{40}BrNO_2$ (514.54)

HRMS: $C_{29}H_{40}NO_2^+$: (434.3059)

Calcd: 434.3059

Found: 434.3058

TLC: R_f 0.22 (CH_2Cl_2/MeOH, 9:1) [I_2]

Preparation of *rel*-(1*S*,3*R*,5*S*,5a*S*,7a*S*,7b*R*) Octahydro-1-(4-methoxy-benzyloxy)-1-isopropyl-3-(1-naphthylmethyl)-5-methyl-7b-methylcyclopenta[*gh*]pyrrolizinium Bromide (V**{*3*,7,*2*})**

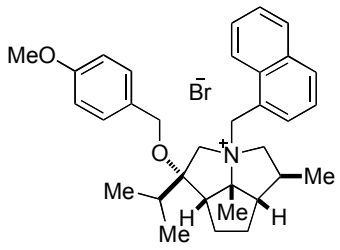

V{*3,7,2*}

Data for **V**{*3*,7,*2*}:

Yield: 42 mg (77%), free-flowing white powder

^{1}H-NMR: (500 MHz, $CDCl_3$)

8.38 (d, *J* = 7.2, 1 H), 8.26 (d, *J* = 8.6, 1 H), 7.88 (t, *J* = 7.34, 2 H), 7.62 (t, *J* = 7.2, 1 H), 7.56–7.46 (m, 2 H), 7.00 (d, *J* = 8.6, 2 H), 6.74 (d, *J* = 8.6, 2 H), 5.73 (d, *J* = 12.8, 1 H), 5.58 (d, *J* = 12.8, 1 H), 4.87 (d, *J* = 13.7, 1 H), 4.38 (d, *J* = 10.6, 1 H), 3.96 (d, *J* = 10.9, 1 H), 3.96-3.92 (m, 1 H), 3.73 (s, 3 H), 3.67 (d, *J* = 13.6, 1 H), 2.93 (dd, *J* = 7.5, 12.2, 1 H), 2.80 (dd, *J* = 6.5, 9.8, 1 H), 2.57–2.40 (m, 3 H), 2.35–2.26 (m, 1 H), 2.16 (s, 3 H), 2.00–1.87 (m, 2 H), 1.79–1.68 (m, 1 H), 1.23 (d, *J* = 6.8, 3 H), 0.94 (d, *J* = 6.8, 3 H), 0.90 (d, *J* = 6.0, 3 H)

MS: (ESI, Q-tof)

484.3 (100)

Mol. Formula: $C_{33}H_{42}BrNO_2$ (564.60)

HRMS: $C_{33}H_{42}NO_2^+$: (484.3216)

Calcd: 484.3216

Found: 484.3215

TLC: R_f 0.25 (CH_2Cl_2/MeOH, 9:1) [I_2]

Preparation of *rel*-(1*S*,3*R*,5*S*,5a*S*,7a*S*,7b*R*) Octahydro-1-(4-methoxybenzyloxy)-1-isopropyl -3-(2-naphthylmethyl)-5-methyl-7b-methylcyclopenta[*gh*]pyrrolizinium Bromide (V{*3*,7,*3*})

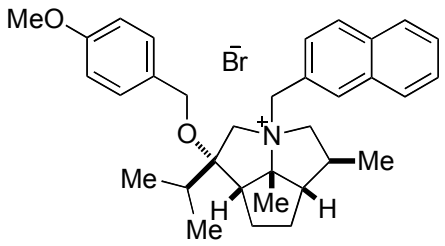

V{*3,7,3*}

Data for **V**{*3*,*7*,*3*}:

Yield: 38 mg (69%), free-flowing white powder

^{1}H-NMR: (500 MHz, $CDCl_3$)

8.35 (s, 1 H), 7.96 (d, *J* = 8.3, 1 H), 7.91 (dd, *J* = 1.7, 8.3, 1 H), 7.85-7.81 (m, 2 H), 7.56–7.45 (m, 2 H), 7.03 (d, *J* = 8.6, 2 H), 6.73 (d, *J* = 8.7, 2 H), 5.47 (d, *J* = 12.1, 1 H), 5.07 (d, *J* = 12.2, 1 H), 4.79 (d, *J* = 13.7, 1 H), 4.41 (d, *J* = 10.6, 1 H), 4.04 (d, *J* = 10.6, 1 H), 3.90 (dd, *J* = 9.2, 12.1, 1 H), 3.71 (s, 3 H), 3.16 (dd, *J* = 7.1, 12.6, 1 H), 2.76 (dd, *J* = 6.9, 9.4, 1 H), 2.52–2.33 (m, 5 H), 2.04 (s, 3 H), 1.96–1.85 (m, 2 H), 1.78–1.69 (m, 1 H), 1.25 (d, *J* = 6.8, 3 H), 1.05 (d, *J* = 6.1, 3 H), 0.99 (d, *J* = 6.8, 3 H)

MS: (ESI, Q-tof)

484.3 (100)

Mol. Formula: $C_{33}H_{42}BrNO_2$ (564.60)

HRMS: $C_{33}H_{42}NO_2^+$: (484.3216)

Calcd: 484.3216

Found: 484.3221

TLC: R_f 0.26 (CH_2Cl_2/MeOH, 9:1) [I_2]

Preparation of *rel*-(1*S*,3*R*,5*S*,5a*S*,7a*S*,7b*R*) Octahydro-1-(4-methoxy-benzyloxy)-1-isopropyl -3-(3,5-trifluoromethlybenzyl)-5-methyl-7b-methylcyclopenta[*gh*]pyrrolizinium Bromide (V**{*3*,*7*,*5*})**

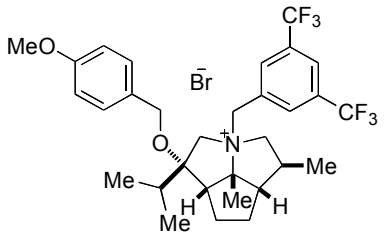

V{*3*,*7*,*5*}

Data for **V**{*3*,*7*,*5*}:

Yield: 52 mg (82%), free-flowing white powder

^{1}H-NMR: (500 MHz, $CDCl_3$)

8.48 (s, 2 H), 7.96 (s, 1 H), 7.07 (d, *J* = 8.6, 2 H), 6.79 (d, *J* = 8.6, 2 H), 5.81 (d, *J* = 12.4, 1 H), 5.27–5.20 (m, 1 H), 4.84 (d, *J* = 13.2, 1 H), 4.48 (d, *J* = 10.8, 1 H), 4.12 (d, *J* = 10.8, 1 H), 3.76 (s, 3 H), 3.62 (dd, *J* = 9.5, 11.9, 1 h), 3.57 (d, *J* = 13.4, 1 H) 3.14 (dd, *J* = 7.51, 11.0, 1 H), 2.75 (dd, *J* = 8.3, 8.3, 1 H), 2.60–2.48 (m, 1 H), 2.48–2.31 (m, 3 H), 2.02 (s, 3 H), 1.95–1.87 (m, 2 H), 1.80–1.71 (m, 1 H), 1.23 (d, *J* = 6.7, 3 H), 1.05 (d, *J* = 6.7, 3 H), 0.99 (d, *J* = 6.8, 3 H)

MS: (ESI, Q-tof)

570.3 (100)

Mol. Formula: $C_{31}H_{38}BrF_6NO_2$ (650.53)

HRMS: $C_{31}H_{38}F_6NO_2^+$: (570.2807)

Calcd: 570.2807

Found: 570.2805

TLC: R_f 0.31 (CH_2Cl_2/MeOH, 9:1) [I_2]

Preparation of *rel*-(1*S*,3*R*,5*S*,5a*S*,7a*S*,7b*R*) Octahydro-1-(4-methoxy-benzyloxy)-1-isopropyl -3-(3,5-*tert*-butylbenzyl)-5-methyl-7b-methycyclopenta[*gh*]pyrrolizinium Bromide (V{*3*,7,*7*})

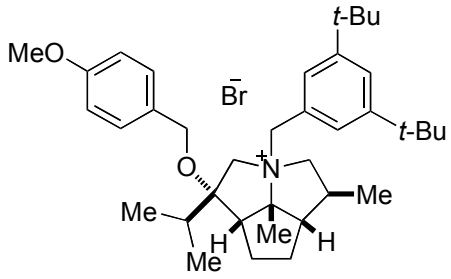

V{*3,7,7*}

Data for **V**{*3*,7,*7*}:

Yield: 47 mg (78%), free-flowing white powder

^{1}H-NMR: (500 MHz, $CDCl_3$)

7.67 (d, *J* = 1.7, 2 H), 7.51 (s, 1 H), 7.11 (d, *J* = 8.6, 2 H), 6.82 (d, *J* = 8.7, 2 H), 5.37 (d, *J* = 12.2, 1 H), 4.87 (d, *J* = 13.7, 1 H), 4.61 (d, *J* = 12.2, 1 H), 4.46 (d, *J* = 10.6, 1 H), 4.17 (d, *J* = 10.6, 1 H), 3.80 (dd, *J* = 8.21, 12.5, 1 H), 3.78 (s, 3 H), 3.68 (d, *J* = 13.7, 1 H), 3.40 (dd, *J* = 8.0, 12.5, 1 H), 2.77 (dd, *J* = 7.54, 8.9, 1 H), 2.45–2.31 (m, 4 H), 2.03 (s, 3 H), 1.99–1.86 (m, 2 H), 1.85–1.76 (m, 1 H), 1.37 (s, 18H), 1.21 (d, *J* = 6.8, 3 H), 1.07 (d, *J* = 6.8, 6 H)

MS: (ESI, Q-tof)

546.4 (100)

Mol. Formula: $C_{37}H_{56}BrNO_2$ (626.75)

HRMS: $C_{37}H_{56}NO_2^+$: (546.4311)

Calcd: 546.4311

Found: 546.4317

TLC: R_f 0.33 (CH_2Cl_2/MeOH, 9:1) [I_2]

Preparation of *rel*-(1*S*,3*R*,5*S*,5a*S*,7a*S*,7b*R*) Octahydro-1-(4-methoxybenzyloxy)-1-isopropyl-3-(4-methoxybenzyl)-5-methyl-7b-methylcyclopenta[*gh*]pyrrolizinium Bromide (V{*3*,7,*8*})

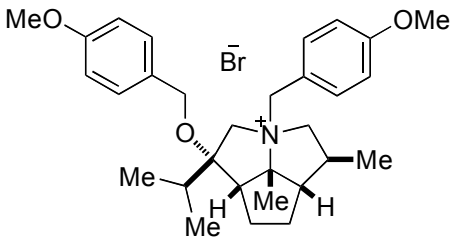

V{*3,7,8*}

Data for **V**{*3*,7,*8*}:

Yield: 35 mg (66%), free-flowing white powder

^{1}H-NMR: (500 MHz, $CDCl_3$)

7.79 (d, *J* = 8.7, 2 H), 7.10 (d, *J* = 8.6, 2 H), 6.95 (d, *J* = 8.6, 2 H), 6.81 (d, *J* = 8.7, 2 H), 5.23 (d, *J* = 12.2, 1 H), 4.75 (d, *J* = 12.4, 1 H), 4.66 (d, *J* = 13.7, 1 H), 4.45 (d, *J* = 10.6, 1 H), 4.12 (d, *J* = 10.6, 1 H), 3.84 (s, 3 H), 3.83–3.73 (m, 1 H), 3.77 (s, 3 H), 3.67 (d, *J* = 13.7, 1 H), 3.20 (dd, *J* = 8.1, 12.2, 1 H), 2.73 (dd, *J* = 6.8, 9.5, 1 H), 2.52–2.28 (m, 4 H), 1.96 (s, 3 H), 1.94–1.85 (m, 2 H), 1.75 (s, 1 H), 1.21 (d, *J* = 6.7, 3 H), 1.04–0.99 (m, 6H)

MS: (ESI, Q-tof)

464.3 (100)

Mol. Formula: $C_{30}H_{42}BrNO_3$ (544.56)

HRMS: $C_{30}H_{42}NO_3^+$: (464.3165)

Calcd: 464.3165

Found: 464.3170

TLC: R_f 0.19 (CH_2Cl_2/MeOH, 9:1) [I_2]

Preparation of Quaternary Ammonium Bromides V{*4,2,R*^{4}}

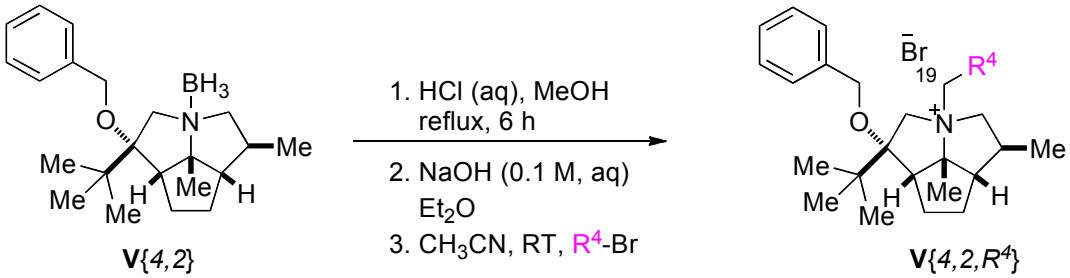

V{*4,2*} **V**{*4,2,R*^{4}}

Following General Procedure II, amino borane **V**{*4,2*} (102 mg, 0.300 mmol) was added to a 25-mL round-bottomed flask as a solution in 0 mL of MeOH (0.03 M). The flask was fitted with a reflux condenser, a magnetic stir bar, and a nitrogen inlet adapter. Lastly, 1.0 N aq. HCl solution (1.5, 5.0 equiv) was added via syringe. The resulting solution was heated and then concentrated by rotary evaporation (15 mm Hg, 20-25 ^{o}C) as described General Procedure II. The resulting free amine was dissolved in acetonitrile and was distributed among one test tube that were subsequently charged with 3,5-bis(trifluoromethyl)benzyl bromide (tube 1, 281 mg, 0.915 mmol, 5.0 equiv). After being agitated for 12 h, the reaction mixtures were worked up and the products isolated and purified as described in General Procedure II.

Preparation of *rel*-(1*R*,3*R*,5*S*,5a*S*,7a*S*,7b*R*) Octahydro-1-benzyloxy-1-*tert*-butyl-3-(3,5-trifluoromethylbenzyl)-5-methyl-7b-methylcyclopenta[*gh*]pyrrolizinium Bromide (V{*4,2,5*})

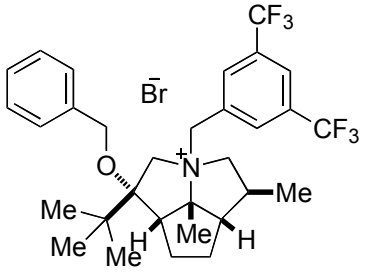

V{*4,2,5*}

Data for **V**{*4,2,5*}:

Yield: 108 mg (93%), free-flowing white powder

^{1}H-NMR: (500 MHz, $CDCl_3$)

8.53 (s, 2 H), 7.97 (s, 1 H), 7.31 (m, 3 H), 7.22-7.19 (m, 2 H), 5.71 (d, *J* = 12.3, 1 H), 5.60 (d, *J* = 12.3, 1 H), 4.80 (d, *J* = 10.8, 1 H), 4.67 (d, *J* = 13.8, 1 H), 4.24 (d, *J* = 10.8, 1 H), 3.84 (dd, *J* = 11.2, 1 H), 3.74 (d, *J* = 13.7, 1 H), 3.12 (dd, 1 H, *J* = 7.9, 11.9, 1 H), 2.97 (dd, *J* = 6.8, 9.5, 1 H), 2.54-2.47 (m, 2 H), 2.36-2.26 (m, 1 H), 2.00 (s, 3 H), 1.92-1.83 (m, 2 H), 1.79-1.72 (m, 1 H), 1.17 (s, 9 H), 0.88 (d, *J* = 6.7, 3 H)

MS: (ESI, Q-tof)

554.2 (100)

Mol. Formula: $C_{31}H_{38}BrF_6NO$ (634.53)

HRMS: $C_{36}H_{37}F_3NO^+$: 554.2858

Calcd: 554.2858

Found: 554.2866

TLC: R_f 0.30 (CH_2Cl_2/MeOH, 9:1) [I_2]

Preparation of Quaternary Ammonium Bromides V{*5,2,R*^{4}}

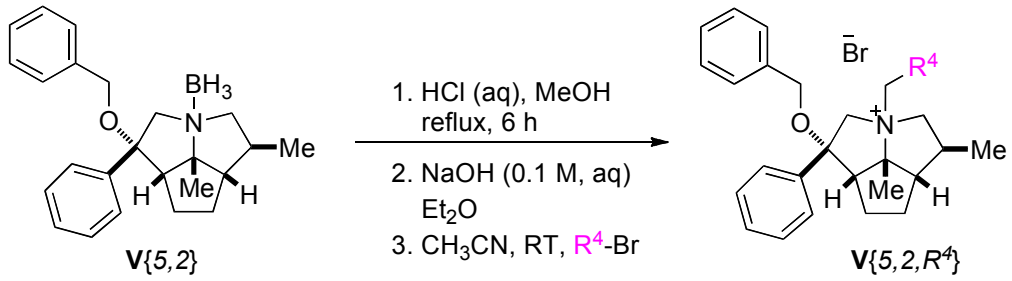

V{*5,2*} **V**{*5,2,R*^{4}}

Following General Procedure II, amino borane **V**{*5,2*} (597 mg, 1.65 mmol) was added to a 100-mL round-bottomed flask as a solution in 50 mL of MeOH (0.03 M). The flask was fitted with a reflux condenser, a magnetic stir bar, and a nitrogen inlet adapter. Lastly, 1.0 N aq. HCl solution (7.5, 5.0 equiv) was added via syringe. The resulting solution was heated and then concentrated by rotary evaporation (15 mm Hg, 20-25 ^{o}C) as described General Procedure II. The resulting free amine was dissolved in acetonitrile and was distributed among eight test tubes that were subsequently charged with benzyl bromide (tube 1, 44 mg, 0.259 mmol, 1.2 equiv), 1-bromomethylnaphthalene (tube 2, 58 mg, 0.259 mmol, 1.2 equiv), 2-bromomethylnaphthalene (tube 3, 58 mg, 0.259 mmol, 1.2 equiv), 3,5-bis(trifluoromethyl)benzyl bromide (tube 4, 80 mg, 0.259 mmol, 1.2 equiv), 3,5-bis(*t*-butyl)benzyl bromide (tube 5, 80 mg, 0.259 mmol, 1.2 equiv), 4-methoxybenzyl bromide (tube 6, 52 mg, 0.259 mmol, 1.2 equiv), 4-trifluoromethylbenzyl bromide (tube 7, 20 mg, 0.085 mmol, 1.2 equiv), 4-cyanobenzyl bromide (tube 8, 17 mg, 0.085 mmol, 1.2 equiv). After being agitated for 12 h, the reaction mixtures were worked up and the products isolated and purified as described in General Procedure II.

Preparation of *rel*-(1*R*,3*R*,5*S*,5a*S*,7a*S*,7b*R*) Octahydro-1-benzyloxy-1-phenyl-3-benzyl-5-methyl-7b-methylcyclopenta[*gh*]pyrrolizinium Bromide (V{*5,2,1*})

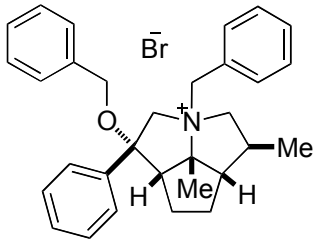

V{*5,2,1*}

Data for **V**{*5,2,1*}:

Yield: 107 mg (95%), free-flowing white powder

^{1}H-NMR: (500 MHz, $CDCl_3$)

7.77 (d, *J* = 8.2, 2 H), 7.67 (t, *J* = 7.5, 2 H), 7.57 (t, *J* = 7.3, 2 H), 7.42 (d, *J* = 7.8, 2 H), 7.40–7.31 (m, 3 H), 7.31–7.24 (m, 2 H), 7.12 (d, *J* = 6.8, 2 H), 5.25 (d, *J* = 12.0, 1 H), 5.03 (dd, *J* = 11.9, 11.9, 1 H), 4.30 (d, *J* = 13.1, 1 H), 3.99 (d, *J* = 10.6, 1 H), 3.82 (d, *J* = 10.7, 1 H), 3.53 (d, *J* = 13.0, 1 H), 3.45 (dd, *J* = 9.3, 9.3, 1 H), 3.36 (d, *J* = 12.1, 1 H), 2.98 (dd, *J* = 6.0, 11.4, 1 H), 2.85 (dd, *J* = 5.72, 9.75, 1 H), 2.49–2.39 (m, 1 H), 2.29 (s, 3 H), 2.27–2.15 (m, 2 H), 1.98–1.91(m, 2 H), 1.30 (d, *J* = 6.3, 3 H)

MS: (ESI, Q-tof)

438.3 (100)

Mol. Formula: $C_{31}H_{36}BrNO$ (518.53)

HRMS: $C_{31}H_{36}NO^+$: (438.2797)

Calcd: 438.2797

Found: 438.2784

TLC: R_f 0.21 (CH_2Cl_2/MeOH, 9:1) [I_2]

Preparation of *rel*-(1*R*,3*R*,5*S*,5a*S*,7a*S*,7b*R*) Octahydro-1-benzyloxy-1-phenyl-3-(1-naphthylmethyl)-5-methyl-7b-methylcyclopenta[*gh*]pyrrolizinium Bromide (V{*5,2,2*})

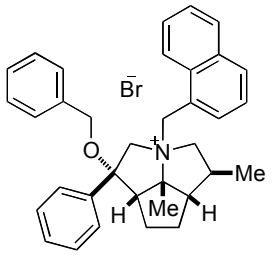

V{*5,2,2*}

Data for **V**{*5,2,2*}:

Yield: 113 mg (92%), free-flowing white powder

^{1}H-NMR: (500 MHz, $CDCl_3$)

7.91 (dd, *J* = 8.4, 14.2, 2 H), 7.85 (t, *J* = 8.3, 2 H), 7.74 (d, *J* = 7.7, 2 H), 7.67 (t, *J* = 7.7, 2 H), 7.58 (d, *J* = 7.4, 1 H), 7.57–7.53 (m, 2 H), 7.51 (d, *J* = 7.2, 1 H), 7.47 (dd, *J* = 5.7, 13.6, 2 H), 7.32–7.23 (m, 1 H), 7.10 (dd, *J* = 2.0, 7.4, 2 H), 5.55 (d, *J* = 12.8, 1 H), 4.74 (d, *J* = 11.9, 1 H), 4.69 (d, *J* = 13.9, 1 H), 4.53 (d, *J* = 12.8, 1 H), 3.98 (d, *J* = 11.0, 1 H), 3.91 (d, *J* = 11.0, 1 H), 3.62 (d, *J* = 13.3, 1 H), 3.39 (dd, *J* = 9.1, 9.1, 1 H), 3.04 (d, *J* = 10.4, 1 H), 2.90 (dd, *J* = 6.4, 11.5, 1 H), 2.55 (dd, *J* = 11.2, 21.0, 1 H), 2.46 (s, 3 H), 2.37–2.27 (m, 1 H), 2.16 (d, *J* = 9.0, 1 H), 2.02–1.95 (m, 2 H), 1.22 (d, *J* = 6.4, 3 H)

MS: (ESI, Q-tof)

488.3 (100)

Mol. Formula: $C_{35}H_{38}BrNO$ (568.59)

HRMS: $C_{35}H_{38}NO^+$: (488.2953)

Calcd: 488.2953

Found: 488.2956

TLC: R_f 0.24 (CH_2Cl_2/MeOH, 9:1) [I_2]

Preparation of *rel*-(1*R*,3*R*,5*S*,5a*S*,7a*S*,7b*R*) Octahydro-1-benzyloxy-1-phenyl-3-(2-naphthylmethyl)-5-methyl-7b-methylcyclopenta[*gh*]pyrrolizinium Bromide (V{*5,2,3*})

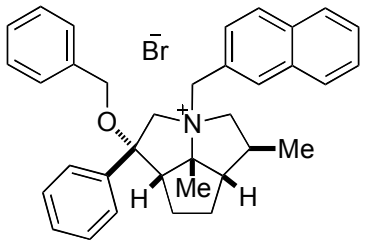

V{*5,2,3*}

Data for **V**{*5,2,3*}:

Yield: 110 mg (90%), free-flowing white powder

^{1}H-NMR: (500 MHz, $CDCl_3$)

7.86–7.79 (m, 5 H), 7.75 (t, *J* = 7.7, 2 H), 7.68–7.60 (m, 3 H), 7.57–7.50 (m, 2 H), 7.31–7.25 (m, 3 H), 7.12 (dd, *J* = 1.9, 7.5, 2 H), 5.48 (d, *J* = 12.1, 1 H), 5.18 (dd, *J* = 11.9, 11.9, 1 H), 4.35 (d, *J* = 13.0, 1 H), 4.00 (d, *J* = 10.7, 1 H), 3.84 (d, *J* = 10.7, 1 H), 3.53 (dd, *J* = 12.4, 12.4, 2 H), 3.47 (dd, *J* = 9.2, 9.2, 1 H), 3.06 (dd, *J* = 6.0, 11.3, 1 H), 2.89 (dt, *J* = 2.75, 5.63, 10.2, 1 H), 2.51–2.40 (m, 1 H), 2.35 (s, 3 H), 2.29–2.15 (m, 2 H), 1.99–1.93 (m, 2 H), 1.32 (d, *J* = 6.4, 3 H)

MS: (ESI, Q-tof)

488.3 (100)

Mol. Formula: $C_{35}H_{38}BrNO$ (568.59)

HRMS: $C_{35}H_{38}NO_3^+$: (488.2953)

Calcd: 488.2953

Found: 488.2943

TLC: R_f 0.25 (CH_2Cl_2/MeOH, 9:1) [I_2]

Preparation of *rel*-(1*R*,3*R*,5*S*,5a*S*,7a*S*,7b*R*) Octahydro-1-benzyloxy-1-phenyl-3-(3,5-trifluoromethylbenzyl)-5-methyl-7b-methylcyclopenta[*gh*]pyrrolizinium Bromide (V{*5,2,5*})

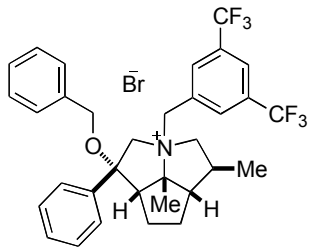

V{*5,2,5*}

Data for V{*5,2,5*}:

Yield: 1 mg (85%), free-flowing white powder

^{1}H-NMR: (500 MHz, $CDCl_3$)

7.93 (s, 2 H), 7.91 (s, 1 H), 7.76 (d, *J* = 7.42, 2 H), 7.72 (t, *J* = 7.7, 2 H), 7.63 (t, *J* = 7.2, 1 H), 7.33–7.27 (m, 3 H), 7.13 (dd, *J* = 2.1, 7.3, 2 H), 5.96 (d, *J* = 12.3, 1 H), 5.34 (dd, *J* = 11.7, 11.7, 1 H), 4.01 (d, *J* = 10.6, 1 H), 3.98 (d, *J* = 13.1, 1 H), 3.84 (d, *J* = 10.6, 1 H), 3.58 (d, *J* = 13.2, 1 H), 3.49 (dd, *J* = 9.4, 9.4, 1 H), 3.39 (d, *J* = 12.4, 1 H), 3.00 (dd, *J* = 6.1, 11.0, 1 H), 2.82 (dd, *J* = 5.8, 10.2, 1 H), 2.51–2.40 (m, 1 H), 2.35 (s, 3 H), 2.31–2.18 (m, 2 H), 2.04–1.92 (m, 2 H), 1.32 (d, *J* = 6.3, 3 H)

MS: (ESI, Q-tof)

574.3 (100)

Mol. Formula: $C_{33}H_{34}BrF_6NO$ (654.52)

HRMS: $C_{33}H_{34}NOF_6^+$: (574.2545)

Calcd: 574.2545

Found: 574.2541

TLC: R_f 0.28 (CH_2Cl_2/MeOH, 9:1) [I_2]

Preparation of *rel*-(1*R*,3*R*,5*S*,5a*S*,7a*S*,7b*R*) Octahydro-1-benzyloxy-1-phenyl-3-(3,5-*tert*-butylbenzyl)-5-methyl-7b-methylcyclopenta[*gh*]pyrrolizinium Bromide (V{*5,2,7*})

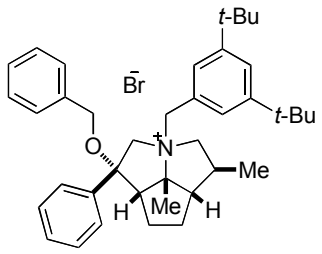

V{*5,2,7*}

Data for V{*5,2,7*}:

Yield: 113 mg (83%), free-flowing white powder

^{1}H-NMR: (500 MHz, $CDCl_3$)

7.78 (d, *J* = 7.4, 2 H), 7.68 (t, *J* = 7.7, 2 H), 7.58 (t, *J* = 7.4, 1 H), 7.40 (s, 1 H), 7.33–7.28 (m, 5 H), 7.18–7.13 (m, 2 H), 5.17 (d, *J* = 11.8, 1 H), 5.10 (dd, *J* = 11.9, 11.9, 1 H), 4.35 (d, *J* = 13.1, 1 H), 4.01 (d, *J* = 10.6, 1 H), 3.80 (d, *J* = 10.6, 1 H), 3.54 (d, *J* = 13.1, 1 H), 3.49 (dd, *J* = 9.4, 9.4, 1 H), 3.25 (d, *J* = 12.0, 1 H), 2.92 (dd, *J* = 5.9, 11.4, 1 H), 2.90–2.85 (m, 1 H), 2.49–2.39 (m, 1 H), 2.30 (s, 3 H), 2.25–2.15 (m, 2 H), 1.98–1.92 (m, 2 H), 1.31 (s, 18H), 1.30 (d, *J* = 6.5, 3 H)

MS: (ESI, Q-tof)

550.4 (100)

Mol. Formula: $C_{39}H_{52}BrNO$ (630.74)

HRMS: $C_{39}H_{52}NO^+$: (550.4049)

Calcd: 550.4049

Found: 550.4048

TLC: R_f 0.31 (CH_2Cl_2/MeOH, 9:1) [I_2]

Preparation of *rel*-(1*R*,3*R*,5*S*,5a*S*,7a*S*,7b*R*) Octahydro-1-benzyloxy-1-phenyl-3-(4-methoxybenzyl)-5-methyl-7b-methylcyclopenta[*gh*]pyrrolizinium Bromide (V{*5,2,8*})

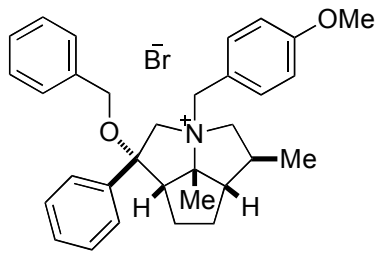

V{*5,2,8*}

Data for **V**{*5,2,8*}:

Yield: 105 mg (89%), free-flowing white powder

^{1}H-NMR: (500 MHz, $CDCl_3$)

7.76 (d, *J* = 7.5, 2 H), 7.67 (t, *J* = 7.7, 2 H), 7.57 (t, *J* = 7.4, 1 H), 7.36 (d, *J* = 8.7, 2 H), 7.32–7.23 (m, 3 H), 7.16–7.10 (m, 2 H), 6.84 (d, *J* = 8.7, 2 H), 5.17 (d, *J* = 12.1, 1 H), 4.98 (t, *J* = 11.9, 1 H), 4.28 (d, *J* = 13.0, 1 H), 3.99 (d, *J* = 10.7, 1 H), 3.82 (d, *J* = 10.6, 1 H), 3.78 (s, 3 H), 3.52 (d, *J* = 13.1, 1 H), 3.44 (dd, *J* = 9.3, 9.3, 1 H), 3.31 (d, *J* = 12.2, 1 H), 2.96 (dd, *J* = 6.0, 11.4, 1 H), 2.84 (dd, *J* = 5.71, 10.1, 1 H), 2.50–2.38 (m, 1 H), 2.26 (s, 3 H), 2.25–2.15 (m, 2 H), 1.98–1.89 (m, 2 H), 1.29 (d, *J* = 6.4, 1 H)

MS: (ESI, Q-tof)

468.3 (100)

Mol. Formula: $C_{32}H_{38}BrNO_2$ (548.55)

HRMS: $C_{32}H_{38}NO_2^+$: (468.2903)

Calcd: 468.2903

Found: 468.2901

TLC: R_f 0.20 (CH_2Cl_2/MeOH, 9:1) [I_2]

Preparation of *rel*-(1*R*,3*R*,5*S*,5a*S*,7a*S*,7b*R*) Octahydro-1-benzyloxy-1-phenyl-3-(4-trifluoromethylbenzyl)-5-methyl-7b-methylcyclopenta[*gh*]pyrrolizinium Bromide (V{*5,2,9*})

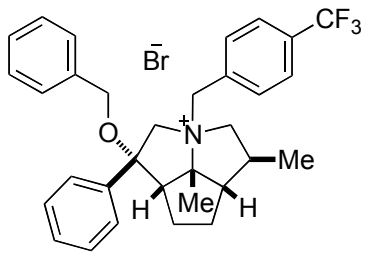

V{*5,2,9*}

Data for **V**{*5,2,9*}:

Yield: 35 mg (89%), free-flowing white powder

^{1}H-NMR: (500 MHz, $CDCl_3$)

7.77 (m, 2 H), 7.69 (dd, *J* = 7.8, 7.8, 2 H), 7.64-7.57 (m, 5 H) 7.30 (m, 3 H), 7.13 (m, 2 H), 5.50 (d, *J* = 12.1, 1 H), 5.12 (dd, *J* = 11.8, 11.8, 1 H), 4.21 (d, *J* = 13.1, 1 H), 4.01 (d, *J* = 10.7, 1 H), 3.84 (d, *J* = 10.7, 1 H), 3.57 (d, *J* = 13.1, 1 1 H), 3.45 (dd, *J* = 9.3, 9.3, 1 H), 3.44 (d, *J* = 12.2, 1 H), 2.97 (dd, *J* = 6.1, 11.3, 1 H), 2.82 (dd, *J* = 5.9, 10.1, 1 H), 2.46 (m, 1 H), 2.31 (s, 3 H), 2.25 (m, 2 H), 1.96 (m, 2 H), 1.30 (d, *J* = 6.4, 3 H)

MS: (ESI, Q-tof)

506.3 (100)

Mol. Formula: $C_{32}H_{35}BrF_3NO$ (586.53)

HRMS: $C_{32}H_{35}F_3NO^+$: (506.2671)

Calcd: 506.2671

Found: 506.2670

TLC: R_f 0.25 (CH_2Cl_2/MeOH, 9:1) [I_2]

Preparation of *rel*-(1*R*,3*R*,5*S*,5a*S*,7a*S*,7b*R*) Octahydro-1-benzyloxy-1-phenyl-3-(4-cyanobenzyl)-5-methyl-7b-methylcyclopenta[*gh*]pyrrolizinium Bromide (V{*5,2,10*})

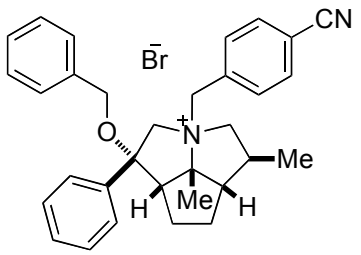

V{*5,2,10*}

Data for V{*5,2,10*}:

Yield: 35 mg (95%), free-flowing white powder

^{1}H-NMR: (500 MHz, $CDCl_3$)

7.77 (d, *J* = 7.4, 2 H), 7.71-7.63 (m, 6H), 7.60 (dd, *J* = 7.3, 7.3, 1 H), 7.31-7.26 (m, 3 H), 7.13-7.10 (m, 2 H), 5.54 (d, *J* = 12.0, 1 H), 5.13 (dd, *J* = 11.8, 11.8, 1 H), 4.16 (d, *J* = 13.2, 1 H), 4.01 (d, *J* = 10.6, 1 H), 3.83 (d, *J* = 10.6, 1 H), 3.58 (d, *J* = 13.1, 1 H), 3.48-3.40 (m, 2 H), 2.94 (dd, *J* = 6.1, 11.2, 1 H), 2.80 (dd, *J* = 5.8, 10.0, 1 H), 2.50-2.40 (m, 1 H), 2.30 (s, 3 H), 2.30-2.17 (m, 2 H), 2.00-1.92 (m, 2 H), 1.29 (d, *J* = 6.3, 1 H)

MS: (ESI, Q-tof)

463.3 (100)

Mol. Formula: $C_{32}H_{35}BrN_2O$ (543.54)

HRMS: $C_{32}H_{35}N_2O^+$: 463.2749)

Calcd: 463.2749

Found: 463.2742

TLC: R_f 0.19 (CH_2Cl_2/MeOH, 9:1) [I_2]

Preparation of Quaternary Ammonium Bromides V{*5,3,R*^{4}}

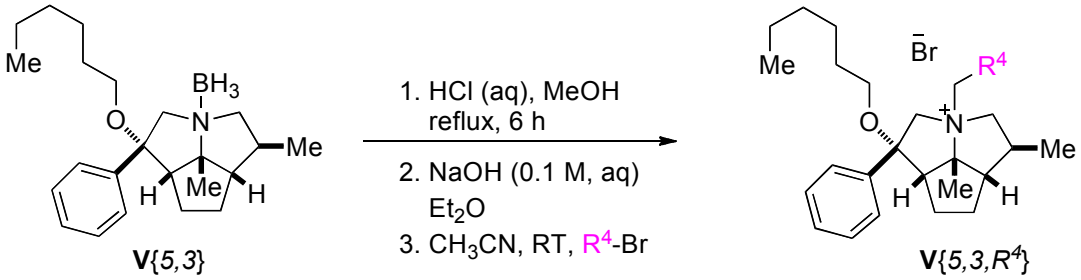

V{*5,3*} **V**{*5,3,R*^{4}}

Following General Procedure II, amino borane **V**{*5,3*} (403 mg, 1.13 mmol) was added to a 100-mL round-bottomed flask as a solution in 43 mL of MeOH (0.03 M). The flask was fitted with a reflux condenser, a magnetic stir bar, and a nitrogen inlet adapter. Lastly, 1.0 N aq. HCl solution (6.9, 5.0 equiv) was added via syringe. The resulting solution was heated and then concentrated by rotary evaporation (15 mm Hg, 20-25 ^{o}C) as described General Procedure II. The resulting free amine was dissolved in acetonitrile and was distributed among six test tubes that were subsequently charged with benzyl bromide (tube 1, 37 mg, 0.215 mmol, 1.2 equiv), 1-bromomethylnaphthalene (tube 2, 48 mg, 0.215 mmol, 1.2 equiv), 2-bromomethylnaphthalene (tube 3, 48 mg, 0.215 mmol, 1.2 equiv), 3,5-bis(trifluoromethyl)benzyl bromide (tube 4, 66 mg, 0.215 mmol, 1.2 equiv), 3,5-bis(*t*-butyl)benzyl bromide (tube 5, 61 mg, 0.215 mmol, 1.2 equiv), 4-methoxybenzyl bromide (tube 6, (43 mg, 0.215 mmol, 1.2 equiv). After being agitated for 12 h, the reaction mixtures were worked up and the products isolated and purified as described in General Procedure II.

Preparation of *rel*-(1*R*,3*R*,5*S*,5a*S*,7a*S*,7b*R*) Octahydro-1-hexyloxy-1-phenyl-3-benzyl-5-methyl-7b-methylcyclopenta[*gh*]pyrrolizinium Bromide (V{*5,3,1*})

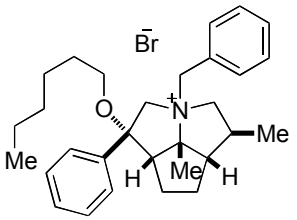

V{*5,3,1*}

Data for **V**{*5,3,1*}:

Yield: 82 mg (89%), free-flowing white powder

^{1}H-NMR: (500 MHz, $CDCl_3$)

7.65 (t, *J* = 8.1, 2 H), 7.62 (d, *J* = 8.07, 2 H), 7.53 (t, *J* = 7.2, 1 H), 7.41 (d, *J* = 6.61, 2 H), 7.39–7.31 (m, 3 H), 5.22 (d, *J* = 12.0, 1 H), 5.02 (dd, *J* = 11.9, 11.9, 1 H), 4.21 (d, *J* = 13.0, 1 H), 3.44 (d, *J* = 13.2, 1 H), 3.34 (d, *J* = 12.0, 1 H), 3.31 (dd, *J* = 9.28, 9.28, 1 H), 2.98 (dd, *J* = 6.1, 11.4, 1 H), 2.90 (ddd, *J* = 6.4, 8.8, 8.8, 1 H), 2.83 (dd, *J* = 6.0, 10.1, 1 H), 2.74 (ddd, *J* = 6.7, 8.8, 8.8, 1 H), 2.40–2.30 (m, 1 H), 2.28–2.19 (m, 1 H), 2.25 (s, 3 H), 2.12–2.03 (m, 1 H), 1.98–1.84 (m, 2 H), 1.41–1.34 (m, 2 H), 1.31 (d, *J* = 6.4, 3 H), 1.27–1.10 (m, 6H), 0.84 (t, *J* = 7.2, 3 H)

MS: (ESI, Q-tof)

432.3 (100)

Mol. Formula: $C_{30}H_{42}BrNO$ (512.56)

HRMS: $C_{30}H_{42}NO^+$: (432.3266)

Calcd: 432.3266

Found: 432.3263

TLC: R_f 0.25 (CH_2Cl_2/MeOH, 9:1) [I_2]

Preparation of *rel*-(1*R*,3*R*,5*S*,5a*S*,7a*S*,7b*R*) Octahydro-1-hexyloxy-1-phenyl-3-(1-naphthylmethyl)-5-methyl-7b-methylcyclopenta[*gh*]pyrrolizinium Bromide (V{*5,3,2*})

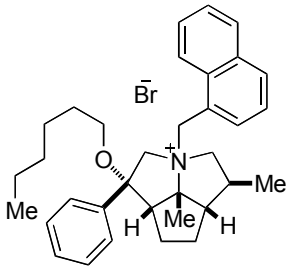

V{*5,3,2*}

Data for **V**{*5,3,2*}:

Yield: 94 mg (93%), free-flowing white powder

^{1}H-NMR: (500 MHz, $CDCl_3$)

7.93–7.87 (m, 3 H), 7.85 (d, *J* = 8.1, 1 H), 7.62-7.59 (m, 4 H), 7.58–7.44 (m, 4 H), 5.54 (d, *J* = 12.8, 1 H), 4.71 (dd, *J* = 11.8, 11.8, 1 H), 4.63 (d, *J* = 13.3, 1 H), 4.57 (d, *J* = 12.8, 1 H), 3.54 (d, *J* = 13.2, 1 H), 3.26 (dd, *J* = 8.9, 8.9, 1 H), 3.01 (dd, *J* = 5.5, 10.1, 1 H), 2.93 (dd, *J* = 6.5, 11.5, 1 H), 2.87–2.87 (m, 2 H), 2.56–2.46 (m, 1 H), 2.43–2.33(m, 1 H), 2.09–2.01 (m, 1 H), 2.01–1.91 (m, 2 H), 1.36 (dd, *J* = 6.9, 14.0, 2 H), 1.26 (d, *J* = 6.4, 2 H), 1.24–1.07 (m, 8H), 0.82 (t, *J* = 7.2, 3 H)

MS: (ESI, Q-tof)

482.3 (100)

Mol. Formula: $C_{34}H_{44}BrNO$ (562.62)

HRMS: $C_{34}H_{44}NO^+$: (482.3423)

Calcd: 482.3423

Found: 482.3428

TLC: R_f 0.28 (CH_2Cl_2/MeOH, 9:1) [I_2]

Preparation of *rel*-(1*R*,3*R*,5*S*,5a*S*,7a*S*,7b*R*) Octahydro-1-hexyloxy-1-phenyl-3-(2-naphthylmethyl)-5-methyl-7b-methylcyclopenta[*gh*]pyrrolizinium Bromide (V{*5,3,3*})

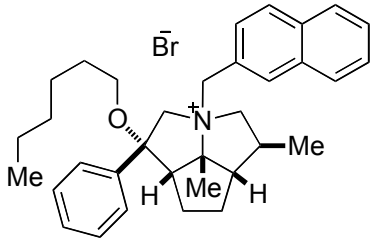

V{*5,3,3*}

Data for **V**{*5,3,3*}:

Yield: 103 mg (99%), free-flowing white powder

^{1}H-NMR: (500 MHz, $CDCl_3$)

7.85–7.79 (m, 3 H), 7.73–7.66 (m, 4 H), 7.65–7.57 (m, 3 H), 7.56–7.50 (m, 2 H), 5.44 (d, *J* = 12.1, 1 H), 5.14 (dd, *J* = 11.9, 11.9, 1 H), 4.27 (d, *J* = 13.0, 1 H), 3.53 (d, *J* = 12.1, 1 H), 3.43 (d, *J* = 13.0, 1 H), 3.34 (dd, *J* = 9.3, 9.3, 1 H), 3.06 (dd, *J* = 6.1, 11.3, 1 H), 2.91 (ddd, *J* = 6.38, 8.90, 8.90, 1 H), 2.87 (dd, *J* = 5.8, 10.2, 1 H), 2.75 (dd, *J* = 6.7, 15.5, 1 H), 2.44–2.19 (m, 2 H), 2.30 (s, 3 H), 2.13–2.05 (m, 1 H), 1.97–1.87 (m, 2 H), 1.40– 1.34 (m, 2 H), 1.33 (d, *J* = 6.4, 3 H), 1.28–1.09 (m, 7H), 0.83 (t, *J* = 7.2, 3 H)

MS: (ESI, Q-tof)

482.3 (100)

Mol. Formula: $C_{34}H_{44}BrNO$ (562.62)

HRMS: $C_{34}H_{44}NO^+$: (482.3423)

Calcd: 482.3423

Found: 482.3423

TLC: R_f 0.29 (CH_2Cl_2/MeOH, 9:1) [I_2]

Preparation of *rel*-(1*R*,3*R*,5*S*,5a*S*,7a*S*,7b*R*) Octahydro-1-hexyloxy-1-phenyl-3-(3,5-trifluoromethyl-benzyl)-5-methyl-7b-methylcyclopenta[*gh*]pyrrolizinium Bromide (V{*5,3,5*})

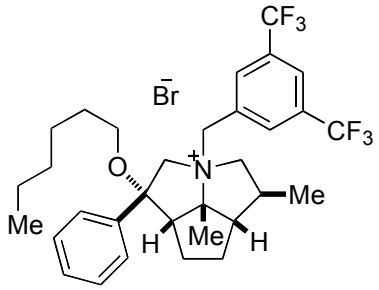

V{*5,3,5*}

Data for **V**{*5,3,5*}:

Yield: 104mg (90%), free-flowing white powder

^{1}H-NMR: (500 MHz, $CDCl_3$)

7.90 (s, 2 H), 7.69–7.63 (m, 4 H), 7.61–7.56 (m, 1 H), 5.92 (d, *J* = 12.3, 1 H), 5.32 (dd, *J* = 11.6, 11.6, 1 H), 3.88 (d, *J* = 13.1, 1 H), 3.49 (d, *J* = 13.1, 1 H), 3.39–3.32 (m, 2 H), 3.00 (dd, *J* = 6.0, 11.0, 1 H), 2.91 (dd, *J* = 6.5, 15.2, 1 H), 2.79 (dd, *J* = 6.19, 10.1, 1 H), 2.75 (dd, *J* = 6.67, 15.4, 1 H), 2.43–2.20 (m, 2 H), 2.30 (s, 3 H), 2.15-2.09 (m, 1 H), 2.00–1.89 (m, 2 H), 1.42-1.35 (m, 2 H), 1.33 (d, *J* = 6.3, 3 H), 1.28–1.12 (m, 6H), 0.84 (t, *J* = 7.2, 3 H)

MS: (ESI, Q-tof)

568.3 (100)

Mol. Formula: $C_{32}H_{40}BrF_6NO$ (648.56)

HRMS: $C_{32}H_{40}NOF_6^+$: (568.3014)

Calcd: 568.3014

Found: 568.3007

TLC: R_f 0.39 (CH_2Cl_2/MeOH, 9:1) [I_2]

Preparation of *rel*-(1*R*,3*R*,5*S*,5a*S*,7a*S*,7b*R*) Octahydro-1-hexyloxy-1-phenyl-3-(3,5-*tert*-butylbenzyl)-5-methyl-7b-methylcyclopenta[*gh*]pyrrolizinium Bromide (V{*5*,*3*,*7*})

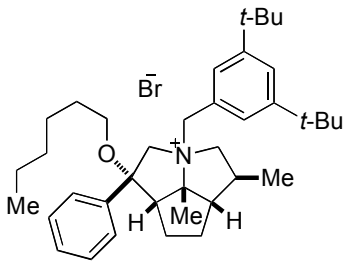

V{*5*,*3*,*7*}

Data for **V**{*5*,*3*,*7*}:

Yield: 105 mg (93%), free-flowing white powder

^{1}H-NMR: (500 MHz, $CDCl_3$)

7.67 (d, *J* = 7.3, 2 H), 7.62 (t, *J* = 7.7, 2 H), 7.52 (t, *J* = 7.2, 1 H), 7.40 (s, 1 H), 7.30 (s, 2 H), 5.16 (d, *J* = 11.9, 1 H), 5.08 (dd, *J* = 11.9, 11.9, 1 H), 4.26 (d, *J* = 12.9, 1 H), 3.44 (d, *J* = 12.9, 1 H), 3.34 (dd, *J* = 9.3, 9.3, 1 H), 3.22 (d, *J* = 12.0, 1 H), 2.95–2.87 (m, 2 H), 2.84 (dd, *J* = 5.8, 9.9, 1 H), 2.73 (dd, *J* = 6.8, 15.5, 1 H), 2.39–2.29 (m, 1 H), 2.26 (s, 3 H), 2.23–2.15 (m, 1 H), 2.12–2.05 (m, 1 H), 1.96–1.86 (m, 2 H), 1.42–1.35 (m, 2 H), 1.35–1.11 (m, 27H), 0.84 (t, *J* = 7.2, 3 H)

MS: (ESI, Q-tof)

544.5 (100)

Mol. Formula: $C_{38}H_{58}BrNO$ (624.68)

HRMS: $C_{38}H_{58}NO^+$: (544.4518)

Calcd: 544.4518

Found: 544.4509

TLC: R_f 0.41 (CH_2Cl_2/MeOH, 9:1) [I_2]

Preparation of *rel*-(1*R*,3*R*,5*S*,5a*S*,7a*S*,7b*R*) Octahydro-1-hexyloxy-1-phenyl-3-(4-methoxybenzyl)-5-methyl-7b-methylcyclopenta[*gh*]pyrrolizinium Bromide (V**{*5,3,8*})**

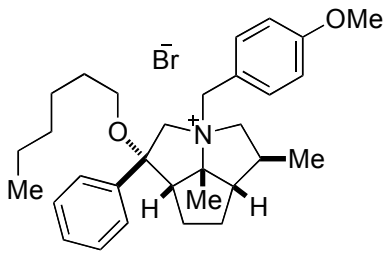

V{*5,3,8*}

Data for **V**{*5,3,8*}:

Yield: 87 mg (90%), free-flowing white powder

^{1}H-NMR: (500 MHz, $CDCl_3$)

7.67–7.59 (m, 4 H), 7.52 (t, *J* = 7.1, 1 H), 7.35 (d, *J* = 8.7, 2 H), 6.84 (d, *J* = 8.8, 2 H), 5.13 (d, *J* = 12.2, 1 H), 4.94 (dd, *J* = 11.9, 11.9, 1 H), 4.19 (d, *J* = 12.8, 1 H), 3.78 (s, 4 H), 3.42 (d, *J* = 13.2, 1 H), 3.33–3.26 (m, 2 H), 2.96 (dd, *J* = 6.0, 11.4, 1 H), 2.90 (ddd, *J* = 6.3, 8.7, 8.7, 1 H), 2.81 (dd, *J* = 6.0, 10.2, 1 H), 2.73 (dd, *J* = 6.7, 15.4, 1 H), 2.42–2.29 (m, 1 H), 2.28–2.16 (m, 1 H), 2.22 (s, 3 H), 2.10-2.03 (m, 1 H), 1.98–1.85 (m, 2 H), 1.40–1.34 (m, 2 H), 1.30 (d, *J* = 6.4, 3 H), 1.27–1.10 (m, 6H), 0.84 (t, *J* = 7.2, 3 H)

MS: (ESI, Q-tof)

462.3 (100)

Mol. Formula: $C_{31}H_{44}BrNO_2$ (542.59)

HRMS: $C_{31}H_{44}NO_2^+$: (462.3372)

Calcd: 462.3372

Found: 462.3372

TLC: R_f 0.25 (CH_2Cl_2/MeOH, 9:1) [I_2]

Preparation of Quaternary Ammonium Bromides V{*5,6,R*^{4}}:

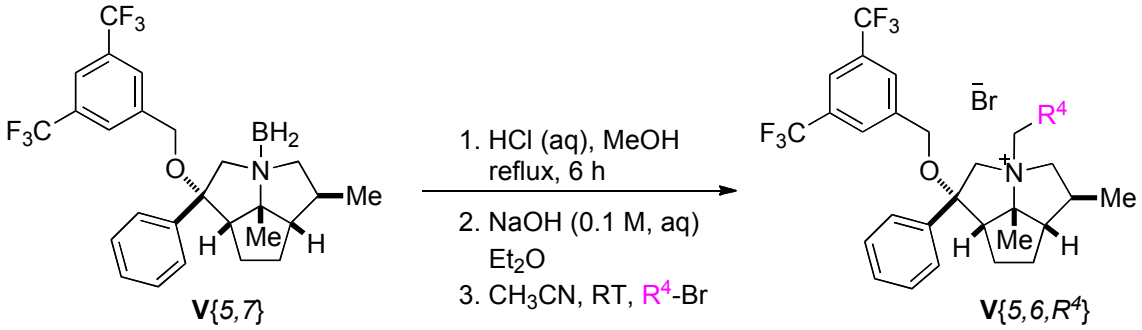

Following General Procedure II, amino borane **V**{*5,6*} (80 mg, 0.161 mmol) was added to a 100-mL round-bottomed flask as a solution in 5.4 mL of MeOH (0.03 M). The flask was fitted with a reflux condenser, a magnetic stir bar, and a nitrogen inlet adapter. Lastly, 1.0 N aq. HCl solution (0.8, 5.0 equiv) was added via syringe. The resulting solution was heated and then concentrated by rotary evaporation (15 mm Hg, 20-25 ^{o}C) as described General Procedure II. The resulting free amine was dissolved in acetonitrile and was distributed among three test tubes that were subsequently charged with benzyl bromide (tube 1, 8 mg, 0.048 mmol, 1.2 equiv), 3,5-bis(*t*-butyl)benzyl bromide (tube 2, 15 mg, 0.048 mmol, 1.2 equiv),), 4-methoxybenzyl bromide (tube 3, 10 mg, 0.048 mmol, 1.2 equiv). After being agitated for 12 h, the reaction mixtures were worked up and the products isolated and purified as described in General Procedure II.

Preparation of *rel*-(1*R*,3*R*,5*S*,5a*S*,7a*S*,7b*R*) Octahydro-1-(3,5-trifluoromethylbenzyloxy)-1-phenyl-3-benzyl-5-methyl-7b-methylcyclopenta[*gh*]pyrrolizinium Bromide (V{*5,6,1*})

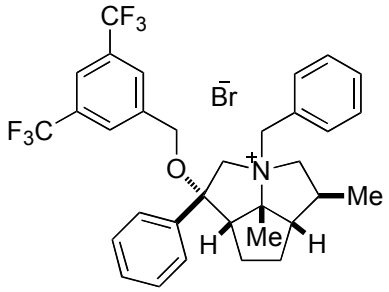

V{*5,6,1*}

Data for **V**{*5,6,1*}:

Yield: 21 mg (79%), free-flowing white powder

^{1}H-NMR: (500 MHz, $CDCl_3$)

7.79–7.75 (m, 2 H), 7.75 (s, 1 H), 7.69 (t, *J* = 7.8, 2 H), 7.60 (t, *J* = 7.3, 1 H), 7.54 (s, 2 H), 7.44–7.33 (m, 5 H), 5.31 (d, *J* = 12.1, 1 H), 5.13 (dd, *J* = 11.9, 11.9, 1 H), 4.34 (d, *J* = 13.0, 1 H), 4.16 (d, *J* = 12.0, 1 H), 3.95 (d, *J* = 12.0, 1 H), 3.59 (d, *J* = 13.1, 1 H), 3.49 (dd, *J* = 9.4, 9.4, 1 H), 3.30 (d, *J* = 12.1, 1 H), 3.04 (dd, *J* = 6.0, 11.4, 1 H), 2.90 (dd, *J* = 5.9, 10.3, 1 H), 2.45–2.20 (m, 2 H), 2.31 (s, 3 H), 2.20–2.10 (m, 1 H), 2.02–1.92 (m, 2 H), 1.33 (d, *J* = 6.4, 3 H)

MS: (ESI, Q-tof)

574.3 (100)

Mol. Formula: $C_{33}H_{34}BrF_6NO$ (654.52)

HRMS: $C_{33}H_{34}NOF_6^+$: 574.2545)

Calcd: 574.2545

Found: 574.2549

TLC: R_f 0.28 (CH_2Cl_2/MeOH, 9:1) [I_2]

Preparation of *rel*-(1*R*,3*R*,5*S*,5a*S*,7a*S*,7b*R*) Octahydro-1-(3,5-trifluoromethylbenzyloxy)-1-phenyl-3-(3,5-trifluoromethylbenzyl)-5-methyl-7b-methylcyclopenta[*gh*]pyrrolizinium Bromide (V{*5,6,5*})

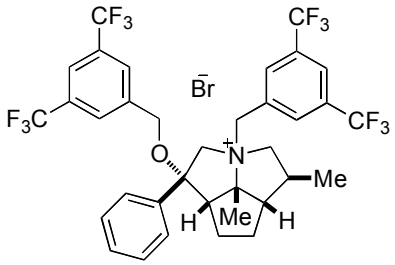

V{*5,6,5*}

Data for **V**{*5,6,5*}:

Yield: 21 mg (66%), free-flowing white powder

^{1}H-NMR: (500 MHz, $CDCl_3$)

7.93 (s, 1 H), 7.89 (s, 2 H), 7.79 (s, 1 H), 7.76–7.70 (m, 3 H), 7.70–7.63 (m, 2 H), 7.55 (s, 2 H), 6.00 (d, *J* = 12.3, 1 H), 5.41 (dd, *J* = 11.7, 11.7, 1 H), 4.16 (d, *J* = 11.9, 1 H), 4.02 (d, *J* = 13.0, 1 H), 3.96 (d, *J* = 12.0, 1 H), 3.65 (d, *J* = 13.1, 1 H), 3.52 (dd, *J* = 9.3, 9.3, 1 H), 3.34 (d, *J* = 12.4, 1 H), 3.09 (dd, *J* = 11.0, 6.0, 1 H), 2.86 (dd, *J* = 5.8, 10.1, 1 H), 2.45–2.26 (m, 2 H), 2.36 (s, 3 H), 2.24–2.15 (m, 1 H), 2.07–1.93 (m, 2 H), 1.35 (d, *J* = 6.3, 3 H)

MS: (ESI, Q-tof)

710.2 (100)

Mol. Formula: $C_{35}H_{32}BrF_{12}NO$ (790.52)

HRMS: $C_{35}H_{32}NOF_{12}^+$: 710.2292)

Calcd: 710.2292

Found: 710.2285

TLC: R_f 0.35 (CH_2Cl_2/MeOH, 9:1) [I_2]

Preparation of *rel*-(1*R*,3*R*,5*S*,5a*S*,7a*S*,7b*R*) Octahydro-1-(3,5-trifluoromethylbenzyloxy)-1-phenyl-3-(4-methoxybenzyl)-5-methyl-7b-methylcyclopenta[*gh*]pyrrolizinium Bromide (V**{*5,6,8*})**

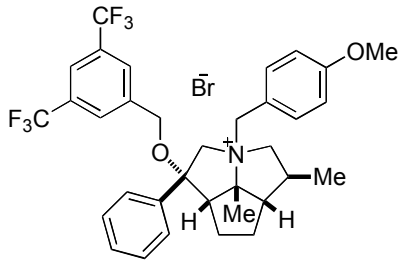

V{*5,6,8*}

Data for **V**{*5,6,8*}:

Yield: 22 mg (82%), free-flowing white powder

^{1}H-NMR: (500 MHz, $CDCl_3$)

7.80–7.72 (m, 3 H), 7.76 (t, *J* = 7.8, 2 H), 7.59 (t, *J* = 7.3, 1 H), 7.54 (s, 2 H), 7.35 (d, *J* = 8.7, 2 H), 6.86 (d, *J* = 8.8, 2 H), 5.22 (d, *J* = 12.1, 1 H), 5.06 (dd, *J* = 12.0, 12.0, 1 H), 4.33 (d, *J* = 13.1, 1 H), 4.16 (d, *J* = 12.0, 1 H), 3.95 (d, *J* = 12.0, 1 H), 3.79 (s, 3 H), 3.56 (d, *J* = 13.1, 1 H), 3.48 (dd, *J* = 9.3, 9.3, 1 H), 3.25 (d, *J* = 12.2, 1 H), 3.02 (dd, *J* = 6.0, 11.5, 1 H), 2.88 (dd, *J* = 5.6, 10.3, 1 H), 2.43–2.31 (m, 1 H), 2.31–2.18 (m, 2 H), 2.28 (s, 3 H), 2.18–2.10 (s, 1 H), 2.01–1.91 (m, 2 H), 1.32 (d, *J* = 6.3, 3 H)

MS: (ESI, Q-tof)

604.3 (100)

Mol. Formula: $C_{34}H_{36}BrF_6NO_2$ (684.55)

HRMS: $C_{34}H_{36}NO_2F_6^+$: 604.2650)

Calcd: 604.2650

Found: 604.2649

TLC: R_f 0.29 (CH_2Cl_2/MeOH, 9:1) [I_2]

Preparation of Quaternary Ammonium Bromides V{*5*,7,R^4}:

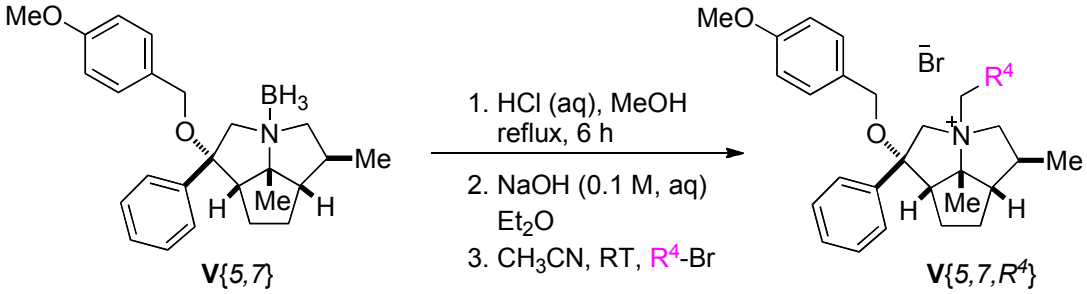

Following General Procedure II, amino borane **V**{*5*,7} (606 mg, 1.55 mmol) was added to a 100-mL round-bottomed flask as a solution in 47 mL of MeOH (0.03 M). The flask was fitted with a reflux condenser, a magnetic stir bar, and a nitrogen inlet adapter. Lastly, 1.0 N aq. HCl solution (7.0, 5.0 equiv) was added via syringe. The resulting solution was heated and then concentrated by rotary evaporation (15 mm Hg, 20-25 ^{o}C) as described General Procedure II. The resulting free amine was dissolved in acetonitrile and was distributed among five test tubes that were subsequently charged with benzyl bromide (tube 1, 34 mg, 0.199 mmol, 1.2 equiv), 1-bromomethylnaphthalene (tube 2, 45 mg, 0.199 mmol, 1.2 equiv), 2-bromomethylnaphthalene (tube 3, 45 mg, 0.199 mmol, 1.2 equiv), 3,5-bis(trifluoromethyl)benzyl bromide (tube 4, 62 mg, 0.199 mmol, 1.2 equiv), 3,5-bis(*t*-butyl)benzyl bromide (tube 5, 57 mg, 0.199 mmol, 1.2 equiv). After being agitated for 12 h, the reaction mixtures were worked up and the products isolated and purified as described in General Procedure II.

Preparation of *rel*-(1*R*,3*R*,5*S*,5a*S*,7a*S*,7b*R*) Octahydro-1-(4-methoxybenzyloxy)-1-phenyl-3-benzyl-5-methyl-7b-methylcyclopenta[*gh*]pyrrolizinium Bromide (V{*5,7,1*})

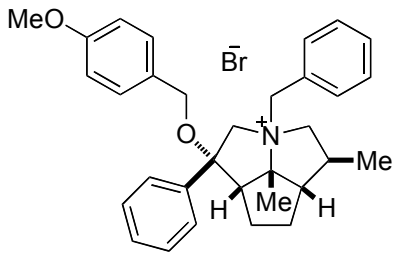

V{*5,7,1*}

Data for **V**{*5,7,1*}**:**

Yield: 89 mg (98%), free-flowing white powder

^{1}H-NMR: (500 MHz, $CDCl_3$)

7.77 (d, *J* = 7.3, 2 H), 7.68 (t, *J* = 7.7, 2 H), 7.57 (t, *J* = 7.3, 1 H), 7.45–7.40 (m, 2 H), 7.39–7.31 (m, 3 H), 7.04 (d, *J* = 8.7, 2 H), 6.81 (d, *J* = 8.7, 2 H), 5.24 (d, *J* = 12.2, 1 H), 5.02 (dd, *J* = 11.9, 11.9, 1 H), 4.27 (d, *J* = 13.2, 1 H), 3.92 (d, *J* = 10.2, 1 H), 3.77 (s, 3 H), 3.70 (d, *J* = 10.2, 1 H), 3.50 (d, *J* = 13.1, 1 H), 3.44 (dd, *J* = 9.0, 9.0, 1 H) 3.35 (d, *J* = 12.1, 1 H), 2.96 (dd, *J* = 6.1, 11.5, 1 H), 2.85 (dd, *J* = 5.5, 9.9, 1 H), 2.49–2.39 (m, 1 H), 2.29 (s, 3 H), 2.25–2.11 (m, 2 H), 1.99–1.89 (m, 2 H), 1.29 (t, *J* = 7.1, 3 H).

MS: (ESI, Q-tof)

468.3 (100)

Mol. Formula: $C_{32}H_{38}BrNO_2$ (548.55)

HRMS: $C_{32}H_{38}NO_2^+$: 468.2903)

Calcd: 468.2903

Found: 468.2899

TLC: R_f 0.21 (CH_2Cl_2/MeOH, 9:1) [I_2]

Preparation of *rel*-(1*R*,3*R*,5*S*,5a*S*,7a*S*,7b*R*) Octahydro-1-(4-methoxy-benzyloxy)-1-phenyl-3-(1-naphthylmethyl)-5-methyl-7b-methylcyclopenta[*gh*]pyrrolizinium Bromide (V{*5,7,2*})

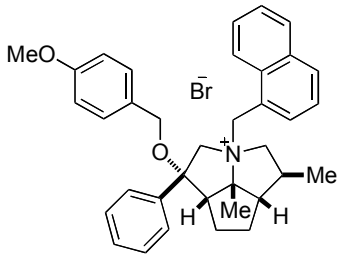

V{*5,7,2*}

Data for **V**{*5,7,2*}**:**

Yield: 95 mg (95%), free-flowing white powder

^{1}H-NMR: (500 MHz, $CDCl_3$)

7.94 (d, *J* = 8.7, 1 H), 7.89 (d, *J* = 8.3, 1 H), 7.86–7.82 (m, 2 H), 7.74 (d, *J* = 7.4, 2 H), 7.67 (t, *J* = 7.7, 2 H), 7.59-7.54 (m, 2 H), 7.52–7.43 (m, 2 H), 7.02 (d, *J* = 8.7, 2 H), 6.78 (d, *J* = 8.7, 2 H), 5.54 (d, *J* = 12.8, 1 H), 4.73–4.64 (m, 2 H), 4.52 (d, *J* = 12.8, 1 H), 3.91 (d, *J* = 10.9, 1 H), 3.83 (d, *J* = 10.9, 1 H), 3.75 (s, 3 H), 3.59 (d, *J* = 13.3, 1 H), 3.38 (dd, *J* = 9.1, 9.1, 1 H), 3.02 (d, *J* = 10.9, 1 H), 2.87 (dd, *J* = 6.2, 11.6, 1 H), 2.61–2.50 (m, 1 H), 2.45 (s, 3 H), 2.35–2.26 (m, 1 H), 2.20–2.11 (m, 1 H), 1.98 (d, *J* = 10.1, 3 H), 1.22 (d, *J* = 6.4, 3 H)

MS: (ESI, Q-tof)

518.3 (100)

Mol. Formula: $C_{36}H_{40}BrNO_2$ (598.61)

HRMS: $C_{36}H_{40}NO_2^+$: 518.3059)

Calcd: 518.3059

Found: 518.3065

TLC: R_f 0.25 (CH_2Cl_2/MeOH, 9:1) [I_2]

Preparation of *rel*-(1*R*,3*R*,5*S*,5a*S*,7a*S*,7b*R*) Octahydro-1-(4-methoxybenzyloxy)-1-phenyl-3-(2-naphthylmethyl)-5-methyl-7b-methylcyclopenta[*gh*]pyrrolizinium Bromide (V{*5*,7,*3*})

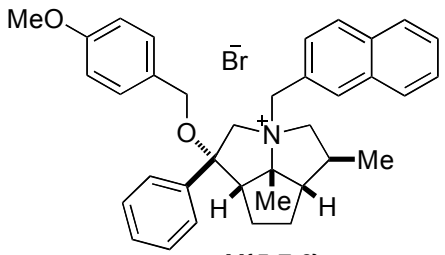

V{*5,7,3*}

Data for **V**{*5*,7,*3*}**:**

Yield: 92 mg (92%), free-flowing white powder

^{1}H-NMR: (500 MHz, $CDCl_3$)

7.86–7.78 (m, 5 H), 7.75 (t, *J* = 7.7, 3 H), 7.69–7.57 (m, 3 H), 7.56–7.48 (m, 2 H), 7.03 (d, *J* = 8.7, 2 H), 6.80 (d, *J* = 8.7, 2 H), 5.46 (d, *J* = 11.9, 1 H), 5.15 (dd, *J* = 11.9, 11.9, 1 H), 4.33 (d, *J* = 12.8, 1 H), 3.93 (d, *J* = 10.2, 1 H), 3.77 (d, *J* = 10.3, 1 H), 3.76 (s, 3 H), 3.54 (d, *J* = 12.1, 1 H), 3.51–3.43 (m, 2 H), 3.03 (dd, *J* = 6.0, 11.3, 1 H), 2.91–2.86 (m, 1 H), 2.51–2.40 (m, 1 H), 2.34 (s, 3 H), 2.27–2.17 (m, 2 H), 1.99–1.93 (m, 2 H), 1.31 (d, *J* = 6.3, 3 H)

MS: (ESI, Q-tof)

518.3 (100)

Mol. Formula: $C_{36}H_{40}BrNO_2$ (598.61)

HRMS: $C_{36}H_{40}NO_2^+$: 518.3059)

Calcd: 518.3059

Found: 518.3071

TLC: R_f 0.26 (CH_2Cl_2/MeOH, 9:1) [I_2]

Preparation of *rel*-(1*R*,3*R*,5*S*,5a*S*,7a*S*,7b*R*) Octahydro-1-(4-methoxybenzyloxy)-1-phenyl-3-(3,5-trifluoromethylbenzyl)-5-methyl-7b-methylcyclopenta[*gh*]pyrrolizinium Bromide (V**{*5*,7,*5*})**

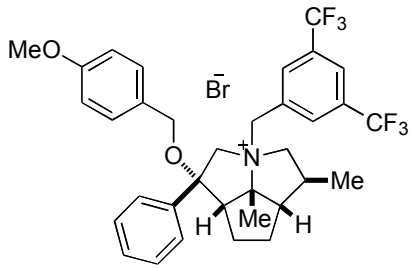

V{*5,7,5*}

Data for **V**{*5*,7,*5*}**:**

Yield: 97 mg (85%), free-flowing white powder

^{1}H-NMR: (500 MHz, $CDCl_3$)

7.92 (s, 2 H), 7.91 (s, 1 H), 7.81–7.68 (m, 4 H), 7.63 (t, *J* = 7.1, 1 H), 7.04 (d, *J* = 8.7, 2 H), 6.82 (d, *J* = 8.7, 2 H), 5.94 (d, *J* = 12.3, 1 H), 5.32 (dd, *J* = 11.6, 11.6, 1 H), 3.94 (d, *J* = 10.3, 2 H), 3.78 (s, 3 H), 3.55 (d, *J* = 13.0, 1 H), 3.48 (dd *J* = 9.4, 9.4, 1 H), 3.36 (d, *J* = 11.4, 1 H), 2.98 (dd, *J* = 5.7, 10.5, 1 H), 2.84–2.78 (m, 1 H), 2.52–2.38 (s, 1 H), 2.34 (s, 3 H), 2.25 (s, 2 H), 2.03–1.93 (m, 2 H), 1.31 (d, *J* = 6.3, 3 H)

MS: (ESI, Q-tof)

604.3 (100)

Mol. Formula: $C_{34}H_{36}BrF_6NO_2$ (684.55)

HRMS: $C_{34}H_{36}NO_2F_6^+$: 604.2650)

Calcd: 604.2650

Found: 604.2635

TLC: R_f 0.29 (CH_2Cl_2/MeOH, 9:1) [I_2]

Preparation of *rel*-(1*R*,3*R*,5*S*,5a*S*,7a*S*,7b*R*) Octahydro-1-(4-methoxybenzyloxy)-1-phenyl-3-(3,5-*tert*-butylbenzyl)-5-methyl-7b-methylcyclopenta[*gh*]pyrrolizinium Bromide (V{*5*,7,*7*})

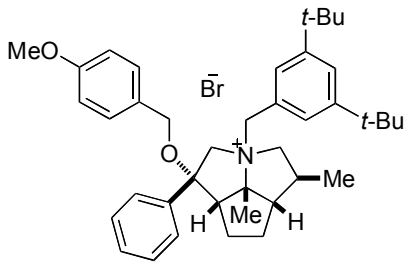

V{*5,7,7*}

Data for **V**{*5*,*7*,*7*}**:**

Yield: 103 mg (94%), free-flowing white powder

^{1}H-NMR: (500 MHz, $CDCl_3$)

7.78 (d, *J* = 7.5, 2 H), 7.68 (t, 2 H, *J* = 7.7), 7.57 (t, *J* = 7.4, 1 H), 7.40 (t, *J* = 1.6, 1 H), 7.33 (d, *J* = 1.4, 2 H), 7.07 (d, *J* = 8.6, 2 H), 6.83 (d, *J* = 8.7, 2 H), 5.17 (d, *J* = 11.7, 1 H), 5.09 (dd, *J* = 12.0, 12.0, 1 H), 4.33 (d, *J* = 13.0, 1 H), 3.95 (d, *J* = 10.2, 1 H), 3.78 (s, 3 H), 3.73 (d, *J* = 10.2, 1 H), 3.51 (d, *J* = 13.6, 1 H), 3.48 (dd, *J* = 9.4, 9.4 1 H), 3.24 (d, *J* = 12.0, 1 H), 2.92–2.84 (m, 2 H), 2.51–2.38 (m, 1 H), 2.30 (s, 3 H), 2.27–2.12 (m, 2 H), 1.98–1.92 (d, *J* = 6.4, 2 H), 1.31 (s, 18H), 1.29 (d, *J* = 6.3, 3 H)

MS: (ESI, Q-tof)

580.4 (100)

Mol. Formula: $C_{40}H_{54}BrNO_2$ (660.77)

HRMS: ($C_{40}H_{54}NO_2^+$: 580.4155)

Calcd: 580.4155

Found: 580.4160

TLC: R_f 0.31 (CH_2Cl_2/MeOH, 9:1) [I_2]

Preparation of Quaternary Ammonium Bromides V{*6,2,R*^{4}}

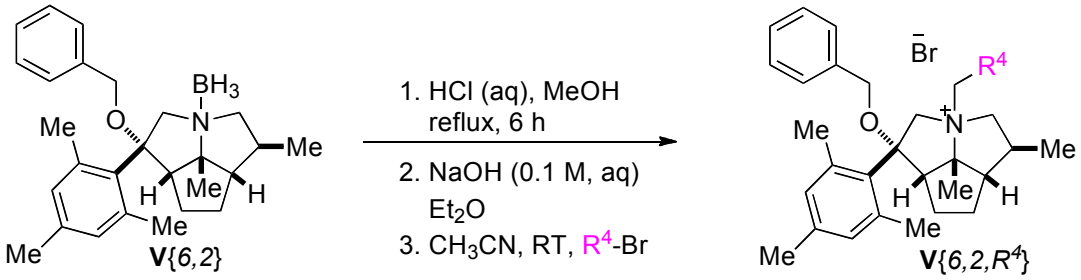

Following General Procedure II, amino borane **V**{*6,2*} (110 mg, 0.273 mmol) was added to a 100-mL round-bottomed flask as a solution in 9.1 mL of MeOH (0.03 M). The flask was fitted with a reflux condenser, a magnetic stir bar, and a nitrogen inlet adapter. Lastly, 1.0 N aq. HCl solution (1.4, 5.0 equiv) was added via syringe. The resulting solution was heated and then concentrated by rotary evaporation (15 mm Hg, 20-25 ^{o}C) as described General Procedure II. The resulting free amine was dissolved in acetonitrile and was distributed among three test tubes that were subsequently charged with benzyl bromide (tube 1, 13 mg, 0.073 mmol, 1.2 equiv), 3,5-bis(trifluoromethyl)benzyl bromide (tube 2, (94 mg, 0.915 mmol, 5.0 equiv), 4-methoxybenzyl bromide (tube 3, 15 mg, 0.073 mmol, 1.2 equiv). After being agitated for 12 h, the reaction mixtures were worked up and the products isolated and purified as described in General Procedure II.

Preparation of *rel*-(1*R*,3*R*,5*S*,5a*S*,7a*S*,7b*R*) Octahydro-1-benzyloxy-1-(2,4,6-methylphenyl)-3-benzyl-5-methyl-7b-methylcyclopenta[*gh*]pyrrolizinium Bromide (V{*6,2,1*}**)**

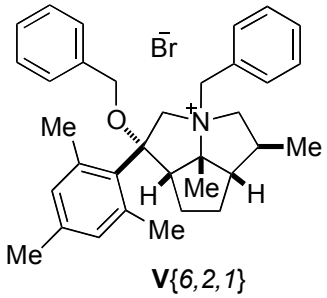

V{*6,2,1*}

Data for **V**{*6,2,1*}:

Yield: 25 mg (74%), free-flowing white powder

^{1}H-NMR: (500 MHz, $CDCl_3$)

7.57-7.43 (m, 2 H), 7.44-7.38 (m, 3 H), 7.32-7.27 (m, 3 H), 7.20-7.14 (m, 3 H), 6.98 (s, 1 H), 5.25 (d, *J* = 12.0, 1 H), 4.94 (dd, *J* = 11.6, 11.6, 1 H), 4.38 (d, *J* = 13.2, 1 H), 4.22 (d, *J* = 10.3, 1 H), 4.13-4.07 (m, 2 H), 3.58 (d, *J* = 13.2, 1 H), 3.37 (d, *J* = 12.0, 1 H), 3.11 (dd, *J* = 6.3, 11.4, 1 H), 2.83 (dd, *J* = 5.9, 9.3, 1 H), 2.74 (s, 3 H), 2.52 (s, 3 H), 2.51-2.42 (m, 1 H), 2.34 (s, 3 H), 2.26-2.17 (m, 2 H), 2.16 (s, 3 H), 1.94-1.83 (m, 2 H), 1.30 (d, *J* = 6.4, 3 H)

MS: (ESI, Q-tof)

480.3 (100)

Mol. Formula: $C_{34}H_{42}BrNO$ (560.61)

HRMS: $C_{34}H_{42}NO^+$: (480.3266)

Calcd: 480.3266

Found: 480.3260

TLC: R_f 0.26 (CH_2Cl_2/MeOH, 9:1) [I_2]

Preparation of *rel*-(1*R*,3*R*,5*S*,5a*S*,7a*S*,7b*R*) Octahydro-1-benzyloxy-1-(2,4,6-trimethyl-phenyl)-3-(3,5-trifluoromethylbenzyl)-5-methyl-7b-methylcyclopenta[*gh*]pyrrolizinium Bromide (V{*6,2,5*})

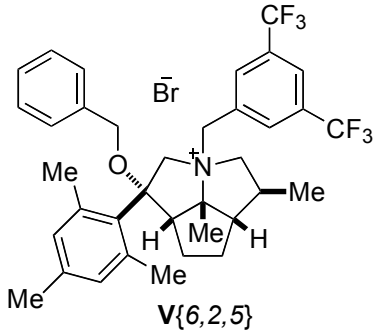

V{*6,2,5*}

Data for V{*6,2,5*}:

Yield: 22 mg (65%), free-flowing white powder

^{1}H-NMR: (500 MHz, $CDCl_3$)

8.11 (s, 2 H), 7.94 (s, 1 H), 7.34-7.29 (m, 3 H), 7.20-7.16 (m, 3 H), 7.02 (s, 1 H), 5.82 (d, *J* = 12.2, 1 H), 5.22 (dd, *J* = 11.5, 11.5, 1 H), 4.25 (d, *J* = 10.3, 1 H), 4.25-4.15 (m, 2 H), 4.13 (d, *J* = 10.2, 1 H), 3.57 (d, *J* = 13.1, 1 H), 3.30 (d, *J* = 12.3, 1 H), 3.07 (dd, *J* = 6.2, 11.0, 1 H), 2.81-2.75 (m, 1 H), 2.76 (s, 3 H), 2.45 (s, 3 H), 2.52-2.42 (m, 1 H), 2.35 (s, 3 H), 2.24 (s, 3 H), 2.28-2.20 (m, 2 H), 1.90-1.84 (m, 2 H), 1.31 (d, *J* = 6.4, 3 H)

MS: (ESI, Q-tof)

616.3 (100)

Mol. Formula: $C_{36}H_{40}BrF_6NO$ (696.60)

HRMS: $C_{36}H_{37}F_3NO^+$: (616.3014)

Calcd: 616.3014

Found: 616.3024

TLC: R_f 0.30 (CH_2Cl_2/MeOH, 9:1) [I_2]

Preparation of *rel*-(1*R*,3*R*,5*S*,5a*S*,7a*S*,7b*R*) Octahydro-1-benzyloxy-1-(2,4,6-methylphenyl)-3-(4-methoxybenzyl)-5-methyl-7b-methylcyclopenta[*gh*]pyrrolizinium Bromide (V{*6,2,8*})

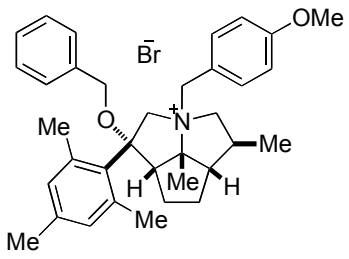

V{*6,2,8*}

Data for **V**{*6,2,8*}:

Yield: 28 mg (78%), free-flowing white powder

^{1}H-NMR: (500 MHz, $CDCl_3$)

7.47 (d, *J* = 8.7, 2 H), 7.33-7.27 (m, 3 H), 7.19-7.16 (m, 2 H), 7.13 (s, 1 H), 6.97 (s, 1 H), 6.90 (d, *J* = 8.7, 2 H), 5.16 (d, *J* = 12.2, 1 H), 4.90 (dd, *J* = 11.6, 11.6, 1 H), 4.37 (d, *J* = 12.9, 1 H), 4.22 (d, *J* = 10.3, 1 H), 4.11 (dd, *J* = 9.3, 9.3, 1 H), 4.09 (d, *J* = 11.3, 1 H), 3.81 (s, 3 H), 3.55 (d, *J* = 13.2, 1 H), 3.31 (d, *J* = 12.2, 1 H), 3.08 (dd, *J* = 6.4, 11.5, 1 H), 2.81 (dd, *J* = 6.0, 9.4, 1 H), 2.73 (s, 3 H), 2.51 (s, 3 H), 2.50-2.42 (m, 1 H), 2.34 (s, 3 H), 2.24-2.16 (m, 2 H), 2.14 (s, 3 H), 1.93-1.81 (m, 2 H), 1.29 (d, *J* = 6.4, 3 H)

MS: (ESI, Q-tof)

510.3 (100)

Mol. Formula: $C_{35}H_{44}BrNO_2$ (590.63)

HRMS: $C_{35}H_{44}NO_2^+$: (510.3372)

Calcd: 510.3372

Found: 510.3382

TLC: R_f 0.25 (CH_2Cl_2/MeOH, 9:1) [I_2]

Preparation of Quaternary Ammonium Bromides V{*7,2,R*^{4}}

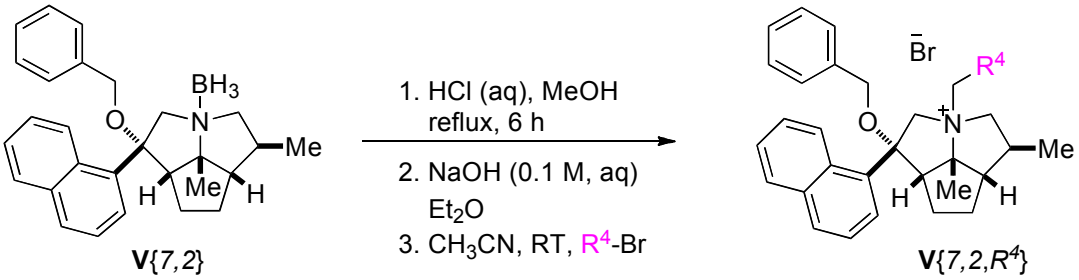

V{*7,2*} **V**{*7,2,R*^{4}}

Following General Procedure II, amino borane **V**{*7,2*} (258 mg, 0.627 mmol) was added to a 50-mL round-bottomed flask as a solution in 21 mL of MeOH (0.03 M). The flask was fitted with a reflux condenser, a magnetic stir bar, and a nitrogen inlet adapter. Lastly, 1.0 N aq. HCl solution (3.1, 5.0 equiv) was added via syringe. The resulting solution was heated and then concentrated by rotary evaporation (15 mm Hg, 20-25 ^{o}C) as described General Procedure II. The resulting free amine was dissolved in acetonitrile and was distributed among five test tubes that were subsequently charged with benzyl bromide (tube 1, 25 mg, 0.149 mmol, 1.2 equiv), 3,5-bis(trifluoromethyl)benzyl bromide (tube 2, 46 mg, 0.149 mmol, 1.2 equiv), 4-methoxybenzyl bromide (tube 3, 30 mg, 0.149 mmol, 1.2 equiv), 4-cyanobenzyl bromide, (tube 4, 29 mg, 0.149 mmol, 1.2 equiv), 4-trifluoromethylbenzyl bromide, (tube 5, 36 mg, 0.149 mmol, 1.2 equiv). After being agitated for 12 h, the reaction mixtures were worked up and the products isolated and purified as described in General Procedure II.

Preparation of *rel*-(1*R*,3*R*,5*S*,5a*S*,7a*S*,7b*R*) Octahydro-1-benzyloxy-1-(1-naphthyl)-3-benzyl-5-methyl-7b-methylcyclopenta[*gh*]pyrrolizinium Bromide (V{*7,2,1*})

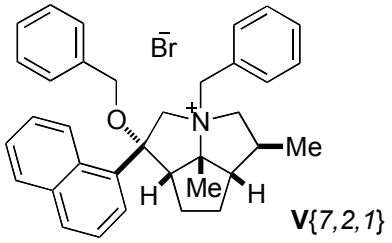

V{*7,2,1*}

Data for **V**{*7,2,1*}:

Yield: 70 mg (97%), free-flowing white powder

^{1}H-NMR: (500 MHz, $CDCl_3$)

8.52 (d, *J* = 8.7, 1 H), 8.13-8.08 (m, 2 H), 8.03 (d, *J* = 7.2, 1 H), 7.74 (dd, *J* = 7.4, 7.4, 1 H), 7.68-7.64 (m, 2 H), 7.29-7.26 (m, 3 H), 7.16 (dd, *J* = 7.5, 7.5, 1 H), 7.11-7.08 (m, 2 H), 6.92 (dd, *J* = 7.8, 7.8, 2 H), 6.37 (d, *J* = 7.4, 1 H), 5.17 (d, *J* = 12.0, 1 H), 5.08 (dd, *J* = 12.0, 12.0, 1 H), 4.65 (d, *J* = 13.0, 1 H), 4.12 (d, *J* = 10.4, 1 H), 3.90 (d, *J* = 10.4, 1 H), 3.83 (dd, *J* = 9.5, 9.5, 1 H), 3.55 (d, *J* = 13.1, 1 H), 2.94 (dd, *J* = 5.9, 11.4, 1 H), 2.90-2.86 (m, 1 H), 2.76 (d, *J* = 12.0, 1 H), 2.59-2.50 (m, 1 H), 2.35 (s, 3 H), 2.30-2.17 (m, 2 H), 1.99-1.95 (m, 2 H), 1.31 (d, *J* = 6.3, 3 H)

MS: (ESI, Q-tof)

488.3 (100)

Mol. Formula: $C_{35}H_{38}BrNO$ (568.59)

HRMS: $C_{35}H_{38}NO^+$: (488.2953)

Calcd: 488.2953

Found: 488.2958

TLC: R_f 0.27 (CH_2Cl_2/MeOH, 9:1) [I_2]

Preparation of *rel*-(1*R*,3*R*,5*S*,5a*S*,7a*S*,7b*R*) Octahydro-1-benzyloxy-1-(1-naphthyl)-3-(3,5-trifluoromethylbenzyl)-5-methyl-7b-methylcyclopenta[*gh*]pyrrolizinium Bromide (V{*7,2,5*})

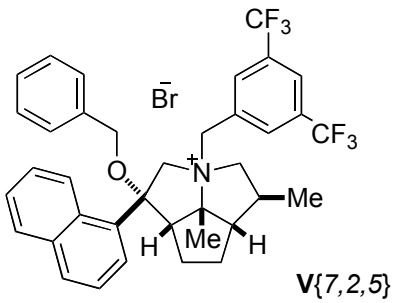

V{*7,2,5*}

Data for **V**{*7,2,5*}:

Yield: 40 mg (45%), free-flowing white powder

^{1}H-NMR: (500 MHz, $CDCl_3$)

8.50 (d, *J* = 8.7, 1 H), 8.04-8.02 (m, 2 H), 8.04 (d, *J* = 7.3, 1 H), 7.77-7.73 (m, 2 H), 7.71-7.63 (m, 2 H), 7.32 (s, 2 H), 7.29-7.27 (m, 3 H), 7.11-7.06 (m, 2 H), 5.66 (d, *J* = 12.1, 1 H), 5.28 (dd, *J* = 11.8, 11.8, 1 H), 4.57 (d, *J* = 12.8, 1 H), 4.09 (d, *J* = 10.3, 1 H), 3.87 (dd, *J* = 9.5, 9.5, 1 H), 3.82 (d, *J* = 10.3, 1 H), 3.70 (d, *J* = 13.1, 1 H), 2.94 (d, *J* = 12.2, 1 H), 2.90-2.82 (m, 2 H), 2.62-2.53 (m, 1 H), 2.46 (s, 3 H), 2.33-2.20 (m, 2 H), 2.03-1.96 (m, 2 H), 1.32 (d, *J* = 6.3, 3 H)

MS: (ESI, Q-tof)

624.3 (100)

Mol. Formula: $C_{37}H_{36}BrF_6NO$ (704.5823)

HRMS: $C_{37}H_{36}F_6NO^+$: (624.6201)

Calcd: 624.6201

Found: 624.2696

TLC: R_f 0.35 (CH_2Cl_2/MeOH, 9:1) [I_2]

Preparation of *rel*-(1*R*,3*R*,5*S*,5a*S*,7a*S*,7b*R*) Octahydro-1-benzyloxy-1-(1-naphthyl)-3-(4-methoxybenzyl)-5-methyl-7b-methylcyclopenta[*gh*]pyrrolizinium Bromide (V{*7,2,8*})

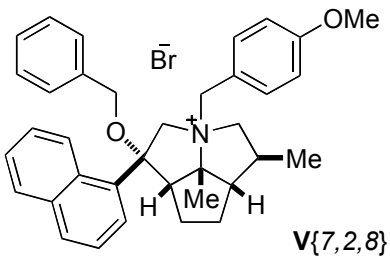

V{*7,2,8*}

Data for **V**{*7,2,8*}:

Yield: 62 mg (82%), free-flowing white powder

^{1}H-NMR: (500 MHz, $CDCl_3$)

8.52 (d, *J* = 8.7, 1 H), 8.12-8.07 (m, 2 H), 8.02 (d, *J* = 7.4, 1 H), 7.74 (dd, *J* = 7.5, 7.5, 1 H), 7.67-7.63 (m, 2 H), 7.30-7.26 (m, 3 H), 7.12-7.09 (m, 2 H), 6.43 (d, *J* = 8.7, 2 H), 6.29 (d, *J* = 7.5, 1 H), 5.08 (d, *J* = 12.1, 1 H), 5.00 (dd, *J* = 12.0, 12.0, 1 H), 4.64 (d, *J* = 13.1, 1 H), 4.12 (d, *J* = 10.3, 1 H), 3.89 (d, *J* = 10.3, 1 H), 3.82 (dd, *J* = 9.4, 9.4, 1 H), 3.67 (s, 3 H), 3.53 (d, *J* = 13.2, 1 H), 2.91 (dd, *J* = 5.9, 11.4, 1 H), 2.90-2.84 (m, 2 H), 2.70 (d, *J* = 12.1, 1 H), 2.60-2.50 (m, 1 H), 2.32 (s, 3 H), 2.30-2.15 (m, 2 H), 1.98-1.94 (m, 2 H), 1.30 (d, *J* = 6.3, 3 H)

MS: (ESI, Q-tof)

518.3 (100)

Mol. Formula: $C_{36}H_{40}BrNO_2$ (598.61)

HRMS: $C_{36}H_{40}NO_2^+$: (518.3059)

Calcd: 518.3059

Found: 518.3065

TLC: R_f 0.28 (CH_2Cl_2/MeOH, 9:1) [I_2]

Preparation of *rel*-(1*R*,3*R*,5*S*,5a*S*,7a*S*,7b*R*) Octahydro-1-benzyloxy-1-(1-naphthyl)-3-(4-trifluoromethylbenzyl)-5-methyl-7b-methylcyclopenta[*gh*]pyrrolizinium Bromide (V{*7,2,9*})

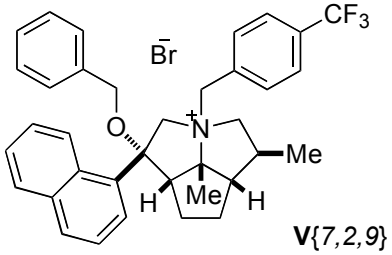

V{*7,2,9*}

Data for **V**{*7,2,9*}:

Yield: 59 mg (74%), free-flowing white powder

^{1}H-NMR: (500 MHz, $CDCl_3$)

8.52 (d, *J* = 8.7, 1 H), 8.15-8.10 (m, 2 H), 8.04 (d, *J* = 7.4, 1 H), 7.79 (dd, *J* = 7.5, 7.5, 1 H), 7.71-7.66 (m, 2 H), 7.30-7.25 (m, 3 H), 7.18 (d, *J* = 8.2, 2 H), 7.12-7.09 (m, 2 H), 6.55 (d, *J* = 7.7, 2 H), 5.39 (d, *J* = 12.0, 1 H), 5.18 (dd, *J* = 11.9, 11.9, 1 H), 4.55 (d, *J* = 13.1, 1 H), 4.14 (d, *J* = 10.3, 1 H), 3.92 (d, *J* = 10.3, 1 H), 3.84 (dd, *J* = 9.3, *J* = 9.3, 1 H), 3.59 (d, *J* = 13.1, 1 H), 2.90 (dd, *J* = 5.9, 11.2, 1 H), 2.87-2.83 (m, 1 H), 2.75 (d, *J* = 12.0, 1 H), 2.60-2.50 (m, 1 H), 2.36 (s, 3 H), 2.32-2.19 (m, 2 H), 2.01-1.95 (m, 2 H), 1.30 (d, *J* = 6.3, 3 H)

MS: (ESI, Q-tof)

556.3

Mol. Formula: $C_{36}H_{37}BrF_3NO$ (636.58)

HRMS: $C_{36}H_{37}F_3NO^+$: (556.2827)

Calcd: 556.2827

Found: 586.2837

TLC: R_f 0.30 (CH_2Cl_2/MeOH, 9:1) [I_2]

Preparation of *rel*-(1*R*,3*R*,5*S*,5a*S*,7a*S*,7b*R*) Octahydro-1-benzyloxy-1-(1-naphthyl)-3-(4-cyanobenzyl)-5-methyl-7b-methylcyclopenta[*gh*]pyrrolizinium Bromide (V{*7,2,10*})

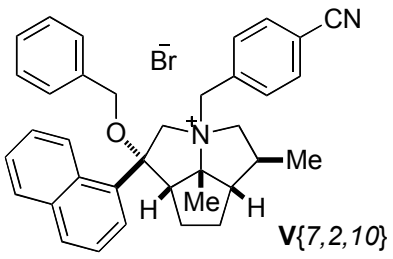

V{*7,2,10*}

Data for V{*7,2,10*}:

Yield: 57 mg (76%), free-flowing white powder

^{1}H-NMR: (500 MHz, $CDCl_3$)

8.50 (d, *J* = 8.6, 1 H), 8.16-8.11 (m, 2 H), 8.04 (d, *J* = 7.3, 1 H), 7.79 (dd, *J* = 7.6, 7.6, 1 H), 7.71-7.66 (m, 2 H), 7.31-7.25 (m, 3 H), 7.22 (d, *J* = 8.5, 2 H), 7.11-7.08 (m, 2 H), 6.54 (d, *J* = 7.9, 2 H), 5.47 (d, *J* = 12.4, 1 H), 5.22 (dd, *J* = 11.7, 11.7, 1 H), 4.48 (d, *J* = 13.1, 1 H), 4.14 (d, *J* = 10.3, 1 H), 3.92 (d, *J* = 10.3, 1 H), 3.84 (dd, *J* = 9.5, 9.5, 1 H), 3.59 (d, *J* = 13.1, 1 H), 2.89 (dd, *J* = 5.9, 11.3, 1 H), 2.85-2.81 (m, 1 H), 2.73 (d, *J* = 11.9, 1 H), 2.59-2.51 (m, 1 H), 2.35 (s, 3 H), 2.33-2.19 (m, 2 H), 2.02-1.96 (m, 2 H), 1.30 (d, *J* = 6.3, 3 H)

MS: (ESI, Q-tof)

513.3 (100)

Mol. Formula: $C_{36}H_{37}BrN_2O$ (593.60)

HRMS: $C_{36}H_{37}N_2O^+$: (513.2906)

Calcd: 513.2906

Found: 513.2899

TLC: R_f 0.26 (CH_2Cl_2/MeOH, 9:1) [I_2]

Preparation of Quaternary Ammonium Bromides β-V{*1*,*2*,*R*^{4}}

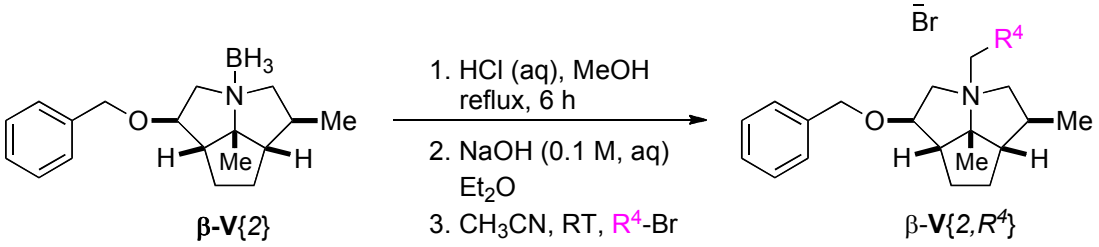

β-V{*2*} β-**V**{*2*,*R*^{4}}

Following General Procedure II, amino borane **β-V**{*2*} (164 mg, 0.589 mmol) was added to a 100-mL round-bottomed flask as a solution in 19 mL of MeOH (0.03 M). The flask was fitted with a reflux condenser, a magnetic stir bar, and a nitrogen inlet adapter. Lastly, 1.0 N aq. HCl solution (2.9, 5.0 equiv) was added via syringe. The resulting solution was heated and then concentrated by rotary evaporation (15 mm Hg, 20-25 ^{o}C) as described General Procedure II. The resulting free amine was dissolved in acetonitrile and was distributed among seven test tubes that were subsequently charged with 1-bromomethylnaphthalene (tube 1, 22 mg, 0.104 mmol, 1.2 equiv), 2-bromomethylnaphthalene (tube 3, 22 mg, 0.104 mmol, 1.2 equiv), 3,5-bis(trifluoromethyl)benzyl bromide (tube 4, 31 mg, 0.104 mmol, 1.2 equiv), 3,5-bis(*t*-butyl)benzyl bromide (tube 5, 29 mg, 0.104 mmol, 1.2 equiv), 4-methoxybenzyl bromide (tube 6, 31 mg, 0.104 mmol, 1.2 equiv), 1-bromohexane (tube 7, 68 mg, 0.435 mmol, 5.0 equiv). After being agitated for 12 h, the reaction mixtures were worked up and the products isolated and purified as described in General Procedure II.

Preparation of *rel*-(1*R*,3*R*,5*S*,5a*S*,7a*S*,7b*R*) Octahydro-1-benzyloxy-3-(1-naphthylmethyl)-5-methyl-7b-methylcyclopenta[*gh*]pyrrolizinium Bromide (β-V{*1,2,2*})

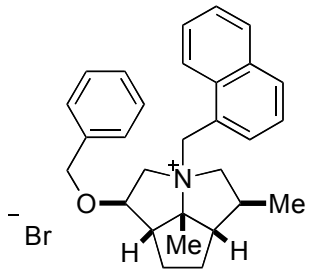

V{*1,2,2*}β

Data for **β-V**{*1,2,2*}:

Yield: 42 mg (98%), free-flowing white powder

^{1}H-NMR: (500 MHz, $CDCl_3$)

8.48 (d, *J* = 8.6, 1 H), 8.30 (d, *J* = 7.2, 1 H), 7.94 (d, *J* = 8.2, 1 H), 7.87 (d, *J* = 8.2, 1 H), 7.56 (dd, *J* = 7.3, 7.3, 1 H), 7.50–7.45 (m, 5 H), 7.43–7.37 (m, 1 H), 7.32 (dd, *J* = 7.8, 7.8, 1 H), 4.87 (d, *J* = 12.6, 1 H), 4.59 (d, *J* = 12.6, 1 H), 4.75 (dd, *J* = 11.9, 11.9, 1 H), 4.92–4.52 (m, 3 H), 4.12 (d, *J* = 3.4, 1 H), 4.03 (d, *J* = 14.1, 1 H), 3.52 (d, *J* = 11.3, 1 H), 3.18 (dd, *J* = 5.8, 11.3, 1 H), 2.82 (dd, *J* = 9.5, 9.5, 1 H), 2.69 (dd, *J* = 5.9, 10.3, 1 H), 2.24 (s, 3 H), 2.19–2.10 (m, 2 H), 1.90–1.77 (m, 2 H), 1.73–1.63 (m, 1 H), 1.25 (d, *J* = 6.3, 3 H).

MS: (ESI, Q-tof)

412.3 (100)

Mol. Formula: $C_{29}H_{34}BrNO$ (492.49)

HRMS: $C_{29}H_{34}NO^+$: (412.2640)

Calcd: 412.2640

Found: 412.2632

TLC: R_f 0.25 (CH_2Cl_2/MeOH, 9:1) [I_2]

Preparation of *rel*-(1*R*,3*R*,5*S*,5a*S*,7a*S*,7b*R*) Octahydro-1-benzyloxy-3-(2-naphthylmethyl)-5-methyl-7b-methylcyclopenta[*gh*]pyrrolizinium Bromide (β-V{*1*,*2*,*3*})

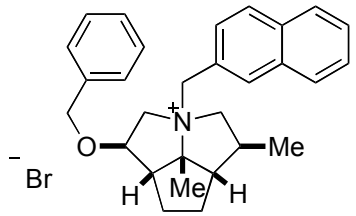

V{*1,2,3*}β

Data for **β-V**{*1*,*2*,*3*}:

Yield: 39 mg (91%), free-flowing white powder

^{1}H-NMR: (500 MHz, $CDCl_3$)

8.09 (s, 1 H), 7.90–7.84 (m, 3 H), 7.73 (dd, *J* = 1.7, 8.4, 1 H), 7.59–7.51 (m, 2 H), 7.48–7.34 (m, 5 H), 5.39 (d, *J* = 11.9, 1 H), 4.79 (d, *J* = 11.8, 1 H), 4.77 (d, *J* = 11.7, 1 H), 4.71 (dd, *J* = 11.9, 11.9, 1 H), 4.64 (d, *J* = 11.7, 1 H), 4.14–4.08 (m, 2 H), 3.53 (d, *J* = 11.1, 1 H), 3.32 (dd, *J* = 6.0, 11.3, 1 H), 2.74 (dd, *J* = 9.2, 9.2, 1 H), 2.59 (dd, *J* = 5.9, 9.9, 1 H), 2.24–2.07 (m, 2 H), 2.10 (s, 3 H), 1.89–1.77 (m, 2 H), 1.73–1.61 (m, 1 H), 1.26 (d, *J* = 6.3, 3 H).

MS: (ESI, Q-tof)

412.3 (100)

Mol. Formula: $C_{29}H_{34}BrNO$ (492.49)

HRMS: $C_{20}H_{38}NO_3^+$: (412.2640)

Calcd: 412.2640

Found: 412.2639

TLC: R_f 0.26 (CH_2Cl_2/MeOH, 9:1) [I_2]

Preparation of *rel*-(1*R*,3*R*,5*S*,5a*S*,7a*S*,7b*R*) Octahydro-1-benzyloxy-3-(3,5-bistrifluoromethylbenzyl)-5-methyl-7b-methylcyclopenta[*gh*]pyrrolizinium Bromide (β-V{*1*,*2*,*5*})

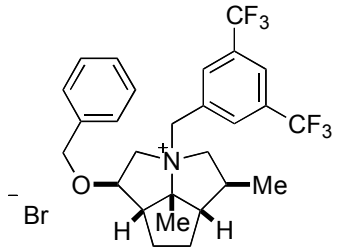

V{*1,2,5*}β

Data for **β-V**{*1*,*2*,*5*}:

Yield: 45mg (89%), free-flowing white powder

^{1}H-NMR: (500 MHz, $CDCl_3$)

8.20 (s, 2 H), 7.94 (s, 1 H), 7.46–7.31 (m, 5 H), 5.84 (d, *J* = 12.1, 1 H), 4.96 (dd, *J* = 11.7, 11.7, 1 H), 4.75 (d, *J* = 11.3, 1 H), 4.69 (d, *J* = 12.1, 1 H), 4.54 (d, *J* = 11.3, 1 H), 4.13 (s, 1 H), 3.68 (dd, *J* = 14.1, 24.4, 2 H), 3.23 (dd, *J* = 6.0, 11.0, 1 H), 2.76 (dd, *J* = 9.5, 9.5, 1 H), 2.57–2.48 (m, 1 H), 2.31–2.22 (m, 1 H), 2.19–2.09 (m, 1 H), 2.11 (s, 3 H), 1.91–1.78 (m, 2 H), 1.75–1.65 (m, 1 H), 1.24 (d, *J* = 6.3, 3 H).

MS: (ESI, Q-tof)

498.2 (100)

Mol. Formula: $C_{27}H_{30}BrF_6NO$ (578.43)

HRMS: $C_{27}H_{30}F_6NO^+$: (498.2232)

Calcd: 498.2232

Found: 498.2214

TLC: R_f 0.29 (CH_2Cl_2/MeOH, 9:1) [I_2]

Preparation of *rel*-(1*R*,3*R*,5*S*,5a*S*,7a*S*,7b*R*) Octahydro-1-benzyloxy-3-hexyl-5-methyl-7b-methylcyclopenta[*gh*]pyrrolizinium Bromide β-V{*1,2,6*}

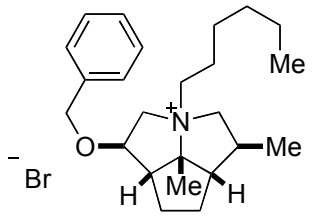

V{*1,2,6*}

Data for **β-V**{*1,2,6*}:

Yield: 33 mg (87%), free-flowing white powder

^{1}H-NMR: (500 MHz, $CDCl_3$)

7.38–7.31 (m, 3 H), 7.27–7.24 (m, 2 H), 4.56 (d, *J* = 11.7, 1 H), 4.48 (d, *J* = 11.7, 1 H), 4.39 (d, *J* = 13.3, 1 H), 4.25 (dd, *J* = 6.1, 11.1, 1 H), 4.12 (s, 1 H), 4.03 (d, *J* = 12.7, 1 H), 3.57–3.50 (m, 1 H), 3.31–3.22 (m, 1 H), 3.05 (dd, *J* = 11.9, 11.9, 1 H), 2.59–2.48 (m, 2 H), 2.17–2.05 (m, 2 H), 1.91–1.70 (m, 5 H), 1.68 (s, 3 H), 1.38 (s, 1 H), 1.32–1.20 (m, 5 H), 1.15 (d, *J* = 6.3, 3 H), 0.86 (t, *J* = 6.8, 3 H)

MS: (ESI, Q-tof)

356.3 (100)

Mol. Formula: $C_{24}H_{38}BrNO$ (436.47)

HRMS: $C_{24}H_{38}NO^+$: (356.2953)

Calcd: 356.2953

Found: 356.2944

TLC: R_f 0.37 (CH_2Cl_2/MeOH, 9/1) [I_2]

Preparation of *rel*-(1*R*,3*R*,5*S*,5a*S*,7a*S*,7b*R*) Octahydro-1-benzyloxy-3-(3,5-*tert*-butylbenzyl)-5-methyl-7b-methylcyclopenta[*gh*]pyrrolizinium Bromide (β-V{*1,2,7*})

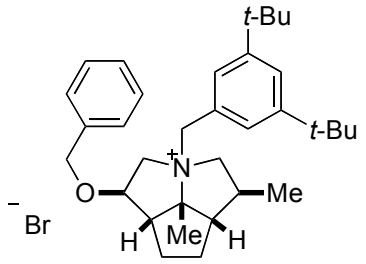

V{*1,2,7*}

Data for **β-V**{*1,2,7*}:

Yield: 42 mg (87%), free-flowing white powder

^{1}H-NMR: (500 MHz, $CDCl_3$)

7.50–7.48 (m, 1 H), 7.41–7.31 (m, 5 H), 7.29 (d, *J* = 1.7, 2 H), 4.71 (d, *J* = 11.3, 1 H), 4.58 (d, *J* = 11.3, 1 H), 4.68 (s, 2 H), 4.23 (s, 1 H), 4.18 (d, *J* = 14.1, 1 H), 4.04 (d, *J* = 14.1, 1 H), 3.82 (dd, *J* = 11.8, 11.8, 1 H), 3.44 (dd, *J* = 5.9, 11.1, 1 H), 2.73 (dd, *J* = 9.6, 9.6, 1 H), 2.70–2.61 (m, 1 H), 2.35 (dd, *J* = 6.5, 10.1, 1 H), 2.16–2.08 (m, 2 H), 1.96–1.90 (m, 1 H), 1.93 (s, 3 H), 1.84–1.75 (m, 1 H), 1.29 (s, 18H), 1.20 (d, *J* = 6.3, 3 H)

MS: (ESI, Q-tof)

474.4 (100)

Mol. Formula: $C_{33}H_{48}BrNO$ (554.64)

HRMS: $C_{33}H_{48}NO^+$: (474.3736)

Calcd: 474.3736

Found: 474.3723

TLC: R_f 0.30 (CH_2Cl_2/MeOH, 9:1) [I_2]

Preparation of *rel*-(1*R*,3*R*,5*S*,5a*S*,7a*S*,7b*R*) Octahydro-1-benzyloxy-3-(4-methoxybenzyl)-5-methyl-7b-methylcyclopenta[*gh*]pyrrolizinium Bromide (β-V{*1,2,8*})

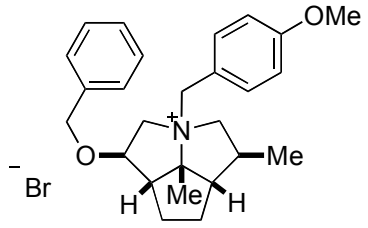

V{*1,2,8*}

Data for **β-V**{*1*,*2*,*8*}:

Yield: 39 mg (92%), free-flowing white powder

^{1}H-NMR: (500 MHz, $CDCl_3$)

7.54 (d, *J* = 8.7, 2 H), 7.44–7.32 (m, 5 H), 6.93 (d, *J* = 8.7, 2 H), 5.07 (d, *J* = 12.0, 1 H), 4.70 (d, *J* = 11.7, 1 H), 4.59 (d, *J* = 11.7, 1 H), 4.58 (d, *J* = 12.1, 1 H), 4.41 (dd, *J* = 11.9, 11.9, 1 H), 4.09 (d, *J* = 3.0, 1 H), 4.02 (d, *J* = 14.0, 1 H), 3.82 (s, 3 H), 3.60 (d, *J* = 11.7, 1 H), 3.25 (dd, *J* = 6.0, 11.3, 1 H), 2.68 (dd, *J* = 9.1, 9.1, 1 H), 2.50 (dd, *J* = 5.8, 10.0, 1 H), 2.27–2.19 (m, 1 H), 2.16–2.07 (m, 1 H), 2.01 (s, 3 H), 1.88–1.65 (m, 3 H), 1.22 (d, *J* = 6.3, 3 H)

MS: (ESI, Q-tof)

392.3 (100)

Mol. Formula: $C_{26}H_{34}BrNO_2$ (472.46)

HRMS: $C_{26}H_{34}NO_2^+$: (392.2590)

Calcd: 392.2590

Found: 392.2582

TLC: R_f 0.19 (CH_2Cl_2/MeOH, 9:1) [I_2]

7.4. Kinetic Analysis from Text.

7.4.1. General Kinetic Analysis Procedure (Half-Life Determinations)

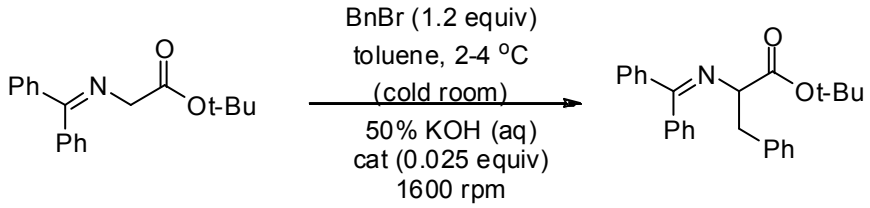

A 2–mL scintillation vial was fitted with a Teflon lined rubber septum and *tert*-butyl 2-(diphenylmethyleneamino) acetate (100 mg, 0.0.34 mmol), and quaternary ammonium salt **x** (x.x mg, 0.025 equiv) were added. The liquid reagents, toluene (0.40 mL) and benzyl bromide (87.1 mg, 0.41 mmol, 1.2 equiv) were added via syringe from stock solutions. Then, a 1.5 cm egg-shaped a magnetic stir bar was placed in the vial, which was then transferred to a cold room that maintained the temperature at 2-4 ^{o}C. The reaction mixture was allowed to equilibrate for at least 1 h with stirring. Lastly, 50% aq. KOH (8.9 M, 0.66 mL, x mmol, 17.8 equiv) was added and the stir rate was set to 1600 rpm. Aliquots were taken at the indicated times and analyzed as follows. Three seconds prior to the indicated time interval, the stirrer was turned off. At the indicated time interval a 5-7 μL aliquot of the organic layer was removed and then was injected into acetonitrile (1-1.2 mL) containing glacial acetic acid (~5 μL). This clear solution was filtered through a small plug of silica gel (0.5 x 1 cm) and the filtrate was analyzed by Reverse Phase-HPLC Method 1.

7.4.2. Analysis and Response Factors

Eq 1: Response factor for **X** = (mmol **3** * area internal standard)
(mmol internal standard * area **3**)
(mmol internal standard *

mmol Product	Area Product	mmol Standard	Area Standard	Response factor
2.34E-04	15.4376	9.73E-04	83.0799	1.296
2.34E-04	15.6277	9.73E-04	83.2519	1.283
2.34E-04	15.5967	9.73E-04	83.6868	1.292
2.34E-04	15.5909	9.73E-04	83.0982	1.283
3.90E-04	23.6288	9.73E-04	75.6462	1.285
3.90E-04	23.1749	9.73E-04	75.2265	1.302
3.90E-04	23.7759	9.73E-04	75.5066	1.274
3.90E-04	23.2827	9.73E-04	75.8688	1.308
6.25E-04	32.9563	9.73E-04	66.1806	1.289
6.25E-04	33.5899	9.73E-04	65.0608	1.244
6.25E-04	33.3643	9.73E-04	65.7796	1.266
6.25E-04	32.0052	9.73E-04	63.2008	1.268
7.81E-04	37.1393	9.73E-04	58.0562	1.254
7.81E-04	36.6825	9.73E-04	57.7248	1.263
7.81E-04	36.9887	9.73E-04	57.9599	1.257
7.81E-04	38.5104	9.73E-04	60.0839	1.252
9.37E-04	40.9315	9.73E-04	53.3471	1.255
9.37E-04	40.8334	9.73E-04	52.9797	1.249
9.37E-04	40.3293	9.73E-04	54.0078	1.290
9.37E-04	40.7821	9.73E-04	53.4912	1.263
			Average Response Factor	1.274

7.4.3. Kinetic data for Libraries IV and V: Table 5 in Text

Table 5. entry 1. catalyst **IV**{*2,2,1*}**: run 1**

time, min	µmol standard	area standard	area product	µmol product	product %
0	256.25	0.00	0.00	0.00	0.00
2	256.25	24.72	0.88	10.88	3.21
6	256.25	19.27	1.24	19.82	5.85
10	256.25	26.00	3.38	39.99	11.80
14	256.25	23.13	4.03	53.62	15.83
20	256.25	29.08	6.96	73.63	21.74
30	256.25	27.11	8.47	96.06	28.36
40	256.25	29.32	10.63	111.46	32.91
91	256.25	3.68	1.80	150.14	44.32
133	256.25	27.68	16.75	186.06	54.93
208	256.25	28.40	20.02	216.70	63.97

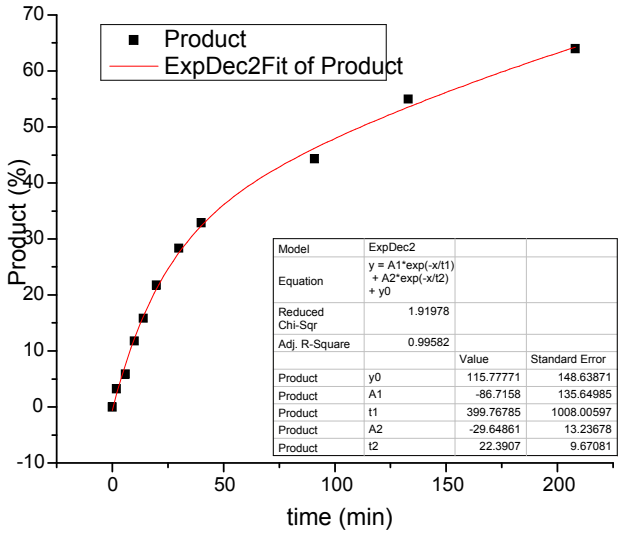

Half-life: 101.71

Table 5. entry 1. catalyst **IV**{*2,2,1*}**: run 2**

time, min	μmol standard	area standard	area product	μmol product	product, %
16	256.25	25.88	4.64	55.07	16.25
20	256.25	26.54	6.50	75.36	22.24
30	256.25	28.39	9.62	104.20	30.75
40	256.25	28.82	11.73	125.14	36.94
60	256.25	26.52	13.16	152.64	45.05
91	256.25	27.25	16.31	184.00	54.31
133	256.25	27.10	18.70	212.15	62.62
208	256.25	27.66	21.58	239.90	70.81

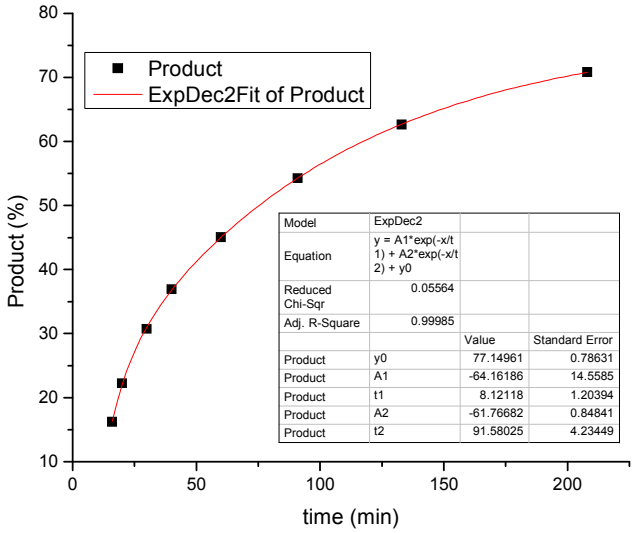

Half-life: 75.3
Average: 93.5

Table 5. entry 2. catalyst **IV**{*2,2,2*}**: run 1**

time, min	µmol standard	area standard	area product	µmol product	product %
0	256.25	0.00	0.00	0.00	0.00
4	256.25	24.76	3.05	37.91	11.19
8	256.25	25.99	6.10	72.15	21.30
12	256.25	24.40	7.68	96.78	28.57
16	256.25	25.72	9.40	112.42	33.19
20	256.25	25.36	10.48	127.08	37.52
30	256.25	25.67	12.80	153.39	45.28
40	256.25	25.86	14.19	168.78	49.83
73	256.25	26.32	16.45	192.13	56.72

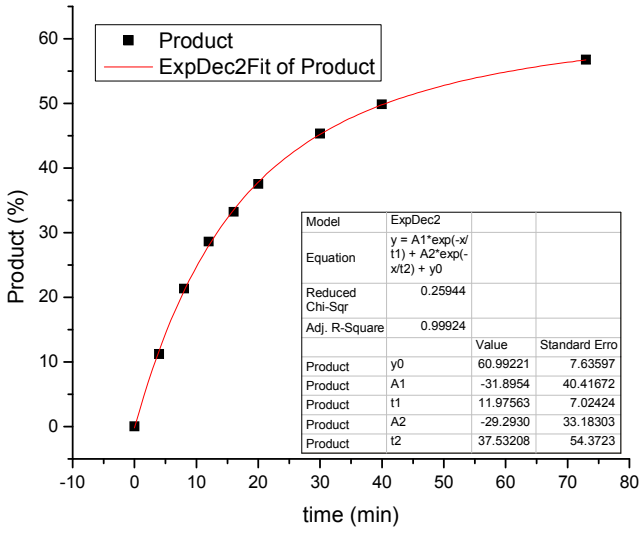

Half-life: 40.64

Table 5. entry 2. catalyst **IV**{*2,2,2*}**: run 2**

time, min	µmol standard	area standard	area product	µmol product	product %
0	256.25	0.00	0.00	0.00	0.00
4	256.25	25.34	2.55	30.96	9.14
8	256.25	25.58	4.96	59.64	17.60
12	256.25	25.75	6.90	82.41	24.32
16	256.25	25.58	8.30	99.71	29.43
20	256.25	26.02	9.80	115.79	34.17
30	256.25	26.67	11.80	136.04	40.15
40	256.25	26.53	12.84	148.82	43.93
73	256.25	25.98	14.83	175.53	51.81
200	256.25	27.08	19.81	224.93	66.39

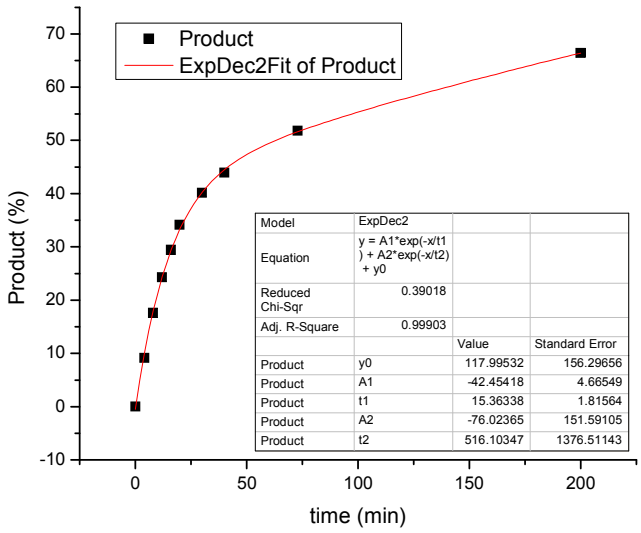

Half-life: 62.97
Average: 51.1

Table 5. entry 3. catalyst **IV**{*3,2,1*}**: run 1**

time, min	µmol standard	area standard	area product	µmol product	product %
0	256.39	0.00	0.00	0.00	0.00
2	256.39	26.76	3.06	35.21	10.38
4	256.39	28.32	5.77	62.71	18.49
6	256.39	28.89	7.71	82.14	24.21
8	256.39	29.19	9.67	101.89	30.04
10	256.39	28.94	11.08	117.77	34.72
12	256.39	28.98	12.57	133.44	39.34
16	256.39	29.59	14.74	153.24	45.17
20	256.39	29.81	17.48	180.37	53.17
30	256.39	28.91	19.85	211.24	62.27
40	256.39	29.20	22.57	237.79	70.10
60	256.39	29.87	26.92	277.28	81.74
102	256.39	30.72	29.40	294.44	86.80

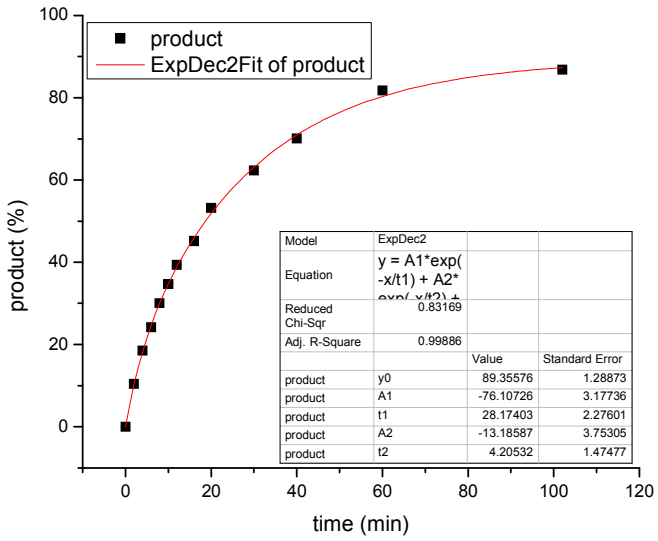

Half-life: 18.69

Table 5. entry 3. catalyst **IV**{*3,2,1*}**: run 2**

time, min	µmol standard	area standard	area product	µmol product	product %
0	256.39	0.00	0.00	0.00	0.00
2	256.39	27.01	3.23	36.82	10.85
4	256.39	29.60	5.96	61.98	18.27
6	256.39	29.77	7.76	80.14	23.63
8	256.39	29.57	9.32	96.94	28.58
10	256.39	30.06	11.14	114.05	33.62
12	256.39	29.95	11.88	121.98	35.96
16	256.39	29.44	14.51	151.61	44.69
20	256.39	30.87	17.11	170.54	50.27
30	256.39	29.86	20.08	206.92	61.00
40	256.39	30.64	21.95	220.44	64.98
60	256.39	30.68	25.33	253.96	74.87
102	256.39	31.08	28.33	280.42	82.67

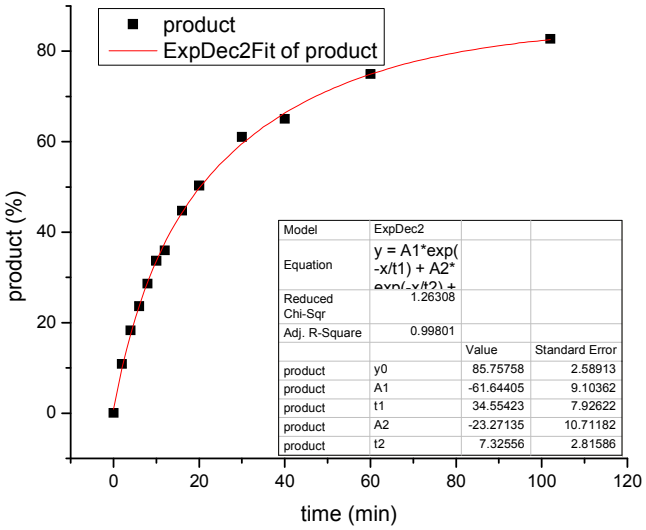

Half-life: 20.26
Average: 19.5

Table 5. entry 4. catalyst **IV**{*3,2,5*}**: run 1**

time, min	µmol standard	area standard	area product	µmol product	produc t %
0	256.25	0.00	0.00	0.00	0.00
2	256.25	24.58	2.35	29.44	8.69
4	256.25	25.57	4.49	53.94	15.93
6	256.25	25.66	6.17	73.91	21.82
8	256.25	25.14	7.20	88.11	26.01
10	256.25	26.04	8.49	100.21	29.58
12	256.25	25.94	9.21	109.12	32.21
16	256.25	26.33	10.93	127.60	37.67
20	256.25	26.23	12.24	143.52	42.37
32	256.25	26.27	14.67	171.71	50.69
44	256.25	26.93	16.44	187.78	55.43

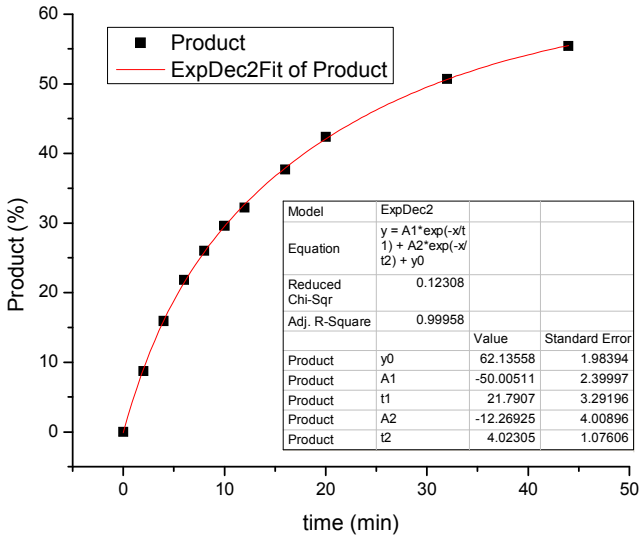

Half-life: 30.87

Table 5. entry 4. catalyst **IV**{*3,2,5*}**: run 2**

time, min	µmol standard	area standard	area product	µmol product	product %
0	256.25	0.00	0.00	0.00	0.00
2	256.25	24.86	2.54	31.40	9.27
4	256.25	24.70	4.76	59.28	17.50
6	256.25	21.18	5.12	74.28	21.92
8	256.25	25.11	7.66	93.81	27.69
10	256.25	24.90	9.01	111.32	32.86
12	256.25	24.74	9.90	123.07	36.32
16	256.25	25.31	11.60	140.98	41.61
20	256.25	25.12	12.98	158.96	46.92
30	256.25	25.71	16.36	195.75	57.77
40	256.25	25.80	18.02	214.78	63.39
60	256.25	26.35	19.94	232.64	68.66

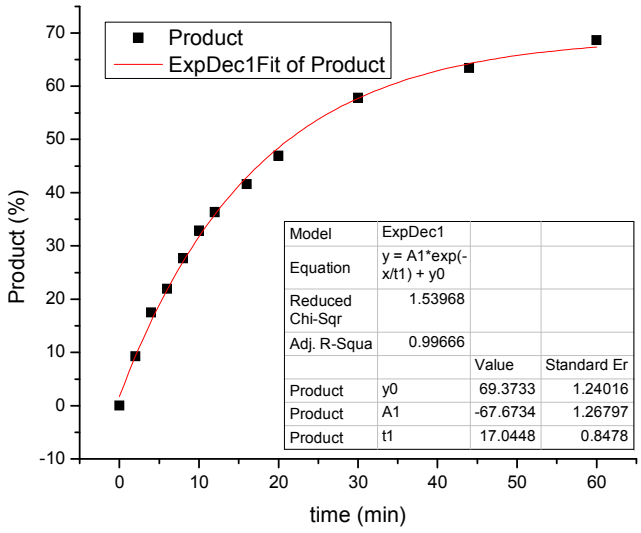

Half-life: 21.32
Average: 26.1

Table 5. entry 5. catalyst **IV**{*5,2,5*}**: run 1**

time, min	µmol standard	area standard	area product	µmol product	product %
0	256.39	0.00	0.00	0.00	0.00
2	256.39	27.19	3.25	36.82	10.85
4	256.39	29.90	6.61	68.03	20.06
6	256.39	30.41	9.04	91.44	26.95
10	256.39	30.58	12.45	125.27	36.93
12	256.39	29.91	13.46	138.48	40.82
16	256.39	30.40	16.26	164.58	48.52
20	256.39	29.42	17.37	181.63	53.54
30	256.39	30.58	20.90	210.26	61.98
40	256.39	30.23	22.73	231.34	68.20
60	256.39	31.58	25.57	249.10	73.43
100	256.39	32.36	28.17	267.80	78.94

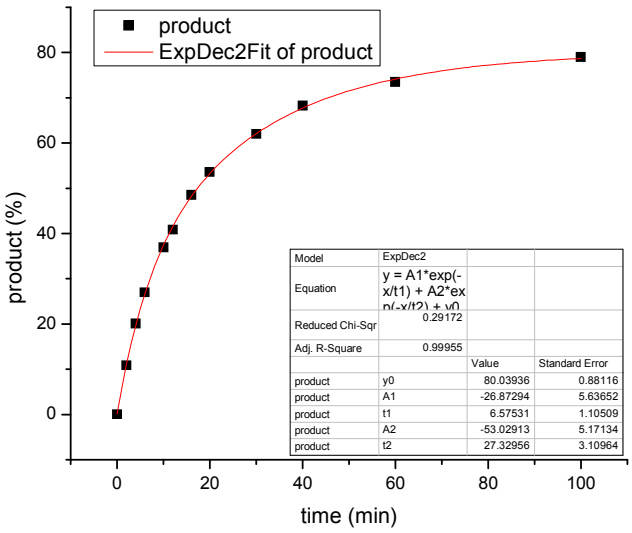

Half-life: 17.34

Table 5. entry 5. catalyst **IV**{*5,2,5*}**: run 2**

time, min	µmol standard	area standard	area product	µmol product	product %
0	256.39	0.00	0.00	0.00	0.00
2	256.39	29.82	4.26	43.93	12.95
4	256.39	27.52	6.65	74.40	21.93
6	256.39	29.95	9.50	97.54	28.76
8	256.39	29.82	11.49	118.56	34.95
10	256.39	29.94	13.13	134.97	39.79
12	256.39	30.30	14.79	150.15	44.26
16	256.39	30.45	17.28	174.60	51.47
20	256.39	30.67	19.13	191.86	56.56
30	256.39	30.16	21.53	219.62	64.74
40	256.39	29.81	23.14	238.82	70.40
60	256.39	31.05	25.51	252.77	74.51
100	256.39	30.92	26.98	268.53	79.16

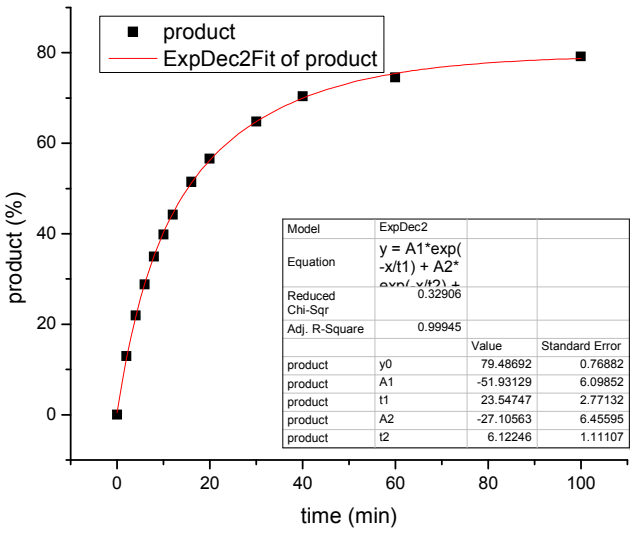

Half-life: 15.21
Average: 16.3

Table 5. entry 6. catalyst **V{*1,2,1*}: run 1**

time, min	µmol standard	area standard	area product	µmol product	product %
0	255.56	0.00	0.00	0.00	0.00
4	255.56	27.21	4.43	49.94	14.74
8	255.56	27.33	6.72	75.41	22.25
12	255.56	27.16	8.73	98.59	29.09
16	255.56	29.91	11.64	119.32	35.21
20	255.56	29.53	13.60	141.24	41.68
30	255.56	29.91	16.36	167.80	49.52
40	255.56	29.90	18.63	191.13	56.40
50	255.56	30.44	20.62	207.69	61.29
60	255.56	30.81	22.69	225.84	66.65
80	255.56	30.07	23.27	237.30	70.03
110	255.56	30.53	25.32	254.36	75.07
171	255.56	31.68	28.12	272.23	80.34

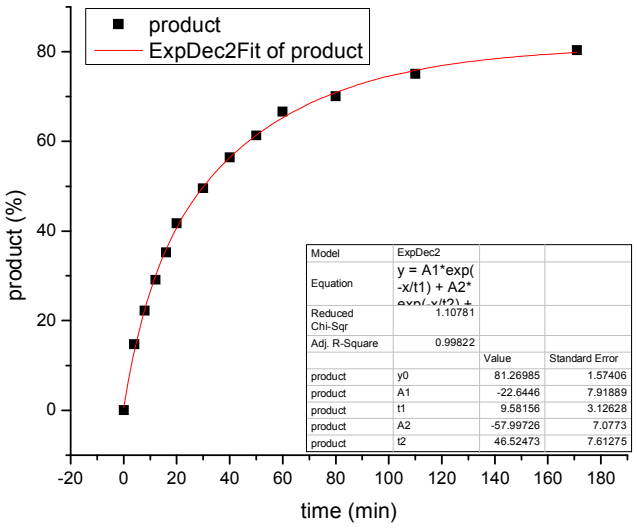

Half-life: 30.20

Table 5. entry 6. catalyst **V{*1,2,1*}: run 2**

time, min	µmol standard	area standard	area product	µmol product	product %
0	255.56	0.00	0.00	0.00	0.00
4	255.56	29.55	4.71	48.90	14.43
8	255.56	29.91	7.42	76.07	22.45
12	255.56	29.44	9.01	93.82	27.69
16	255.56	29.22	10.69	112.13	33.09
20	255.56	29.56	12.35	128.13	37.81
30	255.56	28.61	14.75	158.09	46.66
40	255.56	29.70	17.39	179.60	53.00
50	255.56	29.16	18.54	194.99	57.54
60	255.56	29.42	20.62	214.93	63.43
80	255.56	29.82	22.29	229.24	67.65
110	255.56	30.31	24.38	246.69	72.80
171	255.56	30.50	25.05	251.88	74.33

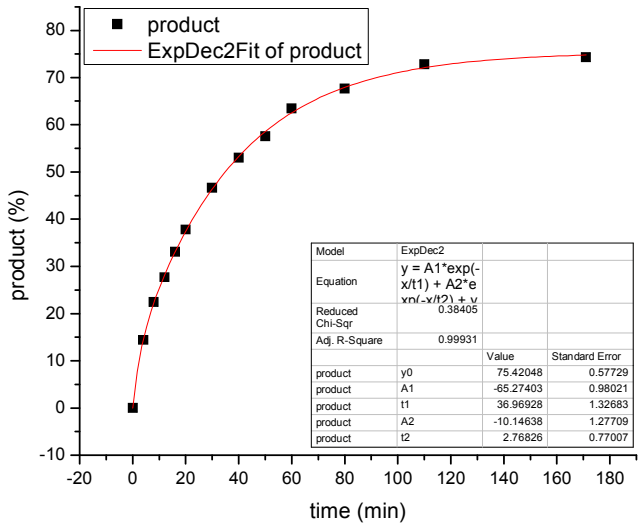

Half-life: 34.86
Average: 32.5

Table 5. entry 7. catalyst **V{*1,2,8*}: run 1**

time, min	µmol standard	area standard	area product	µmol product	product %
0	207.64	0.00	0.00	0.00	0.00
4	207.64	24.85	3.59	36.02	10.63
8	207.64	24.92	6.09	60.85	17.96
12	207.64	25.60	8.37	81.49	24.05
16	207.64	23.43	9.41	100.12	29.55
20	207.64	25.77	11.80	114.07	33.66
30	207.64	25.98	14.70	140.97	41.60
40	207.64	26.53	17.11	160.71	47.43
50	207.64	25.81	18.26	176.26	52.02
60	207.64	24.52	19.22	195.36	57.65
80	207.64	26.25	22.73	215.75	63.67
110	207.64	28.10	26.10	231.51	68.32

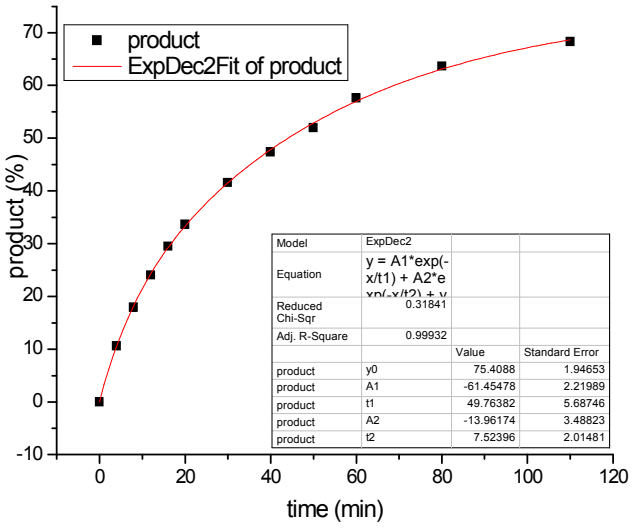

Half-life: 40.03

Table 5. entry 7. catalyst **V{*1,2,8*}: run 2**

time, min	µmol standard	area standard	area product	µmol product	product %
0	207.64	0.00	0.00	0.00	0.00
4	207.64	26.10	3.12	36.65	10.81
8	207.64	26.39	4.94	57.45	16.95
12	207.64	29.65	7.04	72.83	21.49
16	207.64	29.52	8.35	86.78	25.61
20	207.64	27.16	8.76	98.92	29.19
30	207.64	28.96	11.63	123.19	36.36
40	207.64	29.36	13.83	144.42	42.62
50	207.64	29.46	15.03	156.46	46.17
60	207.64	29.47	16.33	169.89	50.14
80	207.64	29.41	17.94	187.08	55.21
110	207.64	29.96	20.93	214.24	63.23

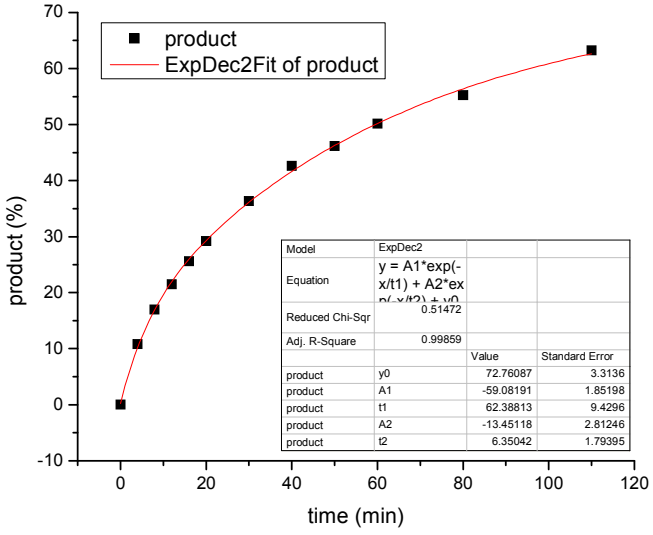

Half-life: 59.51
Average: 51.8

Table 5. entry 8. catalyst **V{*1,2,8*}β: run 1**

time, min	µmol standard	area standard	area product	µmol product	product %
16	256.25	26.34	6.50	75.83	22.39
20	256.25	26.25	7.92	92.75	27.38
30	256.25	26.29	10.74	125.60	37.08
40	256.25	26.64	12.32	142.18	41.97
60	256.25	27.29	16.97	191.19	56.44
98	256.25	27.81	22.36	247.18	72.97

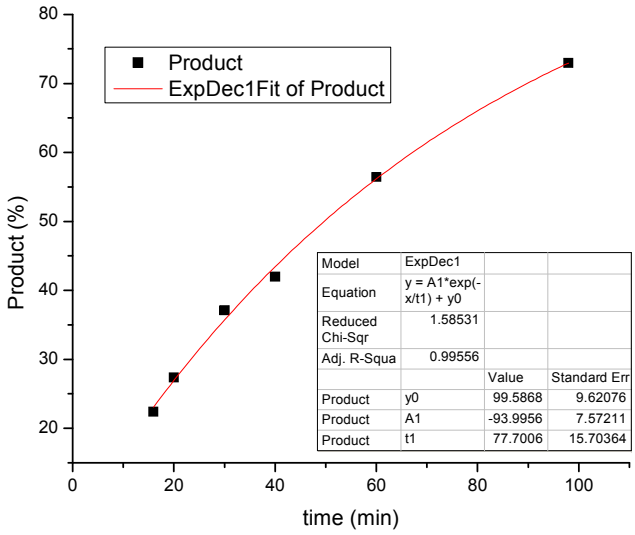

Half-life: 49.69

Table 5. entry 8. catalyst **V{*1,2,8*}β: run 2**

time, min	µmol standard	area standard	area product	µmol product	product %
16	256.25	26.34	6.50	75.83	22.39
20	256.25	26.25	7.92	92.75	27.38
30	256.25	26.29	10.74	125.60	37.08
40	256.25	26.64	12.32	142.18	41.97
60	256.25	27.29	16.97	191.19	56.44
98	256.25	27.81	22.36	247.18	72.97

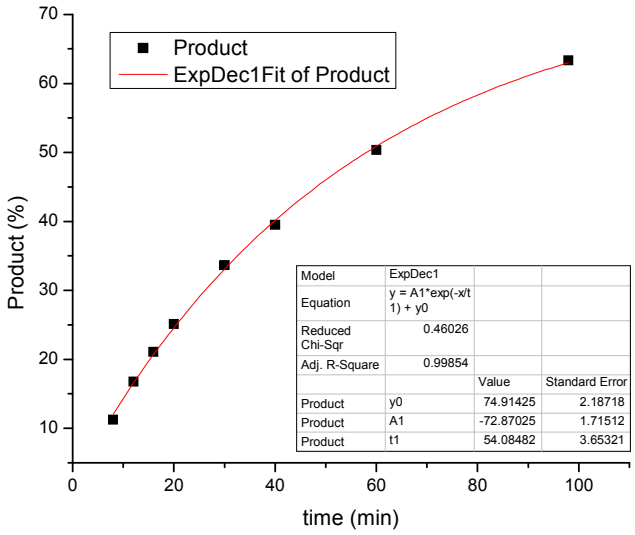

Half-life: 58.05
Average: 53.09

Table 5. entry 9. catalyst **V{*1,2,7*}β: run 1**

time, min	µmol standard	area standard	area product	µmol product	product %
0	256.25	0.00	0.00	0.00	0.00
2	256.25	27.23	4.88	55.14	16.28
4	256.25	26.07	8.62	101.72	30.03
8	256.25	26.65	14.06	162.24	47.90
12	256.25	26.76	16.54	190.02	56.10
20	256.25	26.93	21.61	246.81	72.86
30	256.25	27.28	24.36	274.58	81.06
40	256.25	29.40	27.13	283.70	83.75

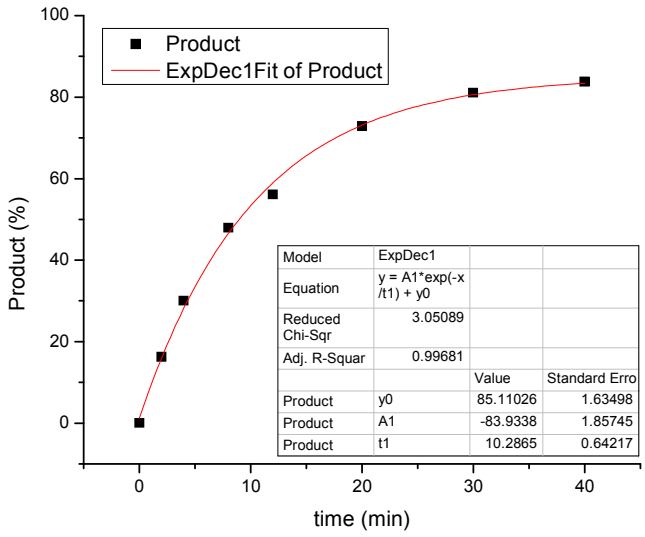

Half-life: 8.97

Table 5. entry 9. catalyst **V{*1,2,7*}β: run 2**

time, min	µmol standard	area standard	area product	µmol product	product %
0	208.20	0.00	0.00	0.00	0.00
2	208.20	23.62	5.95	62.95	18.58
4	208.20	24.23	9.56	98.56	29.09
8	208.20	22.59	13.45	148.72	43.90
12	208.20	22.57	16.33	180.79	53.36
16	208.20	22.94	18.61	202.64	59.81
20	208.20	23.13	21.00	226.82	66.95
30	208.20	23.14	24.78	267.50	78.95
40	208.20	23.55	26.77	283.99	83.82

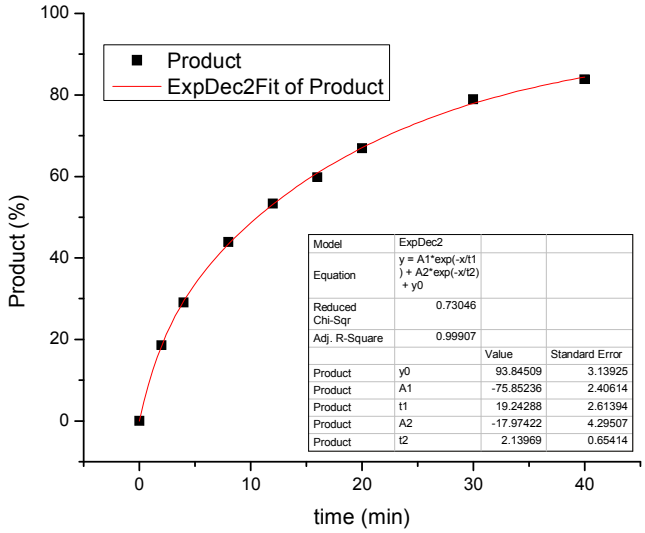

Half-life: 10.60
Average: 9.78

Table 5. entry 10. catalyst **V{*1,2,6*}: run 1**

time, min	µmol standard	area standard	area product	µmol product	product %
0	255.56	0.00	0.00	0.00	0.00
4	255.56	28.44	3.96	42.69	12.60
8	255.56	27.15	6.76	76.36	22.53
12	255.56	29.11	10.32	108.70	32.08
16	255.56	27.97	12.22	134.02	39.55
20	255.56	29.35	14.96	156.34	46.14
30	255.56	28.77	18.14	193.39	57.07
40	255.56	28.95	20.82	220.59	65.10
50	255.56	29.58	22.56	233.80	69.00
60	255.56	29.79	23.99	246.98	72.89
80	255.56	30.14	26.21	266.76	78.72

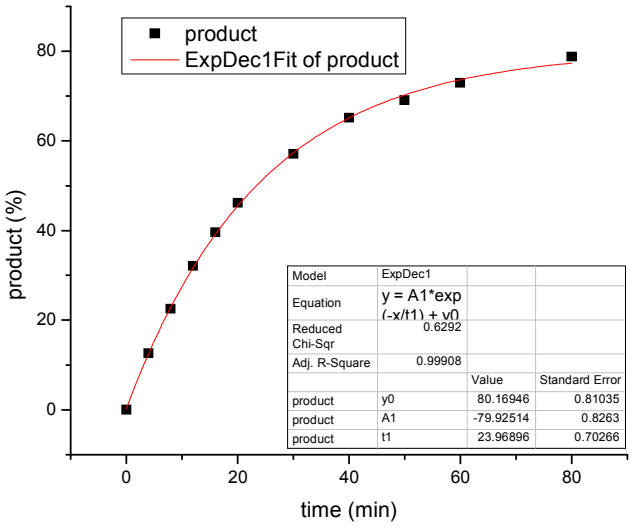

Half-life: 23.35

Table 5. entry 10. catalyst **V{*1,2,6*}: run 2**

time, min	µmol standard	area standard	area product	µmol product	product %
0	255.56	0.00	0.00	0.00	0.00
4	255.56	29.02	4.29	45.31	13.37
8	255.56	29.23	6.90	72.36	21.35
12	255.56	29.93	9.12	93.42	27.57
16	255.56	28.13	10.95	119.36	35.22
20	255.56	28.68	13.29	142.11	41.94
30	255.56	29.54	17.97	186.62	55.07
40	255.56	29.81	21.08	216.85	64.00
50	255.56	30.10	22.38	228.01	67.29
60	255.56	29.93	23.55	241.26	71.20
80	255.56	30.62	25.89	259.29	76.52

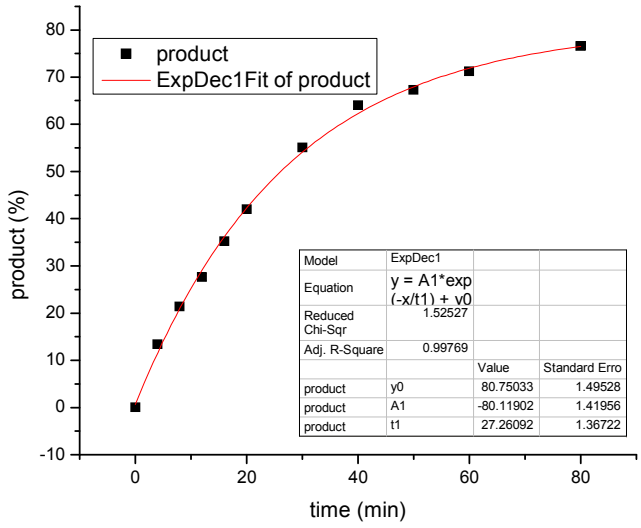

Half-life: 26.11
Average: 24.70

Table 5. entry 11. catalyst **V{*2,2,1*}: run 1**

time, min	µmol standard	area standard	area product	µmol product	product %
0	253.90	0.00	0.00	0.00	0.00
1	253.90	34.13	3.52	31.37	9.25
2	253.90	35.29	6.37	54.90	16.18
3	253.90	35.39	8.42	72.40	21.34
4	253.90	35.35	10.29	88.58	26.11
5	253.90	35.27	11.97	103.26	30.44
6	253.90	34.10	13.60	121.33	35.77
7	253.90	34.07	15.16	135.36	39.90
8	253.90	33.58	22.67	205.42	60.56
9	253.90	33.34	26.12	238.37	70.27
10	253.90	32.67	28.59	266.35	78.52
12	253.90	32.57	29.36	274.33	80.87
15	253.90	32.54	30.89	288.90	85.17
30	253.90	31.83	30.80	294.45	86.80

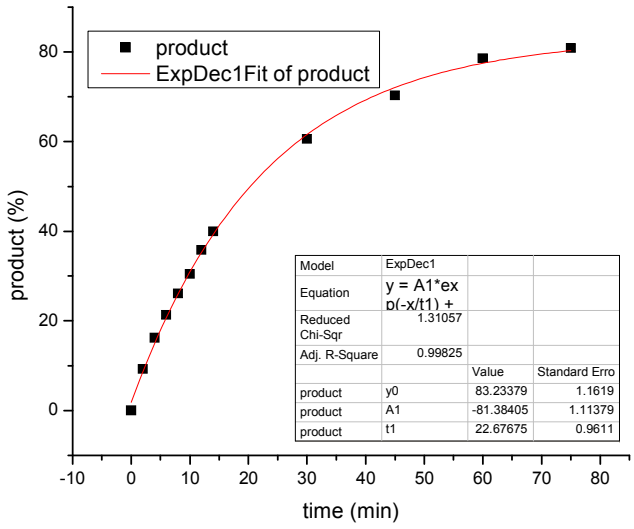

Half-life: 20.31

Table 5. entry 11. catalyst **V{*2,2,I*}: run 2**

time, min	µmol standard	area standard	area product	µmol product	product %
0	253.90	0.00	0.00	0.00	0.00
2	253.90	34.83	3.60	31.44	9.27
4	253.90	36.36	6.40	53.59	15.80
6	253.90	32.64	7.70	71.76	21.15
8	253.90	34.71	10.17	89.20	26.30
10	253.90	33.33	11.47	104.75	30.88
12	253.90	33.93	13.11	117.55	34.65
14	253.90	35.56	15.58	133.37	39.32
30	253.90	33.63	22.09	199.87	58.92
45	253.90	32.88	25.26	233.86	68.94
60	253.90	32.65	27.78	258.92	76.33
75	253.90	32.05	29.32	278.36	82.06

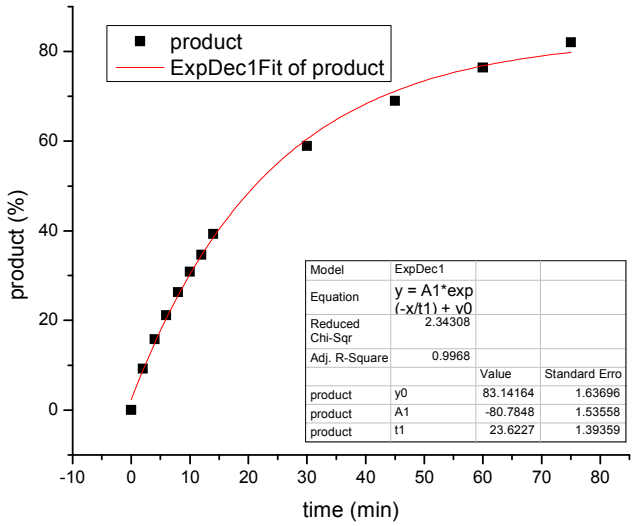

Half-life: 21.05
Average: 20.7

Table 5. entry 12. catalyst **V{*2,2,3*}: run 1**

time, min	µmol standard	area standard	area product	µmol product	product %
0	255.72	0.00	0.00	0.00	0.00
4	255.72	29.68	4.91	50.72	14.98
8.78	255.72	28.67	8.49	90.90	26.86
12	255.72	28.94	10.82	114.74	33.90
16	255.72	29.75	13.06	134.72	39.80
20	255.72	29.62	14.89	154.25	45.57
30	255.72	28.81	18.40	195.96	57.90
40	255.72	31.25	21.00	206.24	60.93
60	255.72	31.16	23.64	232.85	68.80
80	255.72	31.93	25.61	246.18	72.73

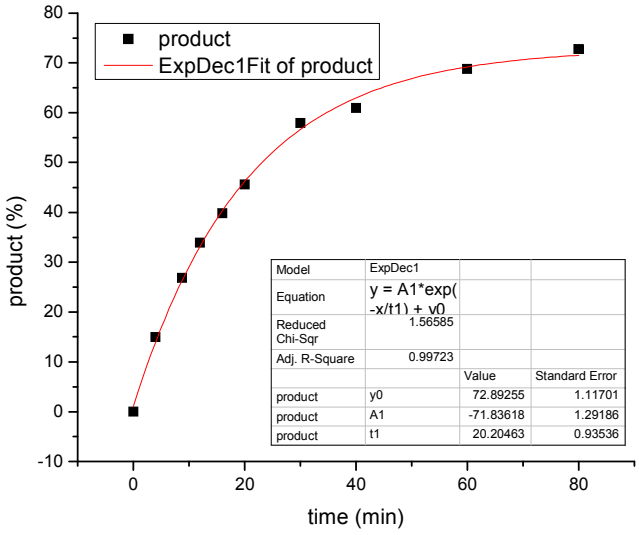

Half-life: 23.11

Table 5. entry 12. catalyst **V{*2,2,3*}: run 2**

time, min	µmol standard	area standard	area product	µmol product	product %
0	255.72	0.00	0.00	0.00	0.00
4	255.72	27.69	4.69	51.97	15.36
8	255.72	28.28	8.18	88.71	26.21
12	255.72	28.93	11.08	117.55	34.73
16	255.72	29.68	13.22	136.72	40.40
20	255.72	29.82	14.99	154.26	45.58
30	255.72	30.43	18.80	189.56	56.01
40	255.72	30.83	20.98	208.84	61.70

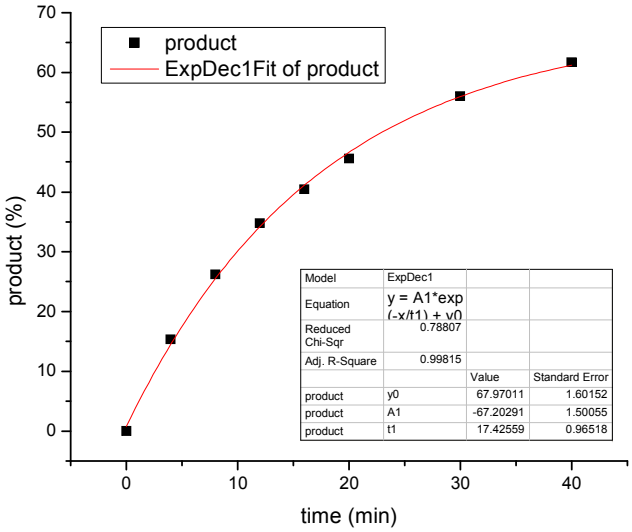

Half-life: 22.98
Average: 23.0

Table 5. entry 13. catalyst **V{*2,2,5*}: run 1**

time, min	µmol standard	area standard	area product	µmol product	product %
60	254.41	36.71	2.62	21.80	6.44
75	254.41	35.66	2.93	25.09	7.41
90	254.41	35.96	3.30	28.02	8.28
105	254.41	35.78	3.55	30.28	8.94
147	254.41	36.21	4.41	37.14	10.97
965	254.41	30.39	18.52	185.78	54.88

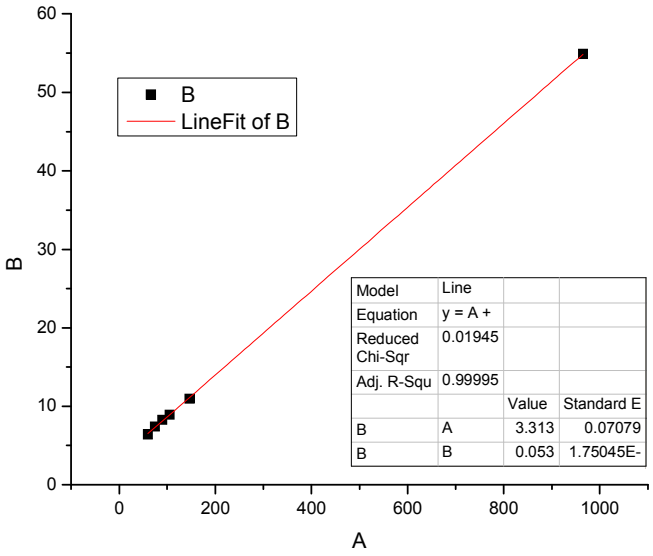

Half-life: 873.94

Table 5. entry 13. catalyst **V{*2,2,5*}: run 2**

time, min	µmol standard	area standard	area product	µmol product	product %
60	253.90	34.92	2.76	24.11	7.12
75	253.90	35.03	3.15	27.44	8.11
90	253.90	35.50	3.65	31.38	9.27
105	253.90	34.23	3.67	32.70	9.66
147	253.90	34.79	4.70	41.20	12.17
965	253.90	30.66	17.67	175.71	51.90

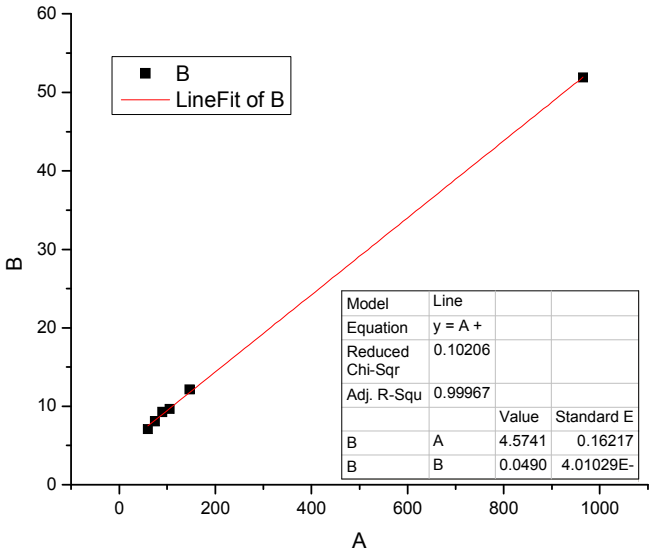

Half-life: 925.55
Average: 899.70

Table 5. entry 14. catalyst **V{*2,2,8*}: run 1**

time, min	µmol standard	area standard	area product	µmol product	product %
2	254.41	33.53	3.73	33.89	9.99
4	254.41	33.08	6.57	60.53	17.84
6	254.41	33.77	8.16	73.64	21.71
8	254.41	32.74	9.76	90.92	26.80
10	254.41	33.14	11.36	104.57	30.83
12	254.41	32.39	12.27	115.56	34.07
14	254.41	31.92	13.39	127.87	37.70
16	254.41	31.72	14.30	137.50	40.53
20	254.41	31.19	16.52	161.49	47.61
30	254.41	30.48	19.93	199.37	58.77
45	254.41	29.91	23.52	239.78	70.68
60	254.41	29.68	25.93	266.33	78.51
75	254.41	29.63	27.19	279.87	82.50
90	254.41	29.43	28.47	294.99	86.96

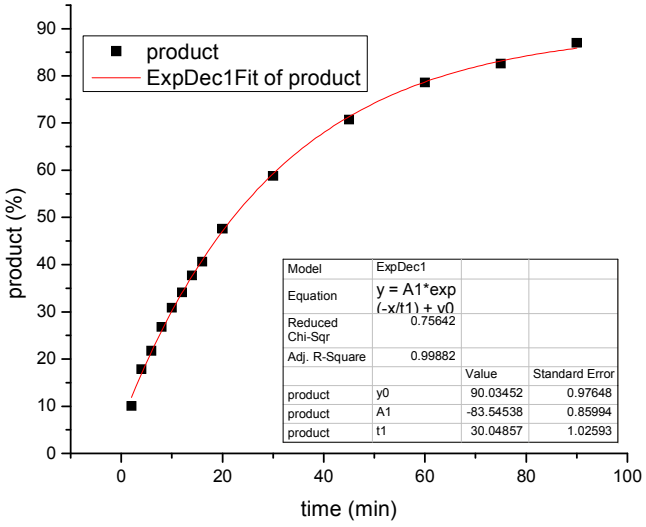

Half-life: 22.11

Table 5. entry 14. catalyst **V{*2,2,8*}: run 2**

time, min	µmol standard	area standard	area product	µmol product	product %
0	254.41	0.00	0.00	0.00	0.00
2	254.41	31.93	3.65	34.84	10.27
4	254.41	31.35	6.57	63.92	18.84
6	254.41	32.35	8.46	79.73	23.50
8	254.41	32.52	10.65	99.91	29.45
10	254.41	32.90	12.39	114.84	33.85
12	254.41	31.52	14.02	135.67	40.00
14	254.41	33.05	15.54	143.33	42.25
16	254.41	31.13	16.03	157.03	46.29
20	254.41	30.42	18.58	186.26	54.91
30	254.41	30.30	22.91	230.50	67.95
45	254.41	30.07	26.39	267.59	78.88
60	254.41	29.40	27.72	287.48	84.75
75	254.41	29.57	29.57	304.93	89.89
90	254.41	29.21	30.03	313.49	92.42

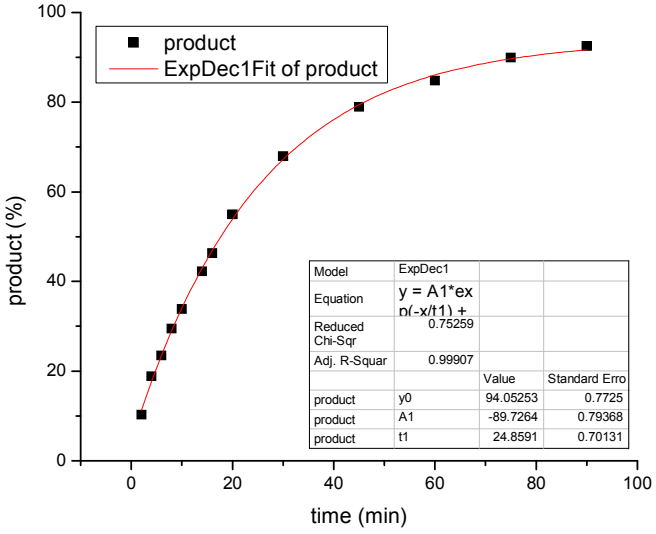

Half-life: 17.68
Average: 19.9

Table 5. entry 15. catalyst **V{*2,2,7*}: run 1**

time, min	µmol standard	area standard	area product	µmol product	product %
0	254.15	0.00	0.00	0.00	0.00
2	254.15	30.56	4.22	40.87	12.08
4	254.15	30.95	7.77	74.29	21.97
6	254.15	30.23	10.27	100.52	29.72
8	254.15	30.23	12.49	122.27	36.15
10	254.15	30.17	14.27	139.88	41.36
15	254.15	30.16	17.81	174.72	51.66
17	254.15	30.08	18.80	184.90	54.67
20	254.15	29.52	20.07	201.15	59.48
30	254.15	29.65	23.63	235.73	69.70
60	254.15	29.91	29.48	291.59	86.22

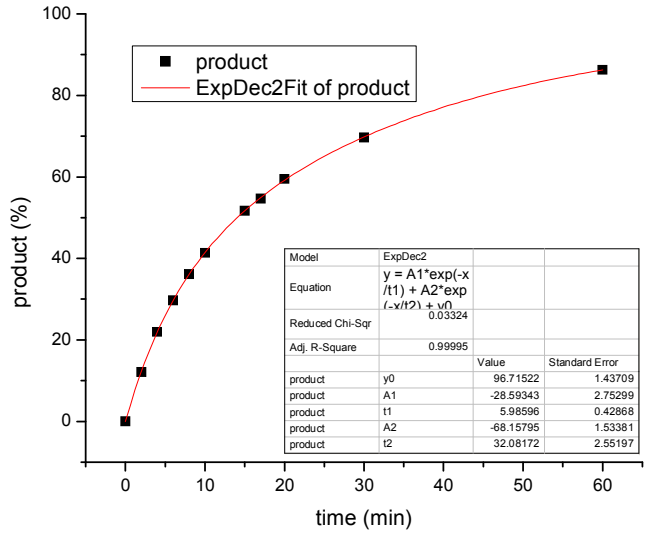

Half-life: 14.41

Table 5. entry 15. catalyst **V{*2,2,7*}: run 2**

time, min	µmol standard	area standard	area product	µmol product	product %
0	254.15	0.00	0.00	0.00	0.00
2	254.15	29.99	3.71	36.58	10.82
4	254.15	29.05	6.76	68.81	20.35
6	254.15	29.29	9.41	95.07	28.11
8	254.15	29.69	11.53	114.88	33.97
10	254.15	29.47	13.27	133.24	39.39
15	254.15	29.61	16.51	164.94	48.77
17	254.15	29.33	17.28	174.23	51.51
20	254.15	29.57	18.80	188.09	55.61
30	254.15	29.73	22.03	219.19	64.81
60	254.15	29.64	27.44	273.88	80.98

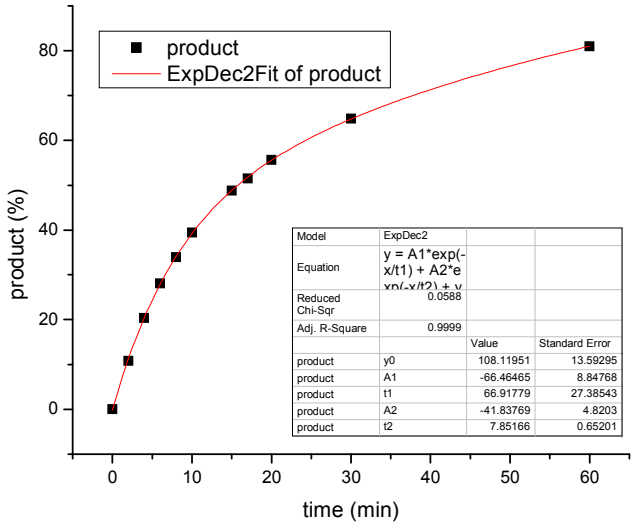

Half-life: 15.77
Average: 15.09

Table 5. entry 16. catalyst **V{*2,2,6*}: run 1**

time, min	µmol standard	area standard	area product	µmol product	product %
0	253.90	0.00	0.00	0.00	0.00
1	253.90	37.44	0.64	5.18	1.53
2	253.90	35.39	1.44	12.38	3.65
3	253.90	37.18	2.35	19.26	5.68
4	253.90	37.90	3.09	24.82	7.32
5	253.90	37.06	3.59	29.51	8.70
6	253.90	37.05	4.40	36.15	10.66
7	253.90	37.04	4.99	41.04	12.10
8	253.90	36.57	5.66	47.08	13.88
9	253.90	33.55	6.07	55.01	16.22
10	253.90	36.15	7.18	60.44	17.82
12	253.90	33.39	8.37	76.33	22.50
15	253.90	33.90	10.56	94.77	27.94
30	253.90	34.54	19.40	170.96	50.40
60	253.90	33.58	25.25	228.79	67.45

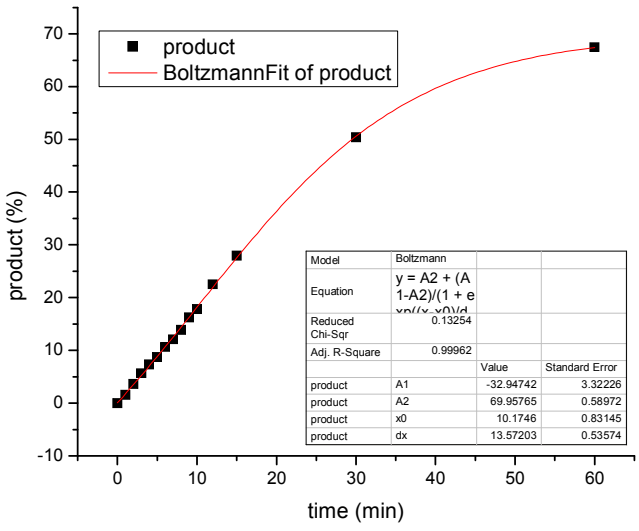

Half-life: 29.51

Table 5. entry 16. catalyst **V{*2,2,6*}: run 2**

time, min	µmol standard	area standard	area product	µmol product	product %
0	253.90	0.00	0.00	0.00	0.00
1	253.90	36.75	0.48	3.95	1.16
2	253.90	37.89	1.27	10.22	3.01
3	253.90	37.46	2.05	16.62	4.90
4	253.90	35.99	2.83	23.90	7.05
5	253.90	34.84	3.43	29.93	8.82
6	253.90	36.78	4.44	36.71	10.82
7	253.90	36.25	5.33	44.71	13.18
8	253.90	34.29	5.54	49.14	14.49
9	253.90	34.90	6.63	57.78	17.03
10	253.90	36.00	7.52	63.55	18.73
12	253.90	35.71	8.87	75.61	22.29
15	253.90	35.54	11.23	96.18	28.35
30	253.90	32.26	20.06	189.29	55.80

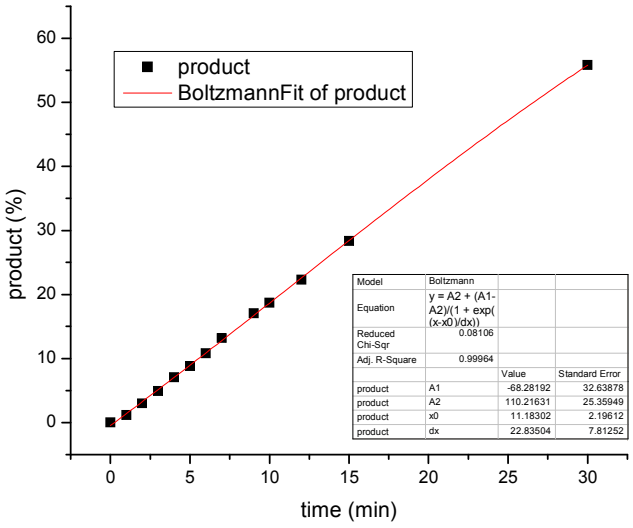

Half-life: 26.60
Average: 28.10

Table 5. entry 17. catalyst **V{*2,3,1*}: run 1**

time, min	µmol standard	area standard	area product	µmol product	product %
0	254.29	0.00	0.00	0.00	0.00
2	254.29	33.61	4.18	37.86	11.11
4	254.29	33.66	6.85	62.05	18.21
6	254.29	33.00	9.12	84.26	24.73
8	254.29	32.81	10.62	98.65	28.96
10	254.29	33.00	12.50	115.48	33.90
12	254.29	32.29	13.60	128.35	37.67
15	254.29	30.85	15.89	156.99	46.08
20	254.29	31.75	17.85	171.34	50.29
30	254.29	30.76	20.88	206.92	60.74
45	254.29	30.50	22.68	226.65	66.53
61	254.29	29.34	23.54	244.52	71.77
75	254.29	29.95	25.98	264.38	77.60
90	254.29	29.85	26.40	269.53	79.12

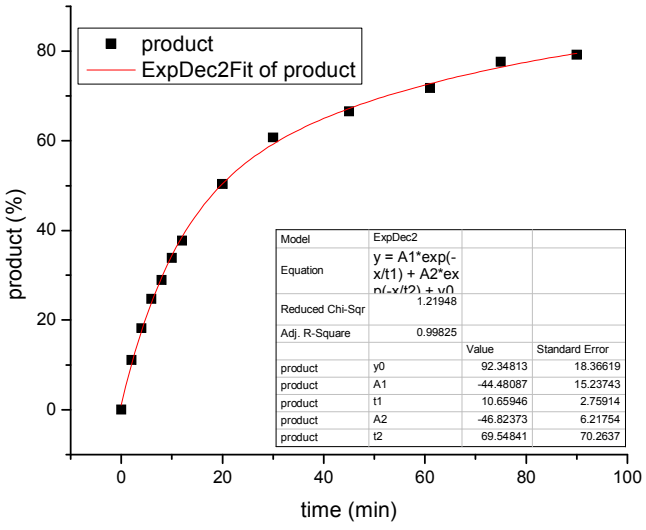

Half-life: 19.64

Table 5. entry 17. catalyst **V{*2,3,1*}: run 2**

time, min	µmol standard	area standard	area product	µmol product	product %
0	254.29	0.00	0.00	0.00	0.00
2	254.29	33.36	3.32	30.37	8.91
4	254.29	34.48	5.80	51.31	15.06
6	254.29	33.33	7.34	67.12	19.70
8	254.29	33.52	8.82	80.19	23.54
10	254.29	31.73	9.63	92.48	27.15
12	254.29	33.09	11.49	105.85	31.07
15	254.29	32.33	13.28	125.22	36.76
20	254.29	32.18	15.43	146.14	42.90
30	254.29	31.99	19.30	183.87	53.97
45	254.29	31.07	21.90	214.87	63.07
61	254.29	30.58	23.85	237.70	69.77
75	254.29	30.08	24.75	250.81	73.62
90	254.29	30.93	26.39	260.08	76.34

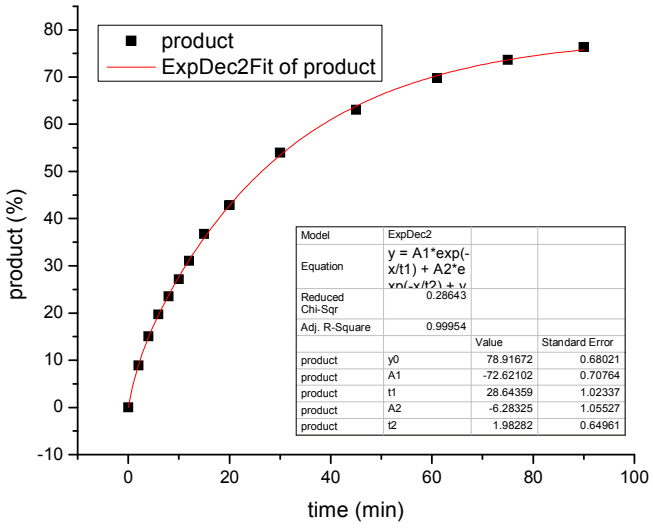

Half-life: 26.38
Average: 23.0

Table 5. entry 18. catalyst **V{*2,3,2*}: run 1**

time, min	µmol standard	area standard	area product	µmol product	product %
0	236.54	0.00	0.00	0.00	0.00
2	236.54	25.92	1.49	16.32	4.82
4	236.54	29.21	3.26	31.65	9.35
8	236.54	28.68	5.53	54.71	16.16
12	236.54	28.98	7.59	74.34	21.96
16	236.54	28.96	8.92	87.41	25.83
20	236.54	27.60	9.64	99.10	29.28
36	236.54	27.81	13.26	135.33	39.98
50	236.54	28.12	14.50	146.39	43.25
75	236.54	28.75	16.84	166.23	49.12
123	236.54	28.73	19.60	193.57	57.19

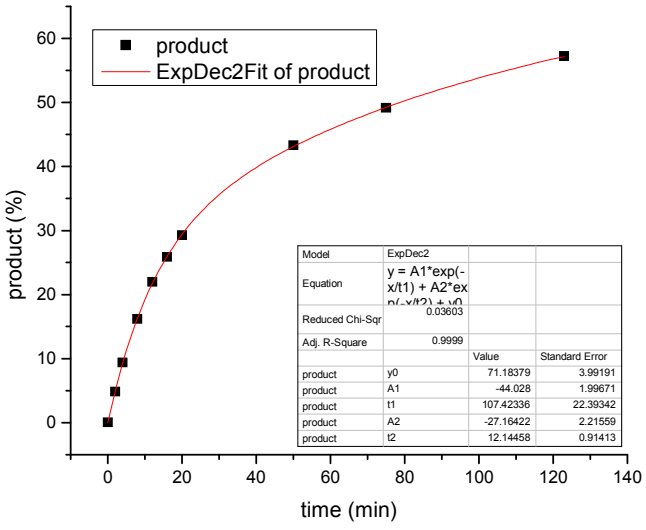

Half-life: 78.80

Table 5. entry 18. catalyst **V{*2,3,2*}: run 2**

time, min	µmol standard	area standard	area product	µmol product	product %
0	256.10	0.00	0.00	0.00	0.00
2	256.10	27.00	1.46	16.59	4.90
4	256.10	29.31	2.81	29.44	8.70
8	256.10	29.90	4.48	46.08	13.61
12	256.10	29.55	5.71	59.39	17.55
20	256.10	29.75	8.10	83.67	24.72
36	256.10	29.76	11.60	119.73	35.37
50	256.10	28.42	12.93	139.79	41.30
75	256.10	29.28	16.26	170.66	50.42
123	256.10	30.53	21.89	220.36	65.11

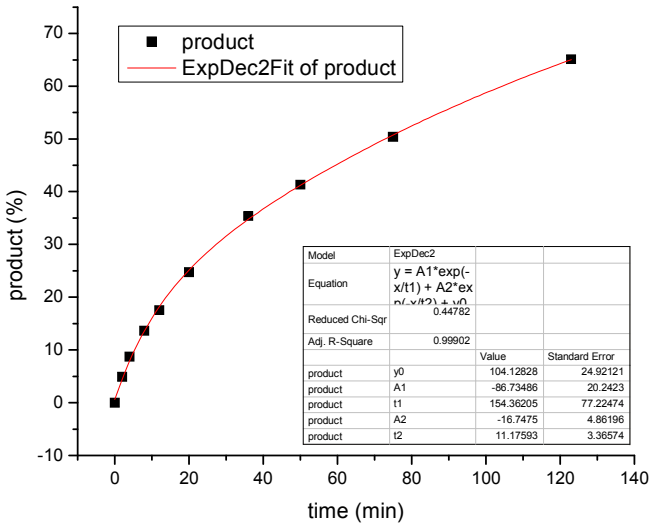

Half-life: 72.85
Average: 75.8

Table 5. entry 19. catalyst **V{*2,3,3*}: run 1**

time, min	µmol standard	area standard	area product	µmol product	product %
0	255.01	0.00	0.00	0.00	0.00
6	255.01	25.99	5.25	61.81	18.28
10	255.01	27.03	7.41	83.90	24.81
16	255.01	26.33	9.68	112.51	33.27
20	255.01	29.01	12.06	127.22	37.62
25	255.01	29.33	14.02	146.24	43.24
30	255.01	28.85	15.10	160.12	47.34
35	255.01	28.43	15.92	171.34	50.66
40	255.01	28.72	16.75	178.40	52.75
50	255.01	28.92	18.01	190.55	56.34
60	255.01	29.23	18.95	198.42	58.67
80	255.01	29.79	21.18	217.54	64.32
170	255.01	30.32	26.47	267.08	78.97

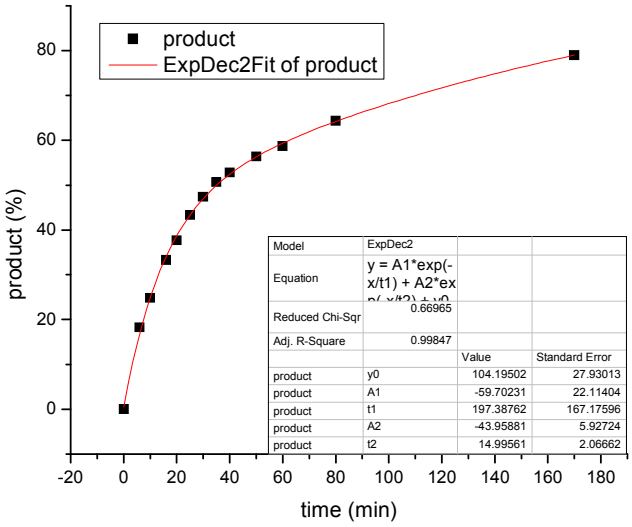

Half-life: 35.12

Table 5. entry 19. catalyst **V{*2,3,3*}: run 2**

time, min	µmol standard	area standard	area product	µmol product	product %
0	255.01	0.00	0.00	0.00	0.00
6	255.01	26.16	5.89	68.91	20.37
10	255.01	29.21	9.38	98.22	29.04
16	255.01	29.34	12.30	128.30	37.94
20	255.01	29.24	13.71	143.44	42.41
25	255.01	29.61	15.64	161.65	47.80
30	255.01	29.73	17.39	178.95	52.91
35	255.01	29.20	18.59	194.89	57.62
40	255.01	29.13	19.14	201.11	59.46
50	255.01	29.87	20.83	213.34	63.08
60	255.01	29.93	22.11	226.09	66.85
80	255.01	30.06	23.42	238.46	70.51
170	255.01	29.85	26.84	275.24	81.38

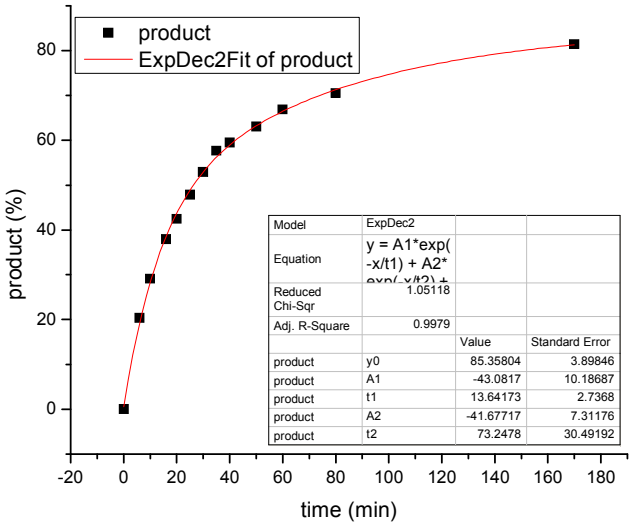

Half-life: 26.32
Average: 30.7

Table 5. entry 20. catalyst **V{*2,3,5*}: run 1**

time, min	µmol standard	area standard	area product	µmol product	product %
0	255.01	0.00	0.00	0.00	0.00
10	255.01	28.52	3.06	32.81	9.70
30	255.01	28.85	6.44	68.32	20.20
90	255.01	30.33	10.69	107.86	31.89
150	255.01	30.70	13.65	136.00	40.21
190	255.01	30.55	15.17	151.89	44.91
250	255.01	31.04	16.84	165.99	49.08
307	255.01	30.36	17.77	179.13	52.97
350	255.01	31.03	19.19	189.18	55.94
402	255.01	30.45	19.76	198.61	58.72
450	255.01	31.55	21.22	205.88	60.87
500	255.01	31.34	21.34	208.38	61.61
552	255.01	31.17	21.57	211.80	62.62

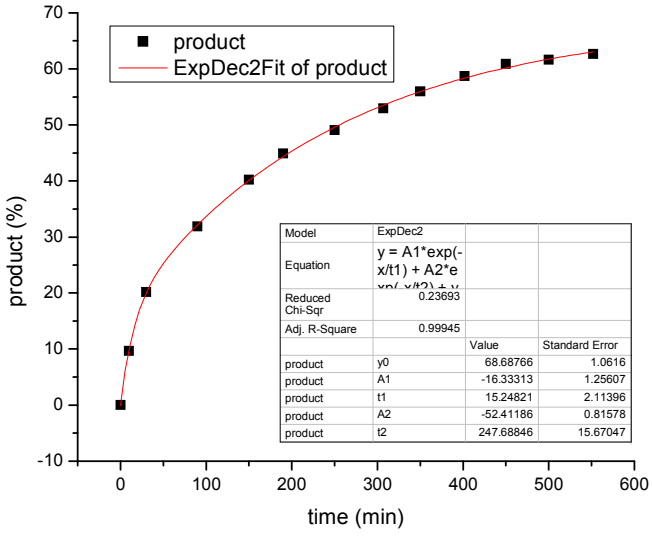

Half-life: 255.43

Table 5. entry 20. catalyst **V{*2,3,5*}: run 2**

time, min	µmol standard	area standard	area product	µmol product	product %
0	255.01	0.00	0.00	0.00	0.00
10	255.01	26.50	2.98	34.35	10.16
90	255.01	28.16	11.13	121.02	35.78
150	255.01	29.78	14.28	146.73	43.38
190	255.01	30.52	16.19	162.30	47.99
250	255.01	30.81	17.66	175.43	51.87
307	255.01	30.74	19.45	193.66	57.26
350	255.01	30.97	20.46	202.15	59.77
402	255.01	31.00	21.96	216.83	64.11
450	255.01	31.37	22.80	222.47	65.78
500	255.01	31.74	23.65	228.02	67.42
552	255.01	31.93	24.47	234.54	69.35

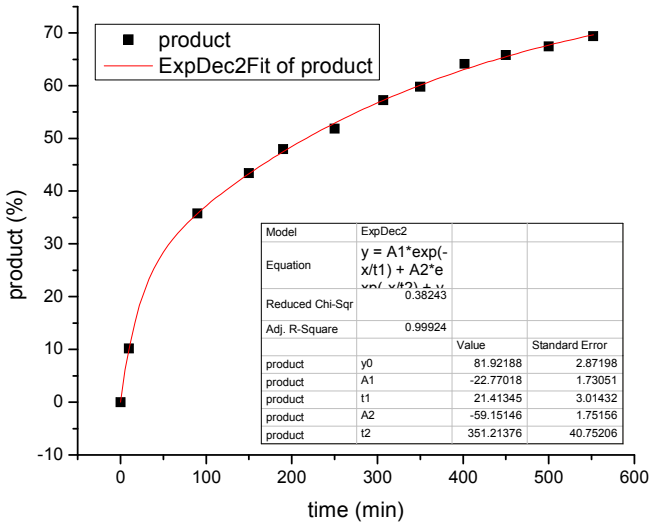

Half-life: 216.64
Average: 236.0

Table 5. entry 21. catalyst **V{*2,3,8*}: run 1**

time, min	µmol standard	area standard	area product	µmol product	product %
0	256.20	0.00	0.00	0.00	0.00
5	256.20	28.79	5.65	60.30	17.81
10	256.20	28.63	9.17	98.50	29.09
15	256.20	28.98	11.81	125.30	37.01
20	256.20	30.28	14.18	143.93	42.51
25	256.20	28.60	15.20	163.43	48.27
30	256.20	28.73	16.75	179.22	52.94
40	256.20	29.92	19.51	200.44	59.21
60	256.20	29.51	22.17	231.00	68.23
80	256.20	29.86	24.33	250.49	73.99
100	256.20	30.22	25.43	258.72	76.42

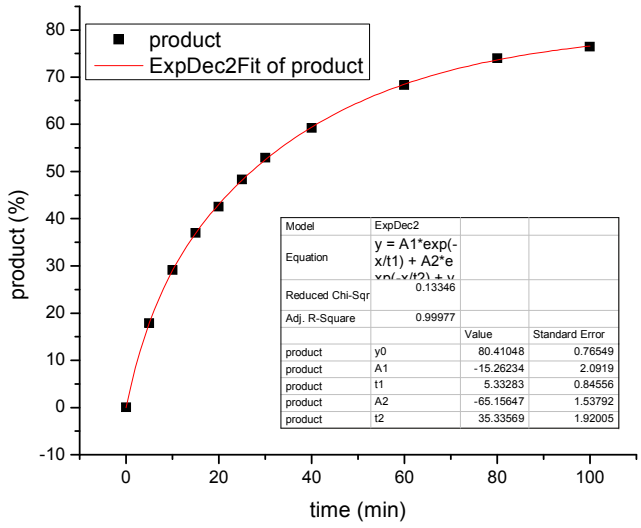

Half-life: 27.04

Table 5. entry 21. catalyst **V{*2,3,8*}: run 2**

time, min	µmol standard	area standard	area product	µmol product	product %
0	256.39	0.00	0.00	0.00	0.00
5	256.39	27.65	6.13	68.17	20.13
10	256.39	30.73	10.12	101.33	29.93
15	256.39	30.30	12.77	129.70	38.31
20	256.39	30.19	14.46	147.41	43.54
25	256.39	28.82	15.36	163.97	48.43
30	256.39	29.41	17.21	179.98	53.16
40	256.39	29.80	20.08	207.31	61.23
60	256.39	30.07	22.71	232.35	68.63
80	256.39	30.46	24.49	247.37	73.07
100	256.39	31.23	26.01	256.23	75.68

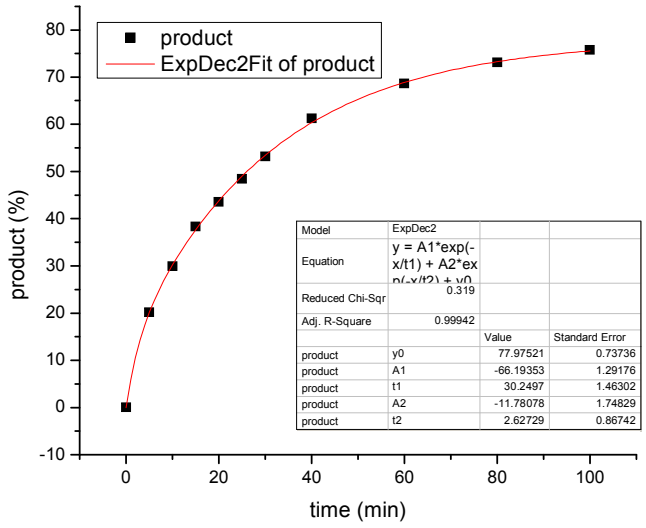

Half-life: 26.05
Average: 26.5

Table 5. entry 22. catalyst **V{*2,3,7*}: run 1**

time, min	µmol standard	area standard	area product	µmol product	product %
0	256.39	0.00	0.00	0.00	0.00
2	256.39	25.91	2.37	28.19	8.33
4	256.39	28.47	4.94	53.39	15.78
6	256.39	28.64	6.28	67.48	19.95
8	256.39	27.17	7.32	82.93	24.52
10	256.39	28.90	9.13	97.21	28.74
12	256.39	29.34	10.30	108.02	31.94
16	256.39	28.77	12.06	129.00	38.14
20	256.39	29.15	13.51	142.56	42.15
30	256.39	29.72	16.86	174.56	51.61
40	256.39	29.78	18.60	192.22	56.84
60	256.39	30.08	21.17	216.60	64.04
94	256.39	30.67	24.57	246.41	72.86

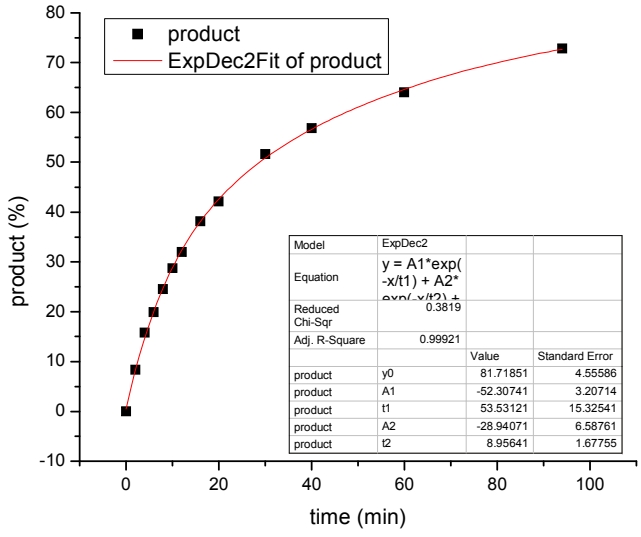

Half-life: 28.78

Table 5. entry 22. catalyst **V{*2,3,7*}: run 2**

time, min	µmol standard	area standard	area product	µmol product	product %
0	256.39	0.00	0.00	0.00	0.00
2	256.39	25.82	2.34	27.91	8.23
4	256.39	26.42	4.64	54.02	15.92
6	256.39	28.33	6.72	72.96	21.51
8	256.39	28.38	8.13	88.18	25.99
10	256.39	28.38	9.42	102.13	30.11
12	256.39	29.07	10.54	111.53	32.88
16	256.39	29.06	12.50	132.34	39.01
20	256.39	29.38	13.98	146.44	43.17
30	256.39	29.19	16.52	174.11	51.33
40	256.39	28.84	17.65	188.34	55.52
60	256.39	30.40	20.94	211.96	62.48
94	256.39	28.88	22.62	240.99	71.04

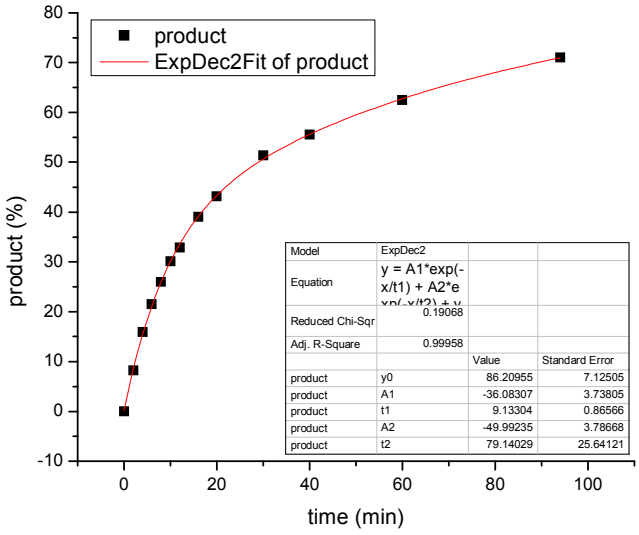

Half-life: 28.92
Average: 28.9

Table 5. entry 23. catalyst **V{*2,3,6*}: run 1**

time, min	µmol standard	area standard	area product	µmol product	product %
0	255.01	0.00	0.00	0.00	0.00
2	255.01	27.08	2.49	28.16	8.32
4	255.01	27.13	4.29	48.34	14.29
6	255.01	29.86	6.51	66.72	19.73
8	255.01	30.07	8.46	86.06	25.45
10	255.01	30.29	9.72	98.22	29.04
12	255.01	27.89	10.32	113.28	33.49
14	255.01	30.06	12.41	126.37	37.36
16	255.01	30.25	13.57	137.26	40.59
20	255.01	30.66	16.02	159.92	47.28
30	255.01	30.65	20.75	207.19	61.26
45	255.01	30.98	24.49	241.87	71.51
80	255.01	30.86	27.09	268.64	79.43

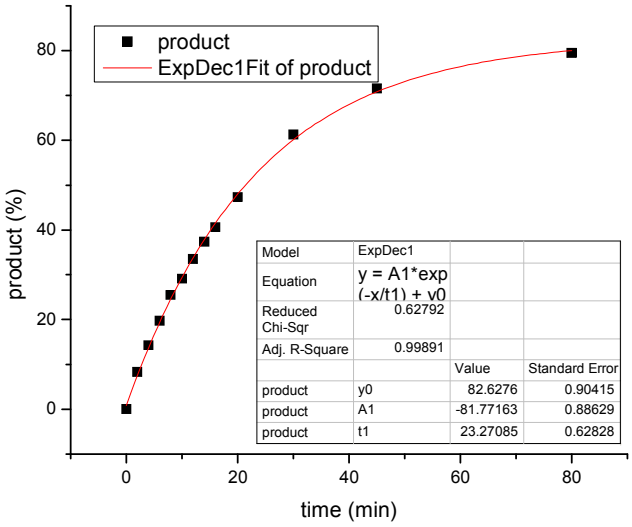

Half-life: 21.38

Table 5. entry 23. catalyst **V{*2,3,6*}: run 2**

time, min	µmol standard	area standard	area product	µmol product	product %
0	255.01	0.00	0.00	0.00	0.00
2	255.01	26.96	2.56	29.07	8.60
4	255.01	27.36	4.59	51.39	15.19
6	255.01	30.57	6.99	69.99	20.69
8	255.01	27.52	7.93	88.13	26.06
10	255.01	28.11	9.15	99.66	29.47
12	255.01	28.49	10.54	113.17	33.46
14	255.01	30.23	12.63	127.88	37.81
16	255.01	30.25	13.91	140.70	41.60
20	255.01	30.89	16.51	163.55	48.36
30	255.01	30.71	21.00	209.22	61.86
45	255.01	30.82	25.08	249.03	73.63
80	255.01	31.85	27.86	267.71	79.16

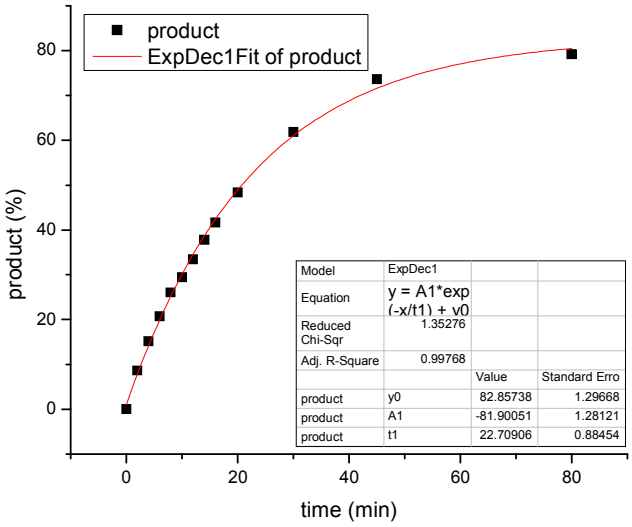

Half-life: 20.74
Average: 21.1

Table 5. entry 24. catalyst **V{*2,7,1*}: run 1**

time, min	µmol standard	area standard	area product	µmol product	product %
0	255.56	0.00	0.00	0.00	0.00
4	255.56	28.62	5.86	62.79	18.53
8	255.56	27.65	9.55	105.89	31.25
12	255.56	28.89	13.00	138.01	40.73
16	255.56	29.77	16.08	165.66	48.89
20.5	255.56	28.83	17.44	185.51	54.75
30	255.56	29.49	21.03	218.67	64.53
40	255.56	29.83	22.61	232.49	68.61
50	255.56	30.37	23.92	241.60	71.30
60	255.56	30.90	25.32	251.30	74.16

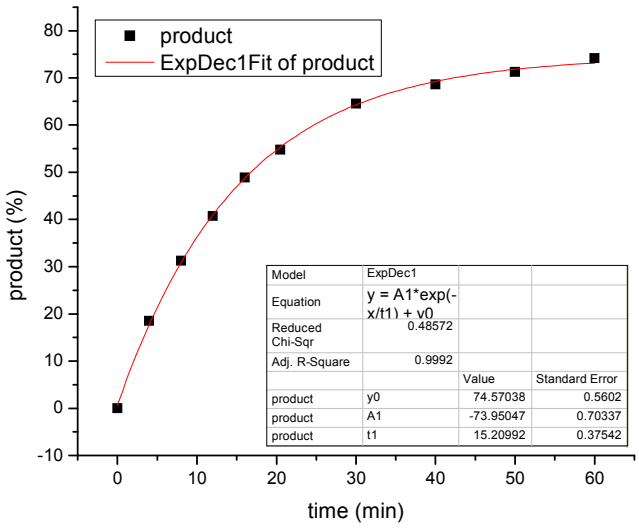

Half-life: 16.76

Table 5. entry 24. catalyst **V{*2,7,1*}: run 2**

time, min	µmol standard	area standard	area product	µmol product	product %
0	255.56	0.00	0.00	0.00	0.00
4	255.56	28.43	5.87	63.27	18.67
8	255.56	27.30	9.34	104.87	30.95
12	255.56	28.46	12.96	139.69	41.23
16	255.56	28.58	14.92	160.05	47.23
20	255.56	29.02	17.14	181.11	53.45
30	255.56	29.95	20.65	211.44	62.40
40	255.56	29.51	22.64	235.26	69.43
50	255.56	29.87	24.16	247.99	73.19
60	255.56	30.33	24.81	250.87	74.04
80	255.56	30.59	26.72	267.88	79.06

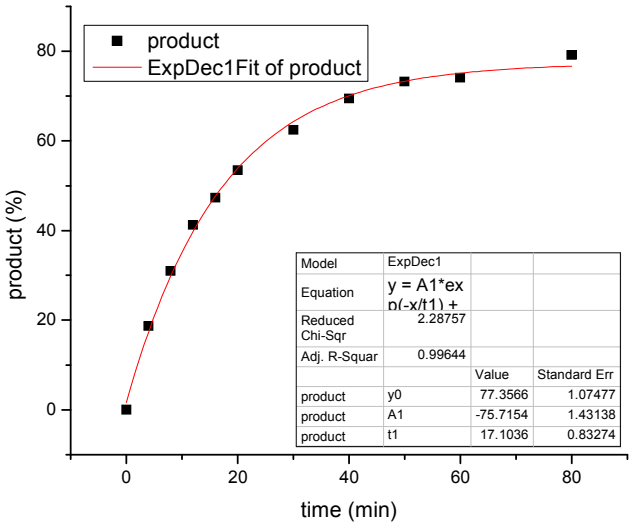

Half-life: 17.41
Average: 17.9

Table 5. entry 25. catalyst **V{*3,2,1*}: run 1**

time, min	µmol standard	area standard	area product	µmol product	product %
0	255.56	0.00	0.00	0.00	0.00
5	255.56	28.69	1.64	17.54	5.18
10	255.56	27.12	3.25	36.73	10.84
20	255.56	30.07	6.76	68.91	20.34
40	255.56	28.65	9.53	102.03	30.12
60	255.56	28.24	11.05	120.02	35.43
80	255.56	28.47	12.45	134.05	39.57
100	255.56	28.27	13.51	146.60	43.28
120	255.56	28.74	15.25	162.75	48.05
140	255.56	28.82	16.24	172.79	51.01
180	255.56	28.53	17.91	192.46	56.82
242	255.56	30.12	21.65	220.42	65.07

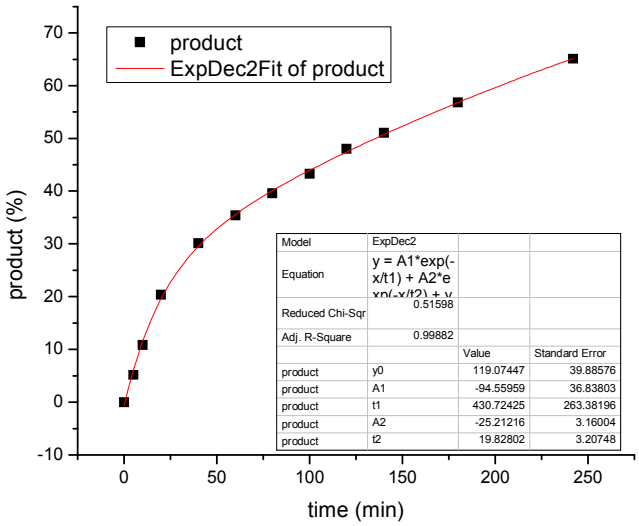

Half-life: 135.44

Table 5. entry 25. catalyst **V{*3,2,1*}: run 2**

time, min	µmol standard	area standard	area product	µmol product	product %
0	255.56	0.00	0.00	0.00	0.00
5	255.56	29.84	1.76	18.08	5.34
10	255.56	29.84	3.63	37.35	11.03
20	255.56	30.44	6.81	68.66	20.27
40	255.56	28.39	9.83	106.18	31.35
60	255.56	29.35	11.44	119.56	35.30
80	255.56	29.11	12.74	134.25	39.63
100	255.56	29.90	14.52	148.93	43.97
120	255.56	30.45	16.03	161.48	47.67
140	255.56	29.84	17.29	177.66	52.45
180	255.56	30.13	19.87	202.24	59.70
242	255.56	31.08	21.97	216.76	63.99

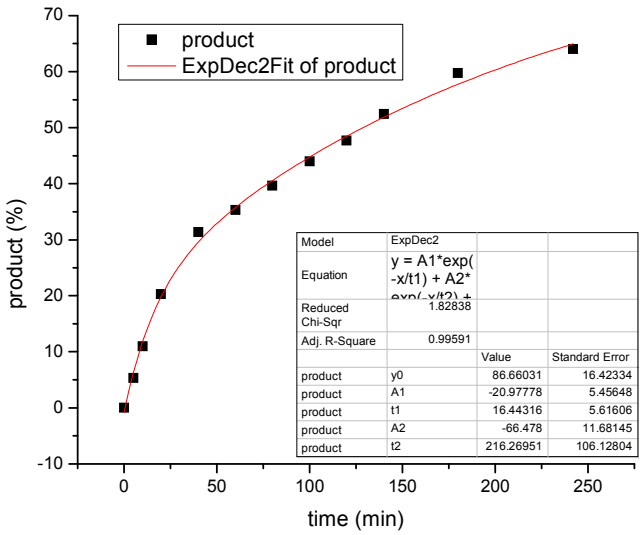

Half-life: 128.77
Average: 132.1

Table 5. entry 26. catalyst **V{*3,2,5*}: run 1**

time, min	µmol standard	area standard	area product	µmol product	product %
0	254.15	0.00	0.00	0.00	0.00
2	254.15	27.34	0.87	9.42	2.78
4	254.15	29.32	2.12	21.34	6.30
6	254.15	29.61	3.19	31.87	9.41
8	254.15	29.72	4.11	40.89	12.08
10	254.15	29.68	4.89	48.72	14.39
15	254.15	29.34	6.54	65.97	19.49
30	254.15	29.45	9.31	93.56	27.64
45	254.15	29.32	11.06	111.57	32.96
60	254.15	29.64	12.53	125.01	36.93
75	254.15	29.58	13.61	136.11	40.20
90	254.15	29.64	14.75	147.16	43.47
105	254.15	29.71	15.69	156.26	46.16
120	254.15	29.75	16.46	163.63	48.33
135	254.15	29.99	17.42	171.78	50.74

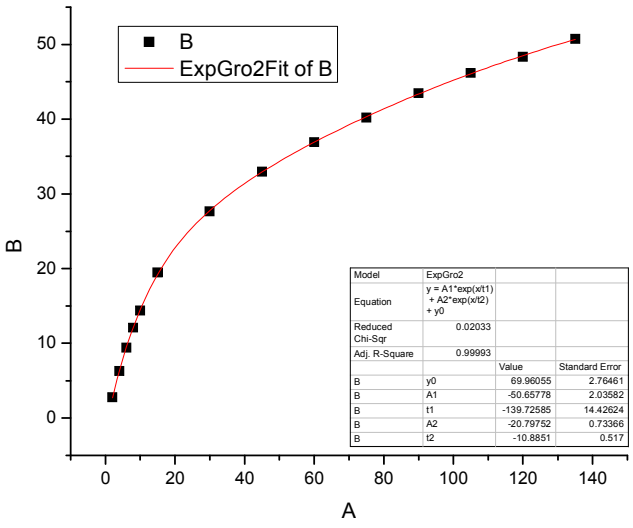

Half-life: 130.13

Table 5. entry 26. catalyst **V{*3,2,5*}: run 2**

time, min	µmol standard	area standard	area product	µmol product	product %
0	254.14	0.00	0.00	0.00	0.00
10	254.14	28.44	3.68	38.25	11.30
15	254.14	28.41	5.99	62.41	18.43
30	254.14	29.07	7.73	78.65	23.23
45	254.14	28.46	10.43	108.41	32.02
60	254.14	28.60	12.20	126.20	37.28
75	254.14	28.54	13.35	138.43	40.89
90	254.14	28.62	14.18	146.56	43.29
105	254.14	28.94	15.28	156.15	46.12
120	254.14	28.57	15.84	163.99	48.44
135	254.14	28.73	16.73	172.26	50.88
150	254.14	28.83	17.52	179.76	53.10
165	254.14	28.91	18.25	186.72	55.15
180	254.14	28.67	18.81	194.07	57.32
180	254.14	28.86	19.37	198.53	58.64

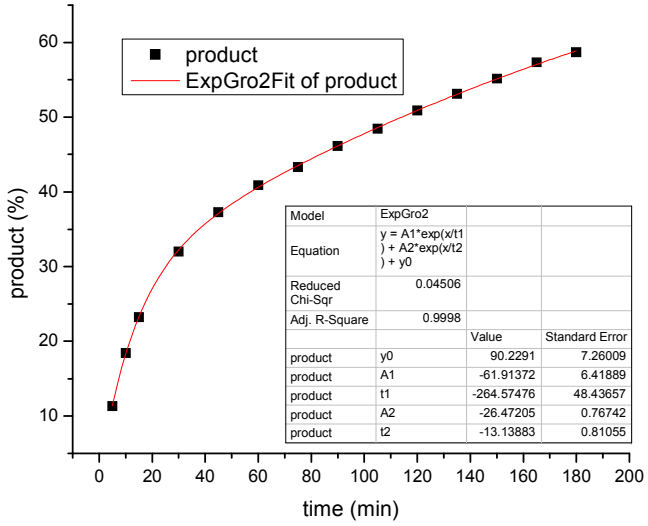

Half-life: 114.10
Average: 122.1

Table 5. entry 27. catalyst **V{*3,2,7*}: run 1**

time, min	µmol standard	area standard	area product	µmol product	product %
0	254.15	0.00	0.00	0.00	0.00
2	254.15	29.86	2.27	22.47	6.63
4	254.15	29.68	4.47	44.52	13.14
6	254.15	29.37	6.45	64.93	19.16
8	254.15	30.37	8.41	81.90	24.17
10	254.15	29.78	9.70	96.39	28.44
15	254.15	29.73	12.58	125.19	36.94
30	254.15	29.26	17.21	173.98	51.34
45	254.15	29.54	19.79	198.16	58.47
60	254.15	29.62	21.81	217.86	64.29
75	254.15	29.58	23.79	237.88	70.20
90	254.15	29.41	25.26	254.06	74.97
105	254.15	29.54	27.15	271.89	80.23
120	254.15	29.48	28.26	283.62	83.69
135	254.15	29.98	29.16	287.66	84.88

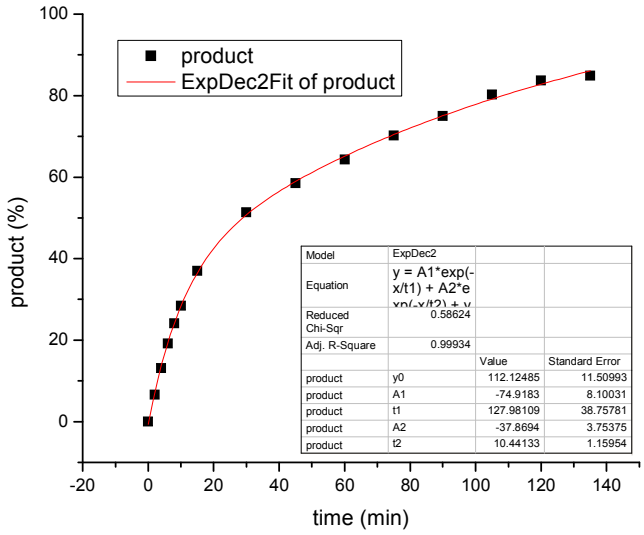

Half-life: 28.94

Table 5. entry 27. catalyst **V{*3,2,7*}: run 2**

time, min	µmol standard	area standard	area product	µmol product	product %
0	254.15	0.00	0.00	0.00	0.00
2	254.15	29.40	2.25	22.67	6.69
4	254.15	29.01	4.53	46.16	13.62
6	254.15	29.07	6.52	66.36	19.58
8	254.15	29.32	8.28	83.49	24.64
10	254.15	29.11	9.62	97.81	28.86
15	254.15	29.09	12.42	126.33	37.28
30	254.15	29.45	17.41	174.90	51.61
45	254.15	29.73	19.99	198.91	58.69
60	254.15	29.74	21.86	217.44	64.16
75	254.15	29.79	23.76	235.95	69.62
90	254.15	29.62	25.49	254.59	75.13
105	254.15	29.94	27.26	269.40	79.50
120	254.15	30.03	28.77	283.42	83.63
135	254.15	29.83	29.48	292.34	86.26

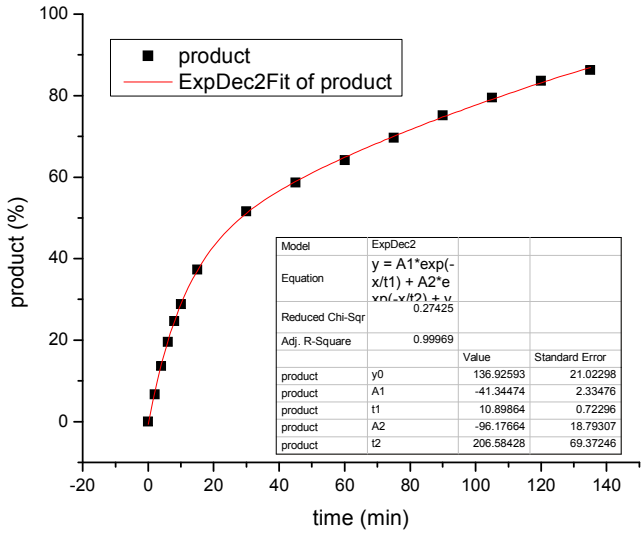

Half-life: 28.33
Average: 28.6

Table 5. entry 28. catalyst **V{*3,3,1*}: run 1**

time, min	µmol standard	area standard	area product	µmol product	product %
0	255.56	0.00	0.00	0.00	0.00
5	255.56	29.16	4.31	49.86	14.74
10	255.56	29.37	6.98	80.11	23.69
20	255.56	29.35	10.33	118.66	35.09
30	255.56	29.09	12.27	142.29	42.07
40	255.56	30.01	14.42	162.06	47.92
50	255.56	28.90	15.11	176.33	52.14
60	255.56	28.93	16.58	193.29	57.15
80	255.56	29.59	19.22	219.08	64.78
100	255.56	29.73	21.92	248.60	73.50
120	255.56	29.89	23.62	266.48	78.79
140	255.56	30.80	24.90	272.64	80.61
180	255.56	30.80	25.47	278.94	82.48

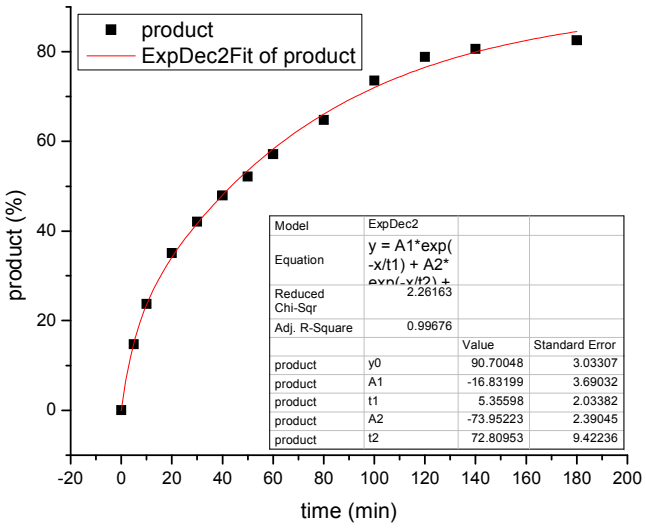

Half-life: 43.49

Table 5. entry 28. catalyst **V{*3,3,1*}: run 2**

time, min	µmol standard	area standard	area product	µmol product	product %
0	255.56	0.00	0.00	0.00	0.00
5	255.56	29.96	3.82	43.01	12.72
10	255.56	30.02	6.59	74.03	21.89
20	255.56	30.27	10.46	116.51	34.45
30	255.56	30.44	13.91	154.08	45.56
40	255.56	29.44	15.26	174.81	51.69
50	255.56	30.40	17.36	192.62	56.95
60	255.56	29.64	18.61	211.73	62.60
80	255.56	30.64	21.87	240.75	71.18
100	255.56	31.73	23.80	252.94	74.79
120	255.56	32.63	25.71	265.77	78.58
140	255.56	30.82	24.68	269.98	79.83
180	255.56	31.04	24.51	266.35	78.75

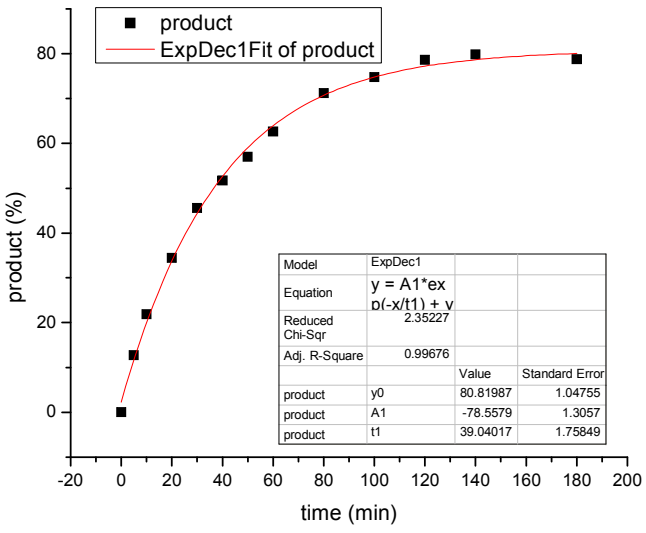

Half-life: 36.53
Average: 41.8

Table 5. entry 29. catalyst **V{*3,3,3*}: run 1**

time, min	µmol standard	area standard	area product	µmol product	produc t %
0	255.56	0.00	0.00	0.00	0.00
4	255.56	27.02	4.25	48.19	14.23
12	255.56	27.82	9.81	108.17	31.93
16	255.56	30.85	13.03	129.53	38.24
20	255.56	30.00	15.05	153.89	45.43
25	255.56	30.97	17.76	175.82	51.91
30	255.56	30.71	20.04	200.16	59.09
40	255.56	30.55	22.70	227.88	67.28
80	255.56	32.48	28.97	273.53	80.75
128	255.56	31.54	28.50	277.06	81.79

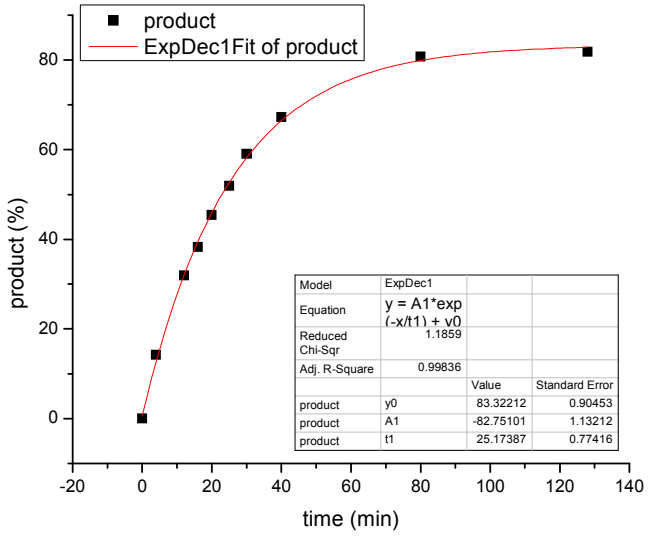

Half-life: 22.90

Table 5. entry 29. catalyst **V{*3,3,3*}: run 2**

time, min	µmol standard	area standard	area product	µmol product	produc t %
0	255.56	0.00	0.00	0.00	0.00
4	255.56	26.40	4.96	57.66	17.02
8	255.56	27.47	8.46	94.45	27.88
12	255.56	27.94	11.37	124.75	36.83
16	255.56	28.30	14.72	159.52	47.09
20	255.56	30.12	17.62	179.39	52.96
25	255.56	30.43	20.59	207.53	61.27
30	255.56	30.47	21.98	221.19	65.30
40	255.56	30.77	24.30	242.20	71.50
60	255.56	31.45	26.51	258.53	76.32
80	255.56	30.09	25.80	263.00	77.64

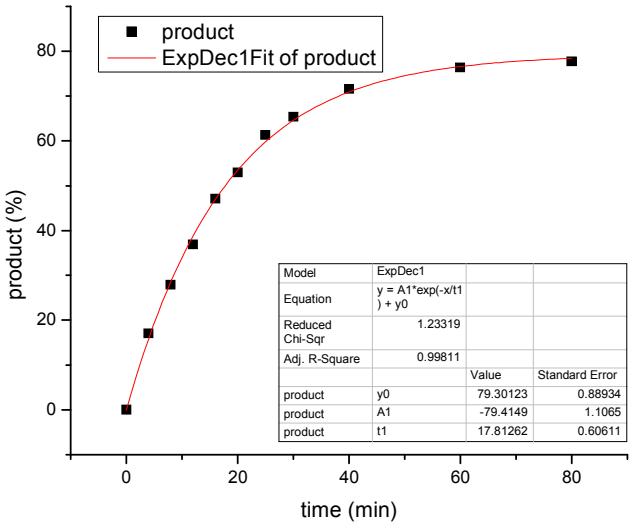

Half-life: 17.76
Average: 20.3

Table 5. entry 30. catalyst **V{*3,3,5*}: run 1**

time, min	µmol standard	area standard	area product	µmol product	product %
0	256.20	0.00	0.00	0.00	0.00
10	256.20	27.23	5.85	66.05	19.53
18	256.20	26.67	8.61	99.32	29.37
38	256.20	29.41	13.47	140.82	41.64
60	256.20	29.58	16.14	167.75	49.60
80	256.20	30.03	18.98	194.29	57.45
100	256.20	29.54	19.32	201.07	59.45
120	256.20	29.89	20.26	208.38	61.61
140	256.20	30.14	21.05	214.71	63.48
160	256.20	29.15	20.97	221.12	65.38
180	256.20	29.91	22.10	227.15	67.16
220	256.20	29.05	22.66	239.84	70.91
240	256.20	29.14	22.88	241.37	71.37

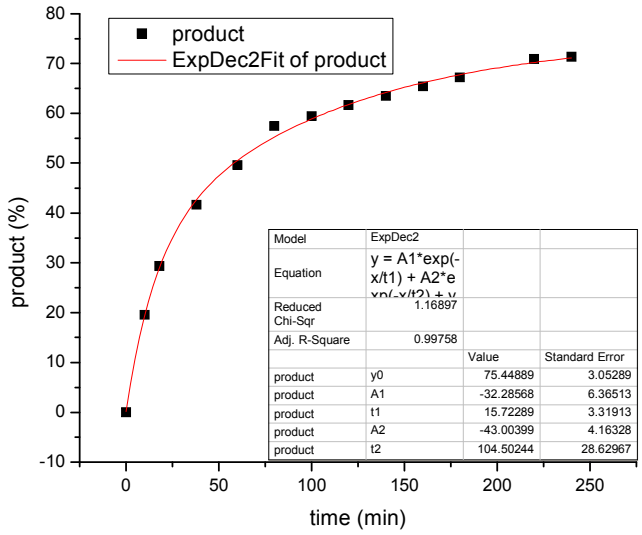

Half-life: 58.16

Table 5. entry 30. catalyst **V{*3,3,5*}: run 2**

time, min	µmol standard	area standard	area product	µmol product	product %
0	256.20	0.00	0.00	0.00	0.00
10	256.20	27.58	5.81	64.73	19.14
18	256.20	28.02	8.68	95.24	28.16
38	256.20	28.07	12.84	140.60	41.57
60	256.20	30.17	15.80	161.04	47.62
80	256.20	30.99	17.93	177.93	52.61
100	256.20	30.60	19.28	193.75	57.29
120	256.20	30.63	20.33	204.06	60.34
140	256.20	30.67	20.95	209.97	62.08
160	256.20	30.37	21.41	216.75	64.09
180	256.20	31.21	22.77	224.31	66.32
220	256.20	30.58	23.05	231.68	68.50
240	256.20	31.26	24.25	238.48	70.51

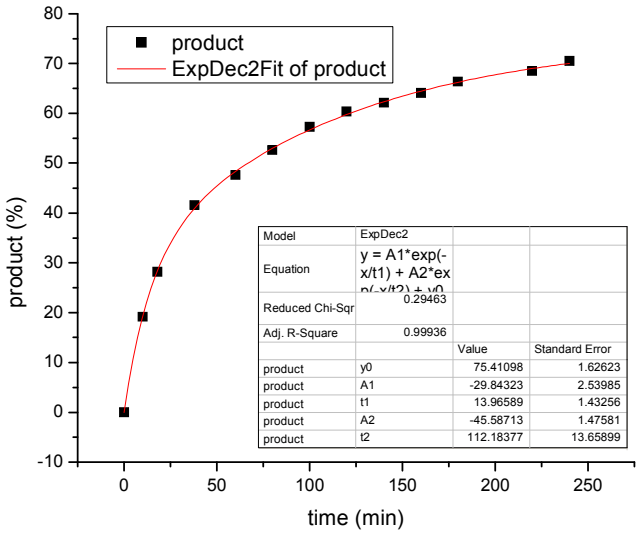

Half-life: 66.68
Average: 62.4

Table 5. entry 31. catalyst **V{*3,3,8*}: run 1**

time, min	µmol standard	area standard	area product	µmol product	product %
0	255.33	0.00	0.00	0.00	0.00
2	255.33	26.52	2.05	23.70	7.00
4	255.33	27.29	3.76	42.19	12.47
6	255.33	27.23	4.95	55.72	16.47
8	255.33	27.28	5.97	67.09	19.83
10	255.33	27.62	7.17	79.56	23.51
12	255.33	27.77	8.01	88.38	26.12
16	255.33	28.69	9.79	104.54	30.89
20	255.33	30.72	11.89	118.56	35.04
30	255.33	29.46	13.66	142.11	42.00
43	255.33	30.90	16.92	167.76	49.58
63	255.33	31.01	18.53	183.14	54.12
118	255.33	31.79	23.73	228.76	67.61

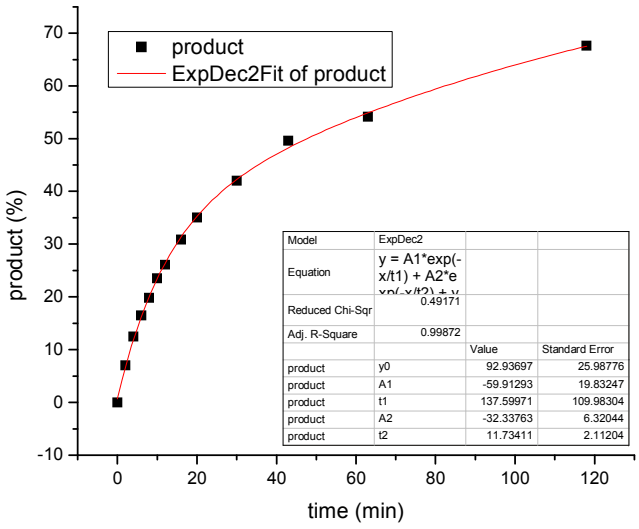

Half-life: 47.64

Table 5. entry 31. catalyst **V{*3,3,8*}: run 2**

time, min	µmol standard	area standard	area product	µmol product	product %
0	255.33	0.00	0.00	0.00	0.00
2	255.33	26.97	2.20	24.97	7.38
4	255.33	27.23	3.76	42.36	12.52
6	255.33	27.48	4.98	55.49	16.40
8	255.33	27.93	6.13	67.24	19.87
10	255.33	27.67	7.04	77.98	23.04
12	255.33	27.43	7.93	88.53	26.16
16	255.33	28.15	9.63	104.82	30.98
20	255.33	30.68	12.26	122.42	36.18
30	255.33	31.09	15.24	150.18	44.38
43	255.33	31.47	18.36	178.79	52.84
63	255.33	30.86	20.97	208.21	61.53
118	255.33	31.49	24.60	239.31	70.72

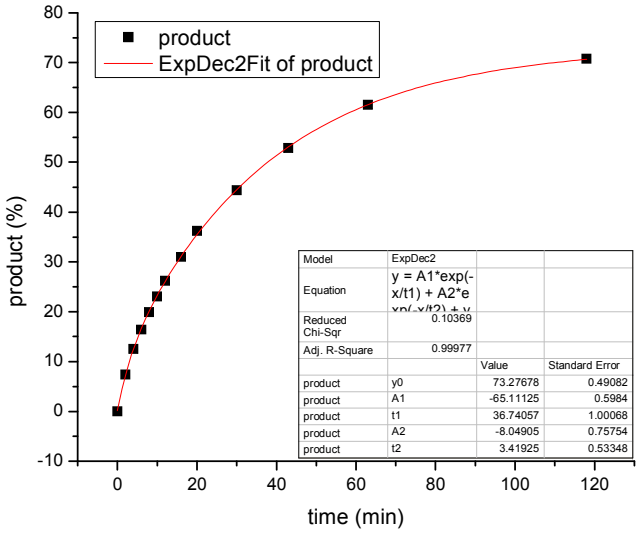

Half-life: 37.79
Average: 42.7

Table 5. entry 32. catalyst **V{*3,2,6*}: run 1**

time, min	µmol standard	area standard	area product	µmol product	product %
10	256.20	26.90	2.13	24.30	7.18
20	256.20	26.70	4.67	53.73	15.89
30	256.20	26.87	7.41	84.81	25.08
40	256.20	29.62	9.75	101.18	29.92
50	256.20	27.70	10.74	119.17	35.24
60	256.20	29.34	12.59	131.94	39.01
80	256.20	29.83	14.85	153.02	45.24
100	256.20	30.27	17.07	173.36	51.26
120	256.20	29.73	18.21	188.32	55.68
150	256.20	29.73	19.35	200.15	59.18

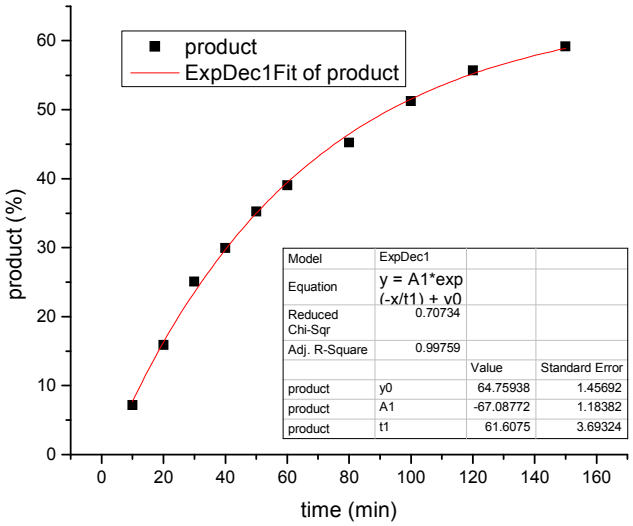

Half-life: 93.28

Table 5. entry 32. catalyst **V{*3,2,6*}: run 2**

time, min	µmol standard	area standard	area product	µmol product	product %
10	256.20	26.73	2.62	30.10	8.90
20	256.20	27.19	5.90	66.74	19.73
30	256.20	29.53	9.86	102.63	30.35
40	256.20	30.28	11.81	119.92	35.46
50	256.20	30.47	12.96	130.75	38.66
60	256.20	29.79	14.17	146.21	43.23
80	256.20	29.94	16.19	166.29	49.17
100	256.20	30.12	18.91	193.07	57.09
120	256.20	30.31	20.74	210.36	62.20
150	256.20	30.16	22.81	232.48	68.74
190	256.20	30.27	25.06	254.48	75.24

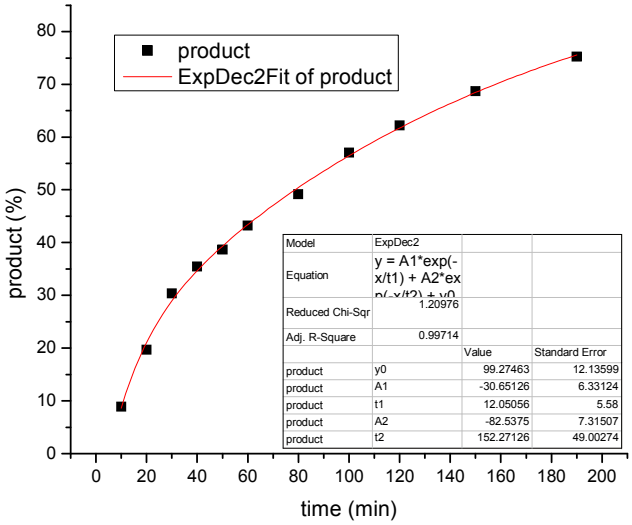

Half-life: 78.69
Average:86.0

Table 5. entry 33. catalyst **V{*3,7,5*}: run 1**

time, min	µmol standard	area standard	area product	µmol product	product %
0	256.39	0.00	0.00	0.00	0.00
5	256.39	26.33	4.17	48.77	14.42
10	256.39	28.79	7.73	82.63	24.43
20	256.39	27.41	10.31	115.72	34.21
30	256.39	29.38	13.63	142.73	42.20
40	256.39	28.17	13.99	152.77	45.17
50	256.39	28.28	15.16	164.92	48.76
60	256.39	28.50	16.19	174.75	51.67
80	256.39	29.22	17.72	186.58	55.17
100	256.39	29.51	18.91	197.21	58.31
130	256.39	29.09	20.33	215.07	63.59
170	256.39	29.65	22.37	232.15	68.64

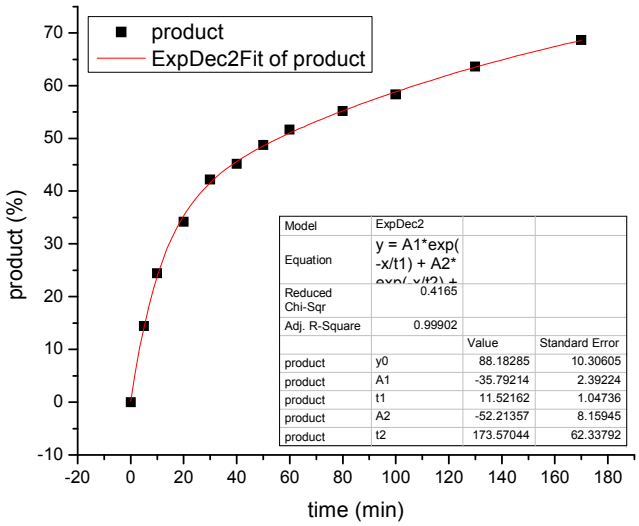

Half-life: 55.63

Table 5. entry 33. catalyst **V{*3,7,5*}: run 2**

time, min	µmol standard	area standard	area product	µmol product	product %
0	256.39	0.00	0.00	0.00	0.00
5	256.39	29.06	4.49	47.58	14.07
10	256.39	27.23	6.98	78.89	23.33
20	256.39	29.71	10.90	112.84	33.36
30	256.39	27.86	12.03	132.79	39.26
40	256.39	28.12	13.50	147.74	43.68
50	256.39	30.09	15.24	155.79	46.06
60	256.39	30.40	16.48	166.85	49.33
80	256.39	30.07	17.15	175.49	51.89
100	256.39	28.97	17.97	190.81	56.42
130	256.39	28.92	19.54	207.84	61.45
170	256.39	29.59	21.27	221.20	65.40

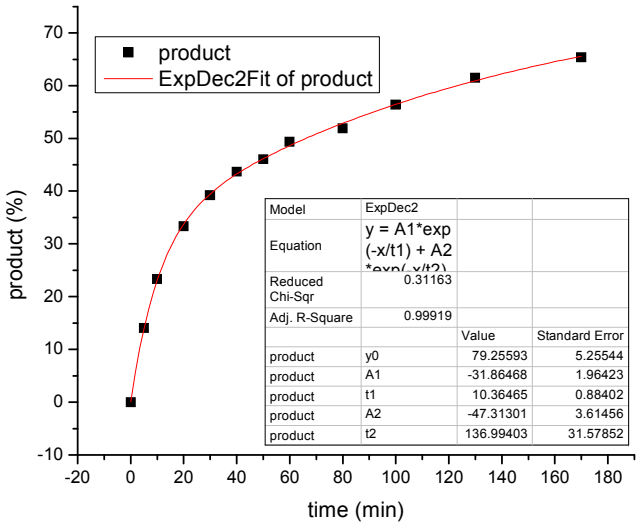

Half-life: 66.11
Average: 60.9

Table 5. entry 34. catalyst **V{*3,7,8*}: run 1**

time, min	µmol standard	area standard	area product	µmol product	product %
0	256.25	0.00	0.00	0.00	0.00
61	256.25	28.63	7.96	85.53	25.24
100	256.25	30.50	11.00	110.89	32.73
140	256.25	30.60	13.27	133.41	39.38
180	256.25	30.39	15.23	154.08	45.48
221	256.25	29.09	16.15	170.70	50.38
260	256.25	30.75	18.01	180.08	53.15
301	256.25	30.64	18.78	188.53	55.64
340	256.25	31.11	19.28	190.56	56.24
403	256.25	30.39	19.77	200.01	59.03

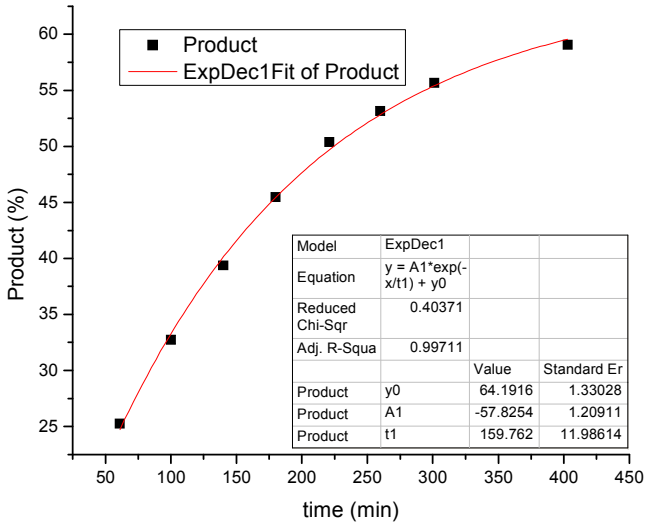

Half-life: 224.43

Table 5. entry 34. catalyst **V{*3,7,8*}: run 2**

time, min	µmol standard	area standard	area product	µmol product	product %
0	338.81	0.00	0.00	0.00	0.00
20	338.81	29.57	3.92	40.76	12.03
61	338.81	30.19	8.52	86.83	25.63
100	338.81	30.56	11.30	113.64	33.54
140	338.81	30.50	13.26	133.64	39.44
180	338.81	29.64	14.82	153.76	45.38
221	338.81	31.68	16.61	161.23	47.59
260	338.81	31.22	16.80	165.45	48.83
301	338.81	31.99	17.95	172.55	50.93
340	338.81	30.87	17.40	173.31	51.15
403	338.81	32.14	18.97	181.46	53.56

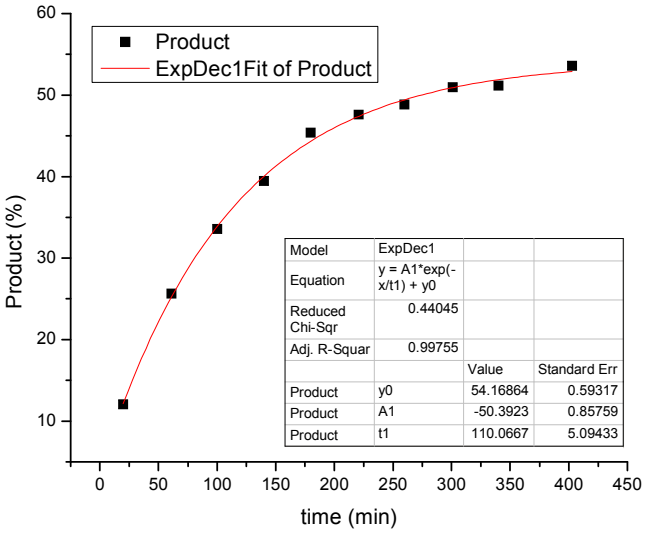

Half-life: 274.31
Average: 249.4

Table 5. entry 35. catalyst **V{*4,2,5*}: run 1**

time, min	µmol standard	area standard	area product	µmol product	product %
0	254.66	0.00	0.00	0.00	0.00
4	254.66	27.50	3.04	33.84	9.98
8	254.66	27.78	5.04	55.54	16.38
12	254.66	27.89	6.11	67.10	19.79
16	254.66	30.42	7.78	78.35	23.11
20	254.66	29.88	8.72	89.41	26.37
30	254.66	30.57	11.05	110.71	32.65
40	254.66	30.90	12.81	127.03	37.46
60	254.66	30.84	15.14	150.45	44.37
80	254.66	30.58	16.29	163.17	48.12
105	254.66	30.82	18.19	180.83	53.33
155	254.66	31.02	20.20	199.53	58.84

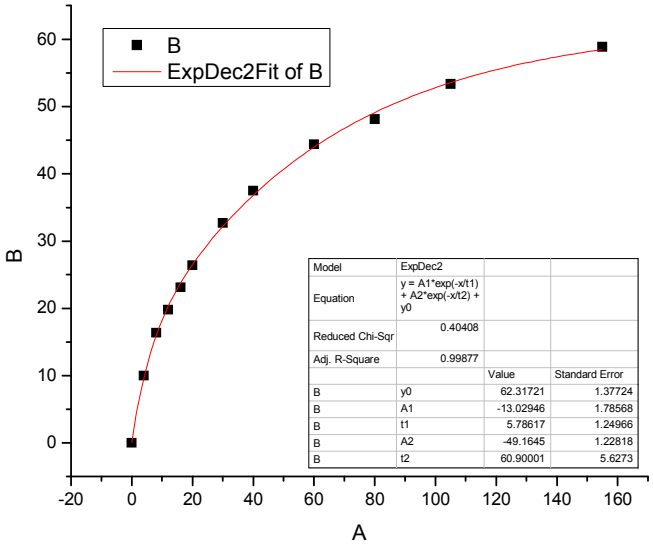

Half-life: 84.30

Table 5. entry 35. catalyst **V{*4,2,5*}: run 2**

time, min	µmol standard	area standard	area product	µmol product	product %
0	254.66	0.00	0.00	0.00	0.00
4	254.66	28.46	2.78	29.88	8.81
8	254.66	28.72	4.92	52.47	15.48
12	254.66	28.94	6.47	68.52	20.21
16	254.66	28.93	7.65	81.03	23.90
20	254.66	29.20	8.49	89.14	26.29
30	254.66	31.70	10.26	99.18	29.25
40	254.66	29.66	10.69	110.45	32.57
60	254.66	31.94	13.00	124.77	36.80
105	254.66	31.89	15.07	144.80	42.70
155	254.66	25.16	12.45	151.57	44.70

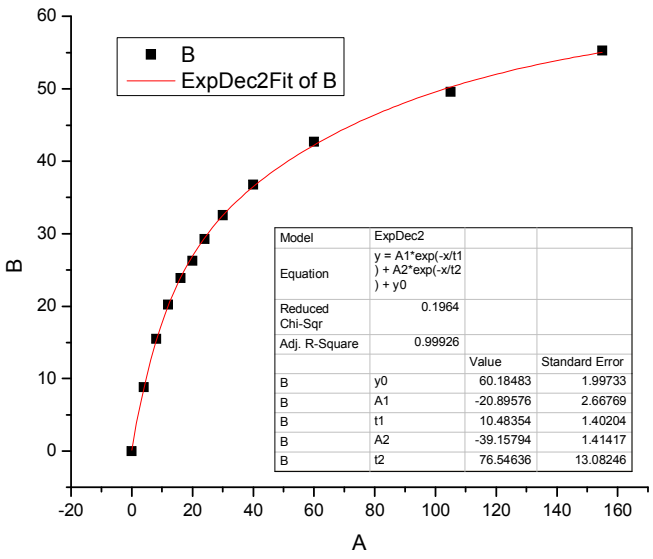

Half-life: 103.94
Average: 93.7

Table 5. entry 36. catalyst **V{*5,2,1*}: run 1**

time, min	µmol standard	area standard	area product	µmol product	product %
0	255.40	0.00	0.00	0.00	0.00
2	255.40	30.92	4.56	45.16	13.36
3	255.40	31.73	6.70	64.71	19.14
4	255.40	30.98	8.65	85.56	25.32
5	255.40	31.00	10.35	102.32	30.27
6	255.40	31.26	12.08	118.43	35.04
7	255.40	31.43	13.68	133.40	39.47
8	255.40	31.08	14.85	146.42	43.32
9	255.40	31.12	15.97	157.30	46.54
10	255.40	31.16	17.20	169.16	50.05
15	255.40	31.40	22.11	215.77	63.84
30	255.40	31.47	30.54	297.42	88.00
60	255.40	31.59	34.53	334.99	99.11

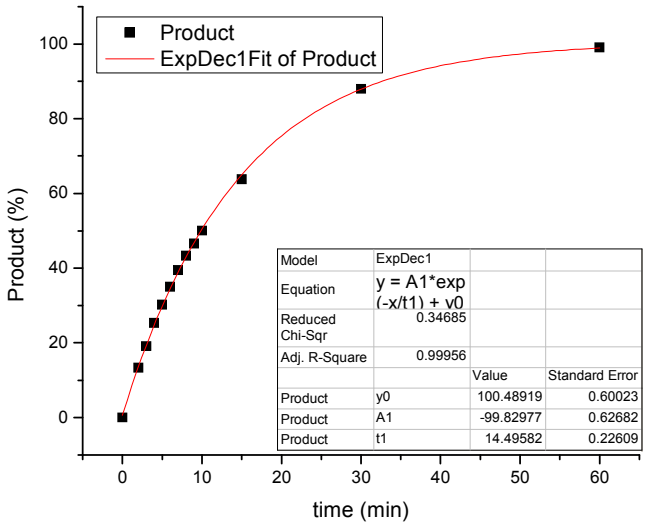

Half-life: 9.88

Table 5. entry 36. catalyst **V{*5,2,1*}: run 2**

time, min	µmol standard	area standard	area product	µmol product	product %
0	255.40	30.32	0.00	0.00	0.00
1	255.40	30.41	2.43	24.52	7.26
2	255.40	31.06	4.39	43.34	12.82
3	255.40	30.71	6.07	60.54	17.91
4	255.40	30.96	7.80	77.19	22.84
5	255.40	31.10	9.37	92.37	27.33
6	255.40	31.36	10.79	105.45	31.20
7	255.40	31.10	12.09	119.14	35.25
8	255.40	31.19	13.31	130.83	38.71
9	255.40	30.90	14.24	141.21	41.78
10	255.40	31.28	15.50	151.89	44.94
15	255.40	31.28	20.04	196.34	58.09
30	255.40	31.48	29.85	290.62	85.98
60	255.40	31.33	34.29	335.42	99.24

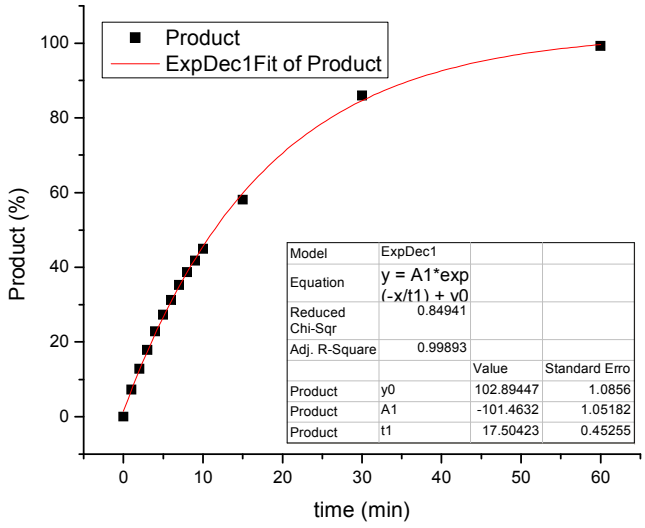

Half-life: 11.40
Average: 10.64

Table 5. entry 37. catalyst **V{*5,2,2*}: run 1**

time, min	µmol standard	area standard	area product	µmol product	product %
0	255.40	30.70	0.00	0.00	0.00
1	255.40	30.18	1.76	17.84	5.28
2	255.40	30.77	3.72	37.09	10.98
3	255.40	30.79	5.35	53.22	15.75
4	255.40	30.61	6.88	68.87	20.38
5	255.40	30.75	8.31	82.80	24.51
6	255.40	30.53	9.58	96.19	28.47
7	255.40	30.72	10.91	108.82	32.21
8	255.40	30.52	11.98	120.30	35.60
9	255.40	30.75	13.19	131.52	38.93
10	255.40	30.68	14.27	142.56	42.18
15	255.40	30.39	19.11	192.70	57.01
30	255.40	30.38	27.82	280.66	83.04
60	255.40	30.88	32.71	324.63	96.05

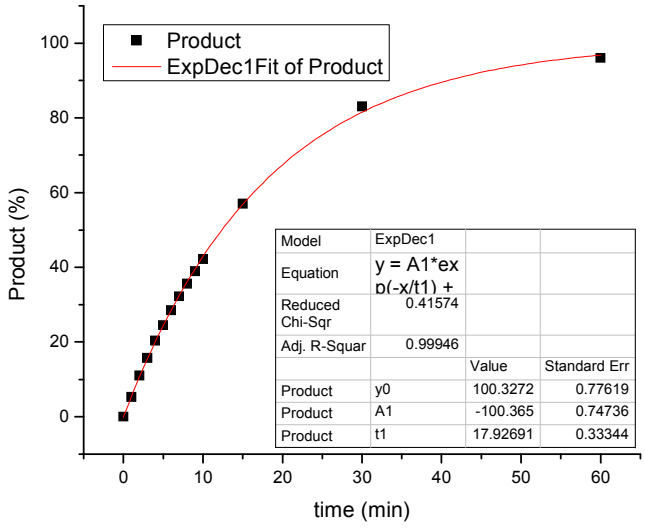

Half-life: 12.37

Table 5. entry 37. catalyst **V{*5,2,2*}: run 2**

time, min	µmol standard	area standard	area product	µmol product	product %
0	255.40	30.35	0.00	0.00	0.00
1	255.40	30.96	1.70	16.84	4.98
2	255.40	31.19	3.83	37.63	11.13
3	255.40	31.31	5.72	55.94	16.54
4	255.40	31.13	7.39	72.80	21.53
5	255.40	31.08	8.92	87.95	26.01
6	255.40	30.90	10.26	101.79	30.10
7	255.40	29.95	11.48	117.43	34.72
8	255.40	30.73	12.82	127.93	37.82
9	255.40	30.08	13.53	137.82	40.75
10	255.40	31.15	14.94	146.98	43.46
15	255.40	30.95	19.19	190.02	56.18
30	255.40	31.37	26.86	262.37	77.58
61	255.40	31.56	31.86	309.37	91.47

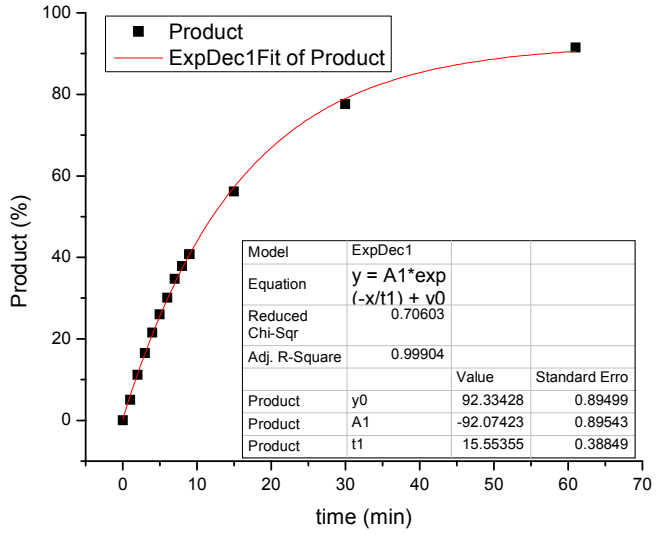

Half-life: 12.09
Average: 12.2

Table 5. entry 38. catalyst **V{*5,2,3*}: run 1**

time, min	µmol standard	area standard	area product	µmol product	product %
0	254.50	30.34	0.00	0.00	0.00
1	254.50	30.93	2.51	24.76	7.30
2	254.50	30.84	4.93	48.77	14.38
3	254.50	30.79	6.86	68.01	20.05
4	254.50	31.01	8.66	85.34	25.16
5	254.50	30.92	10.29	101.67	29.97
6	254.50	30.87	11.67	115.44	34.03
7	254.50	30.94	12.98	128.16	37.78
8	254.50	30.88	14.09	139.31	41.07
9	254.50	30.98	15.15	149.40	44.04
10	254.50	30.72	16.08	159.85	47.12
15	254.50	30.93	20.89	206.29	60.81
30	254.50	31.00	30.27	298.22	87.91
60	254.50	31.44	35.19	341.84	100.77

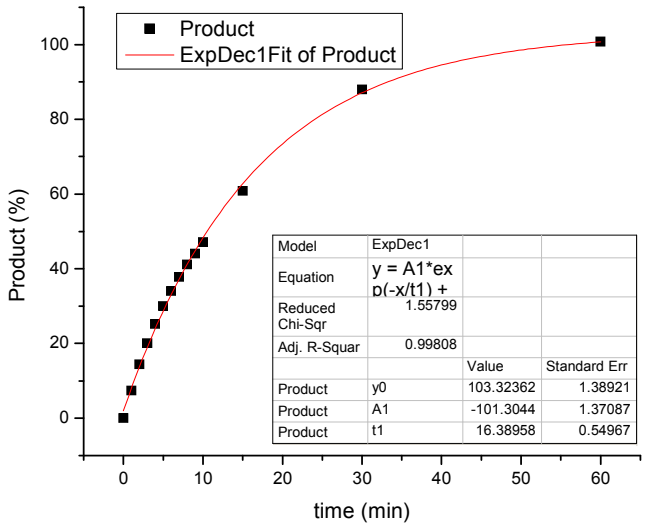

Half-life: 10.52

Table 5. entry 38. catalyst **V{*5,2,3*}: run 2**

time, min	µmol standard	area standard	area product	µmol product	product %
0	254.50	30.36	0.00	0.00	0.00
1	254.50	30.46	2.23	22.33	6.58
2	254.50	30.46	4.29	43.00	12.68
3	254.50	31.04	6.37	62.70	18.48
4	254.50	31.19	8.23	80.56	23.75
5	254.50	30.81	9.87	97.86	28.85
6	254.50	31.00	11.42	112.47	33.16
7	254.50	30.74	12.81	127.22	37.50
8	254.50	31.02	14.30	140.80	41.51
9	254.50	30.91	15.77	155.76	45.92
10	254.50	30.92	17.04	168.32	49.62
15	254.50	30.90	22.60	223.31	65.83
30	254.50	31.27	31.93	311.82	91.92
60	254.50	31.16	35.23	345.31	101.80

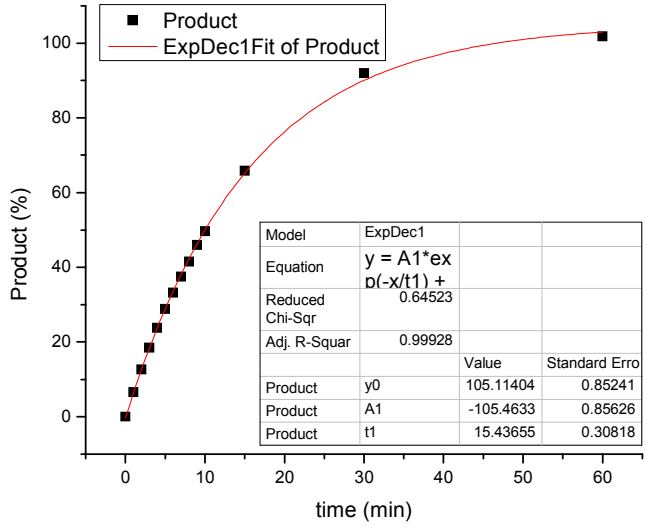

Half-life: 10.02
Average: 10.3

Table 5. entry 39. catalyst **V{*5,2,5*}: run 1**

time, min	µmol standard	area standard	area product	µmol product	product %
0	256.10	0.00	0.00	0.00	0.00
2	256.10	31.79	26.46	255.72	75.55
4	256.10	28.81	8.72	92.99	27.48
6	256.10	29.14	11.82	124.65	36.83
8	256.10	27.37	13.47	151.26	44.69
10	256.10	27.90	15.40	169.59	50.11
12	256.10	18.46	11.89	197.83	58.45
16	256.10	28.43	20.04	216.64	64.01
20	256.10	28.82	22.64	241.45	71.34
30	256.10	28.84	25.73	274.23	81.02

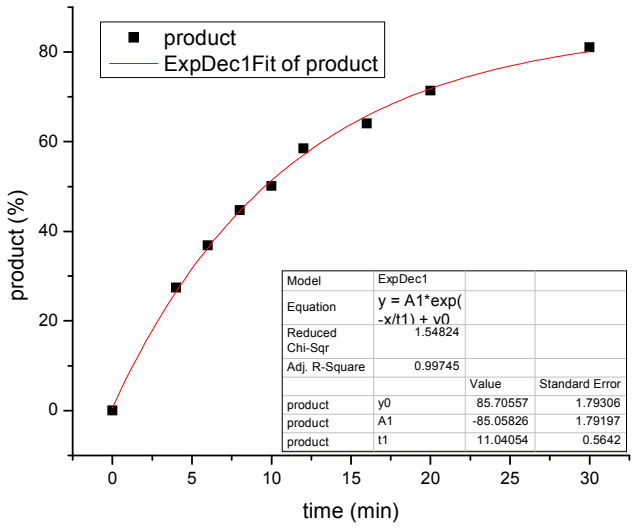

Half-life: 9.58

Table 5. entry 39. catalyst **V{*5,2,5*}: run 2**

time, min	µmol standard	area standard	area product	µmol product	product %
0	256.10	0.00	0.00	0.00	0.00
2	256.10	26.77	5.37	61.65	18.21
4	256.10	27.58	9.07	101.12	29.88
6	256.10	28.43	11.98	129.44	38.24
8	256.10	28.49	14.57	157.20	46.44
10	256.10	28.74	16.21	173.39	51.23
12	256.10	29.15	17.70	186.55	55.12
16	256.10	29.29	20.61	216.19	63.88
20	256.10	29.62	22.41	232.47	68.69
30	256.10	31.16	26.29	259.33	76.62
40	256.10	30.56	26.41	265.63	78.48

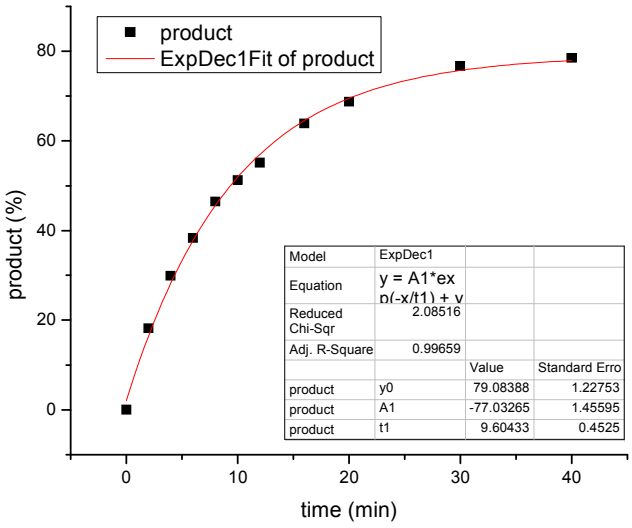

Half-life: 9.36
Average: 9.5

Table 5. entry 40. catalyst **V{*5,2,8*}: run 1**

time, min	µmol standard	area standard	area product	µmol product	product %
0	255.65	0.00	0.00	0.00	0.00
4	255.65	27.72	5.38	59.53	17.60
6	255.65	27.70	7.14	79.03	23.37
8	255.65	27.81	8.83	97.43	28.81
10	255.65	28.59	10.25	109.98	32.52
12	255.65	28.39	11.55	124.79	36.90
14	255.65	30.77	13.87	138.27	40.88
16	255.65	29.02	14.23	150.49	44.50
20	255.65	30.36	17.17	173.46	51.29
30	255.65	31.25	22.12	217.10	64.19
60	255.65	32.07	27.30	261.13	77.21

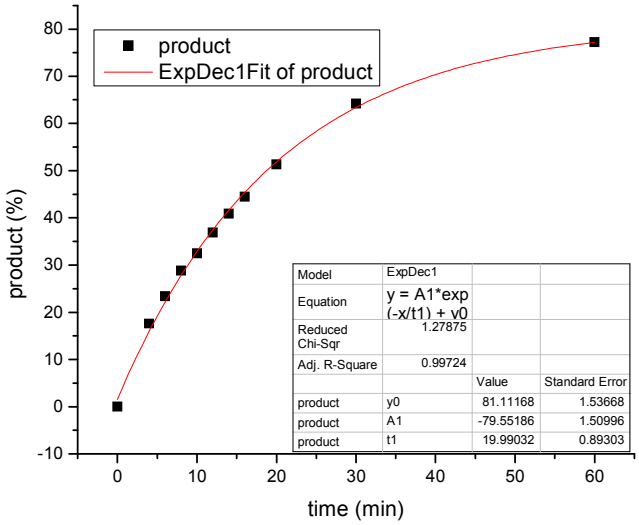

Half-life: 18.77

Table 5. entry 40. catalyst **V{*5,2,8*}: run 2**

time, min	µmol standard	area standard	area product	µmol product	product %
0	255.65	0.00	0.00	0.00	0.00
4	255.65	27.79	5.43	59.41	17.57
6	255.65	28.13	7.80	84.31	24.93
8	255.65	28.11	9.65	104.42	30.88
10	255.65	28.84	11.53	121.70	35.98
12	255.65	28.93	13.05	137.24	40.58
14	255.65	31.19	15.61	152.23	45.01
16	255.65	31.56	16.63	160.35	47.41
20	255.65	30.74	19.24	190.47	56.32
30	255.65	31.02	23.39	229.42	67.83
60	255.65	31.20	26.95	262.83	77.71

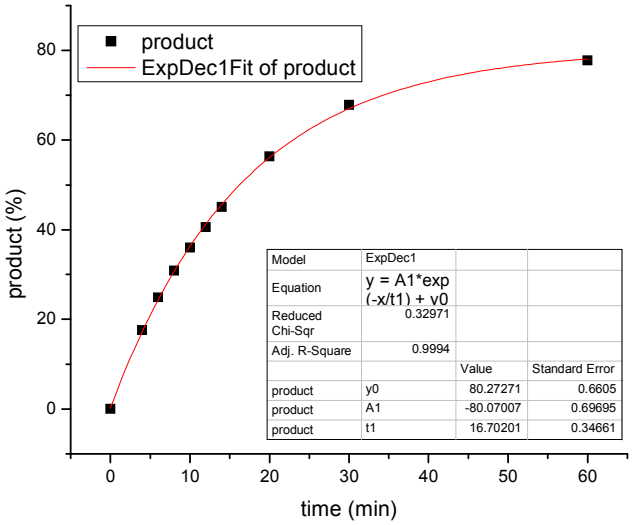

Half-life: 16.25
Average: 17.5

Table 5. entry 41. catalyst **V{*5,2,9*}: run 1**

time, min	µmol standard	area standard	area product	µmol product	product %
0	253.42	0.00	0.00	0.00	0.00
2	253.42	25.50	3.48	41.49	12.27
4	253.42	25.88	5.77	67.85	20.06
6	253.42	26.97	7.84	88.44	26.15
8	253.42	26.88	9.70	109.75	32.45
10	253.42	26.69	11.29	128.70	38.05
12	253.42	27.22	12.46	139.15	41.14
15	253.42	27.32	14.66	163.15	48.24
20	253.42	27.99	17.51	190.27	56.26
30	253.42	28.08	20.93	226.74	67.04
45	253.42	28.64	23.35	247.92	73.30
60	253.42	28.71	24.74	262.05	77.48
75	253.42	29.06	25.50	266.90	78.92
90	253.42	28.85	25.75	271.48	80.27
105	253.42	29.08	25.50	266.62	78.83

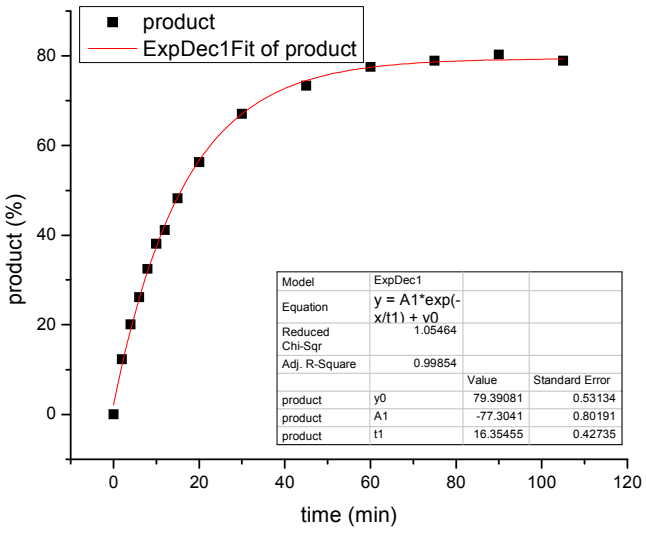

Half-life: 15.82

Table 5. entry 41. catalyst **V{*5,2,9*}: run 2**

time, min	µmol standard	area standard	area product	µmol product	product &
0	253.42	0.00	0.00	0.00	0.00
2	253.42	25.07	3.53	42.87	12.66
4	253.42	25.65	6.09	72.23	21.34
6	253.42	26.76	8.34	94.76	27.99
8	253.42	26.77	9.96	113.12	33.41
10	253.42	27.20	11.47	128.20	37.87
12	253.42	27.46	12.95	143.37	42.35
15	253.42	27.53	14.88	164.32	48.54
20	253.42	27.69	17.72	194.65	57.50
30	253.42	28.88	20.93	220.31	65.08
45	253.42	28.98	23.04	241.74	71.41
60	253.42	28.72	24.77	262.30	77.48
75	253.42	29.23	25.61	266.47	78.71
90	253.42	29.23	25.59	266.29	78.66
105	253.42	28.95	25.91	272.15	80.39

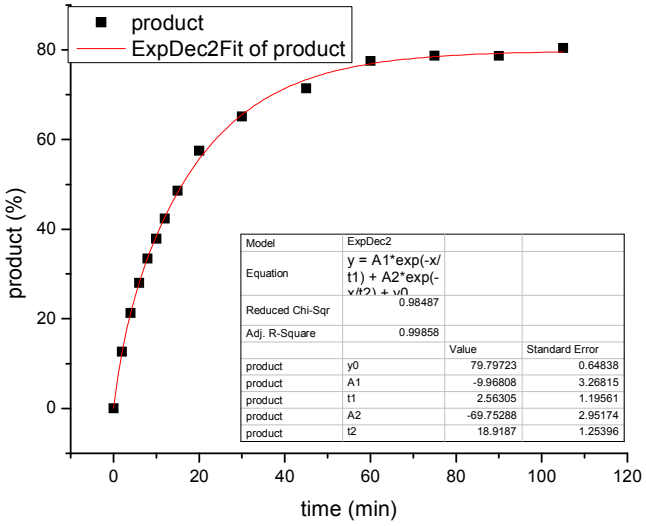

Half-life: 16.15
Average: 16.0

Table 5. entry 42. catalyst **V{*5,2,10*}: run 1**

time, min	µmol standard	area standard	area product	µmol product	product %
0	253.42	0.00	0.00	0.00	0.00
1	253.42	25.96	1.91	22.38	6.62
2	253.42	25.21	3.44	41.54	12.28
3	253.42	25.69	4.52	53.57	15.84
4	253.42	26.55	5.54	63.43	18.75
5	253.42	26.43	6.74	77.52	22.92
6	253.42	26.84	7.95	90.04	26.62
7	253.42	26.59	8.91	101.87	30.12
8	253.42	26.57	9.84	112.67	33.31
9	253.42	26.74	11.18	127.15	37.60
10	253.42	27.04	11.97	134.57	39.79
15	253.42	27.28	15.22	169.64	50.16
30	253.42	28.36	20.31	217.80	64.40
45	253.42	28.39	22.86	244.83	72.39
60	253.42	28.86	24.25	255.46	75.53

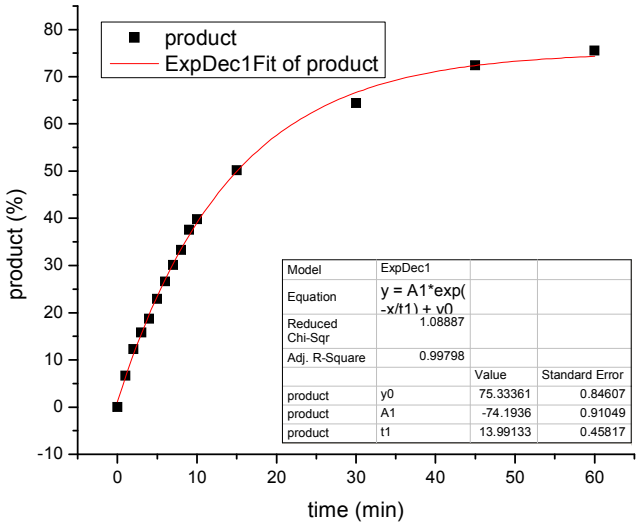

Half-life: 15.03

Table 5. entry 42. catalyst **V{*5,2,10*}: run 2**

time, min	µmol standard	area standard	area product	µmol product	product %
0	253.42	0.00	0.00	0.00	0.00
1	253.42	25.26	2.05	24.72	7.30
2	253.42	25.36	3.67	43.97	12.99
3	253.42	25.34	5.02	60.29	17.81
4	253.42	25.40	6.28	75.18	22.21
5	253.42	25.94	7.37	86.35	25.51
8	253.42	26.95	10.43	117.63	34.74
9	253.42	26.75	11.29	128.30	37.90
10	253.42	26.91	12.00	135.60	40.05
15	253.42	26.99	16.06	180.97	53.46
30	253.42	27.85	20.91	228.38	67.46
45	253.42	28.32	23.34	250.56	74.01
60	253.42	28.77	24.47	258.73	76.42

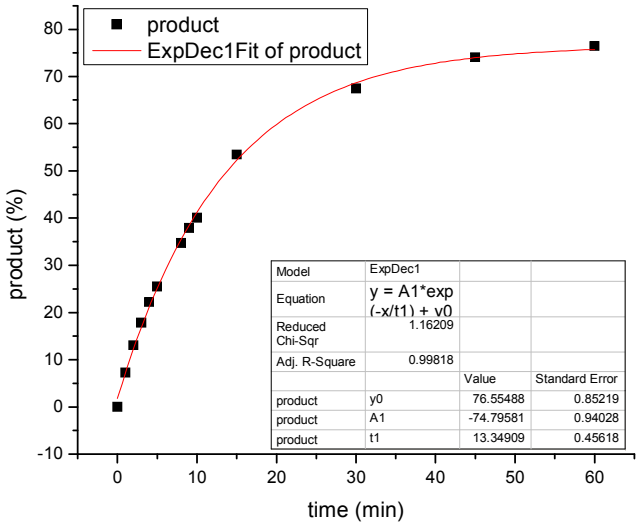

Half-life: 13.82
Average: 14.4

Table 5. entry 43. catalyst **V{*5,3,1*}: run 1**

time, min	µmol standard	area standard	area product	µmol product	product %
0	254.50	30.30	0.00	0.00	0.00
1	254.50	30.28	2.33	23.48	6.91
2	254.50	29.97	4.59	46.77	13.77
3	254.50	30.29	6.56	66.10	19.47
4	254.50	30.48	8.29	83.05	24.46
6	254.50	30.13	11.03	111.78	32.92
7	254.50	31.47	12.39	120.24	35.41
8	254.50	31.69	14.03	135.26	39.83
9	254.50	31.44	15.64	151.90	44.73
10	254.50	31.91	16.71	159.93	47.10
15	254.50	33.40	22.94	209.75	61.77
30	254.50	31.08	30.20	296.73	87.39
60	254.50	31.71	34.34	330.75	97.40

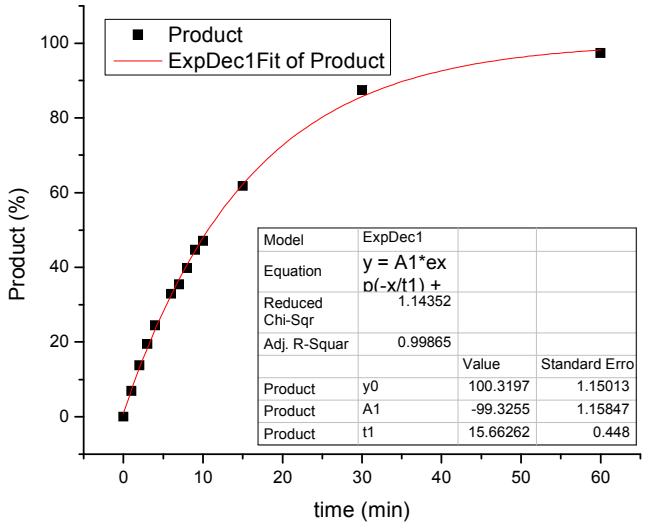

Half-life: 10.65

Table 5. entry 43. catalyst **V{*5,3,1*}: run 2**

time, min	µmol standard	area standard	area product	µmol product	product %
0	254.18	29.59	0.00	0.00	0.00
1	254.18	31.91	3.37	32.22	9.49
2	254.18	29.77	5.79	59.37	17.48
3	254.18	30.90	8.29	81.97	24.14
4	254.18	30.84	10.14	100.43	29.58
5	254.18	31.96	11.92	113.90	33.54
6	254.18	32.07	13.09	124.69	36.72
7	254.18	32.66	16.02	149.83	44.12
8	254.18	31.76	16.98	163.23	48.07
9	254.18	32.52	19.16	179.91	52.98
10	254.18	32.38	20.21	190.57	56.12
15	254.18	32.14	25.34	240.85	70.93
30	254.18	31.21	31.91	312.28	91.97
60	254.18	31.76	35.00	336.64	99.14

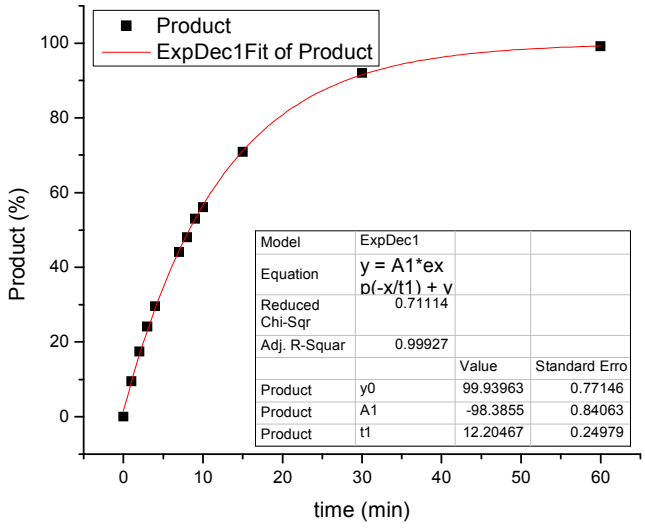

Half-life: 8.28
Average: 9.5

Table 5. entry 44. catalyst **V{*5,3,2*}: run 1**

time, min	µmol standard	area standard	area product	µmol product	product %
0	257.76	0.00	0.00	0.00	0.00
1	257.76	31.00	1.81	17.55	5.17
2	257.76	32.13	3.66	34.16	10.06
3	257.76	31.72	5.19	49.11	14.46
4	257.76	30.77	6.36	62.04	18.27
5	257.76	30.80	7.54	73.40	21.62
6	257.76	31.17	8.83	84.96	25.02
7	257.76	30.81	9.77	95.17	28.03
8	257.76	30.68	10.74	105.03	30.93
9	257.76	31.38	11.90	113.73	33.49
10	257.76	30.79	12.57	122.48	36.07
12	257.76	31.00	14.31	138.48	40.78
15	257.76	30.76	16.22	158.16	46.58
30	257.76	30.76	22.49	219.38	64.61
60	257.76	30.76	28.71	280.03	82.47

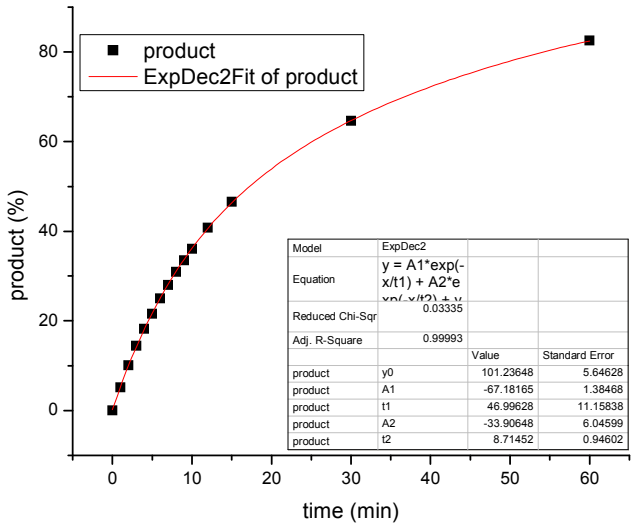

Half-life: 17.24

Table 5. entry 44. catalyst **V{*5,3,2*}: run 2**

time, min	µmol standard	area standard	area product	µmol product	product %
0	257.76	0.00	0.00	0.00	0.00
1	257.76	29.81	1.28	12.88	3.79
2	257.76	29.92	2.86	28.65	8.44
3	257.76	30.28	4.23	41.93	12.35
4	257.76	30.02	5.45	54.47	16.04
5	257.76	29.89	6.55	65.74	19.36
6	257.76	30.49	7.67	75.43	22.21
7	257.76	29.93	8.56	85.82	25.27
8	257.76	30.12	9.52	94.83	27.93
9	257.76	29.93	10.27	102.92	30.31
10	257.76	30.28	11.23	111.26	32.77
12	257.76	30.50	12.71	125.05	36.83
15	257.76	30.63	14.55	142.54	41.98
30	257.76	30.68	21.26	207.87	61.22
60	257.76	30.52	27.41	269.48	79.36

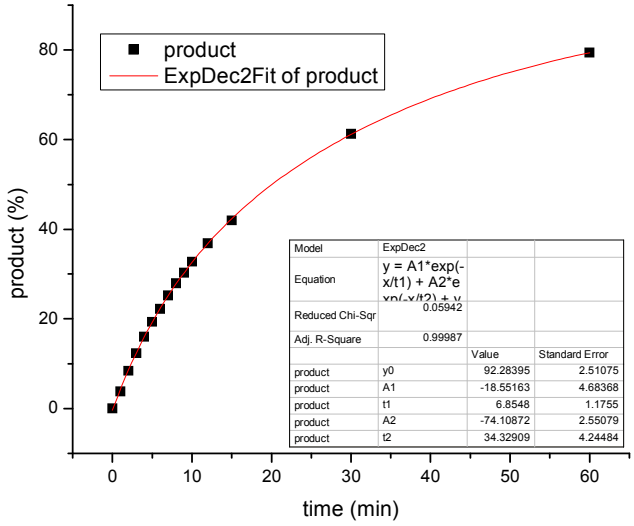

Half-life: 20.08
Average: 18.7

Table 5. entry 45. catalyst **V{*5,3,3*}: run 1**

time, min	µmol standard	area standard	area product	µmol product	product %
0	257.76	0.00	0.00	0.00	0.00
1	257.76	30.12	2.41	24.02	7.07
2	257.76	30.30	4.68	46.31	13.64
3	257.76	30.35	6.69	66.15	19.48
4	257.76	30.55	8.40	82.49	24.29
5	257.76	30.36	10.01	98.90	29.13
6	257.76	30.43	11.43	112.67	33.18
7	257.76	30.47	12.73	125.38	36.92
8	257.76	30.39	13.87	136.91	40.32
9	257.76	30.21	14.91	148.04	43.60
10	257.76	30.65	16.11	157.74	46.45
12	257.76	30.26	17.92	177.72	52.34
15	257.76	30.30	20.48	202.77	59.72
30	257.76	30.38	28.44	280.94	82.73
60	257.76	30.78	32.75	319.26	94.02

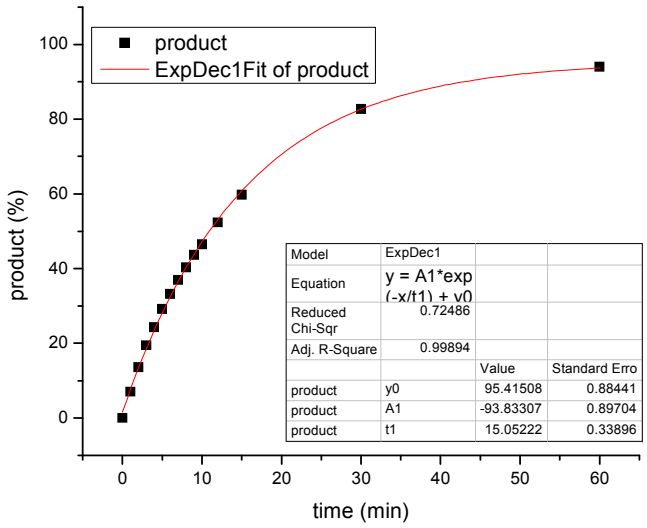

Half-life: 10.92

Table 5. entry 45. catalyst **V{*5,3,3*}: run 2**

time, min	µmol standard	area standard	area product	µmol product	product %
0	257.76	0.00	0.00	0.00	0.00
1	257.76	29.88	2.13	21.42	6.31
2	257.76	29.89	4.12	41.36	12.18
3	257.76	29.96	5.68	56.85	16.74
4	257.76	30.11	7.04	70.11	20.65
5	257.76	29.64	7.99	80.90	23.83
6	257.76	30.32	9.26	91.57	26.97
7	257.76	29.95	10.08	101.02	29.75
8	257.76	30.42	11.33	111.77	32.92
9	257.76	30.15	12.03	119.70	35.25
10	257.76	30.70	13.16	128.65	37.89
12	257.76	30.24	14.71	145.94	42.98
15	257.76	30.51	16.87	165.82	48.83
30	257.76	30.68	25.05	244.97	72.14
60	257.76	30.78	30.88	300.95	88.63

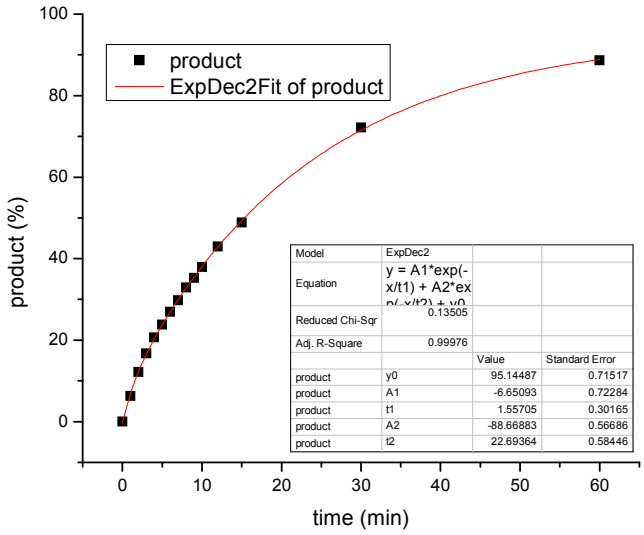

Half-life: 15.32
Average: 13.1

Table 5. entry 46. catalyst **V{*5,3,5*}: run 1**

time, min	µmol standard	area standard	area product	µmol product	product %
0	254.50	30.58	0.00	0.00	0.00
1	254.50	30.50	3.65	35.48	10.45
2	254.50	30.92	7.82	74.90	22.06
3	254.50	31.16	11.93	113.39	33.39
4	254.50	31.22	15.40	146.17	43.05
5	254.50	31.37	18.29	172.71	50.86
6	254.50	31.08	20.12	191.70	56.46
7	254.50	31.39	21.82	205.96	60.65
8	254.50	31.43	23.37	220.29	64.88
9	254.50	31.14	24.16	229.81	67.68
10	254.50	31.13	25.55	243.06	71.58
15	254.50	30.76	29.22	281.35	82.86
30	254.50	31.87	34.41	319.84	94.19
60	254.50	31.57	35.40	332.19	97.83

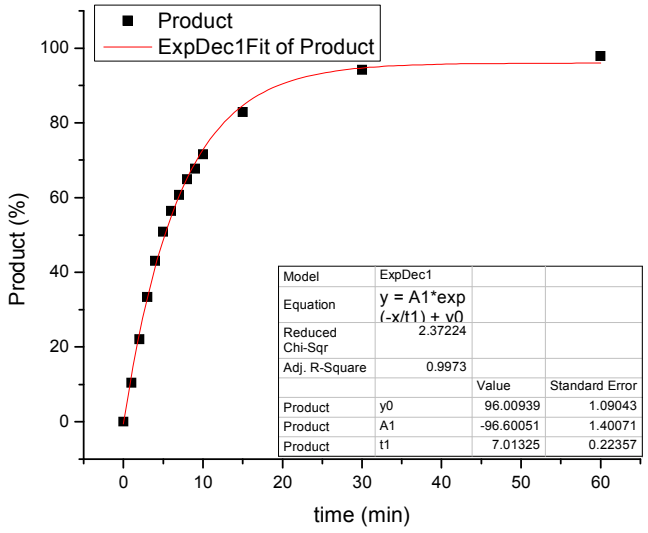

Half-life: 5.20

Table 5. entry 46. catalyst **V{*5,3,5*}: run 2**

time, min	µmol standard	area standard	area product	µmol product	product %
1	254.50	30.04	3.76	37.04	10.91
2	254.50	30.20	8.44	82.74	24.37
3	254.50	30.25	12.64	123.76	36.45
4	254.50	30.14	16.23	159.49	46.97
5	254.50	30.62	18.92	182.98	53.89
6	254.50	31.01	21.74	207.61	61.14
7	254.50	30.85	23.29	223.61	65.85
8	254.50	30.86	24.90	238.97	70.38
9	254.50	30.62	25.81	249.68	73.53
10	254.50	30.59	27.05	261.93	77.14
15	254.50	30.69	30.69	296.27	87.25
30	254.50	31.23	34.88	330.87	97.44

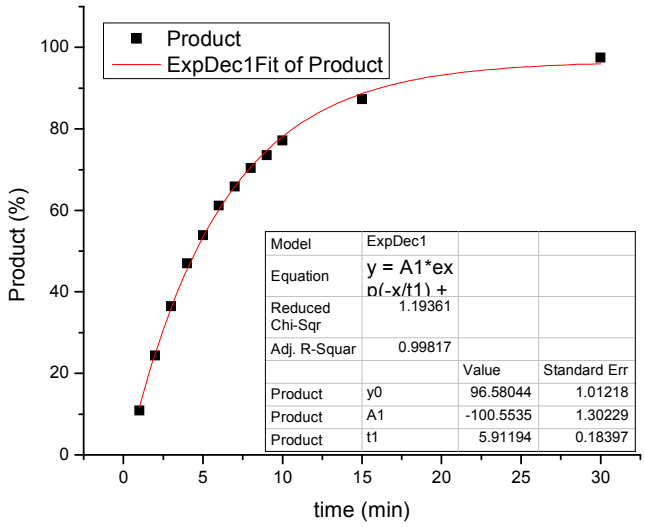

Half-life: 4.55
Average: 4.9

Table 5. entry 47. catalyst **V{*5,3,8*}: run 1**

time, min	µmol standard	area standard	area product	µmol product	product %
0	254.50	29.74	0.00	0.00	0.00
1	254.50	29.99	3.26	33.20	9.79
2	254.50	30.59	5.95	59.44	17.52
3	254.50	30.91	8.06	79.60	23.47
4	254.50	30.38	9.85	99.03	29.19
5	254.50	30.39	11.52	115.82	34.14
6	254.50	30.34	12.97	130.60	38.50
7	254.50	30.39	14.21	142.80	42.10
8	254.50	30.47	15.45	154.90	45.66
9	254.50	30.79	16.53	163.96	48.33
10	254.50	30.65	17.40	173.45	51.13
15	254.50	30.67	21.86	217.63	64.16
30	254.50	30.64	29.95	298.50	88.00
60	254.50	30.96	34.93	344.50	101.56

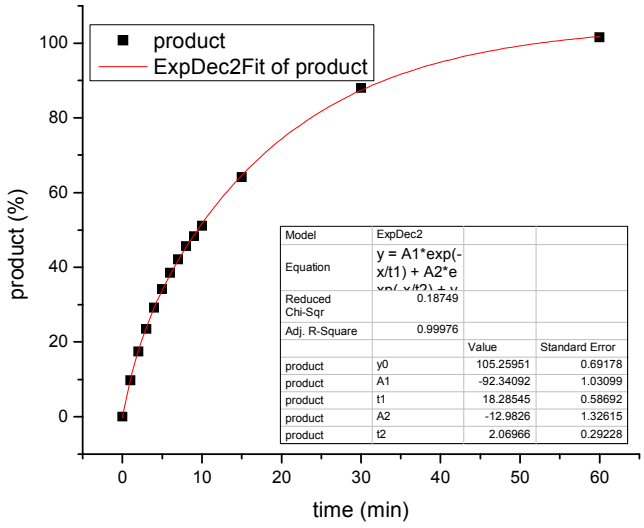

Half-life: 9.43

Table 5. entry 47. catalyst **V{*5,3,8*}: run 2**

time, min	µmol standard	area standard	area product	µmol product	product %
0	254.50	29.91	0.00	0.00	0.00
1	254.50	30.16	2.90	29.40	8.67
2	254.50	30.26	5.46	55.11	16.25
3	254.50	30.60	7.52	75.11	22.14
4	254.50	30.66	9.30	92.67	27.32
5	254.50	30.71	10.93	108.72	32.05
6	254.50	30.90	12.44	122.97	36.25
7	254.50	30.44	13.59	136.34	40.19
8	254.50	30.59	14.88	148.55	43.79
9	254.50	30.69	15.78	157.06	46.30
10	254.50	30.79	16.84	167.07	49.25
15	254.50	30.78	20.74	205.79	60.66
30	254.50	31.10	28.59	280.72	82.75
60	254.50	31.07	34.45	338.70	99.85

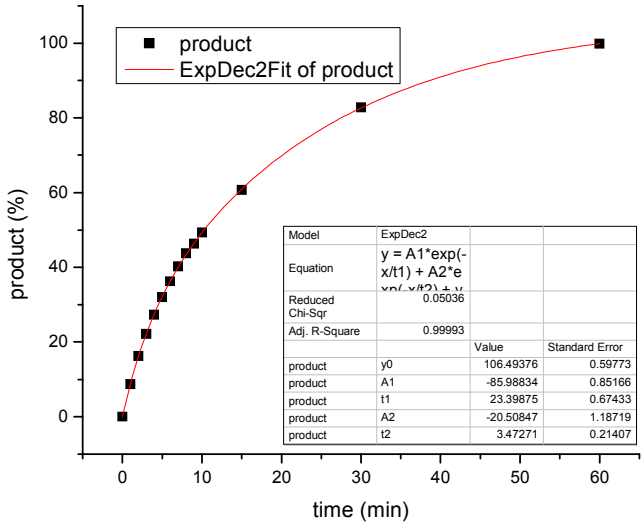

Half-life: 10.27
Average: 9.9

Table 5. entry 48. catalyst **V{*5,3,7*}: run 1**

time, min	µmol standard	area standard	area product	µmol product	product %
0	254.50	30.07	0.00	0.00	0.00
1	254.50	30.50	2.89	28.12	8.27
2	254.50	30.25	5.45	53.36	15.70
3	254.50	30.14	7.83	76.92	22.63
4	254.50	30.30	10.04	98.12	28.87
5	254.50	30.59	11.96	115.84	34.08
6	254.50	30.64	13.60	131.46	38.68
7	254.50	30.59	15.06	145.80	42.90
8	254.50	30.84	16.66	159.98	47.07
9	254.50	30.84	17.90	171.90	50.57
10	254.50	30.83	19.12	183.66	54.03
15	254.50	30.91	23.32	223.45	65.74
30.5	254.50	31.07	31.25	298.00	87.67
60	254.50	31.21	35.34	335.39	98.67

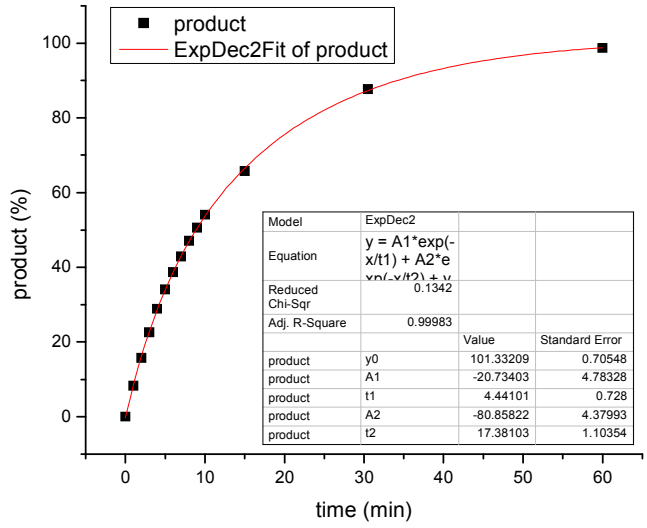

Half-life: 8.88

Table 5. entry 48. catalyst **V{*5,3,7*}: run 2**

time, min	µmol standard	area standard	area product	µmol product	product %
0	254.50	29.87	0.00	0.00	0.00
1	254.50	29.77	3.19	31.75	9.34
2	254.50	29.02	5.77	58.93	17.34
3	254.50	30.24	8.51	83.42	24.54
4	254.50	30.51	10.67	103.54	30.46
5	254.50	30.69	12.69	122.51	36.04
6	254.50	30.81	14.29	137.38	40.42
7	254.50	30.41	15.78	153.66	45.21
8	254.50	31.00	17.58	168.03	49.44
9	254.50	31.02	18.93	180.83	53.20
10	254.50	31.00	20.17	192.74	56.70
15	254.50	31.27	25.19	238.68	70.22
30	254.50	31.05	31.52	300.69	88.46
60	254.50	31.45	35.81	337.26	99.22

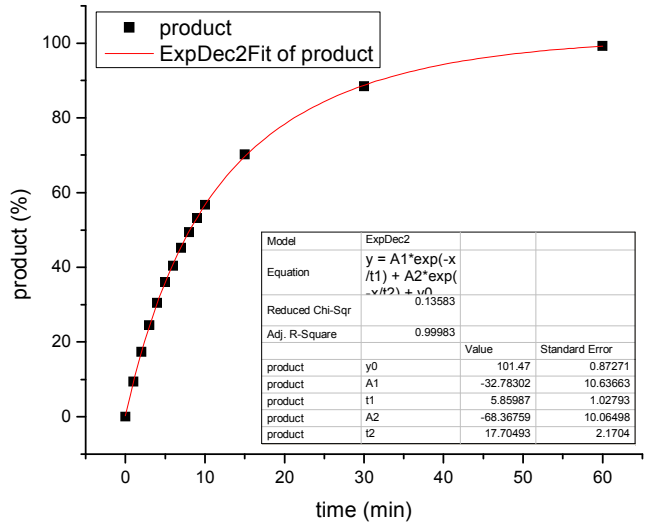

Half-life: 8.11
Average: 8.5

Table 5. entry 49. catalyst **V{*5,6,1*}: run 1**

time, min	µmol standard	area standard	area product	µmol product	product %
0	127.15	0.00	0.00	0.00	0.00
2	127.15	33.05	6.62	30.54	17.94
4	127.15	31.93	11.55	55.14	32.38
6	127.15	30.71	14.89	73.88	43.38
8	127.15	31.05	17.22	84.49	49.62
10	127.15	30.50	19.32	96.55	56.70
12	127.15	29.38	20.46	106.16	62.34
14	127.15	30.37	21.90	109.90	64.54
16	127.15	28.77	22.43	118.83	69.78
20.1	127.15	28.80	23.66	125.20	73.52
29	127.15	28.34	26.12	140.43	82.47
45	127.15	28.56	27.03	144.21	84.69

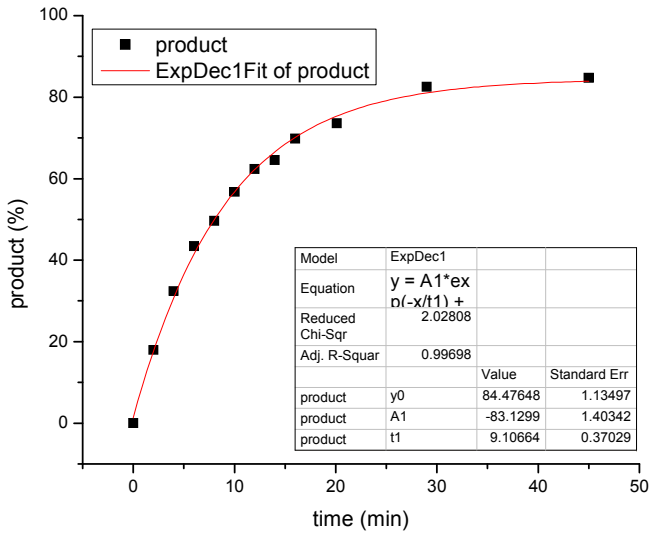

Half-life: 8.02

Table 5. entry 49. catalyst **V{*5,6,1*}: run 2**

time, min	µmol standard	area standard	area product	µmol product	product %
0	127.15	0.00	0.00	0.00	0.00
2	127.15	32.14	7.05	33.45	19.64
4	127.15	29.56	11.27	58.09	34.11
6	127.15	30.08	14.59	73.89	43.39
8	127.15	29.43	16.71	86.51	50.80
10	127.15	29.77	18.83	96.37	56.59
12	127.15	29.16	20.09	105.01	61.66
14	127.15	28.18	21.87	118.31	69.47
16	127.15	28.27	23.59	127.16	74.67
20	127.15	28.10	25.42	137.85	80.95

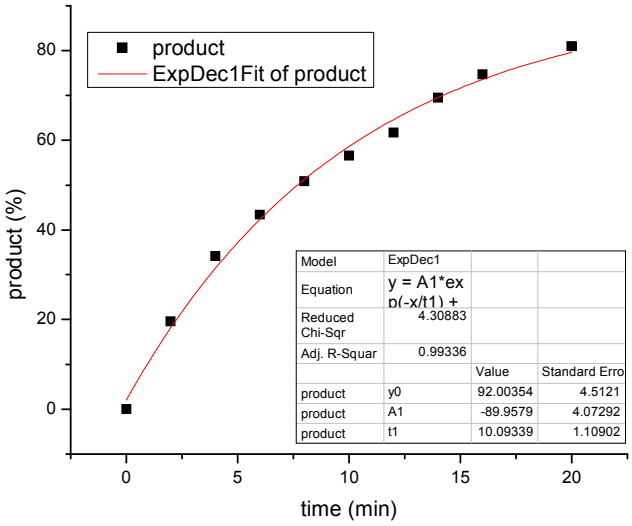

Half-life: 7.69
Average: 7.9

Table 5. entry 50. catalyst **V{*5,6,5*}: run 1**

time, min	µmol standard	area standard	area product	µmol product	product %
0	127.15	0.00	0.00	0.00	0.00
2	127.15	31.62	6.70	32.30	18.97
4	127.15	30.59	12.27	61.15	35.91
6	127.15	29.39	15.31	79.41	46.63
8	127.15	28.92	17.74	93.51	54.91
10	127.15	29.19	19.73	103.02	60.50
12	127.15	28.45	20.43	109.44	64.27
14	127.15	29.24	21.26	110.81	65.07
16	127.15	28.84	22.30	117.80	69.18
20	127.15	28.18	22.78	123.23	72.37
30	127.15	28.84	24.13	127.52	74.89

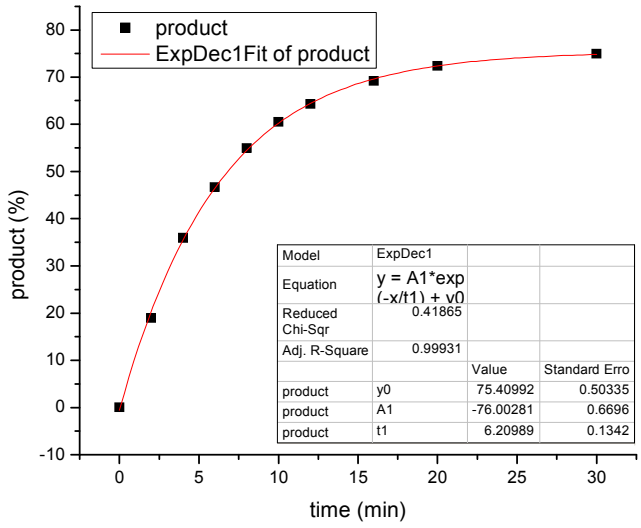

Half-life: 6.80

Table 5. entry 50. catalyst **V{*5,6,5*}: run 2**

time, min	µmol standard	area standard	area product	µmol product	product %
0	127.15	0.00	0.00	0.00	0.00
2	127.15	31.50	6.38	30.85	18.12
4	127.15	30.76	12.01	59.52	34.95
6	127.15	31.10	15.59	76.40	44.86
8	127.15	30.24	17.76	89.49	52.55
10	127.15	29.26	18.94	98.66	57.94
12	127.15	28.78	20.52	108.66	63.81
14	127.15	28.52	21.45	114.63	67.32
16	127.15	28.24	22.11	119.29	70.05
20	127.15	28.80	23.69	125.38	73.63
30	127.15	28.64	24.35	129.59	76.10

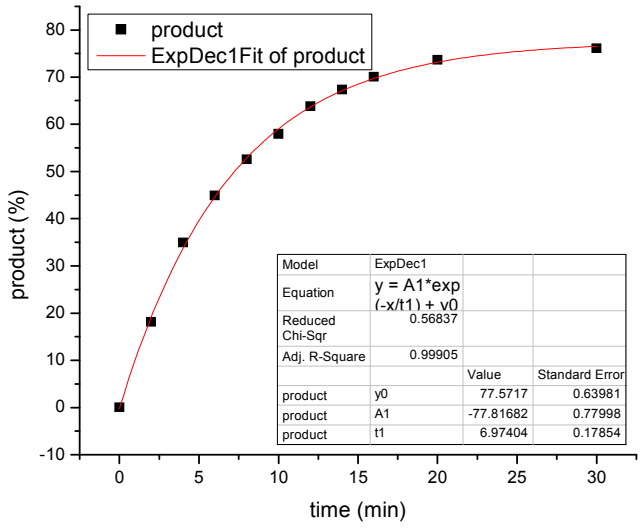

Half-life: 7.24
Average: 7.0

Table 5. entry 51. catalyst **V{*5,6,8*}: run 1**

time, min	µmol standard	area standard	area product	µmol product	product %
0	127.15	0.00	0.00	0.00	0.00
2	127.15	32.43	6.54	30.74	18.05
4	127.15	30.42	11.03	55.24	32.44
6	127.15	29.48	14.20	73.44	43.13
8	127.15	28.65	16.51	87.80	51.56
10	127.15	29.23	18.60	96.95	56.93
12	127.15	28.52	20.38	108.89	63.94
14	127.15	29.10	20.79	108.92	63.96
16	127.15	28.05	21.07	114.47	67.22
20	127.15	27.34	22.60	125.98	73.98

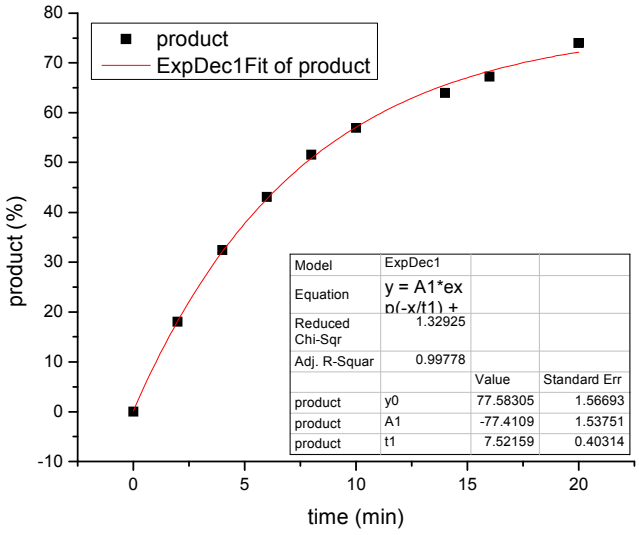

Half-life: 7.76

Table 5. entry 51. catalyst **V{*5,6,8*}: run 2**

time, min	µmol standard	area standard	area product	µmol product	product %
0	127.15	0.00	0.00	0.00	0.00
2	127.15	30.98	8.63	42.44	24.92
4	127.15	30.38	13.06	65.49	38.46
6	127.15	29.47	16.87	87.23	51.22
8	127.15	30.08	18.87	95.62	56.15
10	127.15	29.88	20.33	103.70	60.90
12	127.15	28.57	22.12	118.02	69.31
14	127.15	28.37	23.03	123.74	72.67
16	127.15	28.85	23.15	122.27	71.80
20	127.15	28.15	23.34	126.33	74.18

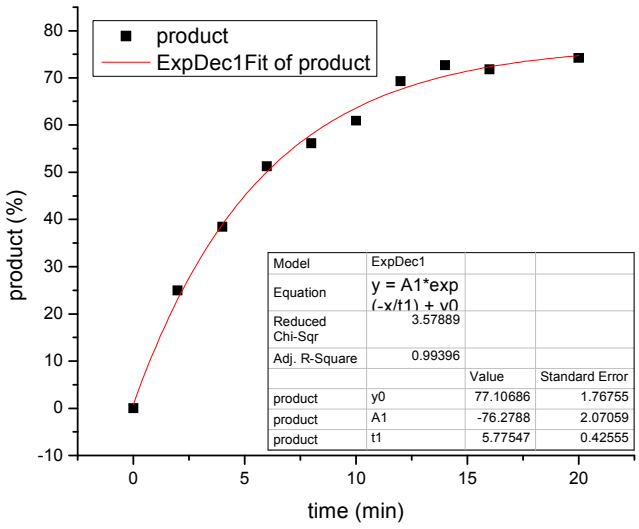

Half-life: 5.98
Average: 6.9

Table 5. entry 52. catalyst **V{*5,7,1*}: run 1**

time, min	µmol standard	area standard	area product	µmol product	product %
0	256.25	0.00	0.00	0.00	0.00
2	256.25	25.44	4.44	53.72	15.86
4	256.25	26.03	6.63	78.31	23.11
6	256.25	25.40	8.12	98.28	29.01
8	256.25	27.12	10.30	116.85	34.49
10	256.25	27.69	11.81	131.21	38.73
12	256.25	28.22	13.50	147.11	43.42
16	256.25	28.69	16.26	174.29	51.44
20	256.25	28.99	18.07	191.66	56.57
30	256.25	29.22	22.53	237.09	69.98
40	256.25	28.80	24.10	257.32	75.95
60	256.25	30.16	28.47	290.23	85.66
100	256.25	29.78	28.46	293.91	86.75

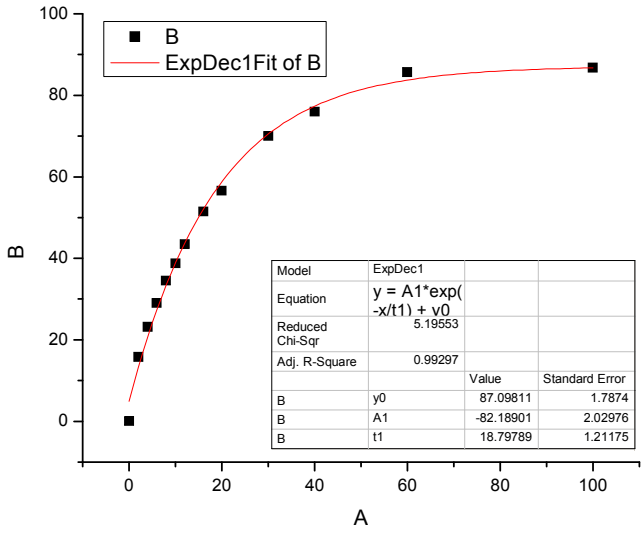

Half-life: 14.95

Table 5. entry 52. catalyst **V{*5,7,1*}: run 2**

time, min	µmol standard	area standard	area product	µmol product	product %
0	256.25	0.00	0.00	0.00	0.00
2	256.25	26.29	3.24	37.89	11.18
4	256.25	26.73	5.11	58.77	17.35
6	256.25	27.04	6.67	75.80	22.37
8	256.25	27.04	7.82	88.96	26.26
10	256.25	28.74	9.73	104.08	30.72
12	256.25	27.43	10.25	114.94	33.92
16	256.25	29.99	13.19	135.21	39.91
20	256.25	28.71	13.99	149.83	44.22
30	256.25	30.03	18.20	186.38	55.01
40	256.25	29.17	20.27	213.69	63.07
60	256.25	30.69	24.98	250.25	73.86

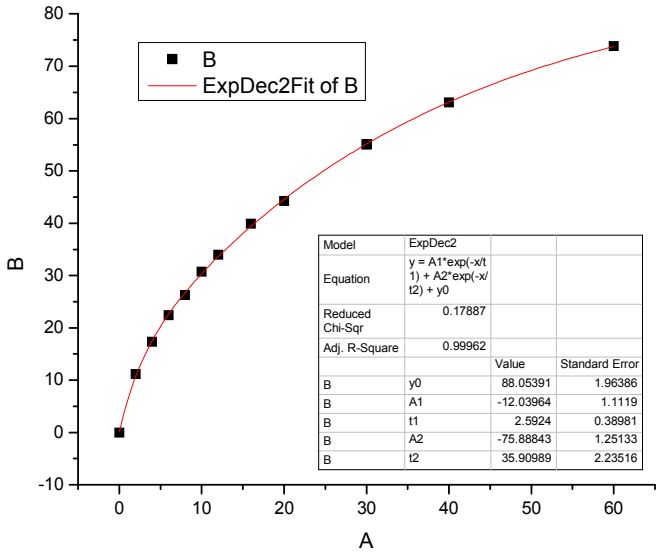

Half-life: 24.79
Average: 19.9

Table 5. entry 53. catalyst **V{*5,7,2*}: run 1**

time, min	µmol standard	area standard	area product	µmol product	product %
2	251.85	30.89	2.92	27.72	8.20
3	251.85	30.66	4.29	41.01	12.12
4	251.85	30.58	5.57	53.42	15.79
5	251.85	30.87	6.87	65.24	19.29
6	251.85	33.65	7.58	66.05	19.53
7	251.85	33.02	8.77	77.88	23.03
8	251.85	30.62	9.88	94.56	27.96
9	251.85	30.92	10.88	103.15	30.50
10	251.85	30.35	11.67	112.71	33.32
15	251.85	29.34	14.85	148.40	43.88
60	251.85	30.99	28.51	269.71	79.75

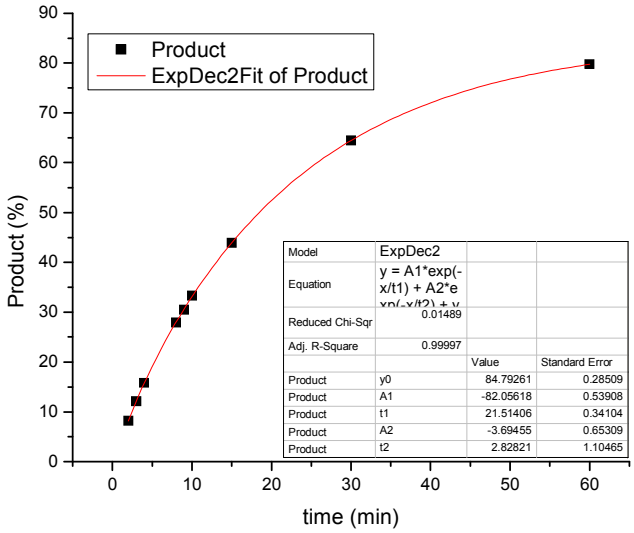

Half-life: 18.65

Table 5. entry 53. catalyst **V{*5,7,2*}: run 2**

time, min	µmol standard	area standard	area product	µmol product	product %
0	251.85	30.39	0.00	0.00	0.00
1	251.85	30.10	2.99	29.14	8.62
2	251.85	30.99	2.98	28.15	8.32
3	251.85	30.65	4.39	41.96	12.41
4	251.85	30.60	5.66	54.23	16.03
5	251.85	30.83	6.90	65.63	19.41
6	251.85	30.67	7.94	75.87	22.43
7	251.85	30.72	9.01	86.02	25.44
8	251.85	30.86	9.97	94.67	27.99
9	251.85	29.99	10.54	102.99	30.45
10	251.85	30.84	11.50	109.33	32.33
15	251.85	30.76	14.86	141.57	41.86
30	251.85	30.67	22.20	212.21	62.75
60	251.85	30.91	29.28	277.67	82.10

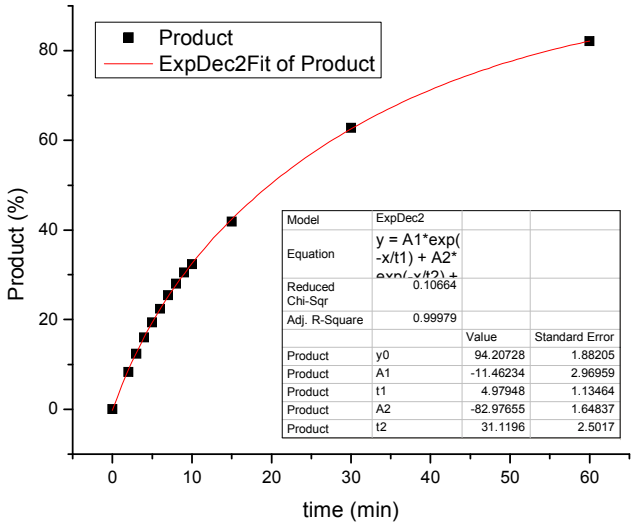

Half-life: 19.75
Average: 19.2

Table 5. entry 54. catalyst **V{*5,7,3*}: run 1**

time, min	µmol standard	area standard	area product	µmol product	product %
0	253.86	32.27	0.00	0.00	0.00
1	253.86	32.35	2.07	18.88	5.58
2	253.86	32.52	4.12	37.46	11.07
3	253.86	32.52	5.86	53.23	15.72
4	253.86	31.81	7.22	67.10	19.82
5	253.86	31.49	8.65	81.14	23.97
6	253.86	31.70	10.04	93.53	27.63
7	253.86	31.87	11.37	105.41	31.14
8	253.86	31.21	12.53	118.65	35.05
9	253.86	30.91	13.69	130.83	38.64
10	253.86	31.46	14.90	139.92	41.33
15	253.86	30.67	19.76	190.33	56.22
30	253.86	30.70	28.99	278.95	82.40
60	253.86	31.25	34.02	321.69	95.02

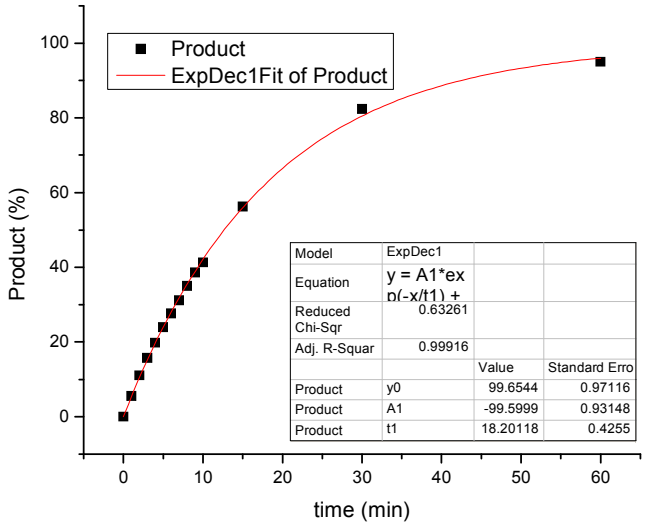

Half-life: 12.67

Table 5. entry 54. catalyst **V{*5,7,3*}: run 2**

time, min	µmol standard	area standard	area product	µmol product	product %
0	253.86	31.54	0.00	0.00	0.00
1	253.86	31.62	2.41	22.53	6.65
2	253.86	31.63	4.65	43.40	12.82
3	253.86	31.62	6.49	60.63	17.91
4	253.86	31.34	8.11	76.51	22.60
5	253.86	31.66	9.81	91.56	27.04
6	253.86	31.75	11.22	104.45	30.85
7	253.86	31.50	12.59	118.07	34.87
8	253.86	31.73	14.08	131.10	38.73
9	253.86	31.75	15.22	141.66	41.84
10	253.86	31.66	16.54	154.41	45.61
15	253.86	30.96	21.53	205.52	60.71
30	253.86	30.96	29.94	285.75	84.40
61	253.86	31.34	35.12	331.08	97.79

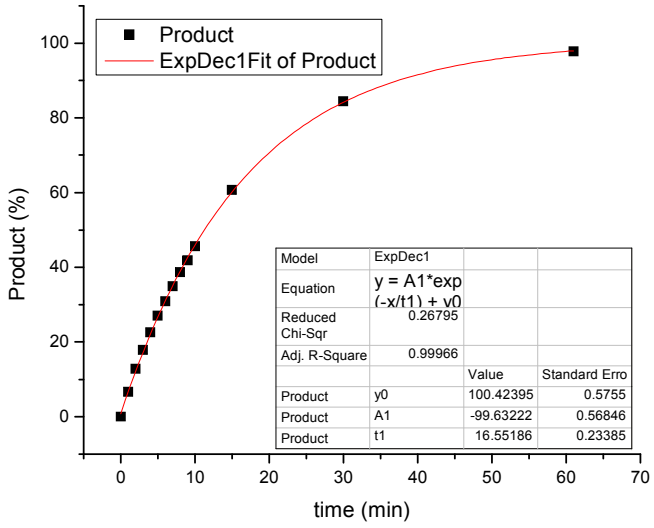

Half-life: 11.27
Average: 12.0

Table 5. entry 55. catalyst **V{*5,7,5*}: run 1**

time, min	µmol standard	area standard	area product	µmol product	product %
0	255.56	0.00	0.00	0.00	0.00
2	255.56	29.45	3.56	37.09	10.95
4	255.56	27.34	6.50	72.89	21.51
6	255.56	30.72	9.91	98.95	29.20
8	255.56	28.30	11.32	122.66	36.20
10	255.56	30.46	13.89	139.82	41.26
12	255.56	30.46	15.07	151.74	44.78
16	255.56	30.57	17.16	172.16	50.81
20	255.56	31.09	18.88	186.30	54.98
30	255.56	30.89	20.78	206.23	60.86
40	255.56	30.58	22.21	222.70	65.72
60	255.56	31.29	25.34	248.30	73.28
91	255.56	31.16	26.21	257.95	76.13

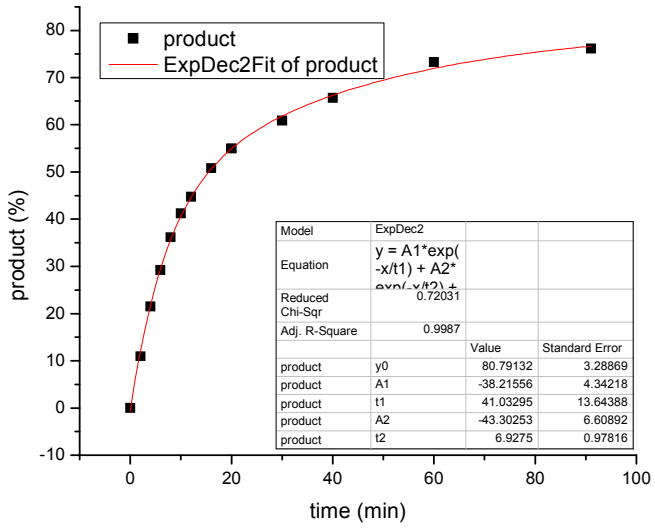

Half-life: 15.52

Table 5. entry 55. catalyst **V{*5,7,5*}: run 2**

time, min	µmol standard	area standard	area product	µmol product	product %
0	255.56	0.00	0.00	0.00	0.00
2	255.56	26.57	2.99	34.56	10.20
4	255.56	27.72	5.40	59.79	17.65
6	255.56	27.49	7.48	83.50	24.64
8	255.56	28.00	9.12	99.84	29.46
10	255.56	30.00	10.97	112.11	33.09
12	255.56	30.18	12.31	125.14	36.93
16	255.56	30.66	14.91	149.17	44.02
20	255.56	31.07	16.58	163.67	48.30
30	255.56	30.81	19.58	194.85	57.50
40	255.56	30.97	21.17	209.59	61.85
60	255.56	31.23	24.07	236.42	69.77
91	255.56	32.76	27.70	259.30	76.52

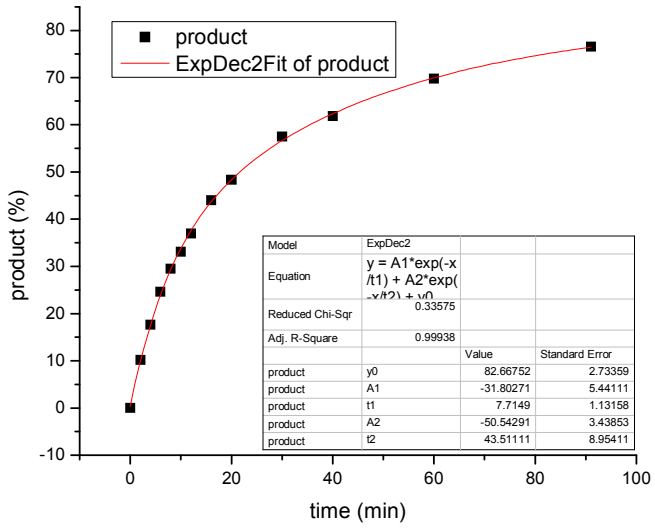

Half-life: 21.63
Average: 18.6

Table 5. entry 56. catalyst **V{*5,7,7*}: run 1**

time, min	µmol standard	area standard	area product	µmol product	product %
0	256.10	0.00	0.00	0.00	0.00
4	256.10	29.89	7.97	81.98	24.22
6	256.10	28.26	9.50	103.27	30.51
8	256.10	28.37	11.39	123.36	36.45
12	256.10	28.78	14.65	156.49	46.23
14	256.10	29.43	16.16	168.79	49.87
16	256.10	29.14	17.32	182.66	53.97
20	256.10	29.35	19.09	199.94	59.07
30	256.10	29.90	22.72	233.47	68.98
40	256.10	30.16	24.90	253.70	74.96
60	256.10	31.00	27.36	271.27	80.15

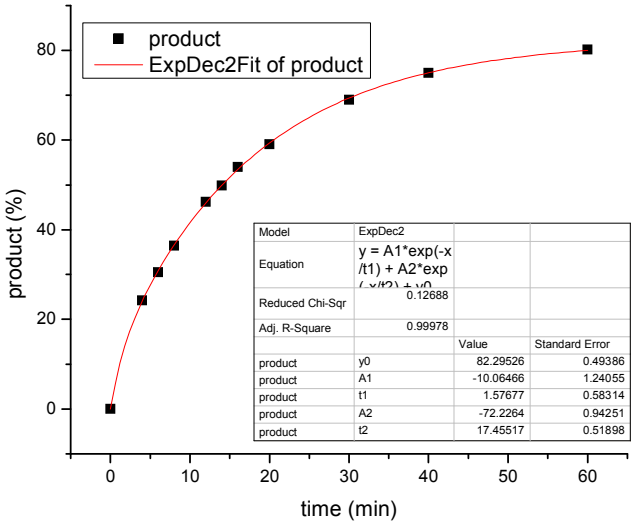

Half-life: 14.05

Table 5. entry 56. catalyst **V{*5,7,7*}: run 2**

time, min	µmol standard	area standard	area product	µmol product	product %
0	256.10	0.00	0.00	0.00	0.00
4	256.10	27.72	6.77	75.04	22.17
6	256.10	27.82	8.87	97.97	28.95
8	256.10	28.73	10.95	117.16	34.61
12	256.10	28.53	14.22	153.17	45.26
14	256.10	29.79	16.41	169.31	50.02
16	256.10	30.08	16.83	171.95	50.80
20	256.10	29.39	18.72	195.82	57.86
30	256.10	29.89	22.72	233.53	69.00

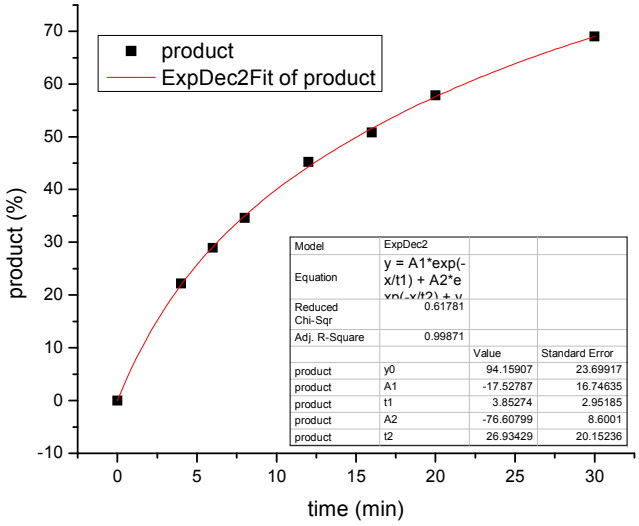

Half-life: 15.05
Average: 14.6

Table 5. entry 57. catalyst **V{*7,2,1*}: run 1**

time, min	µmol standard	area standard	area product	µmol product	product %
0	253.42	0.00	0.00	0.00	0.00
2	253.42	27.63	4.82	52.60	15.55
4	253.42	27.94	7.66	82.68	24.45
6	253.42	24.32	8.64	107.17	31.69
8	253.42	28.15	12.03	128.89	38.11
10	253.42	28.71	13.81	145.08	42.90
12	253.42	28.84	14.91	155.96	46.11
14	253.42	28.70	16.67	175.15	51.79
16	253.42	29.05	18.64	193.56	57.23
20	253.42	29.62	20.48	208.49	61.65
30	253.42	30.02	23.70	238.12	70.41
45	253.42	28.02	25.96	279.36	82.60
60	253.42	29.91	25.28	254.89	75.36

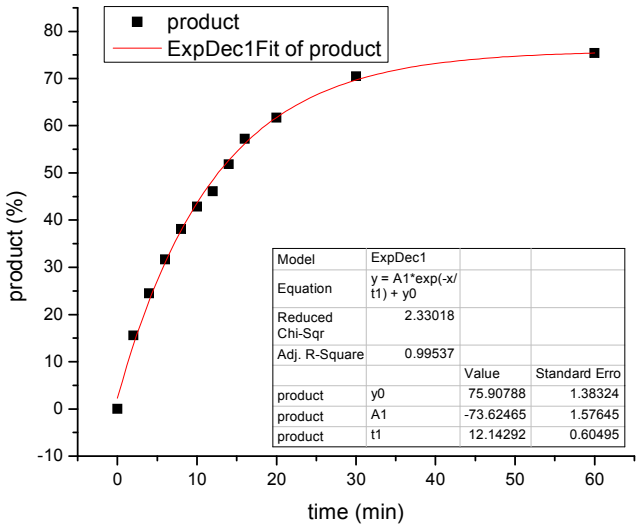

Half-life: 12.68

Table 5. entry 57. catalyst **V{*7,2,1*}: run 2**

time, min	µmol standard	area standard	area product	µmol product	product %
0	254.29	0.00	0.00	0.00	0.00
2	254.29	26.42	3.12	35.70	10.55
4	254.29	26.77	5.71	64.51	19.06
6	254.29	27.34	8.26	91.41	27.00
8	254.29	27.57	10.52	115.54	34.13
10	254.29	27.66	11.65	127.43	37.64
12	254.29	28.05	13.62	146.93	43.40
14	254.29	28.46	15.29	162.62	48.04
16	254.29	28.98	17.20	179.64	53.06
20	254.29	29.28	19.71	203.76	60.19
30	254.29	30.25	23.52	235.27	69.49
45	254.29	30.37	24.70	246.06	72.68
60	254.29	30.28	24.80	247.85	73.21

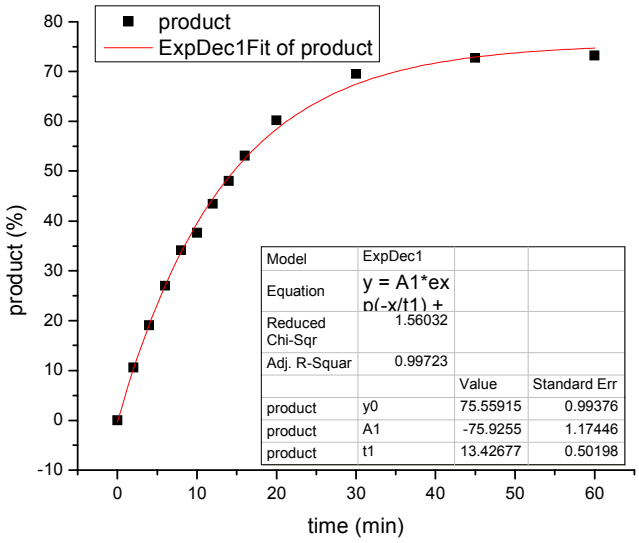

Half-life: 14.62
Average: 13.7

Table 5. entry 58. catalyst **V{*7,2,5*}: run 1**

time, min	µmol standard	area standard	area product	µmol product	product %
0	256.32	0.00	0.00	0.00	0.00
5	256.32	25.60	4.80	57.25	16.93
10	256.32	27.18	8.84	99.23	29.34
15	256.32	27.56	11.99	132.82	39.27
20	256.32	27.80	13.77	151.10	44.68
25	256.32	28.14	14.72	159.61	47.19
30	256.32	27.86	14.56	159.55	47.18
30	256.32	27.86	14.56	159.55	47.18
35	256.32	28.35	16.03	172.59	51.03
40	256.32	28.79	16.96	179.78	53.16
45	256.32	29.12	17.74	185.94	54.98
50	256.32	28.71	18.03	191.69	56.68
85	256.32	29.47	21.12	218.69	64.66
162	256.32	29.58	24.31	250.81	74.16

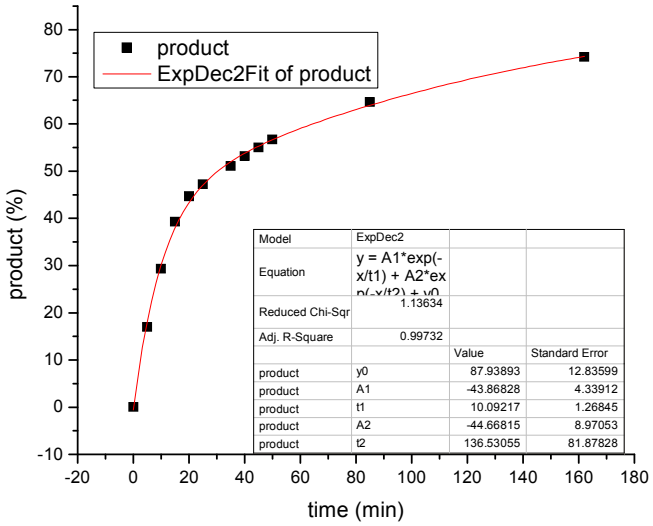

Half-life: 30.34

Table 5. entry 58. catalyst **V{*7,2,5*}: run 2**

time, min	µmol standard	area standard	area product	µmol product	product %
0	256.32	0.00	0.00	0.00	0.00
5	256.32	27.41	5.20	57.86	17.11
10	256.32	27.50	9.67	107.23	31.71
15	256.32	28.66	13.05	138.89	41.07
20	256.32	28.46	15.05	161.32	47.70
25	256.32	24.42	17.36	216.87	64.12
30	256.32	29.62	17.28	177.92	52.61
35	256.32	29.38	18.52	192.33	56.87
40	256.32	27.42	19.53	217.26	64.24
45	256.32	29.80	19.32	197.72	58.46
45	256.32	29.80	19.32	197.72	58.46
50	256.32	27.04	20.92	236.01	69.78
85	256.32	29.91	21.97	224.11	66.26
162	256.32	30.38	24.15	242.53	71.71

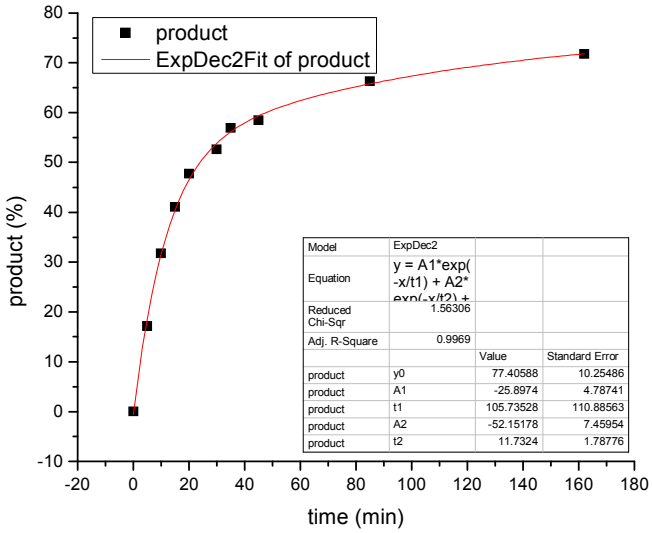

Half-life: 23.97
Average: 28.7

Table 5. entry 59. catalyst **V{*7,2,8*}: run 1**

time, min	µmol standard	area standard	area product	µmol product	product %
0	255.33	0.00	0.00	0.00	0.00
2	255.33	27.67	5.26	58.28	17.22
4	255.33	28.27	8.02	86.91	25.68
6	255.33	28.86	10.62	112.70	33.30
8	255.33	28.75	12.54	133.67	39.50
10	255.33	27.65	13.96	154.72	45.72
12	255.33	28.63	16.32	174.67	51.62
16	255.33	28.00	18.57	203.14	60.03
20	255.33	29.86	22.69	232.81	68.80
30	255.33	30.02	25.53	260.56	77.00

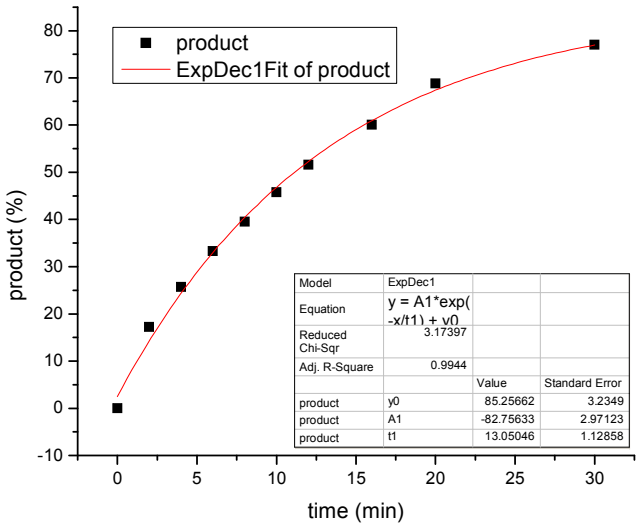

Half-life: 11.14

Table 5. entry 59. catalyst **V{*7,2,8*}: run 2**

time, min	µmol standard	area standard	area product	µmol product	product %
0	255.33	0.00	0.00	0.00	0.00
2	255.33	26.34	4.72	54.86	16.21
4	255.33	26.97	7.96	90.38	26.71
6	255.33	29.27	10.85	113.62	33.58
8	255.33	29.81	12.90	132.54	39.17
10	255.33	29.11	14.81	155.82	46.05
12	255.33	29.59	16.66	172.50	50.98
16	255.33	29.94	19.57	200.27	59.19
20	255.33	30.07	20.44	208.22	61.53
30	255.33	29.17	20.63	216.75	64.05
40	255.33	29.65	21.94	226.79	67.02

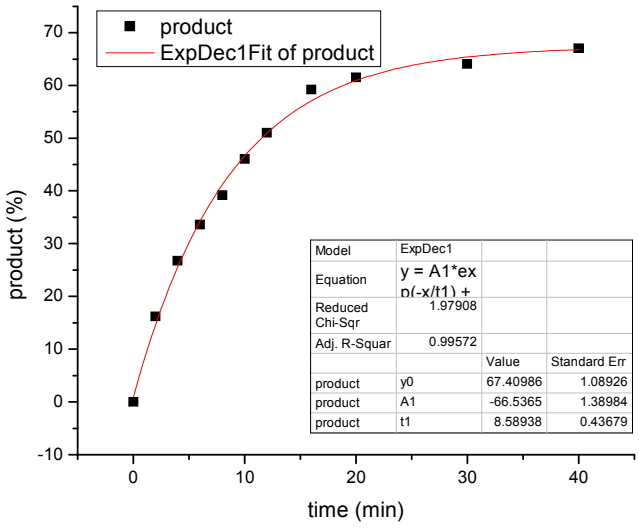

Half-life: 11.52
Average: 11.3

Table 5. entry 60. catalyst **V{*7,2,9*}: run 1**

time, min	µmol standard	area standard	area product	µmol product	product %
0	255.78	0.00	0.00	0.00	0.00
2	255.78	27.62	4.02	44.64	13.18
4	255.78	27.55	6.93	77.19	22.80
6	255.78	27.03	9.16	104.05	30.73
8	255.78	28.48	11.40	122.91	36.30
10	255.78	28.99	13.69	144.96	42.81
12	255.78	31.19	16.39	161.33	47.64
16	255.78	31.05	19.24	190.17	56.16
20	255.78	31.15	22.06	217.35	64.19
30	255.78	31.29	24.96	244.85	72.31
40	255.78	30.88	26.79	266.21	78.62
60	255.78	31.20	27.52	270.70	79.94
100	255.78	30.73	28.15	281.20	83.04

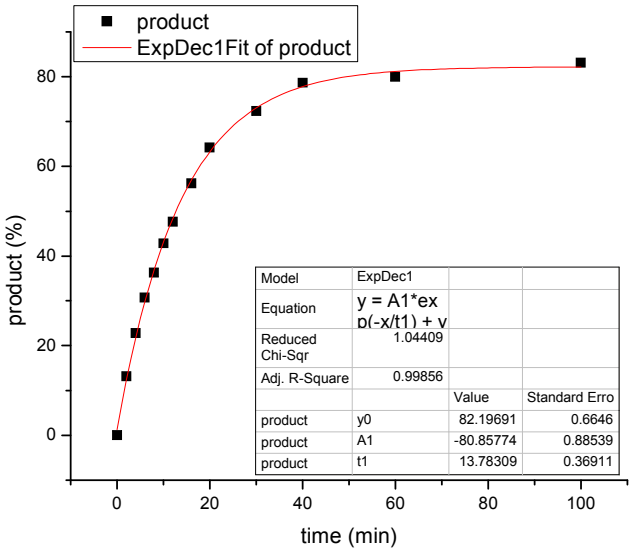

Half-life: 12.69

Table 5. entry 60. catalyst **V{*7,2,9*}: run 2**

time, min	µmol standard	area standard	area product	µmol product	product %
0	255.78	0.00	0.00	0.00	0.00
2	255.78	26.49	4.38	50.77	14.99
4	255.78	30.06	8.31	84.83	25.05
6	255.78	30.17	11.33	115.21	34.02
8	255.78	30.56	13.68	137.38	40.57
10	255.78	29.91	15.26	156.56	46.24
12	255.78	30.54	17.58	176.62	52.16
16	255.78	31.44	20.94	204.44	60.38
20	255.78	31.29	23.44	229.91	67.90
30	255.78	31.34	25.96	254.24	75.08

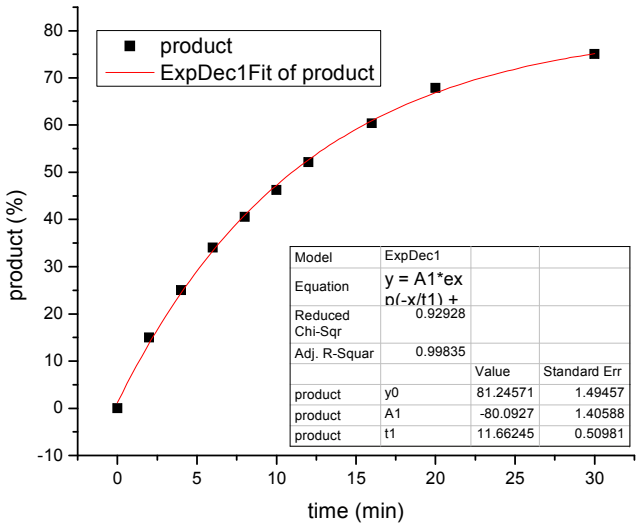

Half-life: 10.91
Average: 11.8

Table 5. entry 61. catalyst **V{*7,2,10*}: run 1**

time, min	µmol standard	area standard	area product	µmol product	product %
5	255.56	0.00	0.00	0.00	0.00
10	255.56	26.68	1.84	21.09	6.22
20	255.56	27.01	4.33	49.14	14.50
30	255.56	18.12	6.64	112.40	33.17
40	255.56	28.13	11.57	126.16	37.23
51	255.56	28.40	13.57	146.51	43.24
60	255.56	29.17	15.34	161.35	47.62
76	255.56	29.27	16.61	174.00	51.35
100	255.56	29.55	18.52	192.26	56.74
156	255.56	29.42	20.25	211.06	62.29
243	255.56	29.90	23.30	239.00	70.53
301	255.56	31.69	26.47	256.14	75.59

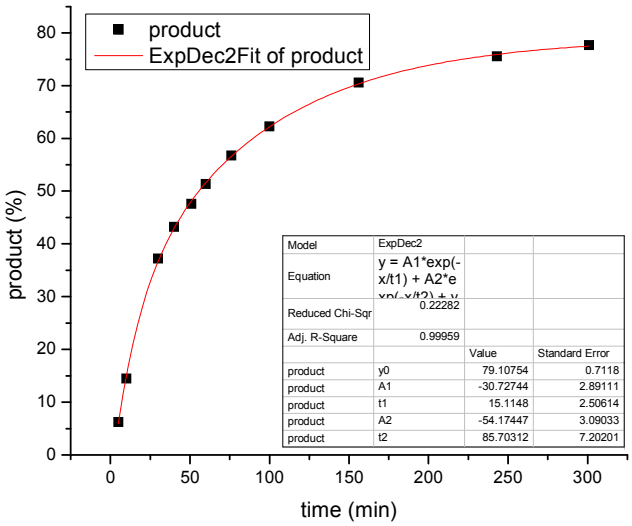

Half-life: 55.56

Table 5. entry 61. catalyst **V{*7,2,10*}: run 2**

time, min	µmol standard	area standard	area product	µmol product	product %
5	255.56	0.00	0.00	0.00	0.00
10	255.56	29.37	2.87	29.95	8.84
20	255.56	29.54	6.34	65.85	19.43
30	255.56	28.55	11.10	119.28	35.20
40	255.56	30.36	14.62	147.67	43.58
51	255.56	30.03	16.23	165.75	48.92
60	255.56	30.69	18.32	183.02	54.01
76	255.56	30.40	19.24	194.07	57.27
100	255.56	30.87	20.75	206.20	60.85
156	255.56	30.88	22.62	224.62	66.29
243	255.56	30.53	24.41	245.24	72.37
301	255.56	32.08	27.11	259.17	76.48

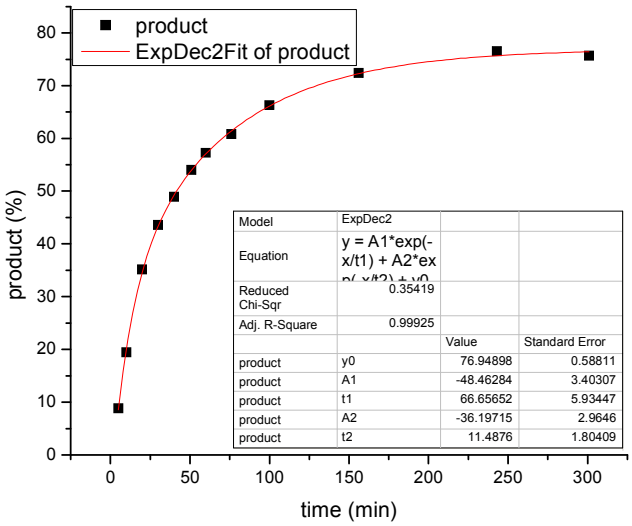

Half-life: 41.56
Average: 48.6

Table 5. entry 62. catalyst **V{*6,2,1*}: run 1**

time, min	µmol standard	area standard	area product	µmol product	product %
0	255.56	0.00	0.00	0.00	0.00
2	255.56	25.94	3.41	40.37	11.92
4	255.56	27.67	6.81	75.46	22.28
6	255.56	28.04	9.36	102.40	30.23
8	255.56	26.94	11.14	126.75	37.42
10	255.56	28.96	14.12	149.50	44.14
12	255.56	28.63	15.62	167.29	49.39
16	255.56	27.38	17.36	194.51	57.42
20	255.56	28.40	20.63	222.76	65.76
28	255.56	29.80	24.84	255.60	75.46
40	255.56	28.98	26.64	281.84	83.21
64	255.56	28.67	26.89	287.62	84.91
84	255.56	29.79	28.53	293.71	86.71

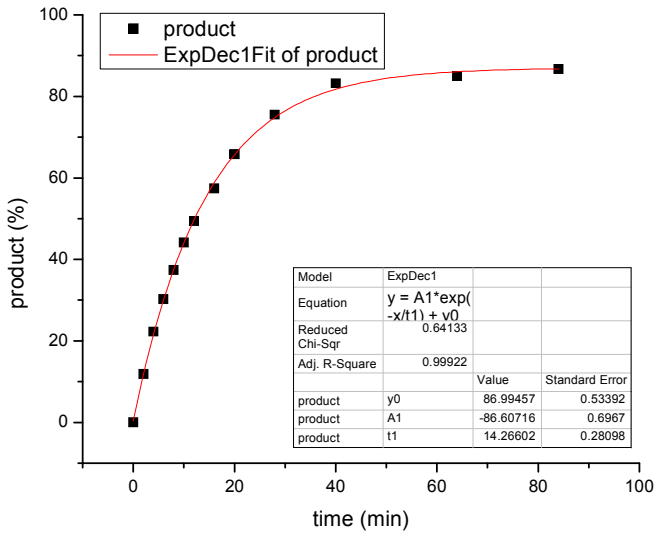

Half-life: 12.13

Table 5. entry 62. catalyst **V{*6,2,1*}: run 1**

time, min	µmol standard	area standard	area product	µmol product	product %
0	255.56	0.00	0.00	0.00	0.00
2	255.56	28.27	4.06	40.75	12.98
4	255.56	26.56	6.91	73.81	23.51
6	255.56	29.02	9.97	97.46	31.04
8	255.56	27.59	11.47	117.98	37.58
10	255.56	27.39	13.30	137.84	43.91
12	255.56	27.83	15.19	154.90	49.34
16	255.56	28.35	18.19	182.13	58.01
20	255.56	30.14	21.18	199.42	63.52
28	255.56	29.97	24.66	233.47	74.37
40	255.56	31.60	29.33	263.38	83.89
64	255.56	30.24	28.13	263.98	84.09
84	255.56	30.01	28.39	268.47	85.52

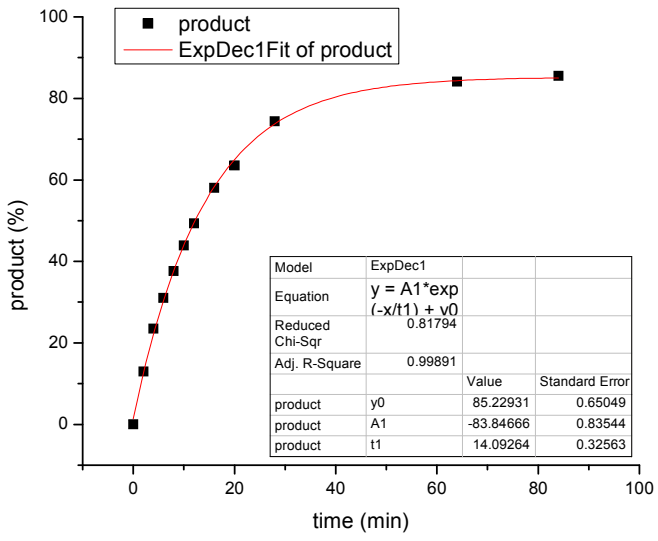

Half-life: 12.22
Average: 12.2

Table 5. entry 63. catalyst **V{*6,2,8*}: run 1**

time, min	µmol standard	area standard	area product	µmol product	product %
0	256.20	0.00	0.00	0.00	0.00
2	256.20	27.02	4.06	46.15	13.64
4	256.20	27.66	7.71	85.67	25.33
6	256.20	30.18	10.90	111.07	32.84
8	256.20	30.18	13.45	136.98	40.50
10	256.20	28.06	13.63	149.31	44.15
12	256.20	30.15	16.70	170.35	50.37
16	256.20	30.63	19.19	192.60	56.95
20	256.20	30.27	20.75	210.74	62.31
30	256.20	30.20	24.46	248.95	73.61
40	256.20	33.80	28.61	260.18	76.93
60	256.20	30.25	27.87	283.29	83.76
100	256.20	31.01	29.49	292.39	86.45

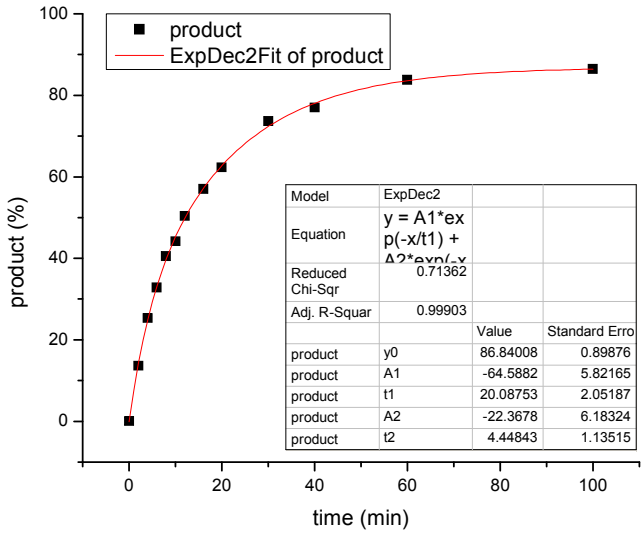

Half-life: 12.10

Table 5. entry 63. catalyst **V{*6,2,8*}: run 2**

time, min	µmol standard	area standard	area product	µmol product	product %
0	256.20	0.00	0.00	0.00	0.00
2	256.20	27.12	4.67	52.94	15.65
4	256.20	28.56	8.38	90.19	26.67
6	256.20	28.66	10.97	117.73	34.81
8	256.20	29.33	13.33	139.66	41.29
10	256.20	28.66	14.37	154.10	45.56
12	256.20	30.25	16.79	170.64	50.45
16	256.20	30.08	18.74	191.52	56.63
20	256.20	30.21	22.10	224.92	66.50
30	256.20	30.88	25.76	256.41	75.82
40	256.20	29.90	26.19	269.29	79.62
60	256.20	29.90	27.53	283.02	83.68
100	256.20	30.66	28.85	289.25	85.52

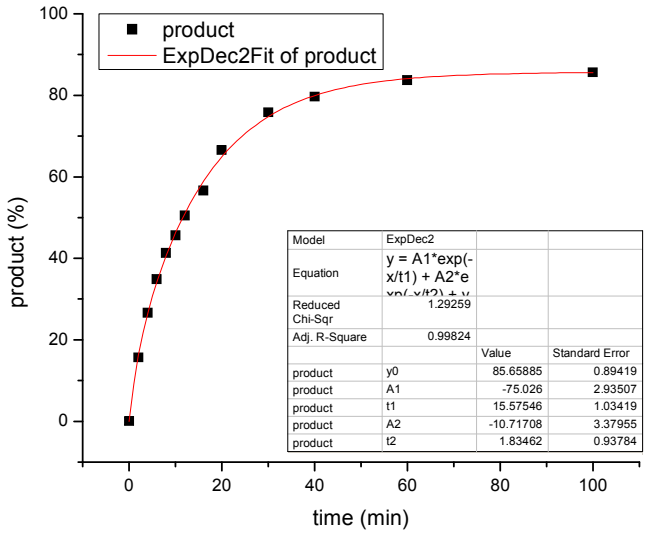

Half-life: 11.59
Average: 11.8

Kinetic data for other Quaternary Ammonium Ions & Library VI: Table 6 in Text

Table 6. entry 1. catalyst Me_4NBr: **run 1**

time, min	standard, µmol	standard, area	product, area	product, µmol	product, %
0	256.52	1.00	0.00	0.00	0.00
945	256.52	26.72	1.38	15.92	4.70
1200	256.52	26.76	1.79	20.60	6.08
1440	256.52	26.29	2.11	24.71	7.30
2400	256.52	26.46	3.52	40.85	12.07
2880	256.52	26.96	4.20	47.92	14.16
3865	256.52	28.87	5.45	57.97	17.12
4320	256.52	26.58	5.11	59.14	17.47
5400	256.52	32.41	7.86	74.51	22.01

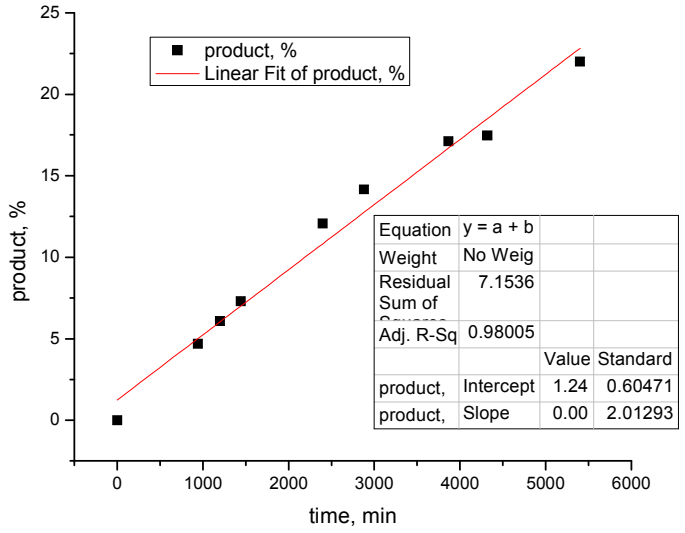

Half Life: 12,189

Table 6. entry 1. catalyst Me_4NBr: **run 2**

time, min	standard, µmol	standard, area	product, area	product, µmol	product, %
0	256.5189	1	0	0	0
945	256.5189	26.4729	1.1692	13.57261	4.009078
1200	256.5189	26.4359	1.4746	17.1418	5.063343
1440	256.5189	26.2949	1.7487	20.43713	6.03672
2400	256.5189	28.4851	3.2886	35.47885	10.47974
2880	256.5189	27.6143	3.5704	39.7337	11.73654
3865	256.5189	26.3943	4.4777	52.134	15.39934
4320	256.5189	30.0689	5.5762	56.98978	16.83364
5400	256.5189	30.4851	6.9026	69.5827	20.55334
6882	256.5189	30.011	8.3029	85.02086	25.11346

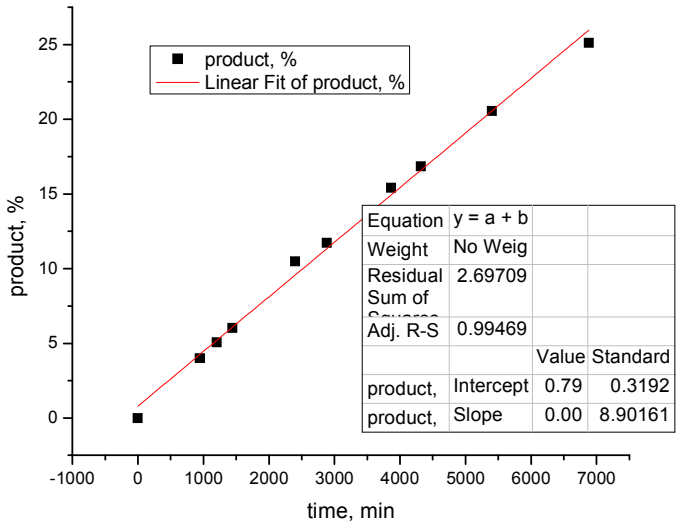

Half Life: 13,298

Average: 12,700

Table 6. entry 2. catalyst $Me_3NC_{16}H_{33}Br$: **run 1**

time, min	standard, µmol	standard, area	product, area	product, µmol	product, %
0	256.52	1.00	0.00	0.00	0.00
945	256.52	27.29	6.38	71.84	21.22
1200	256.52	27.13	6.77	76.69	22.65
1440	256.52	27.65	9.63	107.04	31.62
2400	256.52	28.31	15.90	172.56	50.97
2880	256.52	30.08	17.87	182.59	53.93
3865	256.52	29.61	20.49	212.68	62.82
4320	256.52	30.77	19.11	190.81	56.36
5400	256.52	31.62	25.18	244.74	72.29
6882	256.52	30.06	24.08	246.24	72.74

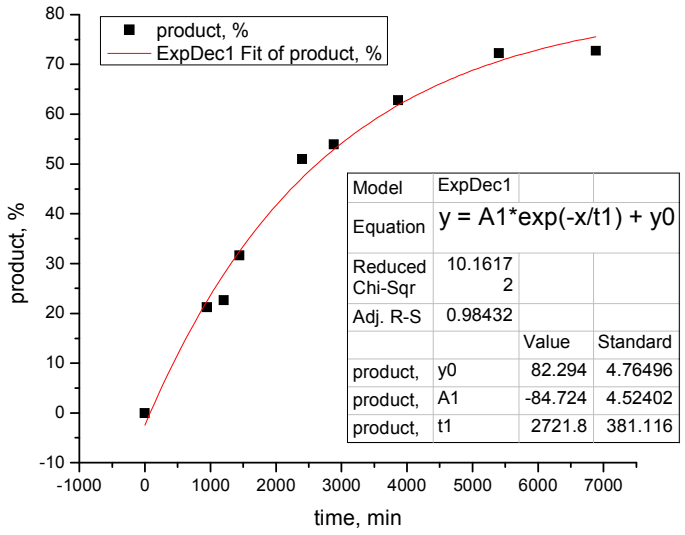

Half Life: 2625.2

Table 6. entry 2. catalyst $Me_3NC_{16}H_{33}Br$: **run 2**

time, min	standard, µmol	standard, area	product, area	product, µmol	product, %
0	256.52	1.00	0.00	0.00	0.00
945	256.52	26.38	3.03	35.29	10.42
1200	256.52	25.72	6.88	82.16	24.27
1440	256.52	27.33	8.40	94.44	27.89
2400	256.52	28.21	14.74	160.57	47.43
2880	256.52	30.30	17.70	179.55	53.03
3865	256.52	29.91	20.96	215.38	63.62
4320	256.52	34.57	26.42	234.85	69.37
6882	256.52	30.34	24.30	246.12	72.70

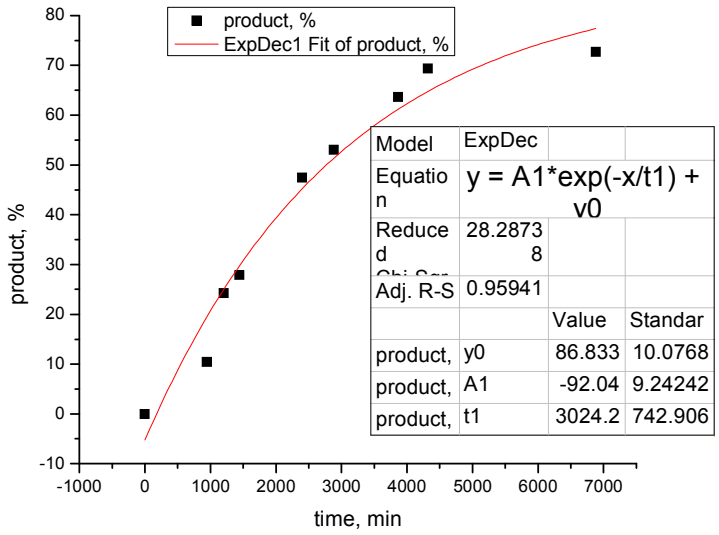

Half Life: 2769.8
Average: 2697.5 (2700)

Table 6. entry 3. catalyst Et_4NBr: **run 1**

time, min	standard, µmol	standard, area	product, area	product, µmol	product, %
0	256.52	30.00	0.00	0.00	0.00
92	256.52	28.28	7.85	85.25	25.18
256	256.52	28.49	12.33	132.95	39.27
335	256.52	29.32	14.69	154.00	45.49
557	256.52	29.61	17.87	185.45	54.78
685	256.52	29.43	17.29	180.60	53.35

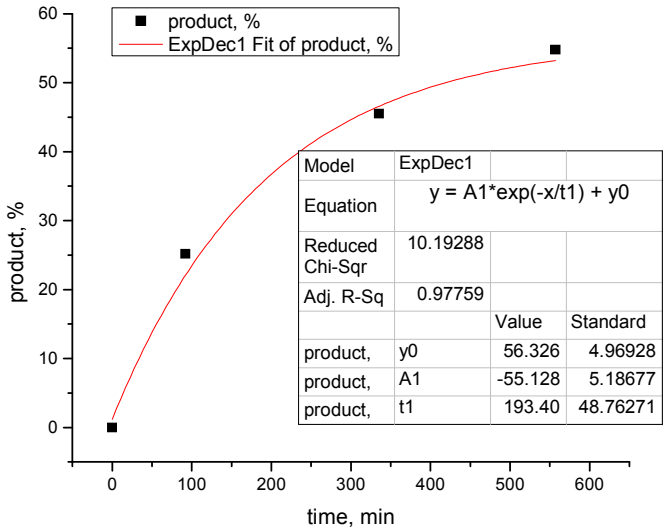

Half Life: 418.7

Table 6. entry 3. catalyst Et_4NBr: **run 2**

time, min	standard, µmol	standard, area	product, area	product, µmol	product, %
0	256.5189			#DIV/0!	#DIV/0!
92	256.5189	28.7187	5.1202	54.78962	16.18376
256	256.5189	27.604	9.1588	101.963	30.11784
335	256.5189	28.396	11.3346	122.6663	36.23317
557	256.5189	29.7893	15.5333	160.2432	47.33264
685	256.5189	32.0585	20.7519	198.9257	58.75867

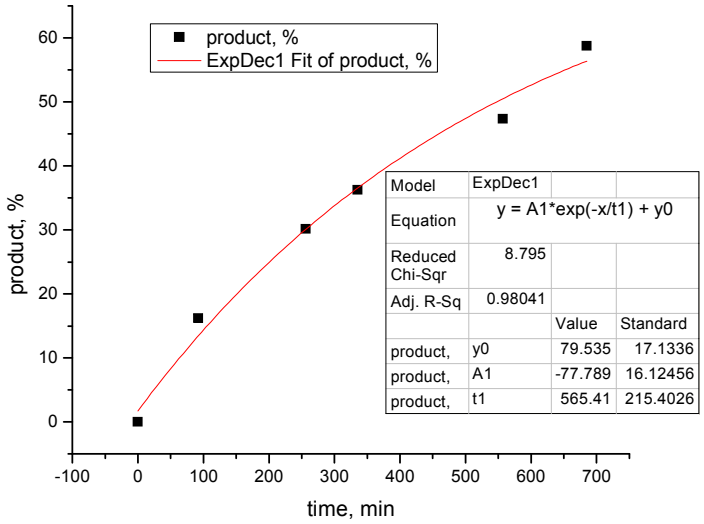

Half Life: 547.6
Average: 480

Table 6. entry 4. catalyst Bu_3NBnBr: **run 1**

time, min	standard, μmol	standard, area	product, area	product, μmol	product, %
0	255.10	21.58	0.00	0.00	0.00
1	255.10	21.28	0.63	5.85	1.73
2	255.10	20.64	1.56	14.99	4.42
3	255.10	21.06	2.73	25.65	7.56
4	255.10	21.46	3.86	35.68	10.52
5	255.10	21.60	5.03	46.17	13.61
6	255.10	21.44	6.11	56.52	16.66
7	255.10	21.17	7.17	67.14	19.79
8	255.10	21.38	8.32	77.10	22.73
9	255.10	21.03	9.27	87.35	25.75
10	255.10	21.42	10.37	95.98	28.29
15	255.10	21.98	16.08	145.01	42.75
30	255.10	21.85	25.67	232.82	68.63
60	255.10	22.05	33.50	301.14	88.77

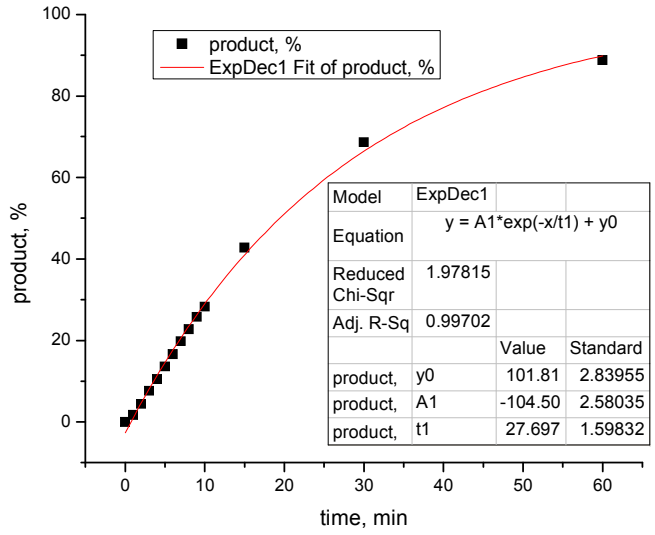

Half Life: 19.43

Table 6. entry 4. catalyst Bu_3NBnBr: **run 2**

time, min	standard, μmol	standard, area	product, area	product, μmol	product, %
0.00	255.10	25.18	0.00	0.00	0.00
1.00	255.10	21.74	0.29	2.66	0.78
2.00	255.10	21.67	0.72	6.63	1.93
3.00	255.10	21.63	1.53	14.00	4.08
4.00	255.10	21.82	2.37	21.55	6.28
5.00	255.10	21.58	3.28	30.18	8.79
6.00	255.10	21.95	4.31	38.89	11.33
7.00	255.10	21.87	5.29	47.90	13.95
8.00	255.10	21.71	6.17	56.31	16.40
9.00	255.10	21.72	7.28	66.42	19.35
10.00	255.10	21.35	7.94	73.72	21.47
15.00	255.10	21.38	13.25	122.81	35.78
30.00	255.10	4.03	4.73	232.74	67.80
60.00	255.10	21.80	34.13	310.28	90.39

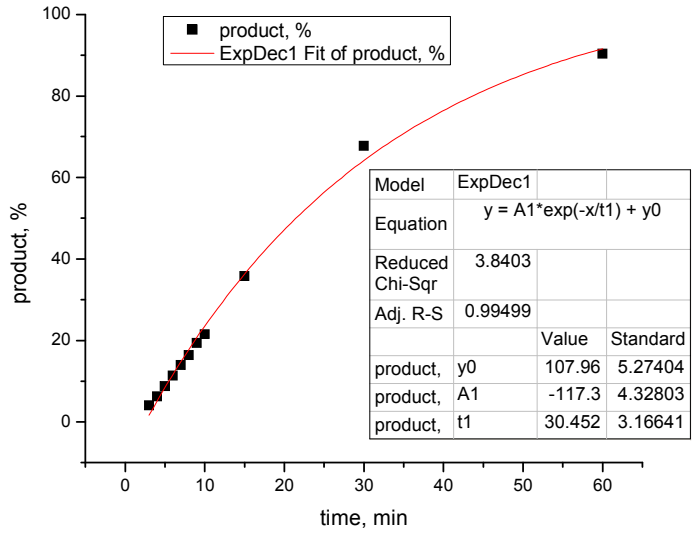

Half Life: 21.46

Average: 20.5

Table 6. entry 5. catalyst **VI**{1}: **run 1**

time, min	standard, μmol	standard, area	product, area	product, μmol	product, %
0	253.41	1.00	0.00	0.00	0.00
30	253.41	25.64	1.48	17.03	5.08
60	253.41	26.35	2.12	23.70	7.07
120	253.41	27.37	3.37	36.29	10.83
210	253.41	31.00	5.97	56.83	16.96
300	253.41	27.21	6.92	75.02	22.38
420	253.41	27.47	11.29	121.21	36.17
600	253.41	28.78	11.18	114.55	34.18
1276	253.41	30.38	18.22	176.93	52.79
1620	253.41	31.46	24.71	231.72	69.14
3640	253.41	32.23	25.41	232.52	69.37

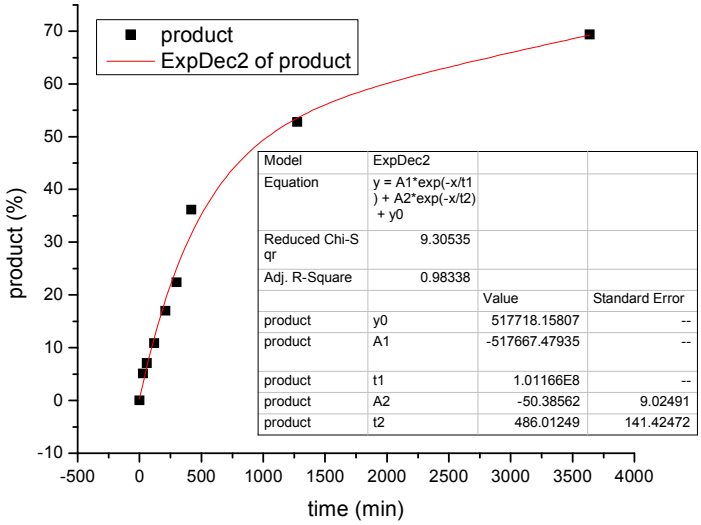

Half Life: 1006.1

Table 6. entry 5. catalyst **VI**{1}: **run 2**

time, min	standard, μmol	standard, area	product, area	product, μmol	product, %
0	253.41	31.27	0.00	0.00	0.00
30	253.41	26.47	1.48	16.47	4.91
60	253.41	30.29	2.75	26.82	8.00
120	253.41	26.39	4.00	44.70	13.34
210	253.41	29.20	7.10	71.67	21.38
300	253.41	27.25	8.66	93.70	27.96
420	253.41	26.73	8.55	94.35	28.15
600	253.41	27.92	14.21	150.11	44.79
1276	253.41	29.31	21.57	217.05	64.76
1620	253.41	29.05	19.09	193.83	57.83
3640	253.41	30.97	26.59	253.17	75.54
4565	253.41	30.53	26.80	258.94	77.26

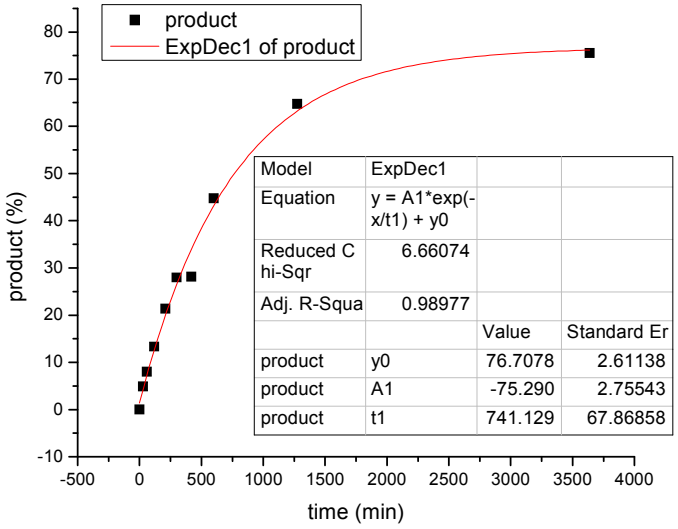

Half Life: 768.1
Average: 887.1

Table 6. entry 6. catalyst **VI**{2}: **run 1**

time, min	standard, µmol	standard, area	product, area	product, µmol	product, %
0	256.52	1.00	0.00	0.00	0.00
3	256.31	30.26	0.05	0.50	0.15
4	256.31	30.28	0.08	0.74	0.22
5	256.31	30.44	0.11	1.04	0.31
6	256.31	30.14	0.14	1.41	0.42
7	256.31	30.31	0.18	1.80	0.53
8	256.31	30.20	0.24	2.39	0.70
10	256.31	30.35	0.33	3.21	0.95
15	256.31	30.72	0.65	6.28	1.85
30	256.31	30.62	1.42	13.79	4.06
60	256.31	30.43	2.31	22.60	6.66
120	256.31	31.17	4.45	42.40	12.49
180	256.31	31.18	5.69	54.23	15.97
240	256.31	30.90	6.99	67.23	19.80
300	256.31	31.92	9.17	85.36	25.14
360	256.31	31.41	10.30	97.47	28.71
420	256.31	31.27	11.52	109.51	32.25
480	256.52	28.27	10.39	112.92	33.35
610	256.52	28.55	11.89	127.91	37.78
795	256.52	28.46	13.83	149.32	44.11
990	256.52	30.28	15.99	162.28	47.93
1210	256.52	30.89	18.60	184.99	54.64
2160	256.52	29.81	22.54	232.30	68.62
2790	256.52	30.60	24.66	247.60	73.14

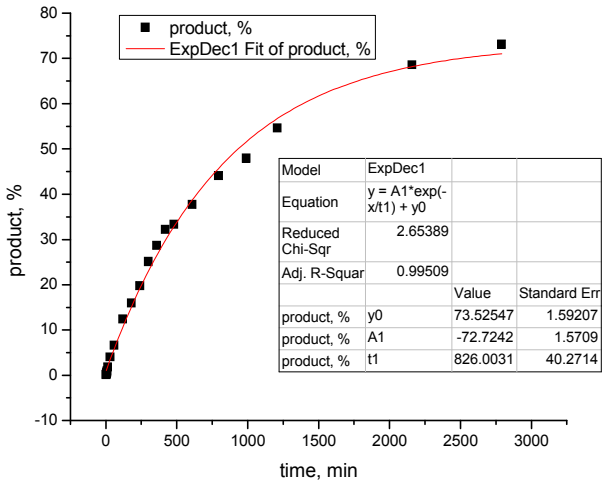

Half Life: 932.2

Table 6. entry 6. catalyst **VI**{2}: **run 2**

time, min	µmol standard	area standard	area product	µmol product	% product
0	256.31	29.94	0.00	0.00	0.00
3	256.31	30.15	0.06	0.60	0.18
5	256.31	30.09	0.13	1.24	0.36
6	256.31	29.90	0.16	1.61	0.47
8	256.31	29.91	0.25	2.49	0.73
9	256.31	30.22	0.30	2.96	0.87
15	256.31	30.46	0.65	6.39	1.88
30	256.31	30.31	1.55	15.20	4.48
60	256.31	30.65	2.80	27.12	7.99
120	256.31	30.61	5.12	49.76	14.65
180	256.31	32.66	7.95	72.32	21.30
240	256.31	30.84	9.51	91.65	26.99
300	256.31	32.80	11.80	106.96	31.50
480	256.52	27.94	11.11	122.17	36.09
610	256.52	28.03	12.61	138.22	40.83
795	256.52	30.03	14.93	152.78	45.13
990	256.52	30.28	15.99	162.28	47.93
1210	256.52	29.93	17.53	179.96	53.16
2160	256.52	29.63	21.04	218.27	64.47
2790	256.52	30.46	23.59	237.96	70.29

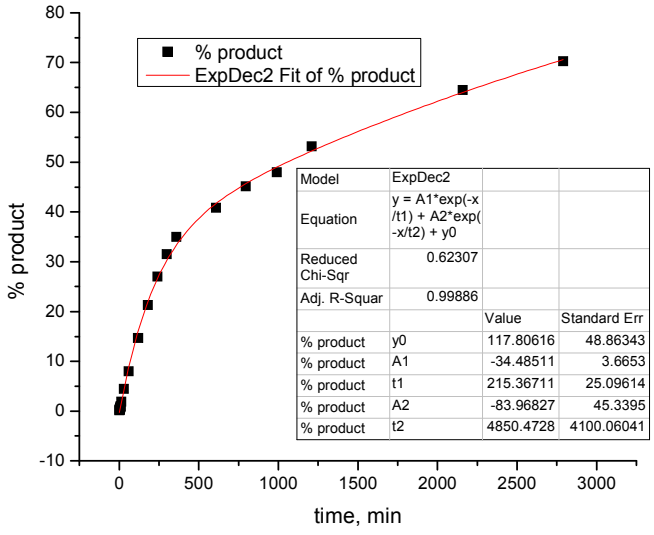

Half Life: 1065.36

Average: 998.8

Table 6. entry 7. catalyst **VI**{3}: **run 1**

time, min	standard, μmol	standard, area	product, area	product, μmol	product, %
0	248.76	30.00	0.00	0.00	0.00
720	248.76	30.53	12.64	0.12	36.16
1020	248.76	33.05	17.40	0.16	45.99
1440	248.76	30.67	20.63	0.20	58.78

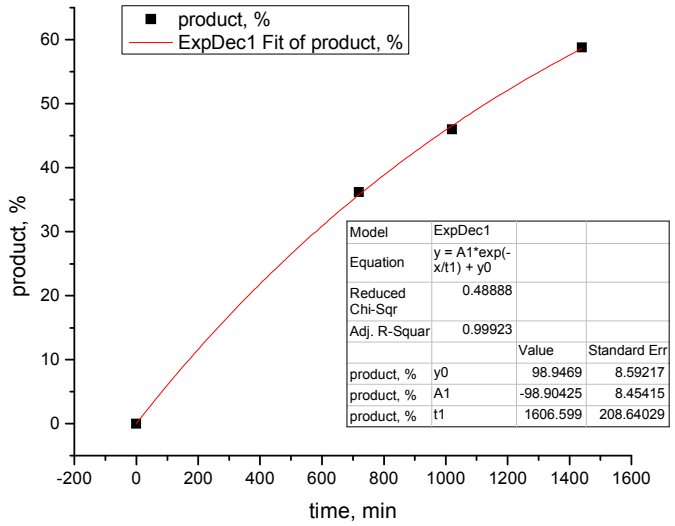

Half Life: 1130.11

Table 6. entry 7. catalyst **VI**{3}: **run 2**

time, min	standard, μmol	standard, area	product, area	product, μmol	product, %
0	248.76	30.00	0.00	0.00	0.00
720	248.76	32.27	14.05	0.13	38.03
1020	248.76	32.11	18.67	0.17	50.80
1440	248.76	31.09	21.04	0.20	59.11

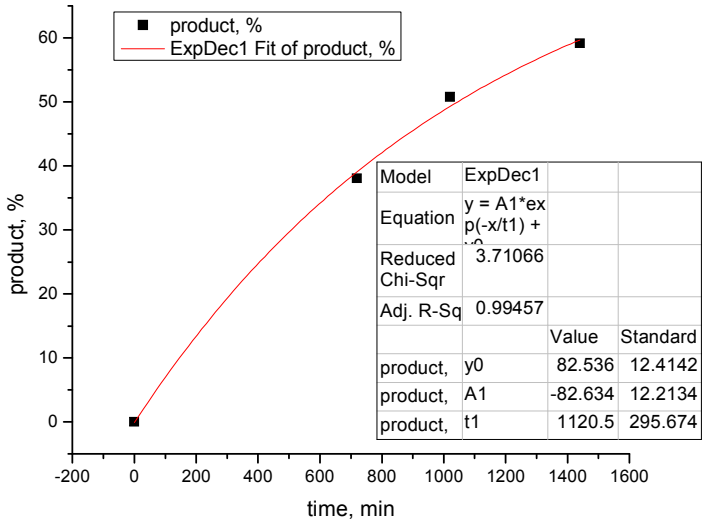

Half Life: 1044.43

Average: 1087

Tabular Summary of Kinetic Data

table	entry	catalyst	**run 1**	**run 2**	log(r1)	log(r2)	Avg. log(t1/2)	deviation in log units
3	1	**I**{*1*}	696.76	1174.28	2.84	3.07	2.96	0.160
3	2	**I**{*2*}	771.90	739.64	2.89	2.87	2.88	0.013
3	4	**I**{*4*}	321.30	328.70	2.51	2.52	2.51	0.007
3	6	**I**{*6*}	10.30	15.80	1.01	1.20	1.11	0.131
4	1	**II**{*1,1*}	199.60	161.90	2.30	2.21	2.25	0.064
4	2	**II**{*1,2*}	190.00	167.20	2.28	2.22	2.25	0.039
4	3	**II**{*1,4*}	269.80	325.60	2.43	2.51	2.47	0.058
4	4	**II**{*1,5*}	325.60	366.30	2.51	2.56	2.54	0.036
4	5	**II**{*1,3*}	216.90	272.80	2.34	2.44	2.39	0.070
4	6	**III**{*1,3*}	70.80	73.80	1.85	1.87	1.86	0.013
4	7	**II**{*2,1*}	9.50	10.70	0.98	1.03	1.00	0.037
4	8	**II**{*2,2*}	23.00	13.60	1.36	1.13	1.25	0.161
4	9	**II**{*2,3*}	12.10	12.10	1.08	1.08	1.08	0.000
4	10	**II**{*3,1*}	10.20	13.10	1.01	1.12	1.06	0.077
4	11	**III**{*3,1*}	10.20	19.40	1.01	1.29	1.15	0.197
4	12	**II**{*3,2*}	6.70	6.50	0.83	0.81	0.82	0.009
4	13	**III**{*3,2*}	10.60	8.40	1.03	0.92	0.97	0.071
4	14	**III**{*3,3*}	14.10	12.90	1.15	1.11	1.13	0.027
4	15	**II**{*3,5*}	20.00	5.40	1.30	0.73	1.02	0.402
4	16	**II**{3,6}	5.00	4.18	0.70	0.62	0.66	0.055
4	17	**III**{*3,6*}	6.70	4.20	0.83	0.62	0.72	0.143
4	18	**II**{*4,1*}	18.40	16.60	1.26	1.22	1.24	0.032
4	19	**II**{*4,2*}	15.40	9.20	1.19	0.96	1.08	0.158
4	20	**II**{*4,3*}	18.20	27.30	1.26	1.44	1.35	0.125
4	21	**II**{*5,1*}	13.56	20.72	1.13	1.32	1.22	0.130
4	22	**III**{*5,1*}	9.20	13.20	0.96	1.12	1.04	0.111
4	23	**II**{*5,2*}	4.80	9.10	0.68	0.96	0.82	0.196
4	24	**III**{*5,2*}	11.90	10.50	1.08	1.02	1.05	0.038
4	25	**II**{*5,3*}	12.90	12.40	1.11	1.09	1.10	0.012
4	26	**II**{*5,4*}	22.60	19.70	1.35	1.29	1.32	0.042
4	27	**II**{*5,5*}	32.40	31.28	1.51	1.50	1.50	0.011
5	1	**IV**{*2,2,1*}	111.70	75.30	2.05	1.88	1.96	0.121
5	2	**IV**{*2,2,2*}	40.64	62.97	1.61	1.80	1.70	0.134
5	3	**IV**{*3,2,1*}	18.69	20.26	1.27	1.31	1.29	0.025
5	4	**IV**{3,*2,5*}	30.87	21.32	1.49	1.33	1.41	0.114
5	5	**IV**{*5,2,5*}	17.34	15.21	1.24	1.18	1.21	0.040
5	6	**V**{*1,2,1*}	30.20	34.86	1.48	1.54	1.51	0.044

Tabular Summary of Kinetic Data (cont.)

5	7	**V**{*1,2,8*}	40.03	59.51	1.60	1.77	1.69	0.122
5	8	**V**{*1,2,8*}b	49.69	58.05	1.70	1.76	1.73	0.048
5	9	**V**{*1,2,7*}b	8.97	10.60	0.95	1.03	0.99	0.051
5	10	**V**{*1,2,6*}	23.35	26.11	1.37	1.42	1.39	0.034
5	11	V{*2,2,1*}	20.31	21.05	1.31	1.32	1.32	0.011
5	12	**V**{*2,2,3*}	23.11	22.98	1.36	1.36	1.36	0.002
5	13	**V**{*2,2,5*}	873.94	925.55	2.94	2.97	2.95	0.018
5	14	**V**{*2,2,8*}	22.11	17.68	1.34	1.25	1.30	0.069
5	15	**V**{*2,2,7*}	14.41	15.77	1.16	1.20	1.18	0.028
5	16	**V**{*2,2,6*}	29.51	26.60	1.47	1.42	1.45	0.032
5	17	**V**{*2,3,1*}	19.64	26.38	1.29	1.42	1.36	0.091
5	18	**V**{*2,3,2*}	78.80	72.85	1.90	1.86	1.88	0.024
5	19	**V**{*2,3,3*}	35.12	26.32	1.55	1.42	1.48	0.089
5	20	**V**{*2,3,5*}	255.43	216.64	2.41	2.34	2.37	0.051
5	21	**V**{*2,3,8*}	27.04	26.05	1.43	1.42	1.42	0.011
5	22	**V**{*2,3,7*}	28.78	28.92	1.46	1.46	1.46	0.001
5	23	**V**{*2,3,6*}	21.38	20.74	1.33	1.32	1.32	0.009
5	24	**V**{*2,7,1*}	16.76	17.41	1.22	1.24	1.23	0.012
5	25	**V**{*3,2,1*}	135.40	128.77	2.13	2.11	2.12	0.015
5	26	**V**{*3,2,5*}	130.13	114.10	2.11	2.06	2.09	0.040
5	27	**V**{*3,2,7*}	28.94	28.33	1.46	1.45	1.46	0.007
5	28	**V**{*3,3,1*}	43.49	36.53	1.64	1.56	1.60	0.054
5	29	**V**{*3,3,3*}	22.90	17.76	1.36	1.25	1.30	0.078
5	30	**V**{*3,3,5*}	58.16	66.68	1.76	1.82	1.79	0.042
5	31	**V**{*3,3,8*}	47.64	37.79	1.68	1.58	1.63	0.071
5	32	**V**{*3,2,6*}	93.28	78.69	1.97	1.90	1.93	0.052
5	33	**V**{*3,7,5*}	55.63	66.11	1.75	1.82	1.78	0.053
5	34	**V**{*3,7,8*}	224.43	274.31	2.35	2.44	2.39	0.062
5	35	**V**{*4,2,5*}	84.30	103.94	1.93	2.02	1.97	0.064
5	36	**V**{*5,2,1*}	9.88	11.40	0.99	1.06	1.03	0.044
5	37	**V**{*5,2,2*}	12.37	12.09	1.09	1.08	1.09	0.007
5	38	**V**{*5,2,3*}	10.52	10.02	1.02	1.00	1.01	0.015
5	39	**V**{*5,2,5*}	9.58	9.36	0.98	0.97	0.98	0.007
5	40	**V**{*5,2,8*}	18.77	16.25	1.27	1.21	1.24	0.044
5	41	**V**{*5,2,9*}	15.82	16.15	1.20	1.21	1.20	0.006
5	42	**V**{*5,2,10*}	15.03	13.82	1.18	1.14	1.16	0.026
5	43	**V**{*5,3,1*}	10.65	8.28	1.03	0.92	0.97	0.077
5	44	**V**{*5,3,2*}	17.24	20.08	1.24	1.30	1.27	0.047
5	45	**V**{*5,3,3*}	10.92	15.32	1.04	1.19	1.11	0.104

Tabular Summary of Kinetic Data (cont.)

5	46	**V**{*5,3,5*}	5.20	4.55	0.72	0.66	0.69	0.041
5	47	**V**{*5,3,8*}	9.43	10.27	0.97	1.01	0.99	0.026
5	48	**V**{*5,3,7*}	8.88	8.11	0.95	0.91	0.93	0.028
5	49	**V**{*5,6,1*}	8.02	7.69	0.90	0.89	0.90	0.013
5	50	**V**{*5,6,5*}	6.80	7.24	0.83	0.86	0.85	0.019
5	51	**V**{*5,6,8*}	7.76	5.98	0.89	0.78	0.83	0.080
5	52	**V**{*5,7,1*}	14.95	24.79	1.17	1.39	1.28	0.155
5	53	**V**{*5,7,2*}	18.65	19.75	1.27	1.30	1.28	0.018
5	54	**V**{*5,7,3*}	12.67	11.27	1.10	1.05	1.08	0.036
5	55	**V**{*5,7,5*}	15.52	21.63	1.19	1.34	1.26	0.102
5	56	**V**{*5,7,7*}	14.05	15.05	1.15	1.18	1.16	0.021
5	57	**V**{*7,2,1*}	12.68	14.62	1.10	1.16	1.13	0.044
5	58	**V**{*7,2,5*}	30.34	23.97	1.48	1.38	1.43	0.072
5	59	**V**{*7,2,8*}	11.14	11.52	1.05	1.06	1.05	0.010
5	60	**V**{*7,2,9*}	12.69	10.91	1.10	1.04	1.07	0.046
5	61	**V**{*7,2,10*}	55.56	41.56	1.74	1.62	1.68	0.089
5	62	**V**{*6,2,1*}	12.13	12.22	1.08	1.09	1.09	0.002
5	63	**V**{*6,2,8*}	12.10	11.59	1.08	1.06	1.07	0.013
6	1	Me4N	12189.00	13298.00	4.09	4.12	4.10	0.027
6	2	Me3Ncetyl	2625.20	2769.80	3.42	3.44	3.43	0.016
6	3	Et4N	418.70	547.60	2.62	2.74	2.68	0.082
6	4	Bu3NBn	19.43	21.46	1.29	1.33	1.31	0.031
6	5	**VI**{*1*}	1006.10	768.10	3.00	2.89	2.94	0.083
6	6	**VI**{*2*}	932.20	1065.36	2.97	3.03	3.00	0.041
6	7	**VI**{*3*}	1044.43	1130.11	3.02	3.05	3.04	0.024
							AVE	0.059
							MAX	0.402
							MIN	0.000
							AVG%[a]	4.52%

[a] Avg% represents the average of the all the %errors for each catalyst where %error = Stdev./$(\log(t_{1/2}))_{avg.}$*100

7.4.4. Stir-Rate Experiments (Figure 9):

Catalyst **V**{3,2,8}; stir-rate 1296 rpm; **run 1**

time, min	µmol standard	area standard	area product	µmol product	product %
130	254.28	26.91	8.47	96.03	28.39
180	254.28	27.23	10.03	112.33	33.21
230	254.28	27.77	11.64	127.90	37.81
342	254.28	29.09	16.11	169.02	49.96

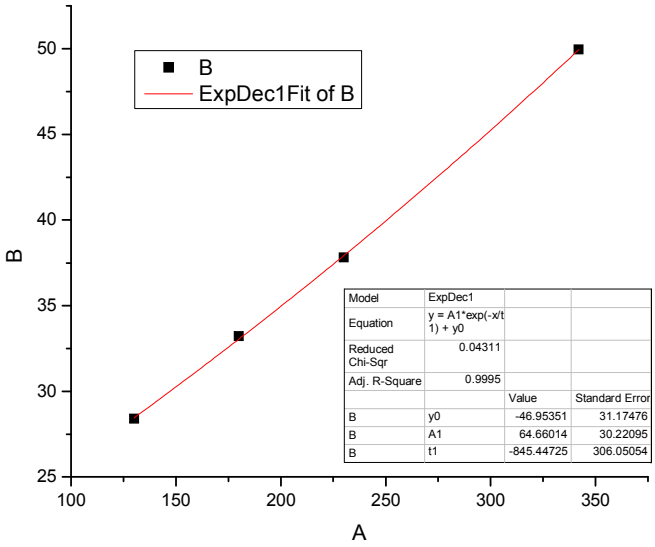

Half-life: 342.44

Catalyst **V**{3,2,8}; stir-rate 1296 rpm; **run 2**

time, min	µmol standard	area standard	area product	µmol product	product %
130	254.28	27.68	9.56	105.41	31.16
180	254.28	27.91	10.95	119.68	35.38
230	254.28	28.83	12.69	134.29	39.70
342	254.28	28.28	15.84	170.86	50.51

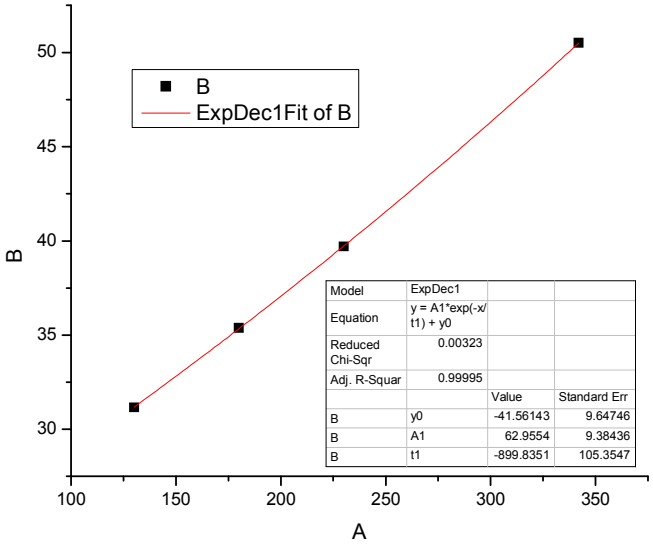

Half-life: 337.06
Avg.: 339.8

Catalyst **V**{3,2,8}; stir-rate 1598 rpm; **run 1**

time, min	µmol standard	area standard	area product	µmol product	product %
0	254.70	0.00	0.00	0.00	0.00
20	254.70	25.82	4.44	52.58	15.54
80	254.70	27.76	8.71	95.93	28.36
157	254.70	29.40	12.62	131.20	38.79
220	254.70	27.92	14.71	161.03	47.60
485	254.70	28.21	20.59	223.11	65.95

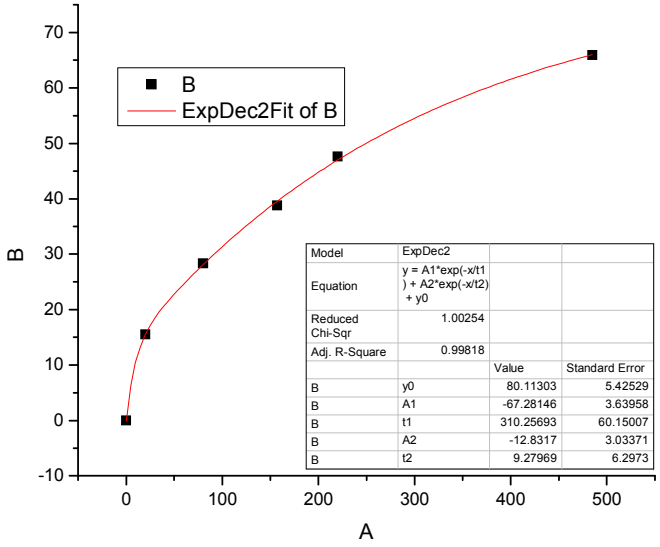

Half-life: 249.42

Catalyst **V**{3,2,8}; stir-rate 1598 rpm; **run 2**

time, min	µmol standard	area standard	area product	µmol product	product %
0	254.70	0.00	0.00	0.00	0.00
20	254.70	29.24	5.58	58.30	17.23
80	254.70	27.51	9.12	101.35	29.96
157	254.70	28.74	13.00	138.26	40.87
220	254.70	29.20	15.55	162.79	48.12
300	254.70	28.83	18.51	196.31	58.03
381	254.70	27.32	18.60	208.04	61.50
485	254.70	29.41	21.81	226.68	67.01

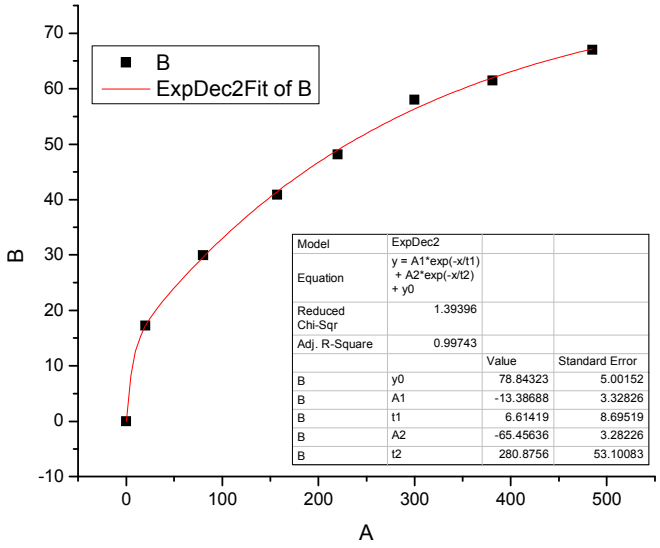

Half-life: 230.18
Average: 240.25

Catalyst **V**{3,2,8}; stir-rate 2000 rpm; **run 1**

time, min	µmol standard	area standard	area product	µmol product	product %
0	254.28	0.00	0.00	0.00	0.00
10	254.28	26.76	4.15	47.31	13.98
42	254.28	26.55	8.19	94.11	27.82
88	254.28	30.38	12.94	129.91	38.40
134	254.28	29.67	15.00	154.23	45.59
219	254.28	30.63	17.72	176.58	52.20
336	254.28	31.52	20.50	198.45	58.66

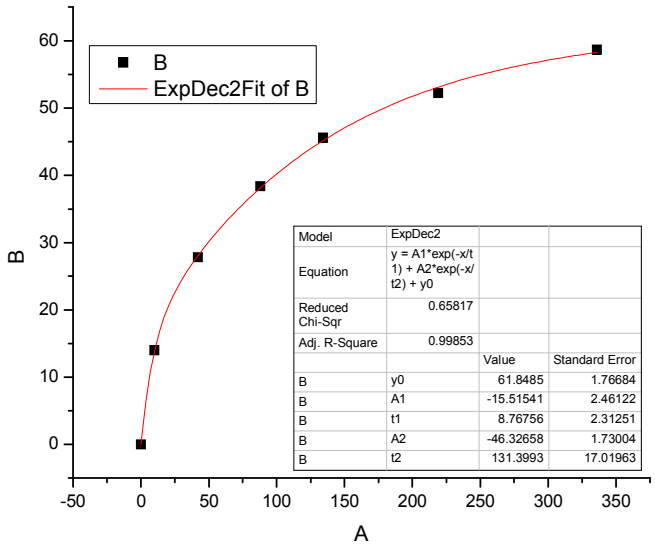

Half-life: 179.17

Catalyst **V**{3,2,8}; stir-rate 2000 rpm; **run 2**

time, min	µmol standard	area standard	area product	µmol product	product %
0	254.28	0.00	0.00	0.00	0.00
10	254.28	20.02	4.46	67.99	20.10
58	254.28	28.13	10.64	115.41	34.12
109	254.28	28.61	13.49	143.93	42.55
205	254.28	30.28	17.49	176.26	52.11
276	254.28	30.95	19.86	195.85	57.90
355	254.28	30.62	21.05	209.83	62.03

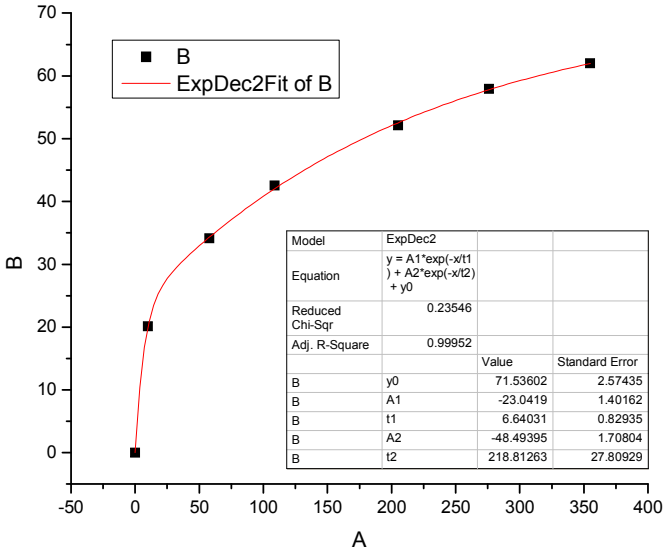

Half-life: 171.61
Average: 175.39

Catalyst **V**{3,2,8}; stir-rate 2500 rpm; **run 1**

time, min	µmol standard	area standard	area product	µmol product	product %
0	254.28	0.00	0.00	0.00	0.00
10	254.28	25.97	4.58	53.83	15.91
30	254.28	27.31	8.10	90.49	26.75
60	254.28	26.71	10.31	117.83	34.83
90	254.28	26.98	12.15	137.38	40.61
114	254.28	27.61	13.80	152.52	45.09
177	254.28	28.32	16.19	174.39	51.55
423	254.28	29.45	21.39	221.55	65.49

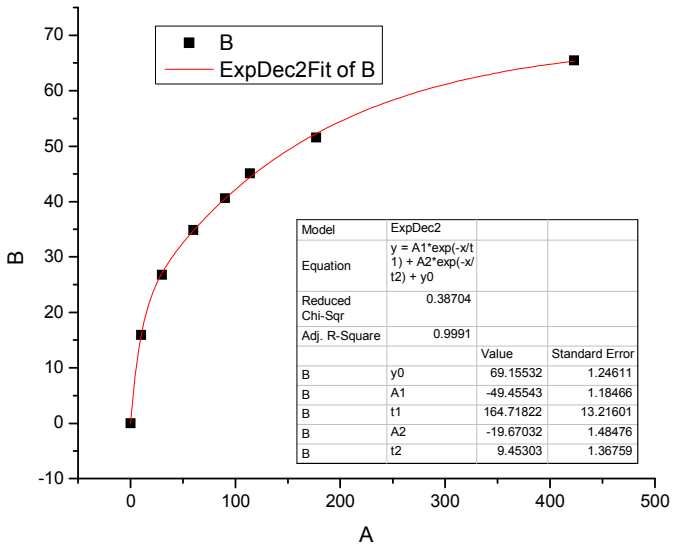

Half-life: 156.23

Catalyst **V**{3,2,8}; stir-rate 2500 rpm; **run 2**

time, min	µmol standard	area standard	area product	µmol product	product %
0	254.28	0.00	0.00	0.00	0.00
10	254.28	25.76	5.30	62.76	18.55
38	254.28	27.04	9.27	104.66	30.94
67	254.28	26.94	10.96	124.19	36.71
123	254.28	27.63	14.59	161.11	47.62
170	254.28	27.70	16.19	178.29	52.70
202	254.28	28.59	18.03	192.49	56.90

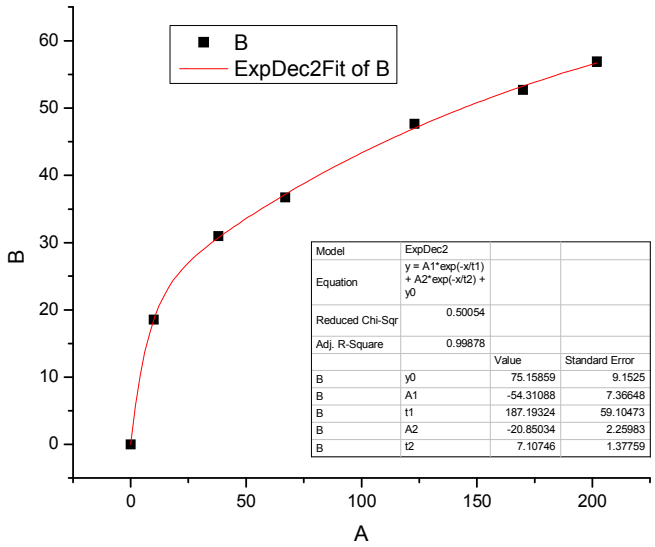

Half-life: 144.05
Average: 150.1

7.5. Supplemental Information for Chapter 3

7.5.1. Structures of Ring Flip Conformations

Structures of Ring Flip Conformers. An annealing algorithm, as implemented in Spartan 08' v.1.2.0 using the MMFF force field, primarily revealed three structurally unique conformers. To obtain relatively accurate populations, the geometry of each conformer was optimized at B3LYP/6-31G(d) and single point calculations (w/ SM8 solvation model) at M06-2X/6-31G(d) were determined.

Table 24.

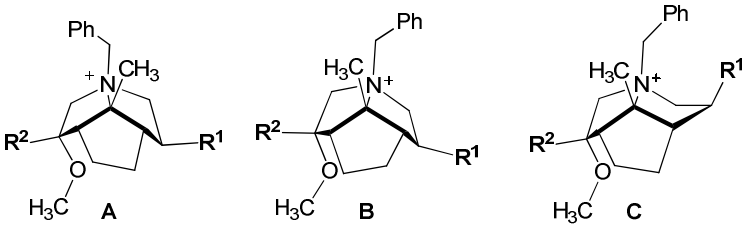

R^2 / R^1	A	B	C
H / H	3.4[a] (3.5[b])	2.6 (2.6)	0.0 (0.0)
H / Me	0.7 (1.0)	0.0 (0.1)	0.1 (0.0)
i-Pr / Me	1.3 (1.1)	0.0 (0.0)	0.9 (0.6)
Me / Me	0.8 (1.2)	0.0 (0.0)	0.2 (0.1)
Ph / H	4.3 (4.3)	2.2 (1.8)	0.0 (0.0)
Ph / Me	1.7 (2.3)	0.0 (0.0)	0.7 (0.8)

[a] Relative energy (kcal/mol) determined geometry optimization at B3LYP/6-31G(d). [b] Relative energy determined of single point M06-2X/6-31G(d) with SM8 solvation model (toluene) on B3LYP geometries.

Coordinates of B3LYP/6-31G(d) structures from Table 24.

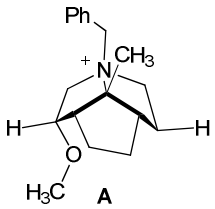

A

1	H	0.5198445	-1.1056888	-1.3509511
2	C	-0.0922583	-1.0082444	-0.4550490
3	N	-0.0157838	0.4589136	-0.0240763
4	C	-1.4168565	1.0991912	-0.4268803
5	C	-2.1797497	-0.0055093	-1.1923938
6	H	0.3437859	-1.6336214	0.3241349
7	H	-2.0365829	0.1039579	-2.2735631
8	C	0.0563812	0.6277901	1.4913207
9	C	-2.1930640	1.2845401	0.9165661
10	H	-2.2133860	2.3507506	1.1668087
11	C	-3.6282226	0.7456975	0.6616719
12	H	-3.8565613	-0.0539597	1.3704370
13	H	-4.3793052	1.5275162	0.8028185
14	C	-3.6526426	0.2007102	-0.7913126
15	H	-4.2275007	-0.7242730	-0.8757283
16	H	-4.1094659	0.9281223	-1.4703696
17	C	-1.3018597	2.4022391	-1.2114489
18	H	-0.8000695	3.1945063	-0.6475354
19	H	-2.3195911	2.7540211	-1.4096019
20	H	-0.8075480	2.2841241	-2.1802766
21	C	1.2048289	1.1224425	-0.6899363
22	H	1.1790829	2.1677920	-0.3812190
23	H	1.0183902	1.0759419	-1.7640275
24	C	2.5366877	0.4936853	-0.3551663
25	C	5.0428903	-0.6376078	0.2187232
26	C	3.1166132	-0.4406959	-1.2267007
27	C	3.2493414	0.8791752	0.7916913
28	C	4.4900542	0.3124526	1.0802872
29	C	4.3581432	-1.0070723	-0.9399430
30	H	2.6105514	-0.7102229	-2.1508980
31	H	2.8457365	1.6409479	1.4542971
32	H	5.0308034	0.6237542	1.9688948
33	H	4.7950535	-1.7251794	-1.6273030
34	H	6.0121381	-1.0740846	0.4401849
35	O	-2.2417650	-1.9173191	0.3263249
36	C	-2.0633721	-3.3239963	0.4746302
37	H	-2.3891679	-3.8573093	-0.4286349
38	H	-2.6842513	-3.6288367	1.3185625
39	C	-1.5549644	-1.3554875	-0.7721557
40	H	-1.0176365	-3.5881612	0.6873306
41	H	0.7495334	-0.1072357	1.9017597
42	H	-1.5816612	-2.0636112	-1.6123288
43	H	0.4651909	1.6261336	1.6645167
44	C	-1.3766292	0.5376448	1.9906408
45	H	-1.4689048	0.9973841	2.9788143
46	H	-1.7004755	-0.5019087	2.0681529

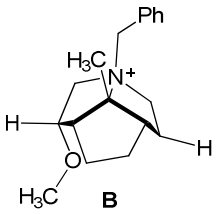

B

1	H	0.2093952	-0.7858366	-1.8801800
2	C	-0.1137017	-0.9618982	-0.8508370
3	N	-0.0821403	0.3860417	-0.1472861
4	C	-1.4825171	1.0460583	-0.4921321
5	C	-2.3795020	-0.1331075	-0.9972988
6	H	0.5924910	-1.6425216	-0.3751505
7	H	-2.5475559	-0.0054101	-2.0713487
8	C	-0.0560873	0.2670642	1.3891273
9	C	-2.1021495	1.4689658	0.8569833
10	H	-1.8617937	2.5108939	1.0988036
11	C	-3.6112610	1.2559445	0.6428609
12	H	-4.0337241	2.1137016	0.1078151
13	C	-3.7167260	-0.0308978	-0.2151844
14	H	-3.8370115	-0.9134266	0.4163686
15	C	-1.3970536	2.1763867	-1.5126602
16	H	-0.8143861	3.0317102	-1.1609900
17	H	-2.4162233	2.5338532	-1.6928925
18	H	-1.0028048	1.8473154	-2.4799400
19	C	1.1378407	1.1981480	-0.6193705
20	H	1.0260163	2.1854731	-0.1680372
21	H	1.0303272	1.3004985	-1.6998953
22	C	2.4799495	0.6013891	-0.2685112
23	C	5.0111290	-0.4476025	0.3509210
24	C	3.0918696	-0.3366924	-1.1150717
25	C	3.1729184	1.0313278	0.8732437
26	C	4.4273531	0.5073033	1.1847495
27	C	4.3445757	-0.8630616	-0.8037503
28	H	2.6026299	-0.6409510	-2.0370631
29	H	2.7451202	1.8005852	1.5117322
30	H	4.9521170	0.8549326	2.0693691
31	H	4.8069261	-1.5845444	-1.4707114
32	H	5.9901625	-0.8525323	0.5887068
33	O	-1.8810550	-2.1097530	0.3780394
34	C	-1.5833281	-3.5039681	0.3769875
35	H	-2.1251987	-4.0199935	-0.4267460

36	H	-1.9117638	-3.8922021	1.3424521
37	C	-1.5655802	-1.4435570	-0.8273356
38	H	-0.5070022	-3.6958786	0.2624823
39	H	0.3591174	-0.7032359	1.6583424
40	H	-4.1535023	1.1757919	1.5900676
41	H	-4.5753771	0.0044679	-0.8901937
42	H	0.6258566	1.0391127	1.7435177
43	C	-1.4742236	0.5180620	1.8924592
44	H	-2.0252552	-0.4215909	1.9457896
45	H	-1.7403469	-2.1185313	-1.6763250
46	H	-1.4530393	0.9582422	2.8933017

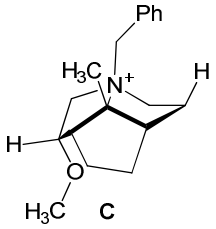

C

1	H	0.1338311	-1.0576225	-1.8025175
2	C	-0.1990450	-1.0853486	-0.7615377
3	N	-0.1152530	0.3244692	-0.2238675
4	C	-1.4834663	1.0171139	-0.6576055
5	C	-2.4261059	-0.1661889	-1.0268952
6	H	0.4705997	-1.7339594	-0.1949898
7	H	-2.6032905	-0.1716323	-2.1074931
8	C	-0.1472951	0.3456877	1.3065666
9	C	-2.0442792	1.6634022	0.6496143
10	H	-2.3451611	2.6950830	0.4432673
11	C	-3.2823530	0.8164953	1.0430758
12	H	-4.0722257	1.4383908	1.4742225
13	C	-3.7282709	0.1098307	-0.2504503
14	H	-4.2956829	-0.8035103	-0.0563771
15	C	-1.3314598	2.0111578	-1.8069816
16	H	-0.7401789	2.8912691	-1.5397746
17	H	-2.3363475	2.3652217	-2.0605168
18	H	-0.9160073	1.5617652	-2.7148929
19	C	1.1366528	1.0577891	-0.7418639
20	H	1.0527359	2.0805340	-0.3719333
21	H	1.0379973	1.0780221	-1.8272565
22	C	2.4604351	0.4583653	-0.3371839
23	C	4.9708171	-0.5751251	0.3796686
24	C	3.0545382	-0.5621667	-1.0957199
25	C	3.1563369	0.9715125	0.7682473
26	C	4.4013893	0.4560843	1.1279512
27	C	4.2980440	-1.0799824	-0.7354188
28	H	2.5585997	-0.9396674	-1.9869271
29	H	2.7346385	1.7963208	1.3382560
30	H	4.9297216	0.8683209	1.9822497
31	H	4.7488798	-1.8655953	-1.3342731
32	H	5.9431813	-0.9732534	0.6535856
33	O	-2.0559042	-1.9696510	0.5865606
34	C	-1.8323920	-3.3664762	0.7762730
35	H	-2.3765723	-3.9542905	0.0251953
36	H	-2.2114240	-3.6090815	1.7702190
37	C	-1.6813343	-1.4839630	-0.6883458
38	H	-0.7650312	-3.6248809	0.7275759
39	H	-0.7108412	-0.5328492	1.6174521
40	H	-1.8918862	-2.2503591	-1.4463753
41	H	0.8747942	0.2657460	1.6748689
42	H	-3.0129458	0.0661176	1.7931020
43	H	-4.3641156	0.7720661	-0.8495520
44	C	-0.8866536	1.6262990	1.6632978
45	H	-0.2390321	2.5046834	1.5624613
46	H	-1.2384054	1.6001599	2.6988295

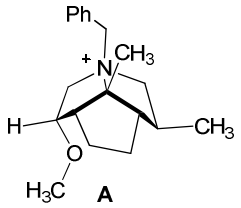

A

1	H	-0.6905810	1.7264974	-0.7987209
2	C	-0.0278715	1.2481814	-0.0786010
3	N	-0.0674870	-0.2551391	-0.3699974
4	C	1.3212009	-0.5958881	-1.0671433
5	C	2.0353184	0.7589253	-1.2709171
6	H	-0.4241415	1.4307501	0.9201390
7	H	1.8450215	1.1441110	-2.2790880
8	C	-0.0650857	-1.1003616	0.9002713
9	C	2.1547709	-1.3517685	0.0126525
10	H	2.1962062	-2.4156710	-0.2505774
11	C	3.5717755	-0.7131774	-0.0151872
12	H	3.8201559	-0.3214382	0.9747308
13	H	4.3387218	-1.4478888	-0.2743001
14	C	3.5269770	0.4393414	-1.0545645
15	H	4.0825548	1.3181728	-0.7200254
16	H	3.9672416	0.1212216	-2.0054465
17	C	1.1880920	-1.3975563	-2.3581337
18	H	0.7269302	-2.3781840	-2.2044837
19	H	2.2008529	-1.5809717	-2.7313956
20	H	0.6460125	-0.8655212	-3.1453895
21	C	-1.3071429	-0.5759583	-1.2255075
22	H	-1.2465072	-1.6410612	-1.4503599
23	H	-1.1755251	-0.0219702	-2.1566672
24	C	-2.6308625	-0.2309901	-0.5859317
25	C	-5.1222135	0.3949249	0.5514531
26	C	-3.2624864	0.9891516	-0.8722103
27	C	-3.2860964	-1.1488640	0.2498740

28	C	-4.5190847	-0.8356515	0.8197504
29	C	-4.4963034	1.3037299	-0.3032429
30	H	-2.8043698	1.6907147	-1.5662536
31	H	-2.8438675	-2.1231168	0.4415414
32	H	-5.0154132	-1.5581556	1.4606088
33	H	-4.9729545	2.2503997	-0.5388231
34	H	-6.0855175	0.6353893	0.9910383
35	O	2.1498981	1.7954849	0.9369293
36	C	1.9365406	2.9666305	1.7205181
37	H	2.1732892	3.8720541	1.1453168
38	H	2.6104459	2.8947178	2.5757419
39	C	1.4117059	1.7542167	-0.2663706
40	H	0.9024961	3.0369729	2.0875082
41	H	-0.7491428	-0.6606352	1.6271034
42	H	1.3812414	2.7633806	-0.7009461
43	H	-0.4496881	-2.0853029	0.6181299
44	C	1.3874424	-1.2092477	1.3474407
45	H	1.6874039	-0.2713042	1.8226601
46	C	1.6119335	-2.3617404	2.3301780
47	H	2.6660636	-2.4188390	2.6197710
48	H	1.3326608	-3.3256430	1.8869846
49	H	1.0267903	-2.2265084	3.2463650

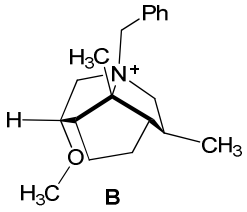

B

1	H	0.3795492	-1.5438976	-1.6036144
2	C	0.0317436	-1.3475491	-0.5860518
3	N	-0.0084202	0.1603680	-0.4245177
4	C	-1.3959606	0.5855237	-1.0597124
5	C	-2.2454313	-0.7292175	-1.1005962
6	H	0.7472647	-1.7739854	0.1171229
7	H	-2.3685585	-1.0287566	-2.1461927
8	C	-0.0757595	0.6121371	1.0453454
9	C	-2.0875192	1.4834502	-0.0162770
10	H	-1.8766012	2.5448059	-0.1998856
11	C	-3.5796816	1.1471183	-0.1891245
12	H	-3.9937256	1.7069780	-1.0354782
13	C	-3.6178230	-0.3782528	-0.4668354
14	H	-3.7495880	-0.9408195	0.4596761
15	C	-1.2745999	1.2267010	-2.4391122
16	H	-0.7118889	2.1637165	-2.4298345
17	H	-2.2880336	1.4614780	-2.7802696
18	H	-0.8390105	0.5540813	-3.1858592
19	C	1.2177828	0.8011849	-1.1018547
20	H	1.0536236	1.8785531	-1.0435447
21	H	1.1719785	0.5005863	-2.1491669
22	C	2.5529470	0.4327942	-0.4999693
23	C	5.0767367	-0.2023017	0.5569308
24	C	3.2336441	-0.7219102	-0.9178283
25	C	3.1730077	1.2813225	0.4296222
26	C	4.4234380	0.9636324	0.9589651
27	C	4.4830548	-1.0415968	-0.3883467
28	H	2.7981947	-1.3648765	-1.6790509
29	H	2.6918702	2.2109862	0.7241899
30	H	4.8919729	1.6335112	1.6735952
31	H	4.9990289	-1.9353913	-0.7257668
32	H	6.0533587	-0.4462632	0.9640085
33	O	-1.7575444	-2.0040790	0.9417739
34	C	-1.4037486	-3.2683464	1.4981121
35	H	-1.8815250	-4.0878313	0.9448150
36	H	-1.7664001	-3.2666244	2.5273342
37	C	-1.4076316	-1.8442980	-0.4175074
38	H	-0.3160153	-3.4269488	1.5031493
39	H	-1.5317076	-2.8004931	-0.9443373
40	H	0.2748672	-0.2034583	1.6762220
41	H	-4.1678771	1.4279870	0.6903183
42	H	-4.4453895	-0.6466024	-1.1283038
43	H	0.6200427	1.4450979	1.1433591
44	C	-1.5077033	1.0605031	1.3512682
45	H	-2.0635799	0.1946441	1.7191921
46	C	-1.5555512	2.1638369	2.4134137
47	H	-2.5899386	2.4632041	2.6106833
48	H	-1.0032386	3.0547797	2.0905456
49	H	-1.1280894	1.8238929	3.3630083

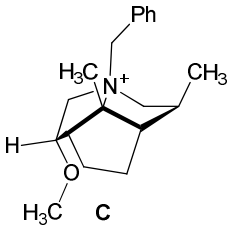

C

1	H	0.2436959	-1.5533281	-1.5343276
2	C	-0.1224335	-1.3518233	-0.5246822
3	N	-0.0951075	0.1516563	-0.3300833
4	C	-1.4798456	0.6695105	-0.9251961
5	C	-2.3580537	-0.6115628	-1.0661739
6	H	0.5503452	-1.8236539	0.1920236
7	H	-2.4723035	-0.8652484	-2.1253882
8	C	-0.1532560	0.5249032	1.1562301
9	C	-2.1247542	1.5338362	0.2072846
10	H	-2.4507427	2.4892965	-0.2168820
11	C	-3.3539517	0.7320422	0.7070126
12	H	-4.1840342	1.3933385	0.9719734
13	C	-3.7098087	-0.2386507	-0.4311493

14	H	-4.2568082	-1.1166756	-0.0792379
15	C	-1.3367478	1.4141391	-2.2506097
16	H	-0.7682022	2.3445640	-2.1650964
17	H	-2.3451865	1.6844739	-2.5807020
18	H	-0.8978475	0.7997121	-3.0435970
19	C	1.1567941	0.7512989	-1.0051627
20	H	1.0848691	1.8284802	-0.8650830
21	H	1.0476603	0.5360171	-2.0679358
22	C	2.4787932	0.2318421	-0.4923538
23	C	4.9711272	-0.6929129	0.4186729
24	C	3.0761721	-0.9003187	-1.0681596
25	C	3.1689628	0.9142793	0.5219388
26	C	4.4027706	0.4516246	0.9797347
27	C	4.3099990	-1.3628858	-0.6126828
28	H	2.5884821	-1.4156251	-1.8923899
29	H	2.7533670	1.8273482	0.9424371
30	H	4.9242987	0.9927072	1.7634516
31	H	4.7604342	-2.2377753	-1.0720031
32	H	5.9340286	-1.0511986	0.7702500
33	O	-1.9962387	-1.9706650	0.9385572
34	C	-1.7343661	-3.2744192	1.4553622
35	H	-2.2223814	-4.0428555	0.8412012
36	H	-2.1516310	-3.2980266	2.4633668
37	C	-1.5890481	-1.7806773	-0.4033584
38	H	-0.6576273	-3.4881782	1.5087722
39	H	-0.6229616	-0.3184057	1.6610420
40	H	-1.7466178	-2.7113494	-0.9655716
41	H	0.8659112	0.6358565	1.5250513
42	H	-3.0920213	0.1597700	1.6017808
43	H	-4.3337428	0.2578413	-1.1836184
44	C	-1.0374508	1.7723399	1.2802389
45	H	-1.4985239	1.7392977	2.2742939
46	C	-0.3173144	3.1236863	1.1613910
47	H	-1.0142053	3.9357341	1.3932860
48	H	0.0734005	3.3218443	0.1575632
49	H	0.5145433	3.1936163	1.8710307

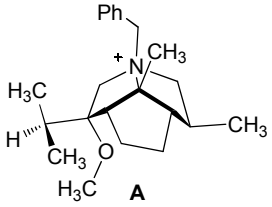

A

1	H	-0.6432235	1.5025948	0.1602147
2	C	-0.0190088	0.6744483	0.4808643
3	N	-0.3880143	-0.5306828	-0.3867244
4	C	0.9402842	-0.9484878	-1.1495549
5	C	1.9587195	0.1830536	-0.9046127
6	H	-0.2886139	0.4457113	1.5109321
7	H	1.9715767	0.8646491	-1.7596537
8	C	-0.7257057	-1.7529578	0.4552609
9	C	1.4774810	-2.1944052	-0.3769865
10	H	1.3170357	-3.0869477	-0.9942425
11	C	2.9901439	-1.9397077	-0.1482767
12	H	3.2088538	-1.9169128	0.9220712
13	H	3.6026667	-2.7315997	-0.5882996
14	C	3.3070667	-0.5644922	-0.7867577
15	H	4.0423028	-0.0005803	-0.2116053
16	H	3.7193865	-0.6972307	-1.7935577
17	C	0.7320570	-1.2471042	-2.6325197
18	H	0.0572010	-2.0916248	-2.8047448
19	H	1.7060468	-1.5325367	-3.0430780
20	H	0.3808699	-0.3838966	-3.2048514
21	C	-1.5588366	-0.1687138	-1.3184927
22	H	-1.7134675	-1.0413709	-1.9531184
23	H	-1.1964401	0.6501103	-1.9425797
24	C	-2.8416276	0.2183103	-0.6215726
25	C	-5.2507081	0.9502137	0.6265446
26	C	-3.1700457	1.5695927	-0.4351519
27	C	-3.7581774	-0.7602935	-0.2048513
28	C	-4.9506347	-0.3979545	0.4198614
29	C	-4.3627343	1.9339281	0.1895587
30	H	-2.5058996	2.3478053	-0.8047645
31	H	-3.5519538	-1.8121013	-0.3856679
32	H	-5.6503395	-1.1672519	0.7324424
33	H	-4.6028224	2.9845594	0.3223402
34	H	-6.1816048	1.2328720	1.1088357
35	O	2.1898802	0.4207643	1.4697239
36	C	2.0272984	1.0197436	2.7520227
37	H	2.5395557	1.9847514	2.8289167
38	H	2.4802481	0.3251824	3.4626214
39	C	1.4962698	0.9855699	0.3484528
40	H	0.9718331	1.1590298	3.0258313
41	H	-1.4046285	-1.4618269	1.2578604
42	H	-1.2452104	-2.4547945	-0.2050597
43	C	0.6133196	-2.3312212	0.8966057
44	H	1.0378015	-1.6911866	1.6769739
45	C	0.4960565	-3.7596277	1.4334794
46	H	1.4813867	-4.1441665	1.7150707
47	H	0.0744367	-4.4362497	0.6803348
48	H	-0.1413015	-3.8006431	2.3232816
49	C	1.7682272	2.5207511	0.2344083
50	H	1.3691538	2.9687047	1.1554036
51	C	1.0588870	3.2263184	-0.9357821
52	H	1.2549675	4.3013639	-0.8761301
53	H	-0.0301074	3.1070230	-0.9290907
54	H	1.4303703	2.8921611	-1.9111721
55	C	3.2751907	2.8260250	0.1729508
56	H	3.4421838	3.9034812	0.2702547

57	H	3.7045097	2.5171695	-0.7875293
58	H	3.8333408	2.3232968	0.9665508

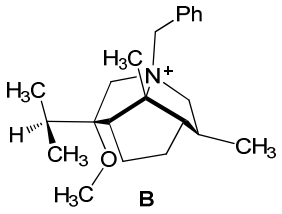

B

1	H	-0.2955992	1.6013457	-0.8962640
2	C	-0.0520100	0.9930126	-0.0251415
3	N	-0.3605642	-0.4415368	-0.4144015
4	C	0.9467804	-0.9324405	-1.1585672
5	C	2.0687598	0.0728062	-0.7322649
6	H	-0.7054995	1.2937989	0.7938824
7	H	2.3568787	0.6501336	-1.6139609
8	C	-0.5282126	-1.3940636	0.7840921
9	C	1.3281674	-2.2783710	-0.5111133
10	H	0.9033408	-3.1218944	-1.0701495
11	C	2.8663625	-2.2701386	-0.5465879
12	H	3.2202747	-2.5842734	-1.5351530
13	C	3.2642847	-0.8012695	-0.2566199
14	H	3.4327380	-0.6476349	0.8095664
15	C	0.8020470	-1.0106000	-2.6760008
16	H	0.0526427	-1.7370440	-3.0019313
17	H	1.7652233	-1.3390175	-3.0797739
18	H	0.5829000	-0.0406862	-3.1346599
19	C	-1.6330663	-0.4885030	-1.2810102
20	H	-1.7402279	-1.5311675	-1.5864391
21	H	-1.4168050	0.1088526	-2.1672303
22	C	-2.8897908	0.0086145	-0.6061184
23	C	-5.2624959	0.9339177	0.5812185
24	C	-3.2493212	1.3635226	-0.6844445
25	C	-3.7587844	-0.8810052	0.0437733
26	C	-4.9328773	-0.4210424	0.6393822
27	C	-4.4228995	1.8249592	-0.0900172
28	H	-2.6238671	2.0617501	-1.2355917
29	H	-3.5354500	-1.9448035	0.0655758
30	H	-5.5964687	-1.1232058	1.1350066
31	H	-4.6887945	2.8750498	-0.1653764
32	H	-6.1803221	1.2906288	1.0388945
33	O	1.6809147	0.5450141	1.6023824
34	C	1.3012252	1.3143002	2.7406084
35	H	2.0006768	2.1337230	2.9380061
36	H	1.3246646	0.6243730	3.5873282
37	C	1.4508276	1.0800656	0.2917957
38	H	0.2873153	1.7281531	2.6540325
39	H	-0.7691053	-0.8054440	1.6681083
40	H	3.2968198	-2.9703080	0.1768092
41	H	4.1880066	-0.5276175	-0.7730321
42	H	-1.3852906	-2.0273483	0.5544348
43	C	0.7381661	-2.2453458	0.9148460
44	H	1.4342974	-1.7219169	1.5732769
45	C	0.4481611	-3.6310416	1.5003883
46	H	1.3705468	-4.2160056	1.5744123
47	H	-0.2572684	-4.1943375	0.8769236
48	H	0.0258760	-3.5573773	2.5085295
49	C	2.0191270	2.5286384	0.1723966
50	H	1.5227917	3.1153537	0.9567315
51	C	1.7218420	3.2450649	-1.1572405
52	H	2.1911118	4.2337311	-1.1439028
53	H	0.6530246	3.4097551	-1.3312313
54	H	2.1331410	2.7113520	-2.0219310
55	C	3.5307925	2.5489033	0.4562939
56	H	3.8783047	3.5813513	0.5632670
57	H	4.0971925	2.0987428	-0.3673859
58	H	3.7840045	2.0095837	1.3727821

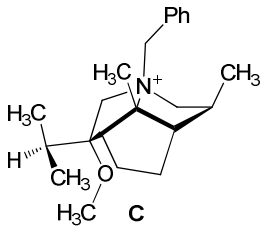

C

1	H	-0.0797628	1.5393565	-0.9356138
2	C	0.1477138	0.9866704	-0.0256314
3	N	-0.3100134	-0.4382642	-0.2656361
4	C	0.9286110	-1.1583006	-0.9510059
5	C	2.1416904	-0.2127706	-0.6914385
6	H	-0.4333409	1.4174983	0.7904206
7	H	2.4557145	0.2273479	-1.6414837
8	C	-0.5204721	-1.2021188	1.0431184
9	C	1.1677011	-2.4616836	-0.1206614
10	H	1.2527239	-3.3110099	-0.8067159
11	C	2.5094288	-2.2478654	0.6260990
12	H	3.0877533	-3.1747868	0.6849650
13	C	3.2475101	-1.1404749	-0.1423265
14	H	3.9680471	-0.6100441	0.4824837
15	C	0.7323153	-1.4224845	-2.4434836
16	H	-0.0707587	-2.1341351	-2.6537826
17	H	1.6607112	-1.8665500	-2.8177637
18	H	0.5618865	-0.5084077	-3.0217737
19	C	-1.5938272	-0.4381733	-1.1218896
20	H	-1.8211810	-1.4835238	-1.3199752
21	H	-1.3185728	0.0356696	-2.0639143
22	C	-2.7885889	0.2533276	-0.5096221
23	C	-5.0693980	1.5070123	0.5496343

24	C	-2.9965556	1.6297692	-0.6891587
25	C	-3.7584202	-0.4893857	0.1814921
26	C	-4.8887769	0.1327503	0.7119187
27	C	-4.1246176	2.2533561	-0.1577348
28	H	-2.2882475	2.2181850	-1.2670662
29	H	-3.6430086	-1.5657041	0.2858106
30	H	-5.6322599	-0.4579745	1.2384537
31	H	-4.2737012	3.3182373	-0.3097271
32	H	-5.9515476	1.9921619	0.9565290
33	O	1.9440046	0.5747507	1.5734088
34	C	1.7055189	1.5146101	2.6201062
35	H	2.4541357	2.3138306	2.6336190
36	H	1.7820228	0.9469329	3.5500104
37	C	1.6689264	0.9621497	0.2178424
38	H	0.7045349	1.9646117	2.5653984
39	H	0.1277051	-0.7208214	1.7727236
40	H	-1.5596260	-1.0856305	1.3507869
41	H	2.3208210	-1.9143841	1.6505357
42	H	3.7997224	-1.5657348	-0.9892708
43	C	-0.0552099	-2.6453432	0.8079834
44	H	0.2839353	-3.0331547	1.7755130
45	C	-1.1139455	-3.6258207	0.2790406
46	H	-0.7008054	-4.6397033	0.2591635
47	H	-1.4506214	-3.4028701	-0.7393349
48	H	-1.9951792	-3.6445397	0.9300331
49	C	2.3427010	2.3329928	-0.1187477
50	H	1.9323299	3.0562987	0.5985646
51	C	2.0370763	2.8975340	-1.5189877
52	H	2.5856058	3.8357740	-1.6511486
53	H	0.9788085	3.1343879	-1.6730490
54	H	2.3600903	2.2285123	-2.3253692
55	C	3.8654269	2.2748045	0.0986014
56	H	4.2867623	3.2843497	0.0611061
57	H	4.3580120	1.6871443	-0.6846865
58	H	4.1255661	1.8328912	1.0640781

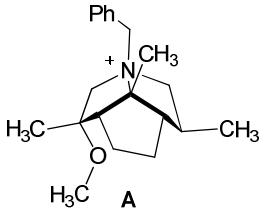

A

1	H	-0.6629321	1.7304631	-0.5540411
2	C	-0.0352914	1.1291275	0.1017335
3	N	-0.1404179	-0.3146996	-0.3926412
4	C	1.2407187	-0.6229844	-1.1195543
5	C	2.0319241	0.7028291	-1.1054352
6	H	-0.4468730	1.1939946	1.1090103
7	H	1.8990303	1.2322650	-2.0553979
8	C	-0.2072390	-1.3357241	0.7377155
9	C	2.0097571	-1.5913864	-0.1695693
10	H	1.9976297	-2.5983002	-0.6038784
11	C	3.4607866	-1.0425577	-0.0826915
12	H	3.7187442	-0.8362329	0.9589263
13	H	4.1865765	-1.7688173	-0.4585682
14	C	3.4977058	0.2666945	-0.9164758
15	H	4.0946973	1.0459458	-0.4373579
16	H	3.9415947	0.0818588	-1.9007984
17	C	1.0850149	-1.2011608	-2.5235903
18	H	0.5696961	-2.1665525	-2.5290999
19	H	2.0923364	-1.3764955	-2.9150155
20	H	0.5828851	-0.5223577	-3.2193263
21	C	-1.3800583	-0.4503683	-1.2977616
22	H	-1.3556586	-1.4690598	-1.6852725
23	H	-1.2176893	0.2372118	-2.1296496
24	C	-2.6998186	-0.1651877	-0.6201560
25	C	-5.1814043	0.3545437	0.5897457
26	C	-3.2862728	1.1068132	-0.7076039
27	C	-3.3950093	-1.1824982	0.0526033
28	C	-4.6232736	-0.9235604	0.6589049
29	C	-4.5153422	1.3671442	-0.1022902
30	H	-2.7958215	1.8955063	-1.2738527
31	H	-2.9877882	-2.1896799	0.0872598
32	H	-5.1498308	-1.7225439	1.1721649
33	H	-4.9579966	2.3553264	-0.1836554
34	H	-6.1410068	0.5552305	1.0566488
35	O	2.1386492	1.3198373	1.2189406
36	C	1.9115741	2.1679835	2.3419853
37	H	2.3218861	3.1714242	2.1865854
38	H	2.4331059	1.6999590	3.1791009
39	C	1.4322797	1.6026975	0.0113089
40	H	0.8452315	2.2533993	2.5964784
41	H	-0.8612846	-0.9593704	1.5255411
42	H	-0.6648051	-2.2337528	0.3122548
43	C	1.2278714	-1.6246961	1.1636432
44	H	1.5850532	-0.8054757	1.7926499
45	C	1.5115742	3.0915640	-0.3587316
46	H	2.5579869	3.4101889	-0.3956057
47	H	0.9878925	3.7263016	0.3625533
48	H	1.0668347	3.2706281	-1.3424659
49	C	1.3508000	-2.9389661	1.9398338
50	H	2.3922189	-3.1204500	2.2241835
51	H	1.0127212	-3.7940954	1.3418788
52	H	0.7593797	-2.9130077	2.8615445

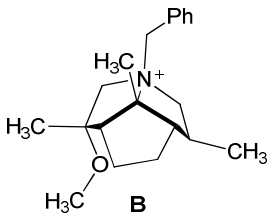

B

1	H	-0.3607072	1.6792425	-1.2934282
2	C	-0.0307064	1.2887369	-0.3272994
3	N	-0.0773439	-0.2238452	-0.4349243
4	C	1.3049537	-0.6117951	-1.1068912
5	C	2.2204490	0.6417676	-0.9171057
6	H	-0.7320972	1.6224304	0.4379670
7	H	2.3885388	1.0941754	-1.8988225
8	C	-0.0796592	-0.9428268	0.9265589
9	C	1.9208315	-1.7097478	-0.2184620
10	H	1.6607605	-2.7105836	-0.5857177
11	C	3.4323939	-1.4334504	-0.3021089
12	H	3.8444432	-1.8761910	-1.2158551
13	C	3.5599319	0.1123524	-0.3338596
14	H	3.7070782	0.5141362	0.6697805
15	C	1.1888400	-1.0087432	-2.5760996
16	H	0.5947127	-1.9126757	-2.7354707
17	H	2.1999312	-1.2211437	-2.9387662
18	H	0.7917497	-0.2052268	-3.2051573
19	C	-1.3147648	-0.6563113	-1.2429179
20	H	-1.2022149	-1.7302589	-1.3989670
21	H	-1.2306731	-0.1589835	-2.2099932
22	C	-2.6441106	-0.3530011	-0.5925668
23	C	-5.1468503	0.1669992	0.5729479
24	C	-3.2558075	0.9017495	-0.7425746
25	C	-3.3235920	-1.3522857	0.1202890
26	C	-4.5639442	-1.0942323	0.7032797
27	C	-4.4942192	1.1622103	-0.1577301
28	H	-2.7776237	1.6749033	-1.3385172
29	H	-2.8949286	-2.3484929	0.2019204
30	H	-5.0781625	-1.8808182	1.2471687
31	H	-4.9564878	2.1363608	-0.2861819
32	H	-6.1146352	0.3686160	1.0221634
33	O	1.7566552	1.4993892	1.3035887
34	C	1.3302693	2.4863707	2.2399319
35	H	1.8898389	3.4215215	2.1314913
36	H	1.5323625	2.0669134	3.2274832
37	C	1.4315457	1.6932881	-0.0722316
38	H	0.2551991	2.7017189	2.1621347
39	H	-0.4386357	-0.2504252	1.6870989
40	H	3.9778781	-1.8800964	0.5353674
41	H	4.4126261	0.4301521	-0.9393254
42	H	-0.7997046	-1.7576331	0.8430077
43	C	1.3234189	-1.4972922	1.1885263
44	H	1.9034773	-0.7300245	1.7050688
45	C	1.7097173	3.1288676	-0.5374393
46	H	2.7514435	3.3927526	-0.3285947
47	H	1.0674877	3.8588053	-0.0353972
48	H	1.5446345	3.2265636	-1.6148371
49	C	1.2953081	-2.7643457	2.0493492
50	H	2.3109686	-3.1367929	2.2174437
51	H	0.7196795	-3.5655098	1.5691823
52	H	0.8525504	-2.5707416	3.0326180

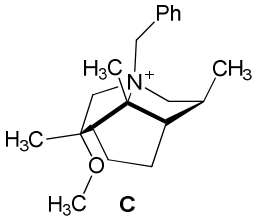

C

1	H	-0.2060110	1.5804765	-1.3290000
2	C	0.1411743	1.2603380	-0.3438143
3	N	0.0025068	-0.2496245	-0.2965731
4	C	1.3579168	-0.8053464	-0.9197838
5	C	2.3285006	0.4113691	-0.9218352
6	H	-0.5043338	1.7073595	0.4132933
7	H	2.4949975	0.7390339	-1.9528243
8	C	-0.0022076	-0.7792598	1.1414496
9	C	1.9111901	-1.8326026	0.1195328
10	H	2.1704515	-2.7608068	-0.4002821
11	C	3.1914254	-1.1882135	0.7150516
12	H	3.9666398	-1.9373365	0.9007899
13	C	3.6346939	-0.1214901	-0.2997603
14	H	4.2286486	0.6732659	0.1581401
15	C	1.1888715	-1.3959653	-2.3187633
16	H	0.5575287	-2.2885321	-2.3366027
17	H	2.1827575	-1.6991631	-2.6641158
18	H	0.8077867	-0.6731801	-3.0477170
19	C	-1.2684662	-0.6844349	-1.0554512
20	H	-1.2683400	-1.7725089	-1.0411795
21	H	-1.1238530	-0.3548026	-2.0843133
22	C	-2.5719754	-0.1539310	-0.5085547
23	C	-5.0520229	0.7698913	0.4333368
24	C	-3.0769039	1.0880252	-0.9241887
25	C	-3.3449931	-0.9386298	0.3613487
26	C	-4.5747279	-0.4790008	0.8331924
27	C	-4.3042458	1.5497871	-0.4512311
28	H	-2.5250547	1.6902276	-1.6415029
29	H	-2.9966454	-1.9270254	0.6522146
30	H	-5.1636022	-1.1014302	1.5001102
31	H	-4.6842904	2.5103351	-0.7861876
32	H	-6.0120245	1.1269278	0.7940847

33	O	2.0163537	1.5333734	1.1966597
34	C	1.7181847	2.6569518	2.0244734
35	H	2.3250919	3.5292316	1.7609603
36	H	1.9658620	2.3496471	3.0423181
37	C	1.6353489	1.5940841	-0.1804808
38	H	0.6552734	2.9350907	1.9891336
39	H	0.5235306	-0.0316659	1.7326937
40	H	-1.0346005	-0.8500916	1.4836549
41	H	2.9615424	-0.7095237	1.6703307
42	H	4.2462218	-0.5725506	-1.0902329
43	C	0.7839435	-2.0978281	1.1442884
44	H	1.2214439	-2.2078387	2.1433621
45	C	-0.0318698	-3.3704425	0.8666255
46	H	0.6040770	-4.2523845	0.9957922
47	H	-0.4349062	-3.4176078	-0.1511470
48	H	-0.8686907	-3.4641177	1.5676163
49	C	1.9837980	2.9457244	-0.8178536
50	H	3.0492283	3.1574423	-0.6822462
51	H	1.4140371	3.7703918	-0.3793124
52	H	1.7747934	2.9320342	-1.8920354

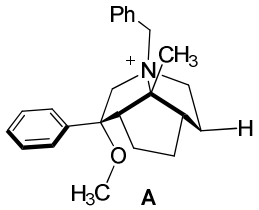

A

1	H	-0.3642392	1.0594903	-0.4555663
2	C	-0.1813268	0.2713646	0.2704891
3	N	-0.9750422	-0.9417811	-0.2092436
4	C	0.0939551	-1.9266605	-0.8504536
5	C	1.4520311	-1.1883273	-0.7731607
6	H	-0.5807332	0.5961642	1.2314140
7	H	1.6634000	-0.6995941	-1.7292592
8	C	-1.6063390	-1.7459444	0.9283295
9	C	0.1968529	-3.1324497	0.1316488
10	H	-0.3296766	-3.9903011	-0.3018607
11	C	1.7107413	-3.4299310	0.2829390
12	H	1.9888112	-3.4278306	1.3398258
13	H	1.9612391	-4.4177350	-0.1131584
14	C	2.4724488	-2.3140894	-0.4824935
15	H	3.3259973	-1.9516907	0.0918845
16	H	2.8578711	-2.6948290	-1.4343054
17	C	-0.2450860	-2.3773191	-2.2696225
18	H	-1.1846556	-2.9355025	-2.3245275
19	H	0.5474279	-3.0612202	-2.5914313
20	H	-0.2717486	-1.5564175	-2.9922822
21	C	-2.0665910	-0.4684511	-1.1869128
22	H	-2.5774077	-1.3712878	-1.5224093
23	H	-1.5342406	-0.0388169	-2.0363856
24	C	-3.0502261	0.5290060	-0.6199524
25	C	-4.9020901	2.3944477	0.3713009
26	C	-2.8710206	1.9031346	-0.8420009
27	C	-4.1914848	0.1021305	0.0768507
28	C	-5.1068346	1.0283347	0.5751265
29	C	-3.7874524	2.8303724	-0.3465937
30	H	-2.0247326	2.2533354	-1.4287490
31	H	-4.3839127	-0.9589627	0.2132926
32	H	-5.9868048	0.6823406	1.1089270
33	H	-3.6372947	3.8895324	-0.5331102
34	H	-5.6191280	3.1148497	0.7535892
35	O	1.6998890	-0.6497491	1.5531458
36	C	1.8607517	0.2209671	2.6721771
37	H	2.6978881	0.9103540	2.5285252
38	H	2.0650217	-0.4296011	3.5247771
39	C	1.3277860	-0.0637346	0.3000829
40	H	0.9518337	0.8033988	2.8809374
41	H	-2.0054891	-1.0587761	1.6751605
42	H	-2.4395663	-2.2942959	0.4825323
43	C	-0.5339215	-2.7034562	1.4185034
44	H	-0.9863081	-3.5513225	1.9411220
45	H	0.1517292	-2.2030941	2.1028574
46	C	2.1855626	1.1689779	-0.0194696
47	C	3.8348758	3.3999598	-0.5216324
48	C	1.7348156	2.4721501	0.2385532
49	C	3.4861701	1.0059961	-0.5195856
50	C	4.3013390	2.1085986	-0.7717612
51	C	2.5492727	3.5781632	-0.0125102
52	H	0.7439772	2.6463853	0.6507629
53	H	3.8727745	0.0125239	-0.7192454
54	H	5.3026654	1.9562939	-1.1639044
55	H	2.1769114	4.5770680	0.1952812
56	H	4.4695319	4.2587696	-0.7187513

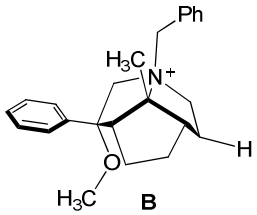

B

1	H	0.1252478	-0.9585853	-1.0528866
2	C	0.1222039	-0.4556126	-0.0837638
3	N	0.9359726	0.8122443	-0.2574655
4	C	-0.0826708	1.8446615	-0.8830538
5	C	-1.5005360	1.2603153	-0.5716566
6	H	0.6128176	-1.0991509	0.6459802
7	H	-1.9537616	0.9414188	-1.5133729
8	C	1.3979506	1.4384865	1.0758356
9	C	0.0320951	3.1316482	-0.0413584

10	H	0.7418724	3.8356235	-0.4905241
11	C	-1.4046121	3.6810911	-0.0291762
12	H	-1.5694651	4.3771091	0.7991394
13	H	-1.5992601	4.2385055	-0.9524582
14	C	-2.3103918	2.4274081	0.0606575
15	H	-2.5410316	2.1900811	1.1000233
16	H	-3.2596406	2.5843625	-0.4588202
17	C	0.1124088	2.0812441	-2.3791967
18	H	1.0824217	2.5226326	-2.6234076
19	H	-0.6544706	2.7944618	-2.6987768
20	H	-0.0308294	1.1754395	-2.9777237
21	C	2.1633380	0.5287916	-1.1425202
22	H	2.6354788	1.4992059	-1.3076057
23	H	1.7676441	0.1720491	-2.0936471
24	C	3.1545051	-0.4598526	-0.5739692
25	C	5.0401623	-2.2920326	0.4169347
26	C	3.0059573	-1.8365172	-0.8065542
27	C	4.2833191	-0.0147644	0.1306234
28	C	5.2166442	-0.9238973	0.6280763
29	C	3.9375970	-2.7466692	-0.3091942
30	H	2.1724267	-2.2019675	-1.4014986
31	H	4.4536324	1.0500846	0.2709884
32	H	6.0868406	-0.5622030	1.1673765
33	H	3.8111522	-3.8076966	-0.5026320
34	H	5.7696470	-3.0000967	0.7987055
35	O	-1.3522796	0.3450197	1.6687250
36	C	-1.4491215	-0.6966656	2.6409370
37	H	-2.4059048	-1.2225251	2.5732368
38	H	-1.3726809	-0.2011765	3.6108909
39	C	-1.3117205	-0.0374651	0.2880316
40	H	-0.6353271	-1.4295853	2.5506360
41	H	1.3363706	0.6788703	1.8529507
42	H	2.4441151	1.7066015	0.9404309
43	C	0.5340485	2.6697901	1.3390055
44	H	1.1193813	3.4477660	1.8372287
45	H	-0.3006355	2.4042862	1.9878795
46	C	-2.3514164	-1.1109597	-0.0362079
47	C	-4.3328261	-3.0434041	-0.5512769
48	C	-2.0066689	-2.4513147	-0.2535097
49	C	-3.7094106	-0.7574692	-0.0652284
50	C	-4.6907188	-1.7128473	-0.3222023
51	C	-2.9887626	-3.4101376	-0.5132016
52	H	-0.9693963	-2.7737039	-0.2168690
53	H	-4.0051934	0.2712642	0.1182488
54	H	-5.7355930	-1.4171810	-0.3445352
55	H	-2.6989696	-4.4431143	-0.6823464
56	H	-5.0969510	-3.7876717	-0.7544690

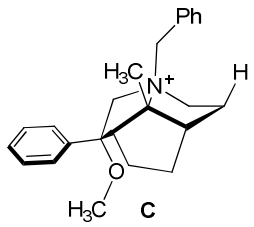

C

1	H	-0.0568727	1.0352842	-0.9471305
2	C	-0.0572682	0.4556547	-0.0224455
3	N	-0.9210149	-0.7562527	-0.2724311
4	C	0.0460223	-1.8198185	-0.9510334
5	C	1.4843082	-1.3213471	-0.6166842
6	H	-0.5065757	1.0571259	0.7682021
7	H	1.9753258	-1.0008057	-1.5390459
8	C	-1.3749088	-1.4295591	1.0236777
9	C	-0.1946627	-3.1460469	-0.1635761
10	H	-0.3457032	-3.9670165	-0.8708962
11	C	1.0906389	-3.3836894	0.6678066
12	H	1.3393650	-4.4474631	0.7250472
13	C	2.1923161	-2.5596292	-0.0202143
14	H	2.9931172	-2.2928888	0.6717945
15	C	-0.1658370	-1.9682953	-2.4565998
16	H	-1.1456969	-2.3797158	-2.7148954
17	H	0.5853751	-2.6782437	-2.8184678
18	H	-0.0108790	-1.0349567	-3.0080085
19	C	-2.1421885	-0.3975819	-1.1391375
20	H	-2.6583632	-1.3398344	-1.3293124
21	H	-1.7364814	-0.0350903	-2.0834872
22	C	-3.0903454	0.6161483	-0.5463884
23	C	-4.9094175	2.4916658	0.4849506
24	C	-2.8979048	1.9902034	-0.7590014
25	C	-4.2263621	0.1959874	0.1630487
26	C	-5.1269934	1.1269375	0.6804352
27	C	-3.7974530	2.9217234	-0.2419630
28	H	-2.0556075	2.3376595	-1.3526983
29	H	-4.4238143	-0.8659384	0.2926456
30	H	-6.0033591	0.7857026	1.2230600
31	H	-3.6384694	3.9810978	-0.4199884
32	H	-5.6134652	3.2171003	0.8815338
33	O	1.4572184	-0.4977373	1.6506641
34	C	1.6164538	0.4942604	2.6665386
35	H	2.5749427	1.0129494	2.5747911
36	H	1.5841951	-0.0487478	3.6130899
37	C	1.3709445	-0.0495108	0.2896304
38	H	0.8068161	1.2378012	2.6558141
39	H	-0.5906161	-1.2446934	1.7555301
40	H	-2.3012697	-0.9624564	1.3556121
41	H	0.9531245	-3.0276788	1.6937038
42	H	2.6408661	-3.1326875	-0.8405664
43	C	-1.4588275	-2.9098197	0.6802507

44	H	-2.3717984	-3.1449258	0.1211513
45	H	-1.4708037	-3.5207937	1.5874312
46	C	2.4411512	0.9996046	-0.0262812
47	C	4.4680773	2.8918975	-0.5240877
48	C	2.1409817	2.3646434	-0.1295841
49	C	3.7800828	0.6013970	-0.1606071
50	C	4.7834181	1.5364126	-0.4086651
51	C	3.1441779	3.3032061	-0.3809053
52	H	1.1220366	2.7221621	-0.0073899
53	H	4.0467502	-0.4468568	-0.0707305
54	H	5.8122347	1.2043438	-0.5131219
55	H	2.8867543	4.3553482	-0.4608027
56	H	5.2490897	3.6202416	-0.7205578

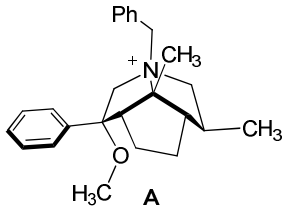

A

1	H	-0.2405960	1.3054757	-0.2959095
2	C	-0.1026377	0.3939335	0.2795629
3	N	-0.9728690	-0.6698657	-0.3891809
4	C	0.0322420	-1.6612055	-1.1129561
5	C	1.4373099	-1.0427879	-0.9460894
6	H	-0.4776782	0.5711585	1.2877448
7	H	1.7029421	-0.4699521	-1.8399084
8	C	-1.7194099	-1.5516410	0.6054632
9	C	0.0188115	-2.9661997	-0.2593704
10	H	-0.5396749	-3.7378826	-0.8032797
11	C	1.5056054	-3.3731506	-0.0832612
12	H	1.7523982	-3.4330705	0.9795028
13	H	1.7061843	-4.3557142	-0.5190738
14	C	2.3563688	-2.2738990	-0.7726460
15	H	3.2525919	-2.0400601	-0.1964660
16	H	2.6859504	-2.6086786	-1.7626558
17	C	-0.3110188	-1.9383292	-2.5751478
18	H	-1.2857275	-2.4201079	-2.7004707
19	H	0.4381726	-2.6403752	-2.9554024
20	H	-0.2652043	-1.0478690	-3.2077763
21	C	-1.9666141	0.0220047	-1.3400152
22	H	-2.5266773	-0.7797893	-1.8217888
23	H	-1.3543559	0.5146382	-2.0967366
24	C	-2.8964998	1.0175020	-0.6867757
25	C	-4.6439400	2.8937723	0.4610574
26	C	-2.6184865	2.3910996	-0.7571841
27	C	-4.0819125	0.6008567	-0.0609805
28	C	-4.9450983	1.5311896	0.5156681
29	C	-3.4838995	3.3234563	-0.1847274
30	H	-1.7337460	2.7402733	-1.2851998
31	H	-4.3468578	-0.4528158	-0.0403638
32	H	-5.8596479	1.1933571	0.9937356
33	H	-3.2575784	4.3831590	-0.2544313
34	H	-5.3210497	3.6182713	0.9035484
35	O	1.7119123	-0.7925380	1.4235051
36	C	1.9607064	-0.0749664	2.6308697
37	H	2.8704050	0.5293132	2.5630027
38	H	2.0870899	-0.8362597	3.4033400
39	C	1.3838191	-0.0399950	0.2479787
40	H	1.1211613	0.5768672	2.9117356
41	H	-2.1222695	-0.9314512	1.4071324
42	H	-2.5568945	-1.9921752	0.0555390
43	C	-0.7476192	-2.6409238	1.0425251
44	H	-0.0445886	-2.2219000	1.7671497
45	C	2.3208014	1.1620641	0.0653530
46	C	4.1076664	3.3252621	-0.2136554
47	C	1.9621848	2.4525843	0.4827316
48	C	3.6019978	0.9740479	-0.4746682
49	C	4.4848671	2.0436968	-0.6174206
50	C	2.8445461	3.5255548	0.3415116
51	H	0.9915723	2.6416344	0.9344833
52	H	3.9195706	-0.0131798	-0.7924838
53	H	5.4681888	1.8738061	-1.0461906
54	H	2.5416808	4.5160114	0.6686531
55	H	4.7938491	4.1591079	-0.3278605
56	C	-1.4609443	-3.8413727	1.6710750
57	H	-0.7372328	-4.6136971	1.9507047
58	H	-2.1787188	-4.2900558	0.9735607
59	H	-2.0023627	-3.5548131	2.5793733

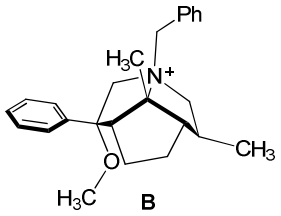

B

1	H	0.0594885	1.2386758	-1.0171604
2	C	-0.0032961	0.6405679	-0.1060544
3	N	-0.9103952	-0.5283804	-0.4272571
4	C	0.0358057	-1.5696973	-1.1457387
5	C	1.4876279	-1.1499448	-0.7407759
6	H	-0.4579816	1.2446208	0.6785910
7	H	2.0011961	-0.7787604	-1.6314551
8	C	-1.4555907	-1.2557243	0.8159127
9	C	-0.2153225	-2.9245762	-0.4574883
10	H	-0.9719738	-3.5118529	-0.9934603

11	C	1.1688415	-3.5963231	-0.4803925
12	H	1.3472515	-4.0549674	-1.4595199
13	C	2.1729975	-2.4446486	-0.2196629
14	H	2.3816517	-2.3454068	0.8468156
15	C	-0.1319917	-1.6126493	-2.6625068
16	H	-1.1267770	-1.9382593	-2.9780182
17	H	0.5841965	-2.3439622	-3.0509954
18	H	0.1035718	-0.6571803	-3.1431720
19	C	-2.0920996	-0.0584890	-1.2961085
20	H	-2.6271523	-0.9675977	-1.5767120
21	H	-1.6523058	0.3718929	-2.1963381
22	C	-3.0255618	0.9307798	-0.6381818
23	C	-4.8018843	2.7745414	0.5185796
24	C	-2.7621274	2.3089042	-0.6916557
25	C	-4.2107478	0.4954646	-0.0268133
26	C	-5.0903061	1.4095671	0.5527932
27	C	-3.6400886	3.2239679	-0.1124037
28	H	-1.8783157	2.6743120	-1.2089990
29	H	-4.4660427	-0.5615210	-0.0249793
30	H	-6.0054720	1.0562544	1.0181903
31	H	-3.4248123	4.2869134	-0.1670367
32	H	-5.4892905	3.4872081	0.9643877
33	O	1.3664501	-0.4534991	1.5785008
34	C	1.4865949	0.4763306	2.6551208
35	H	2.4577835	0.9796750	2.6471338
36	H	1.3913757	-0.1167158	3.5669452
37	C	1.3831030	0.0674969	0.2436111
38	H	0.6924788	1.2367067	2.6427164
39	H	-1.3557243	-0.5962025	1.6765296
40	H	1.2478747	-4.3974252	0.2615765
41	H	3.1258058	-2.6241607	-0.7250953
42	H	-2.5171105	-1.4221721	0.6353513
43	C	-0.7151355	-2.5879411	0.9641186
44	H	0.1513334	-2.4191413	1.6073059
45	C	2.5162200	1.0759527	0.0481580
46	C	4.6647652	2.8709055	-0.2359384
47	C	2.2882698	2.4521549	-0.0775603
48	C	3.8418603	0.6145404	0.0496815
49	C	4.9062453	1.5022202	-0.0936038
50	C	3.3537750	3.3435673	-0.2242953
51	H	1.2788514	2.8529881	-0.0531855
52	H	4.0438773	-0.4455993	0.1701458
53	H	5.9247788	1.1249972	-0.0944461
54	H	3.1550277	4.4066227	-0.3244450
55	H	5.4940109	3.5627155	-0.3497261
56	C	-1.5925730	-3.6760502	1.5907852
57	H	-1.0324119	-4.6112903	1.6919271
58	H	-2.4804193	-3.8815440	0.9796934
59	H	-1.9298862	-3.3886760	2.5927453

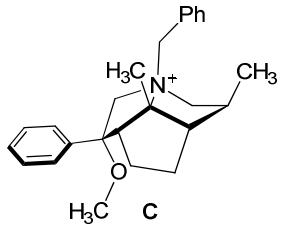

C

1	H	0.1702856	1.1637474	-0.9260466
2	C	0.1065350	0.5657409	-0.0159665
3	N	-0.8809854	-0.5464083	-0.2908206
4	C	-0.0223619	-1.7052103	-0.9570157
5	C	1.4624446	-1.3294480	-0.6609171
6	H	-0.2797949	1.1928429	0.7876361
7	H	1.9495320	-1.0274711	-1.5919401
8	C	-1.4213542	-1.1634410	1.0035621
9	C	-0.3511035	-2.9947494	-0.1361456
10	H	-0.6035575	-3.8039283	-0.8296235
11	C	0.9453806	-3.3474726	0.6351287
12	H	1.0973100	-4.4296450	0.6902226
13	C	2.0842618	-2.6314006	-0.1088768
14	H	2.9423242	-2.4463081	0.5400529
15	C	-0.2716944	-1.8668584	-2.4558639
16	H	-1.2896890	-2.1899877	-2.6899270
17	H	0.4039699	-2.6510170	-2.8131180
18	H	-0.0405430	-0.9634332	-3.0295789
19	C	-2.0299161	-0.0188430	-1.1762875
20	H	-2.6584650	-0.8798932	-1.3945523
21	H	-1.5597345	0.3050620	-2.1045828
22	C	-2.8529616	1.0978227	-0.5792920
23	C	-4.4354462	3.1705272	0.4687473
24	C	-2.4777743	2.4397920	-0.7484643
25	C	-4.0522851	0.8142026	0.0926784
26	C	-4.8355288	1.8419313	0.6182764
27	C	-3.2591321	3.4679629	-0.2227429
28	H	-1.5831252	2.6890856	-1.3138802
29	H	-4.3904383	-0.2151387	0.1866538
30	H	-5.7619611	1.6043550	1.1323765
31	H	-2.9575442	4.5012442	-0.3662706
32	H	-5.0464191	3.9721094	0.8727636
33	O	1.5216987	-0.5681258	1.6272748
34	C	1.7822860	0.3782045	2.6655089
35	H	2.7993662	0.7758332	2.6016101
36	H	1.6634084	-0.1722502	3.6008568
37	C	1.4772241	-0.0785302	0.2773444
38	H	1.0713916	1.2160471	2.6517712
39	H	-0.6584738	-0.9800496	1.7571627
40	H	-2.3374746	-0.6427571	1.2797340
41	H	0.8890022	-2.9716976	1.6603925
42	H	2.4303875	-3.2383667	-0.9537715

43	C	-1.5664703	-2.6705390	0.7630183	52	H	4.0897276	-0.6947440	-0.2674724
44	H	-1.4389218	-3.1650875	1.7331903	53	H	5.9803077	0.8205993	-0.6804229
45	C	2.6336417	0.8824466	-0.0185684	54	H	3.3734237	4.2091990	-0.2203024
46	C	4.8036347	2.6175439	-0.4847088	55	H	5.6398546	3.2854112	-0.6687420
47	C	2.4595622	2.2738572	-0.0011697	56	C	-2.9147761	-3.1380943	0.1927465
48	C	3.9200260	0.3768063	-0.2589370	57	H	-2.9528712	-4.2323050	0.1835404
49	C	4.9940620	1.2345081	-0.4917919	58	H	-3.0893923	-2.8082164	-0.8369045
50	C	3.5331691	3.1350326	-0.2357929	59	H	-3.7499980	-2.7859303	0.8085678
51	H	1.4848277	2.7089357	0.2034966					

7.5.2. Tabular Catalyst Enantioselectivity Data:

name	ln(S/R)
II{2,1}	-0.120
II{2,2}	0.000
II{2,3}	-0.080
II{2,4}	0.000
II{2,5}	0.000
II{2,6}	0.040
II{3,1}	0.080
II{3,2}	0.080
II{3,3}	0.040
II{3,4}	0.040
II{3,5}	0.040
II{3,6}	0.120
II{4,1}	0.040
II{4,2}	0.000
II{4,3}	0.040
II{4,4}	0.000
II{4,5}	0.000
II{4,6}	0.000
II{5,1}	-0.120
II{5,2}	-0.160
II{5,3}	-0.080
II{5,4}	-0.201
II{5,5}	0.000
II{5,6}	-0.080
IV{5,2,5}	0.241
V{1,2,1}	0.080
V{1,2,2}	0.160
V{1,2,3}	0.080
V{1,2,4}	0.241
V{1,2,7}	0.405
V{1,2,8}	0.080
V{1,2,6}	-0.040
V{2,2,1}	-0.120
V{2,2,2}	-0.201
V{2,2,3}	-0.040
V{2,2,5}	0.282
V{2,2,7}	0.282
V{2,2,8}	-0.120
V{2,2,6}	0.040
V{2,7,2}	-0.080
V{2,7,3}	-0.080
V{2,7,5}	0.364
V{2,7,7}	0.282

Tabular Catalyst Enantioselectivity Data: (cont.)

V{2,3,1}	-0.160
V{2,3,2}	-0.080
V{2,3,3}	-0.120
V{2,3,5}	0.282
V{2,3,7}	0.323
V{2,3,8}	-0.201
V{2,3,6}	0.120
V{3,2,1}	-0.282
V{3,2,2}	-0.323
V{3,2,3}	-0.241
V{3,2,5}	-0.575
V{3,2,7}	-0.490
V{3,2,8}	-0.241
V{3,2,6}	-0.282
V{3,7,1}	-0.241
V{3,7,2}	-0.364
V{3,7,3}	-0.323
V{3,7,5}	-0.405
V{3,7,7}	-0.447
V{3,7,8}	-0.405

V{3,7,6}	-0.364
V{3,3,1}	-0.405
V{3,3,2}	-0.282
V{3,3,3}	-0.323
V{3,3,5}	-0.490
V{3,3,7}	-0.405
V{3,3,8}	-0.405
V{3,3,6}	0.040
V{4,2,5}	-0.532
V{5,2,1}	-0.080
V{5,2,2}	-0.040
V{5,2,3}	0.040
V{5,2,5}	1.450
V{5,2,8}	-0.241
V{5,2,9}	-0.040
V{5,2,10}	0.000
V{5,2,11}	0.241
V{5,7,1}	-0.080
V{5,7,2}	0.000
V{5,7,3}	0.040

V{5,7,5}	1.450
V{5,7,7}	0.532
V{5,6,1}	-0.040
V{5,6,5}	1.450
V{5,6,8}	-0.160
V{5,3,1}	-0.201
V{5,3,2}	-0.080
V{5,3,3}	-0.040
V{5,3,5}	1.325
V{5,3,7}	0.447
V{5,3,8}	-0.323
V{7,2,1}	0.040
V{7,2,5}	1.450
V{7,2,8}	-0.080
V{7,2,9}	0.160
V{7,2,10}	0.080
V{6,2,5}	1.153
V{6,2,8}	-0.120

7.5.3. CoMFA Model Development.

All of the CoMFA modeling is performed within the Sybyl X 1.1 software package. Each catalyst geometry is minimized using MMFF with Spartan starting from the desired conformer. Single point calculations are carried out on each MMFF conformer at the desired semi-empirical parameterization level. All structures are then imported as .mol2 files, while retaining electrostatic partial atomic charges, into Sybyl. A rigid-body, root mean square (RMS) alignment, as implemented in Sybyl under the align database option, is then performed on the library in question using the 5-5-5 core as the common substructure and the simplest catalyst (II{1,1}) as the template molecule. The inertial grid orientation option is chosen for the alignment. After the alignment, a region is created to compute the fields for which a grid is created that extends at least 4Å along the Cartesian axes. The volume of the grid is **XXX**. The probe atom used is the standard sp^3 hybridized carbon atom with a +1 atomic charge. The grid spacing within each lattice point is chosen as 2Å. Any grid spacing smaller or larger typically produced worse results, with or without region focusing. Initially, a 2Å grid spacing produced 1584 grid points for the region.

Each conformation library, as defined in table 1, was subjected to a number of CoMFA analyses while investigating different semi-empirical partial charges, cutoff energy combinations and field type (Tripos standard or Indicator). Smoothing functions were not applied in calculating the field values. For the electrostatic field, the distance dependence in the Coulombic expression was set to $1/r^2$. For grid points that exhibit steric energies exceeding the steric cutoff energy, the electrostatic energy for that grid point is set to the average of all the non-excluded electrostatic energies so that these grid points do not contribute to the regression analysis. For the steric energy, the exponent of the repulsive term is set to 12 so as to produce the standard 6-12 Lennard-Jones potential. Other values (8 or 10) generally resulted in poorer result.

After the fields were calculated for all the catalysts in the library, a PLS regression was performed on the calculated interaction energies. All models reported below are generated from 5 components (latent variables). For the Tripos standard fields, the q^2_{LOO} values are reported after 2.0 kcal/mol filtering was applied in which grid points with a standard deviation of less than this value are dropped from the analysis. Column filtering was not applied when Indicator fields were used.

Table 25. The complete investigation semi-empirical partial atomic charges. The data that is boxed represents that in table 2 of the main paper.

	Conformation Library (R^2 / q^2)				
	A	**B**	**C**	**D**	**E**
PM3[a]_30[b]/30[c]_Std[d]	0.699[e] / 0.482[f]	0.686 / 0.446	0.706 / 0.475	**0.813 / 0.612**	0.784 / 0.591
PM3_30/15_Std	0.700 / 0.491	0.690 / 0.441	0.708 / 0.460	0.812 / 0.587	**0.785 / 0.609**
PM3_15/30_Std	0.703 / 0.484	0.692 / 0.468	0.704 / 0.461	**0.797 / 0.642**	**0.804 / 0.609**
PM3_30/30_Ind[e]	0.729 / 0.485	0.734 / 0.533	0.712 / 0.477	**0.799 / 0.640**	0.768 / 0.527
PM3_30/15_Ind	0.783 / 0.463	0.801 / 0.529	**0.879 / 0.621**	**0.870 / 0.621**	**0.868 / 0.618**
PM3_15/30_Ind	0.707 / 0.450	0.694 / 0.454	0.724 / 0.466	**0.811 / 0.609**	0.795 / 0.557
AM1_30/30_Std	0.712 / 0.485	0.683 / 0.440	0.705 / 0.479	**0.810 / 0.621**	0.780 / 0.590
AM1_30/15_Std	0.714 / 0.496	0.685 / 0.429	0.707 / 0.472	**0.812 / 0.607**	0.781 / 0.594
AM1_15/30_Std	0.723 / 0.506	0.688 / 0.452	0.701 / 0.441	**0.791 / 0.634**	**0.801 / 0.613**
AM1_30/30_Ind	0.724 / 0.474	0.697 / 0.423	0.712 / 0.477	**0.813 / 0.653**	0.768 / 0.527
AM1_30/15_Ind	0.796 / 0.503	0.817 / 0.533	**0.906 / 0.671**	**0.896 / 0.635**	**0.866 / 0.641**
AM1_15/30_Ind	0.711 / 0.462	0.693 / 0.416	0.724 / 0.466	**0.811 / 0.609**	0.795 / 0.557
MNDO_30/30_Std	0.728 / 0.547	0.697 / 0.465	0.711 / 0.493	**0.815 / 0.612**	0.794 / 0.574
MNDO_30/15_Std	0.729 / 0.551	0.700 / 0.481	0.711 / 0.485	0.814 / 0.598	0.794 / 0.586
MNDO_15/30_Std	0.734 / 0.545	0.705 / 0.498	0.709 / 0.460	**0.803 / 0.641**	**0.812 / 0.636**
MNDO_30/30_Ind	0.724 / 0.474	0.697 / 0.423	0.712 / 0.477	**0.835 / 0.648**	0.768 / 0.527
MNDO_30/15_Ind	0.797 / 0.484	0.754 / 0.442	**0.835 / 0.619**	**0.924 / 0.778**	0.782 / 0.474
MNDO_15/30_Ind	0.711 / 0.462	0.693 / 0.416	0.724 / 0.466	**0.810 / 0.604**	0.795 / 0.557

[a] Semi-empirical parameterization method for calculating partial atomic charges. [b] Steric cutoff energy (kcal/mol). [c] Electrostatic cutoff energy (kcal/mol). [d] Tripos standard field type. [e] Indicator field type. [e] R^2. [f] q^2_{LOO}.

7.5.4. Internal Cross-validation.

All of the internal cross-validation for the CoMFA models was performed with Sybyl X. q^2_{LMO} represents an average of 100 runs aided by an spl script. Y-scrambling was performed such that 100% of the dependent variable data was scrambled such that each value was paired with the incorrect descriptor values. A PLS regression was then performed on each model. The reported $R^2_{scramb.}$ values are obtained in the absence of column-filtering. The reported $q^2_{LOO,scramb.}$ for models from Tripos Standard fields determined in the presence of 2 kcal/mol column filtering while the $q^2_{LOO,scramb.}$ values for models determined from Indicator fields were determined in the absence of column filtering.

7.5.5. External Cross-validation.

Internal cross-validation is considered a necessary but insufficient condition in assessing

the predictive capacity of a QSAR model (especially for 3-D QSAR).[184] The use of an external dataset that was not used in the model development for prediction is considered to be a more realistic assessment of the predictive power of a model. The entire data set was divided into multiple training sets (data set used to develop the model) and test sets (dataset to be predicted by the model developed from the training set) in accordance with Tropsha's criteria for the rational division of datasets for external validation.184 [b] The primary considerations in the division of the data set were that both the training and test sets would contain five compounds that spanned the range of e.r. and descriptor space of the entire dataset. Addressing the incorporation of catalysts within the entire e.r. range is relatively straightforward, although dividing the data based on their descriptor space is much less straightforward, particularly for 3-D descriptors. There might be hundreds of interaction energies with which to assess the property range which is of a significantly higher order space that is difficult to probe directly. Multi-dimensional descriptor space is difficult to think about and work with. Therefore, on the basis of the assumption that molecules with similar structures (as determined by some shape similarity metric) will have similar properties[185], field similarity was used to segregate molecules based on their fields. This was performed employing a Tanimoto similarity metric (*T*) (Eq. 1) where F_1 and F_2 represent the fields to be compared, E_1 and E_2 represent the interaction energies at grid point *i*, and *n* is the number of grid points.[186]

$$T(F_1, F_2) = \frac{\sum_i^n E_{1,i} E_{2,i}}{\sum_i^n E_{1,i}^2 + \sum_i^n E_{2,i}^2 - \sum_i^n E_{1,i} E_{2,i}} \quad ; \quad -1/3 \leq T \leq 1$$

(Eq. 1)

The catalysts with field properties in the middle of the field property spectrum were identified as having the largest number of of *T* coefficients (100 values generated by comparison to every catalyst in the dataset of 101) greater than a user-defined value ($T = 0.55$ produced a sufficient range of values). With catalysts in the middle of the property spectrum determined, catalysts located at the extremes were approximated (but not yet differentiated) by identifying the catalysts with fields of the lowest similarity (most dissimilar) to catalysts in the middle of the field property region. The extremes were then differentiated by locating catalysts exhibiting the lowest similarity among the catalysts most dissimilar to the catalysts in the middle property region. A similar procedure was performed for indentifying catalysts within the middle and

extremes. A more complete table of the results of all 30 training/test set splits is provided (from table 4 in the main text).

Specific criteria have been suggested for evaluating the predictability of QSAR models based on external validation, which was determined through analyzing a number of QSAR models[184b], and are reiterated here for ease of comparison:

$$q^2 > 0.5 \mid R^2 > 0.6 \mid \frac{(R^2 - R_0^2)}{R^2} > 0.1 \text{ or } \frac{(R^2 - R_0'^2)}{R^2} > 0.1 \mid 0.85 \leq k \leq 1.15 \text{ or } 0.85 \leq k' \leq 1.15$$

where q^2 is that of the training set ($q^2 = q^2_{LOO}$ for this analysis), R^2 is the coefficient of determination for the test set, R^2_0 and R'^2_0 are the squared coefficients of determination for the predicted versus observed and observed versus predicted values respectively, k and k' are the slopes for the predicted versus observed and observed versus predicted values respectively when the intercept is set to zero. These criteria were used to assess the predictive capacity of the CoMFA models for enantioselectivity. Both a complete table of the results of all 30 training/test set splits (Table 26) and a table that summarizes the data (Table 27) are provided.

Table 26. All training/test set splits with correlation parameters.

entry	q^2_{LOO} [a]	R^2 [b]	$(R^2-R^2_0)/R^2$	$(R^2-R'^2_0)/R^2$	k	k'
1	0.883	0.933	0.016	0.021	1.084	0.849
2	0.839	0.915	0.000	0.001	1.041	0.882
3	0.838	0.925	0.000	0.000	1.106	0.925
4	0.819	0.907	0.020	0.025	1.041	0.854
5	0.416	0.793	0.003	0.007	0.913	0.867
6	0.344	0.829	0.001	0.001	1.071	0.774
7	0.632	0.908	0.000	0.000	1.174	0.774
8	0.736	0.885	0.000	0.000	0.887	0.998
9	0.466	0.737	0.007	0.000	0.805	0.922
10	0.777	0.858	0.010	0.014	0.967	0.880
11	0.781	0.900	0.004	0.002	1.011	0.890
12	0.479	0.870	0.000	0.000	1.076	0.808
13	0.917	0.916	0.004	0.002	1.240	0.742
14	0.582	0.855	0.002	0.002	0.967	0.883
15	0.503	0.874	0.001	0.001	1.067	0.873
16	0.893	0.922	0.003	0.001	1.176	0.787
17	0.734	0.877	0.013	0.013	0.948	0.925
18	0.875	0.940	0.001	0.000	1.025	0.918
19	0.814	0.859	0.006	0.008	0.840	1.016
20	0.812	0.923	0.002	0.002	1.105	0.834
21	0.546	0.807	0.006	0.004	0.828	0.911
22	0.356	0.865	0.003	0.002	0.962	0.898
23	0.893	0.917	0.000	0.001	1.046	0.878
24	0.831	0.862	0.000	0.000	1.017	0.848
25	0.837	0.901	0.004	0.006	1.089	0.825
26	0.774	0.873	0.004	0.004	0.865	1.006
27	0.797	0.888	0.001	0.001	0.860	1.032
28	0.877	0.921	0.001	0.001	1.090	0.847
29	0.865	0.897	0.000	0.000	1.027	0.876
30	0.794	0.882	0.001	0.001	0.945	0.934

[a] q^2_{LOO} for the training set. [b] R^2 for the test set.

Table 27. Summary for external validation over 30 training/test set splits (67/34).

	q^2_{LOO}[a]	R^2	$(R^2-R^2_0)/R^2$	$(R^2-R'^2_0)/R^2$	k	k'
Average	0.724	0.881	0.004	0.004	1.01	0.88
C.I.[b]	0.063	0.016	0.002	0.002	0.04	0.03
best q^2_{LOO}[c]	0.917	0.916	0.004	0.002	1.24	0.74
best R^2	0.875	0.940	0.001	0.000	1.02	0.92
worst q^2_{LOO}[d]	0.344	0.829	0.001	0.001	1.07	0.77
worst R^2	0.436	0.737	0.007	0.000	0.81	0.92

[a] q^2_{LOO} for the training set. [b] 95% confidence interval [c] Model containing highest value of q^2_{LOO}. [d] Model containing the lowest value of q^2_{LOO}.

Contour Maps.

For the generation of interpretable contour maps for visualization of the best CoMFA model, 1.0 kcal/mol column filtering was applied to the model after region focusing was applied. The contours maps were similar to those in the absence of column filtering apart from eliminating some of the smaller contours that exhibited low deviation and were seemingly uninterpretable. The model results with 1.0 column filtering (R^2 = 0.922, q^2_{LOO} = 0.868, electrostatic field contribution: 44%; steric field contribution: 56%) are similar to that in the absence of column filtering (R^2 = 0.944, q^2_{LOO} = 0.890, electrostatic field contribution: 55%, steric field contribtution: 45%), so that the contours reflect the model accurately. The contour specifications for the contour maps were based on percent contributions. For the steric contour maps, the volume enclosing regions where increased steric bulk leads to increased enantioselectivity (green) was set to 65% and thus the volumne enclosing regions where decreased steric bulk leads to increased enantioselectivity was set to 35%. Hence, the green contours represent the top 65% of the energy range observed for the van der Walls potential and vice versa for the minimum 35%. For the electrostatic contour maps, the volume enclosing regions where increased positive charge leads to increased enantioselectivity (blue) was set to

75% and thus the volume enclosing regions where decreased positive charge leads to increased enantioselectivity was set to 25%. The physical interpretation of the percentiles remains the same as for the steric contours.

7.6. QSAR Modeling for Chapter 4

Sequence for generating 3D-QSAR model

1. Obtain geometries for each compound
2. Align molecules based on a common core
3. Generate a grid that encompasses all of the molecular with defined lattice spacing and imensions given a point for the origin which could be the center of your scaffold
    a. Spl script **q1.spl** can be used.
4. Calculate electrostatic energies using the grid file as input, using Jaguar, Gaussian, GAMESS, or other to calculate the energies (ie. B3LYP/6-31G(d,p))
5. Calculate steric energies using MMFF94 van der Waals potential using spl script **q2.spl**.
6. Match the electrostatic and steric energy for each grid point and eliminate points based on cutoff energies using spl script **q3.spl** and use **q4.spl** to generate files contained the field data for each catalyst and the standard deviation at each point.
7. Use a graphical user interface (eg. Maestro) to remove grid points that are of no interest and save new grid file.
8. Use spl script **q5.spl** to reduce size of grid points based on a standard deviation threshold.
9. Use spl script **q6.spl** to generate new files with reduced grid point size.
10. Use simulated annealing algorithms in**q7.py** in combination with statistical functions in classes from **q8.py** to generate QSAR models.
11. From the output, obtain the the models with the best correlation (or some other parameter) and visualize the grid point locations with maestro to see if models make sense

Example of Simulated Annealing Run

n=12 data set
Electrostatic scaling factor= 1.0
Steric scaling factor= 1.0
Initial configuration= 1 5
R2= 0.218

Monte-Carlo steps= 1
iteration= 1
temperature= 1000
configuration= 101 5
R2= 0.895
>>>>>>> 0.895 is the new best!! <<<<<<<
clock time= 14:25:13

Monte-Carlo steps= 2
iteration= 2
temperature= 1000
configuration= 134 5
R2= 0.911
>>>>>>> 0.911 is the new best!! <<<<<<<
clock time= 14:26:35

Monte-Carlo steps= 3
iteration= 3
temperature= 984.14539
configuration= 112 5
R2= 0.913
>>>>>>> 0.913 is the new best!! <<<<<<<
clock time= 14:27:43

Monte-Carlo steps= 5
iteration= 4
temperature= 948.42085
configuration= 134 838
R2= 0.938
>>>>>>> 0.938 is the new best!! <<<<<<<
clock time= 14:29:45

Monte-Carlo steps= 6
iteration= 5
temperature= 934.76481
configuration= 28 838
R2= 0.911
clock time= 14:31:07

Monte-Carlo steps= 7
iteration= 6
temperature= 913.2819
configuration= 28 420
R2= 0.901
clock time= 14:32:10

Monte-Carlo steps= 8
iteration= 7
temperature= 895.02801
configuration= 148 420
R2= 0.957
>>>>>>> 0.957 is the new best!! <<<<<<<
clock time= 14:33:45

Monte-Carlo steps= 9
iteration= 8
temperature= 885.2104
configuration= 148 579
R2= 0.958
>>>>>>> 0.958 is the new best!! <<<<<<<
clock time= 14:35:21

Monte-Carlo steps= 10
iteration= 9
temperature= 869.13224
configuration= 110 579
R2= 0.904
clock time= 14:36:51

Monte-Carlo steps= 11
iteration= 10
temperature= 844.45884
configuration= 110 669
R2= 0.926
clock time= 14:37:50

Monte-Carlo steps= 12
iteration= 11
temperature= 831.7584
configuration= 148 669
R2= 0.928
clock time= 14:39:42

Monte-Carlo steps= 13

iteration= 12
temperature= 816.78546
configuration= 111 669
R2= 0.919
clock time= 14:41:32

Monte-Carlo steps= 17
iteration= 13
temperature= 758.50032
configuration= 148 832
R2= 0.958
clock time= 14:47:11

Monte-Carlo steps= 18
iteration= 14
temperature= 747.81851
configuration= 37 832
R2= 0.896
clock time= 14:48:36

Monte-Carlo steps= 20
iteration= 15
temperature= 717.72264
configuration= 148 430
R2= 0.957
clock time= 14:50:57

Monte-Carlo steps= 22
iteration= 16
temperature= 691.67161
configuration= 134 579
R2= 0.915
clock time= 14:53:25

Monte-Carlo steps= 24
iteration= 17
temperature= 665.27818
configuration= 148 572
R2= 0.958
clock time= 14:56:37

Monte-Carlo steps= 26
iteration= 18
temperature= 641.13137
configuration= 124 832
R2= 0.903
clock time= 14:59:03

Monte-Carlo steps= 29
iteration= 19
temperature= 604.50786
configuration= 27 430
R2= 0.904
clock time= 15:02:51

Monte-Carlo steps= 31
iteration= 20
temperature= 580.83447
configuration= 134 430
R2= 0.914
clock time= 15:05:41

Monte-Carlo steps= 32
iteration= 21
temperature= 565.71706
configuration= 134 876
R2= 0.93
clock time= 15:06:35

Monte-Carlo steps= 33
iteration= 22
temperature= 556.72066
configuration= 112 876
R2= 0.913
clock time= 15:08:33

Monte-Carlo steps= 34
iteration= 23
temperature= 544.93406
configuration= 123 876
R2= 0.916
clock time= 15:10:30

Monte-Carlo steps= 37
iteration= 24
temperature= 515.39839
configuration= 112 2
R2= 0.914
clock time= 15:14:28

Monte-Carlo steps= 38
iteration= 25

temperature= 506.04094
configuration= 101 2
R2= 0.899
clock time= 15:15:43

Monte-Carlo steps= 40
iteration= 26
temperature= 486.0803
configuration= 123 5
R2= 0.909
clock time= 15:17:40

Monte-Carlo steps= 41
iteration= 27
temperature= 478.23233
configuration= 123 2
R2= 0.914
clock time= 15:18:31

Monte-Carlo steps= 42
iteration= 28
temperature= 469.8513
configuration= 134 2
R2= 0.926
clock time= 15:19:32

Monte-Carlo steps= 44
iteration= 29
temperature= 454.48385
configuration= 134 822
R2= 0.931
clock time= 15:21:19

Monte-Carlo steps= 45
iteration= 30
temperature= 445.64956
configuration= 112 822
R2= 0.921
clock time= 15:22:44

Monte-Carlo steps= 48
iteration= 31
temperature= 420.86134
configuration= 123 822
R2= 0.917
clock time= 15:26:56

Re-setting temperature to T to T_max = 462.13163

Monte-Carlo steps= 68
iteration= 32
temperature= 357.81805
configuration= 148 838
R2= 0.948
clock time= 15:52:00

Monte-Carlo steps= 73
iteration= 33
temperature= 326.51664
configuration= 134 420
R2= 0.915
clock time= 15:59:08

Monte-Carlo steps= 74
iteration= 34
temperature= 318.08599
configuration= 110 420
R2= 0.912
clock time= 16:01:38

Monte-Carlo steps= 76
iteration= 35
temperature= 307.05445
configuration= 110 571
R2= 0.924
clock time= 16:03:56

Re-setting temperature to T to T_max = 347.1931

Monte-Carlo steps= 80
iteration= 36
temperature= 347.1931
configuration= 36 669
R2= 0.896
clock time= 16:10:22

Monte-Carlo steps= 84
iteration= 37
temperature= 321.74688
configuration= 111 538

R2= 0.919
clock time= 16:17:14

Monte-Carlo steps= 85
iteration= 38
temperature= 315.85388
configuration= 111 447
R2= 0.915
clock time= 16:18:16

Monte-Carlo steps= 86
iteration= 39
temperature= 309.86428
configuration= 221 447
R2= 0.901
clock time= 16:20:05

Monte-Carlo steps= 87
iteration= 40
temperature= 303.45593
configuration= 221 877
R2= 0.9
clock time= 16:21:18

Monte-Carlo steps= 88
iteration= 41
temperature= 297.8484
configuration= 111 877
R2= 0.898
clock time= 16:22:42

Monte-Carlo steps= 89
iteration= 42
temperature= 292.29538
configuration= 111 570
R2= 0.917
clock time= 16:23:42

Monte-Carlo steps= 90
iteration= 43
temperature= 287.78352
configuration= 148 570
R2= 0.925
clock time= 16:25:18

Monte-Carlo steps= 94
iteration= 44
temperature= 268.8683
configuration= 134 832
R2= 0.931
clock time= 16:29:50

Monte-Carlo steps= 101
iteration= 45
temperature= 235.50062
configuration= 134 572
R2= 0.91
clock time= 16:39:30

Monte-Carlo steps= 110
iteration= 46
temperature= 196.71466
configuration= 28 419
R2= 0.907
clock time= 16:53:35

Monte-Carlo steps= 112
iteration= 47
temperature= 189.44858
configuration= 134 419
R2= 0.92
clock time= 16:57:28

Monte-Carlo steps= 113
iteration= 48
temperature= 186.35716
configuration= 148 419
R2= 0.948
clock time= 16:59:01

Monte-Carlo steps= 115
iteration= 49
temperature= 179.44509
configuration= 36 419
R2= 0.91
clock time= 17:02:08

Monte-Carlo steps= 131
iteration= 50
temperature= 133.27666
configuration= 37 838
R2= 0.907

clock time= 17:26:15

Monte-Carlo steps= 137
iteration= 51
temperature= 118.76524
configuration= 110 419
R2= 0.909
clock time= 17:35:47

Monte-Carlo steps= 139
iteration= 52
temperature= 114.50719
configuration= 111 571
R2= 0.917
clock time= 17:38:36

Monte-Carlo steps= 140
iteration= 53
temperature= 112.27939
configuration= 148 571
R2= 0.925
clock time= 17:40:17

Monte-Carlo steps= 156
iteration= 54
temperature= 83.483824
configuration= 27 832
R2= 0.886
clock time= 18:02:23

Monte-Carlo steps= 157
iteration= 55
temperature= 81.253853
configuration= 27 420
R2= 0.912
clock time= 18:03:32

Monte-Carlo steps= 181
iteration= 56
temperature= 51.949478
configuration= 27 587
R2= 0.91
clock time= 18:42:04

Monte-Carlo steps= 182
iteration= 57
temperature= 50.981169
configuration= 148 587
R2= 0.949
clock time= 18:43:32

Monte-Carlo steps= 189
iteration= 58
temperature= 44.815362
configuration= 124 822
R2= 0.894
clock time= 18:51:11

Monte-Carlo steps= 190
iteration= 59
temperature= 43.781149
configuration= 124 298
R2= 0.91
clock time= 18:52:05

Monte-Carlo steps= 191
iteration= 60
temperature= 43.087129
configuration= 148 298
R2= 0.915
clock time= 18:53:06

Monte-Carlo steps= 193
iteration= 61
temperature= 41.522102
configuration= 124 514
R2= 0.935
clock time= 18:55:11

Monte-Carlo steps= 194
iteration= 62
temperature= 40.913489
configuration= 124 883
R2= 0.911
clock time= 18:56:05

Monte-Carlo steps= 195
iteration= 63
temperature= 39.995737
configuration= 148 883
R2= 0.911
clock time= 18:57:17

Monte-Carlo steps= 196
iteration= 64
temperature= 39.26319
configuration= 112 883
R2= 0.888
clock time= 18:58:28

Monte-Carlo steps= 203
iteration= 65
temperature= 34.277884
configuration= 37 420
R2= 0.894
clock time= 19:07:50

7.7. Preparation of Compounds from Chapter 4

7.7.1. Preparation of Compounds from Figure 21

Preparation of (1*S*,3*S*,5*S*,5a*S*,7a*S*,7b*R*)-Octahydro-1-hydroxy-1-(2,3,4-trifluorophenyl)-5-methyl-7b-methyl-2*H*cyclopenta[*gh*] pyrrolizin-2-one (23a)

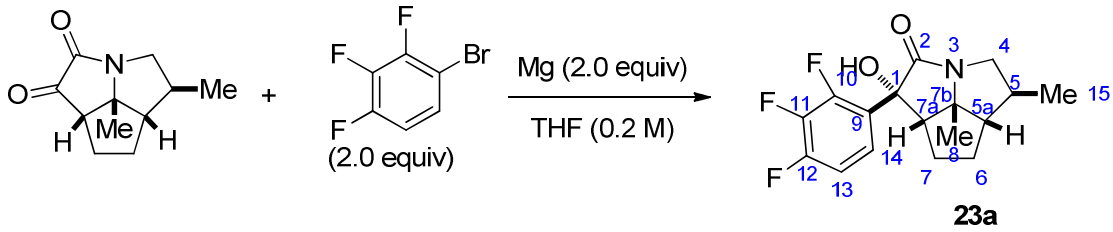

To a 5-mL, two-necked, round-bottomed flask equipped with a nitrogen inlet adapter, a rubber septum and a magnetic stir bar was added **21** (40 mg, 0.207 mmol) followed by THF (400 µL). The flask was immersed in an ice bath and 2,3,4-trifluorophenylmagnesium bromide (600 µL, 0.331 mmol, 1.6 equiv, in THF) was added dropwise via syringe. After being stirred for 10 min, the cooling bath was removed and the reaction was stirred at room temperature for 20 min. The solution was cooled in an ice bath and sat. aq. NH_4Cl (1.0 mL) is added. The resulting mixture was transferred to a 60-mL separatory funnel using an additional 20 mL of water and 20 mL of Et_2O and the aqueous phase was extracted with diethyl ether (3 x 15 mL). The organic extracts were washed with water (2 x 20 mL), and brine (1x 20 mL), then the combinded organic extracts were dried ($NaSO_4$). The mixture was filtered through a cotton plug and concentrated by rotary evaporation (15 mm Hg, 20-25^{o}C). Purification by silica gel chromatography (5.0 cm x 8 cm column, gradient elution, EtOAc/Hexanes, 10, 20, 30, 50%, 25 mL each) afforded 66 mg (98%) of **23a**.

Data for **23a**

^{1}H-NMR: (500 MHz, $CDCl_3$)

6.89 – 6.80 (m, 2H, HC(13), HC(14)), 4.15 (ddd, *J* = 11.7, 7.4, 2.1 Hz, 1H, $H_2C(4)$), 3.68 – 3.52 (m, 1H, OH), 2.73 (td, *J* = 7.3, 3.9 Hz, 1H, HC(7a)), 2.66 – 2.56 (m, 1H, $H_2C(4)$), 2.07 – 1.95 (m, 1H, $H_2C(7)$), 1.86 – 1.62 (m, 4H, HC(5), HC(5a), $H_2C(6)$, $H_2C(7)$), 1.58 – 1.47 (m, 1H, $H_2C(6)$), 1.08 (dd, *J* = 6.6, 2.0 Hz, 3H, $H_3C(15)$), 0.95 (s, 3H, $H_3C(8)$)

^{13}C-NMR: (500 MHz, $CDCl_3$)

175.00 (C(2)), 151.89 (ddd, *J* = 3.2, 10.6, 78.8 Hz, C(12)), 149.89 (ddd, *J* = 2,7, 6.8, 72.7 Hz, C(10)), 140.76 (dt, *J* = 14.1, 252 Hz, C(11)), 128.64 (d, *J* = 8.9 Hz, C(14)), 121.77 (sept, *J* = 3.8 Hz, C(9)), 111.36 (dd, *J* = 3.62, 16.8 Hz, C(13)), 80.75 (C(1) or C(7b)), 75.60 (C(1) or C(7b)), 58.64 (C(5a)), 57.04 (C(7a)), 51.12 (C(4)), 42.06 (C(5)), 30.17 (C(6)), 26.98 (C(7)), 24.11 (C(8)), 17.66 (C(15))

IR: ($CDCl_3$, film)

3271 (s), 3079 (w), 2965 (s), 2928 (s), 2885 (m), 1688 (s), 1631 (m), 1610 (s), 1512 (s), 1477 (s), 1459 (s), 1381 (m), 1329 (w), 1291 (s), 1233 (s), 1202 (m), 1182 (m), 1167 (s), 1149 (m), 1089 (w), 1053 (s), 1030 (m), 989 (m), 953 (m), 908 (s), 866 (w), 838 (w), 826 (m), 733 (s), 679 (m), 649 (m)

MS: (ESI, Q-tof)

326.1 (76) [M+1], 308.1 (100), 260.6 (6), 241.0 (2), 195.0 (2), 163.0 (3), 79.0(2)

Mol. Formula: $C_{17}H_{18}F_3NO_2$ (325.33)

HRMS: $C_{17}H_{19}F_3NO_2^+$, (326.14)

Calcd: 326.1368

Found: 326.1367

TLC: R_f 0.27 (TBME/Hexanes, 3:7) [UV, I_2]

Preparation of (1*R*,3*S*,5*S*,5a*S*,7a*S*,7b*R*)-Octahydro-1-hydroxy-1-(2,3,4-trifluoropheny)-5-methyl-7b-methyl-2*H*cyclopenta[*gh*]pyrrolizine•Borane (23b)

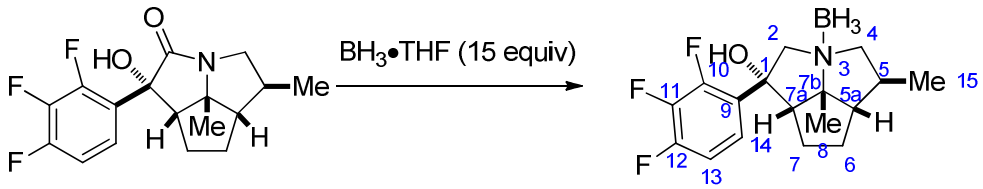

23b

To a 5-mL round-bottomed flask equipped with a nitrogen inlet adapter, a rubber septum, a reflux condenser, and a magnetic stir bar was added **23a** (65 mg, 0.2 mmol) then BH_3•THF complex (3.0 mL, 3.0 mmol, 15 equiv). The reaction flask was immersed in an oil bath and heated to reflux (66 ^oC). After being stirred for 12 h at reflux, the solution was allowed to reach room temperature and was quenched with methanol (5 mL) and concentrated by rotary evaporation (15 mm Hg, 20-25^oC). The resulting colorless oil was purified by silica gel column chromatography (5.0 mm x 8 cm column, gradient elution, TBME/Heaxanes, 5, 10, 15, 20, 25, 30% 25 mL each) to afford 64 mg (98%) of **23b** as a white solid.

Data for **23b**

^{1}H-NMR: (500 MHz, $CDCl_3$)

7.19 – 7.04 (m, 1H, HC(14)), 6.95 (q, *J* = 8.4, 7.6 Hz, 1H, HC(13)), 4.11 (d, *J* = 13.6 Hz, 1H, H_2C(2)), 3.72 (dd, *J* = 13.4, 2.4 Hz, 1H, H_2C(2)), 3.60 (dd, *J* = 12.3, 7.9 Hz, 1H, H_2C(4)), 3.23 (t, *J* = 11.6 Hz, 1H, H_2C(4)), 2.80 (t, *J* = 7.7 Hz, 1H, HC(7a)), 2.47 (dq, *J* = 13.4, 7.1, 6.6 Hz, 1H, HC(5)), 2.26 (m, 2H, H_2C(7), OH), 1.93 (m, 4H, HC(5a), H_2C(6), H_2C(6), H_2C(7)), 1.52 (s, 3H, H_3C(8)), 1.01 (d, *J* = 6.6 Hz, 3H, H_3C(15))

^{13}C-NMR: (500 MHz, $CDCl_3$)

152.48 – 147.50 (m, Ar), 141.58 (t, *J* = 15.7 Hz, Ar), 139.57 (t, *J* = 15.3 Hz, Ar) 129.39 (Ar), 120.74 (dt, *J* = 8.5, 4.4 Hz, Ar), 111.87 (dd, *J* = 17.1, 3.6 Hz, Ar), 89.08 (C(1) or C(7b)), 77.63 (C(1) or C(7b)), 76.63 (d, *J* = 5.3 Hz, (C(2)), 74.39 (C(4)), 61.09 (C(7a)), 60.15 (C(5a)), 34.58 (C(5)), 31.26 (C(6)), 25.05 (C(8)), 24.69 (C(7)), 17.51 (C(15))

IR: ($CDCl_3$, film)

3455 (s), 2962 (s), 2931 (s), 2873 (m), 2383 (s), 2331 (s), 2274 (s), 1634 (m), 1612 (m), 1514 (s), 1469 (s), 1381 (m), 1342 (w), 1299 (s), 1234 (m), 1168

(s), 1133 (m), 1043 (s), 1004 (s), 981 (w), 945 (m), 911 (s), 867 (w), 850 (w), 811 (m), 734 (s), 697 (w), 636 (w)

MS: (ESI, Q-tof)

322.2 (2), 312.1 (100) (M-12)

Mol. Formula: $C_{17}H_{23}BF_3NO$ (325.18)

HRMS: $C_{17}H_{21}F_3NO^+$, (312.16)

Calcd: 312.1575

Found: 312.1565

TLC: R_f 0.27 (TBME/Hexanes, 1:3) [UV, I_2]

Preparation of (1*S*,3*S*,5*S*,5a*S*,7a*S*,7b*R*)-Octahydro-1-benzyloxy-1-(2,3,4-trifluorophenyl)-5-methyl-7b-methyl-2*H*cyclopenta[*gh*]pyrrolizine•Borane (23c)

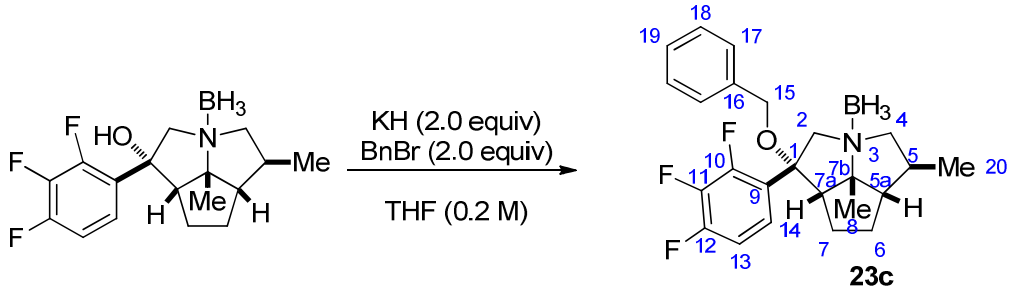

To a two-necked, 5-mL, round-bottomed flask equipped with a nitrogen inlet adapter, a rubber septum and a magnetic stir bar was added washed potassium hydride (15.7 mg, 0.196 mmol, 2.0 equiv) from the drybox followed by THF (200 µL). A solution of alcohol **23b** (63.7 mg, 0.142 mmol) in THF (1.0 mL) is added to the reaction vessel by cannulation. After 15 min of stirring, the flask is immersed in an ice bath. The benzyl bromide (47 µL, 0.392 mmol, 2.0 equiv) is then added dropwise by syringe. The ice bath is removed and the solution is allowed to stir for 2 h at rt. This mixture was cooled in an ice bath and cold sat. aq. NH_4Cl (1.0 mL) is added in one portion. The resulting mixture was transferred to a 60-mL separatory funnel using an additional 15 mL of water and 15 mL of Et_2O and the aqueous phase was extracted with diethyl ether (3 x 15 mL). The organic extracts were washed with water (2 x 20 mL), and brine (1x 20 mL), then the combinded organic extracts were dried ($NaSO_4$). The floculant was filtered through a cotton plug and concentrated by rotary evaporation (15 mm Hg, 20-25^{o}C). Purification by silica gel chromatography (5.0 cm x 8 cm column, gradient elution, TBME/Hexanes, 2, 4, 6, 8, 10, 12%, 25 mL each) afforded 70.8 mg (87%) of ether **23c**.

Data for **23c**

^{1}H-NMR: (500 MHz, $CDCl_3$)

7.34 – 7.27 (m, 3H, Ar), 7.24 – 7.15 (m, 3H, Ar), 7.01 (dd, *J* = 9.1, 16.4 Hz, 1H, HC(13) or HC(14)), 4.18 (d, *J* = 10.9 Hz, 1H, $H_2C(15)$), 4.14 (d, *J* = 13.3 Hz, 1H, $H_2C(2)$), 4.03 (d, *J* = 10.9 Hz, 1H, $H_2C(15)$), 3.94 (d, *J* = 13.2 Hz, 1H, $H_2C(2)$), 3.41 (dd, *J* = 12.5, 7.5 Hz, 1H, $H_2C(4)$), 3.14 (t, *J* = 11.9 Hz, 1H, $H_2C(4)$), 2.94 (t, *J* = 8.7 Hz, 1H, HC(7a)), 2.66 – 2.57 (dq, *J* = 19.8, 8.4 Hz, 1H, $H_2C(7)$), 2.32 (ddt, *J* = 17.7, 13.5, 6.8 Hz, 1H, HC(5)), 2.03 (dt, *J* = 14.5, 8.1 Hz, 1H, HC(7)), 1.99 – 1.80 (m, 3H, HC(5a), $H_2C(6)$, $H_2C(6)$), 1.53 (s, 3H, $H_3C(8)$), 0.99 (d, *J* = 6.4 Hz, 3H, $H_3C(20)$)

^{13}C-NMR: (500 MHz, $CDCl_3$)

150.95 (m, Ar), 141.68 (m, Ar), 139.68 (m, Ar), 137.37 (Ar), 128.54 (Ar), 127.89 (Ar), 127.42 (Ar), 126.25 (m), 122.43 (m), 111.63 (dd, *J* = 3.86, 17.4), 88.11 (C(1) or C(7b)), 82.14 (C(1) or C(7b)), 73.07 (C(4)), 70.60 (C(2)), 66.96 (C(15)), 60.94 (C(5a)), 59.98 (C(7a)), 34.18 (C(5)), 30.38 (C(6)), 25.82 (C(7)), 25.12 (C(8)), 17.00 (C(20)

IR: ($CDCl_3$, film)

3065 (w), 3032 (w), 2960 (s), 2929 (s), 2871 (s), 2393 (s), 2329 (s), 2279 (s), 2242 (w), 1634 (m), 1612 (m), 1516 (s), 1469 (s), 1381 (m), 1340 (m), 1301 (s), 1234 (m), 1172 (s), 1137 (m), 1116 (s), 1081 (s), 1049 (s), 1030 (s), 997 (m), 961 (w), 941 (w), 911 (s), 887 (w), 850 (m), 810 (m), 736 (s), 696 (s), 669 (w), 648 (w), 596 (w)

MS: (ESI, Q-tof)

414.2 (100) [M-1], 412.2 (70), 402.2 (30), 322.2 (12), 214.1 (4)

Mol. Formula: $C_{24}H_{29}BF_3NO$ (415.30)

HRMS: $C_{24}H_{28}BF_3NO^{+}$, (414.22)

Calcd: 414.2216

Found: 414.2213

TLC: R_f 0.35 (TBME/Hexanes, 1:9) [UV, I_2]

Preparation of *rel*-(1*S*,3*R*,5*S*,5a*S*,7a*S*,7b*R*) Octahydro-1-hexyloxy-1-(2,3,4-trifluorophenyl)-3-(3,5-bistrifluoromethylphenylmethyl)-5-methyl-7b-methylcyclopenta[*gh*]pyrrolizinium Bromide (23)

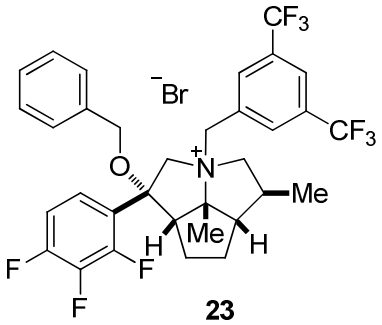

23

Data for **23**:

Yield: 48 mg (91%), free-flowing white powder

^{1}H-NMR: (500 MHz, $CDCl_3$)

8.24 (s, 2H), 7.97 (s, 1H), 7.53 – 7.44 (m, 1H), 7.26 (d, *J* = 3.3 Hz, 6H), 7.14 – 7.02 (m, 2H), 5.79 (bs, 1H), 4.95 (bs, 2H), 4.11 (d, *J* = 10.9 Hz, 1H), 3.94 (d, *J* = 10.9 Hz, 1H), 3.69 (d, *J* = 13.5 Hz, 1H), 3.42 (s, 1H), 2.97 (dd, *J* = 11.2, 6.5 Hz, 1H), 2.70 (s, 1H), 2.48 (d, *J* = 47.6 Hz, 2H), 2.29 – 2.09 (m, 4H), 2.05 – 1.89 (m, 2H), 1.21 (d, *J* = 6.3 Hz, 3H)

MS: (ESI, Q-tof)

628.2 (100) [M-Br^-]

Mol. Formula: $C_{33}H_{31}BrF_9NO$ (708.50)

HRMS: $C_{33}H_{31}F_9NO^+$, (628.23)

Calcd: 628.2262

Found: 628.2258

TLC: R_f 0.23 (CH_2Cl_2/MeOH, 9:1) [I_2]

Preparation of (1*R*,3*S*,5*S*,5a*S*,7a*S*,7b*R*)-Octahydro-1-hydroxy-1-(4-trifluoromethoxyphenyl)-5-methyl-7b-methyl-2*H*cyclopenta[*gh*]pyrrolizine•Borane (24a)

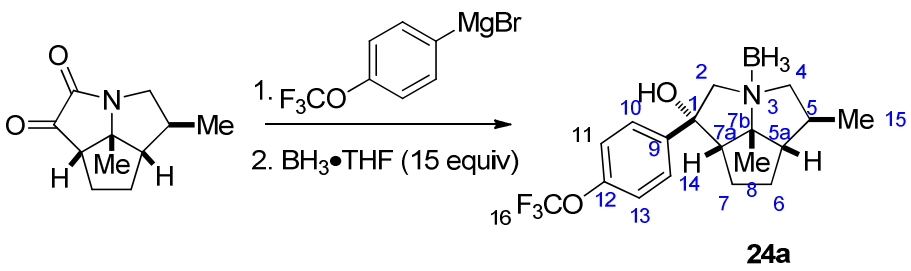

24a

To a 5-mL round-bottomed flask equipped with a nitrogen inlet adapter, a rubber septum, a reflux condenser, and a magnetic stir bar was added 21 (68 mg, 0.191 mmol) then BH_3•THF complex (2.9 mL, 2.9 mmol, 15 equiv). The reaction flask was immersed in an oil bath and heated to reflux (66 ^{o}C). After being stirred for 12 h at reflux, the solution was allowed to reach room temperature and was quenched with methanol (5 mL) and concentrated by rotary evaporation (15 mm Hg, 20-25^{o}C). The resulting colorless oil was purified by silica gel column chromatography (5.0 mm x 8 cm column, gradient elution, TBME/Heaxanes, 5, 10, 15, 20, 25, 30% 25 mL each) to afford 66.7 mg (94%) of 24a as a white solid

Data for **24a**

^{1}H-NMR: (500 MHz, $CDCl_3$)

7.42 (d, 2H, HC(10, HC(14)), 7.19 (d, J = 8.3 Hz, 2H, HC(11), HC(13)), 4.04 (d, J = 13.7 Hz, 1H, $H_2C(2)$), 3.66 (d, J = 13.5 Hz, 1H, $H_2C(4)$), 3.63 (dd, J = 7.6, 12.0, 1H, $H_2C(4)$), 3.25 (t, J = 11.5 Hz, 1H, $H_2C(4)$), 2.69 (dd, J = 9.2, 5.9 Hz, 1H, HC(7a)), 2.63 – 2.49 (m, 1H, HC(5)), 2.34 – 2.21 (m, 1H, $H_2C(7)$), 2.06 – 1.90 (m, 3H, HC(5a), $H_2C(6)$, $H_2C(6)$), 1.90 – 1.75 (m, 1H, $H_2C(7)$), 1.53 (s, 3H, $H_3C(8)$), 1.01 (d, J = 6.6 Hz, 3H, $H_3C(15)$)

^{13}C-NMR: (500 MHz, $CDCl_3$)

148.80 (m, C(12)), 143.71 (C(9)), 126.86 (C(10)), 121.21 (C(11)), 120.51 (q, J = 257.5 Hz, C(16)), 89.74 (C(1) or C(7b)), 79.09 (C(1) or C(7b)), 78.81 (C(2)), 74.52 (C(4)), 62.77 (C(7a)), 60.04 (C(5a)), 34.93 (C(5)), 31.49 (C(6)), 25.16 (C(8)), 24.32 (C(7)), 17.61 (C(15))

IR: ($CDCl_3$, film)

3468 (s), 2961 (s), 2930 (s), 2873 (m), 2381 (s), 2328 (s), 2272 (s), 1609 (w), 1593 (w), 1508 (s), 1458 (s), 1410 (w), 1380 (s), 1335 (w), 1258 (s), 1221 (s), 1169 (s), 1114 (m), 1085 (m), 1060 (m), 1017 (m), 1003 (m), 991 (m), 955

(m), 938 (m), 911 (s), 868 (w), 849 (m), 836 (m), 806 (w), 776 (w), 735 (s)

MS: (ESI, Q-tof)

352.2 (11) [M-3], 342.2 (100)

Mol. Formula: $C_{18}H_{25}BF_3NO_2$ (355.20)

HRMS: $C_{18}H_{22}BF_3NO_2^+$, (352.17)

Calcd: 352.1696

Found: 352.1695

TLC: R_f 0.28 (TBME/Hexanes, 1:3) [UV, I_2]

Preparation of (1*S*,3*S*,5*S*,5a*S*,7a*S*,7b*R*)-Octahydro-1-benzyloxy-1-(4-methoxyphenyl)-5-methyl-7b-methyl-2*H*cyclopenta[*gh*]pyrrolizine•Borane (24b)

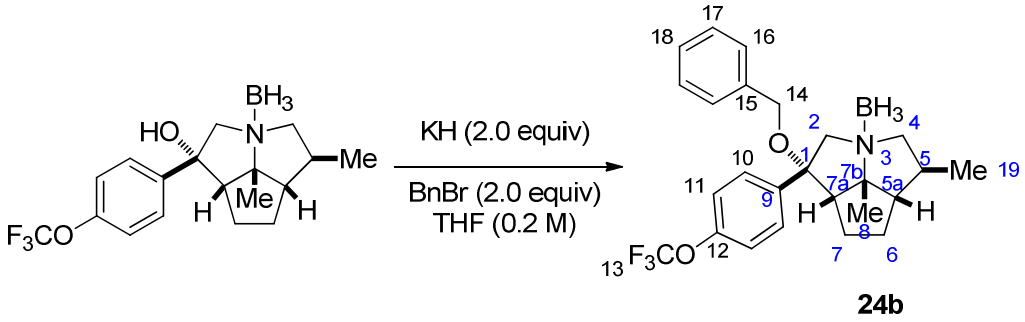

24b

To a two-necked, 5-mL, round-bottomed flask equipped with a nitrogen inlet adapter, a rubber septum and a magnetic stir bar was added washed potassium hydride (14.9 mg, 0.372 mmol, 2.0 equiv) from the drybox followed by THF (200 μL). A solution of alcohol **24a** (66 mg, 0.186 mmol) in THF (1.0 mL) is added to the reaction vessel by cannulation. After 15 min of stirring, the flask is immersed in an ice bath. The benzyl bromide (44.2 μL, 0.372 mmol, 2.0 equiv) is then added dropwise by syringe. The ice bath is removed and the solution is allowed to stir for 2 h at rt. This mixture was cooled in an ice bath and cold sat. aq. NH_4Cl (1.0 mL) is added in one portion. The resulting mixture was transferred to a 60-mL separatory funnel using an additional 15 mL of water and 15 mL of Et_2O and the aqueous phase was extracted with diethyl ether (3 x 15 mL). The organic extracts were washed with water (2 x 20 mL), and brine (1x 20 mL), then the combinded organic extracts were dried ($NaSO_4$). The mixture was filtered through a cotton plug and concentrated by rotary evaporation (15 mm Hg, 20-25°C). Purification by silica gel chromatography (5.0 cm x 8 cm column, gradient elution, TBME/Hexanes, 2, 4, 6, 8, 10, 12%, 25 mL each) afforded 70.8 mg (86%) of ether **24b**.

Data for **24b**

^{1}H-NMR: (500 MHz, $CDCl_3$)

7.47 (d, *J* = 8.8, 2H, HC(10)), 7.39 – 7.27 (m, 3H, HC(17), HC(18)), 7.25 (d, *J* = 8.4 Hz, 2H, HC(11)), 7.21 (d, *J* = 6.9 Hz, 2H, HC(16)), 4.15 (d, *J* = 11.0 Hz, 1H, $H_2C(2)$ or $H_2C(14)$), 4.12 (d, *J* = 13.5 Hz, 1H, $H_2C(2)$ or $H_2C(14)$), 3.99 (d, *J* = 11.0 Hz, 1H, $H_2C(2)$ or $H_2C(14)$), 3.95 (d, *J* = 13.5 Hz, 1H), $H_2C(2)$ or $H_2C(14)$), 3.44 (dd, *J* = 12.4, 7.6 Hz, 1H, $H_2C(4)$), 3.20 (t, *J* = 11.8 Hz, 1H, $H_2C(4)$), 2.80 (t, *J* = 8.0 Hz, 1H, HC(7a)), 2.72 – 2.58 (m, 1H, $H_2C(7)$), 2.43 (ddd, *J* = 16.9, 8.9, 5.5 Hz, 1H, HC(5)), 2.03 – 1.87 (m, 4H, HC(5a), $H_2C(6)$, $H_2C(6)$, $H_2C(7)$), 1.55 (s, 3H, $H_3C(8)$), 0.99 (d, *J* = 6.4 Hz, 3H, $H_3C(5)$).

^{13}C-NMR: (500 MHz, $CDCl_3$)

148.93 (C(12)), 140.49 (C(15)), 137.68 (C(9)), 128.55 (C(17)), 128.16 (C(10)), 127.81 (C(18)), 127.40 (C(16)), 120.93 (C(11)), 120.54 (q, *J* = 257.1 Hz, C(13)) 88.91 (C(1) or C(7b)), 83.10 (C(1) or C(7b)), 73.50 (C(4)), 70.87 (C(2) or C(14)), 66.52 (C(2) or C(14)), 61.59 (C(7a)), 60.61 (C(5a)), 34.48 (C(5)), 30.72 (C(6)), 25.12 (C(8)), 24.69 (C(7)), 17.11 (C(19))

IR: ($CDCl_3$, film)

3065 (w), 3032 (w), 2960 (s), 2929 (s), 2871 (s), 2386 (s), 2330 (s), 2276 (s), 1607 (w), 1594 (w), 1509 (s), 1455 (s), 1411 (w), 1380 (s), 1341 (w), 1258 (s), 1222 (s), 1171 (s), 1117 (s), 1085 (s), 1059 (s), 1016 (s), 992 (m), 956 (w), 912 (m), 844 (m), 810 (w), 810 (w), 734 (s), 698 (s), 647 (w), 602 (w)

MS: (ESI, 70 eV)

442.2 (100) [M-3], 432.2 (28), 271.1 (6)

Mol. Formula: $C_{25}H_{31}BF_3NO_2$ (445.33)

HRMS: $C_{25}H_{28}BF_3NO_2^+$, (442.22)

Calcd: 442.2165

Found: 442.2159

TLC: R_f 0.27 (TBME/Hexanes, 1:9) [UV, I_2]

Preparation of *rel*-(1*S*,3*R*,5*S*,5a*S*,7a*S*,7b*R*) Octahydro-1-hexyloxy-1-(2,3,4-trifluorophenyl)-3-(3-trifluoromethylphenylmethyl)-5-methyl-7b-methylcyclopenta[*gh*]pyrrolizinium Bromide (25)

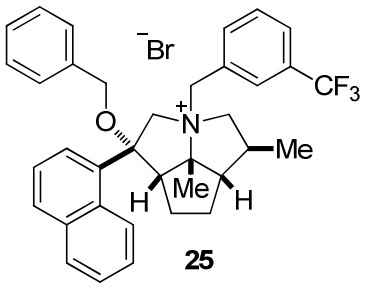

25

Data for **25**:

Yield: 17 mg (64%), free-flowing white powder

^{1}H-NMR: (500 MHz, $CDCl_3$)

8.51 (d, *J* = 8.7 Hz, 1H), 8.10 (d, *J* = 8.0, 2H), 8.02 (d, *J* = 7.4 Hz, 1H), 7.96 (d, *J* = 7.7 Hz, 1H), 7.75 (ddd, *J* = 8.4, 6.8, 1.3 Hz, 1H), 7.72 – 7.62 (m, 2H), 7.47 (d, *J* = 7.8, 1H), 7.33 (t, *J* = 7.8 Hz, 1H), 7.31 – 7.26 (m, 3H), 7.11 – 7.08 (m, 2H), 5.92 (s, 1H), 5.31 (d, *J* = 12.1 Hz, 1H), 5.17 (td, *J* = 12.0, 3.3 Hz, 1H), 4.64 (d, *J* = 13.1 Hz, 1H), 4.09 (d, *J* = 10.3 Hz, 1H), 3.87 – 3.81 (m, 2H), 3.65 (d, *J* = 13.0 Hz, 1H), 2.96 – 2.79 (m, 3H), 2.63 – 2.50 (m, 1H), 2.42 (s, 3H), 2.31 – 2.19 (m, 2H), 2.02 – 1.94 (m, 2H), 1.31 (d, *J* = 6.2 Hz, 3H)

MS: (ESI, Q-tof)

556.3 (100) [M-Br^-]

Mol. Formula: $C_{36}H_{37}BrF_3NO$ (636.58)

HRMS: $C_{36}H_{37}F_3NO^+$, (556.28)

Calcd: 556.2827

Found: 556.2833

TLC: R_f 0.30 (CH_2Cl_2/MeOH, 9:1) [I_2]

Preparation of *rel*-(1*S*,3*R*,5*S*,5a*S*,7a*S*,7b*R*) Octahydro-1-hexyloxy-1-(1-naphthyl)-3-(2,3,4-trifluorophenylmethyl)-5-methyl-7b-methylcyclopenta[*gh*]pyrrolizinium Bromide (26)

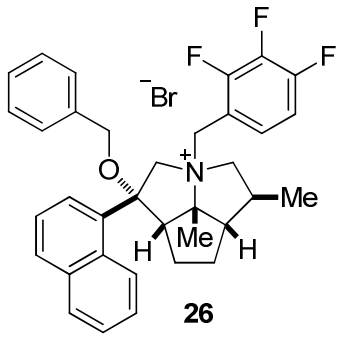

26

Data for **26**:

Yield: 22 mg (83%), free-flowing white powder

^{1}H-NMR: (500 MHz, $CDCl_3$)

8.46 (d, *J* = 8.7 Hz, 1H), 8.07 (t, *J* = 8.3 Hz, 2H), 7.99 (d, *J* = 7.4 Hz, 1H), 7.67 (t, *J* = 7.1 Hz, 1H), 7.63 (t, *J* = 7.7 Hz, 1H), 7.59 (ddd, *J* = 8.5, 6.9, 1.4 Hz, 1H), 7.42 (bs, 1H), 7.31 – 7.23 (m, 4H), 7.12 – 7.06 (m, 2H), 6.79 (dd, *J* = 8.1, 16.4 Hz, 1H), 5.13 (d, *J* = 12.7 Hz, 1H), 4.93 (t, *J* = 11.9 Hz, 1H), 4.47 (d, *J* = 13.0 Hz, 1H), 4.04 (d, *J* = 10.3 Hz, 1H), 3.89 (t, *J* = 9.4 Hz, 1H), 3.81 (d, *J* = 10.3 Hz, 1H), 3.78 (d, *J* = 13.1 Hz, 1H), 3.30 (d, *J* = 12.6 Hz, 1H), 3.03 (dd, *J* = 11.1, 5.8 Hz, 1H), 2.92 (dd, *J* = 10.9, 4.3 Hz, 1H), 2.67 – 2.52 (m, 1H), 2.43 (s, 3H), 2.36 – 2.23 (m, 2H), 2.04 – 1.95 (m, 2H), 1.31 (d, *J* = 6.3 Hz, 3H)

MS: (ESI, Q-tof)

542.3 (100) [M-Br^-]

Mol. Formula: $C_{35}H_{35}BrF_3NO$ (622.56)

HRMS: $C_{35}H_{35}F_3NO^+$, (542.27)

Calcd: 542.2671

Found: 542.2669

TLC: R_f 0.30 (CH_2Cl_2/MeOH, 9:1) [I_2]

Preparation of *rel*-(1*S*,3*R*,5*S*,5a*S*,7a*S*,7b*R*) Octahydro-1-hexyloxy-1-(1-naphthyl)-3-(3,5-bismethylphenylmethyl)-5-methyl-7b-methylcyclopenta[*gh*]pyrrolizinium Bromide (27)

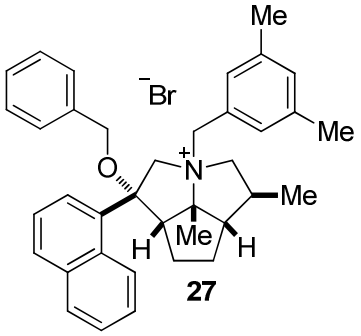

27

Data for **27**:

Yield: 20.4 mg (80%), free-flowing white powder

^{1}H-NMR: (500 MHz, $CDCl_3$)

8.53 (d, *J* = 8.6 Hz, 1H), 8.10 (dd, *J* = 8.2, 6.3 Hz, 2H), 8.03 (d, *J* = 7.3 Hz, 1H), 7.73 (dd, *J* = 8.2, 6.8 Hz, 1H), 7.69 – 7.61 (m, 2H), 7.35 – 7.20 (m, 5H), 7.10 – 7.08 (m, 2H), 6.80 (s, 1H), 6.03 (s, 2H), 5.08 – 4.94 (m, 2H), 4.73 (d, *J* = 13.1 Hz, 1H), 4.08 (d, *J* = 10.4 Hz, 1H), 3.82 (dd, *J* = 10.4, 7.3 Hz, 2H), 3.56 (d, *J* = 13.1 Hz, 1H), 2.98 (dd, *J* = 11.4, 5.8 Hz, 1H), 2.96 – 2.90 (m, 1H), 2.82 (d, *J* = 11.9 Hz, 1H), 2.56 (dq, *J* = 14.0, 11.0, 10.1 Hz, 1H), 2.37 (s, 3H), 2.30 – 2.14 (m, 2H), 2.02 – 1.94 (m, 2H), 1.93 (s, 6H), 1.33 (d, *J* = 6.3 Hz, 3H)

MS: (ESI, Q-tof)

516.3 (100) [M-Br^-]

Mol. Formula: $C_{37}H_{42}BNO$ (596.64)

HRMS: $C_{37}H_{42}NO^+$, (516.33)

Calcd: 516.3266

Found: 516.3259

TLC: R_f 0.33 (CH_2Cl_2/MeOH, 9:1) [I_2]

Preparation of *rel*-(1*S*,3*R*,5*S*,5a*S*,7a*S*,7b*R*) Octahydro-1-hexyloxy-1-(1-naphthyl)-3-(2,3-difluorophenylmethyl)-5-methyl-7b-methylcyclopenta[*gh*]pyrrolizinium Bromide (28)

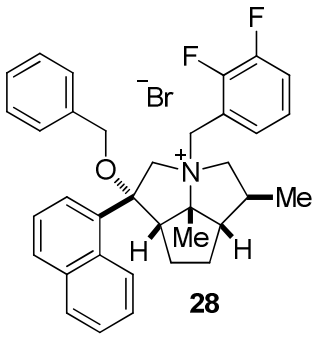

28

Data for **28**:

Yield: 17.5 mg (68%), free-flowing white powder

^{1}H-NMR: (500 MHz, $CDCl_3$)

8.48 (d, *J* = 8.6 Hz, 1H), 8.12 – 7.98 (m, 3H), 7.72 – 7.62 (m, 2H), 7.59 (ddd, *J* = 8.4, 6.9, 1.4 Hz, 1H), 7.30 – 7.24 (m, 3H), 7.16 – 7.00 (m, 4H), 6.87 – 6.82 (m, 1H), 5.04 (d, *J* = 12.7 Hz, 1H), 4.84 – 4.77 (m, 1H), 4.53 (d, *J* = 13.1 Hz, 1H), 4.05 (d, *J* = 10.4 Hz, 1H), 3.95 (t, *J* = 9.3 Hz, 1H), 3.86 – 3.74 (m, 2H), 3.32 (d, *J* = 12.6 Hz, 1H), 3.09 (dd, *J* = 5.8, 11.2 Hz, 1H), 2.94 – 2.89 (m, 1H), 2.65– 2.55 (m, 1H), 2.42 (s, 3H), 2.36 – 2.26 (m, 2H), 2.04 – 1.98 (m, 2H), 1.31 (d, *J* = 6.3 Hz, 3H)

MS: (ESI, Q-tof)

524.3 (100) [M-Br^-]

Mol. Formula: $C_{35}H_{36}BrF_2NO$ (604.57)

HRMS: $C_{35}H_{36}F_2NO^+$, (524.28)

Calcd: 524.2765

Found: 524.2765

TLC: R_f 0.31 (CH_2Cl_2/MeOH, 9:1) [I_2]

7.7.2. Preparation of Compounds for Scheme 22

Preparation of (1*S*,3*S*,5*S*,5a*S*,7a*S*,7b*R*)-Octahydro-1-hydroxy-1-(3-quinoline)-5-methyl-7b-methyl-2*H*cyclopenta[*gh*] pyrrolizin-2-one (30)

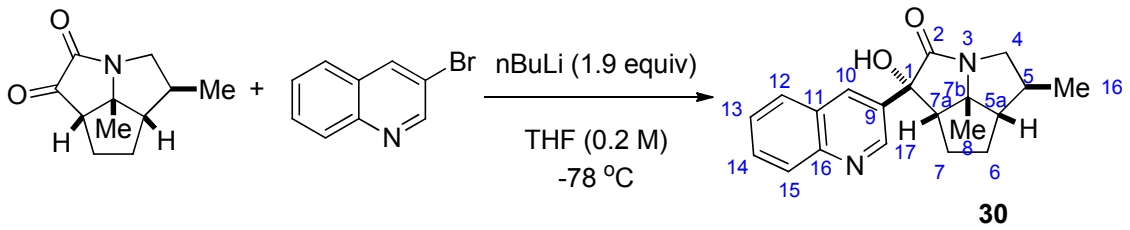

To a 5-mL, two-necked, round-bottomed flask equipped with a nitrogen inlet adapter, a rubber septum and a magnetic stir bar was added THF (0.325 mL) and the flask was immersed in an IPA/$CO_{2(s)}$ bath. Next, n-BuLi (197 μL, 0.492 mmol, 1.9 equiv) is added and then 3-bromoquinoline is added by cannulation as a solution in THF (0.65 mL) dropwise while maintaining an internal temperature < -70 °C. After strring for 1 h at -78 °C, ketoamide **21** is added by cannulation as a solution in THF (325 μL). The solution is allowed to stir for 3 h at -78 °C. The IPA/$CO_{2(s)}$ bath is removed and allowed to stir at rt for 1 h. The solution is cooled in an ice bath and sat. aq. NH_4Cl (1.0 mL) is added. The mixture was transferred to a 60-mL separatory funnel with 20 mL of Et_2O and 20 mL of H_2O. The layers were separated and the aqueous extract was washed with Et_2O (2 x 15 mL). The organic extracts were washed with H_2O (1 x 25 mL), brine (1 x 25 mL), and the combined organic extracts were dried over Na_2SO_4, filtered (cotton plug), and concentrated by rotary evaporation (15 mm Hg, 20-25°C). The resulting oil was purified by silica gel column chromatography (5 mm x 10 cm, gradient elution, EtOAc/Hexanes, 10, 20, 30, 40, 60% 25 mL each) to afford **30** (72.3 mg, 867%) as a pale yellow solid.

Data for **30**:

^{1}H-NMR: (500 MHz, $CDCl_3$)

9.05 (d, *J* = 2.0 Hz, 1H, HC(17)), 8.05 (d, *J* = 8.4 Hz, 1H, HC(15)), 7.95 (s, 1H, HC(10)), 7.75 – 7.59 (m, 2H, HC(12), HC(14)), 7.48 (t, *J* = 7.5 Hz, 1H, HC(13)), 4.20 (dd, *J* = 11.7, 7.2 Hz, 1H, $H_2C(4)$), 4.01 (bs, 1H, OH), 2.69 (dd, *J* = 9.2, 7.2 Hz, 1H, HC(7a)), 2.63 (dd, *J* = 11.7, 10.1 Hz, 1H, $H_2C(4)$), 2.03 (m, 1H, $H_2C(7)$), 1.80 (m, 3H, HC(5a), $H_2C(6)$, $H_2C(7)$), 1.72 – 1.63 (m, 1H, HC(5)), 1.54 – 1.45 (m, 1H, $H_2C(6)$), 1.06 (d, *J* = 6.7 Hz, 3H, $H_3C(16)$), 0.90 (s, 3H, $H_3C(8)$)

^{13}C-NMR: (500 MHz, $CDCl_3$)

175.62 (C(2)), 150.20 (C(17)), 147.55 (C(16)), 136.47 (C(9)), 132.87 (C(10)), 129.76 (C(12) or C(14)), 129.22 (C(15)), 128.19 (C(12) or C(14)), 127.17 (C(11)), 127.01 (C(13)), 81.62 (C(1)), 75.52 (C(7b)), 59.00 (C(5a)), 57.78 (C(7a)), 51.20 (C(4)), 41.84 (C(5)), 30.31 (C(6)), 27.34 (C(7)), 24.23 (C(8)), 17.78 (C(16))

IR: ($CDCl_3$, film)

3358 (s), 3065 (m), 2958 (s), 2929 (s), 2870 (s), 1693 (s), 1622 (w), 1605 (w), 1573 (m), 1495 (s), 1460 (s), 1404 (s), 1378 (s), 1357 (s), 1332 (s), 1313 (m), 1285 (m), 1250 (w), 1230 (s), 1204 (s), 1181 (m), 1136 (s), 1078 (s), 1057 (m), 1035 (m), 1026 (w), 997 (w), 976 (w), 960 (w), 912 (s), 865 (w), 808 (w), 787 (w)

MS: (ESI, Q-tof)

323.2 (100) [M+1]

Mol. Formula: $C_{20}H_{22}N_2O_2$ (322.17)

HRMS: $C_{20}H_{23}N_2O_2^+$, (323.17)

Calcd: 323.1760

Found: 323.1748

TLC: R_f 0.24 (EtOAc/Hexanes, 2:3) [UV, I_2]

Preparation of (1*S*,3*S*,5*S*,5a*S*,7a*S*,7b*R*)-Octahydro-1-benzyloxy-1-(3-quinoline)-5-methyl-7b-methyl-2*H*cyclopenta[*gh*] pyrrolizin-2-one (31)

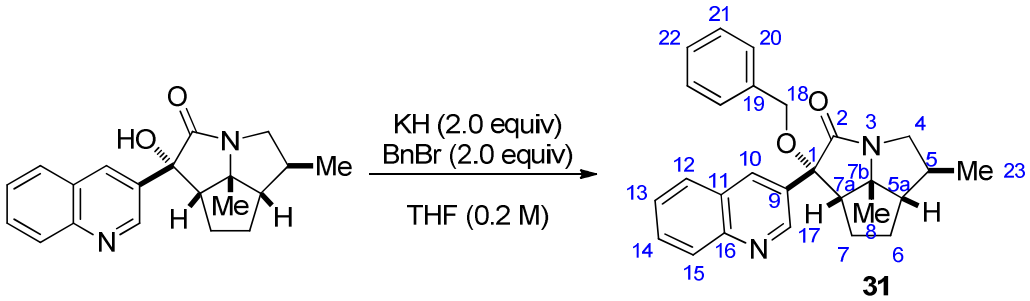

To a two-necked, 5-mL, round-bottomed flask equipped with a nitrogen inlet adapter, a rubber septum and a magnetic stir bar was added washed potassium hydride (17 mg, 0.196 mmol, 2.0 equiv) from the drybox followed by THF (400 μL). A solution of alcohol **30** (70.7 mg, 0.219 mmol) in THF (1.0 mL) is added to the reaction vessel by cannulation. After 15 min

of stirring, the flask is immersed in an ice bath. The benzyl bromide (27.4 μL, 0.230 mmol, 1.05 equiv) is then added dropwise by syringe. The ice bath is removed and the solution is allowed to stir for 2 h at rt. This mixture was cooled in an ice bath and H_2O (1.0 mL) is added in one portion. The resulting mixture was transferred to a 60-mL separatory funnel using an additional 15 mL of water and 15 mL of Et_2O and the aqueous phase was extracted with diethyl ether (3 x 15 mL). The organic extracts were washed with water (2 x 20 mL), and brine (1x 20 mL), then the combinded organic extracts were dried ($NaSO_4$). The mixture was filtered through a cotton plug and concentrated by rotary evaporation (15 mm Hg, 20-25°C). Purification by silica gel chromatography (5.0 cm x 8 cm column, gradient elution, EtOAc/Hexanes, 5, 10, 20, 30, 40%, 25 mL each) afforded 66 mg (73%) of ether **31**.

Data for **31**:

^{1}H-NMR: (500 MHz, $CDCl_3$)

9.15 (d, *J* = 2.3 Hz, 1H, HC(17)), 8.27 (d, *J* = 2.3 Hz, 1H, HC(10)), 8.16 (d, *J* = 8.4 Hz, 1H, HC(12)), 7.88 (dd, *J* = 8.3, 1.5 Hz, 1H, HC(15)), 7.78 (ddd, *J* = 8.4, 6.8, 1.5 Hz, 1H, HC(13)), 7.61 (t, *J* = 7.5 Hz, 1H, HC(14)), 7.36 – 7.16 (m, 5H, HC(20), HC(21), HC(22)), 5.24 (d, *J* = 11.4 Hz, 1H, H_2C(18)), 4.31 (dd, *J* = 11.7, 6.2 Hz, 1H, H_2C(4)), 4.11 (d, *J* = 11.4 Hz, 1H, H_2C(18)), 2.83 (dd, *J* = 9.8, 7.4 Hz, 1H, HC(7a)), 2.64 (dd, *J* = 10.0, 11.7, 1H, H_2C(4)), 2.19 – 2.03 (m, 2H, H_2C(7), H_2C(7)), 1.86 – 1.76 (m, 3H, HC(5), HC(5a), H_2C(6)), 1.59 (m, 1H, H_2C(6)), 1.12 (d, *J* = 5.9 Hz, 3H, H_3C(23)), 0.90 (s, 3H, H_3C(8))

^{13}C-NMR: (500 MHz, $CDCl_3$)

174.60 (C(2)), 150.54 (C(17)), 147.87 (C(16)), 139.01 (C(19)), 135.62 (C(10)), 133.02 (C(9)), 130.20 (C(13)), 129.34 (C(12)), 128.32 (C(15)), 128.20 (C(14)), 127.50 (C(20) or C(21) or C(22)), 127.32 (C(20) or C(21) or C(22)), 127.24 (C(20) or C(21) or C(22)), 127.20 (C(11)), 86.25 (C(1) or C(7b)), 74.48 (C(1) or C(7b)), 66.81 (C(18)), 59.23 (C(5a)), 58.50 (C(7a)), 50.84 (C(4)), 42.13 (C(5)), 30.43 (C(6)), 27.60 (C(7)), 24.31 (C(8)), 17.69 (C(23))

IR: ($CDCl_3$, film)

3089 (w), 3065 (w), 3033 (w), 2959 (s), 2928 (s), 2870 (s), 1693 (s), 1682 (s),

1620 (w), 1606 (w), 1585 (w), 1571 (m), 1495 (s), 1461 (s), 1453 (s), 1394 (s), 1371 (s), 1331 (m), 1312 (w), 1285 (m), 1253 (w), 1230 (s), 1204 (m), 1181 (m), 1145 (s) , 1096 (s), 1065 (s), 1029 (s), 1015 (w), 1000 (s), 959 (w), 909 (s), 864 (w), 832 (w), 810 (w), 789 (w)

MS: (ESI, Q-tof)

413.2 (100) [M+1], 338.3 (18), 307.2 (6)

Mol. Formula: $C_{27}H_{28}N_2O_2$ (412.52)

HRMS: $C_{27}H_{29}N_2O_2^+$, (413.22)

Calcd: 413.2229

Found: 413.2226

TLC: R_f 0.46 (EtOAC/Hexanes, 1:1) [UV, I_2]

Preparation of (1*S*,3*S*,5*S*,5a*S*,7a*S*,7b*R*)-Octahydro-1-benzyloxy-1-(3-quinoline)-5-methyl-7b-methyl-2*H*cyclopenta[*gh*] pyrrolizin-2-thione (32)

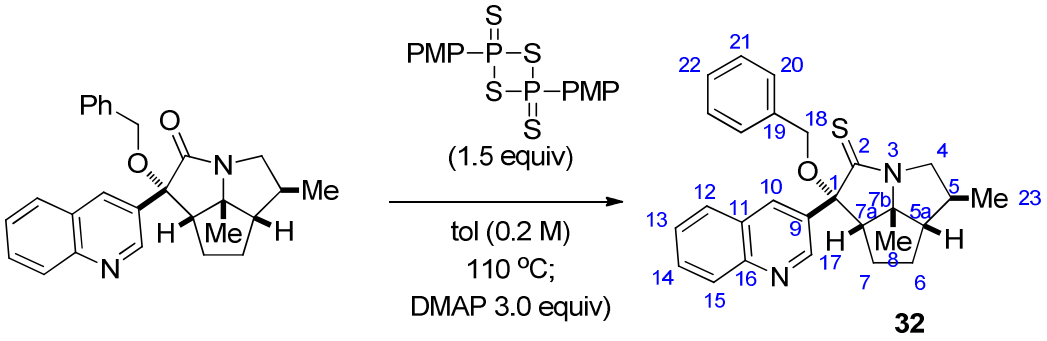

To a 5-mL, two-necked, round-bottomed flask equipped with a nitrogen inlet adapter, a rubber septum and a magnetic stir bar was added **31** (48 mg, 0.116 mmol) followed by Lawesson's reagent (71 mg, 0.175 mmol) and toluene (600 μL). The reaction flask was place in an oil bath at 110 °C. After 4 h, the oil bath is removed and DMAP (42.6 mg, 0.349 mmol) is added. The mixture was concentrated by rotary evaporation (15 mm Hg, 20-25°C). Purification by silica gel chromatography (5 mm x 6 cm column, gradient elution, Et_2O/CH_2Cl_2, 0, 1, 2, 4, 8%, 20 mL each) afforded 48.2 mg (75%) of **32**.

Data for **32**:

^{1}H-NMR: (500 MHz, $CDCl_3$)

9.14 (d, J = 2.3 Hz, 1H, HC(17)), 8.45 (d, J = 2.3 Hz, 1H, HC(10)), 8.14 (d, J

= 8.5 Hz, 1H, HC(12)), 7.88 (d, *J* = 8.1 Hz, 1H, HC(15)), 7.77 (ddd, *J* = 8.5, 6.7, 1.4 Hz, 1H, HC(13)), 7.60 (t, *J* = 7.5 Hz, 1H, HC(14)), 7.27 (dt, *J* = 10.9, 7.2 Hz, 4H, $H_2C(20)$, $H_2C(21)$), 7.21 (t, *J* = 6.9 Hz, 1H, HC(22)), 5.66 (d, *J* = 11.7 Hz, 1H, $H_2C(18)$), 4.88 (dd, *J* = 11.9, 6.3 Hz, 1H, $H_2C(4)$), 4.14 (d, *J* = 11.7 Hz, 1H, $H_2C(18)$), 2.98 (dd, *J* = 9.8, 7.4 Hz, 1H, HC(7a)), 2.92 (t, *J* = 10.4 Hz, 1H, $H_2C(4)$), 2.22 – 2.02 (m, 2H, $H_2C(7)$, $H_2C(7)$), 1.97 – 1.76 (m, 3H, HC(5), HC(5a), $H_2C(6)$), 1.62 – 1.51 (m, 1H, $H_2C(6)$), 1.16 (d, *J* = 5.9 Hz, 3H, $H_3C(23)$), 0.90 (s, 3H, $H_3C(8)$)

^{13}C-NMR: (500 MHz, $CDCl_3$)

201.28 (C(2)), 150.65 (C(17)), 147.76 (C(16)), 139.21 (C(19)), 136.09 (C(10)), 132.94 (C(9)), 130.26 (C(13)), 129.25 (C(12)), 128.51 (C(15)), 128.11 (C(21)), 127.33 (C(20)), 127.28 (C(14)), 127.14 (C(11)), 127.11 (C(22)), 92.81 (C(1) or C(7b)), 80.83 (C(1) or C(7b)), 67.25 (C(18)), 60.63 (C(7a)), 58.59 (C(5)), 54.07 (C(4)), 40.29 (C(5a)), 30.86 (C(6)), 27.73 (C(7)), 23.08 (C(8)), 17.94 (C(23))

IR: ($CDCl_3$ film)

3064 (w), 3030 (w), 2954 (s), 2929 (s), 2869 (s), 1621 (w), 1605 (w), 1572 (m), 1470 (s), 1454 (s), 1431 9s), 1378 (m), 1355 (m), 1330 (m), 1289 (m), 1268 (w), 1251 (s), 1201 (m), 1177 (m), 1154 (w), 1125 (s), 1096 (m), 1054 (m), 1026 (m), 994 (w), 961 (w), 909 (w), 854 (w), 802 (w), 788 (m), 724 9s), 705 (m), 647 (m)

MS: (ESI, Q-tof)

429.2 (100) [M+1], 323.2 (8)

Mol. Formula: $C_{27}H_{28}N_2OS$ (428.59)

HRMS: $C_{27}H_{29}N_2OS^+$: (429.20)

Calcd: 429.2001

Found: 429.2001

TLC: R_f 0.27 (CH_2Cl_2) [UV, I_2]

Preparation of (1*S*,3*S*,5*S*,5a*S*,7a*S*,7b*R*)-Octahydro-1-benzyloxy-1-(3-quinoline)-5-methyl-7b-methyl-2*H*cyclopenta[*gh*] pyrrolizine (33)

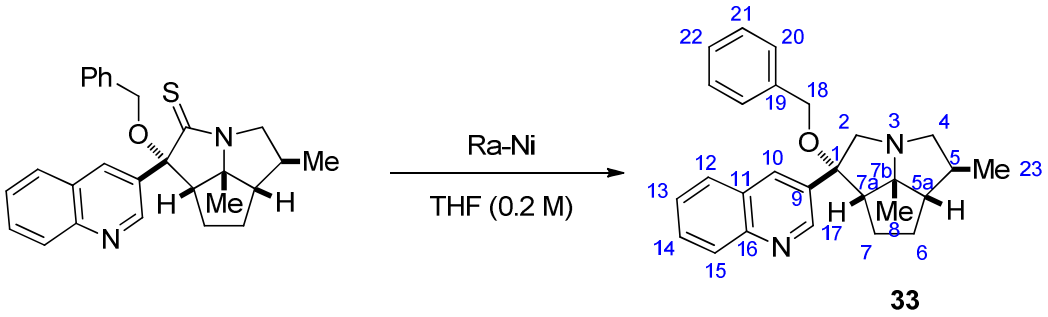

33

To a 5-mL, two-necked, round-bottomed flask equipped with a nitrogen inlet adapter, and a magnetic stir bar was added raney nickel (40 mg) which is then washed with H_2O (3 x 10 mL) followed by THF (3 x 10 mL). Thioamide **32** (57 mg, 0.143 mmol) is added to the reaction flask in THF (1.0 mL). The mixture is stirred vigorously for 12 h at rt. The mixture is filtered with celite and rinsed with ethanol (3 x 20 mL) and concentrated by rotary evaporation (15 mm Hg, 20-25 ^{o}C). The resulting yellow oil is purified by silica gel column chromatography (2 cm x 8 cm, MeOH/CH_2Cl_2, 1, 2, 3, 4, 6, 8%, 25 mL each) to furnish **33** (28.6 mg, 50%) as a white solid.

Data for **33**:

^{1}H-NMR: (500 MHz, $CDCl_3$)

9.25 (d, J = 2.3 Hz, 1H), 8.53 (s, 1H), 8.13 (d, J = 8.4 Hz, 1H), 7.95 (d, J = 7.7 Hz, 1H), 7.73 (ddd, J = 8.5, 6.8, 1.4 Hz, 1H), 7.58 (t, J = 7.5 Hz, 1H), 7.30 (dd, J = 7.9, 6.3 Hz, 2H), 7.28 – 7.21 (m, 3H), 4.11 (s, 2H), 3.92 (s, 1H), 3.34 (d, J = 9.6 Hz, 1H), 3.00 (dd, J = 12.3, 6.2 Hz, 1H), 2.64 (d, J = 14.6 Hz, 1H), 2.46 (t, J = 9.3 Hz, 1H), 2.29 – 2.03 (m, 3H), 1.72 (ddd, J = 15.0, 9.5, 4.4 Hz, 3H), 1.04 (d, J = 6.4 Hz, 3H), 0.94 – 0.76 (m, 3H)

^{13}C-NMR: (500 MHz, $CDCl_3$)

151.28, 147.57, 138.63, 134.42, 129.53, 129.21, 128.43, 127.56, 127.51, 127.34, 126.81, 85.12, 77.41, 77.16, 76.91, 67.31, 62.41, 61.43, 60.61, 60.13, 37.93, 31.73, 29.66, 29.40, 27.85, 22.80, 16.72, 14.26

MS: (ESI, Q-tof)

399.2 (100) [M+1]

Mol. Formula: $C_{27}H_{30}N_2O$ (398.54)

HRMS: $C_{27}H_{31}N_2O^{+}$: (399.24)

Calcd: 399.2436

Found: 399.2432

IR: ($CDCl_3$ film)

3052 (w), 3032 (w), 2952 (s), 2921 (s), 2858 (s), 1618 (w), 1606 (w), 1572 (w), 1495 (s), 1454 (s), 1417 (w), 1372 (s), 1327 (m), 1276 (w), 1246 (m), 1219 (w), 1147 (m), 1116 (s), 1092 (s), 1053 (m), 1040 (m), 1026 (m), 967 (w), 910 (s), 859 (w), 789 (m), 733 (s), 698 (m), 643 (w)

TLC: R_f 0.33 (MeOH/CH_2Cl_2 1:19) [UV, I_2]

Preparation of *rel*-(1*S*,3*R*,5*S*,5a*S*,7a*S*,7b*R*) Octahydro-1-hexyloxy-1-(3-quinoline)-3-(3,5-bistrifluoromethylphenylmethyl)-5-methyl-7b-methylcyclopenta[*gh*]pyrrolizinium Bromide (35)

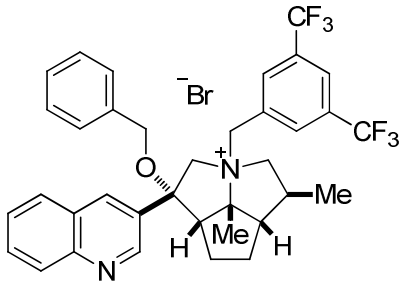

35

Data for **35**:

Yield: 19 mg (38%), free-flowing white powder

^{1}H-NMR: (500 MHz, $CDCl_3$)

9.13 (d, *J* = 2.5 Hz, 1H), 8.82 (s, 1H), 8.19 – 8.17 (m, 3H), 8.11 (d, *J* = 8.1 Hz, 1H), 7.94 (s, 1H), 7.84 (t, *J* = 7.2, 1H), 7.68 (t, *J* = 6.2 Hz, 1H), 7.30 – 7.19 (m, 3H), 7.13 – 7.06 (m, 2H), 5.64 (d, *J* = 12.2 Hz, 1H), 5.06 (bs, 1H), 4.69 (bs, 1H), 4.45 (bs, 1H), 4.19 (d, *J* = 11.0 Hz, 1H), 3.94 (d, *J* = 11.0 Hz, 1H), 3.79 (d, *J* = 13.2 Hz, 1H), 3.46 (t, *J* = 8.7 Hz, 1H), 2.99 (dd, *J* = 11.3, 6.7 Hz, 1H), 2.74 – 2.48 (m, 3H), 2.28 (s, 3H), 2.21 – 2.15 (m, 1H), 2.11 – 1.96 (m, 2H), 1.24 (d, *J* = 6.3 Hz, 3H)

MS: (ESI, Q-tof)

625.3 (100) [M-Br^-]

Mol. Formula: $C_{36}H_{35}BrF_6N_2O$ (705.57)

HRMS: $C_{36}H_{35}F_6N_2O^+$, (625.27)
Calcd: 625.2654
Found: 625.2666

TLC: R_f 0.22 (CH_2Cl_2/MeOH, 9:1) [I_2]

Preparation of Compound 36 from Scheme 23

Preparation of (1*S*,3*S*,5*S*,5a*S*,7a*S*,7b*R*)-Octahydro-1-hydroxy-1-(2-naphthyl)-5-methyl-7b-methyl-2*H*cyclopenta[*gh*] pyrrolizin-2-one (36a)

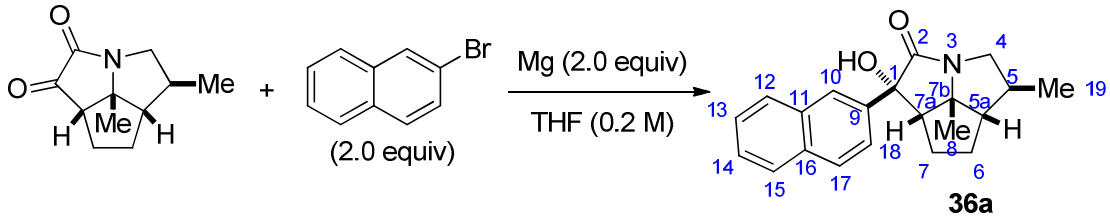

To a 5-mL, two-necked, round-bottomed flask equipped with a nitrogen inlet adapter, a rubber septum and a magnetic stir bar was added **21** (40 mg, 0.207 mmol) followed by THF (400 μL). The flask was immersed in an ice bath and 2-naphthylmagnesium bromide (600 μL, 0.414. mmol, 1.5 equiv, in THF) was added dropwise via syringe. After being stirred for 10 min, the cooling bath was removed and the reaction was stirred at room temperature for 20 min. The solution was cooled in an ice bath and sat. aq. NH_4Cl (1.0 mL) is added. The resulting mixture was transferred to a 60-mL separatory funnel using an additional 20 mL of water and 20 mL of Et_2O and the aqueous phase was extracted with diethyl ether (3 x 15 mL). The organic extracts were washed with water (2 x 20 mL), and brine (1x 20 mL), then the combinded organic extracts were dried ($NaSO_4$). The mixture was filtered through a cotton plug and concentrated by rotary evaporation (15 mm Hg, 20-25°C). Purification by silica gel chromatography (5.0 cm x 8 cm column, gradient elution, EtOAc/Hexanes, 10, 20, 30, 50%, 25 mL each) afforded 63 mg (95%) of **36a**.

Data for **36a**

^{1}H-NMR: (500 MHz, $CDCl_3$)
7.87 – 7.75 (m, 4H, ArH), 7.63 (dd, J = 8.5, 1.9 Hz, 1H, ArH), 7.52 – 7.43 (m, 2H, ArH), 4.25 (dd, J = 11.7, 7.2 Hz, 1H, H_2C(4)), 3.32 (s, 1H, OH), 2.73 (dd,

J = 9.5, 7.2 Hz, 1H, HC(7a)), 2.67 (dd, J = 11.7, 10.1 Hz, 1H, $H_2C(4)$), 2.06 – 2.00 (m, 1H, $H_2C(7)$), 1.90 – 1.66 (m, 4H, HC(5), HC(5a), $H_2C(6)$, $H_2C(7)$), 1.55 – 1.50 (m, 1H, $H_2C(6)$), 1.09 (d, J = 6.6 Hz, 3H, $H_3C(19)$), 0.94 (s, 3H, $H_3C(8)$))

^{13}C-NMR: ($CDCl_3$, 500 MHz)

176.42 (Ar), 141.03 (Ar), 133.04 (Ar), 132.97 (Ar), 128.71 (Ar), 128.47 (Ar), 127.64 (Ar), 126.40 (Ar), 126.33 (Ar), 125.26 (Ar), 124.96 (Ar), 83.05 (C(1) or C(7b)), 75.46 (C(1) or C(7b)), 58.84 (C(5a)), 57.88 (C(7a)), 51.11 (C(4)), 41.94 (C(5)), 30.31 (C(6)), 27.32 (C(7)), 24.08 (C(8)), 17.80 (C(19))

IR: ($CDCl_3$, film)

3306 (s), 3053 (s), 2962 (s), 2926 (s), 2869 (s), 1679 (s), 1632 (m), 1599 (w), 1503 (w), 1451 (s), 1422 (s), 1365 (s), 1352 (s), 1327 (m), 1310 (m), 1292 (m), 1247 (m), 1230 (s), 1207 (s), 1168 (w), 1139 (s), 1115 (w), 1094 (m), 1078 (s), 1062 (m), 1037 (m), 1022 (m), 979 (w), 967 (w), 953 (m), 907 (s), 868 (s), 816 (s), 805 (s), 732 (s), 652 (s)

MS: (ESI, Q-tof)

322.2 (42) [M+1], 304.2 (100), 178.9 (2), 142.0 (2), 100.1 (11)

Mol. Formula: $C_{21}H_{23}NO_2$ (321.41)

HRMS: $C_{21}H_{24}NO_2^+$, (322.18)

Calcd: 322.1807

Found: 322.1812

TLC: R_f 0.18 (EtOAc/Hexanes, 1:3) [UV, I_2]

Preparation of (1*R*,3*S*,5*S*,5a*S*,7a*S*,7b*R*)-Octahydro-1-hydroxy-1-(2-naphthyl)-5-methyl-7b-methyl-2*H*cyclopenta[*gh*]pyrrolizine•Borane (36b)

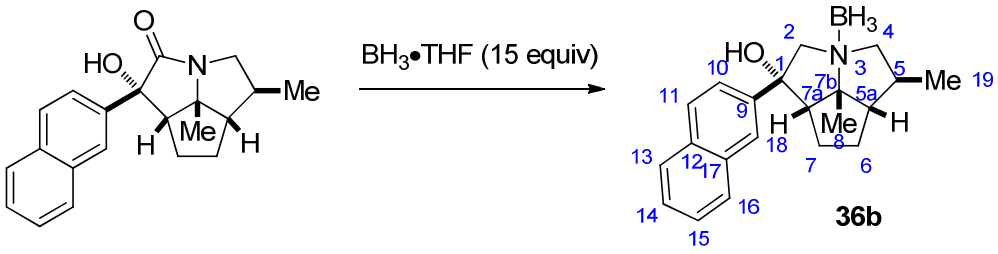

To a 5-mL round-bottomed flask equipped with a nitrogen inlet adapter, a rubber septum, a reflux condenser, and a magnetic stir bar was added sequentially **36a** (84.6 mg, 0.263 mmol) and BH_3•THF complex (4.0 mL, 1.0 M solution, 15 equiv). The reaction flask was immersed in an oil bath and heated to reflux (66 ^oC). After being stirred for 12 h at reflux, the solution was allowed to reach room temperature and was quenched with methanol (5 mL) and concentrated by rotary evaporation (15 mm Hg, 20-25^oC). The resulting colorless oil was purified by silica gel column chromatography (5.0 mm x 8 cm column, gradient elution, hexanes/TBME, 5, 10, 15, 20, 30% 25 mL each) to afford 84.3 mg (98%) of **36b** as a white solid

Data for **36b**

^{1}H-NMR: (500 MHz, $CDCl_3$)

7.86 – 7.77 (m, 4H, ArH), 7.54 – 7.47 (m, 2H, ArH), 7.45 (dd, *J* = 8.6, 2.0 Hz, 1H, ArH), 4.20 (d, *J* = 13.7 Hz, 1H, $H_2C(2)$), 3.72 (d, *J* = 13.6 Hz, 1H, $H_2C(2)$), 3.68 (dd, *J* = 12.2, 8.0 Hz, 1H, $H_2C(4)$), 3.29 (dd, *J* = 12.3, 10.7 Hz, 1H, $H_2C(4)$), 2.82 (dd, *J* = 9.1, 6.0 Hz, 1H, HC(7a)), 2.61 (dddd, *J* = 14.2, 10.4, 6.2, 2.2 Hz, 1H, HC(5)), 2.43 – 2.25 (m, 1H, $H_2C(7)$), 2.03 (s, 1H, OH), 2.0 – 1.86 (m, 4H, $H_2C(6)$, $H_2C(6)$, HC(5a), $H_2C(7)$), 1.57 (s, 3H, $H_3C(8)$), 1.03 (d, *J* = 6.6 Hz, 3H, $H_3C(19)$), 2.0 – 1.4 (m, 3H, H_3B)

^{13}C-NMR: (500 MHz, $CDCl_3$)

142.09 (C(9)), 132.96 (C(12) or C(17)), 132.73 (C(12) or C(17)), 129.00 (ArH), 128.30 (ArH), 127.64 (ArH), 126.72 (ArH), 126.60 (ArH), 123.60 (ArH), 123.45 (ArH), 89.70 (C(1) or C(7b)), 79.47 (C(1) or C(7b)), 78.72 (C(2)), 74.53 (C(4)), 62.64 (C(7a)), 59.91 (C(5a)), 34.82 (C(5)), 31.54 (C(6)), 25.12 (C(8)), 24.22 (C(7)), 17.68 (C(19))

IR: ($CDCl_3$, film)

3466 (s), 3058 (m), 2960 (s), 2928 (s), 2871 (s), 2392 (s), 2351 (s), 2327 (s), 2271 (s), 2241 (s), 1633 (w), 1600 (w), 1505 (m), 1455 (s), 1380 (s), 1341 (m), 1310 (m), 1275 (m), 1233 (m), 1171 (s), 1132 (s), 1060 (m), 1002 (s), 979 (m), 948 (m), 911 (s), 858 (s), 816 (s), 733 (s)

MS: (ESI, Q-tof)

318.2 (70) [M-3], 308.2 (100), 180.2 (3), 100.1 (6)

Mol. Formula:	$C_{21}H_{28}BNO$	(321.26)
HRMS:	$C_{21}H_{25}BNO^{+}$,	(318.20)
	Calcd:	318.2029
	Found:	318.2035
TLC:	R_f 0.22 (TBME/Hexanes, 1:4) [UV, I_2]	

Preparation of (1*S*,3*S*,5*S*,5a*S*,7a*S*,7b*R*)-Octahydro-1-benzyloxy-1-(2-naphthyl)-5-methyl-7b-methyl-2*H*cyclopenta[*gh*]pyrrolizine•Borane (36c)

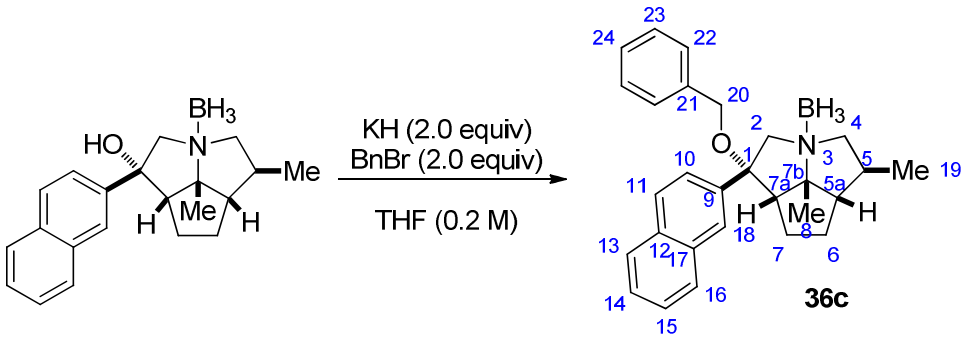

To a two-necked, 5-mL, round-bottomed flask equipped with a nitrogen inlet adapter, a rubber septum and a magnetic stir bar was added washed potassium hydride (21 mg, 2.0 equiv) from the drybox followed by THF (0.4 mL). A solution of alcohol **36b** in THF (0.9 mL) is added to the reaction vessel by cannulation. After 15 min of stirring, the flask is immersed in an ice bath. The benzyl bromide (62 μL, 2.0 equiv) is then added dropwise by syringe. The ice bath is removed and the solution is allowed to stir for 2 h at rt. This mixture was cooled in an ice bath and cold sat. aq. NH_4Cl (1.0 mL) is added in one portion. The resulting mixture was transferred to a 60-mL separatory funnel using an additional 15 mL of water and 15 mL of Et_2O and the aqueous phase was extracted with diethyl ether (3 x 15 mL). The organic extracts were washed with water (2 x 20 mL), and brine (1x 20 mL), then the combinded organic extracts were dried ($NaSO_4$). The floculant was filtered through a cotton plug and concentrated by rotary evaporation (15 mm Hg, 20-25°C). Purification by silica gel chromatography (5.0 cm x 8 cm column, gradient elution, hexanes/TBME, 2, 4, 6, 8, 10%, 25 mL each) afforded 101 mg (94%) of ether **36c**.

Data for **36c**

^{1}H-NMR: (500 MHz, $CDCl_3$)

7.98 – 7.80 (m, 4H, ArH), 7.55 (m, 3H, ArH), 7.32 (m, 3H, HC(23), HC(23), HC(24)), 7.23 (d, *J* = 7.3 Hz, 2H, HC(22), HC(22)), 4.33 (d, *J* = 13.3 Hz, 1H, $H_2C(2)$), 4.21 (d, *J* = 11.1 Hz, 1H, $H_2C(20)$), 4.07 (d, *J* = 13.3 Hz, 1H, $H_2C(2)$), 4.02 (d, *J* = 11.2 Hz, 1H, $H_2C(20)$), 3.52 (dd, *J* = 12.2, 7.8 Hz, 1H, $H_2C(4)$), 3.26 (t, *J* = 11.6 Hz, 1H, $H_2C(4)$), 2.93 (t, *J* = 8.4 Hz, 1H, HC(7a)), 2.85 – 2.71 (m, 1H, $H_2C(7)$), 2.53 (m, 1H, HC(5)), 2.11 – 1.87 (m, 4H, HC(5a), $H_2C(6)$, $H_2C(6)$, $H_2C(7)$), 1.58 (s, 3H, $H_3C(8)$), 1.02 (d, *J* = 6.5 Hz, 3H, $H_3C(19)$)

^{13}C-NMR: (500 MHz, $CDCl_3$)

139.01 (C(19) or C(21), 137.93 (C(19) or (C(21)), 132.93 (C(12) or C(17)), 132.77 (C(12) or C(17)), 129.05 (C(Ar)), 128.46 (C(Ar)), 128.38 (C(Ar)), 127.65 (C(Ar)), 127.45 (C(22)), 126.60 (C(Ar)), 124.89 (C(Ar)), 124.75 (C(Ar)), 88.90 (C(2) or C(20)), 83.40 (C(2) of C(20)), 73.49 (C(4)), 70.51 (C(2)), 66.48 (C(20)), 61.77 (C(7a)), 60.32 (C(5a)), 34.40 (C(5)), 30.85(C(6)), 25.07(C(8)), 24.40(C(7)), 17.26 (C(19))

IR: ($CDCl_3$, film)

3060 (m), 3031 (m), 2958 (s), 2928 (s), 2870 (s), 2385 (s), 2328 (s), 2274 (s), 2241 (m), 1633 (w), 1501 (w), 1497 (m), 1455 (s), 1379 (s), 1348 (w), 1336 (w), 1284 (m), 1271 (m), 1236 (w), 1172 (s), 1136 (s), 1115 (s), 1085 (s), 106 1 (s), 1027 (s), 996 (w) 947 (w), 911 (s), 859 (s), 819 (s), 735 (s)

MS: (ESI, Q-tof)

408.3 (100) [M-3], 398.2 (40), 308.2 (3), 195.0 (4), 180.2 (11), 158.0 (4), 142.0 (4), 100.1 (23), 79.0 (5)

Mol. Formula: $C_{28}H_{34}BNO$ (411.39)

HRMS: $C_{28}H_{31}BNO^+$, (408.25)

Calcd: 408.2499

Found: 408.2500

TLC: R_f 0.32 (TBME/Hexanes, 1:9) [UV, I_2]

Preparation of *rel*-(1*S*,3*R*,5*S*,5a*S*,7a*S*,7b*R*) Octahydro-1-hexyloxy-1-(2-naphthyl)-3-(3,5-bistrifluoromethylphenylmethyl)-5-methyl-7b-methylcyclopenta[*gh*]pyrrolizinium Bromide

(36)

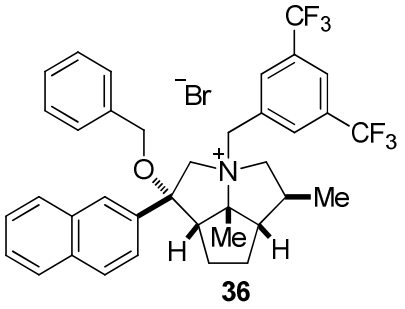

36

Data for **36**:

Yield: 30 mg (74%), free-flowing white powder

^{1}H-NMR: (500 MHz, $CDCl_3$)

8.25 (d, *J* = 1.9 Hz, 1H), 8.22 (d, *J* = 8.6 Hz, 1H), 8.02 – 7.98 (m, 2H), 7.95 (s, 2H), 7.89 (s, 1H), 7.74 (dd, *J* = 8.6, 1.9 Hz, 1H), 7.71 – 7.67 (m, 2H), 7.31 – 7.27 (m, 3H), 7.18 – 7.09 (m, 2H), 5.93 (d, *J* = 12.2 Hz, 1H), 5.36 (t, *J* = 11.6 Hz, 1H), 4.12 (d, *J* = 13.4 Hz, 1H), 4.06 (d, *J* = 10.6 Hz, 1H), 3.84 (d, *J* = 10.5 Hz, 1H), 3.73 – 3.59 (m, 2H), 3.39 (d, *J* = 12.2 Hz, 1H), 2.99 (dd, *J* = 11.1, 6.0 Hz, 1H), 2.87 (dd, *J* = 11.7, 4.7 Hz, 1H), 2.56 – 2.54 (m, 1H), 2.44 (s, 3H), 2.35 – 2.36 (m, 2H), 2.10 – 1.97 (m, 2H), 1.34 (d, *J* = 6.3 Hz, 3H)

MS: (ESI, Q-tof)

624.2 (100) [M-Br^-]

Mol. Formula: $C_{37}H_{36}BrF_6NO$ (704.58)

HRMS: $C_{37}H_{36}F_6NO^+$, (624.27)

Calcd: 624.2701

Found: 624.2693

TLC: R_f 0.28 (CH_2Cl_2/MeOH, 9:1) [I_2]

Preparation of Compounds from Table 18

Preparation of (1*S*,3*S*,5*S*,5a*S*,7a*S*,7b*R*)-Octahydro-1-hydroxy-1-(6-methoxy-2-naphthyl)-5-methyl-7b-methyl-2*H*cyclopenta[*gh*] pyrrolizin-2-one (37a)

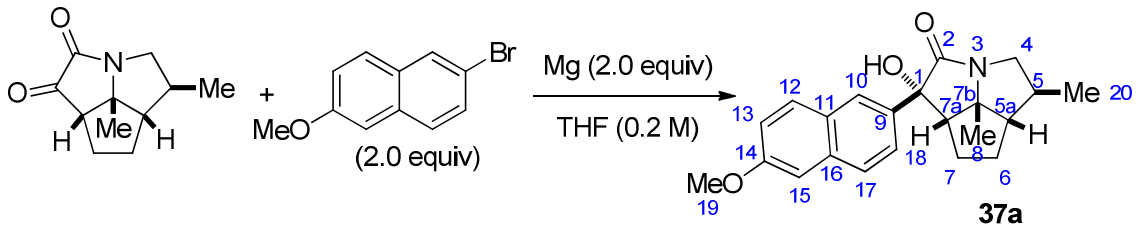

To a 5-mL, two-necked, round-bottomed flask equipped with a nitrogen inlet adapter, a rubber septum and a magnetic stir bar was added **21** (40 mg, 0.207 mmol) followed by THF (400 µL). The flask was immersed in an ice bath and 2-(6-methoxy)-naphthylmagnesium bromide (600 µL, 0.331 mmol, 1.6 equiv, in THF) was added dropwise via syringe. After being stirred for 10 min, the cooling bath was removed and the reaction was stirred at room temperature for 20 min. The solution was cooled in an ice bath and sat. aq. NH_4Cl (1.0 mL) is added. The resulting mixture was transferred to a 60-mL separatory funnel using an additional 20 mL of water and 20 mL of Et_2O and the aqueous phase was extracted with diethyl ether (3 x 15 mL). The organic extracts were washed with water (2 x 20 mL), and brine (1x 20 mL), then the combinded organic extracts were dried ($NaSO_4$). The mixture was filtered through a cotton plug and concentrated by rotary evaporation (15 mm Hg, 20-25°C). Purification by silica gel chromatography (5.0 cm x 8 cm column, gradient elution, EtOAc/Hexanes, 10, 20, 30, 50%, 25 mL each) afforded 58.3 mg (80.1%) of **37a**.

Data for **37a**

^{1}H-NMR: (500 MHz, $CDCl_3$)

7.73 – 7.67 (m, 3H, HC(10), HC(12), HC18)), 7.58 (dd, *J* = 8.6, 1.9 Hz, 1H, HC(17)), 7.13 (dd, *J* = 8.9, 2.5 Hz, 1H, HC(13)), 7.10 (s, 1H, HC(15)), 4.23 (dd, *J* = 11.7, 7.2 Hz, 1H, $H_2C(4)$), 3.91 (s, 3H, $H_3C(19)$), 3.32 (bs, 1H, OH), 2.72 (t, *J* = 7.2 Hz, 1H, HC(7a)), 2.65 (t, *J* = 11.1 Hz, 1H, $H_2C(4)$), 2.07 – 1.96 (m, 1H, $H_2C(7)$), 1.90 – 1.65 (m, 4H, HC(5), HC(5a), $H_2C(6)$, $H_2C(7)$), 1.54 – 1.49 (m, 1H, $H_2C(6)$), 1.09 (d, *J* = 6.6 Hz, 3H, $H_3C(20)$), 0.93 (s, 3H, $H_3C(8)$)

^{13}C-NMR: (500 MHz, $CDCl_3$)

176.53 (C(2)), 158.11 (C(14)), 138.78 (C(9) or C(16)), 134.23 (C(9) or C(16)), 129.91 (C(12)), 128.37, 127.51 (C(18)), 125.48 (C(17)), 125.13

(C(10)), 119.08 (C(13)), 105.68 (C(15)), 83.00 (C(1) or C(7b)), 75.42 (C(1) or C(7b)), 58.85 (C(5a)), 57.92 (C(7a)), 55.42 (C(19)), 51.07 (C(4)), 41.96 (C(5)), 30.32 (C(6)), 27.33 (C(7)), 24.04 (C(8)), 17.78 (C(20)

IR: ($CDCl_3$, film)

3393 (s), 3060 (w), 2957 (s), 2960 (s), 2870 (s), 1693 (s), 1634 (s), 1607 (s), 1504 (m), 1484 (m), 1480 (m), 1392 (s), 1356 (m), 1314 (w), 1267 (s), 1222 (s), 1203 (m), 1179 (m), 1135 (m), 1077 (w), 1034 (s), 910 (s), 853 (s), 810 (m), 732 (s), 698 (w), 667 (w), 646 (m)

MS: (ESI, Q-tof)

352.2 (13) [M+1], 334.2 (100), 178.9 (6), 142.0 (6)

Mol. Formula: $C_{22}H_{25}NO_3$ (351.44)

HRMS: $C_{22}H_{26}NO_3^+$, (352.19)

Calcd: 352.1913

Found: 352.1918

TLC: R_f 0.22 (TBME/Hexanes, 1:3) [UV, I_2]

Preparation of (1*R*,3*S*,5*S*,5a*S*,7a*S*,7b*R*)-Octahydro-1-hydroxy-1-(6-methoxy-2-naphthyl)-5-methyl-7b-methyl-2*H*cyclopenta[*gh*]pyrrolizine•Borane (37b)

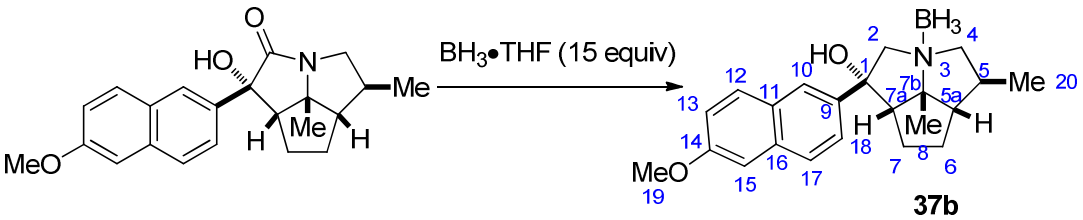

To a 5-mL round-bottomed flask equipped with a nitrogen inlet adapter, a rubber septum, a reflux condenser, and a magnetic stir bar was added **37a** (57 mg, 0.162 mmol) then BH_3•THF complex (2.8 mL, 2.4 mmol, 15 equiv). The reaction flask was immersed in an oil bath and heated to reflux (66 ^oC). After being stirred for 12 h at reflux, the solution was allowed to reach room temperature and was quenched with methanol (5 mL) and concentrated by rotary evaporation (15 mm Hg, 20-25^oC). The resulting colorless oil was purified by silica gel column chromatography (5.0 mm x 8 cm column, gradient elution, hexanes/TBME, 5, 10, 25, 20, 25, 30% 25 mL each) to afford 52 mg (91%) of **37b** as a white solid

Data for **37b**

^{1}H-NMR: (500 MHz, $CDCl_3$)

7.78 – 7.66 (m, 3H, ArH), 7.41 (dd, *J* = 8.5, 2.0 Hz, 1H, ArH), 7.16 (dd, *J* = 8.9, 2.5 Hz, 1H, ArH), 7.10 (d, *J* = 2.5 Hz, 1H, HC(15)), 4.18 (d, *J* = 13.7 Hz, 1H, $H_2C(2)$), 3.91 (s, 3H, $H_3C(19)$), 3.73 (d, *J* = 13.7 Hz, 1H, $H_2C(2)$), 3.69 (dd, *J* = 12.3, 8.2 Hz, 1H, $H_2C(4)$), 3.30 (t, *J* = 11.2 Hz 1H, $H_2C(4)$), 2.83 (dd, *J* = 9.0, 5.9 Hz, 1H, HC(7a)), 2.61 (ddt, *J* = 17.3, 14.5, 7.3 Hz, 1H, HC(5)), 2.35 (m, 1H, $H_2C(7)$), 2.06 – 1.86 (m, 5H, HC(5a), $H_2C(6)$, $H_2C(6)$, $H_2C(7)$, OH), 1.56 (s, 3H, $H_3C(8)$), 1.03 (d, *J* = 6.5 Hz, 3H, $H_3C(20)$)

^{13}C-NMR: (500 MHz, $CDCl_3$)

158.25 (C(14)), 139.92 (Ar), 134.00 (Ar), 129.77 (Ar), 128.40 (Ar), 127.85(Ar), 124.10 (Ar), 123.33 (Ar), 119.56 (C(15)), 105.65 (C(15)), 89.70 (C(1) or C(7b)), 79.46 (C(1) or C(7b)), 78.77 (C(2)), 74.54 (C(4)), 62.55 (C(7a)), 59.95 (C(5a)), 55.48 (C(19)), 34.84 (C(5)), 31.60 (C(6)), 25.16 (C(8)), 24.29 (C(7)), 17.73 (C(20))

IR: ($CDCl_3$, film)

3474 (s), 3060 (w), 2959 (s), 2961 (s), 2871 (m), 2841 (m), 2376 (s), 2328 (s), 2272 (s), 2243 (m), 1633 (s), 1607 (s), 1504 (m), 1485 (s), 1460 (s), 1412 (w), 1388 (s), 1340 (m), 1311 (w), 1258 (s), 1225 (s), 1168 (s), 1135 (s), 1061 (m), 1033 (s), 1002 (m), 980 (w), 938 (m), 910 (s), 854 (s), 812 (m), 732 (s), 679 (m), 648 (m)

MS: (ESI, Q-tof)

348.2 (100) [M-3], 338.2 (47), 238.1 (3), 149.0 (2)

Mol. Formula: $C_{22}H_{30}BNO_2$ (351.29)

HRMS: $C_{22}H_{27}BNO_2^+$, (348.21)

Calcd: 348.2135

Found: 348.2124

TLC: R_f 0.21 (TBME/Hexanes, 1:3) [UV, I_2]

Preparation of (1*S*,3*S*,5*S*,5a*S*,7a*S*,7b*R*)-Octahydro-1-benzyloxy-1-(6-methoxy-2-naphthyl)-5-methyl-7b-methyl-2*H*cyclopenta[*gh*]pyrrolizine•Borane (37c)

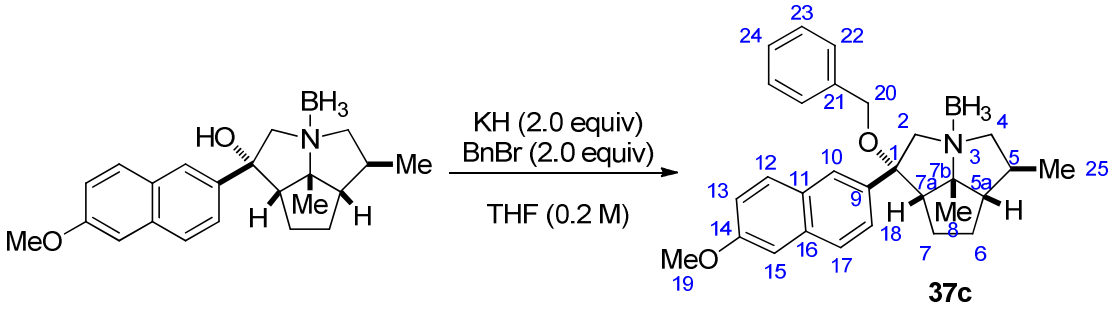

To a two-necked, 5-mL, round-bottomed flask equipped with a nitrogen inlet adapter, a rubber septum and a magnetic stir bar was added washed potassium hydride (11.4 mg, 2.0 equiv) from the drybox followed by THF (400 μL). A solution of alcohol **37b** (50 mg, 0.142 mmol) in THF (1.0 mL) is added to the reaction vessel by cannulation. After 15 min of stirring, the flask is immersed in an ice bath. The benzyl bromide (34 μL, 0.285 mmol, 2.0 equiv) is then added dropwise by syringe. The ice bath is removed and the solution is allowed to stir for 2 h at rt. This mixture was cooled in an ice bath and cold sat. aq. NH_4Cl (1.0 mL) is added in one portion. The resulting mixture was transferred to a 60-mL separatory funnel using an additional 15 mL of water and 15 mL of Et_2O and the aqueous phase was extracted with diethyl ether (3 x 15 mL). The organic extracts were washed with water (2 x 20 mL), and brine (1x 20 mL), then the combinded organic extracts were dried ($NaSO_4$). The floculant was filtered through a cotton plug and concentrated by rotary evaporation (15 mm Hg, 20-25°C). Purification by silica gel chromatography (5.0 cm x 8 cm column, gradient elution, TBME/Hexanes, 2, 4, 6, 8, 10%, 25 mL each) afforded 53.4 mg (85%) of ether **37c**.

Data for **37c**

^{1}H-NMR: (500 MHz, $CDCl_3$)

7.77 (t, *J* = 9.4 Hz, 2H, Ar), 7.74 (s, 1H, HC(10)), 7.49 (dd, *J* = 8.7, 1.9 Hz, 1H, Ar), 7.35 – 7.24 (m, 3H, Ar), 7.24 – 7.18 (m, 3H, Ar), 7.15 (d, *J* = 2.5 Hz, 1H, HC(15)), 4.28 (d, *J* = 13.3 Hz, 1H, $H_2C(2)$), 4.18 (d, *J* = 11.2 Hz, 1H, $H_2C(20)$), 4.03 (d, *J* = 13.3 Hz, 1H, $H_2C(2)$), 3.99 (d, *J* = 11.1 Hz, 1H, $H_2C(20)$), 3.94 (s, 3H, $H_3C(19)$), 3.50 (dd, *J* = 12.3, 7.9 Hz, 1H, $H_2C(4)$), 3.23 (dd, *J* = 8.4, 11.4,1H, $H_2C(4)$), 2.90 (t, *J* = 8.3 Hz, 1H, HC(7a)), 2.81 – 2.70 (m, 1H, $H_2C(7)$), 2.57 – 2.40 (m, 1H, HC(5)), 2.08 – 1.84 (m, 4H, HC(5a), $H_2C(6)$, $H_2C(6)$, $H_2C(7)$), 1.55 (s, 3H, $H_3C(8)$), 0.99 (d, *J* = 6.5 Hz, 3H,

$H_3C(25)$)

^{13}C-NMR: (500 MHz, $CDCl_3$)

158.31 (C(14)), 138.09 (Ar), 136.76 (Ar), 134.16 (Ar), 129.86 (Ar), 128.46 (Ar), 128.19 (Ar), 127.87 (Ar), 127.63 (Ar), 127.47 (Ar), 125.33 (Ar), 124.79 (Ar), 119.33 (C(13)), 105.81 (C(15)), 88.94 (C(1) or C(7b)), 83.42 (C(1) or C(7b)), 73.56 (C(4)), 70.63 (C(2)), 66.43 (C(20)), 62.00 (C(7a)), 60.35 (C(5a)), 55.49 (C(19)), 34.46 (C(5)), 30.94 (C(7)), 25.10 (C(8)), 24.41 (C(6)), 17.31 (C(25))

IR: ($CDCl_3$, film)

3062 (w), 3030 (w), 2959 (s), 2926 (s), 2870 (s), 2385 (s), 2328 (s), 2274 (s), 2241 (s), 1633 (s), 1608 (s), 1503 9s), 1485 (s), 1454 (s), 1412 (w), 1389 (s), 1380 (s), 1339 (m), 1268 (s), 1211 (s), 1168 (s), 1137 (m), 1114 (m), 1085 (s), 1061 (s), 1029 (s), 959 (w), 911 (s), 854 (s), 810 (m), 734 (s), 697 (m), 680 (w), 648 (w)

MS: (ESI, Q-Tof)

438.3 (100) [M-3], 428.3 (25), 269.1 (10)

Mol. Formula: $C_{29}H_{36}BNO_2$ (441.41)

HRMS: $C_{29}H_{33}NO_2^+$, (438.26)

Calcd: 438.2604

Found: 438.2602

TLC: R_f 0.34 (TBME/Hexanes, 1:9) [UV, I_2]

Preparation of *rel*-(1*S*,3*R*,5*S*,5a*S*,7a*S*,7b*R*) Octahydro-1-hexyloxy-1-(6-methoxy-2-naphthyl)-3-(3,5-bistrifluoromethylphenylmethyl)-5-methyl-7b-methylcyclopenta[*gh*]pyrrolizinium Bromide (37)

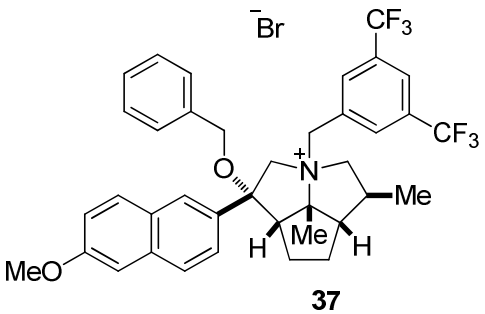

37

Data for **37**

Yield: 34 mg (61%), free-flowing white powder

^{1}H-NMR: (500 MHz, $CDCl_3$)

8.15 (d, J = 2.1 Hz, 1H), 8.10 (d, J = 8.6 Hz, 1H), 7.97 (s, 2H), 7.88 (d, J = 9.3 Hz, 2H), 7.69 (dd, J = 8.5, 2.1 Hz, 1H), 7.33 (dd, J = 8.9, 2.5 Hz, 1H), 7.31 – 7.23 (m, 4H), 7.16 – 7.08 (m, 2H), 5.91 (d, J = 12.5, 1H), 5.35 (t, J = 11.5 Hz, 1H), 4.07 (d, J = 13.7 Hz, 1H), 4.04 (d, J = 10.7 Hz, 1H), 3.99 (s, 3H), 3.83 (d, J = 10.6 Hz, 1H), 3.68 – 3.56 (m, 2H), 3.38 (d, J = 12.3 Hz, 1H), 2.98 (dd, J = 11.0, 6.0 Hz, 1H), 2.85 (dd, J = 10.2, 5.1 Hz, 1H), 2.57 – 2.43 (m, 1H), (s, 3H), 2.31 – 2.24 (m, 2H), 2.06 – 1.94 (m, 2H), 1.33 (d, J = 6.3 Hz, 3H)

MS: (ESI, Q-tof)

654.2 (100) [M-Br^-]

Mol. Formula: $C_{38}H_{38}BrF_6NO_2$ (734.61)

HRMS: $C_{38}H_{38}F_6NO_2^+$, (654.28)

Calcd: 654.2807

Found: 654.2803

TLC: R_f 0.26 (CH_2Cl_2/MeOH, 9:1) [I_2]

Preparation of (1*S*,3*S*,5*S*,5a*S*,7a*S*,7b*R*)-Octahydro-1-hydroxy-1-(2-anthracenyl)-5-methyl-7b-methyl-2*H*cyclopenta[*gh*] pyrrolizin-2-one (38a)

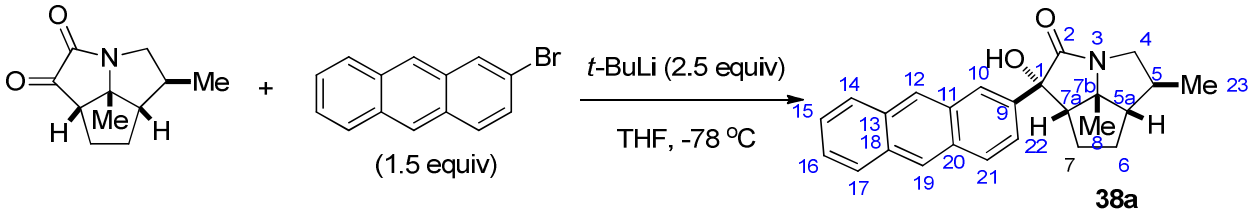

To a 5-mL, two-necked, round-bottomed flask equipped with a nitrogen inlet adapter, a rubber septum and a magnetic stir bar was added 2-bromoanthracene (80 mg, 0.311 mmol, 1.5 equiv) followed by THF (1.0 mL). The flask was immersed in an IPA/$CO_{2(s)}$ bath and stirred for 20 min. Then, *t*-BuLi (304 µL, 0.518 equiv, 2.5 equiv, 1.7 M) was added dropwise over 5 min via syringe. After being stirred for 1 h, **21** (40 mg, 0.207 mmols) in THF (1.1 mL) is added by

cannulation dropwise. After 10 min, the IPA/$CO_{2(s)}$ bath is removed and solution was allowed to reach rt. After 40 min at rt, the solution is cooled in an ice bath and sat. aq. NH_4Cl is added (1.0 mL). The mixture was transferred to a 60-mL separatory funnel with 20 mL of Et_2O and 20 mL of H_2O. The layers were separated and the aqueous extract was washed with Et_2O (2 x 15 mL). The organic extracts were washed with H_2O (1 x 25 mL), brine (1 x 25 mL), and the combined organic extracts were dried over Na_2SO_4, filtered (cotton plug), and concentrated by rotary evaporation (15 mm Hg, 20-25^oC). The resulting pale-yellow oil was purified by silica gel column chromatography (5.0 mm x 5cm, gradient elution, EtOAc/CH_2Cl_2, 0,1,2,3,4% 20 mL each) to afford **38a** (68 mg, 89%) as a white solid.

Data for **38a**

^{1}H-NMR: (500 MHz, $CDCl_3$)

8.36 (s, 1H, HC(12) or HC(19)), 8.34 (s, 1H, HC(12) or HC(19)), 8.03 – 7.93 (m, 3H, HC(14), HC(17), HC(21)), 7.86 (s, 1H, HC(10)), 7.62 (dd, *J* = 8.7, 1.9 Hz, 1H, HC(22)), 7.51 – 7.42 (m, 2H, HC(15), HC(16)), 4.27 (dd, *J* = 11.6, 7.1 Hz, 1H, $H_2C(4)$), 3.44 (bs, 1H, OH), 2.74 (dd, *J* = 9.6, 7.3 Hz, 1H, HC(7a)), 2.68 (t, *J* = 10.9 Hz, 1H, $H_2C(4)$), 2.03 (m, 1H, $H_2C(7)$), 1.91 – 1.67 (m, 4H, HC(5), HC(5a), $H_2C(6)$, $H_2C(7)$), 1.52 (m, 1H, $H_2C(6)$), 1.09 (d, *J* = 6.6 Hz, 3H, $H_3C(23)$), 0.95 (s, 3H, $H_3C(8)$)

^{13}C-NMR: (500 MHz, $CDCl_3$)

176.41 (C(2)), 140.15 (C(9)), 132.08 (C(11) or C(13) or C(18) or C(20)), 132.02 (C(11) or C(13) or C(18) or C(20)), 131.14 (C(11) or C(13) or C(18) or C(20)), 130.97 (C(11) or C(13) or C(18) or C(20)), 129.17 (C(21)), 128.28 (C(14) or C(17)), 128.25 (C(14) or C(17)), 127.02 (C(12) or C(19)), 126.00 (C(12) or C(19)), 125.65 (C(15) or C(16)), 125.59 (C(15) or C(16)), 125.07 (C(10)), 124.69 (C(22)), 83.17 (C(1)), 75.52 (C(7b)), 58.88 (C(5a)), 57.61 (C(7a)), 51.15 (C(4)), 41.94 (C(5)), 30.32 (C(6)), 27.30 (C(7)), 24.08 (C(8)), 17.79 (C(23))

IR: ($CDCl_3$, film)

3312 (s), 3048 (w), 2955 (s), 2923 (w), 2866 (s), 1688 (s), 1460 (m), 1447 (m), 1420 (s), 1358 (m), 1229 (m), 1207 (m), 1139 (s), 1709 (m), 909 (s), 734

(s), 689 (w)

MS: (ESI, Q-tof)

372.2 (55) [M+1], 354.2 (100), 184.1 (3)

Mol. Formula: $C_{25}H_{25}NO_2$ (371.19)

HRMS: $C_{25}H_{26}NO_2^+$, (372.20)

Calcd: 372.1964

Found: 372.1961

TLC: R_f 0.27 (EtOAc/Hexanes, 1:3) [UV]

Preparation of (1*S*,3*S*,5*S*,5a*S*,7a*S*,7b*R*)-Octahydro-1-hydroxy-1-(2-anthracenyl)-5-methyl-7b-methyl-2*H*cyclopenta[*gh*] pyrrolizin•Borane (38b)

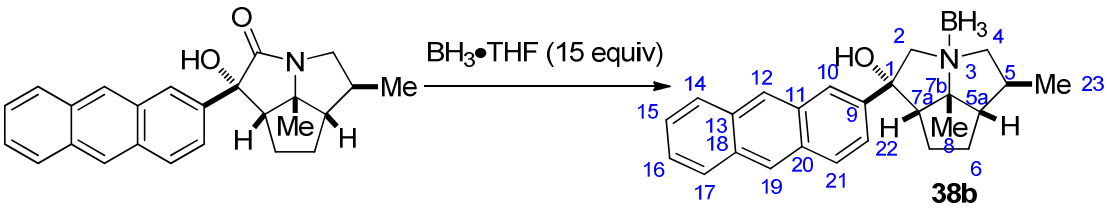

To a 5-mL round-bottomed flask equipped with a nitrogen inlet adapter, a rubber septum, a reflux condenser, and a magnetic stir bar was added **38a** (56 mg, 0.151 mmol) then BH_3•THF complex (1.5 mL, 1.5 mmol, 10 equiv). After being stirred for 12 h at rt, the solution was cooled in an ice bath was quenched with the slow addition of methanol (5 mL) and concentrated by rotary evaporation (15 mm Hg, 20-25°C). The resulting colorless oil was purified by silica gel column chromatography (5.0 mm x 10 cm column, gradient elution, TBME/Hexanes, 2, 4, 6, 8, 10, 12% 25 mL each) to afford 38 mg (68%) of **38b** as a white solid

Data for **38b**

^{1}H-NMR: (500 MHz, $CDCl_3$)

8.39 (d, J = 4.4 Hz, 2H, ArH), 8.07 – 7.96 (m, 3H, ArH), 7.93 (d, J = 2.0 Hz, 1H, ArH), 7.49 (dd, J = 6.5, 3.2 Hz, 2H, ArH), 7.42 (dd, J = 9.0, 1.9 Hz, 1H, ArH), 4.26 (d, J = 13.7 Hz, 1H, $H_2C(2)$), 3.75 (d, J = 13.7 Hz, 1H, $H_2C(2)$), 3.70 (dd, J = 12.3, 8.0 Hz, 1H, $H_2C(4)$), 3.37 – 3.26 (t, J = 11.2, 1H, $H_2C(4)$), 2.87 (dd, J = 9.0, 5.9 Hz, 1H, HC(7a)), 2.71 – 2.54 (m, 1H, HC(5)), 2.36 (m,

1H, $H_2C(7)$), 2.08 – 1.88 (m, 5H, HC(5a), $H_2C(6)$, $H_2C(6)$, $H_2C(7)$, OH), 1.60 (s, 3H, $H_3C(8)$), 1.04 (d, J = 6.5 Hz, 3H, $H_3C(23)$)

^{13}C-NMR: ($CDCl_3$)

141.23 (C(9)), 132.24 (Ar), 132.18 (Ar), 130.95 (Ar), 130.81 (Ar), 129.55 (Ar), 128.31 (Ar), 128.26 (Ar), 126.90 (Ar), 126.17 (Ar), 126.06 (Ar), 125.85 (Ar), 125.83 (Ar), 123.44 (Ar), 123.28 (Ar), 89.78 (C(1) or C(7b)), 79.63 (C(1) or C(7b)), 78.56 (C(2)), 74.61 (C(4)), 62.35 (C(7a)), 60.04 (C(5a)), 34.92 (C(5)), 31.56 (C(6)), 25.21 (C(8)), 24.43 (C(7)), 17.70 (C(23))

IR: ($CDCl_3$, film)

3592 (w), 3516 (m), 3051 (w), 2956 (s), 2960 (s), 2871 (m), 2379 (s), 2327 (s), 2255 (s), 1627 (w), 1458 (s), 1379 (s), 1341 (w), 1307 (w), 1269 (w), 1232 (w), 1176 (s), 1138 (m), 1059 (w), 1003 (m), 979 (w), 948 (m), 908 (s), 836 (w), 808 (w), 733 (s), 650 (s)

MS: (ESI, Q-tof)

370.2 (42) [M-1], 368.2 (44), 358.2 (100), 356.2 (4), 344.2 (5)

Mol. Formula: $C_{25}H_{30}BNO$ (371.32)

HRMS: $C_{25}H_{29}BNO^{+}$, (370.23)

Calcd: 370.2342

Found: 370.2344

TLC: R_f 0.27 (TBME/Hexanes, 1:9) [UV, I_2]

Preparation of (1*S*,3*S*,5*S*,5a*S*,7a*S*,7b*R*)-Octahydro-1-benzyloxy-1-(2-anthracenyl)-5-methyl-7b-methyl-2*H*cyclopenta[*gh*]pyrrolizine•Borane (38c)

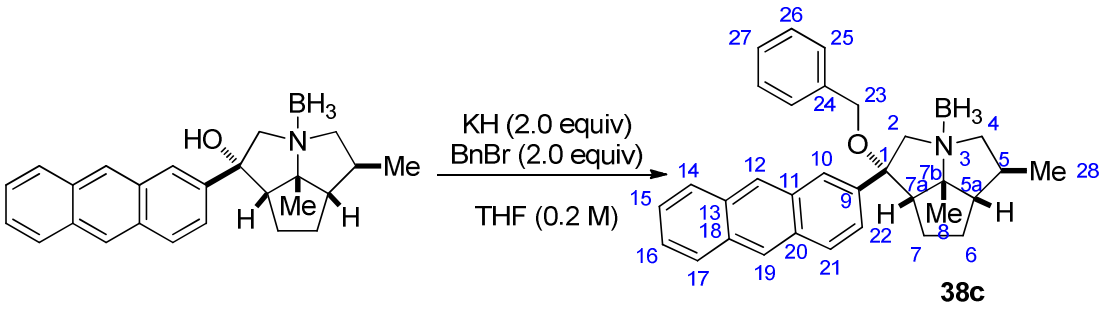

38c

To a two-necked, 5-mL, round-bottomed flask equipped with a nitrogen inlet adapter, a rubber septum and a magnetic stir bar was added washed potassium hydride (8 mg, 2.0 equiv)

from the drybox followed by THF (200 μL). A solution of alcohol **38b** (37 mg, 0.1 mmol) in THF (800 μL) is added to the reaction vessel by cannulation. After 15 min of stirring, the flask is immersed in an ice bath. The benzyl bromide (24 μL, 2.0 equiv) is then added dropwise by syringe. The ice bath is removed and the solution is allowed to stir for 2 h at rt. This mixture was cooled in an ice bath and cold sat. aq. NH_4Cl (1.0 mL) is added in one portion. The resulting mixture was transferred to a 60-mL separatory funnel using an additional 15 mL of water and 15 mL of Et_2O and the aqueous phase was extracted with diethyl ether (3 x 15 mL). The organic extracts were washed with water (2 x 20 mL), and brine (1x 20 mL), then the combinded organic extracts were dried ($NaSO_4$). The floculant was filtered through a cotton plug and concentrated by rotary evaporation (15 mm Hg, 20-25^{o}C). Purification by silica gel chromatography (5.0 cm x 8 cm column, gradient elution, hexanes/TBME, 1, 2, 3, 4, 6%, 25 mL each) afforded 34 mg (75%) of ether **38c**.

Data for 38c

^{1}H-NMR: (500 MHz, $CDCl_3$)

8.44 (s, 1H, ArH), 8.40 (s, 1H, ArH), 8.05 – 8.00 (m, 3H, ArH), 7.96 (s, 1H, ArH), 7.51 – 7.47 (m, 3H, ArH), 7.35 – 7.24 (m, 3H, HC(26), HC(27)), 7.20 (d, J = 7.1 Hz, 2H, HC(25)), 4.33 (d, J = 13.2 Hz, 1H, $H_2C(2)$), 4.20 (d, J = 11.2 Hz, 1H, $H_2C(23)$), 4.04 (d, J = 13.5 Hz, 1H, $H_2C(2)$), 4.03 (d, J = 11.0 Hz, 1H, $H_2C(23)$), 3.49 (dd, J = 12.3, 7.8 Hz, 1H, $H_2C(4)$), 3.22 (t, J = 11.7 Hz, 1H, $H_2C(4)$), 2.94 (t, J = 8.4 Hz, 1H, HC(7a)), 2.83 – 2.68 (m, 1H, $H_2C(7)$), 2.53 – 2.44 (m, 1H, HC(5)), 2.05 – 1.88 (m, 4H, HC(5a), $H_2C(6)$, $H_2C(6)$, $H_2C(7)$), 1.57 (s, 3H, $H_3C(8)$), 0.99 (d, J = 6.5 Hz, 3H, $H_3C(28)$)

^{13}C-NMR: (500 MHz, $CDCl_3$)

138.33 (Ar), 138.00 (Ar), 132.24 (Ar), 131.04 (Ar), 130.83 (Ar), 129.53 (Ar), 128.51 (C(26)), 128.29 (Ar), 127.71 (C(27)), 127.55 (C(25)), 126.98 (Ar), 126.12 (Ar), 125.81 (Ar), 125.79 (Ar), 124.90 (Ar), 124.47 (Ar), 89.00 (C(1) or C(7b)), 83.53 (C(1) or C(7b)), 73.54 (C(4)), 70.43 (C(2)), 66.60 (C(23)), 61.46 (C(7a)), 60.47 (C(5a)), 34.46 (C(5)), 30.89 (C(6)), 25.18 (C(8)), 24.66 (C(7)), 17.28 (C(28))

IR: ($CDCl_3$, film)

3030 (w), 3052 (w), 2958 (s), 2912 (s), 2869 (s), 2383 (s), 2329 (s), 2275 (s), 2222 (w), 1628 (w), 1496 (w), 1454 (s), 1379 (s), 1335 (w), 1307 (w), 1283 (w), 1236 (w), 1170 (s), 1137 (m), 1116 (m), 1083 (s), 1061 (s), 1027 (m), 909 (s), 812 (w), 734 (s), 701 (m), 647 (w)

MS: (ESI, Q-tof)

460.3 (78) [M-1], 458.2 (100), 448.2 (36), 338.3 (4), 297.6 (3), 279.1 (22), 258.1 (3)

Mol. Formula: $C_{32}H_{36}BNO$ (461.45)

HRMS: $C_{32}H_{35}BNO^{+}$, (460.28)

Calcd: 460.2812

Found: 460.2814

TLC: R_f 0.26 (TBME/Hexanes, 1:19) [UV, I_2]

Preparation of *rel*-(1*S*,3*R*,5*S*,5a*S*,7a*S*,7b*R*) Octahydro-1-hexyloxy-1-(2-anthracenyl)-3-(3,5-bistrifluoromethylphenylmethyl)-5-methyl-7b-methylcyclopenta[*gh*]pyrrolizinium Bromide (38)

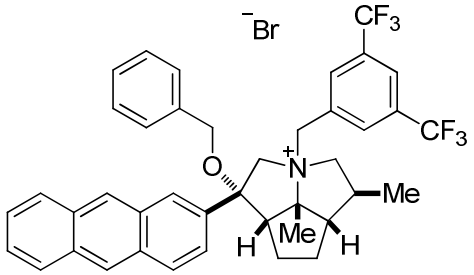

38

Data for **38**

Yield: 39 mg (52%), free-flowing white powder

^{1}H-NMR: (500 MHz, $CDCl_3$)

8.59 (d, *J* = 11.7 Hz, 2H), 8.42 (s, 1H), 8.37 (d, *J* = 8.8 Hz, 1H), 8.09 (dd, *J* = 5.1, 9.0 Hz, 2H), 7.99 (s, 2H), 7.89 (s, 1H), 7.65 (dt, *J* = 9.0, 1.6 Hz, 1H), 7.62 – 7.55 (m, 2H), 7.35 – 7.27 (m, 3H), 7.16 – 7.14 (m, 2H), 5.89 (d, *J* = 12.2 Hz, 1H), 5.36 (t, *J* = 11.6 Hz, 1H), 4.10 (d, *J* = 10.6 Hz, 1H), 3.90 (d, *J* = 10.6 Hz, 1H), 3.72 (t, *J* = 9.3 Hz, 1H), 3.63 (d, *J* = 13.3 Hz, 1H), 3.49 (d, *J* = 11.5 Hz, 1H), 3.01 (dd, *J* = 11.1, 6.0 Hz, 1H), 2.88 (dd, *J* = 8.7, 5.4 Hz, 1H), 2.57 –

2.44 (m, 2H), 2.38 – 2.25 (m, 2H), 2.11 – 2.00 (m, 2H), 1.58 (s, 3H), 1.34 (d, J = 6.3 Hz, 3H)

MS: (ESI, Q-tof)

674.2 (100) [M-Br^-]

Mol. Formula: $C_{41}H_{38}BrF_6NO$ (754.64)

HRMS: $C_{41}H_{38}F_6NO^+$, (674.74)

Calcd: 674.2858

Found: 674.2863

TLC: R_f 0.38 (CH_2Cl_2/MeOH, 9:1) [I_2]

Preparation of (1*S*,3*S*,5*S*,5a*S*,7a*S*,7b*R*)-Octahydro-1-hydroxy-1-(9-phenanthryl)-5-methyl-7b-methyl-2*H*cyclopenta[*gh*] pyrrolizin-2-one (39a)

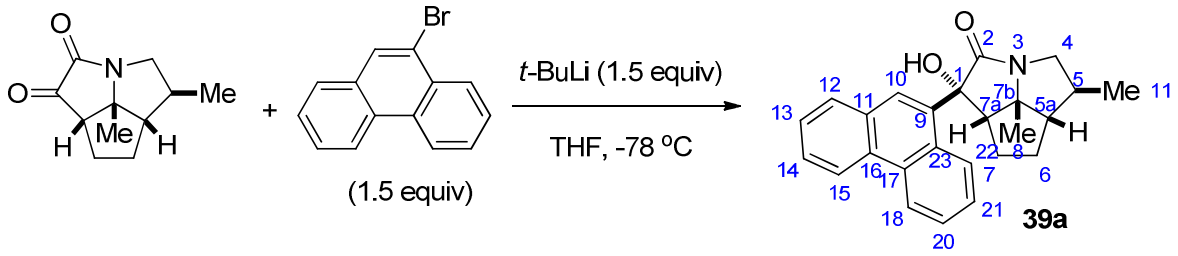

To a 5-mL, two-necked, round-bottomed flask equipped with a nitrogen inlet adapter, a rubber septum and a magnetic stir bar was added 9-bromophenanthrene (100 mg, 0.518 mmol) followed by THF (1.0 mL). The flask was immersed in an IPA/$CO_{2(s)}$ bath and stirred for 20 min. Then, *t*-BuLi (1.6 M, 304 µL, 1.5 equiv) was added dropwise over 5 min via syringe. After being stirred for 1 h, **21** (40 mg, 0.207 mmols) in THF (1.1 mL) is added by cannulation dropwise. After 10 min, the IPA/$CO_{2(s)}$ bath is removed and solution was allowed to reach rt. After 40 min at rt, the solution is cooled in an ice bath and sat. aq. NH_4Cl is added (1.0 mL). The mixture was transferred to a 60-mL separatory funnel with 20 mL of Et_2O and 20 mL of H_2O. The layers were separated and the aqueous extract was washed with Et_2O (2 x 15 mL). The organic extracts were washed with H_2O (1 x 25 mL), brine (1 x 25 mL), and the combined organic extracts were dried over Na_2SO_4, filtered (cotton plug), and concentrated by rotary evaporation (15 mm Hg, 20-25^oC). The resulting pale-yellow oil was purified by silica gel column chromatography (5.0 mm x 5cm, gradient elution, EtOAc/CH_2Cl_2, 0,1,2,3,4% 20 mL each) to afford **39a** (70.4 mg, 92%) as a white solid.

Data for **39a**

mp: 262-264˚C (hexanes)

^{1}H-NMR: (500 MHz, $CDCl_3$)

8.76 – 8.68 (m, 1H, HC(12 or 15 or 22 or 18)), 8.63 (d, *J* = 8.3 Hz, 1H, HC(12 or 15 or 22 or 18)), 8.55 – 8.40 (m, 1H, HC(12 or 15 or 22 or 18)), 7.80 (d, *J* = 7.8 Hz, 1H, HC(12 or 15 or 22 or 18)), 7.73 – 7.60 (m, 3H), 7.57 – 7.53 (m, 3H, HC(13 or 14 or 20 or 21), HC(13 or 14 or 20 or 21), HC(13 or 14 or 20 or 21)), 7.54 (s, 1H, HC(10), HC(13 or 14 or 20 or 21)), 4.31 (dd, *J* = 11.5, 6.4 Hz, 1H, H_2C(4)), 3.60 (bs, 1H, OH), 3.01 (dd, *J* = 10.1, 7.5 Hz, 1H, HC(7a)), 2.74 (dd, *J* = 11.6, 9.5 Hz, 1H, H_2C(4)), 2.27 – 2.12 (m, 1H), 2.08 – 1.90 (m, 1H), 1.87 – 1.68 (m, 3H, HC(5), HC(5a), H_2C(6)), 1.66 – 1.49 (m, 1H, H_2C(6)), 1.11 (d, *J* = 6.1 Hz, 3H, H_3C(11)), 0.89 (s, 3H, H_3C(8))

^{13}C-NMR: (500 MHz, $CDCl_3$)

177.15 (C(2)), 136.81(C(9)), 131.90 (C(11) or C(16) or C(17) of C(23)), 130.77 (C(11) or C(16) or C(17) of C(23)), 130.60 (C(11) or C(16) or C(17) of C(23)), 129.75 (C(11) or C(16) or C(17) of C(23)), 129.29 (C(12) or C(15) or C(22) of C(18)), 127.46 (C(12) or C(15) or C(22) of C(18)), 127.27 (C(13) or C(14) or C(20) of C(21)), 126.89 (C(13) or C(14) or C(20) of C(21)), 126.44 (C(13) or C(14) or C(20) of C(21)), 126.40 (C(13) or C(14) or C(20) of C(21)), 125.77 (C(10)), 123.40 (C(12) or C(15) or C(22) or C(18)), 122.42 (C(12) or C(15) or C(22) of C(18)), 84.26 (C(1) or C(7b)), 76.91 (C(1) or C(7b)), 76.00 (C(1) or C(7b)), 58.89 (HC(5a)), 57.51 (HC(7a)), 51.35 (H_2C(4)), 41.92 (HC(5)), 30.04 (H_2C(6)), 26.97 (H_2C(7)), 24.48(H_3C(8)), 17.71 (H_3C(11))

IR: ($CDCl_3$, film)

3512 (s), 3377 (s), 2959 (s), 2929 (s), 2871 (s), 1692 (s), 1493 (w), 1451 (m), 1404 (m), 1336 (m), 1283 (m), 1213 (m), 1128 (m), 1072 (m), 1045 (m), 1026 (m), 908 (s), 866 (w), 832 (w), 729 (s)

MS: (ESI, Q-tof)

372.2 (30) [M+1], 354.2 (100)

Mol. Formula: $C_{25}H_{25}NO_2$ (371.47)

HRMS: $C_{25}H_{26}NO_2^+$, (372.20)
Calcd: 372.1964
Found: 372.1961
TLC: R_f 0.15 (EtOAc/CH_2Cl_2, 1:4) [UV]

Preparation of (1*S*,3*S*,5*S*,5a*S*,7a*S*,7b*R*)-Octahydro-1-hydroxy-1-(9-phenanthryl)-5-methyl-7b-methyl-2*H*cyclopenta[*gh*] pyrrolizin•Borane (39b)

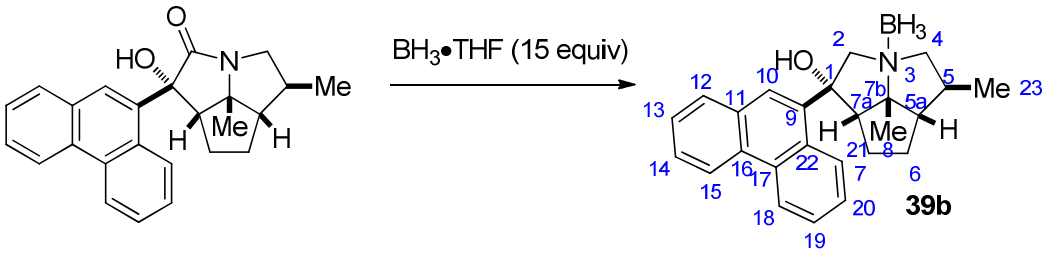

To a 5-mL round-bottomed flask equipped with a nitrogen inlet adapter, a rubber septum, a reflux condenser, and a magnetic stir bar was added **39a** (69 mg, 0.186 mmol) then BH_3•THF complex (2.8 mL, 2.8 mmol, 15 equiv). The reaction flask was immersed in an oil bath and heated to reflux (66 °C). After being stirred for 12 h at reflux, the solution was allowed to reach room temperature and was quenched with methanol (5 mL) and concentrated by rotary evaporation (15 mm Hg, 20-25°C). The resulting colorless oil was purified by silica gel column chromatography (5.0 mm x 8 cm column, gradient elution, hexanes/TBME, 2, 4, 6, 8, 10, 12% 25 mL each) to afford 49 mg (71%) of **39b** as a white solid

Data for **39b**

^{1}H-NMR: (500 MHz, $CDCl_3$)
8.73 (dd, *J* = 8.3, 1.6 Hz, 1H, HC(12) or HC(15) or HC(18) or HC(21)), 8.62 (d, *J* = 8.3 Hz, 1H, HC(12) or HC(15) or HC(18) or HC(21)), 8.50 (dd, *J* = 8.2, 1.6 Hz, 1H, HC(12) or HC(15) or HC(18) or HC(21)), 7.94 (s, 1H, HC(10)), 7.88 (dd, *J* = 7.8, 1.5 Hz, 1H, HC(12) or HC(15) or HC(18) or HC(21)), 7.71 – 7.55 (m, 4H, HC(13), HC(14), HC(19), HC(20)), 4.32 (d, *J* = 13.4 Hz, 1H, H_2C(2)), 4.02 (d, *J* = 13.4 Hz, 1H, H_2C(2)), 3.65 (dd, *J* = 12.3,

7.4 Hz, 1H, $H_2C(4)$), 3.25 (t, J = 8.1 Hz, 1H, HC(7a)), 3.22 (t, J = 12.8 Hz, 1H, $H_2C(4)$), 2.53 (m, 1H, HC(5)), 2.46 – 2.35 (m, 1H, $H_2C(7)$), 2.26 (bs, 1H, OH), 2.12 (m, 1H, $H_2C(7)$), 2.04 – 1.88 (m, 3H, HC(5a), $H_2C(6)$, $H_2C(6)$), 1.53 (s, 3H, $H_3C(8)$), 1.06 (d, J = 6.5 Hz, 3H, $H_3C(23)$)

^{13}C-NMR: (500 MHz, $CDCl_3$)

136.91 (C(9)), 132.05 (C(11) or C(16) or C(17) or C(22)), 130.62 (C(11) or C(16) or C(17) or C(22)), 130.54 (C(11) or C(16) or C(17) or C(22)), 129.72 (C(11) or C(16) or C(17) or C(22)), 129.53 (C(12) or C(15) or C(18) or C(21)), 127.70 (C(13) or C(14) or C(19) or C(20)), 127.18 (C(13) or C(14) or C(19) or C(20)), 127.13 (C(12) or C(15) or C(18) or C(21)), 126.49 (C(13) or C(14) or C(19) or C(20)), 126.44 (C(13) or C(14) or C(19) or C(20)), 125.79 (C(10)), 123.71 (C(12) or C(15) or C(18) or C(21)), 122.42 (C(12) or C(15) or C(18) or C(21)), 88.07 (C(1) or C(7b)), 80.70 (C(1) or C(7b)), 76.11 (C(2)), 74.45 (C(4)), 61.26 (C(5a)), 60.31 (C(7a)), 34.68 (C(5)), 30.75 (C(6)), 27.06 (C(7)), 25.64 (C(8)), 17.33 (C(23))

IR: ($CDCl_3$, film)

3587 (m), 3552 (s), 3448 (s), 3064 (m), 2960 (s), 2928 (s), 2870 (s), 2374 (s), 2343 (s), 2275 (s), 2243 (s), 1599 (w), 1493 (m), 1458 (s), 1379 (s), 1342 (m), 1316 (w), 1273 (w), 1171 (s), 1137 (m), 1110 (m), 1058 (s), 1004 (m), 966 (m), 909 (s), 851 (w), 822 (w), 768 (m), 730

MS: (ESI, Q-tof)

370.2 (100) [M-1], 358.2 (72), 220.0 (2), 195.0 (4), 185.1 (4), 158 (8), 142.0 (5), 126 (10), 107.1 (4), 100.1 (43), 89.1 (4), 79.0 (10)

Mol. Formula: $C_{25}H_{30}BNO$ (371.32)

HRMS: $C_{25}H_{29}BNO^+$, (370.23)

Calcd: 370.2342

Found: 370.2339

TLC: R_f 0.30 (TBME/Hexanes, 1:9) [UV, I_2]

Preparation of (1*S*,3*S*,5*S*,5a*S*,7a*S*,7b*R*)-Octahydro-1-benzyloxy-1-(9-phenanthryl)-5-

methyl-7b-methyl-2*H*cyclopenta[*gh*]pyrrolizine•Borane (39c)

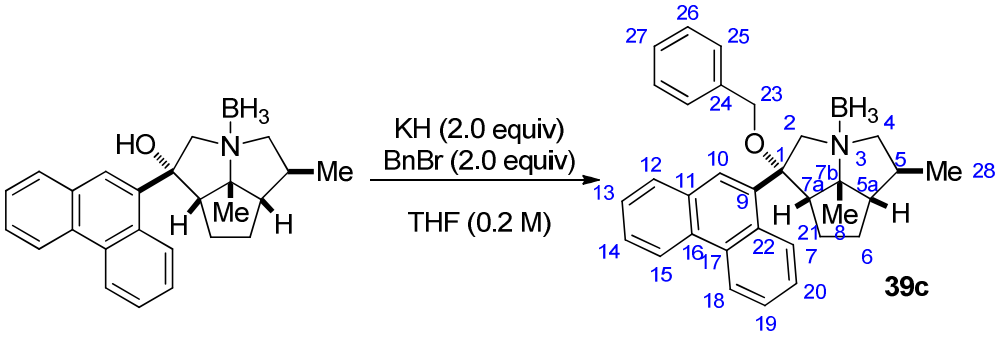

To a two-necked, 5-mL, round-bottomed flask equipped with a nitrogen inlet adapter, a rubber septum and a magnetic stir bar was added washed potassium hydride (10 mg, 2.0 equiv) from the drybox followed by THF (0.4 mL). A solution of alcohol **39b** (48 mg, 0.129 mmol) in THF (0.9 mL) is added to the reaction vessel by cannulation. After 15 min of stirring, the flask is immersed in an ice bath. The benzyl bromide (31 μL, 2.0 equiv) is then added dropwise by syringe. The ice bath is removed and the solution is allowed to stir for 2 h at rt. This mixture was cooled in an ice bath and cold sat. aq. NH_4Cl (1.0 mL) is added in one portion. The resulting mixture was transferred to a 60-mL separatory funnel using an additional 15 mL of water and 15 mL of Et_2O and the aqueous phase was extracted with diethyl ether (3 x 15 mL). The organic extracts were washed with water (2 x 20 mL), and brine (1x 20 mL), then the combinded organic extracts were dried ($NaSO_4$). The floculant was filtered through a cotton plug and concentrated by rotary evaporation (15 mm Hg, 20-25°C). Purification by silica gel chromatography (5.0 cm x 8 cm column, gradient elution, TBME/Hexanes, 1, 2, 3, 4, 6%, 25 mL each) afforded 36 mg (60%) of **39c**.

Data for 39c

^{1}H-NMR: (500 MHz, $CDCl_3$)

8.80 (dd, *J* = 11.3, 8.2 Hz, 2H), 8.75 – 8.65 (m, 2H), 8.62 (d, *J* = 8.5 Hz, 1H), 8.23 (s, 1H), 8.15 (s, 1H), 8.03 (d, *J* = 7.8 Hz, 1H), 7.95 (d, *J* = 7.8 Hz, 1H), 7.78 – 7.56 (m, 7H), 7.40 (s, 0H), 7.28 (pd, *J* = 8.0, 7.0, 2.2 Hz, 5H), 7.16 (d, *J* = 7.1 Hz, 3H), 4.84 (d, *J* = 13.4 Hz, 1H), 4.54 (d, *J* = 11.5 Hz, 1H), 4.29 (d, *J* = 11.2 Hz, 1H), 4.12 (d, *J* = 10.6 Hz, 1H), 4.07 (d, *J* = 13.4 Hz, 1H), 4.02 (d, *J* = 11.2 Hz, 1H), 3.91 (d, *J* = 10.6 Hz, 1H), 3.87 (d, *J* = 11.6 Hz, 1H), 3.77 (q, *J* = 10.9, 9.9 Hz, 2H), 3.33 (t, *J* = 11.1 Hz, 1H), 3.30 – 3.17 (m, 1H), 3.00 (tt,

J = 12.6, 7.5 Hz, 1H), 2.90 (t, *J* = 12.6 Hz, 1H), 2.84 (t, *J* = 8.9 Hz, 1H), 2.66 – 2.50 (m, 1H), 2.50 – 2.37 (m, 1H), 2.35 – 2.13 (m, 3H), 2.13 – 1.89 (m, 5H), 1.76 (s, 4H), 1.35 (s, 3H), 1.32 (s, 0H), 1.11 (d, *J* = 6.5 Hz, 2H), 1.07 (d, *J* = 6.3 Hz, 3H)

^{13}C-NMR: (500 MHz, $CDCl_3$)

138.16, 138.05, 134.34, 133.98, 131.91, 131.65, 131.25, 130.70, 130.55, 130.19, 129.71, 129.28, 128.46, 128.43, 128.25, 127.99, 127.72, 127.62, 127.60, 127.55, 127.21, 126.99, 126.91, 126.69, 126.62, 126.58, 126.33, 123.75, 123.39, 122.72, 122.35, 88.85, 86.83, 85.30, 85.03, 77.41, 77.16, 76.91, 73.60, 72.46, 72.26, 70.90, 67.27, 66.88, 63.74, 63.47, 60.49, 54.80, 34.51, 33.76, 30.96, 28.79, 28.69, 27.85, 25.93, 25.43, 17.80, 16.14

IR: ($CDCl_3$, film)

3069 (m), 3031 (m), 2957 (s), 2927 (s), 2869 (m), 2397 (s), 2333 (s), 2279 (s), 2241 (m), 1602 (w), 1531 (w), 1495 (m), 1454 (s), 1379 (s), 1339 (w), 1292 (w), 1275 (w), 1240 (w), 1170 (s), 1142 (m), 1113 (s), 1077 (s), 1057 (s), 1025 (m), 958 (w), 910 (s), 850 (w), 813 (w), 769 (w), 732 (s), 697 (m), 646 (w), 622 (w)

MS: (EI, 70 eV)

460.3 [M-1] (82), 458.3 (100), 448.3 (58), 279.1 (5), 208.1 (4)

Mol. Formula: $C_{32}H_{36}BNO$ (461.45)

HRMS: $C_{32}H_{35}BNO^+$, (460.28)

Calcd: 460.2812

Found: 460.2811

TLC: R_f 0.24 (TBME/Hexanes, 1:19) [UV, I_2]

Preparation of *rel*-(1*S*,3*R*,5*S*,5a*S*,7a*S*,7b*R*) Octahydro-1-hexyloxy-1-(9-phenanthryl)-3-(3,5-bistrifluoromethylphenylmethyl)-5-methyl-7b-methylcyclopenta[*gh*]pyrrolizinium Bromide (39)

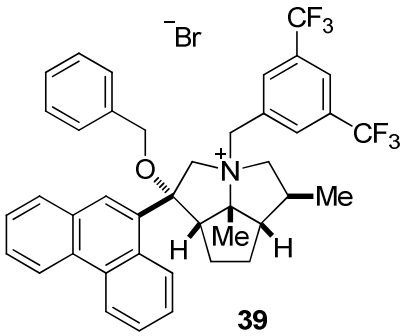

39

Data for **39**

Yield: 42 mg (82%), free-flowing white powder

^{1}H-NMR: (500 MHz, $CDCl_3$)

8.96 (dd, *J* = 8.4, 1.4 Hz, 1H), 8.78 (d, *J* = 8.4 Hz, 1H), 8.63 (dd, *J* = 8.5, 1.3 Hz, 1H), 8.34 (s, 1H), 8.01 (dd, *J* = 7.8, 1.4 Hz, 1H), 7.98 – 7.89 (m, 1H), 7.84 (ddt, *J* = 8.4, 7.1, 1.4 Hz, 1H), 7.75 (dddd, *J* = 11.4, 5.8, 2.5, 1.2 Hz, 3H), 7.38 (s, 2H), 7.30 – 7.27 (m, 3H), 7.17 – 7.07 (m, 2H), 5.63 (d, *J* = 12.2 Hz, 1H), 5.28 (t, *J* = 11.8 Hz, 1H), 4.65 (d, *J* = 13.0 Hz, 1H), 4.19 (d, *J* = 10.3 Hz, 1H), 4.04 (t, *J* = 9.4 Hz, 1H), 3.97 (d, *J* = 10.3 Hz, 1H), 3.72 (d, *J* = 13.1 Hz, 1H), 3.06 (d, *J* = 12.1 Hz, 1H), 2.91 (dt, *J* = 7.4, 3.7 Hz, 1H), 2.85 (dd, *J* = 11.1, 5.9 Hz, 1H), 2.65 – 2.53 (m, 1H), 2.53 (s, 3H), 2.41 – 2.22 (m, 2H), 2.11 – 1.98 (m, 2H), 1.32 (d, *J* = 6.3 Hz, 3H)

MS: (ESI, Q-tof)

674.3 (100) [M-Br^-]

Mol. Formula: $C_{41}H_{38}BrF_6NO$ (754.64)

HRMS: $C_{41}H_{38}F_6NO^+$, (674.29)

Calcd: 674.2858

Found: 674.2839

TLC: R_f 0.38 (CH_2Cl_2/MeOH, 9:1) [I_2]

Preparation of Catalysts from Table 19

Preparation of (1*R*,2*S*)-2-Phenyl-1-(1-butynyloxy)cyclohexane (40a)

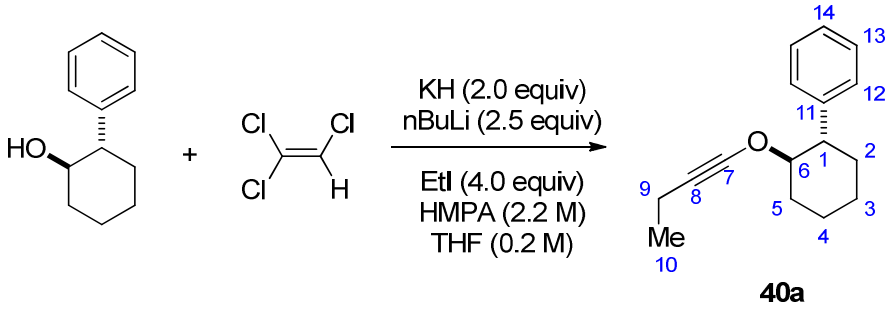

40a

To a two-necked, 25-mL, round-bottomed flask equipped with a nitrogen inlet adapter, a rubber septum and a magnetic stir bar was added washed potassium hydride (182 mg, 4.53 mmol, 2.0 equiv) from the drybox followed by THF (4.5 mL). A solution of **11** (400 mg, 2.27 mmol) in THF (3.4 mL) is added to the reaction vessel by cannulation. After 2 h of stirring, the flask is immersed in IPA/$CO_{2(s)}$ bath. Next, trichloroethylene (224 μL, 4.53 mmol, 2.0 equiv) in THF (3.4 mL) is added dropwise by syringe and the IPA/$CO_{2(s)}$ bath is removed. After 1 h of stirring at rt, the reaction flask is immersed in a IPA/$CO_{2(s)}$ bath and nBuLi (2.3 mL, 5.67 mmols, in hexanes) is added dropwise by syringe and the resulting solution is allowed to stir at -78 ^{o}C for 1 h. Next, iodoethane (730 μL, 9.1 mmol) in HMPA (1.0 mL) is added by cannulation and the IPA/$CO_{2(s)}$ bath is removed. After stirring for 3 h at rt, the solution is poured into a flask containing cold, sat. aq. NH_4Cl (40 mL). The resulting mixture was transferred to a 125-mL separatory funnel and the aqueous phase was extracted with pentane (3 x 40 mL). The organic extracts were washed with water (2 x 40 mL), and brine (1x 20 mL), then the combinded organic extracts were dried ($NaSO_4$). The mixture was filtered through a cotton plug and concentrated by rotary evaporation (15 mm Hg, 20-25^{o}C). Purification by basic alumina chromatography (20 mm x 10 cm column, gradient elution, TBME/Hexanes, 0, 1, 2, 4, 6, 10%, 50 mL each). The resulting white solid was recrystallized from pentane at -78 ^{o}C furnishing 352 mg (68%) of ether **40a**.

Data for **40a**

mp: 60-61 ˚C (pentane)

^{1}H-NMR: (500 MHz, $CDCl_3$)

7.35 (t, *J* = 7.6 Hz, 2H, HC(13)), 7.31 – 7.23 (m, 3H, HC(14), HC(12)), 4.03 (td, *J* = 10.8, 4.4 Hz, 1H, HC(6)), 2.76 (ddd, *J* = 12.5, 10.5, 3.9 Hz, 1H, HC(1)), 2.44 (ddd, *J* = 10.2, 4.7, 2.6 Hz, 1H, HC(5)), 2.10 (q, *J* = 7.4 Hz, 2H,

$H_2C(5)$), 1.96 (tdd, J = 9.4, 4.7, 2.9 Hz, 2H, $H_2C(9)$, $H_2C(9)$), 1.85 – 1.75 (m, 1H, $H_2C(3)$), 1.69 – 1.50 (m, 2H, $H_2C(2)$, $H_2C(5)$), 1.50 – 1.32 (m, 2H, $H_2C(3)$, $H_2C(4)$), 1.07 (t, J = 7.4 Hz, 3H, $H_3C(10)$)

^{13}C-NMR: (500 MHz, $CDCl_3$)

142.94 (C(11)), 128.50 (C(13)), 127.69 (C(12)), 126.67 (C(14)), 88.51 (C(6)), 87.01 (C(7)), 49.21 (C(1)), 40.41 (C(8)), 34.01 (C(2)), 31.10 (C(5)), 25.75 (C(3)), 24.87 (C(4)), 15.27 (C(10)), 11.21 (C(9))

IR: (neat)

3062 (w), 3029 (m), 2971 (s), 2934 (s), 2859 (s), 2254 (s), 1603 (m), 1494 (m), 1462 (m), 1450 (s), 1372 (w), 1354 (w), 1331 (w), 1235 (s), 1209 (s), 1122 (w), 1063 (w), 1031 (w), 999 (s), 976 (m), 929 (m), 900 (w), 867 (), 849 (w), 819 (w), 780 (w), 754 (s)

MS: (ESI, Q-tof)

229.4 (18) [M+1], 209.4 (24), 159.3 (15), 150.3 (13), 139.2 (3), 117 (3)

Opt. Rot.: $[\alpha]_D^{24}$ -68.3, (c = 1.10, EtOH)

Analysis: $C_{16}H_{20}O$ (228.15)

Calcd: C, 84.16; H, 8.83

Found: C, 83.76; H, 9.03

TLC: R_f 0.29 (Hexanes) [UV, $KMnO_4$]

Preparation of (1*R*,2*S*)-2-Phenyl-1-(1-(*Z*)-butenyloxy)cyclohexane (40b)

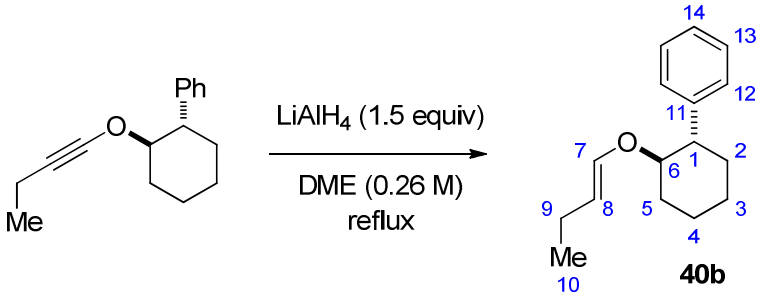

To a two-necked, 50-mL, round-bottomed flask equipped with a nitrogen inlet adapter, a rubber septum and a magnetic stir bar was lithium aluminum hydride (114 mg, 2.85 mmol, 1.5 equiv) followed by dimethoxyethane (5.2 mL). To this solution was added alkyne **40a** (434 mg, 1.9 mmol) in dimethoxyethane (2.2 mL) by cannulation. The reaction flask was placed in an oil

bath at 80 °C. After 1.5 h, the reaction flask is cooled in an ice bath. To the reaction mixture was slowly added 1.0 N NaOH (200 μL) followed by H_2O (200 μL). Sodium sulfate (~300 mg) was added and solution was stirred at rt for 30 min. The suspension was filtered through a plug of deactivated silica gel (5% triethlamine in TBME) and washed with TBME (~25 mL). The filtrate was concentrated by rotary evaporation (15 mm Hg, 20-25°C). Purification by basic alumina chromatography (20 mm x 15 cm column, gradient elution, TBME/Hexanes, 0, 1, 2, 4, 8%, 100 mL each). The colorless oil was distilled (95 °C, 0.06 torr) to afforded 254 mg, 58% of product **40b** as a colorless oil.

Data for **40b**

bp: 95 °C / 0.06 torr

^{1}H-NMR: (500 MHz, $CDCl_3$)

7.33 – 7.27 (m, 2H, HC(13)), 7.24 – 7.17 (m, 3H, HC(14), HC(12)), 5.81 (dt, *J* = 12.3, 1.4 Hz, 1H, HC(7)), 4.72 (dt, *J* = 12.4, 7.0 Hz, 1H, HC(8)), 3.71 (td, *J* = 10.3, 4.3 Hz, 1H, HC(6)), 2.63 (ddd, *J* = 12.4, 10.2, 3.8 Hz, 1H, HC(1)), 1.94 – 1.86 (m, 1H, $H_2C(5)$), 1.96 – 1.85 (m, 2H, $H_2C(2)$, $H_2C(4)$), 1.80 – 1.74 (m, 3H, $H_2C(9)$, $H_2C(9)$, $H_2C(3)$), 1.52 (dtd, *J* = 13.0, 12.2, 11.6, 3.6 Hz, 1H, $H_2C(2)$), 1.45 – 1.29 (m, 3H, $H_2C(3)$, $H_2C(4)$, $H_2C(5)$), 0.84 (t, *J* = 7.4 Hz, 3H, $H_3C(10)$)

^{13}C-NMR: (500 MHz, $CDCl_3$)

144.80 (C(7)), 144.10 (C(11)), 128.33 (C(13)), 127.84 (C(12)), 126.28 (C(14)), 107.81 (C(8)), 82.34 (C(6)), 50.66 (C(1)), 34.29 (C(2)), 32.55 (C(5)), 26.09 (C(3)), 25.04 (C(4)), 20.99 (C(9)), 15.17 (C(10))

IR: (neat)

3029 (m), 2933 (s), 2857 (s), 1668 (s), 1651 (s), 1603 (w), 1494 (m), 1449 (m), 1373 (w), 1337 (w), 1253 (), 1170 (s), 1119 (m), 1066 (w), 1038 (m), 959 (w), 921 (m), 848 (w), 753 (m), 698 (s)

MS: (ESI, Q-tof)

231.2 (15) [M+1], 227.0 (5), 216.9 (10), 198.9 (5), 187.1 (12), 175.1 (5), 160.1 (12), 159.1 (100), 153.1 (15), 129.1 (5), 117.1 (4), 111.1 (10), 91.1 (38), 81.0 (8)

Opt. Rot.: $[\alpha]_D^{24}$ -26.0, (c = 1.04, EtOH)

Analysis: $C_{16}H_{22}O$ (230.17)

Calcd: C, 83.43; H, 9.63

Found: C, 83.34; H, 9.80

TLC: R_f 0.21 (TBME/Hexanes 1:19) [$KMnO_4$]

Preparation of (1*S*,3*S*,5*S*,5a*S*,7a*S*,7b*R*)-Octahydro-1-hydroxy-5-ethyl-7b-methyl-2*H*cyclopenta[*gh*]pyrrolizin-2-one (40c)

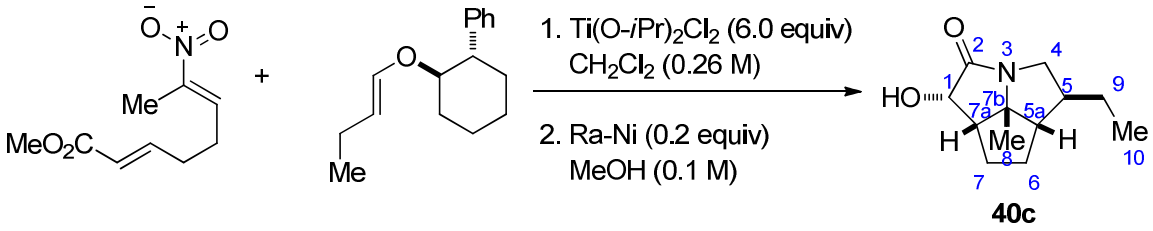

To a 25-mL, two-necked, round-bottomed flask fitted with two rubber septa, a magnetic stir bar, a nitrogen inlet adaptor and an internal temperature probe, was added nitroalkene (E,E)-1 (165 mg, 0.828 mmol) and chiral ether **40b**(210 mg, 0.918 mmol, 1.1 equiv) *via* syringe. The resulting yellow oil was then evacuated under high vacuum (~0.1 mm Hg) for 30 min. The flask was backfilled with N_2 and charged with CH_2Cl_2 (3.3 mL). The solution was cooled to –85 °C (internal temperature) using hexanes/N_2 bath. This yellow solution was sirred for 15 min, then freshly prepared $TiCl_2(O\textit{i}\text{-Pr})_2$ solution (1.2 M in CH_2Cl_2, 1.9 mL, 4.48 mmol, 6.0 equiv) was added dropwise *via* syringe while maintaining an internal temperature ≤ –70 °C (ca. 15 min). After addition of the Lewis acid, the cooling bath was replaced with an acetone/$CO_{2(s)}$ bath and the resulting bright yellow solution was stirred for another 5 h while maintaining an internal temperature ≤ –75 °C. During the course of the reaction, the yellow color gradually faded and a white precipitate formed. After 5 h the reaction was quenched with triethylamine (2.9 mL, 4.5 equiv, 1 M in MeOH) *via* syringe while maintaining an internal temperature of < –40 °C. The cooling bath was then removed and the reaction mixture was allowed to warm to 0 °C (ca. 15 min). The resulting white suspension was then poured onto a biphasic mixture H_2O (30 mL) and TBME (30 mL) in a 125-mL separatory funnel. The aqueous was separated and was washed with TBME (2 x 20 mL). The organic extracts were washed with H_2O (2 x 30 mL) and brine (1 x 30 mL). The combined organic extracts were dried over $NaHCO_3/MgSO_4$ (1/1), filtered (cotton plug), and concentrated by rotary evaporation (15 mm Hg, 20-25 °C). The resulting

residue was filtered through a pad of silica gel (5 mm x 4 cm), eluting with TBME (40 mL) to remove any remaining amine impurities. The resulting clear solution was concentrated by rotary evaporation (15 mm Hg, 20-25 ^{o}C) to a pale-yellow residual oil. The oil was allowed to stand for 8 h. The resulting mixture of nitroso acetals was diluted in MeOH (5 mL) and added to a test tube (5 mm x 14 cm) containing a spatula tip (~20 mg) of Raney Ni (previously washed with H_2O (3 x 10 mL) and MeOH (3 x 10 mL) along with a magnetic stir bar. The tube was placed in a steel autoclave, which was then pressurized with H_2 (350 psi). After 2 days the autoclave was *carefully* vented in a fume hood and the solution was filtered through a plug of Celite (5 cm x 5 cm, cotton plug) with MeOH (25 mL). The resulting clear solution was concentrated by rotary evaporation (15 mm Hg, 20-25 ^{o}C) and purified by silica gel column chromatography (2 cm x 8 cm, EtOAC/Hexanes, 10, 20, 30, 50, 70, 90%, 25 mL each). The white solid was recrystallized from TBME/Hexanes affording 148 mg (85%) of a white crystalline solid.

Data for **40c**

mp: 98-100 ^{o}C (TBME/Hexanes)

^{1}H-NMR: (500 MHz, $CDCl_3$)
4.65 (dd, *J* =2.1, 6.7 Hz, 1H, HC(1)), 4.08 (dd, *J* = 11.8, 6.7 Hz, 1H, $H_2C(4)$), 3.20 – 3.15 (m, 1H, OH), 2.53 (t, *J* = 10.9 Hz, 1H, $H_2C(4)$), 2.52 (dd, *J* = 10.0, 13.9, 1H, HC(7a)), 1.87 (t, *J* = 6.7 Hz, 1H, HC(5a)), 1.84 – 1.72 (m, 2H, $H_2C(6)$, $H_2C(7)$), 1.54 – 1.36 (m, 5H, HC(5), $H_2C(6)$, $H_2C(7)$, $H_2C(9)$, $H_2C(9)$), 1.31 (s, 3H, $H_3C(8)$), 0.90 (t, *J* = 7.1 Hz, 3H, $H_3C(10)$)

^{13}C-NMR: (500 MHz, $CDCl_3$)
175.87 (C(2)), 75.44 (C(7b)), 72.77 (C(1)), 56.48 (C(5a)), 52.12 (C(7a)), 49.56 (C(5)), 49.08 (C(4)), 31.84 (C(6) or C(7)), 26.87 (C(9)), 25.41 (C(6) or C(7)), 24.24 (C(8)), 12.84 (C(10))

MS: (ESI, Q-tof)
210.1 (100) [M+1], 192.1 (5)

Opt. Rot.: $[\alpha]_D^{24}$ -14.0, (c = 1.06, EtOH)

IR: ($CDCl_3$ film)
3306 (s), 3212 (s), 2955 (s), 2919 (s), 2864 (s), 1686 (s), 1458 (w), 1408 (m), 1375 (w), 1329 (w), 1292 (w), 1257 (w), 1225 (m), 1143 (m), 1116 (w), 1053

(w), 913 (w), 879 (w), 799 (w), 722 (w)

Analysis: $C_{12}H_{17}NO_2$ (207.13)

Calcd: C, 68.87; H, 9.15; N, 6.69

Found: C, 68.82; H, 9.33; N, 6.63

TLC: R_f 0.30 (EtOAc/Hexanes 3:2) [I_2, KMnO4]

Preparation of (1*R*,3*R*,5*R*,5a*S*,7a*S*,7b*R*)-Octahydro-1-[*N*-(3,5-Dinitrophenyl)carbamoxy]-5-thyl-7b-methyl-2H-cyclopenta[*gh*]pyrrolizin-2-one (40c-1)

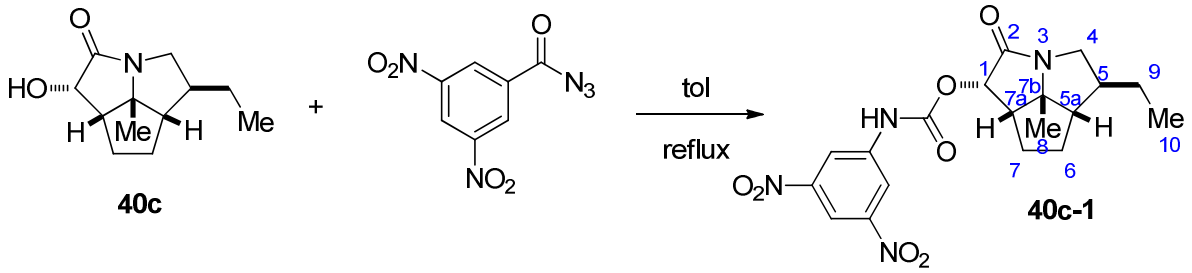

A 25 mL round-bottomed flask (A) was fitted with a reflux condenser, a nitrogen inlet adaptor, a rubber rubber septum and a magnetic stir bar. The apparatus was opened and 3,5-dinitrobenzoylazide (23 mg, 0.097 mmol, 1.5 equiv) was added as a solid. The apparatus was evacuated and backfilled with N_2 three times and toluene (1.8 mL) was added. The clear solution was immersed in a preheated (115 ^oC) oil bath and stirred at reflux for 30 min. In a separate, two-neck, 5 mL conical flask (B) fitted with a triangular a magnetic stir bar, rubber septum and a nitrogen inlet adaptor the starting alcohol was added (10 mg, 0.048 mmol) followed by toluene (1.0 mL). The resulting solution (B) was transferred to flask (A) *via* cannula. The resulting light yellow solution was heated to reflux for 2 h and then allowed to cool to room temperature. The reaction mixture was concentrated *in vacuo*, and the crude product was purified by column chromatography (hexane/EtOAc (3/1, 1/1)) to afford 10.5 mg (52%) of enantioenriched **40c-1** as a white solid. The sample was compared to racemate as previously described.

Data for **40c-1**:

^{1}H-NMR: (500 MHz, $CDCl_3$)

10.20 (s, 1H), 8.59 (s, 1H), 8.53 (s, 1H), 5.92 (d, J = 6.8 Hz, 1H), 4.15 (dd, J = 12.0, 7.1 Hz, 1H), 2.69 (t, J = 10.5 Hz, 2H), 2.02 (t, J = 7.2 Hz, 1H), 1.94 (dt, J = 12.3, 5.9 Hz, 1H), 1.85 (dt, J = 12.1, 6.2 Hz, 1H), 1.63 – 1.38 (m, 8H),

0.95 (t, J = 7.3 Hz, 3H, $H_3C(10)$).

TLC: R_f 0.38 (hexanes/EtOAc, 3:1) [I_2]

CHPLC: *t*R= 10.78 min (<1%) and 28.03 (>99%) (Naphthylleucine, 40 % IPA/Hexanes, 1.5 mL/min, 254 nm, 2 mg/mL)

Preparation of (3*R*,5*S*,5a*S*,7a*S*,7b*R*)-Octahydro-5-ethyl-7b-methyl-2*H*cyclopenta[*gh*]pyrrolizin-1,2-one (40d)

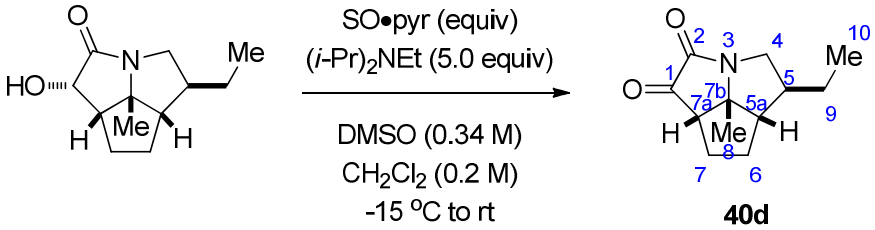

To a 25-mL, three-necked, round-bottomed flask fitted with a nitrogen inlet adapter, a magnetic stir bar, and an internal temperature probe was added **40c** (114 mg, 0.545 mmol), CH_2Cl_2 (2.3 mL), and DMSO (456 μL). The resulting solution was cooled to –12 °C in an ice/salt bath. To this solution was added diisopropylethylamine (475 μL, 2.73 mmol, 5.0 equiv) followed by the dropwise addition of a solution of SO_3•pyridine complex (260 mg, 1.64 mmol, 3.0 equiv) in DMSO (1.1 mL) while maintaining an internal temperature < –5 °C. After being stirred for 20 min at –10 °C, the mixture was allowed to warm to room temperature. The mixture was then cooled to 0 °C and diluted with CH_2Cl_2 (20 mL) and H_2O (25 mL). This mixture was poured into a 60-mL separatory funnel with CH_2Cl_2 (20 mL) and H_2O (20 mL). The aqueous layer was separated washed with CH_2Cl_2 (2 x 25 mL). The organic extracts were washed with 1.0 N. aq. HCl (2 x 20 mL), H_2O (1 x 20 mL), and brine (20 mL), the combined organic extracts dried over $NaSO_4$, filtered (cotton plug), and rinsed with TBME (3 x 10 mL). The mixture was filtered through a cotton plug and concentrated by rotary evaporation (15 mm Hg, 20-25°C). The crude oil was purified by silica gel chromatography (5 mm x 8 cm column, gradient elution, EtOAc/Hexanes, 20, 40, 60, 80, 90%, 25 mL each) to afford **40d** (108 mg, 96%) as a colorless oil.

Data for **40d**

^{1}H-NMR: (500 MHz, $CDCl_3$)

4.36 (dd, J = 12.4, 8.0 Hz, 1H, $H_2C(4)$), 3.00 (dd, J = 12.4, 8.3 Hz, 1H,

$H_2C(4)$), 2.70 (dd, J = 9.0, 5.4 Hz, 1H, HC(7a)), 2.17 – 2.06 (m, 2H, HC(5a), $H_2C(7)$), 2.06 – 1.98 (m, 1H, $H_2C(6)$), 1.80 (qd, J = 7.9, 4.3 Hz, 1H, HC(5)), 1.77 – 1.70 (m, 1H, $H_2C(7)$), 1.62 – 1.48 (m, 2H, $H_2C(9)$, $H_2C(9)$), 1.42 (s, 3H, $H_3C(8)$), 1.40 – 1.31 (m, 1H, $H_2C(6)$), 0.94 (t, J = 7.4 Hz, 3H, $H_3C(10)$)

^{13}C-NMR: (500 MHz, $CDCl_3$)

203.42 (C(1)), 160.21 (C(2)), 74.06 (C(7b)), 55.60 (C(7a)), 54.97 (C(5a)), 50.33 (C(4)), 48.63 (C(5)), 33.41 (C(6)), 30.61 (C(7)), 27.99 (C(9)), 24.89 (C(8)), 12.86 (C(10))

IR: ($CDCl_3$, film)

3501 (w), 3407 (w), 2958 (s), 1875 (s), 1759 (s), 1713 (s), 1461 (s), 1397 (s), 1335 (m), 1311 (m), 1264 (m), 1226 (s), 1180 (s), 1119 (m), 1087 (m), 1053 (m), 1024 (m), 1001 (w), 972 (w), 919 (m), 875 (w), 828 (w), 808 (w), 795 (w), 777 (w), 729 (m), 677 (m), 647 (m), 614 (w)

MS: (EI, 70 eV)

208.1 (100) [M+1], 198.2 (12)

Opt. Rot.: $[\alpha]_D^{24}$ -21.3, (c = 1.02, EtOH)

Mol. Formula: $C_{12}H_{17}NO_2$ (207.07)

HRMS: $C_{12}H_{18}NO_2^+$, (208.13)

Calcd: 208.1338

Found: 208.1342

TLC: R_f 0.38 (EtOAc/Hexanes, 1:1) [UV, I_2]

Preparation of (1*S*,3*S*,5*S*,5a*S*,7a*S*,7b*R*)-Octahydro-1-hydroxy-1-(2-naphthyl)-5-ethyl-7b-methyl-2*H*cyclopenta[*gh*] pyrrolizin-2-one (40e)

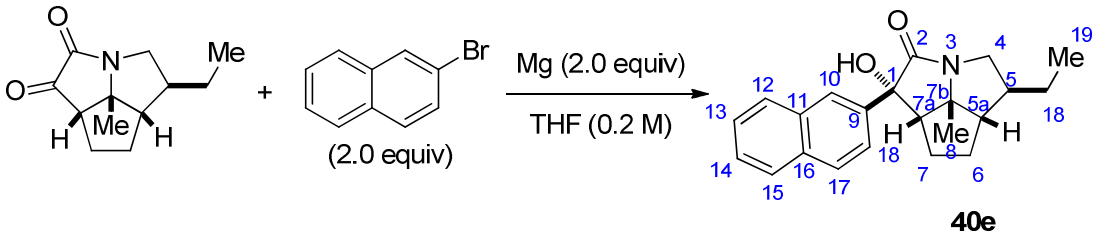

40e

To a 5-mL, two-necked, round-bottomed flask equipped with a nitrogen inlet adapter, a rubber septum and a magnetic stir bar was added **40d** (40 mg, 0.193 mmol) followed by THF

(470 μL). The flask was immersed in an ice bath and 2-naphthylmagnesium bromide (630 μL, 0.386 mmol, 2.0 equiv, in THF) was added dropwise via syringe. After being stirred for 10 min, the cooling bath was removed and the reaction was stirred at room temperature for 20 min. The solution was cooled in an ice bath and sat. aq. NH_4Cl (1.0 mL) is added. The resulting mixture was transferred to a 60-mL separatory funnel using an additional 20 mL of water and 20 mL of Et_2O and the aqueous phase was extracted with diethyl ether (3 x 15 mL). The organic extracts were washed with water (2 x 20 mL), and brine (1x 20 mL), then the combinded organic extracts were dried ($NaSO_4$). The mixture was filtered through a cotton plug and concentrated by rotary evaporation (15 mm Hg, 20-25^oC). Purification by silica gel chromatography (5.0 cm x 6 cm column, gradient elution, EtOAc/Hexanes, 10, 20, 30, 50%, 25 mL each) afforded 57.9 mg (89%) of **40e**.

Data for **40e**

^{1}H-NMR: (500 MHz, $CDCl_3$)

7.91 – 7.72 (m, 4H, ArH), 7.68 – 7.57 (m, 1H, ArH), 7.55 – 7.38 (m, 2H, ArH), 4.29 (dd, J = 11.7, 7.2 Hz, 1H, $H_2C(4)$), 3.39 – 3.37 (m, 1H, OH), 2.73 (t, J = 8.2 Hz, 1H, HC(7a)), 2.68 (t, J = 10.9 Hz, 1H, $H_2C(4)$), 2.06 – 1.99 (m, 1H, $H_2C(7)$), 1.92 – 1.74 (m, 3H, HC(5a), $H_2C(6)$, $H_2C(7)$), 1.64 – 1.55 (m, 1H, HC(5)), 1.54 – 1.40 (m, 3H, $H_2C(6)$, $H_2C(18)$, $H_2C(18)$), 0.95 (t, J = 7.1 Hz, 3H, $H_3C(19)$), 0.92 (s, 3H, $H_3C(8)$)

^{13}C-NMR: (500 MHz, $CDCl_3$)

176.25 (C(2)), 141.03 (C(9) or C(11) or C(16)), 133.05 (C(9) or C(11) or C(16)), 132.98 (C(9) or C(11) or C(16)), 128.69 (Ar), 128.46 (Ar), 127.64 (Ar), 126.38 (Ar), 126.30 (Ar), 125.27 (Ar), 124.96 (Ar), 83.19 (C(1) or C(7b)), 75.32 (C(1) or C(7b)), 57.87 (C(7a)), 57.04 (C(5a)), 49.55 (C(4)), 49.21 (C(5)), 31.17 (C(6)), 27.34 (C(7)), 26.97 (C(18)), 23.98 (C(8)), 12.88 (C(19))

IR: ($CDCl_3$, film)

3306 (s), 3051 (m), 2960 (s), 2926 (s), 2946 (s), 2860 (s), 1680 (s), 1505 (w), 1460 (m), 1438 (w), 1419 (s), 1362 (s), 1316 (m), 1300 (w), 1271 (w), 1250 (w), 1228 (m), 1206 (m), 1186 (w), 1165 (w), 1141 (m), 1113 (w), 1077 (m),

1025 (w), 967 (w), 908 (s), 864 (m), 814 (s), 730 (s), 650 (s), 622 (w)

MS: (ESI, Q-tof)

336.2 (60) [M+1], 318.2 (100)

Mol. Formula: $C_{22}H_{25}NO_2$ (335.44)

HRMS: $C_{22}H_{26}NO_2^+$, (336.20)

Calcd: 336.1964

Found: 336.1968

TLC: R_f 0.24 (EtOAc/Hexanes, 1:3) [UV, I_2]

Preparation of (1*S*,3*S*,5*S*,5a*S*,7a*S*,7b*R*)-Octahydro-1-hydroxy-1-(2-naphthyl)-5-ethyl-7b-methyl-2*H*cyclopenta[*gh*] pyrrolizin•Borane (40f)

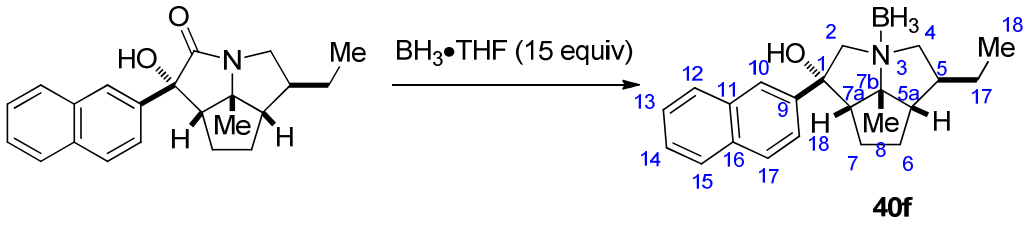

40f

To a 5-mL round-bottomed flask equipped with a nitrogen inlet adapter, a rubber septum, a reflux condenser, and a magnetic stir bar was added **40e** (56 mg, 0.167 mmol) then BH_3•THF complex (2.5 mL, 2.5 mmol, 15 equiv). The reaction flask was immersed in an oil bath and heated to reflux (66 ^oC). After being stirred for 12 h at reflux, the solution was allowed to reach room temperature and was quenched with methanol (5 mL) and concentrated by rotary evaporation (15 mm Hg, 20-25^oC). The resulting colorless oil was purified by silica gel column chromatography (5.0 mm x 8 cm column, gradient elution, TBME/Heaxanes, 5, 10, 15, 20, 25, 30% 25 mL each) to afford 55 mg (98%) of **40f** as a white solid

Data for **40f**

^{1}H-NMR: (500 MHz, $CDCl_3$)

7.88 – 7.78 (m, 4H, ArH), 7.53 – 7.48 (m, 2H, ArH), 7.47 (dd, J = 8.6, 2.0 Hz, 1H, ArH), 4.19 (d, J = 13.7 Hz, 1H, $H_2C(2)$), 3.78 (dd, J = 12.3, 8.2 Hz, 1H, $H_2C(4)$), 3.73 (d, J = 13.7 Hz, 1H, $H_2C(2)$), 3.34 (dd, J = 12.2, 10.2 Hz, 1H, $H_2C(4)$), 2.82 (dd, J = 9.2, 5.9 Hz, 1H, HC(7a)), 2.45 – 2.36 (m, 1H, HC(5)),

2.38 – 2.30 (m, 1H, $H_2C(7)$), 2.06 – 1.98 (m, 4H, HC(5a), $H_2C(6)$, $H_2C(6)$, OH), 1.93 – 1.86 (m, 1H, $H_2C(7)$), 1.57 (s, 3H, $H_3C(8)$), 1.56 – 1.47 (m, 1H, $H_2C(7)$), 1.45 – 1.34 (m, 1H, $H_2C(7)$), 0.92 (t, J = 7.5 Hz, 3H, $H_3C(18)$)

^{13}C-NMR: (500 MHz, $CDCl_3$)

142.14 (C(9) or C(11) or C(16)), 133.00 (C(9) or C(11) or C(16)), 132.75 (C(9) or C(11) or C(16)), 129.00 (Ar), 128.31 (Ar), 127.65 (Ar), 126.73 (Ar), 126.60 (Ar), 123.59 (Ar), 123.47 (Ar), 89.67 (C(1) or C(7b)), 79.70 (C(1) or C(7b)), 78.77 (C(2)), 73.12 (C(4)), 62.80 (C(7a)), 58.47 (C(5a)), 42.38 (C(5)), 32.63 (C(6)), 27.27 (C(17)), 25.32 (C(8)), 24.60 (C(7)), 12.91 (C18))

IR: ($CDCl_3$, film)

3477 (s), 3058 (m), 2962 (s), 2926 (s), 2874 (s), 2383 (s), 2351 (s), 2327 (s), 2272 (s), 2236 (s), 1633 (w), 1600 (m), 1506 (m), 1455 9s), 1379 (s), 1340 (m), 1273 (m), 1232 (m), 1170 (s), 1132 (s), 1061 (m), 1018 (m), 987 (m), 949 (m), 908 (s), 858 (m), 816 (m), 732 (s), 648 (m)

MS: (ESI, Q-tof)

332.2 (100) [M-3], 322.2 (55), 216.1 (12)

Mol. Formula: $C_{22}H_{30}BNO$ (335.29)

HRMS: $C_{22}H_{27}BNO^+$, (322.22)

Calcd: 332.2186

Found: 332.2188

TLC: R_f 0.31 (TBME/Hexanes, 1:4) [UV, I_2]

Preparation of (1*S*,3*S*,5*S*,5a*S*,7a*S*,7b*R*)-Octahydro-1-benzyloxy-1-(2-naphthyl)-5-ethyl-7b-methyl-2*H*cyclopenta[*gh*]pyrrolizine•Borane (40g)

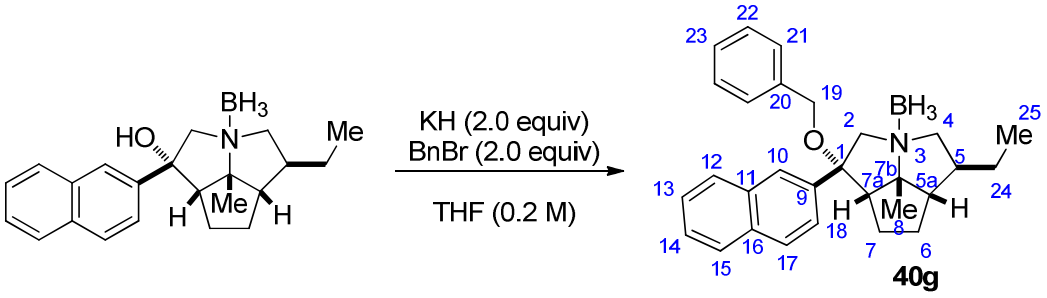

To a two-necked, 5-mL, round-bottomed flask equipped with a nitrogen inlet adapter, a rubber septum and a magnetic stir bar was added washed potassium hydride (13.2 mg, 0.328 mmol, 2.0 equiv) from the drybox followed by THF (400 μL). A solution of alcohol **40f** (55 mg, 0.164 mmol) in THF (1.2 mL) is added to the reaction vessel by cannulation. After 15 min of stirring, the flask is immersed in an ice bath. The benzyl bromide (39 μL, 0.328 mmol, 2.0 equiv) is then added dropwise by syringe. The ice bath is removed and the solution is allowed to stir for 2 h at rt. This mixture was cooled in an ice bath and cold sat. aq. NH_4Cl (1.0 mL) is added in one portion. The resulting mixture was transferred to a 60-mL separatory funnel using an additional 15 mL of water and 15 mL of Et_2O and the aqueous phase was extracted with diethyl ether (3 x 15 mL). The organic extracts were washed with water (2 x 20 mL), and brine (1x 20 mL), then the combinded organic extracts were dried ($NaSO_4$). The mixture was filtered through a cotton plug and concentrated by rotary evaporation (15 mm Hg, 20-25°C). Purification by silica gel chromatography (5.0 cm x 8 cm column, gradient elution, TBME/Hexanes, 2, 4, 6, 8, 10, 12%, 25 mL each) afforded 64.1 mg (92%) of ether **40g**.

Data for **40g**

^{1}H-NMR: (500 MHz, $CDCl_3$)

7.94 – 7.84 (m, 3H, ArH), 7.81 (s, 1H, HC(10)), 7.59 – 7.50 (m, 3H, ArH), 7.37 – 7.26 (m, 3H, HC(21), HC(23)), 7.26 – 7.21 (m, 2H, HC(22)), 4.32 (d, J = 13.4 Hz, 1H, $H_2C(2)$), 4.20 (d, J = 11.0 Hz, 1H, $H_2C(19)$), 4.09 (d, J = 13.4 Hz, 1H, $H_2C(2)$), 3.99 (d, J = 11.0 Hz, 1H, $H_2C(19)$), 3.60 (dd, J = 12.3, 8.1 Hz, 1H, $H_2C(4)$), 3.30 (dd, J = 12.3, 10.6 Hz, 1H, $H_2C(4)$), 2.91 – 2.83 (m, 1H, HC(7a)), 2.80 (dd, J = 12.5, 7.6 Hz, 1H, $H_2C(7)$), 2.38 – 2.27 (m, 1H, HC(5)), 2.07 – 1.84 (m, 4H HC(5a), HC(5), $H_2C(6)$, $H_2C(6)$, $H_2C(7)$), 1.55 (s, 3H, $H_3C(8)$), 1.60 – 1.48 (m, 1H, $H_2C(24)$), 1.39 – 1.25 (m, 1H, $H_2C(24)$), 0.80 (t, J = 7.4 Hz, 3H, $H_3C(25)$)

^{13}C-NMR: (500 MHz, $CDCl_3$)

139.04 (C(9) or C(11) or C(16) or C(20)), 137.85 C(9) or C(11) or C(16) or C(20)), 132.94 C(9) or C(11) or C(16) or C(20)), 132.84 C(9) or C(11) or C(16) or C(20)), 129.06 (Ar), 128.48 (C(28)), 128.39 (Ar), 127.72 (C(23)), 127.68 (C(21)), 127.67 (Ar), 126.65 (Ar), 126.62 (Ar), 124.82 (C(10)), 124.69

(Ar), 88.82 (C(1) or C(7b)), 83.37 (C(1) or C(7b)), 72.40 (C(4)), 70.28 (C(2)), 66.57 (C(19)), 62.57 (C(7a)), 58.63 (C(5a)), 41.68 (C(5)), 31.83 (C(6)), 27.01 (C(24)), 25.08 (C(8)), 24.17 (C(7)), 12.84 (C25))

IR: ($CDCl_3$, film)

3060 (m), 3031 (m), 2929 (s), 2960 (s), 2872 (s), 2390 (s), 2351 (s), 2327 (s), 2274 (s), 2241 (s), 1949 (w), 1808 (w), 1633 (w), 1601 (m), 1497 (m), 1455 (s), 1379 (s), 1350 (m), 1319 (w), 1270 (m), 1235 (m), 1171 (s), 1136 (s), 1083 (s), 1062 (s), 1027 (s), 988 (m), 946 (w), 911 (s), 859 (s), 820 (s), 771 (w), 737 (s), 697 (s), 673 (w), 647 (m), 607 (m)

MS: (ESI, Q-tof)

422.3 (100) [M-3], 412.3 (28), 207.2 (2), 185.1 (5), 180.2 (9), 158.0 (6), 126.0 (6), 100.1 (42), 89.1 (5), 79.0 (10)

Mol. Formula: $C_{29}H_{36}BNO$ (425.41)

HRMS: $C_{29}H_{33}BNO^+$, (422.27)

Calcd: 422.2655

Found: 422.2659

TLC: R_f 0.21 (TBME/Hexanes, 1:9) [UV, I_2]

Preparation of *rel*-(1*S*,3*R*,5*S*,5a*S*,7a*S*,7b*R*) Octahydro-1-hexyloxy-1-(2-naphthyl)-3-(3,5-bistrifluoromethylphenylmethyl)-5-ethyl-7b-methylcyclopenta[*gh*]pyrrolizinium Bromide (40)

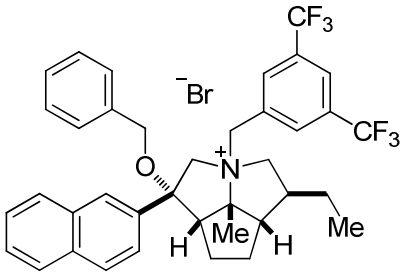

40

Data for **40**

Yield: 51 mg (97%), free-flowing white powder

^{1}H-NMR: (500 MHz, $CDCl_3$)

8.25 (s, 1H), 8.21 (d, J = 8.7 Hz, 1H), 8.03 – 7.94 (m, 4H), 7.89 (s, 1H), 7.74

(dd, J = 8.7, 2.0 Hz, 1H), 7.70 – 7.67 (m, 2H), 7.35 – 7.26 (m, 3H), 7.18 – 7.11 (m, 2H), 5.94 (d, J = 12.3 Hz, 1H), 5.27 (t, J = 11.0 Hz, 1H), 4.13 (d, J = 13.5 Hz, 1H), 4.06 (d, J = 10.7 Hz, 1H), 3.84 (d, J = 10.6 Hz, 1H), 3.71 – 3.60 (m, 2H), 3.42 (d, J = 9.5 Hz, 1H), 3.03 (dd, J = 11.0, 6.0 Hz, 1H), 2.89 (d, J = 6.9 Hz, 1H), 2.60 – 2.45 (m, 1H), 2.44 (s, 3H), 2.33 – 2.23 (m, 1H), 2.19 – 2.00 (m, 3H), 1.82 (p, J = 7.7 Hz, 2H), 0.96 (t, J = 7.4 Hz,, 3H)

MS: (ESI, Q-tof)

638.3 (100) [M-Br^-]

Mol. Formula: $C_{38}H_{38}BrF_6NO$ (718.61)

HRMS: $C_{38}H_{38}F_6NO^+$, (638.29)

Calcd: 638.2858

Found: 638.2872

TLC: R_f 0.32 (CH_2Cl_2/MeOH, 9:1) [I_2]

Preparation of (1*R*,2*S*)-2-Phenyl-1-(2-prenyloxy)cyclohexane (43)

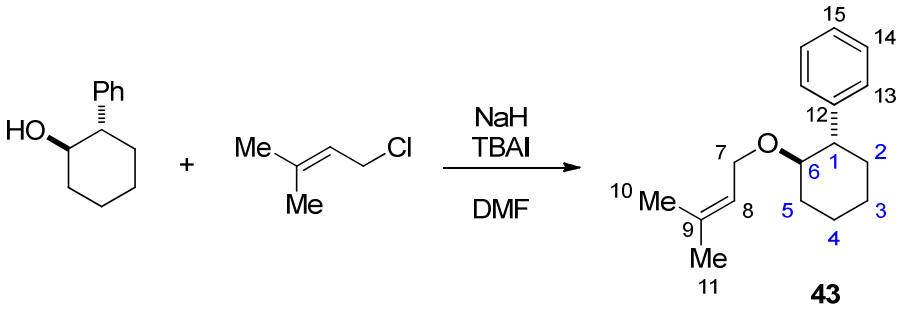

43

To a two-necked, 50-mL, round-bottomed flask equipped with a nitrogen inlet adapter, a rubber septum and a magnetic stir bar was added washed sodium hydride (136 mg, 5.67 mmol, 2.0 equiv) from the drybox followed by DMF (4.5 mL). A solution of alcohol **11** (500 mg, 2.84 mmol) in THF (5.0 mL) is added to the reaction vessel by cannulation. After 10 min of stirring, tetrabutylammonium iodide (105 mg, 0.284 mmol, 0.1 equiv) is added followed by prenyl chloride (639 µL, 5.67 mmols, 2.0 equiv) by syringe. After 12 h of stirring at rt, the reaction flsk is placed in an ice bath and sat. aq. NH_4Cl (5.0 mL) is added. The resulting mixture was transferred to a 125-mL separatory funnel using an additional 40 mL of Et_2O and 40 mL. The aqueous phase was separated and was extracted with Et_2O (2 x 40 mL). The organic extracts were washed with water (3 x320 mL), and brine (1x 20 mL), then the combinded organic

extracts were dried ($NaSO_4$). The mixture was filtered through a cotton plug and concentrated by rotary evaporation (15 mm Hg, 20-25^oC). Purification by silica gel chromatography (20 mm x 10 cm column, gradient elution, TBME/Hexanes, 1, 2, 4, 8, 10%, 100 mL each). The resulting oil was distilled (135 ^oC, 0.13 torr) to afforded 679 mg (98%) of ether **43**.

Data for **43**

bp: 135 ˚C / 0.13 torr

^{1}H-NMR: (500 MHz, $CDCl_3$)

7.33 – 7.22 (m, 4H, HC(13), HC(14)), 7.19 (dtd, *J* = 7.1, 5.0, 2.5 Hz, 1H, HC(15)), 5.02 (t, *J* = 6.9 Hz, 1H, HC(4)), 3.77 (dd, *J* = 11.3, 6.7 Hz, 1H, H_2C(3)), 3.53 (dd, *J* = 11.3, 7.0 Hz, 1H, H_2C(4)), 3.32 (td, *J* = 10.1, 4.6 Hz, 1H, HC(6)), 2.53 (ddd, *J* = 12.2, 10.2, 3.8 Hz, 1H, HC(1)), 2.19 (ddd, *J* = 7.7, 4.2, 1.8 Hz, 1H, H_2C(5)), 1.86 (ddt, *J* = 11.6, 4.6, 2.4 Hz, 2H, H_2C(2), H_2C(4)), 1.78 – 1.70 (m, 1H, H_2C(3)), 1.62 (d, *J* = 1.4 Hz, 3H, H_3C(10)), 1.57 – 1.46 (m, 1H), 1.42 – 1.37 (m, 3H, H_3C(11)), 1.34 (ddd, *J* = 12.4, 7.2, 2.4 Hz, 2H)

^{13}C-NMR: (500 MHz, $CDCl_3$)

145.09 (C(6)), 136.63 (C(9)), 128.16 (C(14)), 127.97 (C(13)), 126.06 (C(15)), 121.65 (C(8)), 81.29 (C(6)), 65.73 (C(7)), 51.43 (C(5)), 34.23 (C(1)), 32.77 (C(2), 26.21, 25.83, 25.37, 17.75 (10)

IR: (neat)

3052 (w), 3027 (m), 2926 (s), 2850 (s), 1670 (w), 1602 (w), 1493 (m), 1447 (s), 1375 (m), 1351 (m), 1240 (w), 1195 (w), 1118 (s), 1080 (s), 1028 (m), 1011 (m), 983 (w), 952 (w), 903 (w), 865 (w), 848 (w), 754 (s), 698 (s)

MS: (ESI, Q-tof)

245 (10) [M+1], 227 (90), 207 (5), 197 (5), 175 (12), 159 (100), 146 (5), 139 (11), 117 (22)

Opt. Rot.: $[\alpha]_D^{24}$ -45.5, (c = 1.02, EtOH)

Analysis: $C_{17}H_{24}O$ (244.18)

Calcd: C, 83.55; H, 9.90

Found: C, 83.52; H, 9.92

TLC: R_f 0.74 (TBME/Hexanes 1:3) [UV, $KMnO_4$]

Preparation of (1*R*,2*S*)-2-Phenyl-1-(1-prenyloxy)cyclohexane (44)

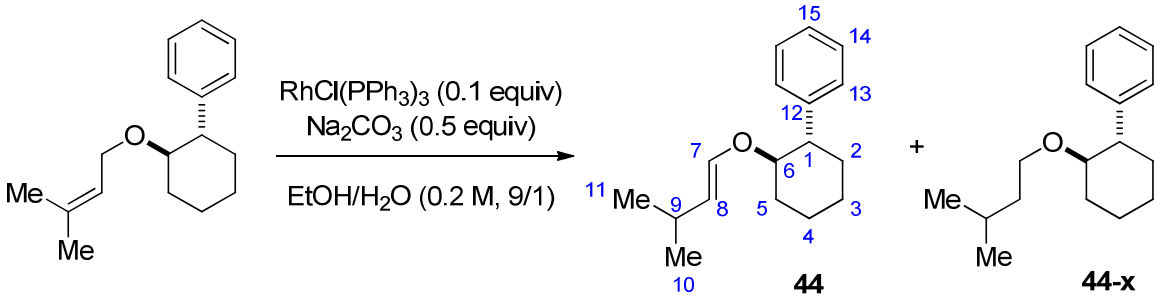

To a two-necked, 50-mL, round-bottomed flask equipped with a nitrogen inlet adapter, a rubber septum and a magnetic stir bar was added ether **43** (663 mg, 2.71 mmol), ethanol (12.2 mL), H_2O (1.4 mL), sodium carbonate (144 mg, 1.36 mmol, 0.5 equiv), and Rhodium(I)tri(triphenylphosphine)Chloride (250.7 mg, 0.271 mmol). The reaction flask is placed in a oil bath at 80 °C. After 2.5 h, the oil bath is removed and the solution is allowed to reach rt. The mixture was concentrated by rotary evaporation (15 mm Hg, 20-25°C). Purification by basic alumina chromatography (20 mm x 15 cm column, gradient elution, TBME/Hexanes, 0, 1, 2, 4, 8%, 100 mL each) to afforded 188 mg of an inseparable mixture of the desired product **44** (129 mg, 20%) and saturated side prouct **44-x**.

Data for **44**

^{1}H-NMR: (500 MHz, $CDCl_3$)

7.34 – 7.28 (m, 3H, ArH), 7.28 – 7.17 (m, 4H, ArH), 5.77 (dt, *J* = 12.5, 0.9 Hz, 1H, HC(7)), 4.67 (dd, *J* = 12.3, 7.4 Hz, 1H, HC(8)), 3.71 (td, *J* = 10.2, 4.2 Hz, 1H, HC(6)), 3.43 (dt, *J* = 9.4, 6.2 Hz, 0.45H), 3.28 (td, *J* = 10.3, 4.2 Hz, 0.45H), 2.98 (dt, *J* = 9.4, 6.8 Hz, 0.45H), 2.64 (ddd, *J* = 12.5, 10.1, 3.8 Hz, 1H, HC(1)), 2.54 (ddd, *J* = 12.5, 10.1, 3.7 Hz, 0.43H), 2.29 – 2.16 (m, 1H, H_2C(5)), 2.04 (sept, *J* = 6.3 Hz, 1H, HC(9)), 1.95 – 1.86 (m, 2H, H_2C(2), H_2C(4)), 1.80 – 1.74 (m, 1H, H_2C(3)), 1.61 – 1.48 (m, 1H, H_2C(2)), 1.47 – 1.28 (m, 3H, H_2C(3), H_2C(4), H_2C(5)), 1.22 (dq, *J* = 13.5, 6.7 Hz, 0.45H), 1.13 (dq, *J* = 13.5, 6.5 Hz, 0.45H), 0.86 (d, *J* = 6.7 Hz, 3H, H_3C(11) or H_3C(10)), 0.83 (d, *J* = 6.7 Hz, 3H, H_3C(10) or H_3C(11)), 0.72 (d, *J* = 6.6 Hz,

11.19H), 0.62 (d, J = 6.5 Hz, 1.12H)

^{13}C-NMR: (500 MHz, $CDCl_3$)

145.11, 144.09, 143.83 (C(7)), 128.34 C(14)), 128.12, 127.92 (C(13)), 127.89, 126.29 (C(15)), 126.03, 113.56 (C(8)), 82.53 (C(6)), 82.48, 67.65, 51.37, 50.85 (C(1)), 38.96, 34.23 (C(2)), 34.09, 34.06, 32.63 (C(5)), 27.30 (C(9)), 26.25, 26.08 (C(3)), 25.32, 25.08 (C(4)), 24.57, 23.62 (C(10) or C(11)), 23.60 (C(10) or C(11)), 22.79, 22.23

IR: (neat)

3066 (w), 3028 (m), 2929 (s), 2856 (s), 1668 (s), 1650 (m), 1603 (w), 1493 (m), 1448 (s), 1375 (w), 1360 (m), 1250 (w), 1168 (s), 1117 (s), 1070 (m), 1036 (w), 948 (w), 923 (m), 871 (w), 848 (w), 815 (w), 754 (s), 698 (s)

TLC: R_f 0.24 (TBME/Hexanes 1:19) [UV, $KMnO_4$]

Preparation of (1*S*,3*S*,5*S*,5a*S*,7a*S*,7b*R*)-Octahydro-1-hydroxy-5-isopropyl-7b-methyl-2*H*cyclopenta[*gh*]pyrrolizin-2-one (41a)

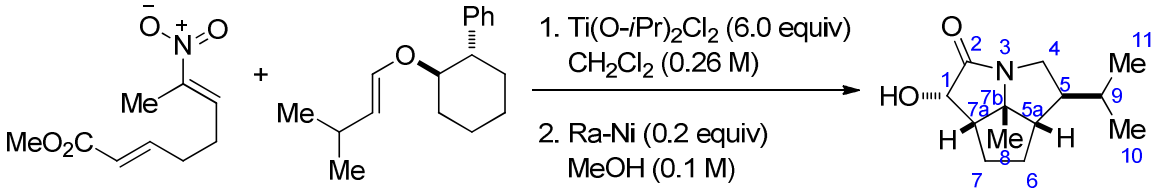

41a

To a 25-mL, two-necked, round-bottomed flask fitted with two rubber septa, a magnetic stir bar, a nitrogen inlet adaptor and an internal temperature probe, was added nitroalkene (E,E)-1 (95.6 mg, 0.48 mmol) and chiral propenyl ether **44** (129 mg, 0.528 mmol, 1.1 equiv) *via* syringe. The resulting yellow oil was then evacuated under high vacuum (~0.1 mm Hg) for 30 min. The flask was backfilled with N_2 and charged with CH_2Cl_2 (2.1 mL). The solution was cooled to –85 ^{o}C (internal temperature) using hexanes/N_2 bath. This yellow solution was sirred for 15 min, then freshly prepared $TiCl_2(O$*i*-Pr)$_2$ solution (1.2 M in CH_2Cl_2, 1.2 mL, 1.44 mmol, 6.0 equiv) was added dropwise *via* syringe while maintaining an internal temperature ≤ –70 ^{o}C (ca. 15 min). After addition of the Lewis acid, the cooling bath was replaced with an acetone/$CO_{2(s)}$ bath and the resulting bright yellow solution was stirred for another 5 h while maintaining an internal temperature ≤ –75 ^{o}C. During the course of the reaction, the yellow

color gradually faded and a white precipitate formed. After 5 h the reaction was quenched with triethylamine (2.9 mL, 6.1 equiv, 1 M in MeOH) *via* syringe while maintaining an internal temperature of < –40 °C. The cooling bath was then removed and the reaction mixture was allowed to warm to 0 °C (ca. 15 min). The resulting white suspension was then poured onto a biphasic mixture H_2O (30 mL) and TBME (30 mL) in a 125-mL separatory funnel. The aqueous was separated and was washed with TBME (2 x 20 mL). The organic extracts were washed with H_2O (2 x 30 mL) and brine (1 x 30 mL). The combined organic extracts were dried over $NaHCO_3/MgSO_4$ (1/1), filtered (cotton plug), and concentrated by rotary evaporation (15 mm Hg, 20-25 °C). The resulting residue was filtered through a pad of silica gel (5 mm x 4 cm), eluting with TBME (40 mL) to remove any remaining amine impurities. The resulting clear solution was concentrated by rotary evaporation (15 mm Hg, 20-25 °C) to a pale-yellow residual oil. The oil was allowed to stand for 8 h. The resulting mixture of nitroso acetals was diluted in MeOH (5 mL) and added to a test tube (5 mm x 14 cm) containing a spatula tip (~20 mg) of Raney Ni (previously washed with H_2O (3 x 10 mL) and MeOH (3 x 10 mL) along with a magnetic stir bar. The tube was placed in a steel autoclave, which was then pressurized with H_2 (350 psi). After 2 days the autoclave was *carefully* vented in a fume hood and the solution was filtered through a plug of Celite (5 cm x 5 cm, cotton plug) with MeOH (25 mL). The resulting clear solution was concentrated by rotary evaporation (15 mm Hg, 20-25 °C) and purified by silica gel column chromatography (2 cm x 8 cm, EtOAC/Hexanes, 10, 20, 30, 50, 70, 90%, 25 mL each). The white solid was recrystallized from TBME/Hexanes affording 89.5 mg (83%) of a white crystalline solid.

Data for **41a**

mp: 127-129 °C (TBME/Hexanes)

^{1}H-NMR: (500 MHz, $CDCl_3$)

4.65(d, *J* = 6.4 Hz, 1H, HC(1)), 4.05 (dd, *J* = 7.4, 11.6 Hz, 1H, $H_2C(4)$), 3.42 (m, 1H, OH), 2.58 (t, *J* = 11.0 Hz, 1H, $H_2C(4)$), 2.50 (dt, *J* = 10.1, 6.8 Hz, 1H, HC(7a)), 1.94 (t, *J* = 7.5 Hz, 1H, HC(5a)), 1.88 – 1.71 (m, 2H, $H_2C(6)$, $H_2C(7)$), 1.58 – 1.37 (m, 3H, $H_2C(6)$, $H_2C(7)$, HC(9)), 1.29 (s, 3H, $H_3C(8)$), 1.33 – 1.25 (m, 1H, HC(5)), 0.92 (dd, *J* = 6.8, 2.4 Hz, 3H, $H_3C(10)$ or $H_3C(11)$), 0.87 (dd, *J* = 6.8, 2.5 Hz, 3H, $H_3C(10)$ or $H_3C(11)$)

^{13}C-NMR: (500 MHz, $CDCl_3$)

175.65 (C(2)), 75.48 (C(7b)), 72.83 (C(1)), 55.10 (C(5)), 54.97 (C(5a)), 52.31 (C(7a)), 47.94 (C(4)), 32.78 (C(9)), 32.60 (C(6)), 25.34 (C(7)), 24.10 (C(8)), 21.45 (C(10) or C(11)), 21.33 (C(10) or C(11))

IR: ($CDCl_3$ film)

3306 (s), 2957 (s), 2871 (s), 1681 (s), 1453 (s), 1416 (s), 1380 (s), 1335 (s), 1297 (m), 1260 (w), 1227 (m), 1179 (w), 1145 (m), 1114 (s), 1096 (m), 1034 (w), 1004 (w), 962 (w), 910 (m), 848 (w), 796 (m), 734 (s), 665 (w), 646 (m)

MS: (ESI, Q-tof)

224.2 (100) [M+1]

Opt. Rot.: $[\alpha]_D^{24}$ -13.0, (c = 1.02, EtOH)

Analysis: $C_{13}H_{21}NO_2$ (223.16)

Calcd: C, 69.92; H, 9.48; N, 6.27

Found: C, 69.85; H, 9.58; N, 6.28

TLC: R_f 0.24 (EtOAc/Hexanes 3:2) [$KMnO_4$]

Preparation of (1*R*,3*R*,5*R*,5a*S*,7a*S*,7b*R*)-Octahydro-1-[*N*-(3,5-Dinitrophenyl)carbamoxy]-5-isopropyl-7b-methyl-2H-cyclopenta[*gh*]pyrrolizin-2-one (40c-1)

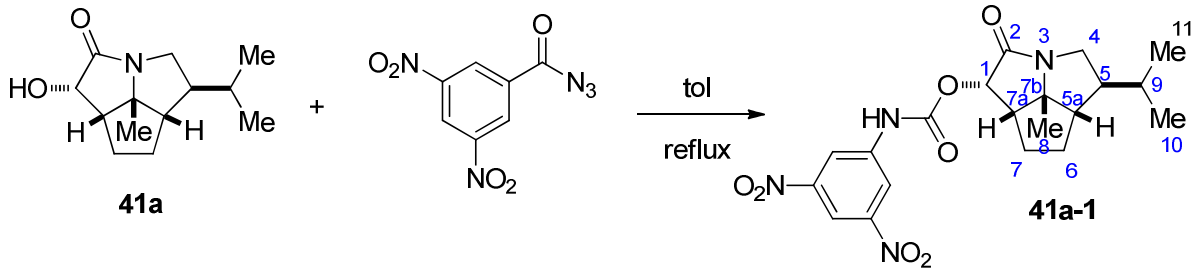

A 25 mL round-bottomed flask (A) was fitted with a reflux condenser, a nitrogen inlet adaptor, a rubber rubber septum and a magnetic stir bar. The apparatus was opened and 3,5-dinitrobenzoylazide (23 mg, 0.097 mmol, 1.5 equiv) was added as a solid. The apparatus was evacuated and backfilled with N_2 three times and toluene (1.8 mL) was added. The clear solution was immersed in a preheated (115 ^oC) oil bath and stirred at reflux for 30 min. In a separate, two-neck, 5 mL conical flask (B) fitted with a triangular a magnetic stir bar, rubber septum and a nitrogen inlet adaptor the starting alcohol was added (10 mg, 0.045 mmol) followed by toluene (1.0 mL). The resulting solution (B) was transferred to flask (A) *via* cannula. The resulting light

yellow solution was heated to reflux for 2 h and then allowed to cool to room temperature. The reaction mixture was concentrated *in vacuo*, and the crude product was purified by column chromatography (hexane/EtOAc (3/1, 1/1)) to afford 11.6 mg (60%) of enantioenriched **41a-1** as a white solid.

Data for **41a-1**:

^{1}H-NMR: (500 MHz, $CDCl_3$)

9.83 (s, 1H), 8.64 – 8.58 (m, 0H), 8.54 (d, J = 2.0 Hz, 2H), 5.89 (d, J = 6.6 Hz, 1H), 4.13 (dd, J = 11.9, 7.4 Hz, 1H), 2.86 – 2.64 (m, 2H), 2.09 (t, J = 7.4 Hz, 1H), 2.01 – 1.92 (m, 1H), 1.92 – 1.78 (m, 1H), 1.73 – 1.59 (m, 2H), 1.59 – 1.50 (m, 2H), 1.44 (s, 4H), 0.97 (d, J = 6.6 Hz, 3H), 0.92 (d, J = 6.6 Hz, 3H).

TLC: R_f 0.40 (hexanes/EtOAc, 3:1) [I_2]

CHPLC: *t*R= 10.56 min (<1%) and 28.64 (>99%) (Naphthylleucine, 40 % IPA/Hexanes, 1.5 mL/min, 254 nm, 2 mg/mL)

Preparation of (3*R*,5*S*,5a*S*,7a*S*,7b*R*)-Octahydro-5-isopropyl-7b-methyl-2*H*cyclopenta[*gh*]pyrrolizin-1,2-one (41b)

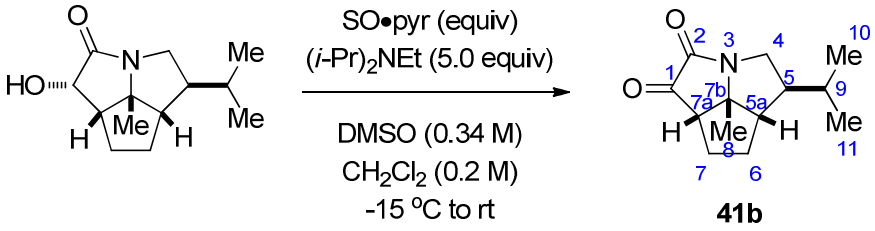

To a 10-mL, three-necked, round-bottomed flask fitted with a nitrogen inlet adapter, a magnetic stir bar, and an internal temperature probe was added **41a** (68.5 mg, 0.307 mmol), CH_2Cl_2 (1.3 mL), and DMSO (257 µL). The resulting solution was cooled to –12 °C in an ice/salt bath. To this solution was added diisopropylethylamine (267 µL, 1.53 mmol, 5.0 equiv) followed by the dropwise addition of a solution of SO_3•pyridine complex (146 mg, 0.92 mmol, 3.0 equiv) in DMSO (636 µL) while maintaining an internal temperature < –5 °C. After being stirred for 20 min at –10 °C, the mixture was allowed to warm to room temperature. The mixture was then cooled to 0 °C and diluted with CH_2Cl_2 (20 mL) and H_2O (25 mL). This mixture was poured into a 60-mL separatory funnel with CH_2Cl_2 (20 mL) and H_2O (20 mL). The aqueous layer was separated washed with CH_2Cl_2 (2 x 25 mL). The organic extracts were washed with 1.0 N. aq. HCl (2 x 20 mL), H_2O (1 x 20 mL), and brine (20 mL), the combined organic extracts

dried over $NaSO_4$, filtered (cotton plug), and rinsed with TBME (3 x 10 mL). The mixture was filtered through a cotton plug and concentrated by rotary evaporation (15 mm Hg, 20-25°C). The crude oil was purified by silica gel chromatography (5 mm x 8 cm column, gradient elution, EtOAc/Hexanes, 20, 40, 60, 80, 90%, 25 mL each) to afford **41b** (66.2 mg, 97%) as a colorless oil.

Data for **41b**

^{1}H-NMR: (500 MHz, $CDCl_3$)

4.32 (dd, *J* = 12.4, 7.8 Hz, 1H, $H_2C(4)$), 3.04 (dd, *J* = 12.3, 9.2 Hz, 1H, $H_2C(4)$), 2.70 (dd, *J* = 8.6, 6.8 Hz, 1H, HC(7a)), 2.15 (dt, *J* = 7.2, 5.1 Hz, 1H, HC(5a)), 2.12 – 1.98 (m, 2H, $H_2C(6)$, $H_2C(7)$), 1.74 – 1.68 (m, 1H, $H_2C(7)$), 1.65 – 1.59 (m, 1H, HC(9)), 1.56 – 1.49 (m, 1H, HC(5)), 1.45 – 1.38 (m, 1H, $H_2C(6)$), 1.40 (s, 3H, $H_3C(8)$), 0.95 (d, *J* = 6.5 Hz, 3H, $H_3C(10)$ or $H_3C(11)$), 0.90 (d, *J* = 6.4 Hz, 3H, $H_3C(10)$ or $H_3C(11)$)

^{13}C-NMR: (500 MHz, $CDCl_3$)

203.01 (C(1)), 159.90 (C(2)), 74.28 (C(7b)), 55.81 (C(7a)), 55.19 (C(5)), 53.60 (C(5a)), 49.31 (C(4)), 34.26 (C(6)), 32.79 (C(9)), 30.07 (C(7)), 25.02 (C(8)), 21.48 (C(10) or C(11)), 21.26 (C(10) or C(11))

IR: (neat)

3411 (m), 2960 (s), 2872 (s), 1764 (s), 1713 (s), 1463 (s), 1402 (s), 1370 (m), 1333 (m), 1265 (w), 1232 (s), 1205 (w), 1182 (s), 1137 (w), 1123 (w), 1090 (m), 1069 (w), 1037 (w), 1000 (w), 961 (w), 914 (s), 852 (w), 828 (w), 794 (w), 730 (s), 678 (s), 646 (s)

MS: (ESI, Q-tof)

222.1 (100) [M+1], 212.2 (28)

Opt. Rot.: $[\alpha]_D^{24}$ -2.2, (c = 1.1, EtOH)

Mol. Formula: $C_{13}H_{19}NO_2$ (221.30)

HRMS: $C_{13}H_{20}NO_2^+$: (350.2120)

Calcd: 222.1494

Found: 222.1501

TLC: R_f 0.21 (EtOAc/Hexanes 2:3) [UV, I_2]

Preparation of (1*S*,3*S*,5*S*,5a*S*,7a*S*,7b*R*)-Octahydro-1-hydroxy-1-(2-naphthyl)-5-isopropyl-7b-methyl-2*H*cyclopenta[*gh*] pyrrolizin-2-one (41c)

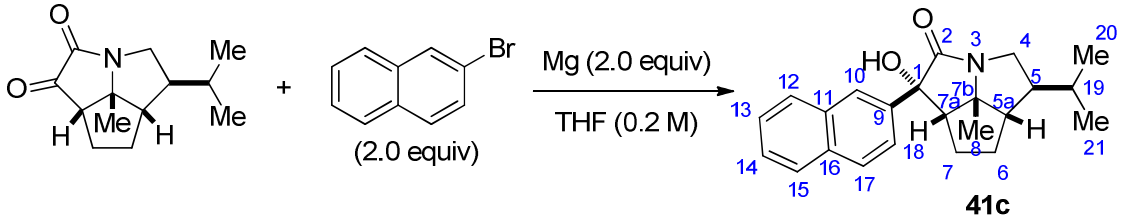

To a 5-mL, two-necked, round-bottomed flask equipped with a nitrogen inlet adapter, a rubber septum and a magnetic stir bar was added **41b** (25 mg, 0.123 mmol) followed by THF (300 µL). The flask was immersed in an ice bath and 2-naphthylmagnesium bromide (400 µL, 0.226. mmol, 2.0 equiv, in THF) was added dropwise via syringe. After being stirred for 10 min, the cooling bath was removed and the reaction was stirred at room temperature for 20 min. The solution was cooled in an ice bath and sat. aq. NH_4Cl (1.0 mL) is added. The resulting mixture was transferred to a 60-mL separatory funnel using an additional 20 mL of water and 20 mL of Et_2O and the aqueous phase was extracted with diethyl ether (3 x 15 mL). The organic extracts were washed with water (2 x 20 mL), and brine (1x 20 mL), then the combinded organic extracts were dried ($NaSO_4$). The mixture was filtered through a cotton plug and concentrated by rotary evaporation (15 mm Hg, 20-25^{o}C). Purification by silica gel chromatography (5.0 cm x 6 cm column, gradient elution, EtOAc/Hexanes, 10, 20, 30, 50%, 25 mL each) afforded 27.5 mg (76%) of **41c**.

Data for **41c**

^{1}H-NMR: (500 MHz, $CDCl_3$)

7.89 – 7.74 (m, 4H, ArH), 7.62 (dd, *J* = 8.6, 1.9 Hz, 1H, ArH), 7.52 – 7.42 (m, 2H, ArH), 4.27 (dd, *J* = 11.7, 7.5 Hz, 1H, H_2C(4)), 3.38 (bs, 1H, OH), 2.74 (t, *J* = 10.5 Hz, 1H, H_2C(4)), 2.74 (t, *J* = 9.2 Hz, 1H, HC(7a)), 2.06 – 2.01 (m, 1H, H_2C(7)), 1.98 – 1.90 (m, 1H, HC(5a)), 1.90 – 1.74 (m, 2H, H_2C(6), H_2C(7)), 1.64 – 1.48 (m, 2H, H_2C(6), HC(19)), 1.48 – 1.35 (m, 1H, HC(5)), 0.96 (d, *J* = 6.7 Hz, 3H, H_3C(20) or H_3C(21)), 0.93 (d, *J* = 6.6 Hz, 3H, H_3C(20) or H_3C(21)), 0.90 (s, 3H, H_3C(8))

^{13}C-NMR: (500 MHz, $CDCl_3$)

176.00 (Ar), 140.91 (Ar), 133.07 (Ar), 133.00 (Ar), 128.70 (Ar), 128.47 (Ar),

127.65 (Ar), 126i.40 (Ar), 126.32 (Ar), 125.34 (Ar), 125.00 (Ar), 83.28 (C(1) or C(7b)), 75.44 (C(1) or C(7b)), 58.02 (C(7a)), 55.59 (C(5a)), 54.83 (C(5)), 48.47 (C(4)), 32.88 (C(19)), 31.93 (C(6)), 27.29 (C(7)), 23.90 (C(8)), 21.49 (C(20) or C(21)), 21.42 (C(20) or C(21))

IR: ($CDCl_3$ film)

3319 (s), 3058 (w), 2951 (s), 2923 (s), 2868 (s), 2360 (w), 1682 (s), 1506 (w), 1461 (m), 1417 (s), 1369 (m), 1279 (w), 1230 (w), 1199 (w), 1138 (m), 1101 (w), 1080 (m), 1028 (w), 973 (w), 954 (w), 908 (s), 861 (w), 843 (w), 813 (s), 732 (s)

MS: (ESI, Q-tof)

350.2 (32) [M+1], 332.2 (100)

Mol. Formula: $C_{23}H_{27}NO_2$ (349.47)

HRMS: $C_{23}H_{28}NO_2^+$: (350.2120)

Calcd: 350.2120

Found: 350.2123

TLC: R_f 0.26 (EtOAc/Hexanes 1:3) [UV, $KMnO_4$]

Preparation of (1*S*,3*S*,5*S*,5a*S*,7a*S*,7b*R*)-Octahydro-1-hydroxy-1-(2-naphthyl)-5-isopropyl-7b-methyl-2*H*cyclopenta[*gh*] pyrrolizin•Borane (41d)

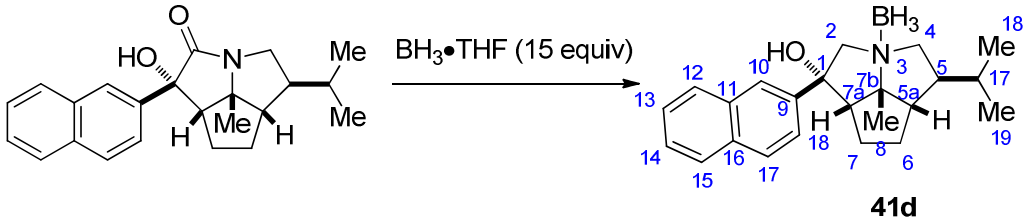

To a 5-mL round-bottomed flask equipped with a nitrogen inlet adapter, a rubber septum, a reflux condenser, and a magnetic stir bar was added **41c** (27 mg, 0.077 mmol) then BH_3•THF complex (1.16 mL, 1.16 mmol, 15 equiv). The reaction flask was immersed in an oil bath and heated to reflux (66 ^oC). After being stirred for 12 h at reflux, the solution was allowed to reach room temperature and was quenched with methanol (5 mL) and concentrated by rotary evaporation (15 mm Hg, 20-25^oC). The resulting colorless oil was purified by silica gel column chromatography (5.0 mm x 8 cm column, gradient elution, TBME/Heaxanes, 5, 10, 15, 20, 25, 30% 25 mL each) to afford 26.5 mg (96%) of **41d** as a white solid

Data for **41d**

^{1}H-NMR: (500 MHz, $CDCl_3$)

7.93 – 7.79 (m, 4H, ArH), 7.58 – 7.46 (m, 3H, ArH), 4.23 (d, *J* = 13.7 Hz, 1H, $H_2C(2)$), 3.74 (dd, *J* = 7.9, 12.5 Hz, 1H, $H_2C(4)$, 3.73 (d, *J* = 14.1, 1H, $H_2C(2)$), 3.43 (dd, *J* = 12.4, 10.3 Hz, 1H, $H_2C(4)$), 2.83 (dd, *J* = 8.9, 5.2 Hz, 1H, HC(7a)), 2.34 (dtd, *J* = 13.3, 7.9, 5.1 Hz, 1H, $H_2C(7)$), 2.27 – 2.19 (m, 1H, HC(5)), 2.16 (td, *J* = 9.1, 4.6 Hz, 1H, HC(5a)), 2.07 – 2.03 (m, 2H, $H_2C(6)$, $H_2C(6)$), 2.01 (bs, 1H, OH), 1.90 (ddt, *J* = 13.5, 9.0, 6.8 Hz, 1H, $H_2C(7)$), 1.58 (s, 3H, $H_3C(8)$) 1.62 – 1.54 (m, 1H, HC(17)), 0.97 (d, *J* = 6.6 Hz, 3H, $H_3C(18)$ or $H_3C(19)$), 0.89 (d, *J* = 6.6 Hz, 3H, $H_3C(18)$ or $H_3C(19)$)

^{13}C-NMR: (500 MHz, $CDCl_3$)

142.13 (Ar), 133.02 (Ar), 132.79 (Ar), 129.03 (Ar), 128.34 (Ar), 127.67 (Ar), 126.74 (Ar), 126.62 (Ar), 123.62 (Ar), 123.53 (Ar), 89.93 (C(1) or C(7b)), 79.96 (C(1) or C(7b)), 79.09 (C(2)), 72.66 (C(4)), 62.88 (C(7a)), 57.36 (C(5a)), 48.11 (C(5)), 33.72 (C(6)), 33.31 (C(17)), 25.60 (C(8)), 25.27 (C(7)), 21.68 (C(18) or C(19)), 21.50 (C(18) or C(19))

IR: ($CDCl_3$, film)

3473 (s), 3058 (w), 2959 (s), 2871 (s), 2383 (s), 2351 (s), 2327 (s), 2272 (s), 1600 (w), 1506 (w), 1469 (s), 1380 (m), 1337 (w), 1268 (w), 1233 (w), 1171 (s), 1133 (m), 1062 (w), 1019 (w), 954 (w), 911 (s), 856 (m), 815 (m), 733 (s), 647 (w)

MS: (EI, 70 eV)

346.2 (100) $[M-3]^+$, 336.2 (50), 318.2 (3), 142.0 (3)

Mol. Formula: $C_{23}H_{32}BNO$ (349.26)

HRMS: $C_{23}H_{29}BNO$, (346.23)

Calcd: 346.2342

Found: 346.2342

TLC: R_f 0.27 (TBME/Hexanes, 1:3) [UV, I_2]

Preparation of (1*S*,3*S*,5*S*,5a*S*,7a*S*,7b*R*)-Octahydro-1-benzyloxy-1-(2-naphthyl)-5-isopropyl-7b-methyl-2*H*cyclopenta[*gh*]pyrrolizine•Borane (41e)

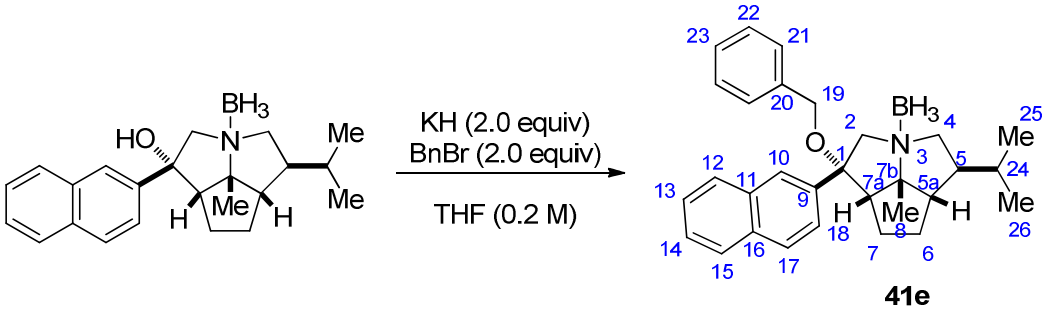

41e

To a two-necked, 5-mL, round-bottomed flask equipped with a nitrogen inlet adapter, a rubber septum and a magnetic stir bar was added washed potassium hydride (6.0 mg, 0.149 mmol, 2.0 equiv) from the drybox followed by THF (200 μL). A solution of alcohol **41d** (26 mg, 0.074 mmol) in THF (0.8 mL) is added to the reaction vessel by cannulation. After 15 min of stirring, the flask is immersed in an ice bath. The benzyl bromide (17.7 μL, 0.149 mmol, 2.0 equiv) is then added dropwise by syringe. The ice bath is removed and the solution is allowed to stir for 2 h at rt. This mixture was cooled in an ice bath and cold sat. aq. NH_4Cl (1.0 mL) is added in one portion. The resulting mixture was transferred to a 60-mL separatory funnel using an additional 15 mL of water and 15 mL of Et_2O and the aqueous phase was extracted with diethyl ether (3 x 15 mL). The organic extracts were washed with water (2 x 20 mL), and brine (1x 20 mL), then the combinded organic extracts were dried ($NaSO_4$). The mixture was filtered through a cotton plug and concentrated by rotary evaporation (15 mm Hg, 20-25°C). Purification by silica gel chromatography (5.0 cm x 8 cm column, gradient elution, TBME/Hexanes, 2, 4, 6, 8, 10, 12%, 25 mL each) afforded 30.5 mg (91%) of ether **41e**.

Data for **41e**

^{1}H-NMR: (500 MHz, $CDCl_3$)

7.91 – 7.82 (m, 3H, ArH), 7.82 – 7.79 (m, 1H, ArH), 7.56 – 7.49 (m, 2H, ArH), 7.34 – 7.27 (m, 2H, ArH), 7.27 – 7.21 (m, 3H, HC(21), HC(22), HC(23)), 4.31 (d, J = 13.4 Hz, 1H, H_2C(2)), 4.18 (d, J = 11.0 Hz, 1H, H_2C(19)), 4.05 (d, J = 13.4 Hz, 1H, H_2C(2)), 3.98 (d, J = 11.0 Hz, 1H, H_2C(19)), 3.56 (dd, J = 12.4, 7.7 Hz, 1H, H_2C(4)), 3.36 (dd, J = 12.4, 10.1 Hz, 1H, H_2C(4)), 2.87 – 2.73 (m, 2H, H_2C(7), HC(7a)), 2.15 – 1.91 (m, 5H,

HC(5), HC(5a), $H_2C(6)$, $H_2C(6)$, $H_2C(7)$), 1.52 (s, 3H, $H_3C(8)$), 1.56 – 1.48 (m, 1H, HC(24)), 0.88 (d, J = 6.7 Hz, 3H, $H_3C(25)$ or $H_3C(26)$), 0.74 (d, J = 6.6 Hz, 3H, $H_3C(25)$ or $H_3C(26)$))

^{13}C-NMR: (500 MHz, $CDCl_3$)

139.11 (Ar), 137.99 (Ar), 133.06 (Ar), 132.98 (Ar), 129.15 (Ar), 128.60 (Ar), 128.53 (Ar), 127.85 (Ar), 127.80 (Ar), 127.78 (Ar), 126.77 (Ar), 126.73 (Ar), 125.02 (Ar), 124.79 (Ar), 89.26 (C(1) or C(7b)), 83.61 (C(1) or C(7b)), 71.82 (C(4)), 70.46, 66.68 (C(2)), 63.09 (C(7a)), 57.34, 47.06, 33.17 (C(8)), 25.44, 25.43 (C(24)), 24.57 (C(7)), 21.77 (C(25) or C(26)), 21.25 (C(25) or C(26))

IR: ($CDCl_3$, film)

3059 (m), 3030 (m), 2960 (s), 2919 (s), 2870 (s), 2369 (s), 2327 (s), 2274 (s), 2240 (m), 1600 (m), 1497 (m), 1454 (s), 1379 (s), 1344 (m), 1295 (w), 1270 (m), 1247 (w), 1170 (s), 1137 (s), 1084 (s), 1066 (s), 1045 (s), 1027 (s), 950 (w), 934 (m), 911 (s), 869 (s), 819 (s), 734 (s), 697 (m), 647 (w), 605 (w)

MS: (EI, 70 eV)

436.3 (100) [M-3], 426.3

Mol. Formula: $C_{30}H_{38}BNO$ (439.44)

HRMS: $C_{30}H_{35}BNO^+$, (436.28)

Calcd: 436.2812

Found: 436.2815

TLC: R_f 0.40 (TBME/Hexanes, 1:9) [UV, I_2]

Preparation of (1*S*,3*S*,5*S*,5a*S*,7a*S*,7b*R*)-Octahydro-1-benzyloxy-1-(2-naphthyl)-5-tertbutyl-7b-methyl-2*H*cyclopenta[*gh*]pyrrolizine•Borane (48)

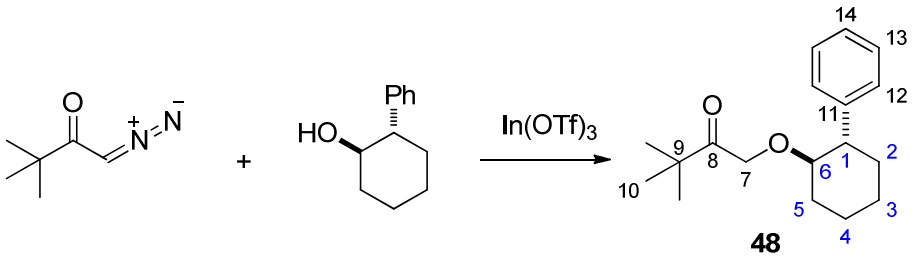

48

To a two-necked, 100-mL, round-bottomed flask equipped with a nitrogen inlet adapter, a

rubber septum and a magnetic stir bar was added α-diazopinacolone (1.1 g, 8.72 mmol, 1.0 equiv) followed by toluene (23.6 mL). Indium(III) triflate (490 mg, 0.87 mmol, 0.1 equiv) is added in one portion. After 1h of stirring, a second portion of indium(III) triflate (490 mg, 0.87 mmol, 0.1 equiv.) is added. After 1.5 h, sat. aq. $NaHCO_3$ is added. The resulting mixture was transferred to a 125-mL separatory funnel using an additional 40 mL of sat. aq. $NaHCO_3$ and 50 mL of Et_2O and the aqueous phase was extracted with diethyl ether (2 x 40 mL). The organic extracts were washed with water (1 x 40 mL), and brine (1x 40 mL), then the combinded organic extracts were dried ($NaSO_4$). The mixture was filtered through a cotton plug and concentrated by rotary evaporation (15 mm Hg, 20-25°C). Purification by silica gel chromatography (20 mm x 10 cm column, gradient elution, TBME/Hexanes, 2, 4, 6, 8, 10, 15%, 50 mL each) afforded 1.51 g (63%) **48**.

Data for **48**

^{1}H-NMR: (500 MHz, $CDCl_3$)

7.32 – 7.21 (m, 4H, ArH), 7.21 – 7.14 (m, 1H, ArH), 3.78 (s, 2H, $H_2HC(7)$), 3.27 (td, J = 10.2, 4.3 Hz, 1H), 2.63 – 2.50 (m, 1H), 2.28 – 2.17 (m, 1H), 1.91 – 1.77 (m, 2H), 1.76 – 1.67 (m, 1H), 1.65 – 1.22 (m, 7H), 1.20 (d, J = 0.8 Hz, 2H), 0.88 (d, J = 0.8 Hz, 9H, $H_3C(10)$).

TLC: R_f 0.22 (TBME/Hexanes, 1:9) [UV, I_2]

Preparation of (1*S*,3*S*,5*S*,5a*S*,7a*S*,7b*R*)-Octahydro-1-benzyloxy-1-(2-naphthyl)-5-tertbutyl-7b-methyl-2*H*cyclopenta[*gh*]pyrrolizine•Borane (49)

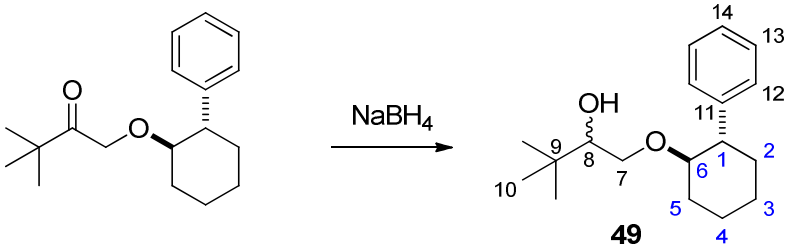

49

To a two-necked, 100-mL, round-bottomed flask equipped with a nitrogen inlet adapter, a rubber septum and a magnetic stir bar was added **48** (429 mg, 1.56 mmol, 1.0 equiv) followed by MeOH (6.5 mL). Solution is cooled in an ice bath. Sodium borohydride (88.5 mg, 2.34 mmol,

1.5 equiv) is added in multiple portions. After 1 h, sat. aq. NH_4Cl (10 mL) is added dropwise. The resulting mixture was transferred to a 125-mL separatory funnel using an additional 30 mL of sat. aq. NH_4Cl and 40 mL of Et_2O and the aqueous phase was extracted with diethyl ether (2 x 30 mL). The organic extracts were washed with water (1 x 30 mL), and brine (1x 30 mL), then the combinded organic extracts were dried ($NaSO_4$). The mixture was filtered through a cotton plug and concentrated by rotary evaporation (15 mm Hg, 20-25°C). Purification by silica gel chromatography (10 mm x 8 cm column, gradient elution, EtOAc/Hexanes, 5, 10, 20, 30%, 50 mL each) afforded 424 mg (89%) of **49**.

Data for **49**

^{1}H-NMR: (500 MHz, $CDCl_3$)

7.35 – 7.28 (m, 2H), 7.25 – 7.18 (m, 3H), 3.69 (dd, J = 9.0, 2.4 Hz, 1H), 3.36 – 3.23 (m, 2H), 3.16 (ddd, J = 9.6, 2.4, 1.5 Hz, 1H), 3.08 (dd, J = 10.0, 3.0 Hz, 0H), 2.96 (dt, J = 8.4, 3.2 Hz, 0H), 2.76 (dd, J = 9.7, 8.9 Hz, 1H), 2.54 (ddd, J = 12.4, 10.1, 3.6 Hz, 1H), 2.31 – 2.13 (m, 1H), 1.97 – 1.82 (m, 3H), 1.82 – 1.66 (m, 3H), 1.65 – 1.47 (m, 3H), 1.42 – 1.28 (m, 5H), 0.77 (s, 9H), 0.74 (s, 3H).

TLC: R_f 0.20 (TBME/Hexanes, 1:4) [UV, I_2]

Preparation of (1*S*,3*S*,5*S*,5a*S*,7a*S*,7b*R*)-Octahydro-1-benzyloxy-1-(2-naphthyl)-5-tertbutyl-7b-methyl-2*H*cyclopenta[*gh*]pyrrolizine•Borane (50)

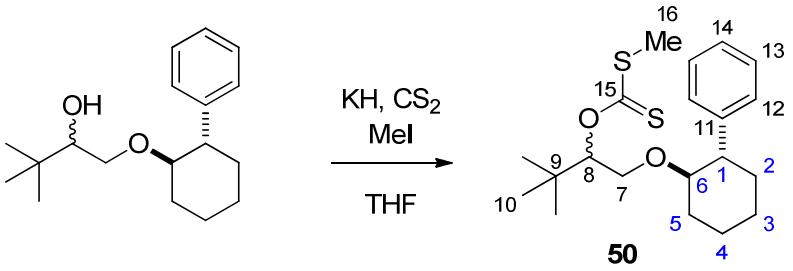

50

To a two-necked, 5-mL, round-bottomed flask equipped with a nitrogen inlet adapter, a rubber septum and a magnetic stir bar was added potassium hydride (11.6 mg, 0.289 mmol, 2.0 equiv) followed by tetrahydrofuran (0.4 mL). Alcohol **49** (40 mg, 0.145mmol) is added as a solution in THF (0.4 mL) to the reaction vessel. After 15 minutes of stirring, the solution is

cooled in an ice bath and carbon disulfide (35 μL, 0.579 mmol, 4.0 equiv.) is added dropwise and the ice bath is removed. After 1.5 h, the solution is cooled in an ice bath and iodomethane (77 μL, 1.23 mmol, 8.5 equiv.) is added and the ice bath is removed. After stirring for 1 h, the solution is cooled in an ice bath and H_2O (1 mL) is added. The resulting mixture was transferred to a 60-mL separatory funnel using an additional 20 mL of H_2O is added and 20 mL of Et_2O and the aqueous phase was extracted with diethyl ether (2 x 20 mL). The organic extracts were washed with water (2 x 20 mL), and brine (1x 20 mL), then the combinded organic extracts were dried ($NaSO_4$). The mixture was filtered through a cotton plug and concentrated by rotary evaporation (15 mm Hg, 20-25°C). Purification by silica gel chromatography (5 mm x 8 cm column, gradient elution, DCM/Hexanes, 5, 10, 15, 20, 40%, 25 mL each) afforded 53 mg (99%) of **50**.

Data for **50**

^{1}H-NMR: (500 MHz, $CDCl_3$)

7.31 – 7.21 (m, 4H), 7.21 – 7.17 (m, 2H), 7.17 – 7.10 (m, 1H), 5.41 (dd, *J* = 5.8, 4.4 Hz, 0.3H), 5.37 (dd, *J* = 5.6, 4.1 Hz, 1H), 3.57 (dd, *J* = 11.4, 4.1 Hz, 1H), 3.42 – 3.31 (m, 1.5H), 3.18 – 3.12 (m, 1H), 2.53 – 2.46 (m, 1.29H), 2.45 (s, 1H), 2.43 (s, 3H), 2.21 – 2.08 (m, 1.48H), 1.87 – 1.75 (m, 3H), 1.75 – 1.65 (m, 1.46H), 1.58 – 1.39 (m, 2H), 1.39 – 1.20 (m, 5.26H), 0.72 (s, 12H).

TLC: R_f 0.25 (DCM/Hexanes, 1:4) [UV, I_2]

Preparation of (1*S*,3*S*,5*S*,5a*S*,7a*S*,7b*R*)-Octahydro-1-benzyloxy-1-(2-naphthyl)-5-tertbutyl-7b-methyl-2*H*cyclopenta[*gh*]pyrrolizine•Borane (51)

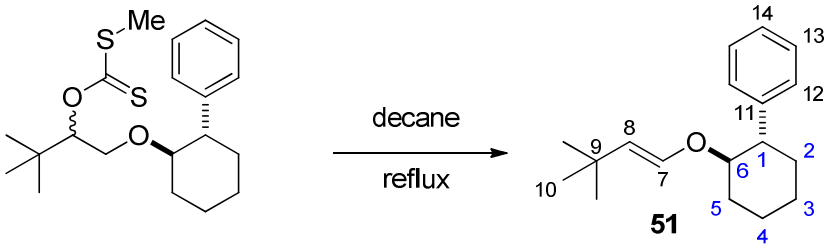

To a two-necked, 5-mL, round-bottomed flask equipped with a nitrogen inlet adapter, a rubber septum and a magnetic stir bar was added **50** (53 mg, 0.145 mmol, 1.0 equiv) followed by

decane (1.45 mL). The solution is warmed to 180 °C. After 24 h, the decane is removed in vauo (0.3 torr). Purification by silica gel chromatography (5 mm x 8 cm column, gradient elution, DCM/Hexanes, 10, 15, 20, 40%, 25 mL each) afforded 14 mg (3%) of **51**.

Data for **51**

^{1}H-NMR: (500 MHz, $CDCl_3$)

7.34 – 7.27 (m, 2H, ArH), 7.27 – 7.19 (m, 3H, ArH), 5.66 (dd, *J* = 12.5, 0.9 Hz, 1H, HC(7)), 4.74 (dd, *J* = 12.5, 1.0 Hz, 1H, HC(8)), 3.69 (td, *J* = 10.0, 4.5 Hz, 1H), 2.64 (ddd, *J* = 11.8, 10.0, 3.7 Hz, 1H), 2.24 – 2.15 (m, 1H), 1.96 – 1.84 (m, 2H), 1.83 – 1.74 (m, 1H), 1.61 – 1.50 (m, 1H), 1.48 – 1.27 (m, 5H), 0.85 (d, *J* = 1.1 Hz, 9H, H_3C(10)).

TLC: R_f 0.24 (DCM/Hexanes, 1:4) [UV, I_2]

Preparation of (1*S*,3*S*,5*S*,5a*S*,7a*S*,7b*R*)-Octahydro-1-hydroxy-5-tertbutyl-7b-methyl-2*H*cyclopenta[*gh*]pyrrolizin-2-one (51a)

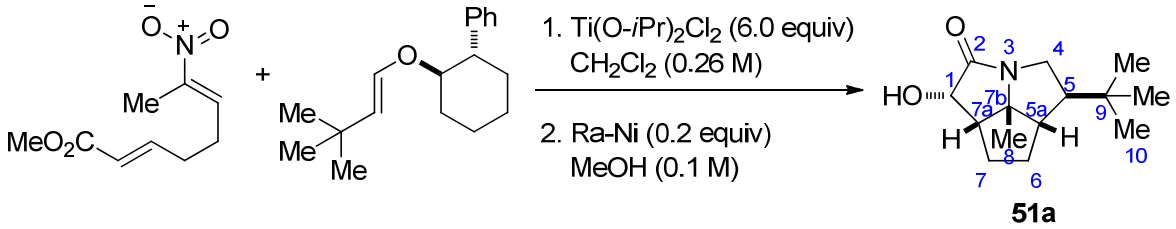

To a 10-mL, two-necked, round-bottomed flask fitted with two rubber septa, a magnetic stir bar, a nitrogen inlet adaptor and an internal temperature probe, was added nitroalkene (E,E)-1 (90.1 mg, 0.452 mmol) and chiral propenyl ether **51** (123 mg, 0.475 mmol, 1.05 equiv) *via* syringe. The resulting yellow oil was then evacuated under high vacuum (~0.1 mm Hg) for 30 min. The flask was backfilled with N_2 and charged with CH_2Cl_2 (2.1 mL). The solution was cooled to –85 °C (internal temperature) using hexanes/N_2 bath. This yellow solution was sirred for 15 min, then freshly prepared $TiCl_2$(O*i*-Pr)$_2$ solution (1.2 M in CH_2Cl_2, 1.2 mL, 1.44 mmol, 6.0 equiv) was added dropwise *via* syringe while maintaining an internal temperature ≤ –70 °C (ca. 15 min). After addition of the Lewis acid, the cooling bath was replaced with an acetone/$CO_{2(s)}$ bath and the resulting bright yellow solution was stirred for another 5 h while maintaining an internal temperature ≤ –75 °C. During the course of the reaction, the yellow

color gradually faded and a white precipitate formed. After 5 h the reaction was quenched with triethylamine (2.9 mL, 6.1 equiv, 1 M in MeOH) *via* syringe while maintaining an internal temperature of < –40 °C. The cooling bath was then removed and the reaction mixture was allowed to warm to 0 °C (ca. 15 min). The resulting white suspension was then poured onto a biphasic mixture H_2O (30 mL) and TBME (30 mL) in a 125-mL separatory funnel. The aqueous was separated and was washed with TBME (2 x 20 mL). The organic extracts were washed with H_2O (2 x 30 mL) and brine (1 x 30 mL). The combined organic extracts were dried over $NaHCO_3/MgSO_4$ (1/1), filtered (cotton plug), and concentrated by rotary evaporation (15 mm Hg, 20-25 °C). The resulting residue was filtered through a pad of silica gel (5 mm x 4 cm), eluting with TBME (40 mL) to remove any remaining amine impurities. The resulting clear solution was concentrated by rotary evaporation (15 mm Hg, 20-25 °C) to a pale-yellow residual oil. The oil was allowed to stand for 8 h. The resulting mixture of nitroso acetals was diluted in MeOH (5 mL) and added to a test tube (5 mm x 14 cm) containing a spatula tip (~20 mg) of Raney Ni (previously washed with H_2O (3 x 10 mL) and MeOH (3 x 10 mL) along with a magnetic stir bar. The tube was placed in a steel autoclave, which was then pressurized with H_2 (350 psi). After 2 days the autoclave was *carefully* vented in a fume hood and the solution was filtered through a plug of Celite (5 cm x 5 cm, cotton plug) with MeOH (25 mL). The resulting clear solution was concentrated by rotary evaporation (15 mm Hg, 20-25 °C) and purified by silica gel column chromatography (2 cm x 8 cm, EtOAC/Hexanes, 20, 30, 40, 60, 80%, 25 mL each) to afford affording 53.9 mg (50%) of a white crystalline solid.

Data for **51a**

^{1}H-NMR: (500 MHz, $CDCl_3$)
4.64 (dd, J = 6.5, 1.3 Hz, 1H), 3.96 (dd, J = 11.9, 7.9 Hz, 1H), 2.74 (ddd, J = 12.0, 10.7, 1.4 Hz, 1H), 2.55 (dt, J = 10.5, 6.7 Hz, 1H), 2.12 – 2.01 (m, 1H), 1.94 – 1.70 (m, 2H), 1.70 – 1.36 (m, 3H), 1.30 (s, 3H, $H_3C(8)$), 0.91 (s, 9H, $H_3C(10)$)

TLC: R_f 0.24 (EtOAc/Hexanes 3:2) [$KMnO_4$]

Preparation of (3*R*,5*S*,5a*S*,7a*S*,7b*R*)-Octahydro-5-tertbutyl-7b-methyl-2*H*cyclopenta[*gh*]pyrrolizin-1,2-one (51b)

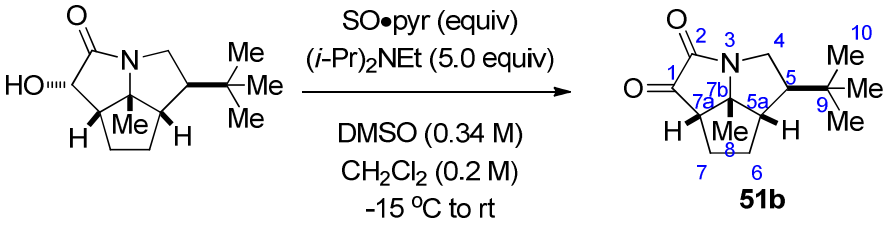

To a 5-mL, three-necked, round-bottomed flask fitted with a nitrogen inlet adapter, a magnetic stir bar, and an internal temperature probe was added **51a** (52 mg, 0.219 mmol), CH_2Cl_2 (1.5 mL), and DMSO (325 μL). The resulting solution was cooled to –12 °C in an ice/salt bath. To this solution was added diisopropylethylamine (179 μL, 1.03 mmol, 5.0 equiv) followed by the dropwise addition of a solution of SO_3•pyridine complex (98 mg, 0.615 mmol, 3.0 equiv) in DMSO (458 μL) while maintaining an internal temperature < –5 °C. After being stirred for 20 min at –10 °C, the mixture was allowed to warm to room temperature. The mixture was then cooled to 0 °C and diluted with CH_2Cl_2 (20 mL) and H_2O (25 mL). This mixture was poured into a 60-mL separatory funnel with CH_2Cl_2 (20 mL) and H_2O (20 mL). The aqueous layer was separated washed with CH_2Cl_2 (2 x 25 mL). The organic extracts were washed with 1.0 N. aq. HCl (2 x 20 mL), H_2O (1 x 20 mL), and brine (20 mL), the combined organic extracts dried over $NaSO_4$, filtered (cotton plug), and rinsed with TBME (3 x 10 mL). The mixture was filtered through a cotton plug and concentrated by rotary evaporation (15 mm Hg, 20-25°C). The crude oil was purified by silica gel chromatography (5 mm x 8 cm column, gradient elution, Et_2O/DCM, 10, 20, 40, 50%, 25 mL each) to afford **b1b** (49 mg, 95%).

Data for **51b**

^{1}H-NMR: (500 MHz, $CDCl_3$)

4.25 (ddd, *J* = 12.3, 8.0, 1.8 Hz, 1H, HC(4)), 3.13 (ddd, *J* = 12.1, 10.2, 1.5 Hz, 1H, HC(4)), 2.72 (dd, *J* = 8.3, 6.7 Hz, 1H), 2.27 – 2.16 (m, 1H), 2.16 – 1.99 (m, 2H), 1.81 – 1.67 (m, 2H), 1.54 – 1.43 (m, 1H), 1.40 (s, 3H, H_3C(8)), 0.93 (s, 9H, H_3C(10)).

TLC: R_f 0.21 (EtOAc/Hexanes 2:3) [UV, I_2]

Preparation of (1*S*,3*S*,5*S*,5a*S*,7a*S*,7b*R*)-Octahydro-1-hydroxy-1-(2-naphthyl)-5-tertbutyl-7b-methyl-2*H*cyclopenta[*gh*] pyrrolizin-2-one (51c)

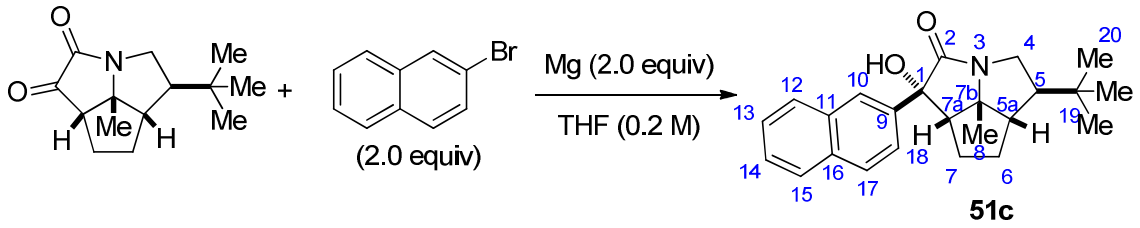

To a 5-mL, two-necked, round-bottomed flask equipped with a nitrogen inlet adapter, a rubber septum and a magnetic stir bar was added **51b** (49 mg, 0.123 mmol) followed by THF (700µL). The flask was immersed in an ice bath and 2-naphthylmagnesium bromide (700 µL, 0.351. mmol, 1.8 equiv, in THF) was added dropwise via syringe. After being stirred for 10 min, the cooling bath was removed and the reaction was stirred at room temperature for 20 min. The solution was cooled in an ice bath and sat. aq. NH_4Cl (1.0 mL) is added. The resulting mixture was transferred to a 60-mL separatory funnel using an additional 20 mL of water and 20 mL of Et_2O and the aqueous phase was extracted with diethyl ether (3 x 15 mL). The organic extracts were washed with water (2 x 20 mL), and brine (1x 20 mL), then the combinded organic extracts were dried ($NaSO_4$). The mixture was filtered through a cotton plug and concentrated by rotary evaporation (15 mm Hg, 20-25°C). Purification by silica gel chromatography (5.0 cm x 6 cm column, gradient elution, EtOAc/Hexanes, 10, 20, 30, 50%, 25 mL each) afforded 68.4 mg (90%) of **51c**.

Data for **51c**

^{1}H-NMR: (500 MHz, $CDCl_3$)

7.88 – 7.83 (m, 1H, ArH), 7.83 – 7.78 (m, 2H, ArH), 7.78 – 7.75 (m, 1H, ArH), 7.62 (dt, *J* = 8.7, 1.5 Hz, 1H, ArH), 7.51 – 7.44 (m, 2H, ArH), 4.16 (dd, *J* = 11.8, 7.9 Hz, 1H, HC(4)), 3.28 (s, 1H), 2.88 (td, *J* = 11.4, 1.3 Hz, 1H), 2.77 (dd, *J* = 9.9, 7.0 Hz, 1H), 1.94 – 1.69 (m, 3H), 1.68 – 1.58 (m, 1H), 1.56 – 1.50 (m, 1H), 1.18 (s, 3H, H_3C(8)), 0.92 (s, 9H, H_3C(20)).

TLC: R_f 0.26 (EtOAc/Hexanes 1:3) [UV, $KMnO_4$]

Preparation of (1*S*,3*S*,5*S*,5a*S*,7a*S*,7b*R*)-Octahydro-1-hydroxy-1-(2-naphthyl)-5-tertbutyl-7b-methyl-2*H*cyclopenta[*gh*] pyrrolizin•Borane (51d)

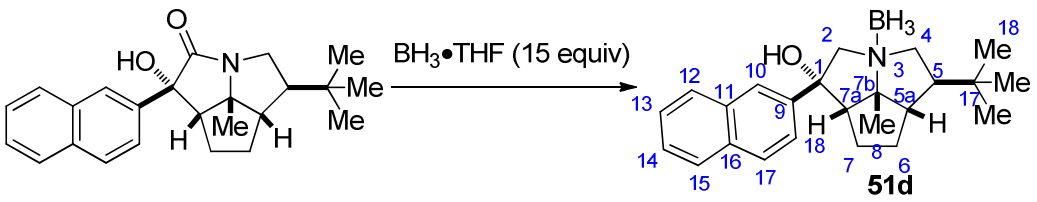

To a 5-mL round-bottomed flask equipped with a nitrogen inlet adapter, a rubber septum, a reflux condenser, and a magnetic stir bar was added **51c** (68.4 mg, 0.188 mmol) then BH_3•THF complex (2.7 mL, 2.7 mmol, 15 equiv). The reaction flask was immersed in an oil bath and heated to reflux (66 ^{o}C). After being stirred for 12 h at reflux, the solution was allowed to reach room temperature and was quenched with methanol (5 mL) and concentrated by rotary evaporation (15 mm Hg, 20-25^{o}C). The resulting colorless oil was purified by silica gel column chromatography (5.0 mm x 8 cm column, gradient elution, TBME/Heaxanes, 5, 10, 15, 20, 25, 30% 25 mL each) to afford 63.9 mg (94%) of **51d** as a white solid

Data for **41d**

^{1}H-NMR: (500 MHz, $CDCl_3$)

7.87 (s, 1H, ArH), 7.86 – 7.77 (m, 2H, ArH), 7.57 – 7.49 (m, 3H, ArH), 4.29 (d, J = 13.7 Hz, 1H, HC(2)), 3.74 (d, J = 13.6 Hz, 1H, HC(2)), 3.64 – 3.50 (m, 2H), 2.84 (dd, J = 8.7, 4.4 Hz, 1H), 2.48 – 2.40 (m, 1H), 2.40 – 2.30 (m, 1H), 2.24 (dt, J = 9.6, 5.6 Hz, 1H), 2.10 – 2.02 (m, 2H), 2.00 – 1.88 (m, 2H), 1.57 (s, 3H), 0.93 (s, 9H).

TLC: R_f 0.27 (TBME/Hexanes, 1:3) [UV, I_2]

Preparation of (1*S*,3*S*,5*S*,5a*S*,7a*S*,7b*R*)-Octahydro-1-benzyloxy-1-(2-naphthyl)-5-isopropyl-7b-methyl-2*H*cyclopenta[*gh*]pyrrolizine•Borane (51e)

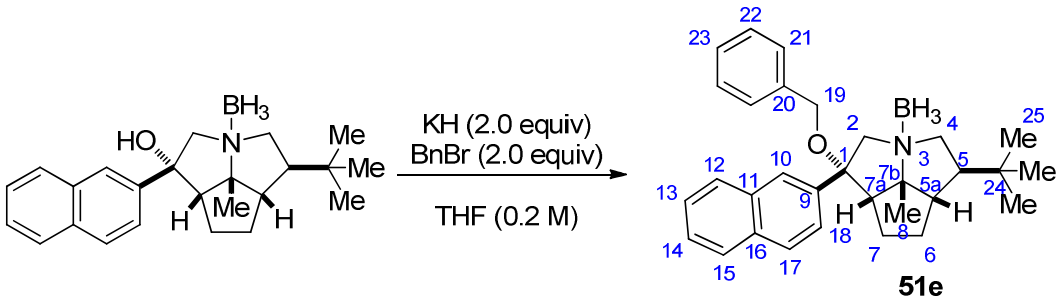

To a two-necked, 5-mL, round-bottomed flask equipped with a nitrogen inlet adapter, a rubber septum and a magnetic stir bar was added washed potassium hydride (6.0 mg, 0.149 mmol, 2.0 equiv) from the drybox followed by THF (200 μL). A solution of alcohol **51d** (26 mg, 0.074 mmol) in THF (0.8 mL) is added to the reaction vessel by cannulation. After 15 min of stirring, the flask is immersed in an ice bath. The benzyl bromide (17.7 μL, 0.149 mmol, 2.0 equiv) is then added dropwise by syringe. The ice bath is removed and the solution is allowed to stir for 2 h at rt. This mixture was cooled in an ice bath and cold sat. aq. NH_4Cl (1.0 mL) is added in one portion. The resulting mixture was transferred to a 60-mL separatory funnel using an additional 15 mL of water and 15 mL of Et_2O and the aqueous phase was extracted with diethyl ether (3 x 15 mL). The organic extracts were washed with water (2 x 20 mL), and brine (1x 20 mL), then the combinded organic extracts were dried ($NaSO_4$). The mixture was filtered through a cotton plug and concentrated by rotary evaporation (15 mm Hg, 20-25°C). Purification by silica gel chromatography (5.0 cm x 8 cm column, gradient elution, TBME/Hexanes, 2, 4, 6, 8, 10, 12%, 25 mL each) afforded 30.5 mg (91%) of ether **51e**.

Data for **51e**

^{1}H-NMR: (500 MHz, $CDCl_3$)

7.89 – 7.79 (m, 4H, ArH), 7.56 – 7.48 (m, 3H, ArH), 7.34 – 7.28 (m, 2H, ArH), 7.28 – 7.22 (m, 1H, ArH), 4.33 (d, J = 13.4 Hz, 1H), 4.18 (d, J = 11.1 Hz, 1H), 4.03 (d, J = 13.4 Hz, 1H), 3.98 (d, J = 11.1 Hz, 1H), 3.52 – 3.39 (m, 2H), 2.86 – 2.81 (m, 1H), 2.81 – 2.75 (m, 1H), 2.30 – 2.21 (m, 1H), 2.21 – 2.15 (m, 1H), 2.10 – 1.90 (m, 3H), 1.50 (s, 3H, H_3C8))), 0.81 (s, 9H, $H_3C(25)$).

TLC: R_f 0.40 (TBME/Hexanes, 1:9) [UV, I_2]

Preparation of *rel*-(1*S*,3*R*,5*S*,5a*S*,7a*S*,7b*R*) Octahydro-1-hexyloxy-1-(2-naphthyl)-3-(3,5-bistrifluoromethylphenylmethyl)-5-isopropyl-7b-methylcyclopenta[*gh*]pyrrolizinium Bromide (42)

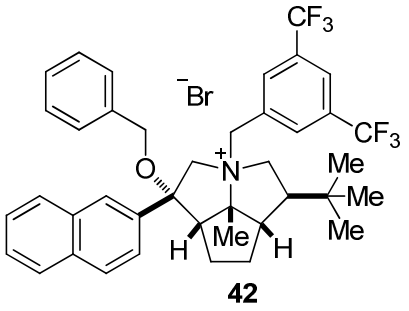

42

Data for **42**

Yield: 64.7 mg (95%), free-flowing white powder

^{1}H-NMR: (500 MHz, $CDCl_3$)

8.26 (s, 1H), 8.20 (d, J = 8.7 Hz, 1H), 8.04 – 7.95 (m, 4H), 7.89 (s, 1H), 7.72 (dd, J = 8.7, 1.9 Hz, 1H), 7.70 – 7.65 (m, 2H), 7.35 – 7.28 (m, 2H), 7.19 – 7.13 (m, 2H), 6.25 (d, J = 12.3 Hz, 1H), 4.86 (t, J = 12.4 Hz, 1H), 4.19 (d, J = 13.0 Hz, 1H), 4.06 (d, J = 10.7 Hz, 1H), 3.89 (d, J = 10.7 Hz, 1H), 3.69 (d, J = 13.1 Hz, 1H), 3.64 (t, J = 9.4 Hz, 2H), 3.02 (dd, J = 11.4, 6.3 Hz, 1H), 2.89 – 2.82 (m, 1H), 2.62 – 2.47 (m, 1H), 2.43 (s, 3H), 2.27 (dt, J = 14.3, 7.3 Hz, 1H), 2.21 – 2.14 (m, 1H), 2.14 – 2.04 (m, 2H), 1.57 (s, 3H), 1.08 (s, 9H).

TLC: R_f 0.35 (CH_2Cl_2/MeOH, 9:1) [I_2]

Preparation of *rel*-(1*S*,3*R*,5*S*,5a*S*,7a*S*,7b*R*) Octahydro-1-hexyloxy-1-(2-naphthyl)-3-(3,5-bistrifluoromethylphenylmethyl)-5-isopropyl-7b-methylcyclopenta[*gh*]pyrrolizinium Bromide (41)

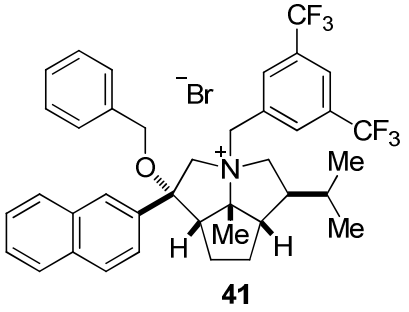

41

Data for **41**

Yield: 95 mg (97%), free-flowing white powder

^{1}H-NMR: (500 MHz, $CDCl_3$)

8.25 (s, 1H), 8.21 (d, *J* = 8.6 Hz, 1H), 8.04 – 7.95 (m, 4H), 7.89 (s, 1H), 7.73 (dd, *J* = 8.6, 2.0 Hz, 1H), 7.70 – 7.67 (m, 2H), 7.32 – 7.27 (m, 3H), 7.15 – 7.13 (m, 2H), 5.99 (d, *J* = 11.8 Hz, 1H), 5.26 (t, *J* = 11.8 Hz, 1H), 4.11 (d, *J* = 12.8 Hz, 1H), 4.06 (d, *J* = 10.7 Hz, 1H), 3.85 (d, *J* = 10.6 Hz, 1H), 3.69 – 3.59 (m, 2H), 3.43 (d, *J* = 12.1 Hz, 1H), 3.03 (dd, *J* = 11.1, 6.2 Hz, 1H), 2.93 (dd, *J* = 10.0, 6.2 Hz, 1H), 2.58 – 2.46 (m, 1H), 2.44 (s, 3H), 2.29 – 2.19 (m, 2H), 2.15 – 2.03 (m, 2H), 1.92 – 1.84 (m, 1H), 1.05 (d, *J* = 6.6 Hz, 3H), 0.88 (d, *J* = 6.5 Hz, 3H)

MS: (ESI, Q-tof)

422.3 (100) [M-3], 412.3 (28), 207.2 (2), 185.1 (5), 180.2 (9), 158.0 (6), 126.0 (6), 100.1 (42), 89.1 (5), 79.0 (10)

Mol. Formula: $C_{39}H_{40}BrF_6NO$ (732.64)

HRMS: $C_{39}H_{40}F_6NO^+$, (652.30)

Calcd: 652.3014

Found: 652.3005

TLC: R_f 0.35 (CH_2Cl_2/MeOH, 9:1) [I_2]

Preparation of Catalysts from Figure 25

Preparation of *rel*-(1*S*,3*R*,5*S*,5a*S*,7a*S*,7b*R*) Octahydro-1-hexyloxy-1-(2-naphthyl)-3-(3,5-bismethoxyphenylmethyl)-5-methyl-7b-methylcyclopenta[*gh*]pyrrolizinium Bromide (49)

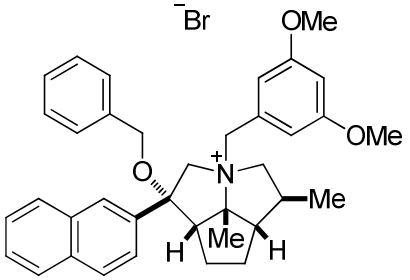

49

Data for **49**

Yield: 38 mg (98%), free-flowing white powder

^{1}H-NMR: (500 MHz, $CDCl_3$)

8.71 (s, 1H), 8.32 – 8.17 (m, 1H), 7.87 (d, *J* = 8.6 Hz, 1H), 7.84 – 7.76 (m, 1H), 7.72 (d, *J* = 8.7 Hz, 1H), 7.57 – 7.45 (m, 2H), 7.38 – 7.23 (m, 4H), 7.23 –

7.13 (m, 4H), 6.50 – 6.43 (m, 1H), 5.95 (d, *J* = 14.6 Hz, 1H), 5.83 (d, *J* = 12.0 Hz, 1H), 4.72 – 4.61 (m, 1H), 4.17 (d, *J* = 11.3 Hz, 1H), 4.11 (d, *J* = 11.5 Hz, 1H), 4.02 – 3.95 (m, 1H), 3.90 (s, 6H), 3.86 – 3.70 (m, 2H), 3.14 – 3.05 (m, 1H), 3.03 – 2.94 (m, 1H), 2.64 (dd, *J* = 7.8, 15.6 Hz, 1H), 2.55 (t, *J* = 9.6 Hz, 1H), 2.18 – 2.09 (m, 1H), 2.12 (s, 3H), 1.92 – 1.80 (m, 1H), 1.00 (d, *J* = 6.5 Hz, 3H)

MS: (ESI, Q-tof)

548.3 (100) [M-Br^-]

Mol. Formula: $C_{37}H_{42}BrNO_3$ (628.64)

HRMS: $C_{37}H_{42}NO_3^+$, (548.32)

Calcd: 548.3165

Found: 548.3153

TLC: R_f 0.25 (CH_2Cl_2/MeOH, 9:1) [I_2]

Preparation of *rel*-(1*S*,3*R*,5*S*,5a*S*,7a*S*,7b*R*) Octahydro-1-hexyloxy-1-(2-naphthyl)-3-(3,5-bisfluorophenylmethyl)-5-methyl-7b-methylcyclopenta[*gh*]pyrrolizinium Bromide (50)

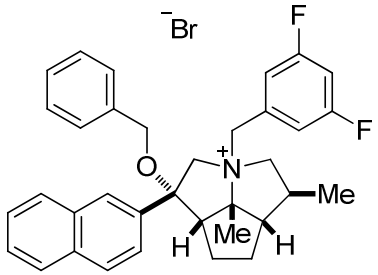

50

Data for **50**

Yield: 47 mg (95%), free-flowing white powder

^{1}H-NMR: (500 MHz, $CDCl_3$)

8.24 (s, 1H), 8.19 (d, *J* = 8.7 Hz, 1H), 8.02 – 7.97 (m, 2H), 7.77 (dt, *J* = 8.7, 1.7 Hz, 1H), 7.68 – 7.65 (m, 2H), 7.35 – 7.22 (m, 3H), 7.17 – 7.09 (m, 2H), 7.09 – 7.00 (m, 2H), 6.80 (t, *J* = 8.5, Hz, 1H), 5.47 (d, *J* = 12.0 Hz, 1H), 5.08 (t, *J* = 6.8 Hz, 1H), 4.34 (d, *J* = 13.2 Hz, 1H), 4.04 (d, *J* = 10.7 Hz, 1H), 3.82 (d, *J* = 10.7 Hz, 1H), 3.71 – 3.55 (m, 2H), 3.32 (d, *J* = 10.2 Hz, 1H), 3.06 (dd,

J = 11.3, 6.1 Hz, 1H), 2.89 – 2.78 (m, 1H), 2.54 – 2.45 (m, 1H), 2.36 (s, 3H) 2.42 – 2.21 (m, 2H), 2.05 – 1.93 (m, 2H), 1.31 (d, J = 6.4 Hz,, 3H)

MS: (ESI, Q-tof)
524.2 (100) [M-Br^-]

Mol. Formula: $C_{35}H_{36}BrF_2NO$ (604.57)

HRMS: $C_{35}H_{36}F_2NO^+$, (524.28)
Calcd: 524.2765
Found: 524.2751

TLC: R_f 0.31 (CH_2Cl_2/MeOH, 9:1) [I_2]

Preparation of *rel*-(1*S*,3*R*,5*S*,5a*S*,7a*S*,7b*R*) Octahydro-1-hexyloxy-1-(2-naphthyl)-3-(3,5-bismethylphenylmethyl)-5-methyl-7b-methylcyclopenta[*gh*]pyrrolizinium Bromide (51)

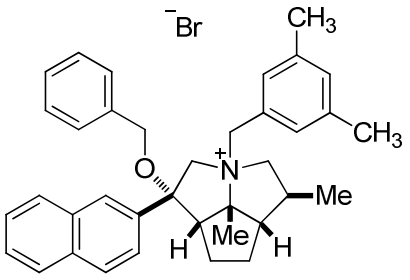

51

Data for **51**

Yield: 82 mg (98%), free-flowing white powder

^{1}H-NMR: (500 MHz, $CDCl_3$)
8.23 (s, 1H), 8.16 (d, J = 8.6 Hz, 1H), 8.05 – 7.95 (m, 2H), 7.80 – 7.74 (d, J = 8.7 Hz, 1H), 7.72 – 7.62 (m, 2H), 7.30 – 7.24 (m, 3H), 7.17 – 7.09 (m, 2H), 6.94 (s, 1H), 6.81 (s, 2H), 5.13 (d, J = 12.1 Hz, 1H), 5.07 – 4.95 (m, 1H), 4.37 (d, J = 13.0 Hz, 1H), 4.03 (d, J = 10.6 Hz, 1H), 3.81 (d, J = 10.6 Hz, 1H), 3.62 (t, J = 9.3 Hz, 1H), 3.55 (d, J = 13.1 Hz, 1H), 3.25 (d, J = 12.2 Hz, 1H), 3.10 (dd, J = 11.4, 5.9 Hz, 1H), 2.93 (d, J = 9.7 Hz, 1H), 2.58 – 2.43 (m, 1H), 2.37 (s, 3H), 2.29 – 2.20 (m, 2H), 2.24 (s, 3H), 2.01 – 1.96 (m, 2H), 1.34 (dd, J = 6.3, 2.3 Hz, 3H)

MS: (ESI, Q-tof)

516.3 (100) [M-Br^-

Mol. Formula: $C_{37}H_{42}BrNO$ (596.64)

HRMS: $C_{37}H_{42}NO^+$, (516.33)

Calcd: 516.3266

Found: 516.3249

TLC: R_f 0.36 (CH_2Cl_2/MeOH, 9:1) [I_2]

7.8. Supporting Information for Chapter 6

Computational Methods

All geometries were fully optimized at the M06-2X[187] level of density functional theory using the 6-31+G(d,p) basis set for all atoms. For the $TiCl_4$ mediated reaction, the M06[187] density functional using the TZV basis set with added 2f polarization functions for titanium and the 6-31+G(d,p) basis set for all other atoms was used. The CPCM model[188] was used for inclusion of dichloromethane for all optimizations. The nature of all stationary points was determined by semi-numerical (numerical differentiation of analytically computed first derivatives) computation of zero-point vibrational energies at 195 K and using the "quasi-harmonic approximation"[189] (with all frequencies below 80 cm^{-1} being replaced by 80 cm^{-1} for computing free energies) for reducing error from the use of the harmonic oscillator approximation for low frequency normal modes. The frequencies were scaled by 0.967 for M06-2X/6-31+G(d,p) and 0.980 for M06/6-31G+(d,p) for calculating ZPE.[190] The electronic energies were further refined using the 6-311+G(2d,2p) basis set. Interaction energy decomposition was performed using the LMO-EDA method.[151] Natural population analysis and perturbation theory energy analysis were performed using NBO 3.1 within Gaussian09.[191] All geometry optimizations and LMO-EDA were performed using the GAMESS[192] program.

7.8.1. Cartesian Coordinates and Energies for Structures from Figure 27, Figure 29, Figure 30, and Figure 32

1-CH_3CHO

C	0.23287	-0.40467	0.00051
H	0.30915	-1.50849	-0.00183
C	-1.15316	0.16091	0.00011
H	-1.69277	-0.20745	0.87931
H	-1.68965	-0.20724	-0.88096
H	-1.12898	1.25109	-0.00002
O	1.24450	0.26617	-0.00025

E(0 K) = -153.770052
E(0 K) + ZPE = -153.715731
H (195 K) = -153.712858
G (195 K) = -153.730761

1-BF_3•OEt_2

B	-0.75702	0.00257	0.00187
O	0.78354	-0.37268	-0.00092
C	1.49277	0.00884	-1.20801
H	2.47927	-0.44931	-1.16253
H	1.56193	1.09782	-1.25137
H	0.92071	-0.38285	-2.04470
C	1.49870	-0.00698	1.20690
H	0.88844	-0.33325	2.04467
H	1.64427	1.07522	1.21998
H	2.45214	-0.53264	1.19200
F	-1.26624	-0.55353	-1.14632
F	-1.26412	-0.55895	1.14844
F	-0.79498	1.38131	-0.00000

E(0 K) = -479.618168
E(0 K) + ZPE = -479.523899
H (195 K) = -479.519407
G (195 K) = -479.542547

2-a

C	3.41041	1.00202	1.01771
H	4.48874	0.80217	1.04498
H	3.20709	2.03561	1.29199
C	2.94577	0.70721	-0.34549
H	3.01740	-0.31117	-0.74551
O	2.48545	1.59761	-1.07308
H	2.94331	0.30163	1.71713
B	2.10236	1.32073	-2.59194
F	3.27695	1.50529	-3.27981
F	1.13716	2.25279	-2.86439
F	1.64365	0.02057	-2.64773

E(0 K) = -478.423414
E(0 K) + ZPE = -478.353511
H (195 K) = -478.349099
G (195 K) = -478.372262

2-b

C	-0.86187	0.03403	0.68575
H	-1.74684	0.02941	1.32786
O	-1.09076	0.03644	-0.53221
C	0.46513	0.02503	1.32491
H	0.56712	-0.93947	1.83914
H	0.46601	0.79082	2.10702
H	1.28512	0.16770	0.62659
B	0.04091	-0.02474	-1.65624
F	0.73425	-1.18921	-1.40906
F	0.80556	1.10514	-1.48525
F	-0.66463	-0.03515	-2.82851

E(0 K) = -478.422059
E(0 K) + ZPE = -478.351673
H (195 K) = -478.347503
G (195 K) = -478.370019

***E*-crotylsilane**

C	0.40795	-0.40440	0.66445
C	-0.56523	0.51416	-0.00946
H	-0.38442	0.54947	-1.09138
H	-0.46621	1.53707	0.37430
Si	-2.36174	-0.05915	0.24876
C	-2.58847	-1.68504	-0.67562
H	-1.92151	-2.45411	-0.27270
H	-2.35544	-1.55743	-1.73837
H	-3.61864	-2.04585	-0.59181
C	-3.52741	1.24848	-0.44786
H	-3.40473	2.19898	0.08149
H	-4.57101	0.93349	-0.34608
H	-3.32617	1.42217	-1.51006
C	-2.69633	-0.30718	2.08676
H	-2.52383	0.61829	2.64611
H	-2.04516	-1.08390	2.50046
H	-3.73479	-0.61393	2.24942

C	1.09793	-1.38184	0.06673
H	0.98915	-1.51392	-1.01172
H	0.51725	-0.28386	1.74472
C	2.02612	-2.32737	0.77316
H	3.04178	-2.26586	0.36733
H	1.69879	-3.36640	0.65580
H	2.07201	-2.10354	1.84298

E(0 K) = -565.832123
E(0 K) + ZPE -565.628236
H (195 K) = -565.621278
G (195 K) = -565.649705

3

C	3.27174	1.07217	0.94194
H	4.27604	1.50992	0.85480
H	2.63208	1.77062	1.48207
C	2.78483	0.86875	-0.43657
H	3.07103	-0.02028	-1.00624
O	2.13687	1.76001	-1.01611
H	3.36705	0.12158	1.46764
B	1.78295	1.61856	-2.54251
F	2.93900	1.95095	-3.21953
F	0.75158	2.50136	-2.74278
F	1.42392	0.29927	-2.74595
C	0.40271	-0.40389	0.66327
C	-0.56652	0.51101	-0.00549
H	-0.39094	0.54340	-1.08761
H	-0.46769	1.53402	0.38031
Si	-2.36644	-0.06183	0.25265
C	-2.58355	-1.68751	-0.67224
H	-1.92027	-2.45806	-0.26582
H	-2.34572	-1.55921	-1.73369
H	-3.61412	-2.04835	-0.59377
C	-3.51454	1.25302	-0.45419
H	-3.38921	2.20284	0.07549
H	-4.56098	0.94536	-0.36033
H	-3.30275	1.42334	-1.51471
C	-2.70226	-0.30618	2.08995
H	-2.52876	0.61909	2.64916
H	-2.05571	-1.08581	2.50576
H	-3.74203	-0.60953	2.25045
C	1.09820	-1.38180	0.06032
H	0.98006	-1.51531	-1.01646
H	0.52118	-0.28197	1.74328
C	2.02817	-2.32240	0.76911
H	3.04562	-2.26609	0.36117
H	1.70352	-3.36132	0.64821
H	2.07328	-2.10247	1.83998

E(0 K) = -1044.266175
E(0 K) + ZPE = -1043.989710
H (195 K) = -1043.978604
G (195 K) = -1044.016383

4‡ (syn-T3-L)

C	3.06882	1.01002	0.94746
H	3.99107	1.54945	0.70848
H	2.40923	1.68931	1.49125
C	2.44735	0.59659	-0.35972
H	3.04982	-0.09608	-0.95826
O	1.88363	1.57782	-1.02967
H	3.32678	0.15269	1.57130
B	1.82851	1.51756	-2.51900
F	3.12533	1.68475	-3.02314
F	0.97784	2.53732	-2.92971
F	1.33980	0.26352	-2.92929
C	0.40742	-0.09172	0.74318
C	-0.60772	0.82289	0.28927
H	-0.49264	1.08488	-0.76881
H	-0.70579	1.71186	0.91935
Si	-2.32815	-0.09677	0.36732
C	-2.21454	-1.57039	-0.78967
H	-1.51703	-2.32278	-0.40731
H	-1.88300	-1.26871	-1.78817
H	-3.19699	-2.04309	-0.88768
C	-3.59712	1.15845	-0.20496
H	-3.62198	2.02452	0.46249
H	-4.59131	0.69987	-0.20756
H	-3.37812	1.50634	-1.21867
C	-2.64765	-0.64943	2.13280
H	-2.61863	0.19394	2.82909
H	-1.90970	-1.39080	2.45560
H	-3.63782	-1.11098	2.20281
C	1.19345	-0.86929	-0.08893
H	0.89080	-0.91882	-1.13402
H	0.59859	-0.14681	1.81795
C	1.98849	-2.03905	0.43538
H	2.92225	-2.16919	-0.12025
H	1.40952	-2.95981	0.31838
H	2.22565	-1.92524	1.49655

E(0 K) = -1044.256951
E(0 K) + ZPE = -1043.979477
H (195 K) = -1043.969449
G (195 K) = -1044.004813

5

C	0.26147	0.63714	0.77449
C	3.03811	1.46763	-0.17584
H	3.66012	1.10252	0.64525
H	3.69278	1.87152	-0.95157
C	-0.79170	1.12291	0.03277
H	-0.81801	0.90261	-1.03624
H	-1.28655	2.03295	0.37333
Si	-2.19875	-0.28551	0.71533

C	-1.67949	-1.95506	0.07824
H	-0.93634	-2.43283	0.72247
H	-1.27861	-1.88640	-0.93856
H	-2.56580	-2.59777	0.05050
C	-3.67121	0.41654	-0.19280
H	-3.87530	1.44895	0.10034
H	-4.54638	-0.19329	0.05676
H	-3.51884	0.37422	-1.27443
C	-2.31133	-0.13790	2.57030
H	-2.41377	0.90505	2.88360
H	-1.44033	-0.57425	3.06750
H	-3.20037	-0.67859	2.91088
O	1.42073	0.88378	-1.81258
H	0.38319	1.02312	1.78990
H	2.40508	2.28265	0.19130
B	1.02044	0.03232	-2.91064
F	2.06411	-0.14427	-3.84760
F	-0.07876	0.64203	-3.54747
F	0.61855	-1.26321	-2.46852
C	2.02737	-1.02539	1.41508
H	2.82306	-1.65064	1.00061
H	1.37743	-1.67002	2.01456
H	2.48414	-0.29289	2.08703
C	1.24620	-0.34935	0.29161
H	0.73130	-1.09221	-0.32282
C	2.18500	0.35949	-0.77620
H	2.83546	-0.45524	-1.13025

E(0 K) = -1044.262065
E(0 K) + ZPE = -1043.982422
H (195 K) = -1043.972469
G (195 K) = -1044.007596

6‡

C	1.93993	2.57444	1.50279
H	2.38365	3.17764	0.70658
H	1.95975	3.15332	2.42914
C	-0.77767	-0.95736	0.64998
H	-1.76745	-0.52461	0.49092
H	-0.73443	-1.74304	1.40546
Si	-0.48700	-1.98671	-1.06560
C	-1.43440	-3.55569	-0.69791
H	-2.47003	-3.33586	-0.42428
H	-0.96625	-4.11531	0.11658
H	-1.44074	-4.18947	-1.59077
C	1.33608	-2.32368	-1.31794
H	1.91991	-1.41853	-1.50470
H	1.45232	-2.97900	-2.18755
H	1.75899	-2.84091	-0.45127
C	-1.28515	-0.98712	-2.42815
H	-0.81157	-0.01549	-2.58592
H	-2.34464	-0.82410	-2.21021
H	-1.21488	-1.54999	-3.36497
H	2.55157	1.67831	1.65001
B	-1.37537	1.69149	2.69876
F	-2.28374	1.50918	1.62406
F	-1.50041	3.02424	3.14614
F	-1.68749	0.80613	3.74014
C	1.36012	1.38448	-1.12360
H	1.40372	2.41264	-1.49273
H	1.13136	0.74105	-1.97589
H	2.35088	1.11574	-0.74584
C	0.29270	1.28373	-0.03077
H	-0.70303	1.46381	-0.44882
C	0.49806	2.21332	1.19346
H	-0.09198	3.12914	1.07543
O	-0.00708	1.42154	2.27291
C	0.27559	-0.03877	0.67700
H	1.22496	-0.36335	1.10665

E(0 K) = -1044.257775
E(0 K) + ZPE = -1043.978259
H (195 K) = -1043.968729
G (195 K) = -1044.003007

7‡

C	0.10020	0.86614	1.75425
H	0.08092	1.55621	0.89707
O	-1.12800	0.16510	1.82548
B	-2.12759	0.54031	0.90795
F	-3.19221	-0.34806	0.91181
F	-1.55741	0.47102	-0.51063
F	-2.56121	1.86163	1.01774
C	1.25178	-0.12839	1.51773
H	2.16248	0.46977	1.39511
C	1.10162	-0.97875	0.27847
H	2.01525	-1.10591	-0.30177
C	0.02730	-1.71436	-0.08770
H	-0.89156	-1.70625	0.48574
H	0.12315	-2.45138	-0.88003
Si	-0.31089	-0.07530	-2.03174
C	-1.79127	-0.92824	-2.77695
H	-2.68287	-0.30446	-2.69643
H	-1.98761	-1.87549	-2.26690
H	-1.58307	-1.14503	-3.82927
C	1.24537	-0.83205	-2.78623
H	2.15193	-0.31950	-2.45389
H	1.14487	-0.65309	-3.86537
H	1.35996	-1.90786	-2.63602
C	-0.04723	1.76522	-2.19864
H	0.42430	1.96618	-3.16568
H	0.63467	2.12206	-1.41930
H	-0.98405	2.31783	-2.11771
C	1.45674	-1.08523	2.70662
H	2.20949	-1.84304	2.47212
H	0.51567	-1.59198	2.93788
H	1.79496	-0.53912	3.59027
C	0.29607	1.69307	3.01816

H	1.27932	2.17409	3.02796
H	0.20175	1.06205	3.90563
H	-0.47385	2.46674	3.06575

E(0 K) = -1044.244049
E(0 K) + ZPE = -1043.964141
H (195 K) = -1043.954595
G (195 K) = -1043.988757

8‡

C	0.89062	2.72791	-1.44472
H	0.41702	3.63327	-1.83446
H	1.78311	3.02153	-0.89064
C	0.57341	-0.47827	-1.89450
H	1.41625	0.18858	-1.75327
H	0.78898	-1.45441	-2.31522
H	1.18512	2.11933	-2.30146
B	0.99484	1.78069	1.70061
F	-0.12886	2.38926	2.28933
F	1.96607	2.75832	1.45215
F	1.49541	0.79716	2.55397
C	-1.86389	1.98801	-2.31986
H	-2.21950	2.95906	-1.96259
H	-2.72295	1.43227	-2.70366
H	-1.16514	2.15329	-3.14386
C	-1.19227	1.22345	-1.17113
H	-1.95955	1.02928	-0.40928
C	-0.07850	2.02196	-0.49416
H	-0.56140	2.78729	0.12116
O	0.60075	1.12474	0.41069
C	-0.70694	-0.11363	-1.65514
H	-1.48793	-0.84334	-1.87242
Si	0.33414	-1.02178	0.50190
C	-0.97072	-0.73296	1.81846
H	-0.92220	-1.59686	2.49194
H	-1.95887	-0.75768	1.34586
H	-0.86783	0.18672	2.38921
C	2.18197	-1.20957	0.74192
H	2.71986	-0.26434	0.69385
H	2.57183	-1.90633	-0.00534
H	2.34248	-1.64543	1.73415
C	-0.20059	-2.75259	-0.09406
H	-1.25498	-2.80013	-0.38392
H	-0.06885	-3.42319	0.76550
H	0.40921	-3.14583	-0.91132

E(0 K) = -1044.258176
E(0 K) + ZPE = -1043.977131
H (195 K) = -1043.967962
G (195 K) = -1044.001218

9‡

Si	-1.16435	-0.33403	1.03095
C	-2.52826	-1.59023	1.25163
H	-2.69279	-1.72882	2.32313
H	-2.24997	-2.55024	0.80992
H	-3.45989	-1.24613	0.79597
C	0.56705	-0.95257	1.35077
H	0.56042	-1.51897	2.28532
H	1.29281	-0.13866	1.43782
H	0.89075	-1.62845	0.55396
C	-1.67334	1.46176	1.14739
H	-2.41014	1.69670	0.37431
H	-0.81714	2.13201	1.02558
H	-2.12673	1.64793	2.12252
C	-1.26636	-0.70271	-1.25811
H	-2.34819	-0.64655	-1.35516
H	-0.79023	-1.68107	-1.27624
C	-0.51324	0.41344	-1.43504
H	-1.03093	1.36981	-1.53647
O	-1.24737	-0.12875	3.51686
C	0.63257	1.09639	-4.06959
H	0.84423	2.14606	-3.84704
H	0.98642	0.88203	-5.08065
O	1.00682	-1.15409	-3.43265
H	-0.45079	0.93950	-4.05289
B	1.71674	-2.24739	-2.81466
F	3.02567	-1.86814	-2.41617
F	1.79323	-3.32447	-3.71607
F	1.04112	-2.69925	-1.63482
C	1.56561	1.77169	-1.09987
H	2.63608	1.80973	-1.31993
H	1.44692	1.88416	-0.01744
H	1.08727	2.63282	-1.57782
C	0.96923	0.45228	-1.59017
H	1.41760	-0.38268	-1.04651
C	1.32548	0.16270	-3.08731
H	2.41302	0.31623	-3.14509
C	-0.36881	0.04191	4.34632
H	0.68634	0.08260	4.02207
C	-0.63020	0.19845	5.80356
H	-0.09988	-0.59433	6.34228
H	-1.69800	0.15539	6.01658
H	-0.20747	1.14978	6.14262

E(0 K) = -1198.089145
E(0 K) + ZPE = -1197.752674
H (195 K) = -1197.740563
G (195 K) = -1197.780258

10

C	1.09769	3.39764	1.18186
H	1.13320	4.14486	0.38341
H	0.75100	3.88286	2.09623
C	-0.89153	-0.71737	0.45490
H	-1.78929	-0.11417	0.27725

H	-1.06651	-1.31508	1.35727
Si	-0.67282	-1.93897	-1.00052
C	-2.08591	-3.17545	-0.90860
H	-3.05176	-2.66363	-0.96701
H	-2.05561	-3.74414	0.02579
H	-2.02427	-3.88235	-1.74214
C	0.98865	-2.80603	-0.82350
H	1.82358	-2.11420	-0.97783
H	1.07732	-3.60530	-1.56643
H	1.09511	-3.25376	0.17013
C	-0.76134	-1.03700	-2.65351
H	0.09596	-0.37793	-2.82156
H	-1.67552	-0.43859	-2.72722
H	-0.77544	-1.77257	-3.46510
H	2.10521	3.00946	1.34518
B	-0.80676	1.11102	2.95407
F	-2.09858	1.14838	2.45858
F	-0.51741	2.23500	3.70603
F	-0.50782	-0.07582	3.58968
C	1.91293	1.41792	-0.94205
H	2.04550	2.35103	-1.49649
H	2.08501	0.58905	-1.63592
H	2.68090	1.36470	-0.16492
C	0.51408	1.32045	-0.35467
H	-0.23839	1.32103	-1.14737
C	0.14925	2.29952	0.78273
H	-0.88229	2.65522	0.71260
O	0.17295	1.18162	1.75308
C	0.30416	0.16648	0.64683
H	1.20893	-0.40178	0.87969

E(0 K) = -1044.281226
E(0 K) + ZPE = -1044.000768
H (195 K) = -1043.990797
G (195 K) = -1044.026120

11‡

Si	-1.17817	-0.38459	1.11895
C	-2.64165	-1.52087	1.35543
H	-3.06457	-1.32600	2.34430
H	-2.34631	-2.57129	1.28846
H	-3.42095	-1.32575	0.61673
C	0.52992	-1.07092	1.44027
H	0.52059	-1.61593	2.38698
H	1.27524	-0.27307	1.51359
H	0.83566	-1.76351	0.65100
C	-1.59656	1.43442	1.26492
H	-2.34152	1.70802	0.51292
H	-0.72474	2.08064	1.12824
H	-2.03120	1.62198	2.24945
C	-1.24069	-0.76797	-1.16164
H	-2.31689	-0.72337	-1.30402
H	-0.75369	-1.74172	-1.16113
C	-0.49669	0.35825	-1.32138
H	-1.02691	1.30473	-1.44899
O	-1.14170	-0.21438	3.65717
C	-0.12952	0.65999	4.14257
H	-0.08374	1.52488	3.47965
H	0.84332	0.15312	4.15326
H	-0.37568	0.99280	5.15658
C	-1.24505	-1.36915	4.47971
H	-2.02190	-2.01392	4.06924
H	-1.51732	-1.07872	5.50027
H	-0.29293	-1.91496	4.50512
C	0.70929	1.09772	-3.91065
H	0.89258	2.14572	-3.65681
H	1.10268	0.91383	-4.91299
O	1.08728	-1.15931	-3.29751
H	-0.37058	0.92011	-3.93673
B	1.80108	-2.25372	-2.68571
F	3.10607	-1.86991	-2.27956
F	1.88657	-3.32263	-3.59689
F	1.12337	-2.72099	-1.51361
C	1.56015	1.73527	-0.90898
H	2.63080	1.79437	-1.12357
H	1.43730	1.82117	0.17534
H	1.07087	2.59967	-1.36957
C	0.98829	0.41783	-1.43142
H	1.43037	-0.42159	-0.88969
C	1.38476	0.15422	-2.92555
H	2.47183	0.31830	-2.95085

E(0 K) = -1199.279589
E(0 K) + ZPE = -1198.918917
H (195 K) = -1198.906721
G (195 K) = -1198.946473

12

Si	-1.20437	-0.30914	1.69436
C	-2.44433	-1.67269	1.46571
H	-2.22198	-2.49255	2.15563
H	-2.40153	-2.06652	0.44750
H	-3.45856	-1.31478	1.66134
C	0.55979	-0.83393	1.44003
H	0.83572	-1.62073	2.15043
H	1.27271	-0.00835	1.52063
H	0.65084	-1.27272	0.44000
C	-1.73322	1.42522	1.26666
H	-2.48611	1.40535	0.47575
H	-0.88534	2.01751	0.91268
H	-2.16581	1.91320	2.14469
C	-1.32560	-0.47579	-1.59680
H	-2.40989	-0.38994	-1.58175
H	-0.88388	-1.46555	-1.50740
C	-0.54895	0.59664	-1.77942
H	-1.02293	1.57354	-1.90423
O	-1.34146	-0.16989	3.54506
C	0.86709	0.99804	-4.40441

H	1.11236	2.05586	-4.27001
H	1.28022	0.66749	-5.36099
O	1.10448	-1.19559	-3.54800
H	-0.22138	0.89035	-4.44487
B	1.73582	-2.25676	-2.81677
F	3.08281	-1.93444	-2.48301
F	1.71953	-3.43178	-3.60252
F	1.06960	-2.55831	-1.58640
C	1.55402	1.91537	-1.44939
H	2.64343	1.91026	-1.55560
H	1.32061	2.13629	-0.40228
H	1.15634	2.73727	-2.05438
C	0.95449	0.57257	-1.87152
H	1.33667	-0.20479	-1.20185
C	1.43855	0.14359	-3.28137
H	2.53403	0.25290	-3.27178
C	-0.44757	-0.16185	4.40749
H	0.59988	-0.25119	4.09222
C	-0.76533	-0.02383	5.83323
H	-0.30457	-0.85961	6.37199
H	-1.84013	0.01066	6.00247
H	-0.28078	0.88855	6.20165

E(0 K) = -1198.101607
E(0 K) + ZPE = -1197.764181
H (195 K) = -1197.751870
G (195 K) = -1197.792040

13

Si	-1.24153	-0.42830	1.81395
C	-2.57862	-1.69328	1.57925
H	-3.48656	-1.41500	2.12295
H	-2.26260	-2.69543	1.88038
H	-2.82504	-1.72891	0.51379
C	0.49182	-1.00146	1.45843
H	0.83609	-1.67502	2.25140
H	1.19058	-0.16157	1.39245
H	0.53430	-1.55509	0.51484
C	-1.73489	1.32426	1.41629
H	-2.48046	1.31522	0.61733
H	-0.88721	1.92198	1.07068
H	-2.18161	1.80427	2.29239
C	-1.32052	-0.49995	-1.53975
H	-2.40249	-0.39621	-1.58048
H	-0.90050	-1.49880	-1.44421
C	-0.52253	0.56451	-1.67034
H	-0.97976	1.54842	-1.80343
O	-1.16865	-0.28575	3.67482
C	-0.14385	0.59961	4.21017
H	0.00871	1.39815	3.48626
H	0.77461	0.02849	4.35853
H	-0.52005	1.00399	5.14848
C	-1.36625	-1.46479	4.50252
H	-2.28254	-1.94547	4.17135
H	-1.47149	-1.12317	5.53159
H	-0.50398	-2.12684	4.39616
C	0.97719	1.04636	-4.21705
H	1.21496	2.09912	-4.03653
H	1.42006	0.75246	-5.17223
O	1.21114	-1.17736	-3.43709
H	-0.10914	0.93881	-4.29442
B	1.81715	-2.25153	-2.70403
F	3.13846	-1.92833	-2.28935
F	1.85179	-3.40718	-3.52211
F	1.08858	-2.60209	-1.51932
C	1.58105	1.84099	-1.19927
H	2.67405	1.81930	-1.25345
H	1.30192	2.02883	-0.15663
H	1.22779	2.69304	-1.79035
C	0.98275	0.52518	-1.70055
H	1.32747	-0.28620	-1.05198
C	1.51895	0.15440	-3.10863
H	2.61232	0.27398	-3.05852

E(0 K) = -1199.293641
E(0 K) + ZPE = -1198.932479
H (195 K) = -1198.919879
G (195 K) = -1198.960580

14

C	-0.30470	2.29567	2.66693
C	-2.13784	-0.05615	1.77928
H	-2.61989	0.79945	2.25768
H	-2.80122	-0.44660	1.00355
C	-0.63547	2.58554	3.92483
H	-0.58356	1.83342	4.70884
H	-0.96478	3.57996	4.20955
O	-0.23180	-0.70796	0.39871
H	-0.36561	3.07409	1.90259
H	-1.97732	-0.83188	2.53161
B	-0.05899	-2.10594	1.06522
F	-1.24020	-2.80391	0.89146
F	0.24798	-1.92673	2.39721
F	0.98865	-2.69876	0.37038
C	1.58410	1.08508	1.58323
H	1.98305	0.11119	1.28781
H	2.27026	1.53947	2.30171
H	1.55316	1.72877	0.69475
C	0.18751	0.94985	2.19833
H	0.22765	0.27276	3.05656
C	-0.82148	0.39740	1.17793
H	-1.00910	1.18135	0.43999
Si	0.00259	-0.61722	-1.37861
C	-0.92607	0.89207	-1.96693
H	-1.98143	0.87374	-1.67818
H	-0.88319	0.87458	-3.06198
H	-0.47993	1.83470	-1.63800
C	1.83506	-0.46709	-1.67382

H	2.03367	-0.57668	-2.74522
H	2.37737	-1.25047	-1.13952
H	2.21422	0.50843	-1.35782
C	-0.76189	-2.17012	-2.06288
H	-0.75928	-2.10705	-3.15600
H	-1.79632	-2.27159	-1.72399
H	-0.20448	-3.05806	-1.75941

E(0 K) = -1044.316487
E(0 K) + ZPE = -1044.036788
H (195 K) = -1044.026622
G (195 K) = -1044.062069

15

C	-2.93577	1.75040	1.46812
C	-0.06188	1.19261	2.23526
H	-0.63033	1.84197	2.90420
H	0.70029	0.66896	2.81779
C	-3.08380	3.05899	1.26336
H	-2.53084	3.57286	0.48012
H	-3.76065	3.65514	1.86757
O	-0.18169	-0.65948	0.72326
H	-3.50713	1.26258	2.26113
H	0.43385	1.81379	1.48272
B	0.01178	-1.95397	0.97895
F	-0.48671	-2.57503	2.05214
F	0.72553	-2.68849	0.12423
C	-2.88189	-0.21227	-0.06440
H	-2.25748	-0.84421	-0.70063
H	-3.63969	0.26133	-0.69346
H	-3.39718	-0.85217	0.66193
C	-2.04327	0.85060	0.65566
H	-1.50928	1.45771	-0.08805
C	-0.98650	0.19759	1.55843
H	-1.49209	-0.42168	2.31142

E(0 K) = -535.152439
E(0 K) + ZPE = -534.986215
H (195 K) = -534.979937
G (195 K) = -535.007643

$(CH_3)_3SiF$

F	-0.06520	-1.08007	0.20261
Si	0.04022	-0.77595	-1.42232
C	-1.09551	0.66686	-1.75926
H	-2.12698	0.42386	-1.48751
H	-1.07531	0.92378	-2.82314
H	-0.78445	1.54782	-1.18990
C	1.82875	-0.36124	-1.75968
H	1.97476	-0.14324	-2.82241
H	2.48121	-1.19716	-1.49071
H	2.13692	0.51799	-1.18608
C	-0.51012	-2.33600	-2.28675
H	-0.46446	-2.20352	-3.37240
H	-1.54014	-2.58736	-2.01688
H	0.13395	-3.17851	-2.01808

E(0 K) = -509.147042
E(0 K) + ZPE = -509.037093
H (195 K) = -509.032061
G (195 K) = -509.055800

CH_3CHO

C	0.22928	-0.40071	0.00055
H	0.29561	-1.51085	-0.00170
C	-1.14977	0.15884	0.00017
H	-1.69480	-0.21302	0.87702
H	-1.69089	-0.21235	-0.87928
H	-1.13557	1.25163	0.00002
O	1.24613	0.26554	-0.00030

E(0 K) = -153.787774
E(0 K) + ZPE = -153.734326
H (195 K) = -153.731440
G (195 K) = -153.749366

$TiCl_4$

Cl	1.02614	1.77141	-0.72328
Cl	1.02614	-1.77141	-0.72328
Cl	-2.04867	0.00000	-0.71926
Cl	-0.00258	0.00000	2.16828
Ti	-0.00075	0.00000	-0.00180

E(0 K) = -2690.508679
E(0 K) + ZPE = -2690.503149
H (195 K) = -2690.498445
G (195 K) = -2690.523568

17

C	0.25374	-0.91430	0.47770
O	-0.25395	0.16768	0.18866
Cl	2.16800	0.85535	-1.39084
Cl	-1.52981	1.33040	-2.15360
Cl	0.75729	3.71682	-2.17461
Cl	0.04019	2.94351	0.95958
H	1.25322	-1.16209	0.07489
C	-0.40872	-1.89847	1.34654
H	0.26836	-2.15736	2.16955
H	-0.55644	-2.82672	0.77947
H	-1.36246	-1.52733	1.72549
Ti	0.25504	1.90454	-0.98246

E(0 K) = -2844.315750

E(0 K) + ZPE = -2844.254045
H (195 K) = -2844.247077
G (195 K) = -2844.276845

***E*-crotylsilane**

C	0.41036	-0.39751	0.66774
C	-0.56064	0.52240	0.00901
H	-0.38541	0.57048	-1.07669
H	-0.47340	1.54609	0.40093
Si	-2.35392	-0.06112	0.25173
C	-2.57521	-1.69200	-0.66207
H	-1.95835	-2.48093	-0.21498
H	-2.28169	-1.58720	-1.71474
H	-3.62216	-2.01797	-0.63136
C	-3.52046	1.23679	-0.45766
H	-3.39371	2.19674	0.05808
H	-4.56584	0.92472	-0.34238
H	-3.32990	1.39665	-1.52609
C	-2.71557	-0.29872	2.08509
H	-2.54566	0.62984	2.64445
H	-2.07980	-1.08087	2.51765
H	-3.76166	-0.59425	2.23303
C	1.09049	-1.37875	0.06128
H	0.96861	-1.50356	-1.02002
H	0.52888	-0.28216	1.75094
C	2.01399	-2.32957	0.74991
H	3.03038	-2.27926	0.33731
H	1.68281	-3.37077	0.63664
H	2.07526	-2.11174	1.82317

E(0 K) = -565.746788
E(0 K) + ZPE = -565.545850
H (195 K) = -565.538857
G (195 K) = -565.567357

18

C	0.71992	-0.00536	1.03915
C	1.41667	3.01648	0.28651
H	1.81881	4.00183	0.00723
H	0.35962	3.13893	0.53682
C	-0.71251	0.19047	0.69430
H	-0.83950	0.35693	-0.38677
H	-1.13550	1.06304	1.21369
Si	-1.78140	-1.31880	1.14939
C	-1.24544	-2.78576	0.10242
H	-0.19564	-3.04220	0.28974
H	-1.35623	-2.56064	-0.96639
H	-1.85701	-3.66740	0.33004
C	-3.57190	-0.88181	0.76704
H	-3.91216	-0.03463	1.37466
H	-4.23761	-1.73105	0.96261
H	-3.67561	-0.60507	-0.29031
C	-1.54994	-1.70409	2.97636
H	-1.82922	-0.84479	3.59853
H	-0.50213	-1.95255	3.18759
H	-2.16802	-2.55796	3.27890
C	1.65289	-0.54012	0.23398
H	1.35180	-0.85634	-0.77113
C	1.59741	2.14141	-0.88659
H	2.57863	1.66084	-1.04717
O	0.72791	2.02339	-1.75700
H	1.02447	0.28006	2.05233
H	1.99468	2.66161	1.14372
C	3.07627	-0.77708	0.61809
H	3.77477	-0.29946	-0.08391
H	3.32221	-1.84712	0.60969
H	3.28861	-0.39099	1.62291
Cl	0.57411	0.71426	-5.92531
Cl	0.54949	3.52384	-4.22090
Cl	2.66069	0.46445	-3.40227
Cl	-1.11781	0.20262	-3.12954
Ti	0.66081	1.35166	-3.78817

E(0 K) = -3410.072102
E(0 K) + ZPE = -3409.807459
H (195 K) = -3409.793829
G (195 K) = -3409.837140

19‡

C	0.62278	0.28152	0.93518
C	1.62161	2.84684	0.19306
H	1.93396	3.75262	-0.34453
H	0.60109	3.01020	0.55207
C	-0.77816	0.36911	0.57800
H	-0.91917	0.46663	-0.50933
H	-1.29703	1.18031	1.10507
Si	-1.73746	-1.25479	1.00616
C	-1.03393	-2.63192	-0.05401
H	0.01600	-2.83280	0.19235
H	-1.09867	-2.37897	-1.11975
H	-1.59905	-3.55716	0.10992
C	-3.51804	-0.88139	0.55291
H	-3.90450	-0.03540	1.13311
H	-4.16215	-1.74795	0.74195
H	-3.59047	-0.62855	-0.51266
C	-1.51737	-1.62399	2.83170
H	-1.83489	-0.77520	3.44901
H	-0.46627	-1.84181	3.05969
H	-2.11257	-2.49718	3.12382
C	1.63480	-0.17177	0.12462
H	1.35347	-0.65047	-0.81751
C	1.69240	1.72482	-0.78883
H	2.70382	1.39834	-1.07806
O	0.79394	1.67707	-1.70658
H	0.91180	0.63255	1.93214
H	2.30507	2.69941	1.03479
C	3.01451	-0.45173	0.63407

H	3.77474	-0.27542	-0.13657
H	3.10684	-1.50304	0.93336
H	3.25495	0.16456	1.50878
Cl	0.52586	0.76208	-5.83900
Cl	0.49161	3.49609	-4.00751
Cl	2.67937	0.36886	-3.46130
Cl	-1.21583	0.12226	-3.14934
Ti	0.63488	1.30347	-3.62755

E(0 K) = -3410.061886
E(0 K) + ZPE = -3409.796492
H (195 K) = -3409.783648
G (195 K) = -3409.825363

20

C	0.14639	0.63629	0.25657
C	2.17075	2.67174	-0.49626
H	2.65645	3.36385	-1.19157
H	1.18490	3.08303	-0.24602
C	-1.01907	0.58102	-0.46497
H	-0.95567	0.31871	-1.52600
H	-1.86603	1.19147	-0.14022
Si	-1.71528	-1.24479	0.33476
C	-0.51183	-2.58964	-0.10851
H	0.41459	-2.54927	0.47473
H	-0.26608	-2.56798	-1.17731
H	-0.99483	-3.55146	0.10457
C	-3.27256	-1.31271	-0.68238
H	-3.93456	-0.46274	-0.49197
H	-3.80979	-2.23596	-0.43199
H	-3.02419	-1.34009	-1.74931
C	-1.92211	-0.94285	2.15946
H	-2.36796	0.03826	2.35884
H	-0.95732	-1.00289	2.67755
H	-2.57965	-1.70409	2.59347
C	1.46291	0.18306	-0.23777
H	1.31307	-0.66216	-0.92652
C	2.04277	1.31277	-1.15669
H	3.04229	0.94893	-1.45839
O	1.24249	1.41739	-2.28986
H	0.11002	1.06170	1.26697
H	2.77832	2.62361	0.41377
C	2.42209	-0.19550	0.88114
H	3.37943	-0.53186	0.46938
H	2.01998	-1.01207	1.49285
H	2.62032	0.65085	1.54909
Cl	1.17348	0.50639	-6.32083
Cl	3.27605	1.75072	-4.23811
Cl	0.22144	-0.98745	-3.60064
Cl	-0.53474	2.64918	-4.38014
Ti	1.07050	1.11811	-4.05343

E(0 K) = -3410.074424
E(0 K) + ZPE = -3409.805758
H (195 K) = -3409.793057
G (195 K) = -3409.834347

S1

C	0.18525	0.28514	0.74531
H	0.82652	0.84143	0.03738
C	-0.35935	1.25090	1.78973
H	-0.99850	2.00159	1.31713
H	0.45139	1.76137	2.31606
H	-0.95672	0.69951	2.52365
C	1.04469	-0.82952	1.36457
H	0.41662	-1.35870	2.09501
C	1.51388	-1.81903	0.29142
H	2.14926	-1.31352	-0.44631
H	0.65831	-2.25036	-0.23320
H	2.09659	-2.62607	0.74347
C	2.23425	-0.24758	2.07807
H	2.89709	0.36887	1.46540
C	2.53806	-0.45566	3.35921
H	1.90153	-1.06582	3.99635
H	3.42767	-0.02615	3.80980
O	-0.90220	-0.31043	0.04562
Si	-1.32357	0.21399	-1.50032
C	0.04232	-0.24810	-2.70573
H	0.98981	0.23227	-2.43866
H	-0.22103	0.06984	-3.71998
H	0.20138	-1.33107	-2.71515
C	-1.55427	2.07890	-1.50547
H	-1.80037	2.42104	-2.51639
H	-0.63966	2.59436	-1.19248
H	-2.36568	2.38092	-0.83579
C	-2.91621	-0.67233	-1.92033
H	-3.26376	-0.37209	-2.91410
H	-3.69893	-0.43149	-1.19503
H	-2.76829	-1.75643	-1.92356

E(0 K) = -719.704914
E(0 K) + ZPE = -719.440443
H (195 K) = -719.432030
G (195 K) = -719.463765

S2‡

C	3.50341	0.69086	-1.98077
H	3.35864	0.44828	-3.03784
H	4.22737	-0.01137	-1.55832
H	3.92253	1.70160	-1.91715
C	0.79247	1.90058	-1.94508
H	-0.07376	2.22719	-1.36608
H	0.43715	1.45179	-2.87908
H	1.39648	2.77504	-2.20630
C	2.28912	0.98586	0.76196
H	3.08967	1.72709	0.84038

H	2.63998	0.05351	1.21759
H	1.41875	1.32942	1.32598
B	0.56864	-1.70763	-0.94904
F	0.75104	-2.65968	0.02483
F	1.90490	-1.27494	-1.45091
F	-0.18750	-2.16828	-1.99659
C	-1.06463	0.04529	0.02497
H	-0.89999	1.06871	0.38750
Si	1.87667	0.67884	-1.03088
O	0.22345	-0.37986	-0.46370
C	-2.08391	0.04548	-1.10446
H	-1.68824	0.56766	-1.97784
H	-2.99781	0.54697	-0.77868
H	-2.33455	-0.97830	-1.39562
C	-1.48349	-0.82933	1.21828
H	-1.61250	-1.85800	0.85357
C	-0.42841	-0.81366	2.33022
H	0.53883	-1.15776	1.95899
H	-0.73813	-1.46822	3.14900
H	-0.31077	0.19894	2.73397
C	-2.80287	-0.34561	1.76032
H	-2.82397	0.69425	2.09533
C	-3.89667	-1.09618	1.88534
H	-4.81193	-0.69746	2.31170
H	-3.90783	-2.13543	1.56428

E(0 K) = -1044.278845
E(0 K) + ZPE = -1043.999193
H (195 K) = -1043.989735
G (195 K) = -1044.023659

S3

C	-0.79190	-0.64487	-0.14748
H	-0.54415	-1.03713	-1.14001
C	-0.60497	-1.73427	0.89339
H	0.45367	-1.96504	1.03014
H	-1.11172	-2.63793	0.54817
H	-1.02749	-1.44382	1.85617
C	-2.20079	-0.04316	-0.21240
H	-2.47832	0.29570	0.79110
C	-2.27439	1.13183	-1.19372
H	-2.03672	0.80252	-2.21169
H	-1.58026	1.93053	-0.91771
H	-3.28602	1.54394	-1.20215
C	-3.15602	-1.13323	-0.62970
H	-2.99352	-1.55740	-1.62302
C	-4.16714	-1.57409	0.11716
H	-4.35261	-1.16941	1.10937
H	-4.83785	-2.34939	-0.23930
O	0.21397	0.44118	0.05031
Si	1.63264	0.40204	-1.07685
B	0.29355	1.17540	1.36713
F	1.57441	0.67388	1.95214
B	1.88242	0.13530	3.49874
F	1.27065	1.06367	4.27037
F	3.23873	0.16123	3.49714
F	1.32421	-1.09787	3.50402
F	-0.72233	0.83836	2.19906
F	0.43299	2.50781	1.13824
C	2.46164	-1.23430	-0.75544
H	2.75766	-1.32412	0.29388
H	3.36796	-1.29027	-1.36717
H	1.83150	-2.08751	-1.02239
C	2.67875	1.87357	-0.64772
H	3.54739	1.85560	-1.31539
H	3.03630	1.85697	0.38307
H	2.13525	2.80543	-0.81997
C	0.91056	0.55990	-2.78566
H	1.74921	0.62534	-3.48804
H	0.32513	1.47920	-2.87797
H	0.29482	-0.28987	-3.09060

E(0 K) = -1368.903620
E(0 K) + ZPE = -1368.609465
H (195 K) = -1368.597402
G (195 K) = -1368.636842

S4‡

B	2.06141	-0.18833	2.72728
F	0.70857	0.10081	2.97989
F	2.17295	-0.26909	1.23916
Si	2.05165	0.63749	-0.57913
B	-0.28095	1.26922	1.43154
F	-1.42811	1.29761	2.09369
F	0.59582	2.26632	1.57482
F	2.40987	-1.42700	3.20114
F	2.88812	0.81801	3.15292
O	-0.04678	0.42451	0.38393
C	-0.90729	-0.69945	0.01528
H	-0.50405	-1.00941	-0.95578
C	2.13883	-1.03349	-1.39673
H	3.18514	-1.23659	-1.64695
H	1.55245	-1.05765	-2.31835
H	1.80203	-1.83034	-0.72974
C	3.63412	1.46119	-0.03656
H	4.05123	2.03599	-0.86873
H	4.36623	0.73150	0.31439
H	3.42110	2.15361	0.78402
C	1.11185	1.90274	-1.58248
H	0.86206	2.78489	-0.98681
H	0.20030	1.49622	-2.02345
H	1.78518	2.22100	-2.38833
C	-0.73946	-1.80989	1.03682
H	0.31801	-2.03414	1.19436
H	-1.24361	-2.71163	0.68381
H	-1.17919	-1.51871	1.99533
C	-2.36830	-0.26439	-0.19301
H	-2.81746	-0.06503	0.78618

C	-2.47763	0.98382	-1.07488
H	-2.05769	0.79296	-2.06921
H	-1.95336	1.84092	-0.64307
H	-3.52687	1.26048	-1.20078
C	-3.11929	-1.40716	-0.82854
H	-2.79398	-1.69368	-1.83095
C	-4.13679	-2.05075	-0.25763
H	-4.48225	-1.78731	0.73947
H	-4.65439	-2.85665	-0.76829

E(0 K) = -1368.862810
E(0 K) + ZPE = -1368.569957
H (195 K) = -1368.557918
G (195 K) = -1368.597312

S5

C	-0.35139	2.41740	0.52276
H	-1.41128	2.34580	0.25092
O	0.18220	1.04713	0.46258
B	-0.05131	-0.02225	1.52752
B	0.01276	0.01125	-0.64229
O	-0.22216	-1.05983	0.42261
F	-1.09329	0.24246	-1.40101
F	1.16680	-0.21212	-1.33190
F	1.05973	-0.19281	2.29415
F	-1.20715	0.13642	2.23045
C	0.32592	-2.42495	0.46740
H	1.39502	-2.33499	0.24033
C	0.09436	-2.96283	1.86960
H	0.58355	-2.35437	2.62873
H	0.49717	-3.97440	1.93227
H	-0.97941	-3.01016	2.07798
C	-0.37941	-3.28891	-0.59029
H	-1.44616	-3.31042	-0.32990
C	-0.16974	2.91149	1.94822
H	-0.57089	3.92274	2.02640
H	0.89574	2.94597	2.19724
H	-0.69050	2.28309	2.66953
C	0.40743	3.29955	-0.48132
H	1.46344	3.29525	-0.17986
C	-0.21854	-2.78121	-2.02970
H	0.83935	-2.67199	-2.28977
H	-0.71617	-1.82476	-2.19007
H	-0.66617	-3.50494	-2.71545
C	0.16421	-4.69448	-0.51433
H	1.23249	-4.80128	-0.71431
C	-0.57176	-5.77759	-0.26978
H	-0.13363	-6.77070	-0.26282
H	-1.63846	-5.70132	-0.07118
C	0.29301	2.83461	-1.93944
H	0.77314	3.57121	-2.58829
H	-0.75606	2.74565	-2.23915
H	0.78581	1.87707	-2.10898
C	-0.11431	4.71222	-0.38700
H	-1.16941	4.84598	-0.63470
C	0.63020	5.77249	-0.07734
H	0.21174	6.77399	-0.06221
H	1.68454	5.66845	0.16877

E(0 K) = -1070.324322
E(0 K) + ZPE = -1069.988662
H (195 K) = -1069.977389
G (195 K) = -1070.015662

S6

C	-2.72997	1.55971	-0.16791
C	-0.16491	0.88764	1.35825
H	-0.84897	1.61833	1.79647
H	0.31775	0.33366	2.16852
C	-2.81793	2.87916	-0.33912
H	-2.05410	3.42704	-0.88681
H	-3.64984	3.45116	0.06042
O	-0.11361	-1.12362	-0.03384
H	-3.51657	1.04051	0.38579
H	0.60436	1.42738	0.79700
C	-2.20984	-0.29911	-1.73561
H	-1.42170	-0.92188	-2.16466
H	-2.71025	0.24052	-2.54429
H	-2.94503	-0.96138	-1.26246
C	-1.63223	0.68643	-0.71365
H	-0.89072	1.32471	-1.21015
C	-0.93305	-0.05931	0.44291
H	-1.71651	-0.55853	1.03011
B	1.10117	-0.91603	-0.68075
F	1.52412	-2.02895	-1.38993
F	1.27417	0.25823	-1.39356
O	2.25837	-0.76433	0.48564
C	3.57315	-0.39302	0.02235
H	4.17836	-0.14667	0.89517
H	3.44763	0.47781	-0.61518
H	4.01172	-1.22623	-0.53277
C	2.29623	-1.83999	1.44501
H	2.83754	-1.48554	2.32262
H	2.79586	-2.70507	1.00154
H	1.26345	-2.07477	1.69178

E(0 K) = -690.176774
E(0 K) + ZPE = -689.929229
H (195 K) = -689.920968
G (195 K) = -689.952681

syn-T1-L

C	-2.67067	-0.94863	-1.36248
H	-2.92463	-1.35089	-0.37847
H	-3.53895	-1.08222	-2.01592
C	-2.40485	0.52667	-1.29981

H	-1.91942	0.97475	-2.16840
O	-3.37997	1.23409	-0.77944
H	-1.83071	-1.49611	-1.78801
C	0.05147	0.14004	-0.64364
C	0.47582	-1.23089	-0.50083
H	0.87389	-1.67649	-1.41647
H	-0.26182	-1.87641	-0.01347
Si	1.97288	-1.19006	0.76578
C	3.25580	0.02952	0.14486
H	2.90482	1.06319	0.22640
H	3.51429	-0.16786	-0.90025
H	4.16934	-0.06174	0.74114
C	2.64822	-2.93920	0.78887
H	1.88824	-3.65922	1.10496
H	3.48817	-2.99945	1.48855
H	3.00886	-3.22689	-0.20316
C	1.27959	-0.67296	2.42939
H	0.45120	-1.31995	2.73445
H	0.92418	0.36221	2.41463
H	2.06327	-0.74600	3.19043
C	-0.96643	0.76162	0.05903
H	-1.44369	0.17131	0.84433
H	0.60704	0.75765	-1.35493
B	-3.73544	2.60040	-1.28080
F	-2.72856	3.06808	-2.13160
F	-3.89465	3.44850	-0.18390
F	-4.94843	2.49712	-1.97197
C	-0.92311	2.25324	0.28739
H	-0.23555	2.47981	1.10853
H	-1.90918	2.63083	0.55887
H	-0.58046	2.78356	-0.60583

E(0 K) = -1044.249076
E(0 K) + ZPE = -1043.972308
H (195 K) = -1043.962023
G (195 K) = -1043.998071

syn-T2-L

C	-3.56981	0.83241	-0.07775
H	-3.60301	1.91143	0.08243
H	-4.46679	0.54137	-0.63487
C	-2.39504	0.43151	-0.93510
H	-2.23044	-0.64599	-0.98657
O	-2.32756	1.07602	-2.08331
H	-3.56927	0.30750	0.87769
C	-0.09650	0.10768	-0.35038
C	0.14835	-1.22876	0.14336
H	0.24425	-1.95788	-0.66742
H	-0.57374	-1.55820	0.89809
Si	1.89043	-1.22306	1.02945
C	3.14972	-0.53522	-0.17908
H	2.98161	0.52925	-0.37101
H	3.10965	-1.06840	-1.13455
H	4.16008	-0.64763	0.22626
C	2.25080	-3.01067	1.46189
H	1.45645	-3.43518	2.08243
H	3.19155	-3.07475	2.01836
H	2.34883	-3.61843	0.55736
C	1.70859	-0.13912	2.54854
H	0.96913	-0.55662	3.23894
H	1.38706	0.86945	2.26831
H	2.66163	-0.05471	3.07956
C	-0.94048	1.05045	0.21610
H	-1.34940	0.80180	1.19637
H	0.41218	0.39580	-1.27267
B	-1.45471	0.57709	-3.18309
F	-1.02901	-0.72998	-2.88954
F	-0.33325	1.41957	-3.26461
F	-2.18218	0.59775	-4.36622
C	-0.79439	2.51665	-0.10767
H	-0.07429	2.97544	0.57632
H	-1.74251	3.04809	0.00571
H	-0.44244	2.64672	-1.13282

E(0 K) = -1044.255851
E(0 K) + ZPE = -1043.978159
H (195 K) = -1043.968079
G (195 K) = -1044.003588

anti-T1-L

C	-0.69565	0.01315	0.06863
C	-1.98013	2.60978	-0.43867
H	-2.34990	2.79414	0.57268
H	-2.20286	3.49457	-1.04307
C	-0.12082	-0.72137	-1.03291
H	0.82049	-0.29370	-1.39351
H	-0.82264	-0.90774	-1.85197
Si	0.33719	-2.50658	-0.36261
C	1.41068	-2.27957	1.15813
H	0.83972	-1.84312	1.98414
H	2.26100	-1.62422	0.94465
H	1.80209	-3.24580	1.49160
C	1.26524	-3.32586	-1.76835
H	0.66460	-3.33569	-2.68253
H	1.50538	-4.36084	-1.50484
H	2.20118	-2.79733	-1.97187
C	-1.26612	-3.38906	0.04946
H	-1.93167	-3.42034	-0.81846
H	-1.79258	-2.89938	0.87468
H	-1.05475	-4.41961	0.35196
C	-0.03777	0.98596	0.80045
H	1.03452	1.07398	0.62498
C	-0.48811	2.43464	-0.44328
H	-0.05318	2.01023	-1.35318
O	0.16688	3.45300	0.07075
H	-1.73527	-0.20012	0.32942
H	-2.49000	1.74721	-0.87151
B	1.56470	3.71566	-0.38582

F	1.57663	3.72380	-1.78770
F	2.42021	2.70200	0.07909
F	1.93579	4.94699	0.13816
C	-0.52517	1.43869	2.15189
H	-1.59839	1.26722	2.27382
H	-0.31276	2.50215	2.29556
H	-0.00339	0.88503	2.93792

E(0 K) = -1044.253716
E(0 K) + ZPE = -1043.976119
H (195 K) = -1043.966090
G (195 K) = -1044.001628

anti-T2-L

C	2.37598	1.88849	-0.07874
H	3.12646	2.62746	-0.37867
H	1.64295	2.38754	0.55753
C	1.75523	1.37383	-1.34524
H	2.45246	0.85538	-2.01097
O	0.93269	2.21322	-1.94202
H	2.88149	1.09754	0.47866
C	-0.00090	0.23260	-0.18735
C	0.05134	0.25674	1.25434
H	-0.29587	1.19674	1.69523
H	1.01870	-0.05216	1.66125
Si	-1.23401	-1.08596	1.88057
C	-2.95799	-0.40613	1.59517
H	-3.15630	-0.23152	0.53349
H	-3.10185	0.53613	2.13285
H	-3.70136	-1.12148	1.96158
C	-0.86720	-1.30182	3.70571
H	0.14080	-1.69718	3.86121
H	-1.58278	-2.00296	4.14730
H	-0.95276	-0.34775	4.23414
C	-0.94376	-2.66078	0.90258
H	0.10948	-2.95844	0.93233
H	-1.23506	-2.53220	-0.14492
H	-1.53863	-3.47882	1.32029
C	0.92270	-0.36889	-1.02293
H	1.74523	-0.89230	-0.53111
H	-0.83688	0.74499	-0.66941
B	0.78099	2.30963	-3.41974
F	1.78121	1.55098	-4.04694
F	0.91160	3.65751	-3.75862
F	-0.48661	1.84407	-3.78642
C	0.55666	-0.85921	-2.40245
H	1.42864	-0.86864	-3.06059
H	-0.21116	-0.22926	-2.85660
H	0.17519	-1.88225	-2.33040

E(0 K) = -1044.251666
E(0 K) + ZPE = -1043.974577
H (195 K) = -1043.964530
G (195 K) = -1043.999981

anti-T3-L

C	-0.16914	-0.15851	-0.58182
C	0.81658	0.63577	-1.13858
C	2.13769	-0.85989	-1.32784
H	1.69620	-1.27771	-2.23691
O	2.18244	-1.64675	-0.28138
B	1.49162	-2.96915	-0.29523
F	1.31419	-3.34500	1.03097
F	0.25879	-2.85540	-0.96585
F	2.29722	-3.88854	-0.97419
C	3.39201	-0.04046	-1.48470
H	4.16995	-0.73852	-1.81433
H	3.68895	0.36889	-0.51735
H	3.31109	0.75465	-2.22256
H	-0.89865	-0.60233	-1.26151
C	-0.28356	-0.48875	0.81441
H	0.63785	-0.30358	1.37617
H	-0.65005	-1.50687	0.97269
Si	-1.63475	0.68270	1.59416
C	-3.19925	0.56468	0.56425
H	-3.05444	0.98677	-0.43534
H	-4.00634	1.12218	1.05037
H	-3.52444	-0.47503	0.45693
C	-0.93592	2.42428	1.59905
H	-0.72171	2.77107	0.58319
H	-0.01149	2.47265	2.18294
H	-1.65660	3.11659	2.04595
C	-1.91605	0.03598	3.33200
H	-2.30531	-0.98616	3.30533
H	-2.64590	0.66650	3.84996
H	-0.98823	0.03874	3.91147
H	1.42047	1.21579	-0.43876
C	0.62361	1.20631	-2.52561
H	1.56659	1.35350	-3.05515
H	0.13123	2.18137	-2.46415
H	-0.00755	0.54760	-3.12906

E(0 K) = -1044.252924
E(0 K) + ZPE = -1043.977111
H (195 K) = -1043.966562
G (195 K) = -1044.003233

syn-T1-H

C	-2.66964	-0.99510	-1.12003
H	-2.95569	-1.34382	-0.12518
H	-3.52557	-1.14223	-1.78900
C	-2.38941	0.46685	-1.12421
H	-1.83658	0.89871	-1.95920
O	-3.31749	1.22048	-0.60611
H	-3.24647	2.17083	-0.94618
H	-1.83034	-1.57101	-1.50406

H	-2.85252	4.31721	-1.15466
O	-3.01402	3.51775	-1.67354
H	-3.70039	3.74737	-2.31546
C	0.08339	0.13296	-0.38123
C	0.47425	-1.26745	-0.28601
H	0.73512	-1.70520	-1.25507
H	-0.26748	-1.88265	0.23508
Si	2.07787	-1.38884	0.81089
C	3.40651	-0.28938	0.06787
H	3.12634	0.76734	0.12358
H	3.59743	-0.54271	-0.97939
H	4.34280	-0.41582	0.62094
C	2.58245	-3.19477	0.79982
H	1.78558	-3.82843	1.20035
H	3.47347	-3.33497	1.42016
H	2.81721	-3.53045	-0.21456
C	1.60922	-0.80317	2.53154
H	0.84207	-1.44540	2.97552
H	1.22688	0.22252	2.50688
H	2.48556	-0.81888	3.18727
C	-0.86724	0.75760	0.38311
H	-1.36622	0.16439	1.15163
H	0.62934	0.74878	-1.10098
C	-0.90755	2.25147	0.55251
H	-0.23661	2.54965	1.36405
H	-1.91009	2.58763	0.82884
H	-0.58541	2.76878	-0.35715

E(0 K) = -796.4989445
E(0 K) + ZPE = -796.200629
H (195 K) = -796.190480
G (195 K) = -796.225902

syn-T2-H

C	1.57186	1.59597	-0.95941
O	1.15702	2.41135	-1.91013
H	0.55934	3.09917	-1.50811
H	0.11273	4.64209	0.05939
O	-0.34342	3.93917	-0.42286
H	-1.16477	4.33469	-0.74594
C	-0.20633	0.58367	0.04071
C	0.13939	0.26446	1.42412
H	0.17119	1.15671	2.05843
H	1.08203	-0.28871	1.50292
Si	-1.22316	-0.88487	2.19805
C	-2.89150	-0.05357	1.97905
H	-3.17357	0.00275	0.92294
H	-2.88676	0.95969	2.39294
H	-3.66482	-0.62659	2.50058
C	-0.77048	-1.05198	4.01092
H	0.24328	-1.44523	4.13236
H	-1.46322	-1.73546	4.51175
H	-0.82817	-0.08148	4.51304
C	-1.15691	-2.53024	1.29804
H	-0.18839	-3.01952	1.44056
H	-1.32574	-2.40219	0.22393
H	-1.93347	-3.19941	1.68221
C	0.30338	-0.04232	-1.07181
H	0.99849	-0.86386	-0.90261
H	-0.94537	1.37267	-0.11994
C	-0.28969	0.06521	-2.44250
H	0.48987	0.14443	-3.20552
H	-0.95448	0.92674	-2.52759
H	-0.86538	-0.84242	-2.64918
C	2.83198	0.84184	-1.26782
H	3.63475	1.58700	-1.28896
H	2.78086	0.35828	-2.24521
H	3.06099	0.11018	-0.49271
H	1.50687	1.99106	0.05504

E(0 K) = -796.5023165
E(0 K) + ZPE = -796.202799
H (195 K) = -796.192753
G (195 K) = -796.228001

syn-T2-H (*Z*-CH_3CHOH^+)

C	1.42526	1.61445	-0.93207
O	0.92451	2.41139	-1.84939
H	1.25028	2.19191	-2.77221
H	1.21747	1.95491	-4.97572
O	1.81509	1.80383	-4.23079
H	2.65905	2.20056	-4.48658
C	-0.32900	0.52261	0.08264
C	0.01107	0.26994	1.48173
H	-0.05636	1.17376	2.09613
H	0.99934	-0.19154	1.59316
Si	-1.22898	-1.01683	2.23878
C	-2.98194	-0.37967	2.02443
H	-3.26673	-0.33551	0.96836
H	-3.09985	0.61881	2.45688
H	-3.68324	-1.05098	2.53044
C	-0.75654	-1.16292	4.04808
H	0.28545	-1.47891	4.15620
H	-1.39083	-1.90049	4.54922
H	-0.88102	-0.20297	4.55825
C	-0.98423	-2.62575	1.30249
H	0.05416	-2.96719	1.36193
H	-1.25055	-2.50917	0.24669
H	-1.62136	-3.41003	1.72304
C	0.23658	-0.11072	-0.99654
H	0.97122	-0.88855	-0.79020
H	-1.11150	1.25740	-0.12174
C	-0.33376	-0.08331	-2.38142
H	0.45964	-0.05766	-3.13513
H	-0.99674	0.77255	-2.52484
H	-0.90891	-0.99967	-2.54762
C	2.72423	0.90696	-1.20294
H	3.50086	1.67981	-1.22318
H	2.71508	0.38500	-2.16222

H	2.96707	0.20985	-0.40044
H	1.32210	2.02416	0.06932

E(0 K) = -796.5027299
E(0 K) + ZPE = -796.203743
H (195 K) = -796.193766
G (195 K) = -796.228748

syn-T3-H

C	0.44494	-0.16671	0.69417
C	2.91384	1.27474	1.03042
H	3.81686	1.88064	0.88815
H	2.14539	1.90837	1.47561
C	-0.58628	0.80369	0.31723
H	-0.49744	1.11651	-0.72948
H	-0.57059	1.68615	0.96708
Si	-2.33787	0.00533	0.48695
C	-2.45020	-1.38438	-0.77151
H	-1.70445	-2.16028	-0.57082
H	-2.29397	-1.01118	-1.78877
H	-3.44002	-1.84987	-0.73025
C	-3.58087	1.36507	0.12444
H	-3.48708	2.18043	0.84837
H	-4.60080	0.97238	0.18474
H	-3.43245	1.77593	-0.87893
C	-2.53758	-0.64972	2.23615
H	-2.41627	0.15072	2.97285
H	-1.80440	-1.43289	2.45446
H	-3.53598	-1.07954	2.36507
C	1.14148	-0.97486	-0.15445
H	0.90441	-0.94010	-1.21978
C	2.50419	0.79933	-0.31905
H	3.09314	0.01400	-0.79569
O	1.92090	1.65091	-1.09403
H	1.88889	1.29975	-2.04840
H	0.65608	-0.27093	1.76075
H	3.16403	0.44044	1.68600
H	1.14156	0.55408	-3.92565
O	1.91184	0.48383	-3.34527
H	2.68922	0.55344	-3.91680
C	2.02439	-2.09676	0.30998
H	2.99360	-2.09545	-0.20036
H	1.55135	-3.05770	0.08529
H	2.19629	-2.04744	1.38838

E(0 K) = -796.5039829
E(0 K) + ZPE = -796.205445
H (195 K) = -796.195332
G (195 K) = -796.230671

anti-T1-H

C	-0.08313	-0.15429	-0.76380
C	-2.68386	0.57734	-2.01638
H	-2.91132	-0.41264	-2.41904
H	-3.55006	1.22103	-2.20554
C	0.67061	0.93113	-0.14815
H	0.23203	1.26659	0.79890
H	0.82106	1.77867	-0.82543
Si	2.45291	0.28938	0.30429
C	2.23907	-1.22788	1.38931
H	1.76717	-2.04652	0.83622
H	1.62174	-1.00286	2.26503
H	3.21337	-1.57816	1.74422
C	3.28085	1.69412	1.22906
H	3.29549	2.60646	0.62554
H	4.31472	1.42744	1.47034
H	2.75537	1.90526	2.16521
C	3.34314	-0.13230	-1.29286
H	3.37923	0.73298	-1.96159
H	2.85018	-0.95643	-1.81790
H	4.37200	-0.43851	-1.07888
C	-1.00670	-0.93768	-0.12389
C	-2.50773	0.51639	-0.53825
H	-1.98529	1.32575	-0.02466
O	-3.49989	-0.03663	0.10515
H	-3.40694	0.13843	1.09167
H	0.10169	-0.35346	-1.82214
H	-1.81206	0.99883	-2.51535
H	-2.86511	-0.17309	3.21267
O	-2.83355	0.50475	2.52366
H	-3.12459	1.32581	2.94243
H	-1.11017	-0.79471	0.95369
C	-1.56235	-2.20763	-0.69834
H	-2.63873	-2.28075	-0.51095
H	-1.08829	-3.06978	-0.21956
H	-1.38075	-2.27423	-1.77415

E(0 K) = -796.501713
E(0 K) + ZPE = -796.201519
H (195 K) = -796.191867
G (195 K) = -796.226274

anti-T2-H

C	2.21611	2.00656	0.09013
H	3.03377	2.70013	-0.13989
H	1.44364	2.55032	0.63555
C	1.71823	1.50916	-1.22223
H	2.40696	0.89217	-1.80460
O	0.94324	2.31523	-1.89479
H	0.96209	2.13282	-2.88899
H	2.61950	1.19836	0.70038
H	0.40301	1.68951	-4.96646
O	1.16730	1.88121	-4.40700
H	1.69027	2.54068	-4.88271
C	-0.02601	0.23895	-0.07401
C	0.15625	0.06501	1.36396

H	0.04231	1.00098	1.92272
H	1.10432	-0.42065	1.61730
Si	-1.24815	-1.10355	2.02124
C	-2.90731	-0.29985	1.66185
H	-3.10324	-0.25268	0.58589
H	-2.95624	0.71572	2.06707
H	-3.71044	-0.88506	2.12120
C	-0.95661	-1.29177	3.86427
H	0.03176	-1.71558	4.06605
H	-1.70892	-1.95941	4.29643
H	-1.02813	-0.32443	4.37043
C	-1.10292	-2.74177	1.11538
H	-0.11840	-3.19681	1.26380
H	-1.26209	-2.60924	0.04010
H	-1.85827	-3.44385	1.48288
C	0.69695	-0.38188	-1.05702
H	1.51930	-1.03054	-0.74954
H	-0.84650	0.88643	-0.39479
C	0.21452	-0.52797	-2.47202
H	1.03411	-0.44339	-3.19180
H	-0.55518	0.21272	-2.70657
H	-0.22865	-1.52031	-2.60061

E(0 K) = -796.5017622
E(0 K) + ZPE = -796.202831
H (195 K) = -796.192843
G (195 K) = -796.227835

anti-T3-H

C	0.26005	0.56497	0.72401
C	-0.83618	0.96382	-0.15297
H	-0.70992	0.58332	-1.17284
H	-0.99800	2.04717	-0.15521
Si	-2.48644	0.16627	0.48825
C	-3.81956	0.71811	-0.71148
H	-3.59966	0.36538	-1.72398
H	-3.90728	1.80827	-0.73570
H	-4.78807	0.30559	-0.41221
C	-2.80892	0.77935	2.23266
H	-2.03630	0.43319	2.92666
H	-3.77133	0.39858	2.58920
H	-2.84408	1.87245	2.27150
C	-2.27306	-1.69859	0.44488
H	-1.51354	-2.03961	1.15535
H	-1.98760	-2.03822	-0.55592
H	-3.21803	-2.18476	0.70819
C	1.16634	-0.43451	0.47060
H	1.06634	-0.98445	-0.46580
C	2.16309	1.19597	-0.47761
O	1.74668	1.11798	-1.71966
H	1.09058	1.84153	-1.96223
H	0.33354	1.07643	1.68632
H	0.68522	3.78682	-2.82567
O	0.20035	3.07726	-2.38145
H	-0.56725	2.89614	-2.94023
C	1.98606	-1.07676	1.55178
H	2.93685	-1.45823	1.17557
H	1.42959	-1.93610	1.94184
H	2.17355	-0.39199	2.38305
C	3.55646	0.70552	-0.23796
H	4.20804	1.43902	-0.72717
H	3.72715	-0.26794	-0.70062
H	3.80565	0.68302	0.82166
H	1.87359	2.09040	0.07624

E(0 K) = -796.5007433
E(0 K) + ZPE = -796.200894
H (195 K) = -796.191156
G (195 K) = -796.225727

anti-T3-H (*Z*-CH_3CHOH^+)

C	0.24208	0.57109	0.74330
C	-0.87041	0.95928	-0.12015
H	-0.72685	0.61691	-1.15029
H	-1.04889	2.04003	-0.10135
Si	-2.50300	0.12834	0.50995
C	-3.83715	0.63501	-0.70903
H	-3.59507	0.27863	-1.71504
H	-3.94689	1.72281	-0.74597
H	-4.80069	0.20501	-0.41848
C	-2.85348	0.75674	2.24406
H	-2.07488	0.44010	2.94562
H	-3.80834	0.36080	2.60412
H	-2.91214	1.84953	2.26411
C	-2.25049	-1.73301	0.49860
H	-1.48669	-2.04353	1.21864
H	-1.95207	-2.08322	-0.49482
H	-3.18528	-2.23627	0.76630
C	1.13970	-0.43745	0.49818
H	1.01595	-1.01688	-0.41784
C	2.10018	1.19168	-0.53249
O	1.64276	1.06447	-1.75419
H	2.09783	0.32236	-2.26080
H	0.34605	1.10428	1.69146
H	2.26376	-1.45827	-3.52559
O	2.81589	-0.89719	-2.96377
H	3.59818	-0.68571	-3.49197
C	1.99412	-1.04944	1.56906
H	2.95096	-1.40400	1.18062
H	1.47099	-1.92364	1.97219
H	2.17360	-0.35490	2.39389
C	3.51188	0.79818	-0.22492
H	4.14232	1.53880	-0.73212
H	3.76143	-0.19314	-0.60835
H	3.71805	0.85671	0.84294
H	1.74141	2.10124	-0.05764

E(0 K) = -796.5007181

E(0 K) + ZPE = -796.200648
H (195 K) = -796.190879
G (195 K) = -796.225525

syn-T1-F

C	0.68424	0.08931	0.43550
C	-0.33136	0.98513	0.09252
H	-0.49568	1.21423	-0.95998
H	-0.61503	1.76292	0.79840
C	1.47248	-0.69977	-0.39473
H	1.23987	-0.68400	-1.46135
C	3.27992	0.70173	-0.65881
H	0.89275	-0.01291	1.50676
Si	-2.51166	-0.26411	0.36443
C	-1.94320	-1.24153	-1.14728
H	-0.96393	-1.69602	-0.96822
H	-1.84019	-0.57909	-2.01345
H	-2.67111	-2.02168	-1.38607
C	-3.23575	1.46432	0.09701
H	-2.79215	1.95628	-0.77286
H	-3.04281	2.09674	0.97000
H	-4.31813	1.39317	-0.04545
C	-1.87946	-0.73587	2.08413
H	-1.45180	0.12301	2.60898
H	-1.09083	-1.49056	1.99089
H	-2.69582	-1.15398	2.68000
F	-4.04267	-1.06654	0.53704
O	4.25051	-0.04442	-0.90640
C	2.18953	-1.91846	0.11276
H	3.19493	-1.99287	-0.32511
H	1.65422	-2.85082	-0.11487
H	2.30717	-1.86733	1.20279
H	3.14383	1.08059	0.36890
C	2.65664	1.55380	-1.73864
H	3.26283	2.46159	-1.85563
H	1.63888	1.85260	-1.47561
H	2.66155	1.01382	-2.68965

E(0 K) = -819.6120356
E(0 K) + ZPE = -819.349891
H (195 K) = -819.340850
G (195 K) = -819.373933

syn-T2-F

C	0.58677	0.35226	0.59175
C	-0.40645	1.16478	0.04129
H	-0.55496	1.16504	-1.03854
H	-0.68460	2.07806	0.56186
C	1.36778	-0.62120	-0.02135
H	1.11869	-0.89222	-1.04757
C	3.09591	0.76009	-0.57244
H	0.80233	0.51449	1.65369
Si	-2.63564	0.03850	0.46798
C	-2.11669	-1.10772	-0.93693
H	-1.09093	-1.45861	-0.79529
H	-2.15548	-0.56608	-1.88833
H	-2.79352	-1.96490	-0.99520
C	-3.31262	1.75261	0.03084
H	-2.73850	2.24554	-0.75673
H	-3.28785	2.39696	0.91726
H	-4.35423	1.65822	-0.29153
C	-2.01193	-0.30117	2.22043
H	-1.60735	0.60319	2.68344
H	-1.20584	-1.04203	2.18584
H	-2.82683	-0.69055	2.83741
F	-4.20329	-0.66895	0.71496
C	2.15597	-1.62066	0.77893
H	3.04434	-1.96054	0.23061
H	1.58013	-2.51547	1.05371
H	2.51447	-1.15417	1.70367
O	3.95884	0.69464	0.32656
H	2.38047	1.59978	-0.59308
C	3.35921	0.10399	-1.91490
H	3.66836	-0.93637	-1.77444
H	4.18732	0.63940	-2.39694
H	2.48537	0.14648	-2.56883

E(0 K) = -819.6100459
E(0 K) + ZPE = -819.347694
H (195 K) = -819.338619
G (195 K) = -819.371906

syn-T3-F

C	0.61813	0.10317	0.31185
C	3.46672	1.14629	0.41552
H	4.41263	1.69033	0.29639
H	2.73128	1.82576	0.85452
C	-0.34521	0.99474	-0.17103
H	-0.38029	1.16491	-1.24744
H	-0.60703	1.84910	0.45216
C	1.42179	-0.76690	-0.41090
H	1.21521	-0.86969	-1.47575
C	2.99153	0.70267	-0.95282
H	3.48835	-0.20540	-1.34337
O	2.52007	1.53552	-1.75351
H	0.77785	0.09732	1.39541
H	3.63713	0.29892	1.08557
Si	-2.52694	-0.10565	0.07027
C	-1.98983	-1.18368	-1.38458
H	-0.99891	-1.61199	-1.21016
H	-1.92706	-0.57116	-2.29095
H	-2.71340	-1.98588	-1.55378
C	-3.21697	1.61960	-0.30291
H	-2.63594	2.13950	-1.06837
H	-3.19477	2.23168	0.60628
H	-4.25663	1.53812	-0.63430

C	-1.99824	-0.52383	1.84307
H	-1.55472	0.34143	2.34438
H	-1.23810	-1.31269	1.82082
H	-2.85506	-0.87886	2.42235
F	-4.09961	-0.84780	0.24675
C	2.16247	-1.90040	0.24858
H	3.20079	-1.98326	-0.10975
H	1.69016	-2.87523	0.06981
H	2.20405	-1.75350	1.33425

E(0 K) = -819.6116318
E(0 K) + ZPE = -819.349190
H (195 K) = -819.340065
G (195 K) = -819.373428

anti-T1-F

C	0.68424	0.08931	0.43550
C	-0.33136	0.98513	0.09252
H	-0.49568	1.21423	-0.95998
H	-0.61503	1.76292	0.79840
C	1.47248	-0.69977	-0.39473
H	1.23987	-0.68400	-1.46135
C	3.27992	0.70173	-0.65881
H	0.89275	-0.01291	1.50676
Si	-2.51166	-0.26411	0.36443
C	-1.94320	-1.24153	-1.14728
H	-0.96393	-1.69602	-0.96822
H	-1.84019	-0.57909	-2.01345
H	-2.67111	-2.02168	-1.38607
C	-3.23575	1.46432	0.09701
H	-2.79215	1.95628	-0.77286
H	-3.04281	2.09674	0.97000
H	-4.31813	1.39317	-0.04545
C	-1.87946	-0.73587	2.08413
H	-1.45180	0.12301	2.60898
H	-1.09083	-1.49056	1.99089
H	-2.69582	-1.15398	2.68000
F	-4.04267	-1.06654	0.53704
O	4.25051	-0.04442	-0.90640
C	2.18953	-1.91846	0.11276
H	3.19493	-1.99287	-0.32511
H	1.65422	-2.85082	-0.11487
H	2.30717	-1.86733	1.20279
H	3.14383	1.08059	0.36890
C	2.65664	1.55380	-1.73864
H	3.26283	2.46159	-1.85563
H	1.63888	1.85260	-1.47561
H	2.66155	1.01382	-2.68965

E(0 K) = -819.6134605
E(0 K) + ZPE = -819.351442
H (195 K) = -819.342288
G (195 K) = -819.375729

anti-T2-F

C	0.68357	0.12422	0.41983
C	-0.34745	0.95148	-0.03785
H	-0.48397	1.04840	-1.11591
H	-0.59879	1.83756	0.54334
C	1.46430	-0.77558	-0.29678
H	1.21694	-0.91590	-1.35137
C	3.28826	0.43987	-0.66310
H	3.51281	-0.37828	-1.37507
H	0.90391	0.17567	1.49148
Si	-2.47215	-0.17427	0.39870
C	-1.97379	-1.36151	-0.98361
H	-0.96724	-1.75465	-0.81463
H	-1.96198	-0.82945	-1.94146
H	-2.68593	-2.18842	-1.05259
C	-3.21774	1.50898	-0.06168
H	-2.66979	2.01406	-0.86054
H	-3.20901	2.16489	0.81692
H	-4.25821	1.37296	-0.37139
C	-1.86452	-0.47839	2.16654
H	-1.40986	0.41907	2.59626
H	-1.09831	-1.26213	2.15723
H	-2.69206	-0.80327	2.80327
F	-4.04015	-0.90572	0.67207
C	2.15631	-1.91913	0.39991
H	3.00296	-2.29824	-0.18686
H	1.48966	-2.76981	0.59755
H	2.55820	-1.57605	1.36057
O	3.96737	0.52569	0.38410
C	2.67789	1.66493	-1.29968
H	3.48418	2.24707	-1.76352
H	2.18241	2.28350	-0.54682
H	1.94862	1.39677	-2.06907

E(0 K) = -819.6094134
E(0 K) + ZPE = -819.347678
H (195 K) = -819.338664
G (195 K) = -819.371722

anti-T3-F

C	0.59417	0.33992	0.52508
C	3.41199	-0.13330	-2.01442
H	3.46648	-1.19602	-1.76930
C	-0.38803	1.16564	-0.01624
H	-0.54858	1.16716	-1.09404
H	-0.67692	2.06921	0.51449
C	1.36027	-0.63160	-0.10711
H	1.10440	-0.88167	-1.13691
C	3.07085	0.73427	-0.81725
O	2.71408	1.91285	-0.99700
H	0.80510	0.47888	1.59120
H	2.67287	0.02771	-2.80378

Si	-2.60481	0.04958	0.49576
C	-2.12747	-1.18234	-0.85006
H	-1.05107	-1.36090	-0.88402
H	-2.44151	-0.78487	-1.82257
H	-2.65151	-2.12949	-0.68904
C	-3.29625	1.74061	-0.00590
H	-2.73681	2.20936	-0.81821
H	-3.26690	2.41750	0.85593
H	-4.34096	1.62506	-0.31064
C	-1.96944	-0.19185	2.25945
H	-1.51126	0.72270	2.64679
H	-1.20352	-0.97504	2.27166
H	-2.79131	-0.48968	2.91700
F	-4.17439	-0.64659	0.78902

TS-a1

E(195 K) = -872.714264
G(195 K) = -872.409913

C	6.0	0.4368091839	-0.6264807398	-0.6893720498
C	6.0	-0.5724557795	-2.6587123862	0.4040993718
C	6.0	1.0241093939	-0.1749654226	0.6565121235
C	6.0	0.3144514037	-2.1534382257	-0.7551977615
H	1.0	1.3062016937	-2.6111993687	-0.7146126083
H	1.0	-0.1164008265	-3.5237439681	0.8971881195
H	1.0	1.1832506358	0.9110119238	0.6948495705
H	1.0	-0.1203295873	-2.4414827061	-1.7161052227
C	6.0	-0.9819665849	-0.0182761670	-0.8031516183
H	1.0	-1.4977590189	-0.4335846664	-1.6733167094
H	1.0	-0.9058097909	1.0648785635	-0.9331133896
SI	14.0	2.8229847500	-0.8458955211	1.0713560702
C	6.0	3.5082836161	0.2993732670	2.3887379086
H	1.0	3.5747930016	1.3308215529	2.0303703994
H	1.0	4.5142758137	-0.0276504041	2.6706937215
H	1.0	2.8875273225	0.2851622105	3.2903619174
C	6.0	2.7636976762	-2.6025500540	1.7398498976
H	1.0	2.4607713658	-3.3386818350	0.9908677021
H	1.0	2.0866299515	-2.6818963821	2.5968663014
H	1.0	3.7670624124	-2.8748048725	2.0844721366
C	6.0	3.7876665937	-0.7367557278	-0.5319277511
H	1.0	3.3939422717	-1.4235313279	-1.2875801499
H	1.0	4.8324838374	-1.0044151880	-0.3441717129
H	1.0	3.7643656677	0.2788281119	-0.9386406622
H	1.0	-1.5518410655	-2.9884937470	0.0452718805
C	6.0	-1.8605503205	-0.2833517426	0.4042123882
C	6.0	-0.7934070923	-1.6055858363	1.4681164037
H	1.0	-1.4719462680	-1.8738528790	2.2753772907
H	1.0	1.0501817520	-0.2576747378	-1.5154281730
H	1.0	-2.0095114852	0.5336607258	1.1101341971
O	8.0	-2.9556965213	-0.9924650626	0.1576565253
C	6.0	0.1143132096	-0.5925105119	1.7068738499
H	1.0	0.0545500683	-0.0309002520	2.6392084600
H	1.0	-3.6328940523	-0.8576505736	0.8792792424
H	1.0	-5.5497327733	-0.2388048931	1.8069629335
O	8.0	-4.6310365337	-0.4022444878	2.0579524887
H	1.0	-4.6612572367	-0.8690160754	2.9028181250

TS-a2

E(195 K) = -872.717268
G(195 K) = -872.413289

H	1.0	0.3162195211	-0.7892937744	0.0768247203
C	6.0	0.0512508130	-0.6144496108	1.1225350136
C	6.0	2.12681	-1.66326	0.68016
H	1.0	3.13064	-1.84876	0.26902
H	1.0	1.62325	-2.63889	0.72498
H	1.0	2.26343	-1.32293	1.71376
H	1.0	4.39208	0.18237	-2.39510
H	1.0	3.55302	0.44526	0.13439

E(0 K) = -819.6083625
E(0 K) + ZPE = -819.345360
H (195 K) = -819.336376
G (195 K) = -819.369424

C	6.0	-0.0112707011	1.0930280477	2.9910626805
C	6.0	-1.6830483595	-0.7968925071	2.7838653887
C	6.0	-0.8649576603	-0.0146550657	3.5746324426
C	6.0	-1.4383952233	-0.9148933005	1.3569635978
C	6.0	0.3971945383	0.8222368969	1.5235619534
H	1.0	-1.0846288031	0.0484687717	4.6384919806
H	1.0	-0.1093518103	1.5213088513	0.8524367619
H	1.0	-0.5860789556	2.0216645289	3.0708592976
H	1.0	-2.4314618118	-1.4269915283	3.2618031166
H	1.0	-1.7046234820	-1.9241102437	1.0145080105
H	1.0	1.4696448201	0.9896802681	1.3906822150
C	6.0	0.8211685427	-1.6146060473	2.0162534340
H	1.0	1.8989132386	-1.4374021431	1.9325291232
H	1.0	0.6133493036	-2.6381924524	1.6926815531
SI	14.0	-2.6977765853	0.1950709508	0.3502729144
C	6.0	-4.3121446765	-0.7600409074	0.3173418192
H	1.0	-4.1829122004	-1.7467826564	-0.1374283299
H	1.0	-5.0514757129	-0.2088679943	-0.2726719473
H	1.0	-4.7202673407	-0.8924293225	1.3244917997
C	6.0	-2.9753285714	1.8562633087	1.1850423305
H	1.0	-2.1178725323	2.5302872901	1.1084569633
H	1.0	-3.2268944375	1.7293741987	2.2434082164
H	1.0	-3.8252825810	2.3473478734	0.6988770319
C	6.0	-1.9747547897	0.3770154501	-1.3699585853
H	1.0	-1.0361002447	0.9391401034	-1.3661434390
H	1.0	-2.6870117503	0.9168085437	-2.0026619691
H	1.0	-1.7924535748	-0.6017593169	-1.8246387640
C	6.0	0.4448012967	-1.5126420254	3.4752696344
H	1.0	1.0818164073	-0.8891793510	4.1073870754
O	8.0	0.0538906898	-2.6466923119	4.0429014854
H	1.0	0.8705218510	1.2332028304	3.6246450903
H	1.0	0.0949944414	-2.5551282076	5.0340731482
H	1.0	-0.5529237896	-2.1584880328	7.1464569604
O	8.0	0.2153714893	-2.0354998448	6.5733816904
H	1.0	0.9807052562	-2.3294926073	7.0847851933

TS-b1

E(195 K) = -757.189334
G(195 K) = -756.935374

C	6.0	-2.9427756569	-2.0622451355	-0.5188670145
H	1.0	-3.2101322331	-2.5064662551	0.4425594369
H	1.0	-3.7833355550	-2.2118355145	-1.2078439704
C	6.0	-2.7653340415	-0.5938918279	-0.3974987901
H	1.0	-2.2278209804	-0.0498053576	-1.1740511636
O	8.0	-3.6937931788	0.0471660140	0.2339185418
H	1.0	-3.6118021957	1.0509679598	0.0736209432
H	1.0	-2.0607372877	-2.5453443223	-0.9352650431
H	1.0	-3.4390684994	3.1635810236	0.3667648544

O	8.0	-3.2194034792	2.4742657991	-0.2760376538
H	1.0	-3.4727992987	2.8280220729	-1.1400769737
C	6.0	-0.1737354416	-1.0700919756	0.4024754169
C	6.0	0.1435239897	-2.4677016912	0.6753177744
H	1.0	0.4108090189	-3.0222905167	-0.2306249941
H	1.0	-0.6536129074	-2.9846514075	1.2211816940
SI	14.0	1.7123811382	-2.5570324547	1.8197890625
C	6.0	3.1114186816	-1.6282733520	0.9793241547
H	1.0	2.8874602567	-0.5599193280	0.8984305213
H	1.0	3.3006595974	-2.0192548577	-0.0254260399
H	1.0	4.0325910921	-1.7345791799	1.5610229049
C	6.0	2.1149234259	-4.3793451255	2.0140818998
H	1.0	1.2808771254	-4.9216483486	2.4695410271
H	1.0	2.9918681307	-4.5000429140	2.6581936356
H	1.0	2.3387611638	-4.8376844262	1.0459421079
C	6.0	1.2612519834	-1.7628619286	3.4592787289
H	1.0	0.4348576030	-2.2942296959	3.9417899619
H	1.0	0.9654789644	-0.7180964154	3.3206346198
H	1.0	2.1201940503	-1.7835395668	4.1373275922
C	6.0	-1.1369441151	-0.3369575705	1.0331151504
H	1.0	-1.1549689351	0.7431263516	0.9209533925
H	1.0	-1.6932182253	-0.7617570083	1.8662222134
H	1.0	0.4196732606	-0.5738924354	-0.3672183402

TS-b2

E(195 K) = -757.191168
G(195 K) = -756.935409

C	6.0	3.2978863346	1.0867330920	0.9782481766
H	1.0	4.1656082702	1.7359011044	0.8071661550
H	1.0	2.5224514448	1.6683666383	1.4790084403
C	6.0	2.8478241645	0.6265449785	-0.3604268155
H	1.0	3.4961601925	-0.0523886867	-0.9171070661
O	8.0	2.1005374069	1.4291320084	-1.0434007719
H	1.0	2.0205580522	1.1195110184	-2.0101485968
H	1.0	3.6172003668	0.2538994806	1.6040028867
H	1.0	1.1645266625	0.4697540809	-3.8642997234
O	8.0	1.9809481309	0.3951694911	-3.3509564162
H	1.0	2.7080267275	0.5343984385	-3.9734140384
C	6.0	0.9392291627	-0.6558446804	0.8511103409
C	6.0	1.0978985936	-0.8759789685	2.2876860063
H	1.0	0.9630363567	0.0422481937	2.8707139659
H	1.0	2.0535863570	-1.3504395250	2.5361426854
SI	14.0	-0.2749272859	-2.1016205653	2.9002488008
C	6.0	-1.9549670655	-1.3370335586	2.5535380665
H	1.0	-2.1409379004	-1.2617627277	1.4773591351
H	1.0	-2.0357522067	-0.3362226988	2.9892478515
H	1.0	-2.7454662099	-1.9585216166	2.9862031431
C	6.0	0.0139760765	-2.3340572687	4.7392737769
H	1.0	1.0073301678	-2.7505986415	4.9318107620
H	1.0	-0.7304644984	-3.0213747235	5.1537052374
H	1.0	-0.0692319062	-1.3803562514	5.2691052388
C	6.0	-0.0674552391	-3.7064424503	1.9477335694
H	1.0	0.9454527429	-4.1069445613	2.0583896467
H	1.0	-0.2628102206	-3.5553036526	0.8812369959
H	1.0	-0.7705032828	-4.4599938047	2.3165497087
C	6.0	1.6877610758	-1.2423323503	-0.1237172670
H	1.0	1.3827623757	-1.2107674376	-1.1652041664
H	1.0	2.4672169160	-1.9553450536	0.1391471791
H	1.0	0.1444365725	0.0250914288	0.5407853064

TS-c1

E(195 K) = -757.189449
G(195 K) = -756.934111

C	6.0	-0.1676418667	-0.8325579049	0.3755505841
C	6.0	-2.8281001452	-2.1201898483	-0.3766226030
H	1.0	-3.0555647520	-2.5132124337	0.6161899471
H	1.0	-3.6704564115	-2.3564751407	-1.0381976960
C	6.0	0.6277535167	-0.2288455296	-0.6926807789
H	1.0	0.2179782565	0.7315128339	-1.0266913740
H	1.0	0.7541046144	-0.9045537211	-1.5464779635
SI	14.0	2.4246650507	0.1390327908	-0.0578828840
C	6.0	2.2808902710	1.2672993660	1.4351087455
H	1.0	1.7373382071	0.7781723758	2.2494468034
H	1.0	1.7563985301	2.1928464209	1.1770145374
H	1.0	3.2763603969	1.5345567937	1.8033767622
C	6.0	3.3119014653	0.9769993316	-1.4833492519
H	1.0	3.3084067837	0.3419720974	-2.3744064057
H	1.0	4.3529654857	1.1816320895	-1.2144012385
H	1.0	2.8319983612	1.9279600581	-1.7339182045
C	6.0	3.2271468823	-1.4976414111	0.3944322903
H	1.0	3.2190048028	-2.1875346985	-0.4552734765
H	1.0	2.7126241114	-1.9758826482	1.2338730895
H	1.0	4.2690941487	-1.3364572245	0.6887805736
C	6.0	-1.1197700228	-0.1871542919	1.1041567644
H	1.0	-1.2527527380	0.8876245853	0.9951237036
C	6.0	-2.7195937249	-0.6382853661	-0.3488861841
H	1.0	-2.1708795200	-0.1172126634	-1.1363810150
O	8.0	-3.6924609120	-0.0034860326	0.2102360637
H	1.0	-3.6333529338	0.9967473938	0.0081435614
H	1.0	0.0078034081	-1.8881598757	0.5883744161
H	1.0	-1.9262756530	-2.5836014357	-0.7741776848
H	1.0	-1.5826709055	-0.6643241426	1.9621198469
H	1.0	-3.4487951845	3.1029633554	0.2811171091
O	8.0	-3.2303215846	2.4074103598	-0.3552617183
H	1.0	-3.4728329231	2.7584139222	-1.2236882093

TS-c2

E(195 K) = -757.192915
G(195 K) = -756.937875

C	6.0	0.6730404514	-0.4293965984	0.7725663210
C	6.0	3.1848839704	1.0431993882	1.0508041278
H	1.0	4.0785687317	1.6656749175	0.9179593344
H	1.0	2.3966181408	1.6659044561	1.4762069578
C	6.0	-0.3551281882	0.5507306448	0.4217065961
H	1.0	-0.2575058709	0.8989186921	-0.6134671012
H	1.0	-0.3550054211	1.4066741342	1.1061489986
SI	14.0	-2.1105468936	-0.2522562115	0.5444938620
C	6.0	-2.1991299251	-1.6338967137	-0.7241220704
H	1.0	-1.4559177905	-2.4102632751	-0.5172897134
H	1.0	-2.0285119601	-1.2544018827	-1.7367138190
H	1.0	-3.1895745108	-2.0994588437	-0.7002650791
C	6.0	-3.3453910242	1.1090560219	0.1604390122
H	1.0	-3.2685278757	1.9227442352	0.8881404746
H	1.0	-4.3653933358	0.7135251299	0.1989765061
H	1.0	-3.1779602666	1.5224212692	-0.8388731905
C	6.0	-2.3540874043	-0.9116773349	2.2860190857
H	1.0	-2.2389747933	-0.1145724566	3.0272785667
H	1.0	-1.6368293413	-1.7053619101	2.5181486110
H	1.0	-3.3609837861	-1.3281573903	2.3908245741
C	6.0	1.3862099517	-1.1794369696	-0.1091461625
H	1.0	1.1639294419	-1.1597085872	-1.1743258381
C	6.0	2.8124605304	0.5566338435	-0.3033823934
H	1.0	3.4043246537	-0.2334886299	-0.7667509131
O	8.0	2.2081484660	1.3835802262	-1.0816138730
H	1.0	2.1836403237	1.0304706064	-2.0409331535
H	1.0	2.0492330823	-1.9646915640	0.2417505784
H	1.0	0.8820182954	-0.5683928283	1.8338948232
H	1.0	3.4382273132	0.2178986978	1.7150710786
H	1.0	1.4346109795	0.3280412024	-3.9122658776
O	8.0	2.2047498291	0.2484516445	-3.3328812474
H	1.0	2.9833671990	0.3185557351	-3.9028410343

Table S1. Energy components at varying bond lengths along the intrinsic reaction coordinate for all three activation. Units are in kcal/mol.

$d_{C\text{-}C}$	ΔE_{es}	ΔE_{ex}	ΔE_{rep}	ΔE_{ste}	ΔE_{orb}	ΔE_{disp}	ΔE_{int}	ΔE_{d}
syn-T1-L								
1.92	-41.97	-73.62	213.30	139.68	-102.59	-30.63	-35.50	39.54
1.97	-36.50	-66.35	192.48	126.13	-89.85	-29.95	-30.17	34.26
2.02	-31.70	-59.87	174.03	114.16	-78.71	-29.29	-25.54	29.50
2.15	-21.80	-46.15	135.24	89.09	-56.41	-27.60	-16.73	19.78
2.28	-14.64	-35.97	106.44	70.47	-41.45	-25.89	-11.51	13.29
2.54	-4.97	-22.37	68.05	45.68	-25.47	-22.52	-7.28	6.31
2.80	1.73	-13.22	42.64	29.42	-19.39	-18.44	-6.68	3.64
syn-T2-L								
1.92	-48.32	-80.60	233.95	153.35	-106.96	-33.67	-35.60	35.43
1.97	-42.95	-73.47	213.35	139.88	-94.75	-33.01	-30.83	30.61
2.02	-38.17	-67.04	194.86	127.82	-83.98	-32.35	-26.68	26.27
2.15	-27.86	-52.97	154.77	101.80	-61.86	-30.60	-18.53	17.29
2.28	-19.55	-41.73	123.12	81.39	-46.36	-28.79	-13.31	11.01
2.54	-7.72	-25.56	77.93	52.37	-28.31	-25.03	-8.68	4.18
2.80	0.14	-14.49	47.19	32.70	-20.45	-20.41	-8.02	1.59
syn-T3-L								
1.92	-44.94	-76.69	221.98	145.29	-103.42	-31.16	-34.24	33.40
1.97	-39.78	-69.75	201.95	132.20	-91.43	-30.48	-29.48	28.52
2.02	-35.16	-63.49	183.96	120.47	-80.98	-29.79	-25.46	24.28
2.15	-25.11	-49.75	144.76	95.01	-59.92	-27.96	-17.98	15.98
2.28	-16.90	-38.60	113.35	74.75	-45.16	-26.05	-13.36	10.49
2.54	-4.95	-22.24	67.84	45.60	-27.34	-22.07	-8.77	4.35
2.80	1.91	-12.29	40.22	27.93	-19.61	-18.01	-7.77	2.12
anti-T1-L								
1.92	-43.08	-74.09	213.64	139.55	-100.34	-29.29	-33.17	34.37
1.97	-37.72	-66.92	193.12	126.20	-88.24	-28.60	-28.36	29.48
2.02	-32.96	-60.46	174.78	114.32	-77.67	-27.92	-24.23	25.14
2.15	-22.88	-46.61	135.69	89.08	-56.47	-26.17	-16.44	16.48
2.28	-15.26	-36.02	105.95	69.93	-42.01	-24.42	-11.75	10.74
2.54	-4.59	-21.42	64.99	43.57	-25.86	-20.88	-7.77	4.63
2.80	2.42	-11.62	37.65	26.03	-19.00	-16.56	-7.11	2.39
anti-T2-L								
1.92	-47.15	-78.49	228.51	150.02	-105.29	-31.81	-34.23	36.72
1.97	-41.67	-71.43	208.02	136.59	-93.18	-31.14	-29.40	31.80
2.02	-36.76	-65.04	189.60	124.56	-82.62	-30.48	-25.31	27.50
2.15	-26.20	-51.05	149.60	98.55	-61.09	-28.73	-17.46	18.82
2.28	-17.84	-39.95	118.15	78.20	-45.87	-26.90	-12.40	12.73

Table S1. (cont.) Energy components at varying bond lengths along the intrinsic reaction coordinate for all three activation. Units are in kcal/mol.

2.54	-6.11	-24.11	73.62	49.51	-27.58	-23.27	-7.45	5.52
2.80	1.29	-13.67	44.39	30.72	-19.96	-19.04	-6.99	2.80
anti-T3-L								
1.92	-42.27	-75.57	220.48	144.91	-107.07	-32.45	-36.88	27.15
1.97	-36.74	-68.40	199.74	131.34	-94.26	-31.77	-31.42	23.66
2.02	-31.87	-61.98	181.30	119.32	-83.06	-31.09	-26.70	20.47
2.15	-21.80	-48.28	142.15	93.87	-60.43	-29.33	-17.69	13.76
2.28	-14.38	-37.87	112.61	74.74	-44.96	-27.53	-12.14	8.94
2.54	-4.05	-23.35	71.65	48.30	-27.71	-23.92	-7.37	3.33
2.80	2.60	-13.58	44.27	30.69	-20.76	-19.60	-7.06	1.48

$d_{C\text{-}C}$	ΔE_{es}	ΔE_{ex}	ΔE_{rep}	ΔE_{ste}	ΔE_{orb}	ΔE_{disp}	ΔE_{int}	ΔE_{d}
syn-T1-H								
2.10	6.73	-48.02	142.65	94.63	-101.12	-25.77	-25.53	23.63
2.16	11.36	-42.46	126.78	84.32	-92.15	-25.01	-21.49	19.61
2.22	15.40	-37.62	112.92	75.30	-84.58	-24.25	-18.13	16.16
2.31	20.60	-31.48	95.33	63.85	-75.45	-23.14	-14.14	11.90
2.40	24.98	-26.44	80.82	54.38	-68.55	-22.04	-11.23	8.61
2.58	32.05	-18.56	58.18	39.62	-60.04	-19.80	-8.17	4.53
2.76	37.24	-12.55	41.10	28.55	-55.65	-17.23	-7.10	2.55
syn-T2-H								
2.10	-1.98	-59.63	174.64	115.01	-113.60	-27.38	-27.94	23.91
2.16	3.14	-53.45	156.90	103.45	-104.38	-26.56	-24.35	20.25
2.22	7.95	-47.65	140.37	92.72	-96.29	-25.68	-21.30	17.12
2.31	14.65	-39.65	117.63	77.98	-85.76	-24.25	-17.38	13.06
2.40	20.47	-32.75	98.01	65.26	-77.03	-22.83	-14.14	9.66
2.58	29.74	-21.96	67.38	45.42	-64.79	-20.10	-9.73	4.84
2.76	36.66	-13.49	43.27	29.78	-57.62	-16.71	-7.88	2.52
syn-T3-H								
2.10	4.69	-52.39	154.09	101.70	-105.51	-26.12	-25.24	20.20
2.16	9.46	-46.59	137.37	90.78	-96.65	-25.25	-21.66	16.64
2.22	13.84	-41.30	122.16	80.86	-89.04	-24.33	-18.68	13.64
2.31	19.76	-34.24	101.95	67.71	-79.63	-22.90	-15.06	9.98
2.40	24.99	-28.11	84.53	56.42	-72.17	-21.46	-12.22	7.09
2.58	33.22	-18.41	57.11	38.70	-62.17	-18.58	-8.82	3.46
2.76	38.67	-11.82	38.40	26.58	-57.03	-15.82	-7.60	1.93
anti-T1-H								

Table S1. (cont.) Energy components at varying bond lengths along the intrinsic reaction coordinate for all three activation. Units are in kcal/mol.

2.10	7.30	-48.88	144.16	95.28	-101.25	-25.28	-23.94	20.34
2.16	11.93	-43.24	128.09	84.85	-92.62	-24.50	-20.34	16.69
2.22	16.05	-38.25	113.84	75.59	-85.35	-23.68	-17.39	13.62
2.31	21.44	-31.74	95.33	63.59	-76.51	-22.45	-13.93	9.94
2.40	26.07	-26.24	79.67	53.43	-69.67	-21.20	-11.36	7.10
2.58	33.42	-17.49	54.79	37.30	-60.78	-18.55	-8.61	3.74
2.76	38.95	-10.70	35.38	24.68	-55.98	-15.27	-7.62	2.26
anti-T2-H								
2.10	2.61	-53.42	158.08	104.66	-105.83	-27.63	-26.19	22.52
2.16	7.57	-47.58	141.34	93.76	-96.91	-26.82	-22.39	18.74
2.22	12.11	-42.30	126.22	83.92	-89.12	-25.98	-19.07	15.36
2.31	18.19	-35.22	105.94	70.72	-79.51	-24.67	-15.27	11.43
2.40	23.28	-29.33	89.05	59.72	-71.87	-23.42	-12.29	8.27
2.58	31.20	-20.22	63.10	42.88	-61.76	-20.97	-8.65	4.02
2.76	36.89	-13.37	43.70	30.33	-56.42	-18.14	-7.34	2.12
anti-T3-H								
2.10	-2.00	-58.68	172.16	113.48	-111.96	-28.42	-28.90	25.89
2.16	3.15	-52.53	154.57	102.04	-102.81	-27.61	-25.22	22.19
2.22	7.82	-46.94	138.64	91.70	-94.83	-26.77	-22.08	18.98
2.31	14.12	-39.46	117.34	77.88	-84.55	-25.47	-18.02	14.77
2.40	19.65	-32.99	98.98	65.99	-76.12	-24.16	-14.64	11.16
2.58	28.62	-22.89	70.34	47.45	-64.32	-21.65	-9.90	5.65
2.76	35.10	-15.39	49.09	33.70	-58.13	-18.88	-8.20	3.10

$d_{C\text{-}C}$	ΔE_{es}	ΔE_{ex}	ΔE_{rep}	ΔE_{ste}	ΔE_{orb}	ΔE_{disp}	ΔE_{int}	ΔE_{d}
syn-T1-F								
2.18	-7.67	-61.82	160.64	98.82	-88.65	-21.91	-19.41	23.91
2.23	-1.69	-54.90	143.02	88.12	-80.95	-21.33	-15.84	20.66
2.28	3.58	-48.78	127.49	78.71	-74.38	-20.74	-12.82	17.75
2.38	12.64	-38.50	101.53	63.03	-63.80	-19.57	-7.70	12.35
2.48	19.74	-30.62	81.65	51.03	-56.91	-18.42	-4.57	8.09
2.68	30.77	-19.02	52.27	33.25	-51.12	-15.76	-2.86	2.56
2.88	37.47	-11.69	33.53	21.84	-49.67	-13.00	-3.35	0.56
syn-T2-F								
2.18	-6.82	-62.12	161.17	99.05	-88.06	-21.04	-16.87	22.77
2.23	-0.66	-55.01	143.11	88.10	-80.64	-20.49	-13.68	19.82

Table S1. (cont.) Energy components at varying bond lengths along the intrinsic reaction coordinate for all three activation. Units are in kcal/mol.

2.28	4.89	-48.60	126.95	78.35	-74.22	-19.94	-10.93	17.13
2.38	14.44	-37.68	99.63	61.95	-63.93	-18.90	-6.44	12.08
2.48	22.14	-29.23	78.53	49.30	-57.40	-17.88	-3.85	7.95
2.68	33.27	-17.55	49.02	31.47	-52.35	-15.50	-3.11	2.86
2.88	39.18	-10.48	30.83	20.35	-50.51	-12.85	-3.84	1.43
syn-T3-F								
2.18	3.64	-55.45	146.93	91.48	-86.57	-22.13	-13.58	18.77
2.23	9.18	-49.11	130.62	81.51	-79.65	-21.54	-10.50	15.68
2.28	14.10	-43.47	116.14	72.67	-73.75	-20.95	-7.93	12.90
2.38	22.52	-33.95	91.86	57.91	-64.84	-19.79	-4.20	8.06
2.48	29.04	-26.68	73.18	46.50	-59.69	-18.56	-2.71	4.86
2.68	38.15	-16.25	46.13	29.88	-55.22	-15.71	-2.89	1.82
2.88	42.28	-9.87	29.23	19.36	-52.80	-12.62	-3.77	1.28
anti-T1-F								
2.18	-2.22	-55.31	146.05	90.74	-81.91	-22.18	-15.56	19.55
2.23	3.38	-48.91	129.69	80.78	-74.89	-21.64	-12.37	16.42
2.28	8.32	-43.29	115.35	72.06	-69.04	-21.10	-9.76	13.66
2.38	16.82	-33.84	91.31	57.47	-60.18	-19.99	-5.89	8.85
2.48	23.60	-26.56	72.70	46.14	-55.17	-18.85	-4.27	5.47
2.68	33.50	-16.11	45.77	29.66	-51.43	-16.04	-4.30	2.02
2.88	38.60	-9.06	27.34	18.28	-49.32	-12.57	-4.99	1.51
anti-T2-F								
2.18	-3.11	-59.25	155.28	96.03	-84.67	-21.85	-13.59	20.12
2.23	3.00	-52.35	137.62	85.27	-77.22	-21.29	-10.23	16.81
2.28	8.60	-46.00	121.57	75.57	-70.83	-20.73	-7.40	13.75
2.38	18.38	-35.32	94.92	59.60	-62.89	-19.63	-4.53	8.57
2.48	24.78	-27.84	75.63	47.79	-56.58	-18.46	-2.47	5.59
2.68	34.43	-16.98	47.80	30.82	-52.27	-15.86	-2.88	2.37
2.88	39.38	-10.46	30.90	20.44	-50.35	-13.13	-3.67	1.15
anti-T3-F								
2.18	-0.08	-60.67	157.58	96.91	-93.17	-20.84	-17.18	24.03
2.23	5.16	-53.25	139.19	85.94	-85.42	-20.39	-14.71	21.98
2.28	10.56	-47.07	123.48	76.41	-78.95	-19.82	-11.80	19.16
2.38	20.50	-36.66	97.02	60.36	-68.48	-18.55	-6.17	13.16
2.48	27.18	-28.13	75.89	47.76	-60.73	-17.51	-3.29	9.01
2.68	37.70	-16.70	46.80	30.10	-55.08	-14.86	-2.14	3.28
2.88	42.84	-9.85	28.96	19.11	-53.15	-12.04	-3.25	1.92

Models for Arriving at Data in Table 22

For each transition state, a plot of each component of the interaction energy as a function of the total distortion energy is constructed. From these plots, each interaction energy component is interpolated at a total distortion energy that leads to the optimum correlation coefficient between the electronic activation energy ($\Delta E^{\ddagger}$) and the sum of the interaction energy (the sum of the interapolated interaction energy components) and the chosen total distortion energy (Figure 9). This procedure is performed for each activation manifold. Table 2 consists of all the interpolated interaction energy components at the indicated distortion energy.

BF_3-mediated transition states. Interpolated at $\Delta E_d^{\ddagger}$= 33.0 kcal/mol.

syn-T1-L

$\Delta E_{es,d} = -1.071 - 1.036\Delta E_d$ $R^2 = 0.9997$

$\Delta E_{ste,d} = 36.391 + 2.622\Delta E_d$ $R^2 = 0.9993$

$\Delta E_{orb,d} = -10.458 - 2.322\Delta E_d$ $R^2 = 0.9999$

$\Delta E_{disp,d} = -21.899 - 0.347\Delta E_d + 3.21\text{E-}3(\Delta E_d)^2$ $R^2 = 0.9974$

$\Delta E_{int,d} = -1.939 - 0.652\Delta E_d - 5.00\text{E-}3(\Delta E_d)^2$ $R^2 = 0.9974$

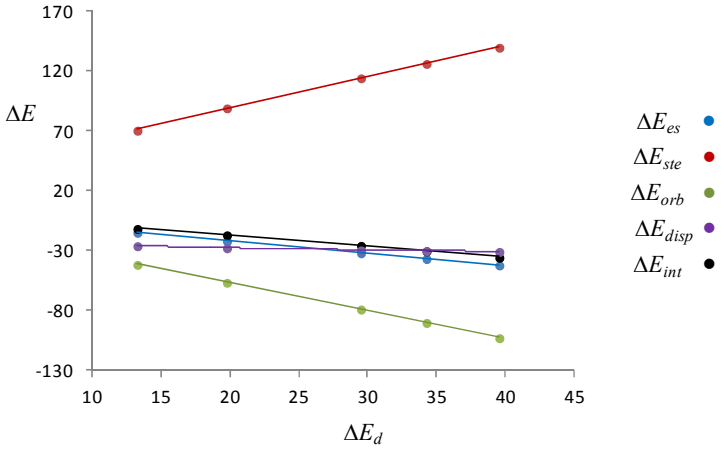

syn-T2-L

$\Delta E_{es,d} = -4.656 - 1.423\Delta E_d + 5.46\text{E-}3(\Delta E_d)^2$ $R^2 = 0.9996$

$\Delta E_{ste,d} = 44.647 + 3.488\Delta E_d - 1.20\text{E-}2(\Delta E_d)^2$ $R^2 = 0.9998$

$\Delta E_{orb,d} = -19.01 - 2.478\Delta E_d$ $R^2 = 0.9999$

$\Delta E_{disp,d} = -25.11 - 0.381\Delta E_d - 3.97\text{E-}3(\Delta E_d)^2$ $R^2 = 0.999$

$\Delta E_{int,d} = -4.854 - 0.721\Delta E_d - 4.20\text{E-}3(\Delta E_d)^2$ $R^2 = 1.0$

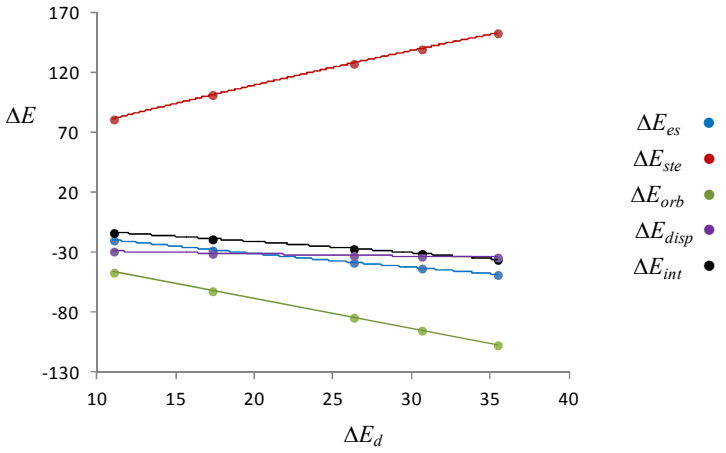

syn-T3-L

$\Delta E_{es,d} = -0.170 - 1.733\Delta E_d + 1.19\text{E-}2(\Delta E_d)^2$ $R^2 = 0.9994$

$\Delta E_{ste,d} = 33.329 + 4.265\Delta E_d - 2.76\text{E-}2(\Delta E_d)^2$ $R^2 = 1.0$

$\Delta E_{orb,d} = -16.414 - 2.814\Delta E_d + 6.30\text{E-}3(\Delta E_d)^2$ $R^2 = 1.0$

$\Delta E_{disp,d} = -21.83 - 0.467\Delta E_d + 5.65\text{E-}3(\Delta E_d)^2$ $R^2 = 0.9973$

$\Delta E_{int,d} = -5.112 - 0.746\Delta E_d - 3.89\text{E-}3(\Delta E_d)^2$ $R^2 = 1.0$

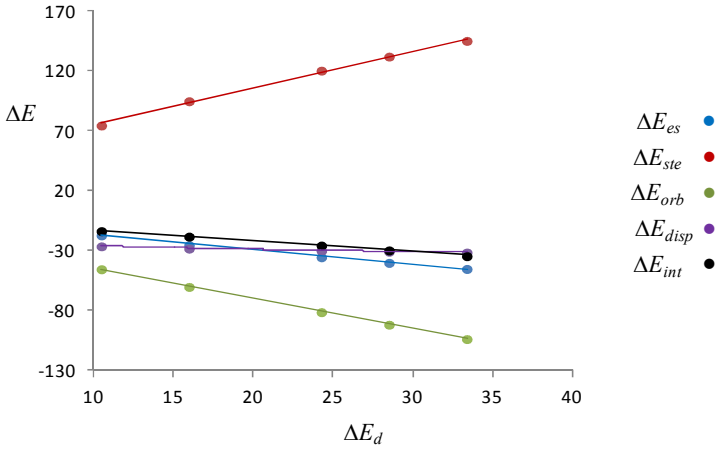

anti-T1-L

$\Delta E_{es,d} = -0.516 - 1.447\Delta E_d + 6.14\text{E-}3(\Delta E_d)^2$ $R^2 = 0.9998$

$\Delta E_{ste,d} = 32.77 + 3.655\Delta E_d - 1.61\text{E-}2(\Delta E_d)^2$ $R^2 = 0.9997$

$\Delta E_{orb,d} = -15.69 - 2.464\Delta E_d$ $R^2 = 1.0$

$\Delta E_{disp,d} = -20.70 - 0.398\Delta E_d + 4.33\text{E-}3(\Delta E_d)^2$ $R^2 = 0.9977$

$\Delta E_{int,d} = -3.635 - 0.705\Delta E_d - 4.50\text{E-}3(\Delta E_d)^2$ $R^2 = 1.0$

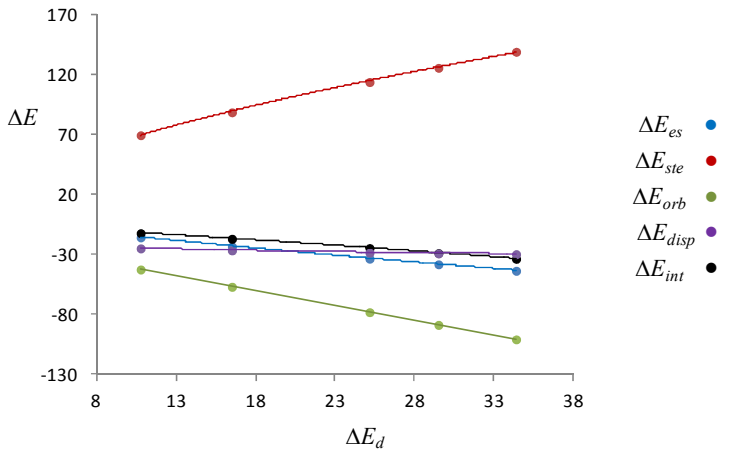

anti-T2-L

$\Delta E_{es,d} = 0.823 - 1.559\Delta E_d + 6.92\text{E-}3(\Delta E_d)^2$ $R^2 = 0.9999$

$\Delta E_{ste,d} = 32.577 + 3.804\Delta E_d - 1.66\text{E-}2(\Delta E_d)^2$ $R^2 = 0.9999$

$\Delta E_{orb,d} = -14.410 - 2.477\Delta E_d$ $R^2 = 1.0000$

$\Delta E_{disp,d} = -22.32 - 0.419\Delta E_d + 4.39\text{E-}3(\Delta E_d)^2$ $R^2 = 0.9982$

$\Delta E_{int,d} = -2.659 - 0.713\Delta E_d - 4.02\text{E-}3(\Delta E_d)^2$ $R^2 = 1.0000$

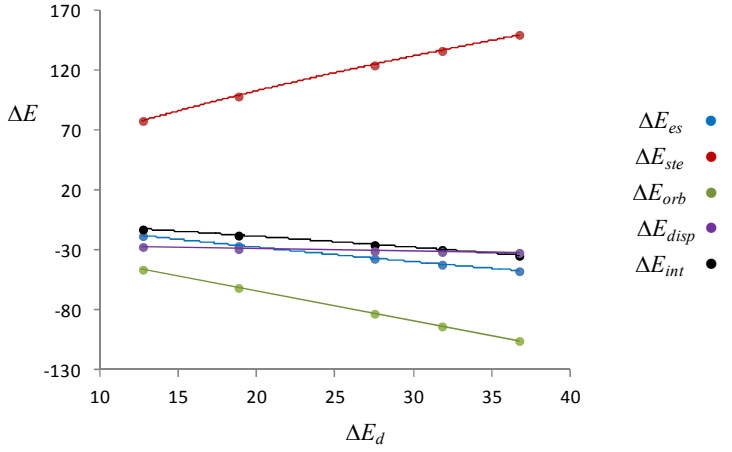

anti-T3-L

$\Delta E_{es,d} = -2.072 - 1.048\Delta E_d$ $R^2 = 0.9996$

$\Delta E_{ste,d} = 39.273 + 3.085\Delta E_d - 8.94\text{E-}3(\Delta E_d)^2$ $R^2 = 0.9999$

$\Delta E_{orb,d} = -16.93 - 2.339\Delta E_d$ $R^2 = 1.0000$

$\Delta E_{disp,d} = -23.8 - 0.357\Delta E_d + 3.46\text{E-}3(\Delta E_d)^2$ $R^2 = 0.9980$

$\Delta E_{int,d} = -2.894 - 0.719\Delta E_d - 4.27\text{E-}3(\Delta E_d)^2$ $R^2 = 1.0000$

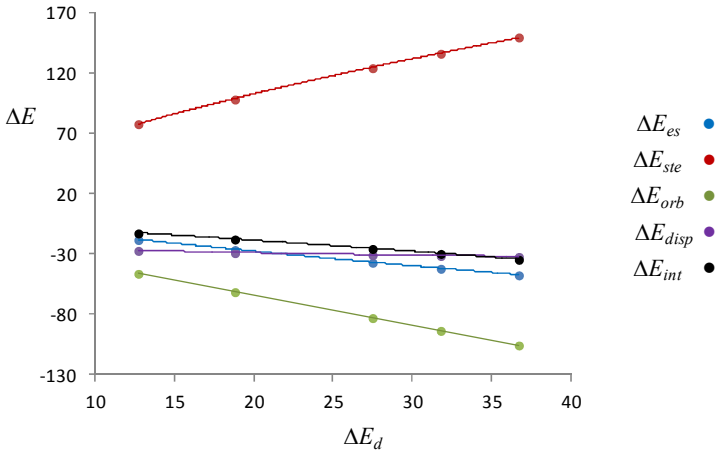

Brønsted acid-mediated transition states interpolated at $\Delta E_d^{\ddagger}$= 17.7 kcal/mol.

syn-T1-H

$\Delta E_{es,d} = 36.87 - 1.448\Delta E_d - 7.36\text{E-}3(\Delta E_d)^2$ $R^2 = 1.0000$

$\Delta E_{ste,d} = 28.82 + 3.083\Delta E_d - 1.27\text{E-}2(\Delta E_d)^2$ $R^2 = 1.0000$

$\Delta E_{orb,d} = -51.03 - 1.983\Delta E_d - 6.04\text{E-}3(\Delta E_d)^2$ $R^2 = 1.0000$

$\Delta E_{disp,d} = -18.71 - 0.441\Delta E_d - 5.78\text{E-}3(\Delta E_d)^2$ $R^2 = 0.9997$

$\Delta E_{int,d} = -4.033 - 0.791\Delta E_d - 5.05\text{E-}3(\Delta E_d)^2$ $R^2 = 1.0000$

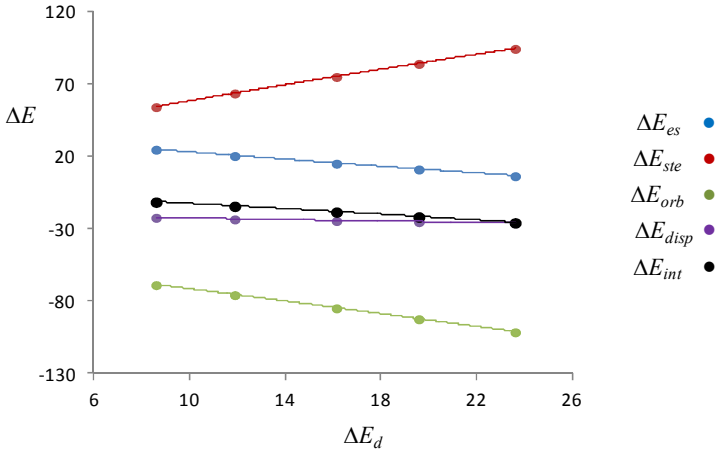

syn-T2-H

$\Delta E_{es,d} = 39.24 - 2.085\Delta E_d + 1.51\text{E-}2(\Delta E_d)^2$ $R^2 = 1.0000$

$\Delta E_{ste,d} = 24.49 + 4.437\Delta E_d - 2.79\text{E-}2(\Delta E_d)^2$ $R^2 = 1.0000$

$\Delta E_{orb,d} = -51.60 - 2.653\Delta E_d + 2.48\text{E-}3(\Delta E_d)^2$ $R^2 = 1.0000$

$\Delta E_{disp,d} = -17.63 - 0.627\Delta E_d + 9.16\text{E-}3(\Delta E_d)^2$ $R^2 = 1.0000$

$\Delta E_{int,d} = -5.069 - 0.927\Delta E_d - 1.23\text{E-}3(\Delta E_d)^2$ $R^2 = 1.0000$

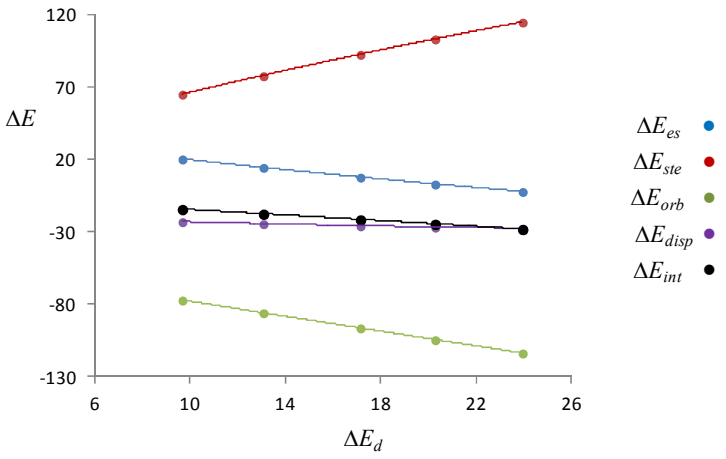

syn-T3-H

$\Delta E_{es,d} = 39.23 - 2.176\Delta E_d + 2.31\text{E-}2(\Delta E_d)^2$ $R^2 = 1.0000$
$\Delta E_{ste,d} = 26.03 + 4.587\Delta E_d - 4.16\text{E-}2(\Delta E_d)^2$ $R^2 = 1.0000$
$\Delta E_{orb,d} = -53.46 - 2.671\Delta E_d + 4.61\text{E-}3(\Delta E_d)^2$ $R^2 = 1.0000$
$\Delta E_{disp,d} = -17.18 - 0.695\Delta E_d + 1.25\text{E-}2(\Delta E_d)^2$ $R^2 = 0.9999$
$\Delta E_{int,d} = -5.363 - 0.959\Delta E_d - 1.25\text{E-}3(\Delta E_d)^2$ $R^2 = 1.0000$

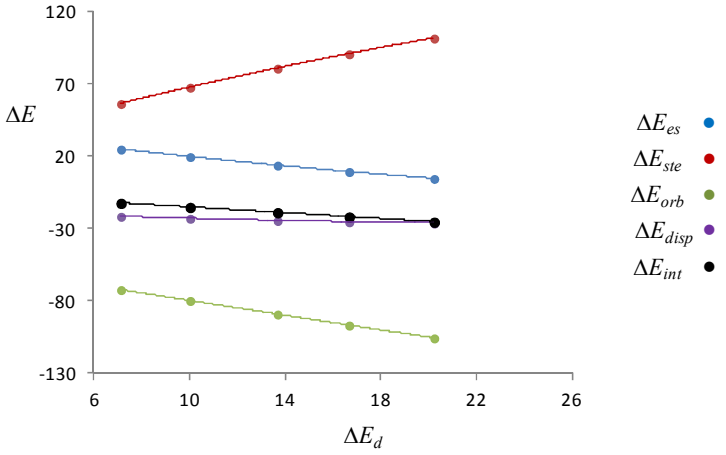

anti-T1-H

$\Delta E_{es,d} = 36.87 - 1.448\Delta E_d + 7.36\text{E-}3(\Delta E_d)^2$ $R^2 = 1.0000$
$\Delta E_{ste,d} = 28.82 + 3.084\Delta E_d - 1.\text{E-}227(\Delta E_d)^2$ $R^2 = 1.0000$
$\Delta E_{orb,d} = -51.03 - 1.983\Delta E_d - 5.78\text{E-}3(\Delta E_d)^2$ $R^2 = 1.0000$
$\Delta E_{disp,d} = -18.71 - 0.441\Delta E_d + 6.04\text{E-}3(\Delta E_d)^2$ $R^2 = 0.9997$
$\Delta E_{int,d} = -4.033 - 0.791\Delta E_d - 5.05\text{E-}3(\Delta E_d)^2$ $R^2 = 1.0000$

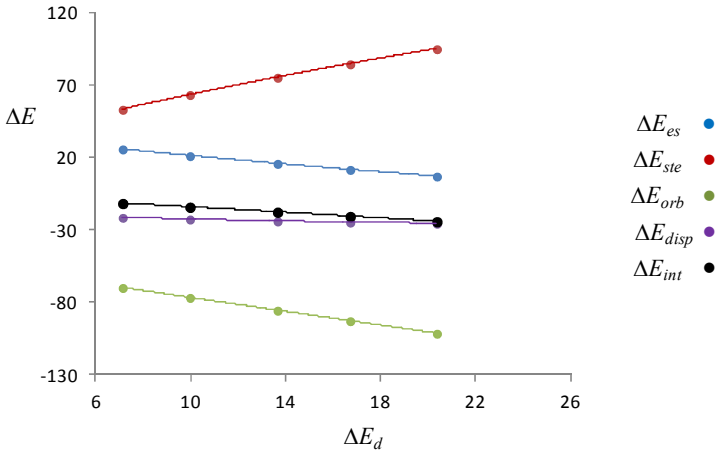

anti-T2-H

$\Delta E_{es,d} = 38.21 - 1.935\Delta E_d + 0.0158(\Delta E_d)^2$ $R^2 = 0.9999$

$\Delta E_{ste,d} = 27.66 + 4.143\Delta E_d - 3.23\text{E-}2(\Delta E_d)^2$ $R^2 = 0.9999$

$\Delta E_{orb,d} = -51.24 - 2.535\Delta E_d - 4.97\text{E-}3(\Delta E_d)^2$ $R^2 = 1.0000$

$\Delta E_{disp,d} = -19.36 - 0.564\Delta E_d + 8.76\text{E-}3(\Delta E_d)^2$ $R^2 = 0.9998$

$\Delta E_{int,d} = -4.749 - 0.888\Delta E_d - 2.83\text{E-}3(\Delta E_d)^2$ $R^2 = 1.0000$

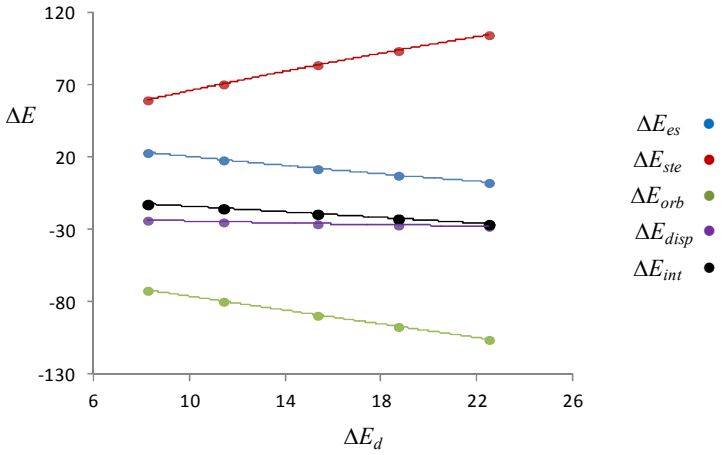

anti-T3-H

$\Delta E_{es,d} = 37.87 - 1.701\Delta E_d + 6.19\text{E-}3(\Delta E_d)^2$ $R^2 = 1.0000$

$\Delta E_{ste,d} = 27.29 + 3.564\Delta E_d - 9.02\text{E-}3(\Delta E_d)^2$ $R^2 = 1.0000$

$\Delta E_{orb,d} = -50.63 - 2.212\Delta E_d - 6.13\text{E-}3(\Delta E_d)^2$ $R^2 = 1.0000$

$\Delta E_{disp,d} = -19.07 - 0.528\Delta E_d + 6.45\text{E-}3(\Delta E_d)^2$ $R^2 = 1.0000$

$\Delta E_{int,d} = -4.564 - 0.874\Delta E_d - 2.55\text{E-}3(\Delta E_d)^2$ $R^2 = 1.0000$

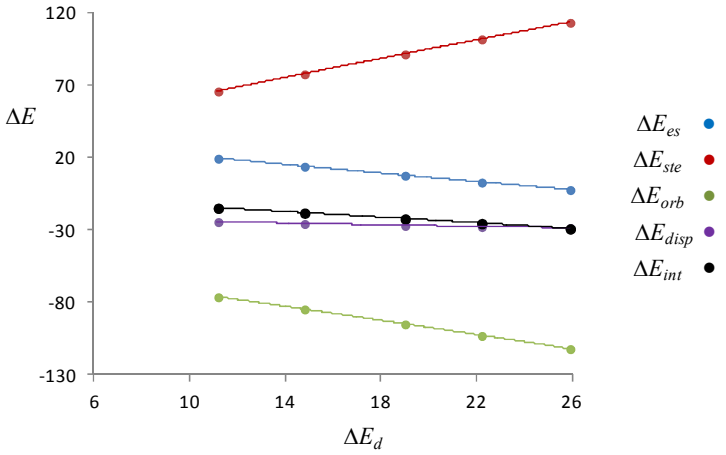

Fluoride-mediated transition states interpolated at $\Delta E_d^{\ddagger}$= 18.1 kcal/mol.

syn-T1-F

$\Delta E_{es,d} = 32.13 - 1.471\Delta E_d - 8.06\text{E-}3(\Delta E_d)^2$ $R^2 = 1.0000$

$\Delta E_{ste,d} = 30.95 + 2.312\Delta E_d + 2.20\text{E-}3(\Delta E_d)^2$ $R^2 = 0.9999$

$\Delta E_{orb,d} = -46.77 - 0.991\Delta E_d - 3.19\text{E-}2(\Delta E_d)^2$ $R^2 = 1.0000$

$\Delta E_{disp,d} = -15.97 - 0.334\Delta E_d + 3.57\text{E-}3(\Delta E_d)^2$ $R^2 = 0.9998$

$\Delta E_{int,d} = 0.292 - 0.476\Delta E_d - 1.46\text{E-}2(\Delta E_d)^2$ $R^2 = 1.0000$

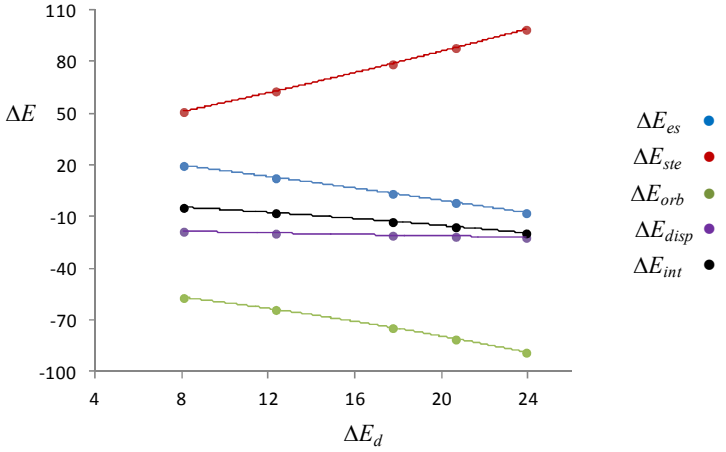

syn-T2-F

$\Delta E_{es,d} = 35.54 - 1.601\Delta E_d - 1.14\text{E-}2(\Delta E_d)^2$ $R^2 = 1.0000$

$\Delta E_{ste,d} = 28.37 + 2.391\Delta E_d + 3.13\text{E-}2(\Delta E_d)^2$ $R^2 = 1.0000$

$\Delta E_{orb,d} = -48.55 - 0.768\Delta E_d - 4.26\text{E-}2(\Delta E_d)^2$ $R^2 = 0.9999$

$\Delta E_{disp,d} = -15.77 - 0.286\Delta E_d + 2.41\text{E-}3(\Delta E_d)^2$ $R^2 = 0.9998$

$\Delta E_{int,d} = -0.428 - 0.263\Delta E_d - 2.03\text{E-}2(\Delta E_d)^2$ $R^2 = 0.9997$

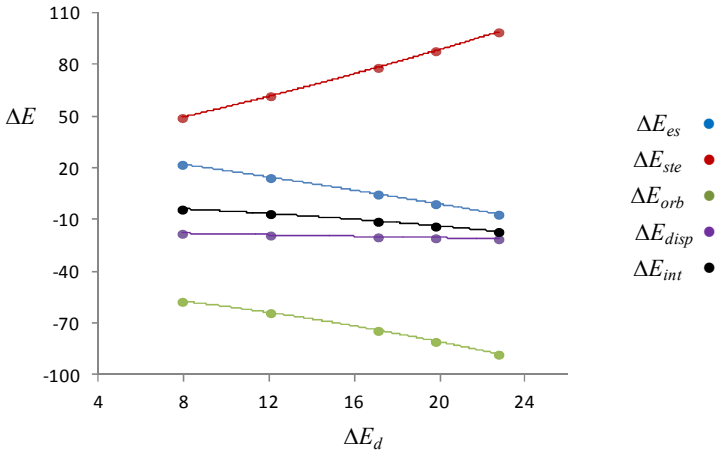

syn-T3-F

$\Delta E_{es,d} = 38.41 - 2.000\Delta E_d + 8.10\text{E-}3(\Delta E_d)^2$ $R^2 = 0.9996$

$\Delta E_{ste,d} = 30.41 + 3.413\Delta E_d - 8.96\text{E-}3(\Delta E_d)^2$ $R^2 = 1.0000$

$\Delta E_{orb,d} = -53.09 - 1.210\Delta E_d - 3.07\text{E-}2(\Delta E_d)^2$ $R^2 = 0.9999$

$\Delta E_{disp,d} = -16.68 - 0.436\Delta E_d + 7.86\text{E-}3(\Delta E_d)^2$ $R^2 = 0.9977$

$\Delta E_{int,d} = -0.941 - 0.233\Delta E_d - 2.37\text{E-}3(\Delta E_d)^2$ $R^2 = 0.9994$

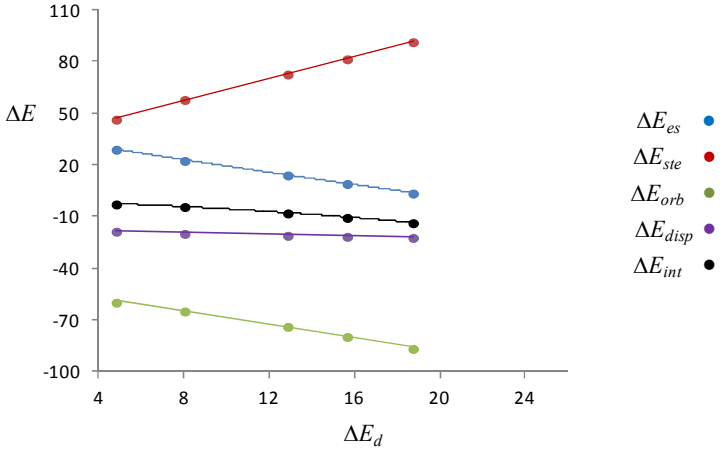

anti-T1-F

$\Delta E_{es,d} = 34.30 - 2.019\Delta E_d + 7.96\text{E-}3(\Delta E_d)^2$ $R^2 = 0.9998$

$\Delta E_{ste,d} = 28.68 + 3.246\Delta E_d - 4.00\text{E-}3(\Delta E_d)^2$ $R^2 = 0.9998$

$\Delta E_{orb,d} = -48.43 - 1.030\Delta E_d - 3.50\text{E-}2(\Delta E_d)^2$ $R^2 = 0.9999$

$\Delta E_{disp,d} = -16.85 - 0.410\Delta E_d + 7.11\text{E-}3(\Delta E_d)^2$ $R^2 = 0.9989$

$\Delta E_{int,d} = -2.265 - 0.221\Delta E_d - 2.37\text{E-}2(\Delta E_d)^2$ $R^2 = 0.9993$

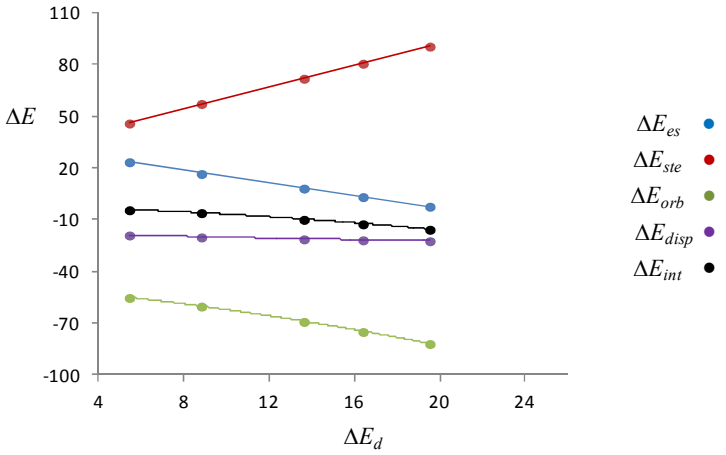

anti-T2-F

$\Delta E_{es,d} = 36.55 - 2.190\Delta E_d + 1.11\text{E-}2(\Delta E_d)^2$ $R^2 = 0.9998$

$\Delta E_{ste,d} = 27.87 + 3.759\Delta E_d - 1.92\text{E-}2(\Delta E_d)^2$ $R^2 = 0.9990$

$\Delta E_{orb,d} = -48.95 - 1.333\Delta E_d - 2.14\text{E-}2(\Delta E_d)^2$ $R^2 = 0.9971$

$\Delta E_{disp,d} = -16.39 - 0.428\Delta E_d + 7.93\text{E-}3(\Delta E_d)^2$ $R^2 = 0.9949$

$\Delta E_{int,d} = -0.904 - 0.195\Delta E_d - 2.15\text{E-}2(\Delta E_d)^2$ $R^2 = 0.9969$

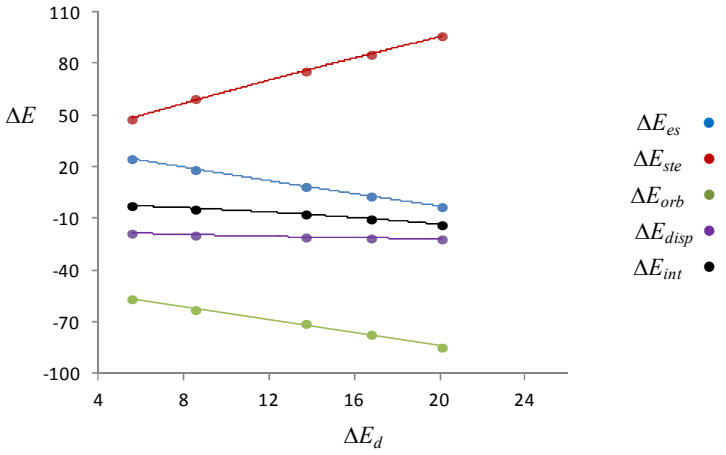

anti-T3-F

$\Delta E_{es,d} = 36.58 - 0.801\Delta E_d - 2.95\text{E-}2(\Delta E_d)^2$ $R^2 = 0.9988$

$\Delta E_{ste,d} = 34.23 + 1.012\Delta E_d + 6.41\text{E-}2(\Delta E_d)^2$ $R^2 = 0.9947$

$\Delta E_{orb,d} = -54.28 - 0.216\Delta E_d - 5.58\text{E-}2(\Delta E_d)^2$ $R^2 = 0.9941$

$\Delta E_{disp,d} = -15.16 - 0.278\Delta E_d + 1.79\text{E-}3(\Delta E_d)^2$ $R^2 = 0.9996$

$\Delta E_{int,d} = -0.897 - 0.288\Delta E_d - 1.93\text{E-}2(\Delta E_d)^2$ $R^2 = 0.9999$

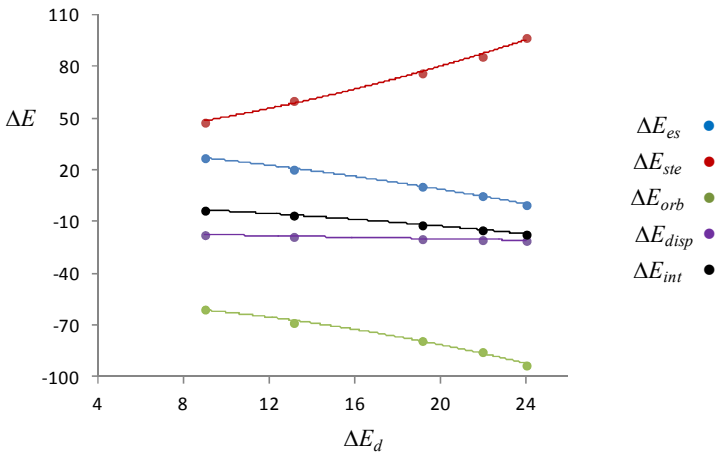

Models for Arriving at Data in Table 23

BF_3-mediated transition states. Interpolated at $\Delta E_d^{\ddagger}$= 33.0 kcal/mol.

syn-T1-L

$\varepsilon_{HOMO}^{\ddagger} = -0.291 - 8.90E\text{-}4\Delta E_d + 4.96E\text{-}6(\Delta E_d)^2$ $R^2 = 0.9998$

$\varepsilon_{HOMO} = -0.277 - 5.34E\text{-}4\Delta E_d - 3.88E\text{-}6(\Delta E_d)^2$ $R^2 = 0.9999$

$\varepsilon_{LUMO} = -5.79E\text{-}2 - 1.99E\text{-}3\Delta E_d + 1.35E\text{-}5(\Delta E_d)^2$ $R^2 = 1.0000$

$\Delta q = 2.32E\text{-}2 + 2.395E\text{-}2\Delta E_d - 2.698E\text{-}4(\Delta E_d)^2$ $R^2 = 0.9991$

syn-T2-L

$\varepsilon_{HOMO}^{\ddagger} = -0.293 - 9.85E\text{-}4\Delta E_d + 4.97E\text{-}6(\Delta E_d)^2$ $R^2 = 1.0000$

$\varepsilon_{HOMO} = -0.278 - 5.49E\text{-}4\Delta E_d - 4.20E\text{-}6(\Delta E_d)^2$ $R^2 = 0.9998$

$\varepsilon_{LUMO} = -6.09E\text{-}2 - 1.96E\text{-}3\Delta E_d + 1.31E\text{-}5(\Delta E_d)^2$ $R^2 = 0.9999$

$\Delta q = 9.55E\text{-}2 + 1.75E\text{-}2\Delta E_d - 1.34E\text{-}4(\Delta E_d)^2$ $R^2 = 0.9999$

syn-T3-L

$\varepsilon_{HOMO}^{\ddagger} = -0.294 - 1.08E\text{-}3\Delta E_d + 8.05E\text{-}6(\Delta E_d)^2$ $R^2 = 1.0000$

$\varepsilon_{HOMO} = -0.276 - 4.73E\text{-}4\Delta E_d - 2.90E\text{-}6(\Delta E_d)^2$ $R^2 = 1.0000$

$\varepsilon_{LUMO} = -6.16E\text{-}2 - 2.19E\text{-}3\Delta E_d + 1.82E\text{-}5(\Delta E_d)^2$ $R^2 = 0.9999$

$\Delta q = 9.31E\text{-}2 + 1.91E\text{-}2\Delta E_d - 1.67E\text{-}4(\Delta E_d)^2$ $R^2 = 0.9997$

anti-T1-L

$\varepsilon_{HOMO}^{\ddagger} = -0.294 - 1.08E\text{-}3\Delta E_d + 8.05E\text{-}6(\Delta E_d)^2$ $R^2 = 0.9997$

$\varepsilon_{HOMO} = -0.276 - 4.73E\text{-}4\Delta E_d - 2.90E\text{-}6(\Delta E_d)^2$ $R^2 = 1.0000$

$\varepsilon_{LUMO} = -6.16E\text{-}2 - 2.19E\text{-}3\Delta E_d + 1.815E\text{-}5(\Delta E_d)^2$ $R^2 = 0.9999$

$\Delta q = 7.04E\text{-}2 + 1.845E\text{-}2\Delta E_d - 1.445E\text{-}4(\Delta E_d)^2$ $R^2 = 0.9998$

anti-T2-L

$\varepsilon_{HOMO}^{\ddagger} = -0.293 - 1.03E\text{-}3\Delta E_d + 7.84E\text{-}6(\Delta E_d)^2$ $R^2 = 0.9997$

$\varepsilon_{HOMO} = -0.277 - 4.63E\text{-}4\Delta E_d - 2.82E\text{-}6(\Delta E_d)^2$ $R^2 = 0.9999$

$\varepsilon_{LUMO} = -5.69E\text{-}2 - 2.18E\text{-}3\Delta E_d + 1.66E\text{-}5(\Delta E_d)^2$ $R^2 = 0.9998$

$\Delta q = 6.25E\text{-}2 + 1.88E\text{-}2\Delta E_d - 1.43E\text{-}4(\Delta E_d)^2$ $R^2 = 0.9999$

anti-T3-L

$\varepsilon_{HOMO}^{\ddagger} = -0.295 - 1.13E\text{-}3\Delta E_d + 9.14E\text{-}6(\Delta E_d)^2$ $R^2 = 0.9998$

ε_{HOMO}= –0.278 – 5.62E-4ΔE_d – 4.05E-6$(\Delta E_d)^2$ R^2 = 1.0000
ε_{LUMO}= –6.20E-2 – 2.19E-3ΔE_d + 1.83E-5$(\Delta E_d)^2$ R^2 = 1.0000
Δq = 7.97E-2 + 1.71E-2ΔE_d – 1.195E-4$(\Delta E_d)^2$ R^2 = 0.9999

Brønsted acid-mediated transition states interpolated at $\Delta E_d^{\ddagger}$= 17.7 kcal/mol.
syn-T1-H
$\varepsilon_{HOMO}^{\ddagger}$= –0.308 – 1.26E-3$\Delta E_d$ + 1.24E-5$(\Delta E_d)^2$ R^2 = 0.9997
ε_{HOMO}= –0.277 + 6.53E-4ΔE_d – 7.05E-6$(\Delta E_d)^2$ R^2 = 1.0000
ε_{LUMO}= –8.32E-2 – 2.44E-3ΔE_d + 2.63E-5$(\Delta E_d)^2$ R^2 = 1.0000
Δq = 1 – 0.939 + 2.09E-2ΔE_d – 2.14E-4$(\Delta E_d)^2$ R^2 = 0.9999
syn-T2-H
$\varepsilon_{HOMO}^{\ddagger}$= –0.310 – 1.62E-3$\Delta E_d$ + 1.79E-5$(\Delta E_d)^2$ R^2 = 0.9992
ε_{HOMO}= –0.276 + 3.70E-4ΔE_d – 3.27E-7$(\Delta E_d)^2$ R^2 = 0.9999
ε_{LUMO}= –8.61E-2 – 2.50E-3ΔE_d + 2.44E-5$(\Delta E_d)^2$ R^2 = 1.0000
Δq = 1 – 0.926 + 2.29E-2ΔE_d – 2.69E-4$(\Delta E_d)^2$ R^2 = 1.0000

syn-T3-H
$\varepsilon_{HOMO}^{\ddagger}$= –0.309 – 1.76E-3$\Delta E_d$ + 2.47E-5$(\Delta E_d)^2$ R^2 = 0.9999
ε_{HOMO}= –0.278 + 6.12E-4ΔE_d – 5.97E-6$(\Delta E_d)^2$ R^2 = 1.0000
ε_{LUMO}= –8.39E-2 – 2.76E-3ΔE_d + 3.80E-5$(\Delta E_d)^2$ R^2 = 0.9999
Δq = 1 – 0.921 + 2.43E-2ΔE_d – 3.30E-4$(\Delta E_d)^2$ R^2 = 0.9999
anti-T1-H
$\varepsilon_{HOMO}^{\ddagger}$= –0.308 – 1.64E-3$\Delta E_d$ + 2.27E-5$(\Delta E_d)^2$ R^2 = 0.9995
ε_{HOMO}= –0.276 + 6.07E-4ΔE_d – 6.58E-6$(\Delta E_d)^2$ R^2 = 0.9996
ε_{LUMO}= –8.41E-2 – 2.68E-3ΔE_d + 3.64E-5$(\Delta E_d)^2$ R^2 = 0.9999
Δq = 1 – 0.945 + 2.50E-2ΔE_d – 3.44E-4$(\Delta E_d)^2$ R^2 = 0.9998
anti-T2-H
$\varepsilon_{HOMO}^{\ddagger}$= –0.308 – 1.53E-3$\Delta E_d$ + 1.73E-5$(\Delta E_d)^2$ R^2 = 0.9999
ε_{HOMO}= –0.276 + 4.74E-4ΔE_d – 3.61E-6$(\Delta E_d)^2$ R^2 = 0.9997
ε_{LUMO}= –8.22E-2 – 2.58E-3ΔE_d + 2.76E-5$(\Delta E_d)^2$ R^2 = 1.0000
Δq = 1 – 0.930 + 2.33E-2ΔE_d – 2.86E-4$(\Delta E_d)^2$ R^2 = 0.9998
anti-T3-H
$\varepsilon_{HOMO}^{\ddagger}$= –0.305 – 1.83E-3$\Delta E_d$ + 2.24E-5$(\Delta E_d)^2$ R^2 = 0.9839
ε_{HOMO}= –0.276 + 3.51E-4ΔE_d – 6.86E-6$(\Delta E_d)^2$ R^2 = 1.0000
ε_{LUMO}= –8.33E-2 – 2.43E-3ΔE_d + 2.20E-5$(\Delta E_d)^2$ R^2 = 1.0000
Δq = 1 – 0.936 + 2.125E-2ΔE_d – 2.13E-4$(\Delta E_d)^2$ R^2 = 1.0000

Fluoride-mediated transition states interpolated at $\Delta E_d^{\ddagger}$= 18.1 kcal/mol.
syn-T1-F
$\varepsilon_{HOMO}^{\ddagger}$= –0.1883 + 1.44E-3$\Delta E_d$ – 5.08E-5$(\Delta E_d)^2$ R^2 = 0.9934
ε_{HOMO}= –0.189 + 2.86E-3ΔE_d – 5.70E-5$(\Delta E_d)^2$ R^2 = 0.9996
ε_{LUMO}= 2.23E-2 – 2.63E-4ΔE_d + 2.19E-6$(\Delta E_d)^2$ R^2 = 0.9992
Δq = – 4.69E-3 + 1.99E-2ΔE_d – 1.215E-4$(\Delta E_d)^2$ R^2 = 1.0000
syn-T2-F

$\varepsilon_{HOMO}^{\ddagger} = -0.200 + 2.71E\text{-}3\Delta E_d - 8.49E\text{-}5(\Delta E_d)^2$ $R^2 = 0.9882$
$\varepsilon_{HOMO} = -0.199 + 3.93E\text{-}3\Delta E_d - 8.76E\text{-}5(\Delta E_d)^2$ $R^2 = 0.9993$
$\varepsilon_{LUMO} = 2.17E\text{-}2 - 1.852E\text{-}4\Delta E_d + 1.19E\text{-}8(\Delta E_d)^2$ $R^2 = 0.9992$
$\Delta q = -2.53E\text{-}2 + 2.06E\text{-}2\Delta E_d - 9.91E\text{-}5(\Delta E_d)^2$ $R^2 = 1.0000$

syn-T3-F

$\varepsilon_{HOMO}^{\ddagger} = -0.203 + 2.66E\text{-}3\Delta E_d - 9.12E\text{-}5(\Delta E_d)^2$ $R^2 = 0.9974$
$\varepsilon_{HOMO} = -0.199 + 3.88E\text{-}3\Delta E_d - 9.28E\text{-}5(\Delta E_d)^2$ $R^2 = 0.9996$
$\varepsilon_{LUMO} = 2.18E\text{-}2 - 1.03E\text{-}4\Delta E_d - 1.26E\text{-}6(\Delta E_d)^2$ $R^2 = 0.9975$
$\Delta q = -1.04E\text{-}2 + 2.06E\text{-}2\Delta E_d - 1.60E\text{-}4(\Delta E_d)^2$ $R^2 = 1.0000$

anti-T1-F

$\varepsilon_{HOMO}^{\ddagger} = -0.202 + 2.74E\text{-}3\Delta E_d - 9.31E\text{-}5(\Delta E_d)^2$ $R^2 = 0.9831$
$\varepsilon_{HOMO} = -0.199 + 4.05E\text{-}3\Delta E_d - 9.67E\text{-}5(\Delta E_d)^2$ $R^2 = 0.9983$
$\varepsilon_{LUMO} = 2.14E\text{-}2 - 1.52E\text{-}4\Delta E_d - 7.635E\text{-}7(\Delta E_d)^2$ $R^2 = 0.9986$
$\Delta q = -9.48E\text{-}3 - 2.07E\text{-}2\Delta E_d + 1.46E\text{-}4(\Delta E_d)^2$ $R^2 = 1.0000$

anti-T2-F

$\varepsilon_{HOMO}^{\ddagger} = -0.204 + 2.415E\text{-}3\Delta E_d - 7.16E\text{-}5(\Delta E_d)^2$ $R^2 = 0.9974$
$\varepsilon_{HOMO} = -0.202 + 3.42E\text{-}3\Delta E_d - 7.40E\text{-}5(\Delta E_d)^2$ $R^2 = 0.9978$
$\varepsilon_{LUMO} = 2.17E\text{-}2 - 1.81E\text{-}4\Delta E_d - 2.67E\text{-}7(\Delta E_d)^2$ $R^2 = 0.9992$
$\Delta q = -1.06E\text{-}2 - 2.155E\text{-}2\Delta E_d + 1.64E\text{-}4(\Delta E_d)^2$ $R^2 = 0.9996$

anti-T3-F

$\varepsilon_{HOMO}^{\ddagger} = -0.203 + 3.18E\text{-}3\Delta E_d - 9.73E\text{-}5(\Delta E_d)^2$ $R^2 = 0.9784$
$\varepsilon_{HOMO} = -0.205 + 4.78E\text{-}3\Delta E_d - 1.10E\text{-}4(\Delta E_d)^2$ $R^2 = 0.9924$
$\varepsilon_{LUMO} = 2.22E\text{-}2 - 1.89E\text{-}4\Delta E_d - 1.13E\text{-}6(\Delta E_d)^2$ $R^2 = 0.9999$
$\Delta q = 1.93E\text{-}2 - 1.80E\text{-}2\Delta E_d + 2.65E\text{-}5(\Delta E_d)^2$ $R^2 = 0.9956$

Chapter 8: *References*

(1) Dehmlow, E. V.; Dehmlow, S. Monographs in Modern Chemistry, Vol: 11: Phase Transfer Catalysis.; Verlag Chemie, 1980.

(2) Yammamoto, H.; Ed. *Lewis Acids in Organic Synthesis*; Wiley-VCH: Weinheim, 2001.

(3) a) Normat, H. *Angew. Chem. Int. Ed.* **1967**, *6*, 1046-1067. b) Stephenson, B.; Solladie, G.; Mosher, H. S. *J. Am. Chem. Soc.* **1972**, *94*, 4184-4188. c) Sowinski, A. F.; Whitesides, G. M. *J. Org. Chem.* **1979**, *44*, 2369-2376.

(4) C. M. Starks *J. Am. Chem. Soc.* **1971**, *93*, 195-199.

(5) (a) Williamson, W. *Liebigs Ann. Chem*. **1851**, *77*, 37-49. b) Williamson, W. *J. Chem. Soc*. **1852**, *106*, 229-239.

(6) (a) Merz A. *Angew. Chem. Int. Ed.* **1973**, *12*, 846-947. b) Freedman, H. H.; Dubois, R. A. Tetrahedron Lett. **1975**, *38*, 3251-3254.

(7) M. Halpern; Phase-Transfer Catalysis Mechanisms and Syntheses. 1997; p 18

(8) For an insightful analysis of hydroxide-initiated PTC reactions see: Starks, C. M.; Liotta, C. L.; Halpern, M., *Phase-Transfer Catalysis: Fundamentals, Applications and Industrial Perspectives*. Chapman and Hall: New York, 1994, pp 89-108.

(9) (a) Brandstrom, A. *Adv. Phys. Org. Chem.* **1977**, *15*, 267-330. (b) Rabinovitz, M.; Cohen, Y.; Halpern, M. *Angew. Chem., Int. Ed. Engl.* **1986**, *25*, 960-970.

(10) (a) Naik, S. D.; Doraiswamy, L. K. *Amer. Inst. Chem. Eng. J*. **1998**, *44*, 612-646. (b) Yang, H.-M. and Wu H.-S. *Catalysis Reviews* **2003**, *45*, 463-540.

(11) (a) Makosza, M. *Tetrahedron Lett*. **1966**, *38*, 4261-4624. (b) Makosza, M.; Serafin, B.; *Roczn. Chem*. **1965**, *39*, 1805-1810. (c) Makosza, M.; Serafin, B. *Roczn. Chem*. **1965**, *39*, 1799-1803. (d) Makosza, M.; Serafin, B. *Roczn. Chem*. **1965**, *39*, 1595-1601. (e) Makosza, M.; Serafin, B. *Roczn. Chem*. **1965**, *39*, 1401-1409. (f) Makosza, M.; Serafin, B. *Roczn. Chem.* **1965**, *39*, 1223-1230. (g) Makosza, M.; Serafin, B. *Roczn. Chem.* **1975**, *43*, 439-462.

(12) (a) Starks, C. M. *J. Am. Chem. Soc*. **1971**, *93*, 195-199. (b) Starks, Charles M.; Owens, Robert M. *J. Am. Chem. Soc.* **1973**, *95*, 3613-3617.

(13) (a) Herriot, A.; Picker, D. *J. Am. Chem. Soc*. **1975**, *97*, 2345-2349. (b) Herriot, A. W.; Picker D. *Tet. Lett*. **1972**, *44*, 4521-4524. (c) Landini, D.; Maia, A.; Montanari, F. *J. Am.*

Chem. Soc. **1978**, *100*, 2796-2801. (d) Gordon, J.; Kutina, R. *J. Am. Chem. Soc*. **1978**, *100*, 2796-2801.

(14) Landini, D.; Maia, A.; and Montanari, F. *J. Chem. Soc*., *Chem. Commun*. **1977**, 112-113.

(15) For a monograph style overview see: Starks, C. In *Phase-Transfer Catalysis, Mechanism and Synthesis*, ACS Symposium Series 659; Halpern, M. E., Ed.; ACS: Washington, D.C., 1996; Chapt. 2.

(16) For an overview of PTC kinetics see: (a) Liotta, C. L. in Chapter 3 of reference 8. (b) Wang, M.-L. in Chap. 2 of *Handbook of Phase Transfer Catalysis*; Sasson, Y., Neumann, R., Eds.; Chapman & Hall: London, 1997.

(17) (a) Starks, C. *Tetrahedron* **1999**, *55*, 6261-6274. (b) Makosza, M. and Lasek, W. *J. Phys. Org. Chem.* **1993**, *6*, 412-420.

(18) (a) Halpern, M.; Sasson, Y.; Willner, I.; Rabinovitz, M. *Tetrahedron Lett*. **1981**, *22*, 1719-1722. (b) Halpern, M.; Sasson, Y.; Rabinovitz, M. *J. Org. Chem*. **1983**, *48*, 1022-1025. (c) Halpern, M.; Sasson, Y.; Rabinovitz, M. *J. Org. Chem*. **1984**, *49*, 2011-2012. (d) Halpern, M.; Feldman, D.; Sasson, Y.; Rabinovitz, M. *Angew. Chem.* **1984**, *96*, 79-80. (e) Halpern, M.; Z.; Hayder A.; Sasson, Y.; Rabinovitz, M. *J. Org. Chem*. **1985**, *50*, 5088-5092. (f) Feldman, D.; Halpern, M.; Rabinovitz, M. *J. Org. Chem.* **1985**, *50*, 1746-1749.

(19) Starks, C. *Chemtech,* **1980**, *10*, 110-117.

(20) Bordwell, F. G.; Hughes, D. L. The pK_a of thiophenol is 6.5: *J. Org. Chem.* **1982**, *47*, 3224-3232.

(21) (a) Brändström, A.; Junggren, U. *Acta Chem. Scand.* **1969**, *23*, 2203-2204. (b) Brändström, A;. Junggren, U. *Acta Chem. Scand.* **1969**, *23*, 2204-2205. (c) Brändström, A.; Junggren, U. *Acta Chem. Scand.* **2969**, *23*, 2536-2537. (d) Brändström, A.; Junggren, U. *Acta Chem. Scand.* **1969**, *23*, 3585-3586. (e) Brändström, A. *Pure Appl. Chem.* **1982**, *54*, 1769-1782. (f) Dockx, J. *Synthesis* **1973**, *8*, 441-456. and references cited therein. It should be noted that the use of stoichiometric ion pair extraction utilizes 1 equivalent of ammonium ion, and does not require the ammonium ion to "turn over".

(22) For an overview and discussion of theoretical derivations of ammonium ion pair reactivity see ref. . (a) Ions and ion pairs in organic reactions; Szwarc, M., Ed.; John Wiley & Sons: New York, 1974; Vols. 1 and 2.

(23) (a) Makosza, M. *Pure Appl. Chem.* **1975**, *43*, 439-462 and references cited therein. (b) Makosza, M.; Fedorynski, M. *Adv. Catal*. **1987**, *35*, 375-422.

(24) (a) Masson, D.; Magdassi, S.; Sasson, Y. *J. Org. Chem.* **1990**, *55*, 2714-2717. (b) Moberg, R.; Bokman, F.; Bohman, O.; Siegbahn, H. O. G. *J. Am. Chem. Soc*. **1991**, *113*, 3663-3667.

(25) Halpern, M.; Sasson, Y.; Rabinovitz, M. *Tetrahedron*, **1982**, *38*, 3183-3187.

(26) For a discussion of the use of this relationship see ref) Starks, C. M.; Liotta, C. L.; Halpern, M., *Phase-Transfer Catalysis: Fundamentals, Applications and Industrial Perspectives*. Chapman and Hall: New York, 1994. pp 270-287.

(27) Halpern, M. In *Phase-Transfer Catalysis, Mechanism and Synthesis*, ACS Symposium Series 659; Halpern, M. E., Ed.; ACS: Washington, D.C., 1996; Chapt. 8.

(28) (a) Jackman, L. M.; Lange, B. C. *Tetrahedron* **1977**, *33*, 2737-2769. (b) Seebach, D. *Angew. Chem., Int. Ed.* **1988**, *27*, 1624-1654. (c) Gregory, K.; von R. Schleyer, P.; Snaith, R. *Adv. Inorg. Chem.* **1991**, *37*, 47-142. (d) Collum, D. B. *Acc. Chem. Res.* **1993**, *26*, 227-234. (e) Lucht, B. L.; Collum, D. B. *Acc. Chem. Res.* **1999**, *32*, 1035-1042. (f) Valnot, J.-Y.; Maddaluno, J. In *The Chemistry of Organolithium Compounds, Vol. 2*; Rapoport, Z., Marek, I., Eds.; Wiley-Interscience: Chichester, 2006; Chapt. 8. (g) Collum, D. B.; McNeil, A. J.; Ramirez, A. *Angew. Chem., Int. Ed.* **2007**, *46*, 3002-3017.

(29) (a) Bergbreiter, D. E.; Newcomb, M. In *Asymmetric Synthesis, Vol. 2*, *Stereodifferentiating Reactions, Part B*; Morrison, J. D., Ed.; Academic Press: New York, 1984, Chapt. 9. (b) Evans, D. A. In *Asymmetric Synthesis, Vol. 3, Stereodifferentiating Reactions, Part B*; Morrison, J. D., Ed.; Academic Press: New York, 1984, Chapt. 1. (c) Lutomsky, K. A.; Meyers, A. I. In *Asymmetric Synthesis, Vol. 3, Stereodifferentiating Reactions, Part B*; Morrison, J. D., Ed.; Academic Press: New York, 1984, Chapt. 3. (d) Enders, D. In *Asymmetric Synthesis, Vol. 3, Stereodifferentiating Reactions, Part B*; Morrison, J. D., Ed.; Academic Press: New York, 1984, Chapt. 4. (f) Seyden-Penne, J. *Chiral Auxiliaries and Ligands in Asymmetric Synthesis*; Wiley-Interscience: New York,

1995. (g) Job, A.; Janeck, C. F.; Bettray, W.; Peters, R.; Enders, D. *Tetrahedron* **2002**, *58*, 2253-2329. (h) Ager, D.J., Prakash., I., Schaad, D.R. *Chem. Rev*. **1996**, *96*, 835-876. (i) *Stereoselective Synthesis, Methods of Organic Chemistry (Houben-Weyl); E21*; Helmchen, G.; Hoffmann, R.; Mulzer, J.; Schaumann, E. Eds.; Thieme: Stuttgart, 1996; Vol. 2; pp 645-1126. (j) Gnas, Y.; Glorius, F. *Synthesis* **2006**, 1899-1930.

(30) (a) Hughes, D. L. In *Comprehensive Asymmetric Catalysis*, *Vol. III*; Jacobsen, E. N.; Pfaltz, A.; Yamamoto, H., Eds.; Springer Verlag: Heidelberg, 1999; Chapt. 34.1. (b) Hughes, D. L. *Comprehensive Asymmetric Catalysis, Suppl*. *1*; Jacobsen, E. N.; Pfaltz, A.; Yamamoto, H., Eds.; Springer Verlag: Heidelberg, 2004; pp 161-170. (c) Helmchen, G. In *Asymmetric Synthesis-The Essentials*; Christmann, M., Bräse, S., Eds.; Wiley-VCH: Weinheim, 2006; pp. 95-99.

(31) For a thorough and insightful analysis of this strategy see ref. 4b.

(32) (a) Weber, W. P.; Gokel, G. W. *Phase Transfer Catalysis in Organic Synthesis*. Springer-Verlag: Berlin; New York, 1977; Vol. 4. (b) Dehmlow, E. V.; Dehmlow, S. S., *Phase Transfer Catalysis*. Verlag Chemie: Weinheim; Deerfield Beach, 1983; Vol. 11. (c) *Phase-Transfer Catalysis: New Chemistry, Catalysts, and Applications*; American Chemical Society: Washington, DC, 1985. (d) Starks, C. M.; Liotta, C. L.; Halpern, M., *Phase-Transfer Catalysis: Fundamentals, Applications and Industrial Perspectives*. Chapman and Hall: New York, 1994. (e) *Phase-Transfer Catalysis: Mechanisms and Syntheses*; American Chemical Society: Washington, DC, 1997. (g) *Handbook of Phase Transfer Catalysis*; Sasson, Y., Neumann, R., Eds.; Chapman & Hall: London, 1997. (h) O'Donnell, M. J. In *Catalytic Asymmetric Synthesis*, *2nd Ed.*; Ojima, I., Ed.; Wiley-VCH: New York, 2000; Chapt. 10. (i) Jones, R. A., *Quaternary Ammonium Salts: Their Use in Phase-Transfer Catalysed Reactions*; Academic Press: San Diego, 2001. (j) Lygo, B. *Phase-Transfer Reactions*; In Rodd's Chemistry of Carbon Compounds, Elsevier Science Ltd.: Oxford, 2001; Vol. 5, pp 101-149. (k) Hashimoto, T.; Maruoka, K. *Chem. Rev.* **2007**, *107*, 5656-5682. (l) Ooi, T.; Maruoka, K. *Angew. Chem., Int. Ed.* **2007,** *46*, 4222-4266. (m) *Asymmetric Phase Transfer Catalysis*; Maruoka, K. Ed.; Wiley-VCH: New York, 2008. (n) Maruoka, K. *Org. Proc. Res. Dev.* **2008**, *12*, 679-697.

(33) (a) Dolling, U. H.; Davis, P.; Grabowski, E. J. J. *J. Am. Chem. Soc*. **1984**, *106*, 446-447. (b) Bhattacharya, A.; Dolling, U.-H.; Ryan, K.; Grabowski, E. J. J.; Karady, S.; Weinstock, L. *Angew. Chem., Int. Ed.* **1986,** *25*, 476-477. (c) Hughes, D. L.; Dolling, U.-H.; Ryan, K. M.; Schoenewaldt, E. F.; Grabowski, E. J. J. *J. Org. Chem.* **1987**, 52, 4745-4752.

(34) (a) O'Donnell, M. J.; Bennett, W. D.; Wu, S. D. *J. Am. Chem. Soc.* **1989**, *111*, 2353-2355. (b) O'Donnell, M. J.; Bordwell, F. G.; Benet, W. D.; Bruder, W. A.; Jacobsen, W. N.; Knuth, K.; LeClef, B.; Polt, R. L.; Mrozack, S. R.; Cripe, T. A. *J. Am. Chem. Soc.* **1988**, *110*, 8520-8525. (c) O'Donnell, M. J. *Acc. Chem. Res.* **2004**, *37*, 506-517.

(35) Ooi, T. In *Asymmetric Phase Transfer Catalysis*; Maruoka, K. Ed.; Wiley-VCH: New York, 2008, Chapt 2. pp 9-33.

(36) (a) Lygo, B.; Wainwright, P. G. *Tetrahedron Lett*. **1997**, *38*, 8595-8598. (b) Lygo, B.; Crosby, J.; Lowdon, T. R.; Wainwright, P. G. *Tetrahedron* **2001**, *57*, 2391-2402. (c) Lygo, B.; Allbutt, B.; James, S. R. *Tetrahedron Lett.* **2003**, *44*, 5629-5632. (d) Lygo, B.; Andrews, B. I. *Acc. Chem. Res.* **2004**, *37*, 518-525.

(37) (a) Corey, E. J.; Bo, Y.; Busch-Petersen, J. *J. Am. Chem. Soc*. **1998**, *120*, 13000-13001. (b) Corey, E. J.; Xu, F.; Noe, M. C. *J. Am. Chem. Soc*. **1997**, *119*, 12414-12415.

(38) (a) Jew, S.-s.; Yoo, M.-S.; Jeong, B.-S.; Park, H.-g. Park, *Org. Lett.* **2002**, *4*, 4245-4248. (b) Jew, S.-s.; Lee, J.-H.; Jeong, B.-S.; Yoo, M.-S.; Kim, M.-J.; Lee, Y.-J.; Lee, J.; Choi, S.-h.; Lee, K.; Lah, M. S.; Park, H.-g. *Angew. Chem., Int. Ed.* **2005**, *44*, 1383-1385.

(39) (a) Maruoka, K.; Ooi, T. *Chem. Rev*. **2003**, *103*, 3013-3028. (b) Ooi, T.; Maruoka, K. *Acc. Chem. Res.* **2004**, *37*, 526-533. (c) Maruoka, K. *Pure Appl. Chem.* **2005**, *77*, 1285-1296. (d) Maruoka, K.; Ooi, T.; Kano, T. *Chem. Commun.* **2006**, 1487-1495.

(40) (a) Ohshima, T.; Gnanadesikan, V.; Shibuguchi, T.; Fukuta, Y.; Nemoto, T.; Shibasaki, M. *J. Am. Chem. Soc*. **2003**, *125*, 1206-11207. (b) Shibasaki, M.; Fukuta, Y.; Shibuguchi, T.; Ohshima, T. *Tetrahedron* **2004**, *60*, 7743-7754. (c) Okada, A.; Shibuguchi, T.; Masu, H.; Yamaguchi, K.; Shibasaki, M. *Angew. Chem., Int. Ed*. **2005**, *44*, 4564-4567.

(41) Sasai, H. (Jpn. Kokai Tokkyo Koho), JP2003335780, **2003**.

(42) (a) Arai, S.; Tsuji, R.; Nishida, A. *Tetrahedron Lett.* **2002**, *43*, 9535-9538. (b) Arai, S.; Takahashi, F.; Tsuji, R.; Nishida, A. *Heterocycles* **2006,** *67*, 495-501.

(43) For leading references, see: (a) Oslob, J. D.; Akermark, B.; Helquist, P.; Norrby, P.-O. *Organometallics* **1997**, *16*, 3015-3021. (b) Lipkowitz,K. B.; D'Hue, C. A.; Sakamoto, T.; Stack, J. N. *J. Am. Chem. Soc*. **2002**, *124*, 14255-14267. (c) Kozlowski, M. C.; Panda, M. *J. Org. Chem*. **2003**, *68*, 2061-2076. (d) Alvarez, S.; Schefzick, S.; Lipkowitz, K.; Avnir, D. *Chem. Eur. J*. **2003**, *9*, 5832-5837. (e) Kozlowski, M. C.; Dixon, S. L.; Panda, M.; Lauri, G. *J. Am. Chem. Soc*. **2003**, *125*, 6614-6615. (f) Lipkowitz, K. B.; Kozlowski, M.C. *Synlett* **2003**, 1547-1565. (g) Chen, J.; Jiwu, W.; Mingzong, L.; You, T. *J. Mol.Catal. A:Chem*. **2006**, *258*, 191-197. (h) Urbano-Cuadrado,M.; Carbo, J. J.; Maldonado, A. G.; Bo, C. *J. Chem. Inf. Model*. **2007**, *47*, 2228-2234. (i) Sigman, M. S.; Miller, J. J. *J. Org. Chem.* **2009**, *74*, 7633-7643. (j) Alvarez, S.; Alemany, P.; Avnir, D.. *Chem. Soc. Rev.* **2005**, *34*, 313-326.

(44) (a) Lygo, B.; Crosby, J.; Lowdon, T. R.; Peterson, J. A.; Wainwright, P. G. *Tetrahedron* **2001**, *57*, 2403-2409. (b) Cannizzaro; C. E.; Houk, K. N. *J. Am. Chem. Soc.* **2002**, *124*, 7163-7169. (c) Lygo, B.; Allbutt, B.; Beaumont, D. J.; Butt, U.; Gilks, J. A. R. *Synlett*, **2009**, 675-680.

(45) Lipkowitz, K. B.; Cavanaugh, M. W.; Baker, B.; O'Donnell, M. J. *J. Org. Chem.* **1991**, *56*, 5181-5192.

(46) (a) Pochapsky, T. C.; Stone, P. M.; Pochapsky, S. S. *J. Am. Chem. Soc.* **1991**, *113*, 1460-1462. (b) Hofstetter, C.; Wilkinson, P.S.; Pochapsky, T. C. *J. Org. Chem.* **1999**, *64*, 8794-8800. (c) Pochapsky, T. C.; Hofstetter, C. *Mag. Res*. *Chem.* **2000**, *38,* 90-94.

(47) (a) Reetz, M.; Huttle, S.; Goddard, R. *J. Am. Chem. Soc*. **1993**, 119, 9339-9340. (b) Goddard, R.; Herzog, H. M.; Reetz, M. T. *Tetrahedron*, **2002**, *58*, 7847-7850. (c) Reetz, M. T.; Huette, S.; Goddard, R.; Minet, U. *J. Chem. Soc., Chem. Commun*. **1995**, 275-277. (d) Reetz, M. T.; Bingel, C.; Harms, K. *J. Chem. Soc., Chem. Commun*. **1993**, 1558-1560. (e) Reetz, M. T.; Hutte, S.; Goddard, R. *Eur. J. Org. Chem*. **1999**, 2475-2478. (f) Goddard, R.; Hutte, S.; Reetz, M. T. *Acta Crystallogr., Sect. C: Cryst. Struct. Commun*. **2000**, C56, 878-880.

(48) Cook, T. C.; Andrus, M. B.; Ess, D. H. *Org. Lett.* **2012**, *14*, 5836-5839.

(49) (a) Miller, J. J.; Sigman, M. S. *Angew. Chem. Int. Ed.* **2008**, *47*, 771-774. (b) Sigman, M. S.; Miller, J. J. *J. Org. Chem.* **2009**, *74*, 7633-7643.

(50) Jiang, C.; Li, Y.; Tian, Q.; You, T. *J. Chem. Inf. Comput. Sci.* **2003**, *43*, 1876-1881.

(51) (a) Lipkowitz, K. B. *J. Am. Chem. Soc.* **2001**, *123*, 6710-6711. (b) Alvarez, S.; Schefzick, S.; Lipkowitz, K.; Avnir, D. *Chem. Eur. J.* **2003**, *9*, 5832-5837.

(52) *Molecular Interaction Fields: Applications in Drug Discovery and ADME Prediction*; Cruciani, G., Ed.; Series: Methods and Principles in Medicinal Chemistry; Wiley-VCH: Weinheim, 2006; Vol 27.

(53) Cramer, R. D., III; Patterson, D. E.; Bunce, J. D. *J. Am. Chem. Soc.* **1988**, *110*, 5959-5967.

(54) Lipkowitz, K. B.; Pradhan, M. *J. Org. Chem.* **2003**, *68*, 4648-4656.

(55) Dixon, S.; Merz, K. M., Jr.; Lauri, G.; Ianni, J. C. *J. Comput. Chem.* **2004**, *26*, 23-24.

(56) Phaun, P. –W.; Ianni, J. C.; Kozlowski, M. C. *J. Am. Chem. Soc.* **2004**, *126*, 15473-15479.

(57) (a) Kozlowski, M. C.; Dixon, S. L.; Panda, M.; Lauri, G. *J. Am. Chem. Soc.* **2003**, *125*, 6614-6615. (b) Ianni, J. C.; Annamalai, V.; Phuan, P-W.; Panda, M.; Kozlowski, M. C. *Angew. Chem., Int. Ed.* **2006**, *45*, 5502-5505. (d) Huang, J.; Ianni, J. C.; Antoline, J. E.; Hsung, R. P.; Kozlowski, M. C. *Org. Lett.* **2006**, *8*, 1565-1568. (e) Urbano-Cuadrado, M.; Carbo, J. J.; Maldonado, A. G.; Bo, C. *J. Chem. Inf. Model.* **2007**, *47*, 2228-2234.

(58) (a) Melville, J. L.; Andrews, B. I.; Lygo, B.; Hirst, J. D. *Chem.Commun.* **2004**, 1410-1411. (b) Melville, J. L.; Lovelock, K. R. J.; Wilson, J.; Allbutt, B.; Burke, E. K.; Lygo, B.; Hirst, J. D. *J. Chem. Inf. Model.* **2005**, *45*, 971-981.

(59) Lygo, B.; Allbutt, B.; James, R. S. *Tetrahedron Lett.* **2003**, *44*, 5629-5632.

(60) Lipkowitz, K. B.; Cavanaugh, M. W.; Baker, B.; O'Donnell, M. J. *J. Org. Chem.* **1991**, *56*, 5181-5192.

(61) (a) Denmark, S. E.; Thorarensen, A. Chem. Rev. **1996**, 96, 137-165; (b) Denmark, S. E.; Cottell, J. In The Chemistry of Heterocyclic Compounds: Synthetic Applications of 1,3-Dipolar Cycloaddition Chemistry Toward Heterocycles and Natural Products; Padwa, A.; Pearson,W. H., Eds.;Wiley-Interscience: New York, NY, 2002; pp 83-167.

(62) Denmark, S. E.; Schnute, M. E. *J. Org. Chem.* **1991**, *56*, 6738.

(63) Denmark, S. E. Schnute, M. E.; Thorarensen, A. Middletone, D. S.; Stolle, A. *Pure & Appl. Chem*. **1994**, *66*, 2041-2044.

(64) Lygo, B.; Allbutt, B.; Beaumont, D. J.; Butt, U.; Gilks, J. A. R. *Synlett*, **2009**, 675-680.

(65) Kitamura, K.; Arimura, Y.; Shirakawa, S.; Maruoka, K. *Tetrahedron Lett.* **2008**, *49*, 2026-2030. (b) Lygo, B.; Andrews, B. I.; Hirst, J. D.; Melville, J. L.; Peterson, J. A.; Slack, D. *Chim. Oggi* **2004**, *22*, 8-10. (c) Lygo, B.; Andrews, B. I.; Crosby, J.; Peterson, J. A. *Tetrahedron Lett.* **2002**, *43*, 8015-8018.

(66) The hydration of 2,3-dihydrofuran has been reported numerous times; for sample procedures see: (a) Saito, T.; Nishimoto, Y.; Yasuda, M.; Baba, A. *J. Org. Chem.* **2006**, *71*, 8516-8522. (b) Kojima, K.; Kimura, M.; Ueda, S.; Tamaru, Y. *Tetrahedron* **2006**, *62*, 7512-7520. (c) Kodato, S.; Nakagawa, M,; Nakayama, K.; Hino, T. *Tetrahedron* **1989**, *45*, 7247-7262. (d) Bergman, N. A.; Jansson, M.; Chiang, Y.; Kresge, J.; Yin, Y. *J. Org. Chem*. **1987**, *52*, 4449-4453. (e) Bates, H. A.; Farina, J. *J. Org. Chem*. **1985**, *50*, 3843-3845.

(67) (a) Parikh, J. R.; Doering, W. E. *J. Am. Chem. Soc*. **1967**, *89*, 5505-5507. b) Chen, L.; Lee, S.; Renner, M.; Tian, Q.; Nayyar, N. *Org. Proc. Res. Dev*. **2006**, *10*, 163-164.

(68) Still, W. C.; Gennari, C. *Tetrahedron Lett*. **1983**, *24*, 4405-4408.

(69) Chow, H.-F.; Fleming, I. *J. Chem. Soc., Perkin Trans. 1*. **1984**, *8*, 1815-1819.

(70) Reich, H. J.; Renga, J. M.; Reich, I. L. *J. Am. Chem. Soc*. **1975**, *97*, 5434-5447.

(71) See for example: Ludvig, E. B.; Belenkaya, B. G. *J. Macrom. Sci., Part A: Pure and Appl. Chem.*, **1974**, *8*, 819-828.

(72) (a) Floc'h, Y. Le; Yvergnaux, F.; Toupet, L.; Gree, R. *Bull. Soc. Chim. France*, **1991**, *5*, 742-759. (b) Moriarty, R. M.; Vaid, R. K.; Hopkins, T. E.; Vaid, B. K.; Prakash, O. *Tetrahedron Lett.* **1990**, *31*, 197-200. (c) Chatterjee, A. K.; Morgan, J. P.; Scholl, M.; Grubbs, R. H. *J. Am. Chem. Soc*. **2000**, *122*, 3783-3784. (d) Fouque, E.; Rousseau, G.; Seyden-Penne, J. *J. Org. Chem.* **1990**, *55*, 4807-4017. (e) Bierling, B.; Krischke, K.; Oberender, H.; Schulz, M. *J. Prakt. Chem*. **1972**, *314*, 170-180. (f) Ito, Y.; Hirao, T.; Saegusa, T. *J. Org. Chem.* **1978**, *43*, 1011-1013.

(73) (a) Rubottom, G. M.; Gruber, J. M.; Marrero, R.; Juve, H. D. Jr.; Kim, C. W. *J. Org. Chem.* **1983**, *48*, 4940-4944. (b) Christoffers, J. O.; H. Fischer, P.; Frey, W. *Tetrahedron* **2003**, *59*, 3769-3778. (c) Paterson, I. *Tetrahedron*, **1988**, *44*, 4207-4219.

(74) (a) Tsuji, J.; Takahashi, K.; Minami, I.; Shimizu, I. *Tetrahedron Lett.* **1984**, *42*, 4783-4786. (b) *Handbook of Organopalladium Chemistry for Organic Synthesis*; Negishi, E.-I., Ed.; Wiley-Interscience: New York, 2002.

(75) Denmark, S. E.; Seierstad, M. E. *J. Org. Chem.* **1999**, *64*, 1610-1619. (b) Denmark, S. E.; Schnute, M. E.; Senanayake, C. B. W. *J. Org. Chem.* **1993**, *58*, 1859-1874.

(76) Denmark, S. E.; Senanayake, C. B. W.; Ho, G.-D. *Tetrahedron* **1990**, *46*, 4857-4876.

(77) Schlaf, M.; Bosch, M. *J. Org. Chem*. **2003**, *68*, 5225-5227.

(78) Enantiomeric composition of the lactams was determined CSP-SFC after derivatization as their 3,5-dinitrobenzoyl carbamates, as previously reported.[75,76]

(79) Barton, D. H. R.; Dorchak, J.; Jaszberenyi, J. C. *Tetrahedron* **1992**, *48*, 7435-7446

(80) Dehmlow, E. V.; Wagner, S.; Muller, A. *Tetrahedron* **1999**, *55*, 6335-6346.

(81) Ooi, T.; Kameda, M.; Maruoka, K. *J. Am. Chem. Soc.* **2003**, *125*, 5139-5151.

(82) (a) Bayer, J. L.; Alazard, J. P.; Thal, C. *Tetrahedron* **1990**, *46*, 5187-5198. (b) Swain, C. J.; Kneed, C.; Herbert, R.; Baker, R. *J. Chem. Soc., Perkin Trans. 1* **1990**, 3183-3186

(83) (a) Williamson, W. *Liebigs Ann. Chem*. **1851**, *77*, 37-49. b) Williamson, W. *J. Chem. Soc*. **1852**, *106*, 229-239.

(84) (a) Miller, N. E. *J. Am. Chem. Soc.* **1996**, *88*, 4284-4285. Kessar, S. V.; Singh, P.; Vohra, R.; Kaur, N. P.; Singh, K. N. *J. Chem. Soc., Chem. Commun.* **1997**, *97*, 568-570. Vedejs, E.; Kendall, J. T. *J. Am. Chem. Soc.* **1997**, *119*, 6941-6942

(85) (a) Imamoto, T. *Lanthanides in Organic Synthesis.*, Academic Press: London, 1994. (b) Imamoto, in *Comprehensive Organic Synthesis, Vol. 1*; Trost, B. M., Fleming, I. Eds.; Pergamon Press: Oxford, 1991, (c) Imamoto, T.; Takiya, N.; Nakamura, K.; Hatajima, T.; Kamiya, Y. *J. Am. Chem. Soc.* **1989**, *111*, 4392-4398.

(86) Preliminary results from Libraries **II** and **III** indicated that the 9-anthrylmethyl group exhibited the lowest enantioselectivity and the catalysts were difficult to store and handle due to photooxidation.

(87) Another common method for mixing of biphasic mixtures is a ball mill. The forces involved in this process are quite different from disruption of a biphase by shearing. For an overview see: Lynch, A.; Rowland C (**2005**). *The history of grinding*. SME

(88) We chose to hold the temperature at 2-4 ^{o}C out of convenience, since the temperature could be controlled simply running the reactions in a cold room, alleviating the need for re-circulating baths or cryogenics.

(89) S. S. Yufit, S. S.; Zinovyev, S. S. *J. Phys. Org. Chem.* **2001**, *14*, 343-348.

(90) (a) Starks, C. *Tetrahedron* **1999**, *55*, 6261-6274. (b) Makosza, M. and Lasek, W. *J. Phys. Org. Chem.* **1993**, *6*, 412-420.

(91) (a) Masson, D.; Magdassi, S.; Sasson, Y. *J. Org. Chem.* **1990**, *55*, 2714-2717. (b) Moberg, R.; Bokman, F.; Bohman, O.; Siegbahn, H. O. G. *J. Am. Chem. Soc*. **1991**, *113*, 3663-3667.

(92) *Foye's Principles of Medicinal Chemistry;* Lemke, T.; Williams, D., Eds.; Lippincott Williams & Wilkins: Philadelphia, PA, **2008**.

(93) Pharmacokinetic-pharmacodynamic modeling and simulation; Bonate, P.; Springer: New York, NY, **2005**.

(94) The error is represented as %error = Stdev./$(\log(t_{1/2}))_{avg.}$*100. See the Supplemental Information for percent errors for each catalyst as well as a histogram illustrating the distribution of error across all of the catalysts.

(95) This data point was extrapolated after monitoring the reaction for 1 week (~25%) to ensure a linear initial rate.

(96) It is important to note that this analysis incorporates a weighting factor in order to take into account how many of each catalyst is in each representative group. See the Experimental Section for the statistical formulae used. Deviations were normalized to 1 for convenience.

(97) (a) For a brief summary of this rational see ref 13d pp. 151-153. (b) Balcells, J.; Collona, S.; Fornasier, R. *Synthesis*, **1976**, *8*, 266-267.

(98) *Ion Exchange Separation in Analytical Chemistry*, O. Samuelson, Ed.; Wiley: New York, 1963.

(99) (a) Maruoka, K.; Xisheng, W.; Kitamura, M. *J. Am. Chem. Soc.* **2007**, *129*, 1038-1039. (b) Kanger, T.; Lippur, K.; Kriis, K.; Kailas, T.; Müürisepp, A-M.; Pehk, T.; Lopp, M. *Tetrahedron: Asymmetry*, **2007**, *18*, 137-141. (c) Nagasawa, K.; Kita, T.; Georgieva, A.; Hashimoto, Y.; Nakata, T. *Angew. Chem., Int.Ed.* **2002**, *41*, 2832-2834. (d) Takabe, K.;

Mase, N.; Ohno, T.; Hoshikawa, N.; Ohishi, K.; Morimoto, H.; Yoda, H. *Tetrahedron Lett.* **2003**, *44*, 4073-4075. (e) MacFarland, D. K.; Kowtoniuk, W. E.; Grover, G. N. *Tetrahedron Lett.* **2006**, *47*, 57-60. (f) Ramachandran, U.; Kumar, S. *Tetrahedron*, **2005**, *61*, 4141-4148. (g) Arai, S.; Nishida, A.; Tsuji, R. *Tetrahedron Lett.* **2002**, *43*, 9535-9537.

(100) (a) Liu. Z.; Chen, X. *Huaxue Shijie* **1982**, *23*, 104-106. (b) Afanas'eva, V. L.; Bagreeva, M. R.; Lyubeshkin, V. V.; Pechenina, V. M.; Epshtein, N. A.; Glushkov, R. G. *Khim. – Farm. Zh.* **1987**, *21*, 1114-1119.

(101) Neither Taft nor Charton steric values are available for all of the R^2 groups. Calculated molar refractivity values are commonly utilized in place of experimentally determined steric values. See for example: Wildman, S.A., Crippen, G.M. *J. Chem. Inf. Comput. Sci.* **1999**, *39*, 868–873.

(102) Williams, A. "Free Energy Relationships in Organic and Bio-Organic Chemistry," Royal Soc. Of Chem., Cambridge, England.

(103) Lill, M. A. *Drug Discovery Today* **2007**, *12*, 1012.

(104) Hansch, C.; Fujita, T. *J. Am. Chem. Soc.* **1964**, *86*, 1616.

(105) Wilson, J. W.; Free, S. M. *J. Med. Chem.* **1964**, *7*, 395.

(106) Harper, K. C.; Sigman, M. S. *PNAS* **2011**, *108*, 2179-2183.

(107) Harper, K. C.; Bess, E. N.; Sigman, M. S. *Nature Chem.* **2012**, *4*, 366-374.

(108) Harper, K. C.; Sigman, M. S. *Science* **2011**, *333*, 1875-1878.

(109) Su, P. Li, H. *J. Chem. Phys.* **2009**, *131*, 1-15.

(110) Duncon-Gould, N. (2011) *An Investigation of Phase Transfer Catalyis Employing Quantitative Structure-Activity Relationships.* Doctoral dissertation, University of Illinois at Urbana-Champaign, Urbana, Illinois.

(111) Spartan '08 is a product of Wavefunction, Inc. 18401 Von Karman Ave., Suite 370. Irvine, CA 92612 USA, http://www.wavefun.com/index.html.

(112) Cramer, C.; Truhlar, D. G. *Acc. Chem. Res.* **2008**, *41*, 760-768.

(113) Mittal R. R.; Harris, L.; McKinnon, R. A.; Sorich, M. J. *J. Chem. Inf. Model.* **2009**, *49*, 704-709.

(114) Kroemer, R. T.; Hecht, P. *J. Comput.-Aided Mol. Des.* **1995**, *9*, 205-212.

(115) (a) Golbraikh, A.; Tropsha, A. *J. Mol. Graphics Modell.* **2002** , *20*, 269-276. (b) Golbraikh, A.; Tropsha, A. *J. Comput.-Aided Mol. Des.* **2002**, *16*, 357-369. (c) Tropsha, A.; Gramatica, P.; Gombar, V. K. *QSAR Comb. Sci.* **2003**, *22*, 69-77.

(116) Wold, S.; Eriksson, L. In *Chemometric Methods in Molecular Design*; van de Waterbeemd, H., Ed.; Wiley-VCH: Weinheim, 1995; pp 309-318.

(117) (a) Hopfinger, A. J.; Wang, S.; Tokarski, J. S.; Jin, B.; Albuquerque, M.; Madhav, P. J.; Duraiswami, C. *J. Am. Chem. Soc.* **1997**, *119*, 10509-10524. (b) See ref. 58b for an implementation of the method of 51a and variants thereof applied to APTC.

(118) The energy difference between conformations **A** and **B** is calculated to be 2.4 kcal in favor of **A** (B3LYP/6-31G(d)//M06-2x/6-31G(d) in toluene solvent (SM8)). This difference is presumed to be larger when R2 ≠ H . Preliminary modeling studies in the presence of an anion support a significantly larger energy difference between **A** and **B**.

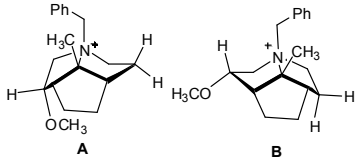

(119) The energy difference ranges from 2.6 kcal (R1=R2=H) favoring the **up** conformation to 0.8 kcal favoring the **dn** conformation depending on the identities of R1 and R2 (B3LYP/6-31G(d)//M06-2X/6-31G(d) in toluene solvent (SM8), without a counterion, and with R3 = Me; R4 = Ph for reduction in the number of basis functions since R3 is unlikely to influence the ring conformation significantly).

(120) A full table including the investigation of different semi-empirical partial charges (including PM3, AM1) is available in the Experimental Section.

(121) Additional data relating to the external cross-validation and the methods by which it was performed are available in the Experimental Section.

(122) The 3D coordinates for all molecules included in the enantioselectivity and activity data set are included in the Experimental Section

(123) See the discussion in the previous paper in this issue for a comparison of electrostatic potential maps.

(124) Anslyn, E. V.; Dougherty, D. A. *Modern Physical Organic Chemistry*. University Science: Sausalito, 2006; p 181.

(125) Cherkasov, R. A.; Kutyrev, G. A.; Pudovik, A. N., *Tetrahedron* **1985**, *41*, 2567-2624

(126) Halgren, T. A. *J. Comput. Chem.* **1996**, *17*, 520-552.

(127) Molander, G. A.; Harris, C. R. *J. Org. Chem.* **1998**, *63*, 812-816

(128) Muthusamy, S.; Babu, S. A.; Gunanathan, C. Tetrahedron Lett. 2002, 43, 3133-3136.

(129) Meulemans, T. M. Stork, G. A. Macaev, F. Z., Jansen, G. J. M.; de Groot, A. *J. Org. Chem.* **1999**, *64*, 9178-9188.

(130) a) Snarey, M.; Terrett, N. K.; Willett, P.; Wilton, D. J., "Comparison of Algorithms for Dissimilarity-Based Compound Selection". *J. Mol. Graphics Model.* **1997,** *15*, 372-385. b) Khanna, V.; Ranganathan, S., "Molecular Similarity and Diversity Approaches in Chemoinformatics". *Drug Dev. Res.* **2011,** *72*, 74-84.

(131) Seebach, D.; Goliński, J. *Helv. Chim. Acta* **1981**, *64*, 1413-1423.

(132) (a) Heathcock, C. H.; Buse, C. T.; Kleshick, W. A.; Pirrung, M. C.; Sohn, J. E.; Lampe, J. *J. Org. Chem.* **1980**, *45*, 1066-1081. (b) Lam, Y.-H.; Houk, K. N.; Scheffler, U.; Mahrwald, R. *J. Am. Chem. Soc.* **2012**, *134*, 6286-6295.

(133) (a) Rondan, N. G.; Paddon-Row, M. N.; Caramella, P.; Houk, K. N. *J. Am. Chem. Soc.* **1981**, *103*, 2436-2438. (b) Houk, K. N. *Pure Appl. Chem.* **1983**, *55*, 277-282.

(134) Mulzer, J.; Brüntrup; Finke, J.; Zippel, M. *J. Am. Chem. Soc.* **1979**, *101*, 7723-7725.

(135) Schlosser, M. *Bull. Soc. Chim. Fr.* **1971**, 453-459.

(136) Reviews: (a) Sakurai, H. *Pure Appl. Chem.* **1982**, *54*, 1-22. (b) Majetich, G. In *Organic Synthesis: Theory and Application*s; Hudlicky, T., Ed.; JAI Press: Greenwich, 1989; Vol. 1, p. 173-240. (c) Hosomi, A. *Acc. Chem. Res.* **1988**, *21*, 200-206. (d) Schinzer, D. *Synthesis* **1988**, 263-273. (e) Fleming, I.; Dunogués, J.; Smithers, R. *Org. React.* **1989**, *37*, 57-575. (f) Yamamoto, Y.; Asao, N. *Chem. Rev.* **1993**, *93*, 2207-2293. (g) Langkopf, E.; Schinzer, D. *Chem. Rev.* **1995**, *95*, 1375-1408. (h) Masse, C. E.; Panek, J. S. *Chem. Rev.* **1995**, *95*, 1293-1316. (i) Fleming, I.; Barbero, A.; Walter, D. *Chem. Rev.* **1997**, *97*, 2063-2192. (j) Yanagisawa, A. In *Comprehensive Asymmetric Catalysis*; Jacobsen, E. N.; Pfaltz, A.; Yamamoto, H., Eds.; Springer-Verlag: Berlin, 1999; Vol. 2, Chapter 27. (k) Denmark, S. E.; Almstead, N. G. In *Modern Carbonyl Chemistry*, Otera, *J.*, Ed.; Wiley-VCH: Weinheim, 2000; Chapter 10. (l) Denmark, S. E.; Fu, *J. Chem. Rev.* **2003**, *103*,

2763-2793. (m) Yus, M.; Gonzalez-Gomez, J. C.; Foubelo, F. *Chem. Rev.* **2011**, *111*, 7774-7854.

(137) (a) *Modern Carbonyl Chemistry*; Otera, *J.*, Ed.; Wiley-VCH: Weinheim, 2000. (b) *Modern Aldol Reactions*; Mahrwald, R., Ed.; Wiley-VCH: Weinheim, 2004.

(138) For a thorough disquisition on the state of the art in S_E' reactions see: (a) Matassa, V. G.; Jenkins, P. R.; Kümin, A.; Damm, L.; Schreiber, *J.*; Felix, D.; Zass, E.; Eschenmoser, A. *Isr. J. Chem.* **1989**, *29*, 321-343. (b) Denmark, S. E.; Werner, N. S. *J. Am. Chem. Soc.* **2010**, *132*, 3612-3620. (c) Denmark, S. E.; Weber, E. J.; Almstead, N. G.; Wolf, L. M. *Tetrahedron* **2012**, *68*, 7701-7718.

(139) Reviews: (a) Hoffmann, R. W. In *Stereocontrolled Organic Synthesis*; Trost, B. M., Ed.; Blackwell Scientific Publications: Cambridge; 1994; pp 259-274. (b) Roush, W. R. In *Stereoselective Synthesis, Methods of Organic Chemistry (Houben-Weyl)*; E21; Helmchen, G.; Hoffmann, R. W.; Mulzer, J.; Schaumann, E., Eds.; Thieme Stuttgart: New York, 1996; Vol. 3; pp 1410-1486. (c) Hall, D. G.; Lachance, H. *Org. React.* **2008**, *73*, 1-573.

(140) (a) Reetz, M. T.; Hüllmann, M.; Massa, W.; Berger, S.; Rademacher, P.; Heymanns, P. *J. Am. Chem. Soc.* **1986**, *108*, 2405-2408. (b) Denmark, S. E.; Henke, B. R.; Weber, E. J. *Am. Chem. Soc.* **1987**, *109*, 2512-2514. (c) Shambayati, S.; Crowe, W. E.; Schreiber, S. L. *Angew. Chem. Int. Ed.* **1990**, *29*, 256-272. (d) Ooi, T.; Maruoka, K. In *Modern Carbonyl Chemistry*; Otera, *J.*, Ed.; Wiley-VCH: Weinheim, 2000; Chapter 1. (e) Saito, S.; Yamamoto, H. In *Modern Carbonyl Chemistry*; Otera, J., Ed.; Wiley-VCH: Weinheim, 2000; Chapter 2. (f) Denmark, S. E.; Almstead, N. G. *J. Am. Chem. Soc.* **1993**, *115*, 3133-3139.

(141) Denmark, S. E.; Fu, J.; *Chem. Commun.* **2003**, 167-170.

(142) (a) Denmark, S. E.; Weber, E. J. *Helv. Chim. Acta.* **1983**, *66*, 1655-1660. (b) Denmark, S. E.; Weber, E. J. *J. Am. Chem. Soc.* **1984**, *106*, 7970-7971. (c) Denmark, S. E.; Henke, B. R.; Weber, E. J. *J. Am. Chem. Soc.* **1987**, *109*, 2512-2514. (d) Denmark, S. E.; Weber, E. J.; Wilson, T. M.; Willson, T. M. *Tetrahedron* **1989**, *45*, 1053-1065. (e) Denmark, S. E.; Almstead, N. G. *J. Org. Chem.* **1994***, 59,* 5130-5132. (f) Denmark, S. E.; Hosoi, S. *J.*

Org. Chem. **1994***, 59,* 5133-5135. (g) Denmark, S. E.; Almstead, N. G. *J. Mex. Chem. Soc.* **2009,** *53*, 174-192.

(143) Tietze, L. F.; Kinzel, T.; Schmatz, S. *Chem. Eur. J.* **2009**, *15*, 1706-1712.

(144) Bottoni, A.; Costa, A. L.; Di Tommaso, D.; Rossi, I.; Tagliavini, E. *J. Am. Chem. Soc.* **1997,** *119,* 12131-12135.1

(145) Tietze, L. F.; Kinzel, T.; Schmatz, S. *J. Am. Chem. Soc.* **2006**, *128*, 11483-11495.

(146) Morokuma, K. *J. Chem. Phys.* **1971**, *55*, 1236-1235.

(147) Kitaura, K.; Morokuma, K. *Int. J. Quantum Chem.* **1976**, *10*, 325-340.

(148) (a) Jeziorski, B.; Moszynski, R.; Szalewicz, K. *Chem. Rev.* **1994**, *94*, 1887-1930. (b) Frenking, G. Solá; Vyboishchikov, S. F. *J. Oranomet. Chem.* **2005**, *690*, 6178-6204.

(149) (a) Bickelhaupt, F. M. *J. Comput. Chem.* **1999**, *20*, 114-128. (b) Diefenbach, A.; Bickelhaupt, F. M. *J. Chem. Phys.* **2001**, *115*, 4030-4040. (c) Diefenbach, A.; Bickelhaupt, F. M. *J. Phys. Chem. A* **2004**, *108*, 8460-8466. (d) de Jong, G. T.; Bickelhaupt, F. M. *Chem. Phys. Chem.* **2007**, *8*, 1170-1181.

(150) (a) Ess, D. H.; Houk, K. N. *J. Am. Chem. Soc.* **2007**, *129*, 6894-6898. (b) Ess, D. H.; Houk, K. N. *J. Am. Chem. Soc.* **2008**, *130*, 10187-10198. (c) Ess, D. H.; Jones, G. O.; Houk, K. N. *Org. Lett.* **2008**, *10*, 1633-1636. (d) Hayden, A. E.; Houk, K. N. *J. Am. Chem. Soc.* **2009**, *131*, 4084-4089.

(151) Su, P.; Li, H. *J. Chem. Phys.* **2009**, *131*, 1-15.

(152) Mukaiyama, T.; Matsuo J. In Modern Aldol Reactions Vol 1: Enolates, Organocatalysis, Biocatalysis and Natural Product Syntesis, Mahrwald, R., Ed.; Wiley-VCH: Weinheim, 2004; Chapter 3.

(153) Tomioka, K. In *Modern Carbonyl Chemistry*; Otera, J., Ed.; Wiley-VCH: Weinheim, 2000; Chapter 12.

(154) (a) Akiyama, T.; Kirino, M. *Chem. Lett.* **1995**, 723-724. (b) Akiyama, T.; Yamanaka, M. *Synlett* **1996**, 1095-1096.

(155) Bottoni, A.; Costa, A. L.; Tommaso, D. D.; Rossi, I.; Tagliavini, E. *J. Am. Chem. Soc.* **1997**, *119*, 12131-12135.

(156) Laurence, C.; Gal, J-F. *Lewis Basicity and Affinity Scales: Data and Measurement*, John Wiley & Sons: West Sussex, 2010; Chapter 3.

(157) The numbering system is independent of that used in previous chapters.

(158) (a) Reetz, M. T.; Hullmann, M.; Massa, W.; Berger, S.; Rademacher, P.; Heymanns, P. *J. Am. Chem. Soc.* **1986**, *108*, 2405-2408. (b) Denmark, S. E.; Henke, B. R.; Weber, E. *J. Am. Chem. Soc.* **1987**, *109*, 2512-2514. (c) Corey, E. J.; Loh, T.–P.; Sarshar, S.; Azimioara, M. *Tetrahedron Lett.* **1992**, *33*, 6945-6948. (d) Denmark, S. E.; Almstead, N. G. *J. Am. Chem. Soc.* **1993**, *115*, 3133-3139. (e) Ishihara, K.; Gao, Q.; Yamamoto, H. *J. Am. Chem. Soc.* **1993**, *115*, 10412-10413.

(159) Bürgi, H. B.; Dunitz, D. J.; Lehn, J. M.; Wipff, G. *Tetrahedron* **1974**, *30*, 1563-1572.

(160) Wong, C. T.; Wong, M. W. *J. Org. Chem.* **2006**, *72*, 1425-1430.

(161) (a) Gerrard, W.; Mooney, E. F.; Peterson, W. G. *J. Inorg. Nucl. Chem.* **1966**, *29*, 943-949. (b) Rasul, G.; Williams, R. E. *Collect. Czech. Chem. Commun.* **1999**, *64*, 847-855.

(162) Laurence, C.; Gal, J-F. *Lewis Basicity and Affinity Scales: Data and Measurement*, John Wiley & Sons: West Sussex, 2010; Chapter 3.

(163) Kelly, D. R.; Roberts, S. M. *Synth. Commun.* **1979**, *9*, 295-299.

(164) Akiyama, T.; Nakano, M.; Kanatani, J.–Y; Ozaki, S. *Chem. Lett.* **1997**, 385-386.

(165) (a) Akiyama, T.; Ishikawa, K.; Ozaki, S. *Chem. Lett.* **1994**, 627-630. (b) Danheiser, R. L.; Takahashi, T.; Bertók, B. Dixon, B. *Tetrahedron Lett.* **1993**, *34*, 3845-3848.

(166) (a) Angle, S. R.; El-said, N. A.; *J. Am. Chem. Soc.* **1999**, *121*, 10211-10212. (b) Angle, S. R.; Belanger, D. S.; El-Said, N. A. *J. Org. Chem.* **2002**, *67*, 7699-7705.

(167) See the Experimental Section for computed pathways for conversion of **14** to **15.**

(168) (a) Weber, R.; Susz, B. P. *Helv. Chim. Acta* **1967**, *50*, 2226-2232. (b) Susz, B.-P.; Weber, R. *Helv. Chim. Acta* **1970**, 53, 2085-2097. (c) Paul, R. C.; Singal, H. R.; Chadha, S. L. *Ind. J. Chem*. **1971**, *9*, 985-988. (d) Filippini. F.; Susz, B.-P. *Helv. Chim. Acta* **1971**, *54*, 1175-1178. (e) Dabrowski, J.; Katcka, M. *J. Mol. Structure* **1972**, *12*, 179-183. (f) Childs, R. F.; Mulholland, D. L.; Nixon, A. *Can. J. Chem*. **1982**, *60*, 801-808. (g) Bachand, B.; Wuest, J. D. *Organometallics* **1991**, *10*, 2015-2025. (h) Denmark, S. E.; Almstead, N. G. *Tetrahedron* **1992**, *48*, 5565-5578. (i) Cozzi, P. G.; Solari, E.; Floriani, C.; Chiesi-Villa, A.; Rizzoli, C. *Chem. Ber.* **1996**, *129*, 1361-1368. (j) Gau H-M.; Le, C-G.; Liu, C-C.; Jiang, M-K.; Ho Y-C.; Kuo, C-N *J. Am. Chem. Soc.* **1996**, *118*, 2936-2941.

(169) Fluoride-promoted desilylation in the BF_3-promoted reaction by free fluoride is less likely on the basis of the greater heterolytic bond dissociation energy of a B-F (110 kcal/mol) versus a Ti-Cl (102 kcal/mol). BDE data is taken from; Luo, R-Y *Comprehensive Handbook of Chemical Bond Energies* CRC Press: Boca Raton, 2007.

(170) Denmark, S. E.; Weber, E. J.; Almstead, N. G.; Wolf, L. M. *Tetrahedron* **2012**, *68*, 7701-7718.

(171) The system of nomenclature for the transition states used herein designates the following: (1) syn or anti describe the relative topicity of the reacting double bonds in terms of the product stereostructure, (2) T = a transition state, (3) 1 = antiperiplanar, 2 = (+)-synclinal, 3 = (–)-synclinal arrangement of double bonds, and L = Lewis acid promoted; H = Brønsted acid promoted; F = fluoride promoted.

(172) See the Experimental Section for energy comparisons of geometries of the protonated acetaldehyde.

(173) Olah, G. A.; O'Brian, D. H; Calin, M. *J. Am. Chem. Soc.* **1967**, *89*, 3582-3586.

(174) The distortion energy of the aldehyde component is represented as ΔE_{dist}(A) while the distortion energy of the crotylsilane component is represented as ΔE_{dist}(B).

(175) Whereas **syn-T3-L** and **syn-T3-H** are the lowest energy pathways, **syn-T3-F** is not the lowest energy pathway, even though it possesses the strongest orbital interactions (Section 2.2.).

(176) (a) Klopman, G. *J. Am. Chem. Soc.* **1968**, *90*, 223-234. (b) Salem, L. *J. Am. Chem. Soc.* **1968**, *90*, 543-552. (c) Salem, L. *J. Am. Chem. Soc.* **1968**, *90*, 553-566.

(177) This statement is supported by the fact that the orbital interaction energy component (ΔE_{orb}) favors **syn-T3-L** compared to **anti-T1-L** under constant distortion (ΔE_{orb}(**syn-T3-L**) – ΔE_{orb}(**anti-T1-L**) = -5.4 kcal/mol) (Table 2).

(178) Anh, N. T.; Thanh, B. T. *Nouv. J. Chim.* **1986**, *10*, 681-683.

(179) The quantities are calculated at constant levels of distortion from Table 2.

(180) Since the contribution from orbital energy gap is non-existent from both equalities Δ_x(**syn-T3**) = Δ_x(**anti-T1**) and Δ_x(**anti-T2**) = Δ_x(**syn-T1**) for both electrophilic activation modes, the approach outlined in Figure 12 is acceptable for isolating overlap contributions rather than differences in orbital energy gaps.

(181) Negative values of Δq_L^{SOI} and $\Delta_L^{\ddagger,SOI}$, and a positive value for ΔE_{orb}^{SOI} indicate greater stabilizing interactions in **anti-T2** which implies the lack of stabilizing SOIs in **syn-T3**. A negative value for ΔE_{int}^{SOI} may indicate a small stabilizing contribution from SOIs.

(182) This additional distortion does not lead to an increase in the HOMO energy of **anti-T2-L** relative to **syn-T3-L**, i.e. the HOMO energies of these transition states are equal. Thus, the lesser distortion in **syn-T3-L** arises from greater orbital overlap rather than a narrowing of the HOMO-LUMO gap.

(183) Denmark, S. E.; Schnute, M. E.; Senanayake, C. B. W. *J. Org. Chem.* **1993***, 58,* 1853-1858.

(184) (a) Golbraikh, A.; Tropsha A. *J. Mol. Graphics. Modell.* **2002**, *20*, 269-276. (b) Tropsha, A.; Gramatica, P.; Gombar, V. K. *QSAR Comb. Sci.* **2003**, *22*, 69-77.

(185) *Concepts and Applications of Molecular Similarity*; Johnson, M. A., Maggiora, G. M.; Eds; John Wiley & Sons, Inc.: New York, 1990.

(186) As calculated from an spl script

(187) Zhao, Y.; Truhlar, D. G. *Theor. Chem. Acc.* **2008**, *120*, 215-241.

(188) Barone, V.; Cossi, M. J. Phys. Chem. A **1998**, *102*, 1995-2001.

(189) Ribeiro, R. F.; Marenich, A. V.; Cramer, C. J.; Truhlar, D. G. *J. Phys. Chem. B* **2011**, *115*, 14556-14562.

(190) Alecu, I. M.; Zheng, J.; Zhao, Y.; Truhlar, D. G. *J. Comput. Theory Comput.* **2010**, *6*, 2872-2887.

(191) Frisch, M. J. T., G. W.; Schlegel, H. B.; Scuseria, G. E.; Robb, M. A.; Cheeseman, J. R.; Scalmani, G.; Barone, V.; Mennucci, B.; Petersson, G. A.; Nakatsuji, H.; et al. Gaussian 09, Revision A.01; Gaussian, Inc.: Wallingford, CT, 2010.

(192) Schmidt, M. W.; Baldridge, K. K.; Boatz, J. A.; Elbert, S. T.; Gordon, M. S.; Jensen, J. H.; Koseki, S.; Matsunaga, N.; Nguyen, L. A.; Su, S.; Windus, T. L.; Dupuis, M.; Montgomery, J. A. *J. Comput. Chem.* **1993**, *14*, 1347-1363.